The Long Island Sound Habitat Mapping Initiative Phase II – Eastern Long Island Sound

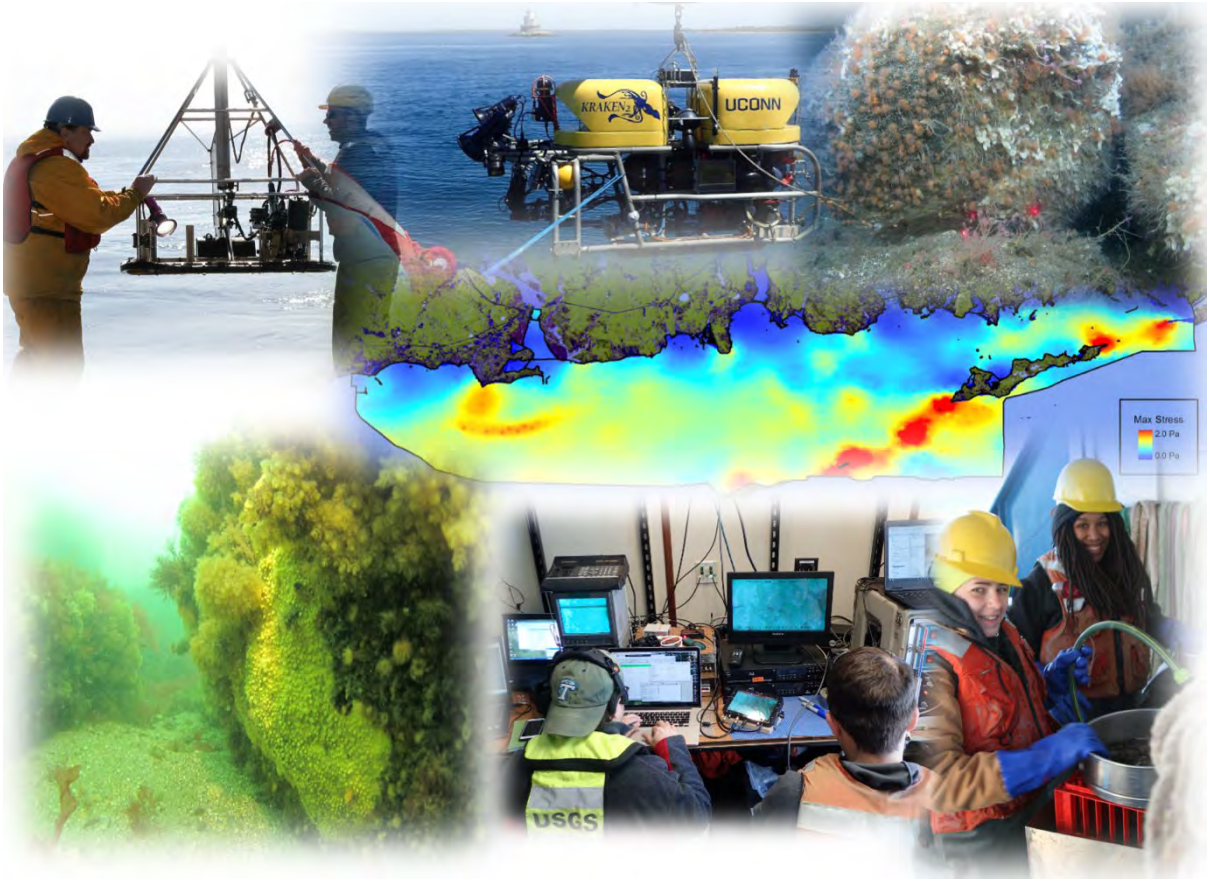

Final Report

Submitted by:
The Long Island Sound Mapping and Research Collaborative (LISMaRC)

August 23, 2021
Revised April 7, 2022

Long Island Sound Study
A Partnership to Restore and Protect the Sound

Connecticut Department of
ENERGY & ENVIRONMENTAL PROTECTION

TABLE OF CONTENTS

LIST OF FIGURES

LIST OF TABLES

Long Island Sound Cable Fund Steering Committee Organizations and Members

US Environmental Protection Agency, Long Island Sound Study
888 Washington Blvd, Stamford, CT 06901 (203) 977-1541

- Mark Tedesco

Connecticut Department of Energy and Environmental Protection, Land and Water Resources Division 79 Elm St., Hartford CT 06106 (860) 424-3034

- Brian Thompson
- Kevin O'Brien
- DeAva Lambert

New York Department of Environmental Conservation, Division of Marine Resources 205 North Belle Mead Road, Suite 1, East Setauket, New York 11733 (631) 444-0430

- Dawn McReynolds
- Victoria O'Neill
- Cassandra Bauer

New York Department of State, Office of Planning and Development
One Commerce Plaza Suite 1010, 99 Washington Ave., Albany, NY 12231-0001
(518) 474-6000

- Jeff Herter

Connecticut Sea Grant, University of Connecticut - Avery Point Marine Science Building
1080 Shennecossett Rd, Groton, Connecticut 06340-6048 (860) 405-9128

- Sylvain De Guise, Ph.D.

New York Sea Grant 125 Nassau Hall, Stony Brook University, Stony Brook, NY 11794-5001 (631) 632-6905

- Rebecca L. Shuford, Ph.D.

Collaborative Project Mapping Teams and Members

Long Island Sound Mapping and Research Collaborative (LISMARC):

University of Connecticut Avery Point, Marine Sciences Department
1080 Shennecossett Rd, Groton, Connecticut 06340-6048 (860) 405-9128.

- Ivar G. Babb, Principal Investigator
- Dennis Arbige

- Peter J. Auster, Ph.D.
- Chris W. Conroy, Ph.D.
- Todd Fake
- Kay Howard-Strobel
- Grant McCardell, Ph.D.
- Jim O'Donnell, Ph.D.

University of New Haven
300 Boston Post Rd, West Haven, CT 06516 (203) 932-7000.

- Roman N. Zajac, Ph.D.
- Chris Conroy, Ph.D.
- Nicole Govert
- Courtney Schneeburger
- Olivia Walton

U.S. Geological Survey
384 Woods Hole Rd., Woods Hole, MA 02543-1598
(508) 548-8700

- Seth Ackermann
- Dann Blackwood

Mystic Aquarium
55 Coogan Blvd.
Mystic, CT 06355

- Peter J. Auster, PhD.

General Acknowledgements

This project was made possible by the Long Island Sound Research and Restoration Fund, established by a Memorandum of Understanding among the members of the Policy Committee of the Long Island Sound Management Conference and administered by Long Island Sound Cable Fund Steering Committee.

The Steering Committee would like to thank and acknowledge the following:

- Katie Dykes: Commissioner, Connecticut Department of Energy & Environmental Protection
- Basil Seggos: Commissioner, New York Department of Environmental Conservation
- Deborah Szaro: Acting Regional Administrator, U.S. Environmental Protection Agency, New England-Region 1
- Walter Mugdan: Acting Regional Administrator, U.S. Environmental Protection Agency, New York-Region 2
- Benjamin Friedman, Acting NOAA Administrator and Under Secretary of Commerce for Oceans and Atmosphere

- Northeast Utilities Services Company
- Long Island Power Authority
- Cross Sound Cable, Inc.

LISMaRC Acknowledgements

The LISMaRc Team would like to thank the crew of the Research Vessel *Connecticut*, (Marc Liebig, Captain), the operators of the Kraken2 remotely operated vehicle (Kevin Joy, Dennis Arbige) the operators of the USGS SEABOSS (Dann Blackwood, Seth Ackerman), UConn Diving Safety Officer (Jeff Godfrey) and Research Vessel *Osprey* (Charles Woods, Captain).

We also thank the following for their assistance in the field and/or laboratory:

Nicole Adrion, Shaina Harkins, Tyler Fountain, Alexis Guitard, Annalee Mears, Marisa Thompson, and Amanda Tucker.

Citations

The recommended citations for the overall work and appendices are:

Long Island Sound Mapping and Research Collaborative (LISMaRC). (2021). "The Long Island Sound Habitat Mapping Initiative Phase II – Eastern Long Island Sound – Final Report." (Unpublished project report).

Long Island Sound Mapping and Research Collaborative (LISMaRC). (2021). "The Long Island Sound Habitat Mapping Initiative Phase II – Eastern Long Island Sound – Appendices." (Unpublished project report).

The recommended citations for the individual chapters that follow are provided at the beginning of each section.

EXECUTIVE SUMMARY

This report compiles the efforts of the Long Island Sound Mapping and Research Collaborative (LISMaRC) conducted from 2017 to present in the Phase II area of eastern Long Island Sound (LIS). LISMaRC is a partnership between the University of Connecticut, the University of New Haven and the U.S. Geological Survey. Funded by the Long Island Sound Cable Fund and administered by the Cable Fund Steering Committee the initiative this is the second of three phases focusing on areas identified by managers and scientists as high priority areas for habitat mapping. The comprehensive information needed to manage Long Island Sound and its resources must be gathered at a range of scales as the Sound is diverse in its topography, which in turn supports a diversity of life and natural resources. LISMaRC therefore used a variety of technologies and methodologies to provide data on a range of scales, from big picture acoustic maps of the features of the underwater landscape to the fine scale distribution of organisms living on and in the seafloor. Similar to the Phase I Pilot project the Phase II effort focused on: 1) acoustic shallow water mapping, 2) sediment grain size characterization, 3) ecological characterization and 4) physical oceanographic characterization.

Shallow Water Acoustic Mapping

The University of Connecticut led the LISMaRC shallow water acoustic mapping effort utilizing its Geoswath Phase Differencing Bathymetric Sonar (PDBS) deployed on the Research Vessel Lowell P. Weicker in 2017 and 2018. Prior to the mapping effort Val Schmidt from the Center for Coastal Ocean Mapping at the University of New Hampshire visited UConn and reviewed the equipment setup and spent a day at sea and provided recommendations for the subsequent surveys. Shallow water acoustic mapping efforts in the Phase II area were coordinated with Roger Flood, Stony Brook University, and the decision was made that UConn would map three areas (Survey Blocks 23, 24 and 25) identified by NOAA as gap areas. The newly acquired data were originally processed using the Geoswath software that was incompatible with existing data formats. The CARIS software was later acquired and the data were re-processed in this compatible format. Given time constraints, however, these data were not integrated into the unified data set developed by NOAA. Further, given the inherent noise generated by the Geoswath PDBS system and the challenges associated with trying to filter this raw data (both bathymetry and backscatter) using both the Geoswath and the CARIS software suites, it is not recommended to utilize this system for future Long Island Sound mapping efforts.

Sediment Texture and Grain Size Distribution

The goal of the Sediment Characterization effort was actually three-fold: 1) provide additional data on the sediment grain size in the Phase II area, 2) provide sediment samples taken by the SEABOSS' modified Van Veen grab for subsequent analysis by the Infaunal Ecological Characterization team of the Long Island Sound Mapping and Research Collaborative (LISMaRC) and 3) provide digital still images and videos for subsequent analysis by the LISMaRC Epifaunal Ecological Characterization team. Two surveys were conducted in the Phase II area in fall 2017 and spring 2018 using the U.S. Geological Survey's SEABed Observation and Sampling System (SEABOSS) deployed from the Research Vessel (R/V) Connecticut. Sea-floor images and videos were collected at 210 sampling sites within the survey area, and surficial sediment samples were collected at 179 of the sites. The samples from each survey were analyzed in the sediment laboratory at the

USGS Woods Hole Coastal and Marine Science Center using two different methods: the Beckman Coulter Multisizer 3 and sieving of the >= 4-phi fraction, and the HORIBA LA-960 laser diffraction analyzer and sieving of the >= -2-phi fraction. Separate subsamples were taken from each sample, stored and then sent to the Lamont Doherty Earth Observatory team (Tim Kenna) for separate grain size analyses. The results of the sediment grain size analyses revealed the preponderance of sand as the primary seafloor constituent representing 74% (by weight) of the overall samples. Furthermore there is a widespread geographic distribution of sand as the major seafloor constituent throughout the Phase II area.

The LISMaRC Sediment Texture and Grain Size element provided a comprehensive dataset to assist with several other elements of the overall Long Island Sound Cable Fund Habitat Mapping Initiative. These include: 1) acoustic backscatter groundtruth data, 2) sedimentary environments, 3) both infaunal and epifaunal ecological characterization, and 4) additional groundtruth data to assist with the physical oceanography component of the initiative. Furthermore, the USGS Data Release (Ackerman et al., 2020) has already been utilized as part of the data sets assisting the Equinor Corporation with its power cable routing in support of the Beacon Wind offshore windfarm they are permitted to develop.

Ecological Characterization

As in the Phase I Pilot, the Ecological Characterization of the Phase II area comprised a comprehensive approach built upon multiple scale technologies and methods required to assess the spatial complexity of the seafloor habitats in the area. The following elements were implemented to address this challenge.

Seafloor/Habitat Characterization

Based on previous studies, many at coarse scales, the Phase II study is known to be highly dynamic in terms of sedimentary processes, has a complex geomorphology in some areas, and is dominated by primarily sandy and coarser grained sediments, which is supported by the seafloor characterization in the current study. For the current effort several types of data representing different seafloor characteristics were used to classify and subsequently characterize the seafloor in the study area. These included a multibeam backscatter mosaic, bathymetry, seafloor rugosity as measured by the Terrain Roughness Index (TRI), maximum physical bottom stress, and sediment grain-size composition. The integrated backscatter mosaic of the seafloor was analyzed using eCognition that segments the mosaic into meaningful objects (image-objects) of various sizes based on spectral and spatial characteristics to identify regions with similar pixel values based on mean pixel brightness. Five classes (A – E) were designated based on general sedimentary groups (gravel, gravelly sand, sand, silty sand, and sandy silt) used by the USGS for analysis of sediment samples obtained at the Phase II sampling sites. Patch type D (gravelly sand) represented 45.1% of the study area, Patch C (sand) 41%, Patch B (silty sand), 11.3%, Patch E (sandy gravel), 1.7% and Patch A (sandy silt), 0.86%.

The distribution of the patch types is spatially complex throughout most of the Phase II study area; however, some broader trends do emerge that are similar to previous mappings of sediment distributions in this portion of LIS. There are also boulder areas at a few sampling locations but these were not considered within the overall characterization, which was based solely on sediment composition, depth, maximum seabed stress, and topographic roughness. There are also a number of relatively large sand wave fields in the Phase II area, particularly

in the western portion. The acoustic patch types represent general habitat areas that have certain environmental characteristics with regard to sediment grain size composition, topographic roughness, and maximum hydrodynamic stresses on the seafloor. These characteristics are potential determinants of the kinds of infaunal and epifaunal communities that may be found within the acoustic patch types.

Infaunal Ecological Characterization

The main focus of this portion of the study was to characterize the infaunal communities across the different sea floor environments found in the Phase II project study area, to assess differences in infaunal community structure among the large-scale acoustic patch types identified through the Seafloor/Habitat Characterization process and also ecological variability within these patch types. Infaunal grab samples (160) were collected for infaunal analyses using the USGS SEABOSS system during the fall, 2017 and spring, 2018 field campaigns. In the lab, samples were sorted under a dissecting microscope and individuals were identified to the lowest possible taxon.

After the data sets were assembled, several sets of statistical and GIS-based analyses were conducted to assess the characteristics of infaunal communities (total abundance [total number of identified organisms per sample], taxonomic/species richness [species richness and taxonomic richness are used interchangeably here and represent the number of taxa that were differentiated to the lowest possible taxonomic level], taxonomic/species diversity [as Shannon Diversity Index, a measure that accounts for both total number of taxa/species and relative proportion/evenness], community composition and related metrics [multivariate analyses measuring similarities and trends within and among samples]) among and within the large-scale acoustic patches that were identified, and to map the spatial trends in community structure and biodiversity relative to sea floor habitat structure.

A total of 289 infaunal taxa were identified in all the samples collected in the LIS Phase II area, 85% of these were identified to the species level. Two sets of analyses were conducted to assess the general infaunal community characteristics (taxonomic richness, total abundance and diversity): one using the entire data set from both sampling periods and also for each sampling period separately to assess potential seasonal differences among the large-scale patch types. Infaunal mean total abundances in the patch types generally ranged from ~ 175 to 225 individuals $0.1m^{-2}$ (Figure 5.2-1). Mean taxonomic richness ranged between 20 and 30 taxa $0.1m^{-2}$ using data from both sampling periods (Figure 5.2-5). The overall range was quite large, with some sites having upwards of 40 to 50 taxa, whereas others had as few as 4 to 5 taxa. Mean taxonomic diversity, which takes into account both the number of taxa and their proportional abundance and measured by Shannon diversity index H′, ranged from approximately 0.6 to 1.0, although at some sites it was higher approaching approximately 1.4

Infaunal community structure is spatially heterogenous in the Phase II Area and was variable within each of the patch types. Classification (cluster) analyses identified 13 community types, some of which were relatively distinct from the others, and others that were more similar. The distributions of the ten most abundant taxa were also spatially variable. This variation can likely be attributed, in part, to the environmental differences found among the acoustic patch types and environmental variability within each acoustic patch type relative to the large-scale environmental gradients across this portion of LIS. There are, however, some general trends that can be identified. Total abundance, taxonomic richness and diversity were highest in the central and eastern portions of the Phase II study area (Figure 5.2-26). High

abundances were found in the central portion of fishers Island sound and also within a large, deeper water area of the central portion of the study area. High taxonomic richness was found in the western portion of Fishers Island Sound, south of the Thames River, and in central portion of the study area. High taxonomic diversity followed a similar pattern as taxonomic richness although they were not spatially congruent. The infaunal community patterns discussed above exhibit a number of similarities to those found in previous studies.

Epifaunal Ecological Characterization

This element of the project is an extension of studies to develop spatially comprehensive seafloor habitat maps and interpretive products for Long Island Sound that includes emergent- and epi-faunal elements of seafloor habitats. There are inherent difficulties sampling hard substratum habitats upon which epi-faunal organisms depend, as well as the fragility of those emergent taxa and biogenic structures that occur on the surface of both hard substratum and fine-grained sediments. Specialized sampling tools and approaches for imaging and collection of physical samples (*e.g.,* integrated cameras/grabs, remotely operated vehicles, divers with quadrat cameras and airlift samplers) were used to address these issues. The majority of the samples for ecological characterization were collected during 2 sampling periods, between November 28 and December 3, 2017 and May 8 and 15, 2018 using the United States Geological Survey's (USGS) SEABOSS. Locations with high rugosity and complex topographies were sampled via still and video imagery with the Kraken2 ROV during 1 cruise conducted during May 2018, again using the RV Connecticut. Scuba was employed to collect quadrat camera still images and associated suction samples to assess and contrast patterns of diversity using visual versus direct sample approaches. This wet-diving component of the project was conducted between August 2017 and August 2018.

Epifaunal and emergent seafloor organisms and associated biogenic features were characterized using seafloor imagery and suction sampling by divers. Images were collected during SEABOSS and ROV transects (n = 602 SEABOSS images fall 2017, n = 595 SEABOSS images spring 2018, n = 110 ROV images spring 2018, n = 87 wet-diving images 2017-18).

A total of 119 taxa were identified to the lowest possible taxonomic unit and an additional 33 biogenic features, structures formed by organisms (*e.g.,* shell, tubes, burrows) and used as habitat by vagile fauna were observed in the study region. Multivariate analyses were implemented to test for differences in the composition of taxa and biogenic features based on eCognition patch assignments for image samples. The eCognition patches exhibit significant differences in both taxa and biogenic features such that each class has distinct characteristics useful to differentiate and map elements of habitats.

The distribution and abundance of taxa and features did not, however, follow uniform geographic trends, reflecting the varied seafloor habitats characterized by eCognition patches as described above, although a number of spatial patterns were identified that provide important insights on this region of Long Island Sound. Multiple taxa and biogenic habitat features were identified that represent larger gradients and general relationships with physical characteristics of seafloor environments, as well as ecological responses to on-going changes in local and regional environmental conditions. Some of these taxa are worthy of specific consideration due to their role as an ecosystem engineer or biogenic habitat, or their vulnerability, conservation status, or dominance in the community. These taxa are: hydrozoan and bryozoan turfs, ghost anemone *Diadumene leucolena*, macroalgal taxa

aggregated as Laminariaceae and Rhodopyhta, and the solitary hydroid *Corymorpha pendula.* These are identified in the analyses and GIS datasets as "Select Taxa."

A series of maps and brief descriptions were developed that illustrate the distribution and abundance of epifaunal and emergent taxa with diverse life histories as well as biogenic features that fill important functional roles as seafloor habitat. Most of these taxa are structure forming, serving an "ecosystem engineering" role, while the biogenic features are themselves structure. These maps and descriptions also describe many unique ecological relationships and trends occurring in this part of the Sound.

This component of the study also identified multiple sites with notable biological and geological features that were described and included associated imagery to visualize local conditions. These include Ellis Reef, Ram Island Reef, Black Ledge, Varved Lake Clays and Deltaic Deposits, Deep Boulder Morraines and south of the Race and Fishers Island

Integrated Ecological Characterization

The ecosystem dynamics of the seafloor and bottom waters are shaped by both the infaunal and epifaunal communities that are found in any particular habitat/bottom type. Both sets of organisms are critical in seafloor and demersal food webs, and are often key ecosystem engineers generating a variety of habitats, both when live and dead (e.g. shell hash from bivalves) that are critical to different life stages of the full biotic diversity of the seafloor. Thus, being able to determine patterns of joint infaunal and epifaunal community structure can provide insights into ecosystem function and also assessments for conservation and management.

In order to show the joint trends in several community characteristics for both infauna and epifauna in the Phase II study area, mean taxonomic richness and mean diversity were calculated at the sampling block (SB) and single sample site (NB) levels and plotted together in GIS.

An integrated habitat map links acoustic patch types to generalized physical and the defining ecological characteristics of biogenic features, infauna, and epi- and emergent fauna. It is notable that patterns of faunal composition and abundance (cover) follow the general grain size composition that is evident in the acoustic patch types (*i.e.*, finer to coarser sediments) along with the concomitant physical attributes.

The ecological pattern in this area comports with the similarity of sediment composition (a gradient of sand-gravel) such that patterns of diversity and dominance shift across patches but are drawn from a similar species pool. Depth, tidal stress, and related measures are correlated with such changes but species life-histories will be important for predicting the effects of ecological disturbance to human-caused impacts and patterns of resilience (e.g., acute versus chronic stresses and small versus large spatial scales).

Seafloor/Habitat Classification

In 2012, the Coastal and Marine Ecological Classification Standard (CMECS) was adopted by the Federal Geographic Data Committee. Sub-components and modifiers included in the CMECS documentation do not necessarily apply in all seafloor environments, which was recognized by its developers, so our approach was to adhere to the extent possible to CMECS modifiers but also to define our own as necessary to accurately describe biotic components

specific to the Phase II area. Our selections of sub-components and modifiers for the classification are based on the in-depth analyses conducted of the infaunal and epifaunal communities, as well as the analyses of the sediment and environmental data associated with characterization of the seafloor patch structure (Section 4.0).

We developed CMECS classifications at two levels of resolution, at the sample level and at the acoustic patch level. At the sample level, this included a CMECS classification for each sediment sample grab used for infaunal analyses and for those digital images used for epifaunal analyses. Having classifications at two levels of detail provides for more specific information at the scale of a sample site/image location. The CMECS classifications of the acoustic patch types summarize the results from the analyses of both the infaunal and epifaunal communities and associated environmental characteristics, such as surficial features that are ecologically relevant. Several classification levels were added to provide details about the habitat and ecological characteristics in the acoustic patch types.

The CMECS classification for the acoustic patch types attempts to capture their general attributes across the Phase II study area. As such, it should be used as a starting point for a more detailed consideration of ecological characteristics in any specific portion of the area using the more in-depth analyses presented in the Infaunal and Epifaunal Characterizations and their associated GIS databases.

Overall Discussion and Conclusions

Habitat Mapping

The seafloor environment in the Phase II study area is spatially complex, reflecting the mix of large-scale hydrodynamic and geomorphological features that influence its features.

The dominance of sands and coarser sediments in the Phase II study area is evident in the backscatter mosaic that was used for the characterization of sea floor habitat structure. Much of the mosaic has a complex pattern of image characteristics that are primarily associated with sandy/harder sediments than that of muddy/finer sediments. This is in contrast to the Phase I area where there are large areas of muddy sediments that were distinct features in the backscatter mosaic. Sea floor characterization, which can be used as a basis for habitat mapping, can be difficult in an area such as eastern LIS.

The acoustic patch types can be designated as habitat types, and their mapped distribution forms the basis of an overall habitat map for the Phase II study area (Figure 4.3-1 and see below). This also forms the framework for subsequent research and surveys that can assess the accuracy of the characteristics of these habitat types as determined in this study, and also the extent of the distribution of seafloor habitats in this portion of LIS.

Infaunal Communities

Infaunal community characteristics vary across the Phase II study area, but there are some general trends, notably higher total abundance and taxonomic richness from west to east. There are several areas of relatively high diversity throughout the study area. Infaunal community composition for each acoustic patch type, is relatively distinct, but variable within acoustic patch types, predominantly due to changes in taxonomic dominance.

Analysis of community structure without grouping by acoustic patch type revealed that differences were most notable between the south/central, and north coastal portions of the Phase II area. The eastern central portion of the study area is comprised of a variable mix of community types but their similarity is relatively high.

Apart from the community types that were indicated by the analyses, and the dominant species, there are portions of the Phase II study area that support infauna that occur in low numbers but can have important ecological functions and can be considered as indicators of relatively un-impacted environmental conditions. These include taxa such as ophiuroids, deep burrowing shrimp, sand dollars and large polychaetes.

Epifaunal Communities

The communities of attached and emergent taxa associated with each acoustic patch type were distinct principally based on changes in dominance and not wholesale differences in composition. As with infaunal community characteristics linked to sediment size fractions, epi- and emergent taxa were associated with multiple grain-sizes differentially represented within each acoustic patch type.

Management Considerations and Implications

The habitat and ecological characterization of the Phase II study area can inform managers, stakeholders, and policymakers about several important issues related to assessing risk and benefits of human activities in this region. These include:

- The results indicate complexity in the distribution of taxa at multiple spatial scales.
- The maps and data products represent a snapshot in time.
- In addition to the seasonal differences in benthic communities observed over the duration of Phase II, comparing results to past studies and sampling efforts reveal longer-term changes in seafloor ecology.
- The integrated habitat map, diversity, and community and taxon-specific maps, and the aggregate of supporting analyses, can inform decisions related to the spatial and temporal extent of potential impacts from human activities.

Physical Oceanographic Characterization

Springtime and wintertime deployments were executed using bottom-moored tripods with an array of instruments measuring temperature, salinity, currents, and stresses and two ship surveys were also executed to measure salinity, temperature, density structure and current patterns.

The Long Island Sound (LIS) FVCOM model uses a ‘nesting’ approach that is computationally efficient since it allows the effect of the larger-scale processes to be simulated at coarse resolution and allows UCONN computing resources to focus on the smaller-scale structures in LIS and Block Island Sound (BIS). LIS-FVCOM was initialized using a temperature and salinity climatology data set derived via objective interpolation of CTDEEP station data and the data in the NOAA archives. Skill assessments of the model were conducted for sea surface height, temperature and salinity. The skill assessments and model-data comparisons indicate that the model shows good agreement with both existing data and newly acquired data.

The model output was used to create monthly maps of near-bottom salinity and temperature within the study area as well as maps of both mean and maximum bottom-stresses. The model was also used to produce estimates of along-track MSL and water heights to support the acoustic surveys conducted by Roger Flood, Stony Brook University as well as provide further validation of the model results.

The model was used to produce maps of:

- The bottom temperature distributions throughout the study area for each month
- The bottom salinity distributions throughout the study area for each month
- The spatial structure of the maximum bottom stress magnitude due to (mainly) tidal currents
- The spatial structure of the mean bottom stress magnitude due to (mainly) tidal currents

Appendices

A comprehensive Appendix has been developed as a stand-alone document, largely due to the size of this document and the Appendices document as well as to follow the precedent established in the Phase I Pilot reporting structure. The Appendix comprises three major sections: 1) Map Products developed in the standard format provided by the Long Island Sound Cable Fund Steering Committee and 2) Metadata files also drafted using the template provided by the Steering Committee and 3) Field Logs and Data.

1.0 INTRODUCTION

1.1 Background

In June 2004, a settlement fund was created for the purpose of mapping the benthic environment of Long Island Sound (LIS) to identify areas of special resource concern, as well as areas that may be more suitable for the placement of energy and other infrastructure. This activity shall assist managers in the State of Connecticut, the State of New York, Connecticut and New York Sea Grant, and the U.S. Environmental Protection (USEPA) agency with their mandates to preserve and protect coastal and estuarine environments and water quality of Long Island Sound, while balancing competing human and energy needs with protection and restoration of essential ecological function and habitats.

In 2004, the Long Island Sound Study Policy Committee signed a Memorandum of Understanding on administering the fund for research and restoration projects to enhance the waters and related natural resources of Long Island Sound. In 2006, the Long Island Sound Study Policy Committee signed a second Memorandum of Understanding formally establishing a framework for the fund's use. The Policy Committee agreed that the Fund be used to: "Emphasize benthic mapping as a priority need, essential to an improved scientific basis for management and mitigation decisions." A LIS Cable Fund Steering committee, comprised of representatives from the Connecticut Department of Energy & Environmental Protection, the State of New York Department of Environmental Conservation, the State of New York Department of State, the U.S. Environmental Protection Agency Regions 1 and 2, the Connecticut Sea Grant and the New York Sea Grant, was convened to provide management and guidance for use of the fund.

Between 2004 and 2012, numerous workshops and meetings were held to help refine the vision for a benthic mapping effort. Additionally, a spatial planning exercise (Battista and O'Brien, 2015) was conducted to identify areas of LIS to concentrate data collections and analysis with the understanding that:

- Current funding was insufficient to have operations cover the entirety of LIS;
- By concentrating in areas where there were multiple interests from a range of stakeholders the utility of data collected and presented can be maximized.

The results identified three distinct geographic areas (Figure 1-1) The Pilot area is shown in green. The remaining areas have been designated as Phase 2 (eastern area in red) and Phase 3 (western area in red). Workshops and other meetings also defined the complementary topical areas necessary for a comprehensive habitat mapping effort for Long Island Sound and include:

- Acoustic Intensity - Acoustic intensity products are able to depict valuable properties about the composition, roughness, and texture of the seafloor to provide meaningful information to managers about the distribution and composition of seafloor habitats.
- Seafloor Topography - Seafloor topography products showing bathymetry and terrain relief are able to depict important features and seafloor changes to better explain physical, geological, and ecological processes.
- Benthic Habitat and Ecological Processes - Maps depicting seafloor habitats and their ecological communities are critical for many environmental management,

Figure 1- 1 Map of LIS depicting the three priority areas identified for habitat mapping.

- conservation, and research activities, and for the growing focus on coastal and marine spatial planning. Such maps depict either separately or in combination the spatial distribution and extent of benthic habitats classified based on physical, geological, geomorphological, and biological attributes and the benthic communities that reside in the mapped habitats. Additionally, maps can be produced that depict ecological process across the sea floor.
- Sediment Texture and Grain Size Distribution - Mud, sand, and gravel dominated areas provide very different habitats and the main grain size often determines many seafloor characteristics. Therefore, grain size composition and sediment texture of the seafloor are essential elements of any habitat classification and detailed knowledge of grain size distribution is the basis for many management decisions.
- Sedimentary Environments - Besides grain size the stability and suitability for different habitats for various species depend on the dominating sedimentary environment characterized by processes such as erosion, deposition, and transportation. Mapping and understanding these processes in detail is important for understanding habitats as well as their potential to change.
- Physical and Chemical Environments - Products that depict the distributions and variability of environmental characteristics like temperature, salinity, dissolved oxygen and bottom stress are central elements of habitat classification. They are also important to wise regulation and planning for dredging and other engineering activities in the coastal ocean.

1.2 Phase I Pilot Project

The Pilot Project was carried out from 2012 – 2014 for a section in LIS ranging from Bridgeport, CT to Port Jefferson, NY that includes the Stratford Shoals formation, and was implemented through a partnership of three consortiums consisting of:

- *National Oceanic and Atmospheric Administration (NOAA) Ocean Services Collaborative:* a partnership between the National Center for Coastal and Ocean Science (NCCOS) Biogeography Branch and the Office of Coast Survey;
- *Long Island Sound Mapping and Research Collaborative (LISMARC):* a partnership between the University of Connecticut, the U.S. Geological Survey, the University of New Haven, and the University of Rhode Island; and
- *Lamont-Doherty Earth Observatory (LDEO) of Columbia University Collaborative*: a partnership of LDEO, Stony Brook University, and Queens College – City University of New York

The teams worked together to address all of the critical elements for habitat mapping identified above and produced a comprehensive report and numerous map products aligned with each element. The results of the Phase I effort (Final Report and Appendixes) are available online (Long Island Sound Cable Fund Steering Committee, eds. 2015) at the Long Island Sound Habitat Mapping website (see links in Reference section below). The Steering Committee conducted a thorough internal and external review of the report and provided several recommendations that were incorporated into the Phase II scope of work and products reported and presented in this report.

1.3 Phase II Statement of Work

The overarching goal of the Phase II workplan is to provide environmental data and information to help better understand and manage the benthic resources of Long Island Sound by continuing in and improving on the efforts conducted in the pilot. The original statement of work (SOW) submitted on December 22, 2016 described the tasks to be conducted by LISMaRC for the Phase II area of the Long Island Sound Cable Fund Mapping Initiative. These included: 1) acoustic mapping of some of the shallow water areas of the Phase II region, 2) sediment grain size characterization, 3) ecological characterization, 4) physical oceanographic characterization and 5) database management and public access data portal development. As proposed, portions of some of these components (Acoustics and Sediment Grain Size) were done in collaboration with other project partners in the data collection and analysis phase. Summaries of each component conducted by LISMaRC are detailed below.

1.4 The Phase II Area of Interest

The Phase II area was defined by the process summarized above and illustrated in Figure 1-2 below. This area stretches from Duck Island west of the Connecticut River east to the Rhode Island border including Fishers Island Sound and areas to the south of Fishers Island, including the Race. This area comprises approximately 518 square kilometers.

Figure 1- 2 Map of the Phase II area outlined in the green polygon.

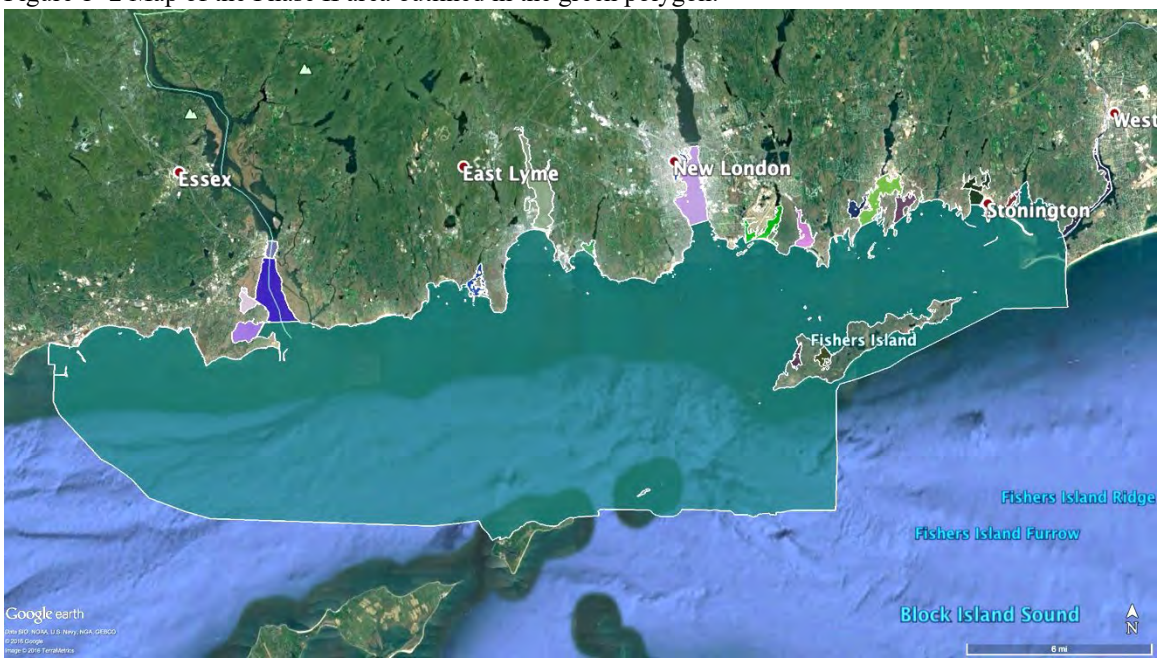

1.5 References

Battista, Tim & O'Brien, Kevin. (2015). "Spatially Prioritizing Seafloor Mapping for Coastal and Marine Planning." *Coastal Management* 43(1), 35-51. DOI: 10.1080/08920753.2014.985177

Long Island Sound Cable Fund Steering Committee, eds. (2015). *Seafloor mapping of long island sound – Final report: phase 1 pilot project.* (Unpublished project report). U. S. Environmental Protection Agency Long Island Sound Study, Stamford, CT. https://lismap.uconn.edu/wp-content/uploads/sites/2333/2019/01/LISCF_PilotMappingProject_Report_Final_June2015.pdf

Long Island Sound Cable Fund Steering Committee, eds. (2015). *Seafloor mapping of long island sound – Final report: phase 1 pilot project appendices.* (Unpublished project report). U. S. Environmental Protection Agency Long Island Sound Study, Stamford, CT. https://lismap.uconn.edu/wp-content/uploads/sites/2333/2019/01/LISCF_PilotMappingProject_Report_Final_Appendices_June2015.pdf

2.0 SHALLOW WATER ACOUSTIC MAPPING

Recommended Citations:

Babb, I and Arbige, D. (2021). Objectives. Section 2.1 in "Shallow Water Acoustic Mapping" p. 16 in "The Long Island Sound Habitat Mapping Initiative Phase II – Eastern Long Island Sound – Final Report" (Unpublished project report).

Babb, I and Arbige, D. (2021). Historical Context. Section 2.2 in "Shallow Water Acoustic Mapping" p. 17-20 in "The Long Island Sound Habitat Mapping Initiative Phase II – Eastern Long Island Sound – Final Report" (Unpublished project report).

Babb, I and Arbige, D. (2021). New Data Acquisition. Section 2.3 in "Shallow Water Acoustic Mapping" p. 20-26 in "The Long Island Sound Habitat Mapping Initiative Phase II – Eastern Long Island Sound – Final Report" (Unpublished project report).

Babb, I and Arbige, D. (2021). Data Processing Results and Integration. Section 2.4 in "Shallow Water Acoustic Mapping" p. 26-29 in "The Long Island Sound Habitat Mapping Initiative Phase II – Eastern Long Island Sound – Final Report" (Unpublished project report).

Babb, I and Arbige, D. (2021). Discussion. Section 2.5 in "Shallow Water Acoustic Mapping" p. 30 in "The Long Island Sound Habitat Mapping Initiative Phase II – Eastern Long Island Sound – Final Report" (Unpublished project report).

Babb, I and Arbige, D. (2021). Summary/Conclusions. Section 2.6 in "Shallow Water Acoustic Mapping" p. 30 in "The Long Island Sound Habitat Mapping Initiative Phase II – Eastern Long Island Sound – Final Report" (Unpublished project report).

Babb, I and Arbige, D. (2021). References. Section 2.7 in "Shallow Water Acoustic Mapping" p. 31 in "The Long Island Sound Habitat Mapping Initiative Phase II – Eastern Long Island Sound – Final Report" (Unpublished project report).

2.1 Objectives

As with the Phase I Pilot, a principal focal topic for the Long Island Sound Mapping and Research Collaborative (LISMaRC) was the acquisition of acoustic data to map the seafloor. The acquisition of high-resolution bathymetry and backscatter data provide the stepping off point for all subsequent elements of the habitat mapping initiative. The bathymetry provides detailed information on the seafloor topography, while at the same time providing quantitative data that can be used to develop a number of derived products such as slope, rugosity and topographic roughness indices. The backscatter data provides a proxy for the nature of the seafloor with harder substrates providing a stronger acoustic return from the seafloor contrasted to the softer sediments that absorb much more of the sound from the acoustic survey systems. These variable seafloor reflectance values are typically displayed as gray-scale, with the harder substrates displayed as lighter shades, while the softer sediments are displayed with darker tones.

2.2 Historical Context

At detailed review of existing data was conducted by NOAA's National Centers for Coastal Ocean Science (NCCOS) prior to developing the scope of work (SOW) for the Phase II Acoustic Mapping element. This analysis generated a report (NCCOS, 2015) that listed existing acoustic data surveys (Figure 2.2-1). NCCOS utilized the existing surveys to develop unified bathymetry (Figure 2.2-2) and backscatter (Figure 2.2-3) mosaics for the Phase II area. These unified maps served as the baseline of existing acoustic data in the Phase II area to which newly acquired data was to be integrated.

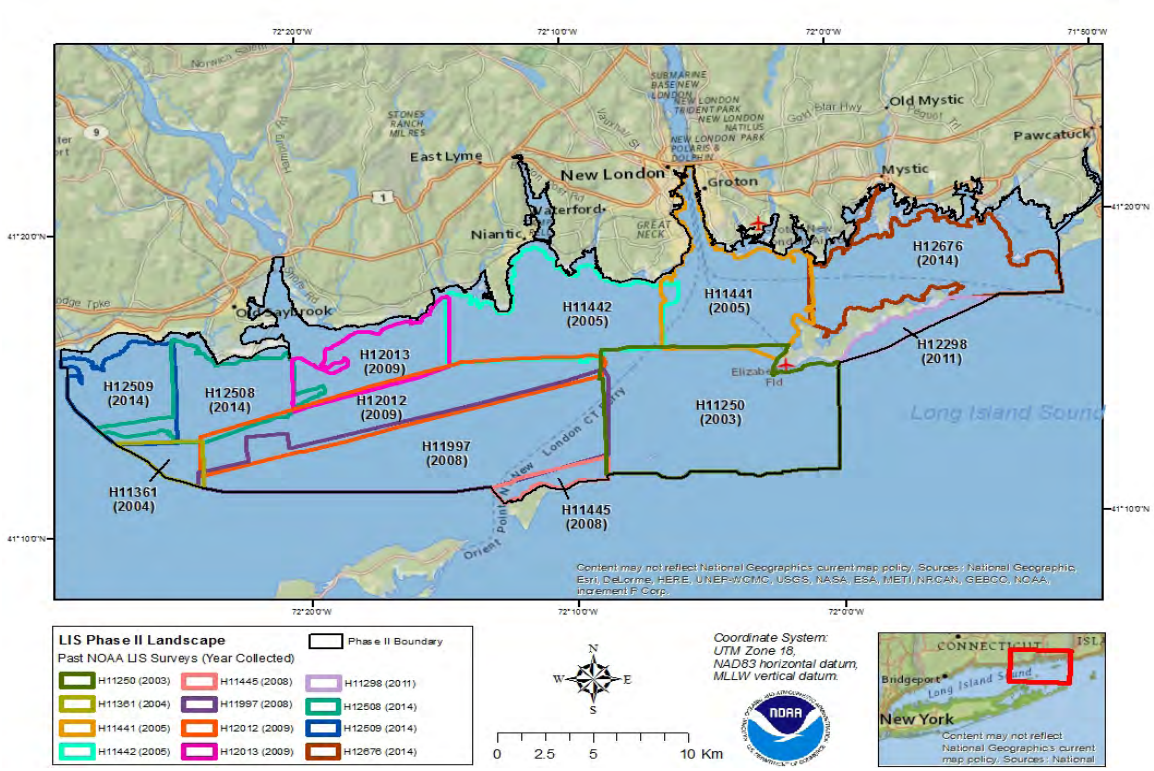

Figure 2.2-1 Map of previous NOAA surveys in the Phase II area.

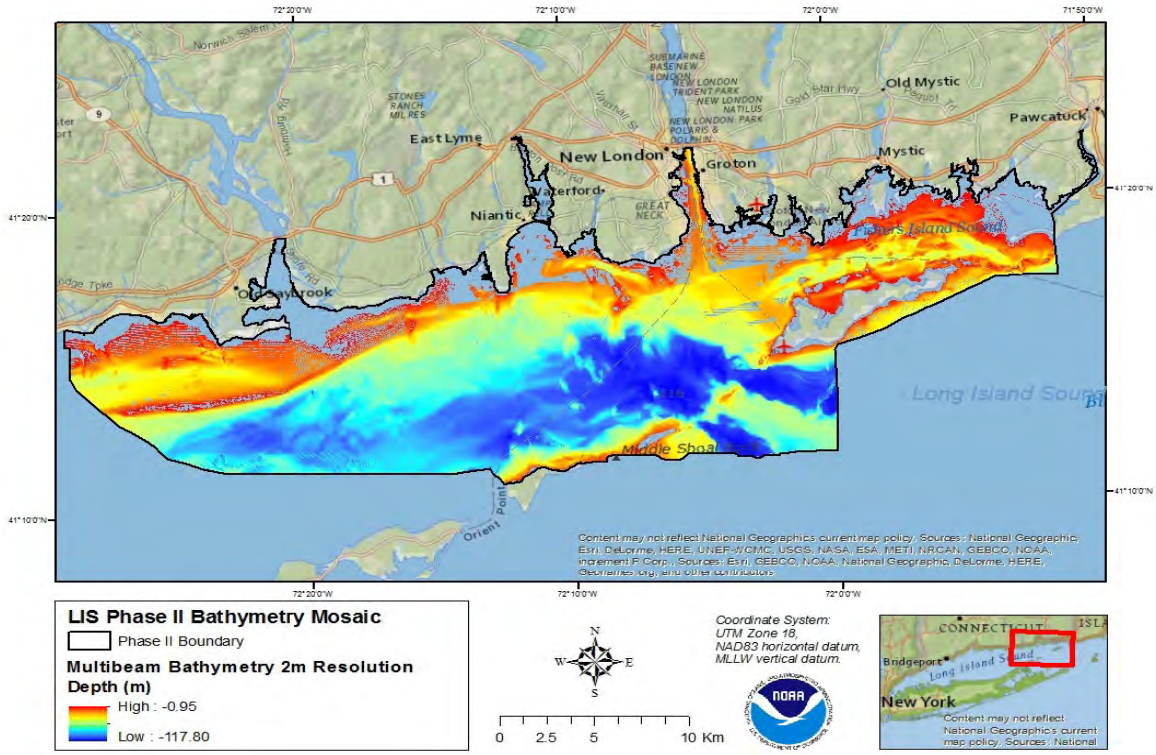

Figure 2.2-2 Unified bathymetry mosaic developed by NCCOS

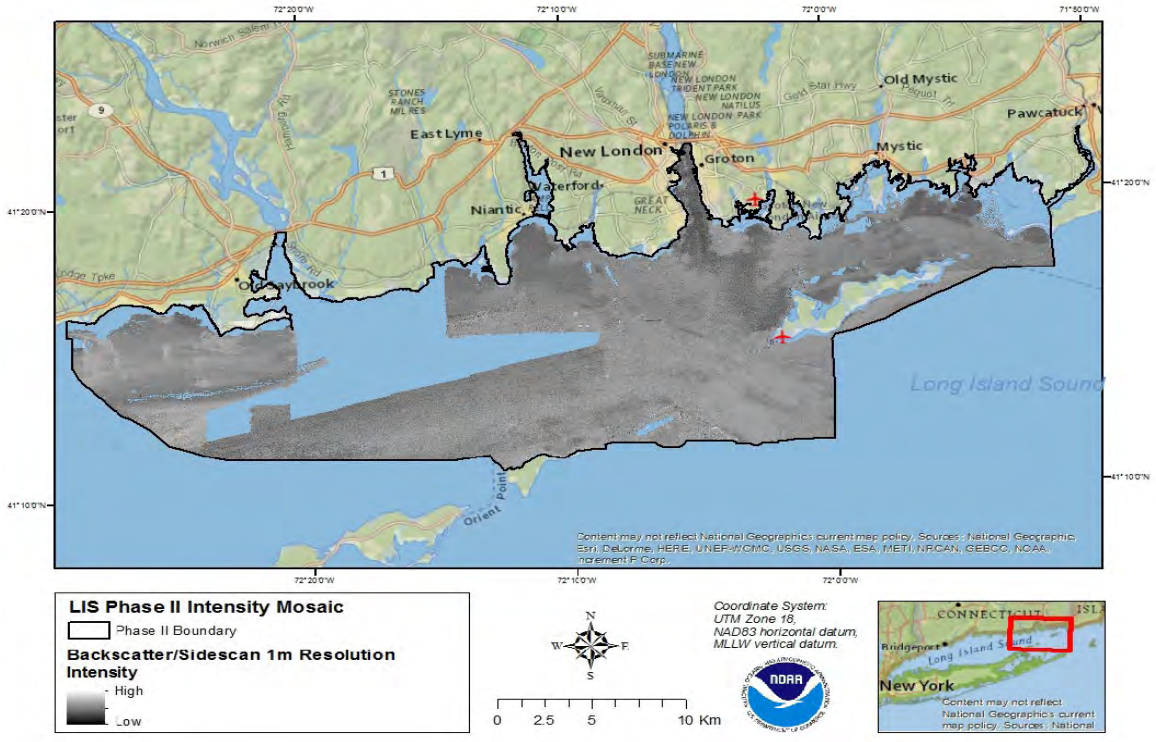

Figure 2.2-3 Unified backscatter mosaic developed by NCCOS

2.2.1 Gap Analysis and Survey Block Selection

The NCCOS 2015 report also identified remaining data gaps for both bathymetry and backscatter and previously un-surveyed areas in the Phase II area (Figure 2.2-4).

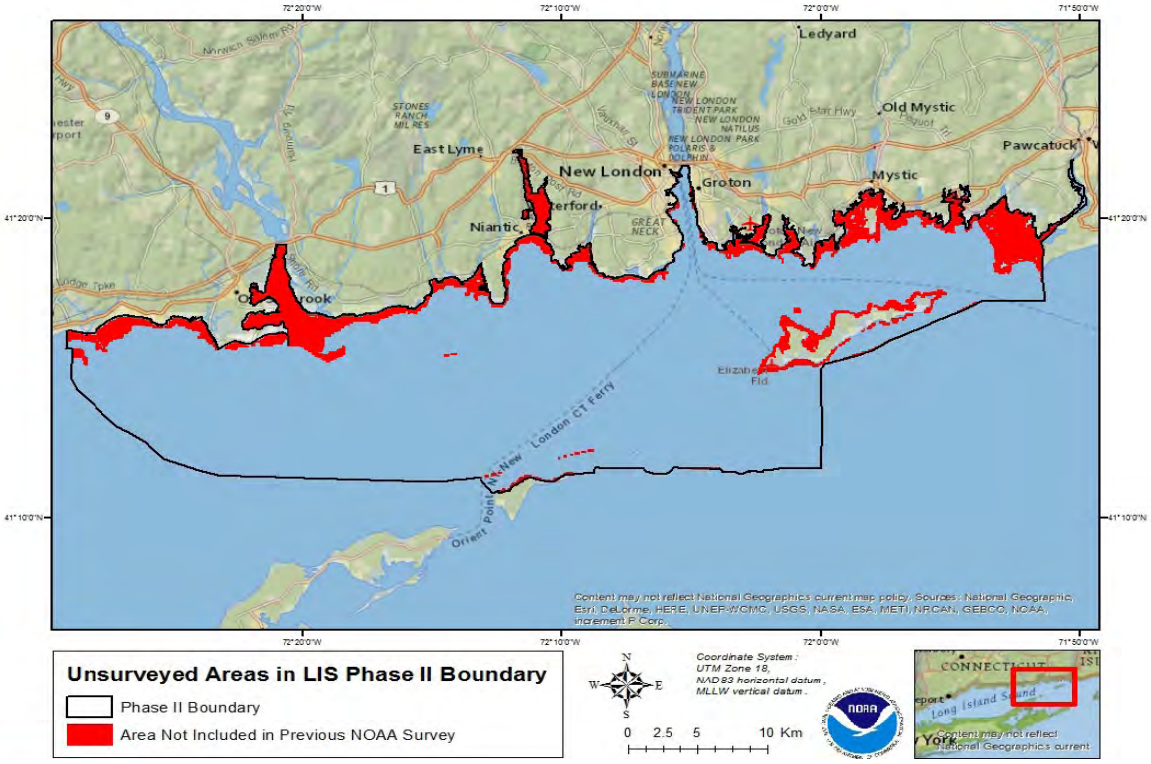

Figure 2.2-4 Map of areas within the Phase II region not previously surveyed by NOAA.

Each of these areas were prioritized by the gap density, i.e. areas with most data gaps were the highest priority, as opposed to some other determinant e.g. management or ecological priority.

The unmapped areas were parsed into two shallow blocks (1-3 fathoms) and 30 deeper blocks (>3 fathoms) (Figure 2.2-5). The decision was made not to attempt to map the two shallow blocks due primarily to the challenging nature of working in these areas (ie. minimum water depths of 1.4 meters less than the survey vessels' draft and the degree of effort needed to map these areas, ie. shallower waters require tighter678 line spacing and therefore more time on the water to complete). Teams from the Lamont-Doherty Earth Observatory (LDEO) consortium (Stony Brook University) and the Long Island Sound Mapping and Research Collaborative (LISMaRC) (UConn) coordinated efforts to map the deeper water priority sites using their respective technologies. Stony Brook utilized a Kongsberg EM3000D dual-head multibeam sonar system deployed from their RV Pritchard, while UConn utilized its Geoswath Phase-Differencing Bathymetric Sonar (PDBS, also called an interferometric system) from the RV Weicker.

This collaboration manifest in a division of labor between the LISMaRC UConn and SOMAS teams to collect new acoustic data in the gap areas (Survey Blocks) identified by NOAA for new data acquisition. The LISMaRC team surveyed Blocks 23, 24 and 25, which were adjacent to the UConn Avery Point campus. This resulted in the acquisition of 1.35 square miles (3.49 square kilometers) for Block 23 and 4.95 square miles (12.8 square kilometers) for Blocks 24 and 25, for a total of 6.3 square miles (16.29 square kilometers). The SoMAS team surveyed the remaining Blocks, and also collected some new data in Blocks 24 and 25

for comparison purposes, acquiring 35.1 square miles of new bathymetry and backscatter data (91.0 square kilometers). The total area of new bathymetry and backscatter data collected for the Phase 2 study was thus 41.4 square miles (107.2 square kilometers).

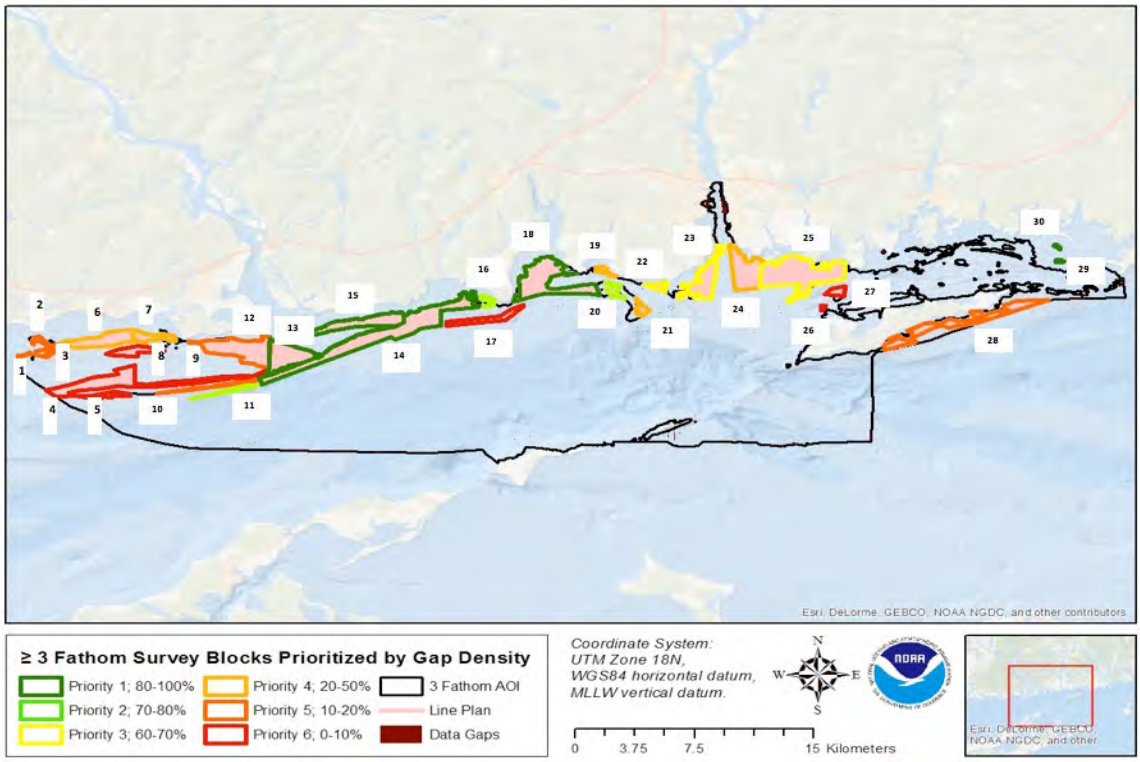

Figure 2.2-5 Map of the deeper (>3 fathom) shallow water gaps prioritized by NOAA.

2.3 New Data Acquisition

2.3.1 Survey Methods

Prior to conducting the acoustic surveys of the selected blocks, LISMaRC contacted the Center for Coastal Ocean Mapping at the University of New Hampshire to provide an on-site consultation of the technologies and proposed approach to mapping. This visit took place on May 4th, 2017 and involved a review of the Geoswath PDBS sonar installation on board the RV Weicker, a review of system configuration and data acquisition settings. Several hours were spent on board the vessel with Val providing insights and recommended strategies for the system's operation. Most significant was the importance of keeping the gain, pulse length and power at same levels throughout the entire survey.

The Geoswath system was mounted in the moonpool on the RV Weicker and the acquisition system located on nearby workbench (Figure 2.3-1).

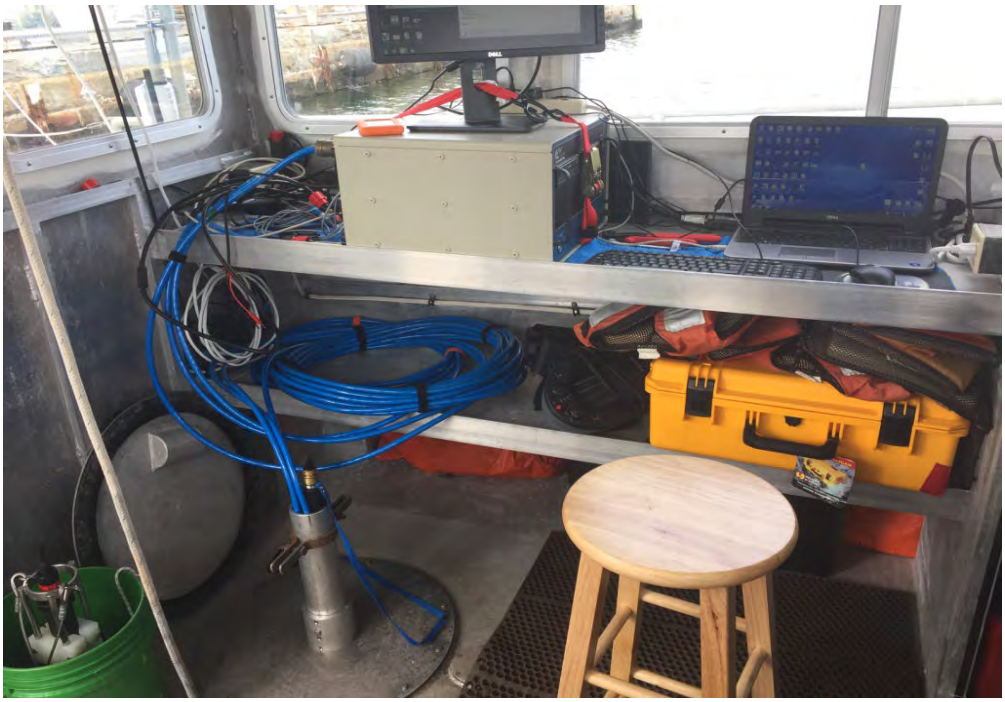

Figure 2.3-1 Geoswath setup on the RV Weicker, moonpool cover is in the lower left.

The surveys were conducted at a vessel speed between 4-5 knots (10 km/hr) to ensure data density sufficient to meet the NOAA recommendations. Due to the sampling gap at nadir generated by the PDBS a 100% swath overlap was implemented to provide the recommended 100% coverage of bathymetric and backscatter data. The swath width (line spacing) was also maintained to not exceed the 5 times water depth, which in reality is a conservative approach for an interferometric system (Figure 2.3-2). A survey line spacing of 25 meters/side was used in shallow areas, while a 30-meter spacing was adopted for deeper areas.

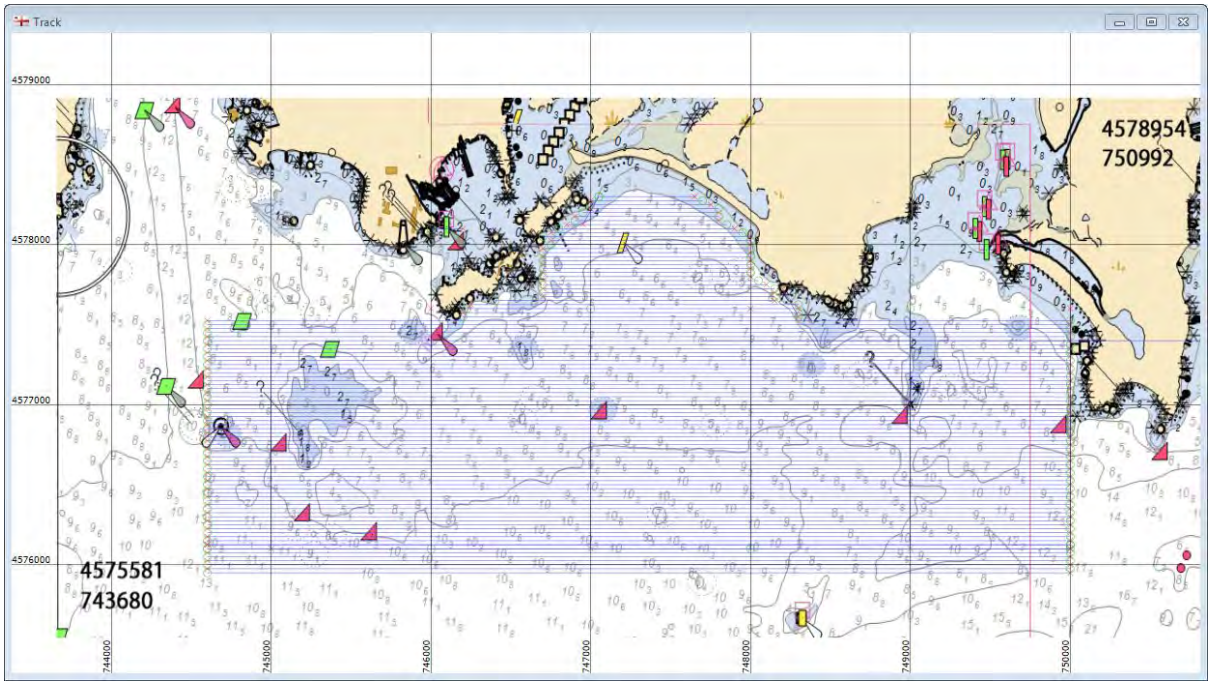

Figure 2.3-2 Screen capture from the RV Weicker's navigation system illustrating the tight spacing of the survey lines for Survey Blocks 24 and 25.

To improve survey accuracy and precision LISMaRC utilized UConn's ACORN (Advanced Continuously Operating Reference Network) that is composed of several receivers (GPS) that stream data to on-campus computers. The computers distribute the information to surveyors and mappers to help them in their work. ACORN allows highly accurate positioning in real time. This means that a location anywhere on or above the earth can be pinpointed within the space of a dime. The ACORN maintains nine base stations in the state of Connecticut including two that provide coverage within the Phase II area. LISMaRC worked with ACORN staff to integrate this real-time network (RTN) into the navigation system on the Weicker to provide this much improved accuracy. A description of the ACORN can be found at: http://naturally.uconn.edu/2014/07/29/this-is-not-your-cars-gps/ and the site network is http://acorn.uconn.edu

Sound velocity profiles (SVP) were conducted every three hours to acquire sound speed data using UConn's Valeport SVP system. Sound velocity data was imported into the processing software for sound speed corrections.

Data acquisition was performed using the Geoswath+ acquisition software and saved as .rff files for subsequent post-processing. The system recorded bathymetry and side scan sonar data along with heave, pitch and roll data from a Seatex MRU-5 mounted on the Geoswath transducer.

2.3.2 Field Survey Results

The acoustic surveys were conducted over the course of approximately one year from 2017-2018. Seasonal considerations, ship and crew schedules were the primary drivers for the protracted survey period. Table 2.3-1 lists the dates and times for the survey legs, showing a total survey investment of about 15 days to map the Survey Blocks 23, 24 and 25. LISMaRC had originally estimated a 20-day mapping period as part of its contribution to the new acoustic data acquisition.

Table 2.3- 1. Survey Log from UConn Geoswath Surveys 2017-2018.

Date	Depart (UTC)	Return (UTC)	Hours	Comments
4/31/2017	13:00	18:50	5.833	
5/4/2017	12:00	15:30	3.500	Engine problems
5/8/2017	13:00	17:48	4.800	Rerun lines from 5/4
5/17/2017	13:00	20:05	7.083	
5/18/2017	12:55	19:30	6.583	
6/21/2017	14:57	19:09	4.200	
6/22/2017	13:00	18:38	5.633	
6/23/2017	13:00	17:17	4.283	
Subtotal			41.917	
7/26/2017	15:00	20:31	5.517	
7/27/2017	13:00	19:07	6.117	
7/28/2017	16:00	19:00	3.000	
7/31/2017	16:00	20:06	4.100	
Subtotal			18.733	

8/14/2017	13:00	15:00	2.000	Overheat problems with transmitter
8/15/2017	14:00	17:10	3.167	
8/16/2017	11:30	16:45	5.250	
8/17/2017	12:00	16:50	4.833	
Subtotal			15.250	
6/5/2018	13:30	19:30	6.000	
6/6/2018	13:30	19:30	6.000	
6/7/2018	13:50	20:15	6.417	
6/11/2018	14:00	19:00	5.000	
6/19/2018	14:00	15:00	1.000	Overheat problems with deckbox
6/20/2018	14:20	18:32	4.200	
6/21/2018	14:10	18:55	4.750	
Subtotal			33.367	
7/17/2018	14:30	17:10	2.667	
7/18/2018	14:30	17:20	2.833	Overheat problems with deckbox
7/19/2018	13:00	18:38	5.633	
Subtotal			11.133	
Grand Total Hours			120.400	
Grand Total Days (8 hour days)			15.050	

2.3.3 Data Processing

2.3.3.1 Geoswath Data Processing

Processing of the acoustic data collected via the Geoswath+ system to develop the data products recommended by NOAA was problematic. Prior to the surveys UConn upgraded the software to Geoswath GS4 that generated data in a format that was unreadable by earlier versions of the CARIS software that uses the CUBE (Combined Uncertainty and Bathymetric Estimator) algorithm. According to the Center for Coastal and Ocean Mapping: "CUBE (Combined Uncertainty and Bathymetric Estimator), is an error-model based, direct DTM generator that estimates the depth plus a confidence interval directly on each node point of a bathymetric grid. In doing this, the approach provides a mechanism for automatically "processing" most of the data and, most importantly, the technique produces an estimate of uncertainty associated with each grid node." (CCOM: http://ccom.unh.edu/theme/data-processing/cube.) This feature is built into the CARIS software, recommended by NOAA for acoustic data processing, however, UConn's CARIS license had lapsed at the time of the survey.

Therefore, the bathymetry data were originally processed using the Geoswath GS4 software, while the backscatter data was processed using Kongsberg's Geotexture software. These data products were reviewed by NOAA and were deemed to be very "stripy" and several conversations were had to explore how to address this result. Over the course of several months in 2018-2019 UConn worked with NOAA to test several approaches to improve the output. Suggestions were made to export the Geoswath data in a .gsf (general sonar file)

format to perhaps allow NOAA technicians to import the data into CARIS, which was done and sent to NOAA in September, 2018. An issue arose from this attempt as all of the necessary survey offsets were removed during the generation of the .gsf file format, essentially forcing them to work with unfiltered data. Further Webex meetings were held in October, 2018 to discuss other methods to address the issues with the data. Another suggestion was to attempt additional nadir filtering. To that end a three-meter gap along the nadir was filtered out, since there was additional data to fill in the gaps from the adjacent overlapping lines. However, in the final analysis, the striping was still just as evident. UConn felt that the major part of the striping was from the density (and noise/scatter) of the data at the edges of the swaths, even though the swath width was trimmed very aggressively; essentially using only 4 to 5 times water depth for usable swath width (vs the 10-12 times water depth claimed by Geoswath). The Geoswatch backscatter (side scan sonar) data was also problematic to process, and several attempts to work with NOAA (LTJG Jennifer Kraus) were made, including sending geotiff files for import into CARIS. No improved results were returned.

2.3.3.2 CARIS Data Processing

Ultimately, the decision was made to acquire the latest version of the CARIS software to ascertain how well it could address the striping issue, along with its capability to run the CUBE algorithm to address the data uncertainty. The CARIS software was acquired in late 2019 and a second round of data processing was initiated. There were several upgrade issues, hardware problems and operating system incompatibilities that had to be addressed before the CARIS software was finally operational on one of UConn's computers.

A schematic of the CARIS processing workflow is illustrated in Figure 2.3-3. The first step is to create a Vessel File (eg., RV_Weicker.hvf). This vessel file contains all the physical offsets between the various sensors used in the data acquisition (transducers, GPS antennas, gyro, heave sensor, pitch sensor, roll sensor, etc.). It also contains timing delays, and transducer error corrections for pitch, roll, and yaw which are determined during pre-survey "Patch Tests." The vessel file also contains the uncertainty values (standard deviation) for the various sensors and measurements which are then used to compute the horizontal and vertical Total Propagated Uncertainty (TPU). Note the creation of a "HIPS file" is also an automatic part of CARIS processing. Figure 2.3-4 is a screen shot of the TPU values that were input into the .hvf file as part of the CARIS processing.

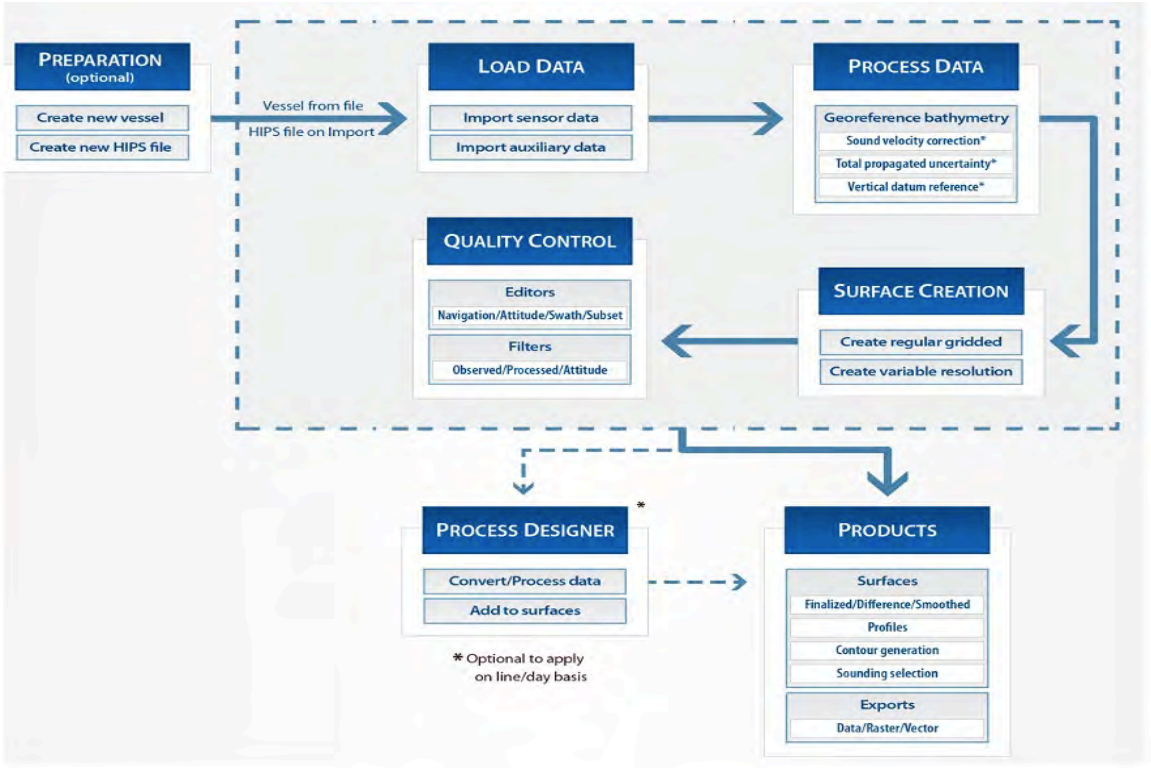

Figure 2.3-3 Schematic of the CARIS data processing workflow (from Teledyne CARIS 2021 Version 11)

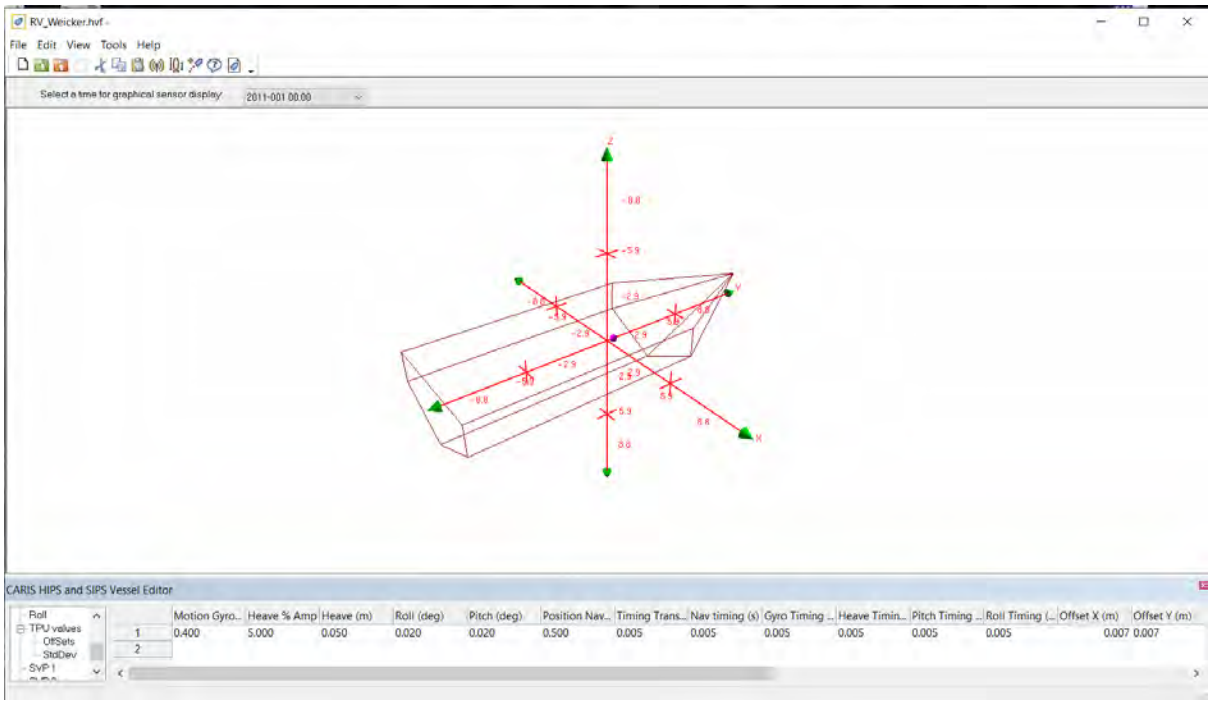

Figure 2.3-4 Screenshot from the CARIS software's Vessel Editor used to input the uncertainty values for the RV Weicker used for the LISMaRC acoustic acquisition.

The next processing step was to load the sensor data. The Geoswath acquisition software uses the original "linename" supplied by the operator, then creates 9 support files using that "linename.xxx" format. Of these files, the .rff file is the raw sensor data that CARIS imports

to begin its processing. The tide and sound velocity profile data were then formatted for CARIS and imported as the auxiliary data. These raw data files have been uploaded to the Lamont Doherty Earth Observatory (LDEO) LIS Map Archive.

The next box in the flow diagram is the Process Data. This step is known as "Georeferencing Bathymetry." This process converts the raw data trackline depths into latitude, longitude, and depth by combining the ship navigation with horizontal and vertical offsets from the vessel file. This geographically references the sounding position and depth. Other corrections such as Sound Velocity Correction, Total Propagated Uncertainty (TPU), and Vertical Datum Reference are added at this step.

The CARIS processing software then allows for the generation of four different types of Regular Gridded Surfaces. These are Swath Angle, Shoalest Depth True Position, Uncertainty, and CUBE (Combined Uncertainty and Bathymetry Estimator). The CUBE was selected as the method of choice for generating the gridded surface, as this met the NOAA requirements.

The next step in the process was quality control editing. After creation of a "regular gridded surface", it was necessary to review and edit/clean the raw data before it could be used to create Final Products. This was done with a series of automatic and manual editing tools; including Navigation Editor, Attitude Editor, Swath Editor, and Subset Editor.

The final step was to generate the Geotiff imagery and .PDF standardized map template data products proposed in the original scope of work.

2.4 Data Processing Results and Integration

The results below represent the map products generated by the above processing procedures and represent new acquisition of 3.49 km2 for Block 23 and 12.8 km2 for Blocks 24 and 25 combined (Table 2.4-1). The map images included in this report have been reduced significantly for this report and the .PDF standard map template versions are provided in Appendix One. Full size images are available on the Long Island Sound Mapping website (https://lismap.uconn.edu) or the Lamont Doherty Earth Observatory Long Island Sound Data Portal: MGDS (http://www.marine-geo.org/portals/lis/). These results were also provided to NOAA via a Google Drive.

Table 2-4-1 LISMaRC Phase II New Acoustic Data Acquisition

Survey Name	Survey Blocks	Survey Area (km^2)	Deployment		Blocks Completed?
		Total UConn Survey Area: 16.29 km ^{2}	May - August, 2017 & June, 2018 (MJ)	June-July 2018 (JJ)	C = Complete P = Partial
B2, B3, B4, B5, B6,	24, 25	12.8	MJ		C
A1, A2, A3, A5, A6	23	3.49		JJ	C

2.4.1 Geoswath Processing Results

A mosaic of the bathymetry data from Survey Blocks 23, 24 and 25 generated by Geoswath GS4 software is seen in Figure 2.4-1. The striping of the data generated from the survey lines is evident in this image. The color ramp has orange as the shallowest water ranging to the blue deeper areas. Despite the striping issue the bathymetry map does provide a very good representation of the seafloor topography of this part of the Long Island Sound. This Geoswath image has a "shaded relief image" that has slightly exaggerated "z" elevation and "sun lighting" which give it the dramatic shadow effects.

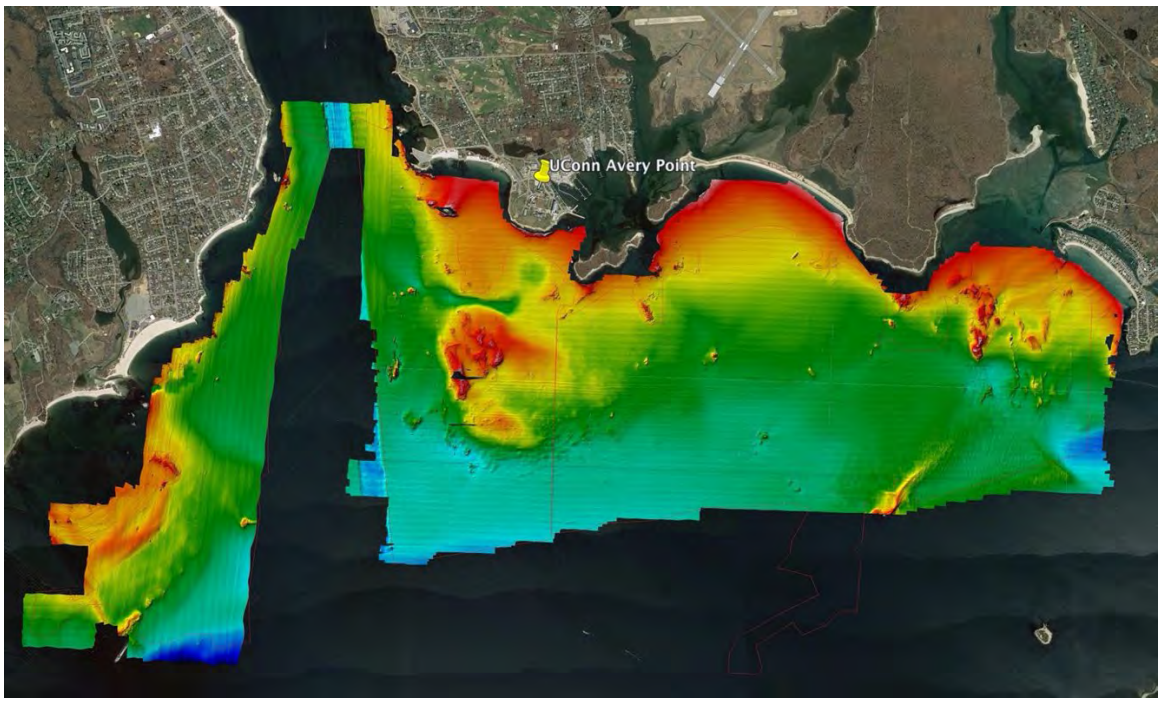

Figure 2.4-1Mosaic of bathymetry data from Survey Blocks 23, 24 and 25 generated by the Geoswath GS4 processing.

As described above, the Geoswath backscatter data was more problematic and the striping issue is evident in the output seen in Figure 2.4-2. However, the image does provide useful information on the nature of the seafloor in this part of the Sound. For these maps the reflectance value was used (vs absorption) with higher reflectance producing darker color areas to depict harder bottom areas and lighter reflectance in areas with softer substrates.

Figure 2.4-2 Mosaic of backscatter data from Survey Blocks 23, 24 and 25 generated by the Geoswath GS4 processing.

2.4.2 CARIS Processing Results

The results of the CARIS processing for the Survey Blocks 23, 24 and 25 can be seen in Figure 2.4-3 and Figure 2.4-4. As can be seen in Figure 2.4-3 the filtering applied to the surface reduced the striping issue at the expense of topographic resolution. This is particularly evident in the shallower (orange-red) and rougher seafloor areas. Figure 2.4-3 was generated with only "color shaded" by depth, lacking the sun illumination and hill shading seen the in Geoswath imagery. Figure 2.4-4 was generated with a 5x vertical exaggeration, which does provide greater relief, but also enhances the striping. Also of note is that the CARIS processed data includes additional data to the south of Survey Blocks 24 and 25, which was acquired after the decision was made to process the data using CARIS, and was therefore missing in the Geoswath processed images.

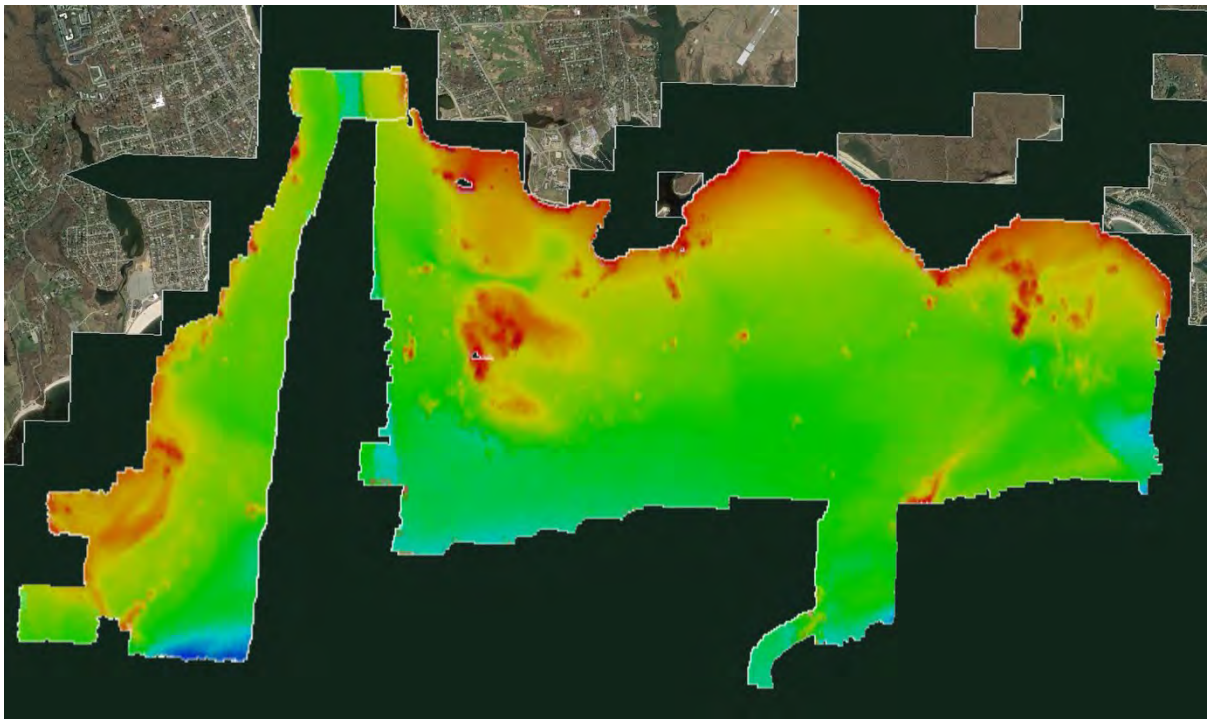

Figure 2.4-3 Mosaic of bathymetry data from Survey Blocks 23, 24 and 25 generated by the CARIS processing.

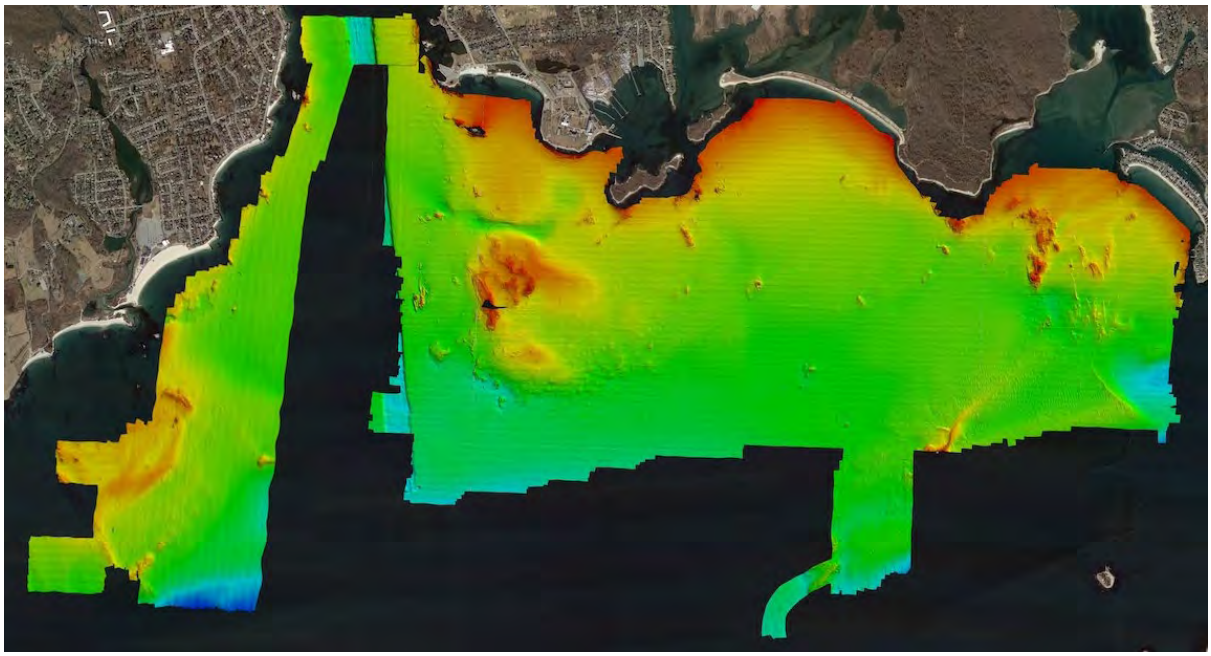

Figure 2.4-4 Mosaic of bathymetry data from Survey Blocks 23, 24 and 25 generated by the CARIS processing with a 5x vertical exaggeration applied.

The results of CARIS processing of the backscatter data can be seen in Figure 2.4-5. It appears that this image presents a bit more striping, particularly in the lighter (lower reflectance) areas.

Figure 2.4-5 Mosaic of backscatter data from Survey Blocks 23, 24 and 25 generated by the CARIS processing.

2.5 Discussion

All of the original raw data files, tide, sound velocity profiles, field logs and all of the CARIS files and subdirectories and final Geotiff data products were copied onto an external hard drive and sent to Frank Nitsche at the Lamont Doherty Earth Observatory (LDEO) at Columbia University for upload to their Long Island Sound data depository. Delivery of the data was confirmed by Dr. Nitsche on 6/2/2020. Subsequently, metadata files using the recommended LIS Cable Fund Word Doc template were developed and also sent to the LDEO repository. Due to all of the back and forth with NOAA during most of 2019, they were not able to integrate LISMaRC's CARIS data into their final unified map products they generated as part of their deliverables. No decision has been made as to how to further proceed with any future integration of this data.

There is a part of the Block #24 that was surveyed with the LISMaRC Geoswath system and by Roger Flood using the Kongsberg beam-forming multibeam sonar. There have been discussions about developing an overlay map of this area to compare the results of the two systems directly, however, fiscal and temporal resources are lacking to conduct this comparison.

2.6 Summary/Conclusions

The process of identifying the gap areas to be mapped in the Phase II area was very effective, as was the division of labor to conduct the new data acquisition between LISMaRC and Stony Brook University. The UConn Geoswath Phase Differencing Bathymetric Sonar was able to acquire data within the three sample blocks (23, 24 and 25) from the RV Lowell Weicker over an extended time period from 2017-2018. The processing of the newly acquired data, however, was challenging, owing primarily to ongoing system and software

updates by the Geoswath company that affected integration of the data to the standards established by NOAA in the original scope of work. Acquisition of the latest version of the CARIS software allowed for the required process steps to meet the requirements and generate a product that could be integrated with the existing and newly acquired (by the Stony Brook University group) acoustic data.

However, given the inherent noise generated by the Geoswath Phase Differencing Bathymetric Sonar (interferometric) system and the challenges associated with trying to filter this raw data (both bathymetry and backscatter) using both the Geoswath and the CARIS software suites, it is not recommended to utilize this system for future Long Island Sound mapping efforts. This is particularly the case since there is currently a proposal being processed as part of the EPA's Long Island Sound Study Enhancement Grant (LISS EG) program for acquisition of a new dual head Kongsberg multibeam sonar for use in LIS. This effort is being led by Roger Flood at Stony Brook University (SBU) and the University of Connecticut is also involved to be part of the operations team to operate this new system. Furthermore, the proposal includes time to install, test and utilize this new system on both SBU's RV Seawolf and UConn's RV Connecticut to demonstrate that it can serve as a truly regional resource for seafloor mapping in the Sound. It is envisioned that future acquisition of acoustic data as part of the LISS EG as well as the Phase III of the Long Island Sound Cable Fund will be conducted using this new, state of the art system.

2.7 References

Center for Coastal and Ocean Mapping – Joint Hydrographic Center: CUBE http://ccom.unh.edu/theme/data-processing/cube

National Centers for Coastal Ocean Science (NCCOS) (2015). *NOAA phase2 summary report final*. NCCOS.

Teledyne Caris (2021). *HIPS and SIPS*. https://www.teledynecaris.com/en/products/hips-and-sips/

3.0 SEDIMENT TEXTURE AND GRAIN SIZE DISTRIBUTION

Recommended Citation:

Ackerman, S. and Babb, I. (2021). Objectives. Section 3.1 in "Sediment Texture and Grain Size Distribution" p. 32-33 in "The Long Island Sound Habitat Mapping Initiative Phase II – Eastern Long Island Sound – Final Report" (Unpublished project report).

Ackerman, S. and Babb, I. (2021). Historical Context. Section 3.2 in "Sediment Texture and Grain Size Distribution" p. 33-35 in "The Long Island Sound Habitat Mapping Initiative Phase II – Eastern Long Island Sound – Final Report" (Unpublished project report).

Ackerman, S. and Babb, I. (2021). New Data Acquisition. Section 3.3 in "Sediment Texture and Grain Size Distribution" p. 35-38 in "The Long Island Sound Habitat Mapping Initiative Phase II – Eastern Long Island Sound – Final Report" (Unpublished project report).

Ackerman, S. and Babb, I. (2021). Data Processing. Section 3.4 in "Sediment Texture and Grain Size Distribution" p. 38-40 in "The Long Island Sound Habitat Mapping Initiative Phase II – Eastern Long Island Sound – Final Report" (Unpublished project report).

Ackerman, S. and Babb, I. (2021). Results. Section 3.5 in "Sediment Texture and Grain Size Distribution" p. 40-44 in "The Long Island Sound Habitat Mapping Initiative Phase II – Eastern Long Island Sound – Final Report" (Unpublished project report).

Ackerman, S. and Babb, I. (2021). Discussion. Section 3.5 in "Sediment Texture and Grain Size Distribution" p. 44 in "The Long Island Sound Habitat Mapping Initiative Phase II – Eastern Long Island Sound – Final Report" (Unpublished project report).

Ackerman, S. and Babb, I. (2021). Summary/Conclusions. Section 3.6 in "Sediment Texture and Grain Size Distribution" p. 45 in "The Long Island Sound Habitat Mapping Initiative Phase II – Eastern Long Island Sound – Final Report" (Unpublished project report).

Ackerman, S. and Babb, I. (2021). References. Section 3.7 in "Sediment Texture and Grain Size Distribution" p. 45-46 in "The Long Island Sound Habitat Mapping Initiative Phase II – Eastern Long Island Sound – Final Report" (Unpublished project report).

3.1 Objectives

Sediment texture, which includes shape, size and three-dimensional arrangement of sediment particles, is an essential element of any habitat classification. Gravel, sand, mud and various mixtures of these major grain size classes provide very different habitats (Galparsoro et al., 2013). Besides its importance for habitats, the surface sediment classification is a key element for managing different resources in LIS. In fact, different bottom types can themselves be considered a valuable resource (e.g. sand). Further, sediment grain size is one of the main factors influencing the distribution of heavy metal contaminant levels (Bastami et al., 2015; McHugh and Kenna, 2015).

Acoustic data, especially backscatter or reflectance can provide broad-scale information on the range of grain size composition of the seafloor (coarse sediments such as gravel usually correspond to high backscatter and finer sediments are less reflective (i.e. absorb more sound)

and thus correspond to lower backscatter). This acoustic information on its own, however, is insufficient to discriminate all differences in grain size that might be relevant for benthic habitats. In some cases, (e.g. in mud-dominated areas) differences in the backscatter can be caused by fine-scale morphology rather than by differences in grain size content (Ferrini and Flood, 2006; Nitsche et al., 2004). Therefore, sediment grain size distribution requires analysis of actual samples.

3.2 Historical Context

Sediment texture has been studied in LIS for many decades because it provides the basis for other studies and management applications. In 2000 USGS compiled existing grain size data and produced a sediment texture map for the entire LIS (Figure. 3.2-1).

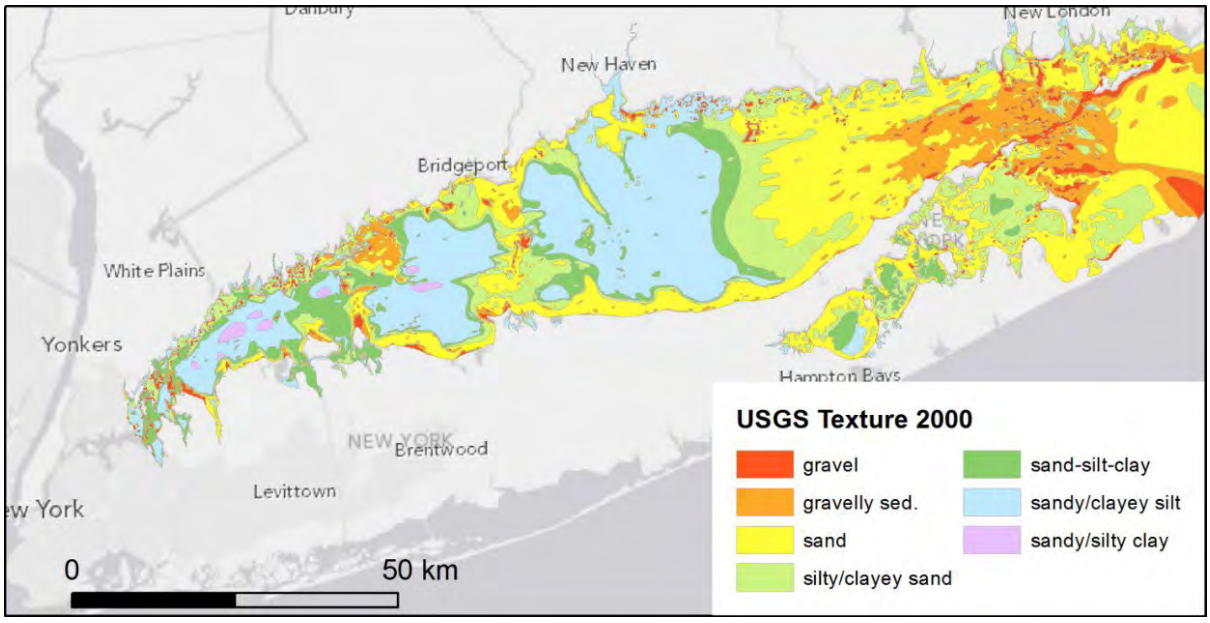

Figure 3.2-1 USGS grain size map of LIS from 2000 (Poppe et al., 2000).

This compilation is based on a large number of grain size data in combination with a limited amount sidescan data where those were available (Poppe et al., 2000). The grain size sample information is compiled in two USGS databases. The LIS Surficial Sediment Sample Database (LISSEDDATA, Poppe et al. 2004) counts >14,000 entries between 1930 and 1998 with a majority ~10,000 from the 1930s (Figure 3.2-2). The second database is the East Coast Sediment Texture Database which contains ~2420 entries for LIS between 1980 and 2010 (McMullen et al., 2014). The large majority of these data are from sediment grabs and few are from sediment cores and images sources.

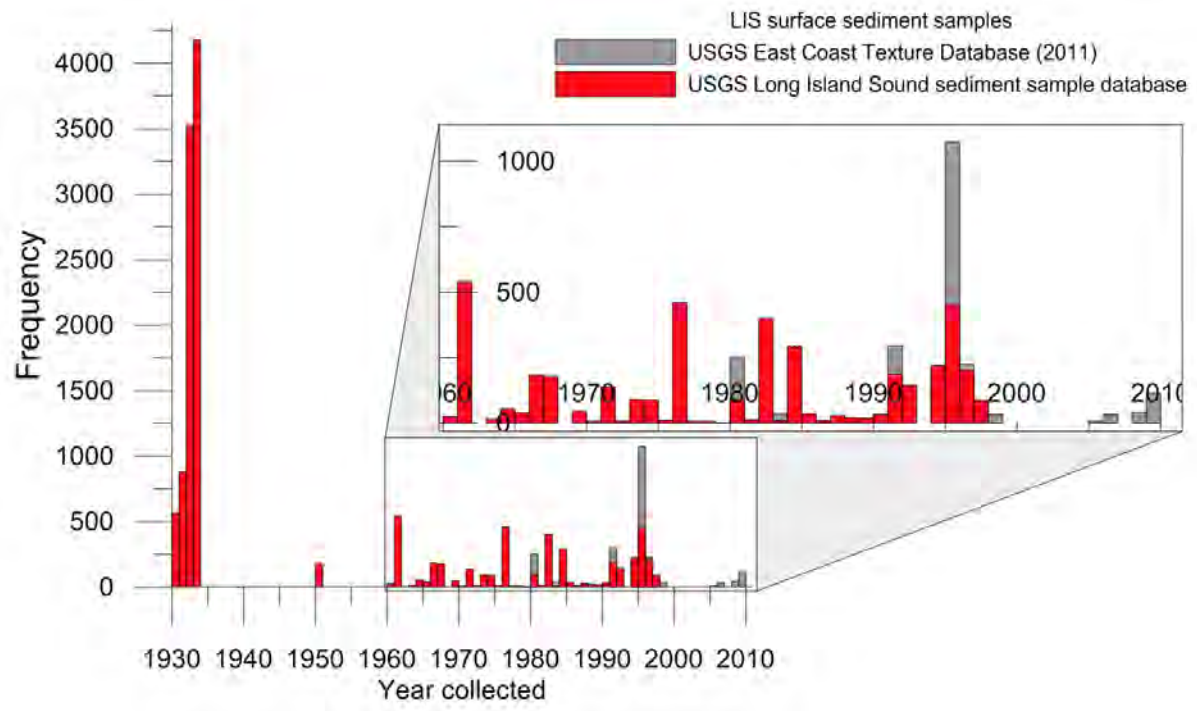

Figure 3.2-2 Number of existing sediment texture data from the USGS LIS Surficial Sediment Sample Database and the East Coast Sediment Texture Database.

While the density of older grain size data is high, the majority of these samples are older than 20 years. It is unclear to what extent older sediment samples from the 1930s reflect the present condition and if their grain size classification follows the present standards for sediment analyses. Samples from the 1930s to 1990s might not represent any changes of the LIS bottom environments during and after this period. On the other hand, grain size data from the 1990s and 2000s might still represent current conditions in some areas that have not changed much. However, the description of biological habitats requires an accurate description of the substrate texture and we cannot be sure beforehand, if the older data still reflect the present state. The distribution of these sediment samples from both databases within the Phase II area can be seen in Figure 3.2-3.

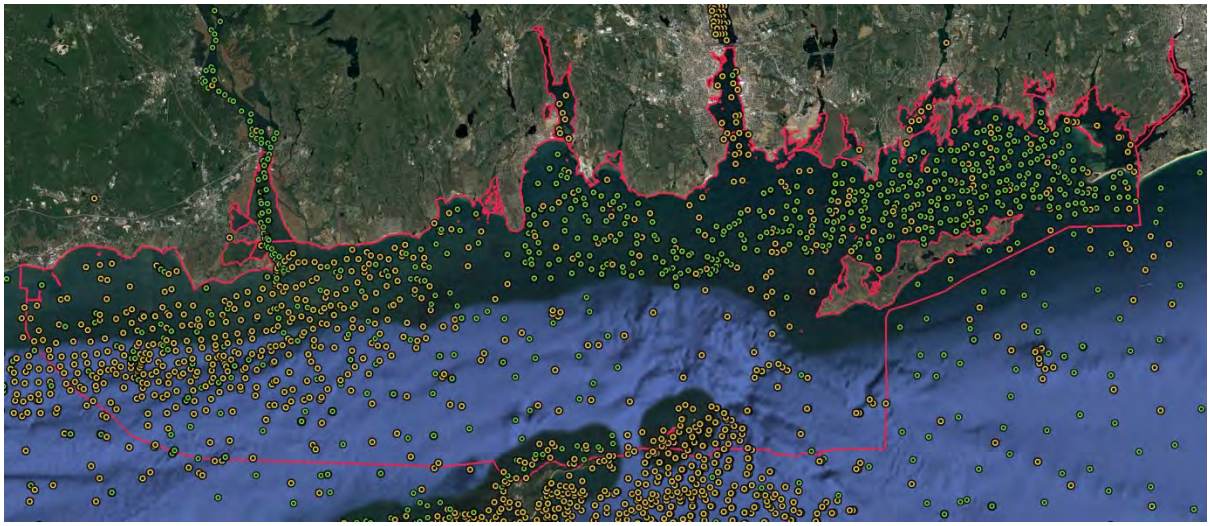

Figure 3.2-3 Map of the Phase II area with locations of the sediment grain size data from the LISSEDDATA database (yellow circles) and the east-coast sediment database (green circles).

3.3 New Data Acquisition:

The following sections are excerpted from Ackerman et al. 2020:

Ackerman, S.D., Huntley, E.C., Blackwood, D.S., Babb, I.G., Zajac, R.N., Conroy, C.W., Auster, P.J., Schneeberger, C.L., and Walton, O.L., (2020). *Sea-floor sediment and imagery data collected in Long Island Sound, Connecticut and New York, 2017 and 2018: U.S. Geological Survey data release*. https://doi.org/10.5066/P9GK29NM)

Two marine geological surveys were conducted in Long Island Sound, Connecticut and New York, in fall 2017 and spring 2018 by the U.S. Geological Survey, University of Connecticut, and University of New Haven through the Long Island Sound Mapping and Research Collaborative (LISMaRC) (Figure 3.3-1). The SEABed Observation and Sampling System (SEABOSS) (Figure 3.3-2) was deployed from the Research Vessel (R/V) Connecticut. Sea-floor images and videos were collected at 210 sampling sites within the survey area, and surficial sediment samples were collected at 179 of the sites. The sediment data and the observations from the images and videos were used to identify sediment texture and sea-floor habitats.

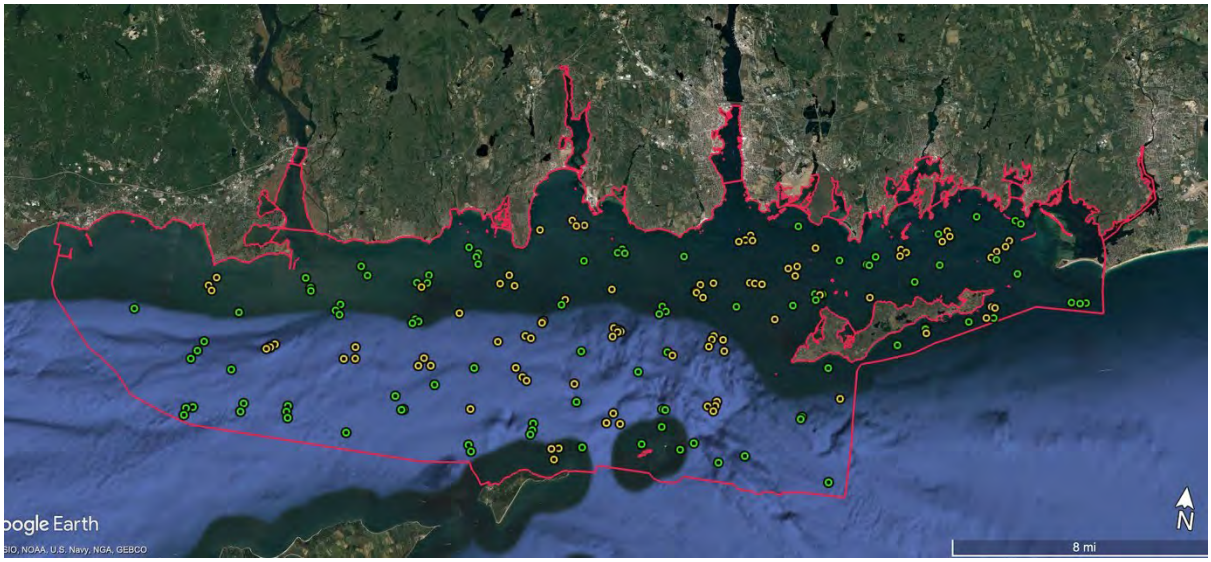

Figure 3.3-1 Map of the Phase II area showing the SEABOSS deployment sites for Fall 2017 (yellow circles) and Spring 2018 (green circles).

3.3.1 Sampling

The R/V Connecticut occupied one of the target sites identified by the LISMaRC Ecological Characterization team and the SEABOSS was deployed off the vessel's A-frame on the stern of the ship. The SEABOSS was equipped with a modified Van Veen grab sampler, a Nikon D300 digital still camera with a Photosea strobe, two video cameras (one forward-looking so that a shipboard operator could monitor for proper tow depth and obstacles, and one downward-looking, a Kongsberg Simrad OE1365 in this setup, that overlapped with the field of view of the still camera) with a topside feed, a GoPro HERO4 Black camera recording backup video, and lights to illuminate the sea floor for video and photograph collection. The elements of this particular SEABOSS were held within a stainless-steel frame that measured 1.15 x 1.15 meters. The frame had a stabilizer fin that oriented the system as it drifted over the seabed. The winch operator lowered the SEABOSS until the sea floor was observed in the topside live video feed. For those sites that were primarily targeted for a sediment grab, the vessel and SEABOSS then drifted with wind and current for up to a few minutes to ensure a decent image with a clear view of the sea floor was acquired; for those sites that were targeted for both a video transect of the sea floor and a sediment grab, the vessel was navigated along a planned transect for up to an hour. A scientist monitored the real-time bottom video and acquired bottom photographs at points of interest by remotely triggering the Nikon camera shutter. Bottom video was also recorded during the drift from the downward-looking video camera. Then, at most sites the winch operator lowered the Van Veen grab sampler until it rested on the sea floor. When the system was raised, the Van Veen grab sampler closed and collected a sample as it was lifted off the sea floor. Times for the sampler retrieval, which would later be used to derive the sample locations, were manually recorded in the survey log when the sampler was lifted off the seabed. The sampler was recovered to the deck of the survey vessel where a subsample was taken for grain-size analysis at the sediment laboratory at the USGS Woods Hole Coastal and Marine Science Center. Sediment samples were only attempted in areas where collecting a sample would not damage the SEABOSS; therefore, no samples were collected in areas with a cobble, boulder, or rocky seabed, as identified in real time using the topside live video feed. Samples were

also not attempted if the current was too strong, if the deployment was aborted due to the strobe malfunctioning, or if the grab sampler accidentally tripped earlier in the deployment. A total of 210 sites were occupied aboard the R/V Connecticut with the SEABOSS: 93 sites were occupied in fall 2017 during field activity 2017-056-FA, and 117 sites were occupied in spring 2018 during field activity 2018-018-FA. Sediment samples were collected at 179 of the 210 sites. Duplicate sediment samples were collected for collaborators (ie Tim Kenna, LDEO) as requested.

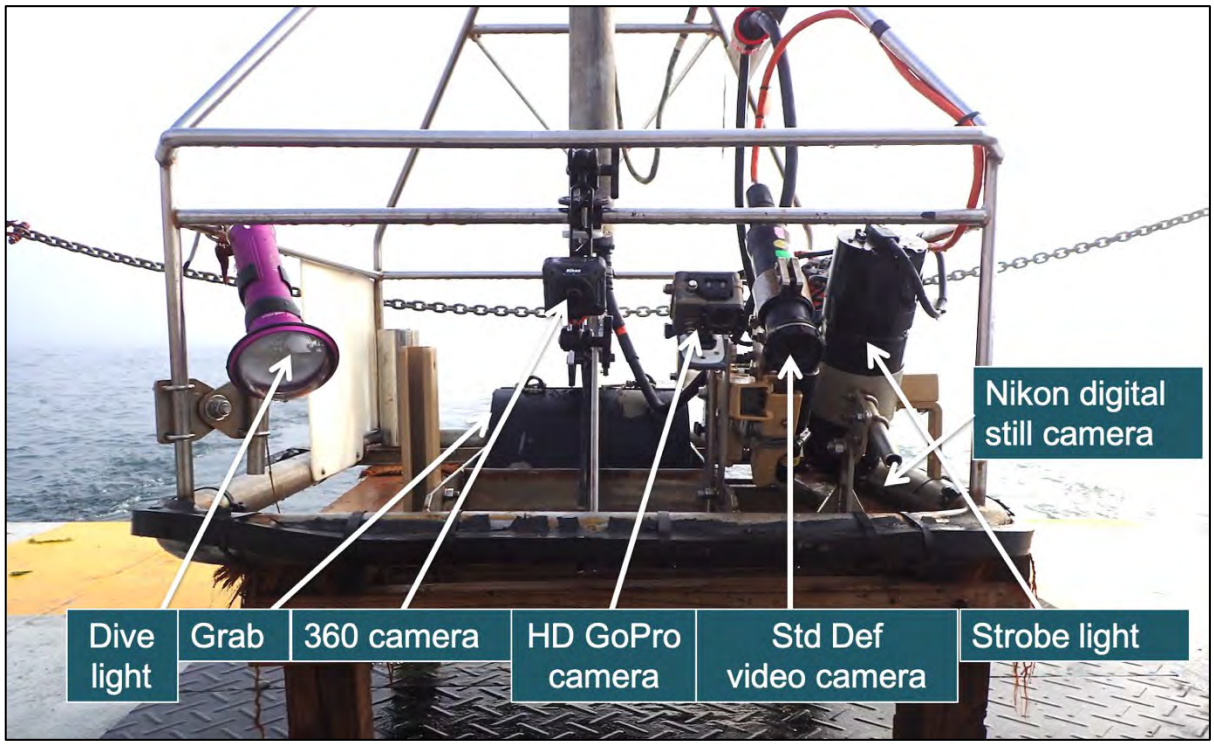

Figure 3.3-2 The USGS' SEABed Observation and Sampling System (SEABOSS) illustrating the imaging and sampling systems.

3.3.2 Acquired and processed navigation

During the surveys, WAAS-enabled GPS navigation from a Garmin GPSMAP 76C receiver was logged through a DataBridge data logger and ArcMap GPS. The GPS was set to receive fixes at a 2-second interval in geographic coordinates (WGS 84). Dates and times were recorded in Coordinated Universal Time (UTC). Log files were saved for each Julian day in text format. An AWK script (parsegprmc17056.awk for the fall 2017 log files and parsegprmc18018.awk for the spring 2018 log files) was used to parse the GPRMC navigation string from the log files for each survey and create ASCII Comma Separated Values (CSV) text files. The output files were merged for each survey and then reformatted using an AWK script (navtimereformat.awk), creating a processed navigation CSV text file for each sampling survey.

3.3.3 Assembled sample information for sediment laboratory

The sediment sample times (as recorded in the survey logs) were used to parse GPS positions for each sediment sample from the logged GPS data. Approximate depths for each sample were derived from an unpublished composite bathymetry dataset used by the Long Island

Sound Mapping and Research Collaborative project. This information was then provided to the sediment laboratory at the USGS Woods Hole Coastal and Marine Science Center with the sample analysis request form for each survey.

Duplicate samples were collected for collaborators at the Lamont Doherty Earth Observatory (LDEO) team (Tim Kenna, LDEO) as requested.

3.4 Data processing

3.4.1 Sediment Analyses

The samples from each survey were analyzed in the sediment laboratory at the USGS Woods Hole Coastal and Marine Science Center using two different methods: the Beckman Coulter Multisizer 3 and sieving of the >= 4-phi fraction, and the HORIBA LA-960 laser diffraction analyzer and sieving of the >= -2-phi fraction. Separate subsamples were taken from each sample submitted to the sediment analysis laboratory for each method.

3.4.1.1 Beckman Coulter Multisizer 3 Analyses

The subsamples for grain-size analysis using the Beckman Coulter Multisizer 3 and sieving of the >= 4-phi fraction were assigned unique analysis identifiers (ANALYSISID), and a macro-enabled Microsoft Excel data entry spreadsheet (GrainSizeWorksheetxxxx.xlsm, where xxxx is the batch number assigned to the sample submission) was created for each survey to record the measurement data. About 50 grams of wet sediment were placed in a pre-weighed beaker, weighed, oven dried at 100 degrees Celsius, and reweighed to correct for salt. The dried sample was wet sieved through a 0.062 mm (No. 230) sieve. The coarse fraction remaining in the sieve was oven dried at 100 degrees Celsius (until completely dried) and weighed. The fine fraction in water was collected in a plastic Nalgene bottle and sealed with a screw lid (stored for no longer than one week). The coarse fraction was dry sieved to determine the individual weights of the 4- to -5-phi fractions, and the weights were recorded in the data entry spreadsheet. The fine fraction was run and combined using the 200-micron and 30-micron Coulter analyses using the Multisizer 3 software to get the fine fraction grain-size distribution for each survey. The fine fraction distribution data were added to the data entry spreadsheet for each survey. The spreadsheet for each survey was used to calculate a continuous phi class distribution from the original fractions.

3.4.1.2 HORIBA LA-960 Analyses

For the sediments analyzed using the HORIBA LA-960 laser diffraction analyzer and sieving of the >= -2-phi fraction, the subsamples for grain-size analysis were assigned unique analysis identifiers (ANALYSISID) and divided into batches of no more than 30 samples. Each batch was entered into a Microsoft Excel data entry spreadsheet (LD Worksheet Templatexxxx.xlsx, where xxxx is the identifier assigned to the sample submission) to record the initial and dried sample weights, as well as the sieved coarse fraction weights. Each batch was also entered into macro-enabled Microsoft Excel data entry spreadsheets (GrainSizeWorksheetLD1-30xxxx(batchyy).xlsm or GrainSizeWorksheetLD31-60xxxx(batchyy).xlsm, where xxxx is the identifier assigned to the sample submission, "LD1-30" and "LD31-60" refer to the pre-labeled and weighed glass laser diffraction vials in which the samples will be run, and "batchyy" refers to the sample batch) to record the measurement data coming from the laser diffraction unit and incorporate the initial, dried,

and sieved weights. About 10-15 grams of wet sediment were placed in a pre-weighed beaker and the gross weight was recorded. The sample was wet sieved through a 4 mm (No. 5) sieve. If there was any coarse fraction remaining in the sieve, the coarse material was oven dried at 100 degrees Celsius in a pre-weighed beaker, and weighed again when dry. This coarse fraction was dry sieved to determine the individual weights of the -2- to -5-phi fractions, and the weights were recorded in the data entry spreadsheet LD Worksheet Templatexxxx.xlsx. The fine fraction in water was collected in a pre-labeled and weighed glass laser diffraction vial. If there was any coarse fraction remaining in the sieve from wet sieving, this vial was also oven dried at 100 degrees Celsius and weighed when dry. If there was no coarse fraction remaining from wet sieving, the sample can proceed directly to processing for analyses by the HORIBA LA-960 laser diffraction unit. Fine fractions ready for analysis by the HORIBA laser diffraction unit were rehydrated with distilled water if they had been dry. Fifteen (15) ml of pre-mixed 40 g/l sodium hexametaphosphate [(NaPO3)6] were added to each sample. If the height of the fluid in the laser diffraction vial was less than 5 cm, more distilled water was added to raise the level to no more than 8 cm in the vial. The samples were gently stirred, covered, and allowed to soak for at least 1 hour (for samples that were not dried) or up to 24 hours (for samples that were dried). Soaked vials were placed into an ultrasonic bath and run for 10 minutes at a frequency of 37 Hz with a power level of 100. If the samples appeared to be fully disaggregated, they were placed into pre-determined autosampler locations and were run using the HORIBA LA-960 for Windows software to get the fine fraction grain-size distributions. The fine fraction distribution data were added to the appropriate data entry spreadsheets (GrainSizeWorksheetLD1-30xxxx(batchyy).xlsm or GrainSizeWorksheetLD31-60xxxx(batchyy).xlsm) for each survey. The spreadsheet for each survey was used to calculate a continuous phi class distribution from the original fractions.

3.4.2 Calculated grain-size classification and statistical analyses.

Sediment grain size classification was based on a rigorous definition (Shepard [1954] as modified by Schlee and Webster [1967], Schlee [1973], and Poppe and others [2005]). In the definitions below, gravel is defined as particles with nominal diameters greater than 2 mm; sand consists of particles with nominal diameters less than 2 mm, but greater than or equal to 0.0625 mm; silt consists of particles with nominal diameters less than 0.0625 mm, but greater than or equal to 0.004 mm; and clay consists of particles with nominal diameters less than 0.004 mm.

A continuous phi class distribution from the original fractions was transposed to the "results" tab in the macro-enabled Microsoft Excel data entry workbook (GrainSizeWorksheetLD1-30xxxx(batchyy).xlsm or GrainSizeWorksheetLD31-60xxxx(batchyy).xlsm for the laser diffraction results, where xxxx is the identifier assigned to the sample submission, "LD1-30" and "LD31-60" refer to the pre-labeled and weighed glass laser diffraction vials in which the samples were run, and "batchyy" refers to the sample batch; or GrainSizeWorksheetxxxx.xlsm for the Multisizer results, where xxxx is the identifier assigned to the sample submission) for each survey. Macros in the workbook ("GSMoMArithmatic," "GSstatistics," and "sedimentname" for the laser diffraction results, and "GSstatistics" and "sedimentname" for the Multisizer results) were run to calculate grain-size classification and statistical analyses and finish processing the data. Sample, navigation, and field identifiers along with continuous phi class distribution data, grain-size classification, and statistical analysis results were copied and pasted into a final Microsoft Excel spreadsheet (xxxxGS-LDresults.xlsx for the laser diffraction results and xxxxGS-MSresults.xlsx for the Multisizer results, where xxxx is the batch number assigned to the

sample submission) for each survey. The processed data were quality control checked and assigned a quality grade based on the examination of the analytical data. Processed data were released to the submitter and incorporated into the laboratory's database. All raw analytical data generated by the samples were archived in the sediment analysis laboratory.

3.4.3 Final sediment grain-size analysis results CSV files

For the laser diffraction results, the sediment grain-size analysis results spreadsheets for each survey were merged in Microsoft Excel 2016 for Mac and then edited to remove the quality grade and metric distribution fields and to format fields. The Microsoft Excel spreadsheet was then saved as a CSV file (2017-056-FAand2018-018-FAsamplesGS-LD.csv). For the Multisizer results, the sediment grain-size analysis results spreadsheets for each survey were merged in Microsoft Excel 2016 for Mac and then edited to remove some fields, format fields, add site locations for those sites where no sample was successfully collected, and add a no data value (-9999) to empty attributes as needed. The sites with no successful grab were located using the start time of the sampler retrieval from the survey logs; the sampler retrieval position was chosen as the sample location because the video clip is considered the sample in the absence of a physical sample. Some of these site locations from the survey logs did not intersect a bottom video trackline, so they were moved to the last navigation fix along the site's bottom video trackline. Finally, the Microsoft Excel spreadsheet was saved as a CSV file (2017-056-FAand2018-018-FAsamplesGS-MS.csv).

3.4.4 Simplified sediment grain-size analysis results shapefile from the Multisizer analysis.

The CSV file of the sediment grain-size analysis results from the Multisizer analysis was copied and edited to create a simplified version of the CSV file with fewer attribute fields (specifically, STDEV, SKEWNESS, KURTOSIS, and the individual phi measurements [e.g., PHI11] were removed). A shapefile was created using the simplified version of the CSV file in Esri ArcGIS (version 10.3.1), and XTools Pro (version 12.0) for Esri ArcGIS was used to modify some field parameters in the point shapefile (Table Operations - Table Restructure).

3.5 Results

The goal of the Sediment Characterization effort was actually three-fold: 1) provide additional data on the sediment grain size in the Phase II area, 2) provide sediment samples taken by the SEABOSS' modified Van Veen grab for subsequent analysis by the Infaunal Ecological Characterization team of the Long Island Sound Mapping and Research Collaborative (LISMaRC) and 3) provide digital still images and videos for subsequent analysis by the LISMaRC Epifaunal Ecological Characterization team.

3.5.1 Sediment Grain Size

The sediment grain size data were collected to explore the nature of the sea floor and to characterize the seabed by identifying sediment texture. The sediments were analyzed using two different methods: the Beckman Coulter Multisizer 3 and sieving of the >= 4-phi fraction as was done in the Phase I Pilot area, and the HORIBA LA-960 laser diffraction analyzer and sieving of the >= -2-phi fraction. The HORIBA LA-960 laser diffraction analyzer is a new method for analyzing grain-size distribution at the sediment laboratory at the USGS Woods Hole Coastal and Marine Science Center. This dataset was analyzed using both methods so that the results could be compared, but no comparison was presented in the data release.

The results of the sediment grain size analyses revealed the preponderance of sand as the primary seafloor constituent. Figure 3.5-1 illustrates the percent (by weight) of the major components of each of the samples taken in 2017 and 2018. Figure 3.5-2 presents the results of the sediment classification based on Shepard (1954).

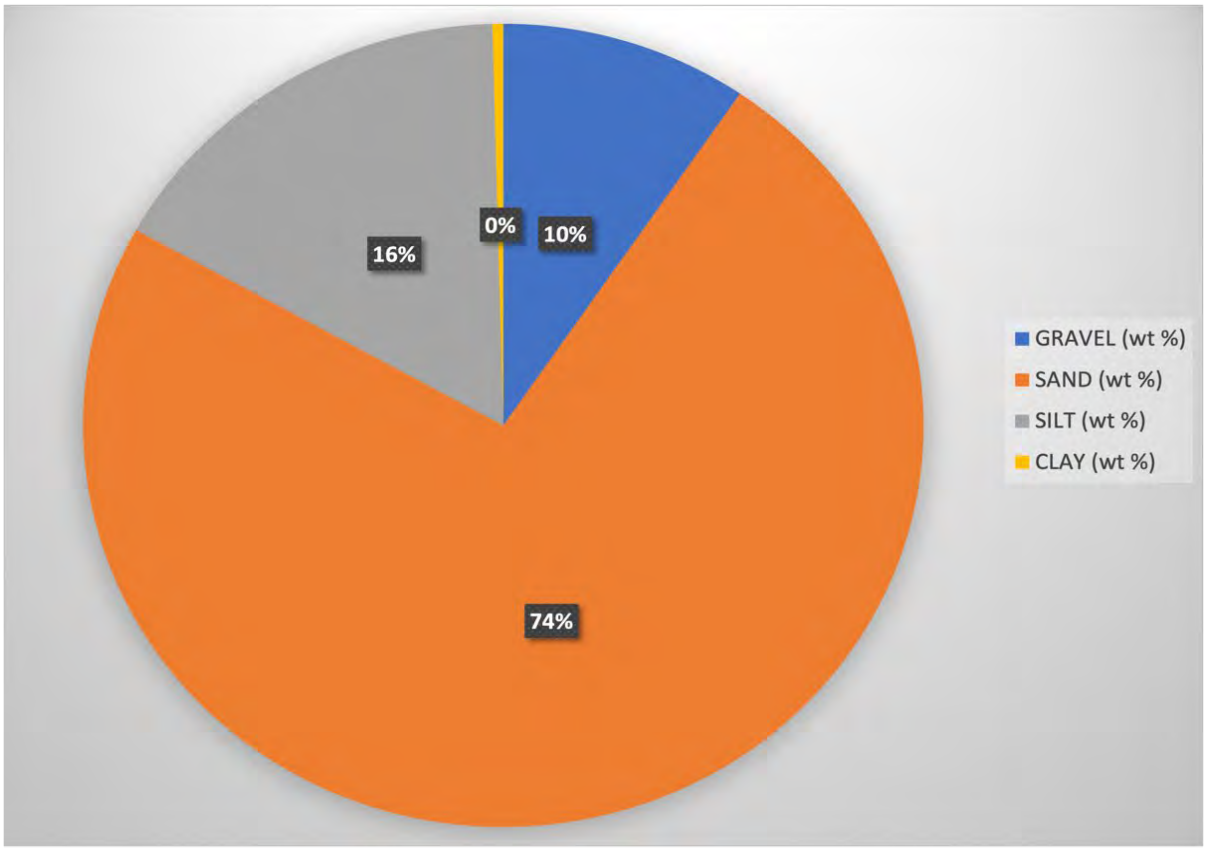

Figure 3.5-1 Percent (by weight) of the main constituents of the sediment samples collected by the USGS' SEABOSS in 2017 and 2018.

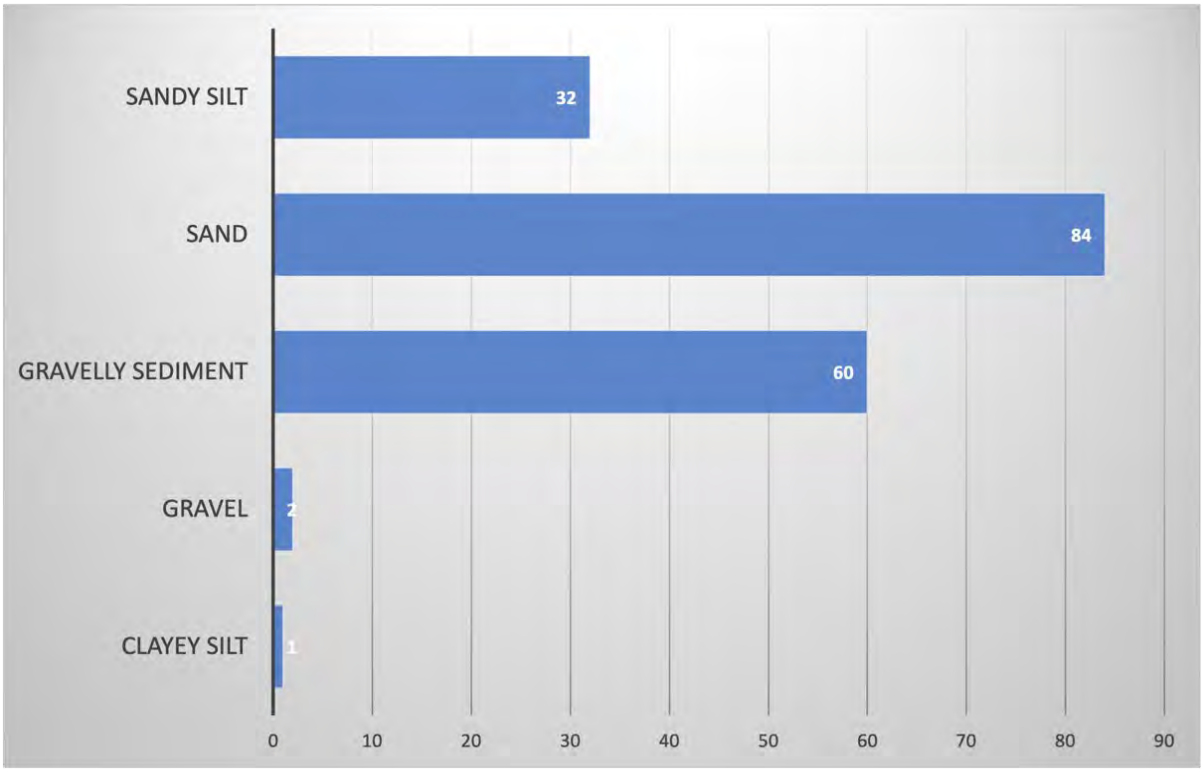

Figure 3.5-2 Sediment classification (Shepard, 1954) of 2017 and 2018 samples.

The series of maps below (Figures 3.5-3, 3.5-4 and 3.5-5) illustrate the distribution of the major sediment types in the Phase II area. As can be seen in each map there is a widespread geographic distribution of sand as the major seafloor constituent throughout the Phase II area.

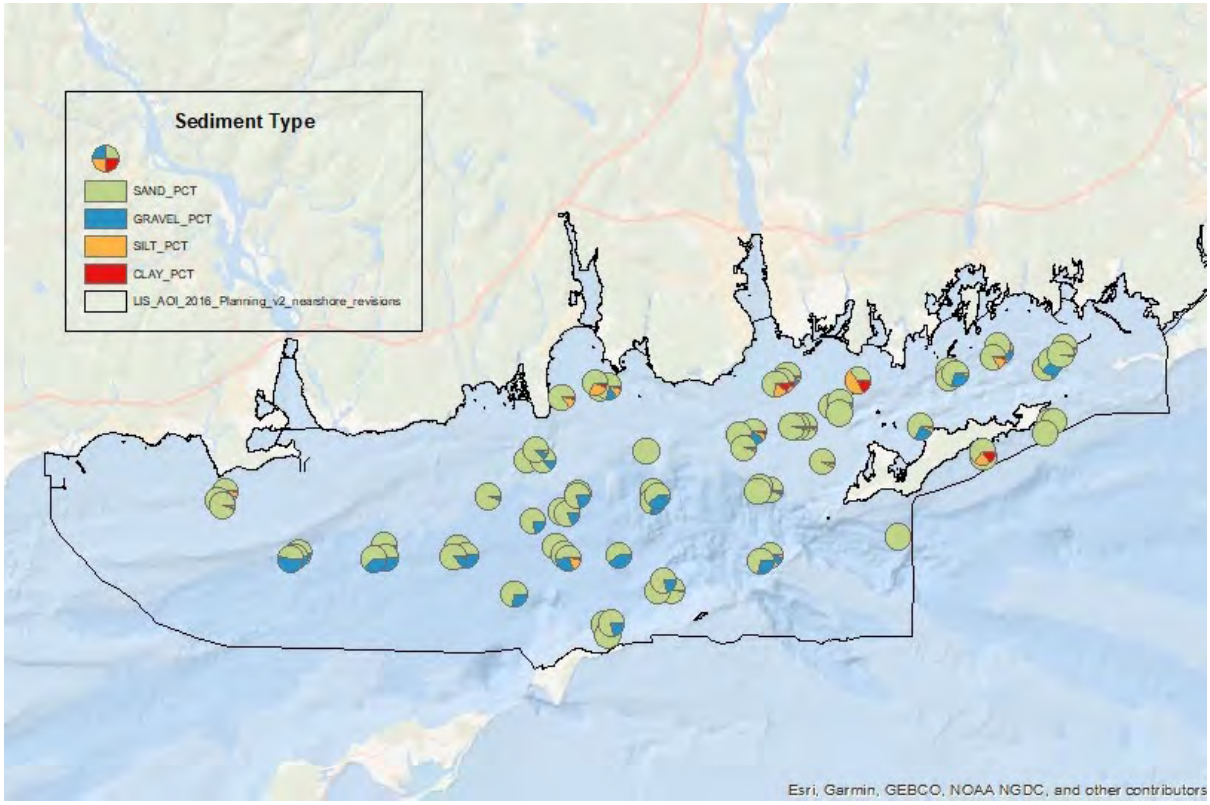

Figure 3.5-3 Map showing the percent (by weight) of the major sediment types in each of the samples collected in the Fall, 2017.

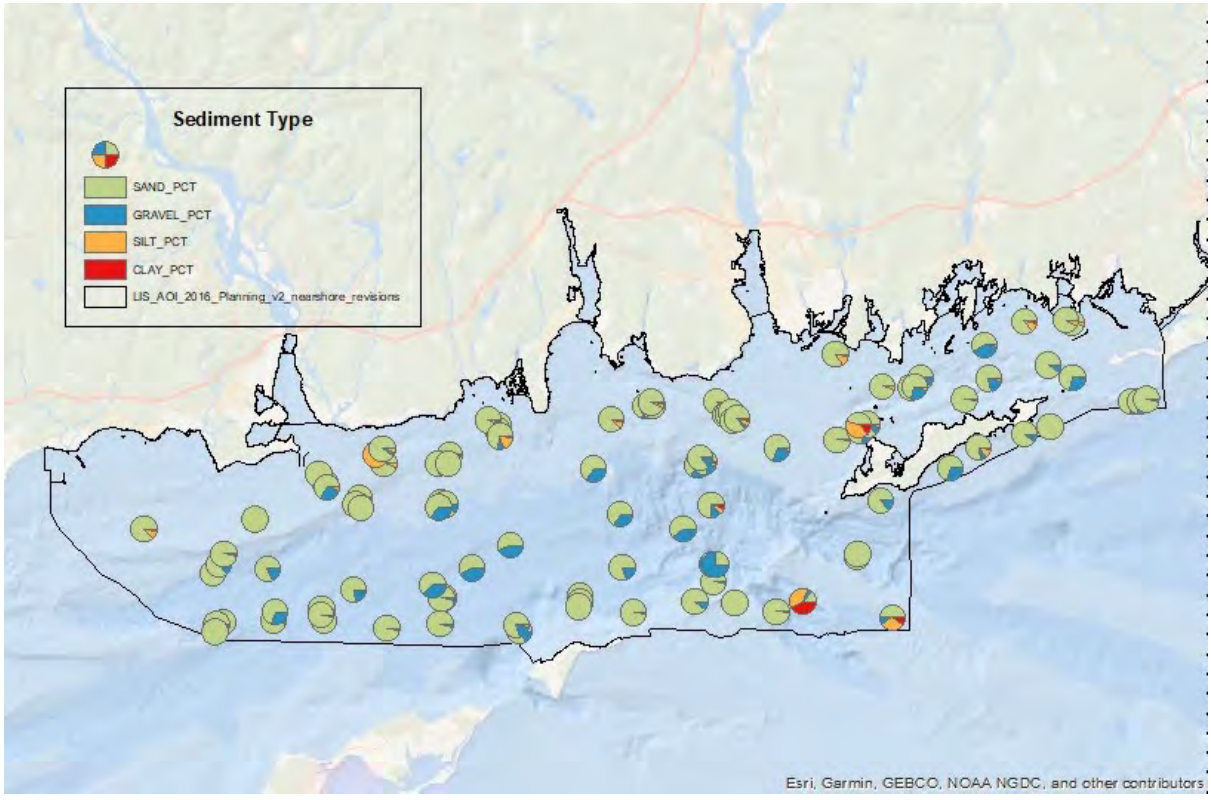

Figure 3.5-4 Map showing the percent (by weight) of the major sediment types in each of the samples collected in the Spring, 2018.

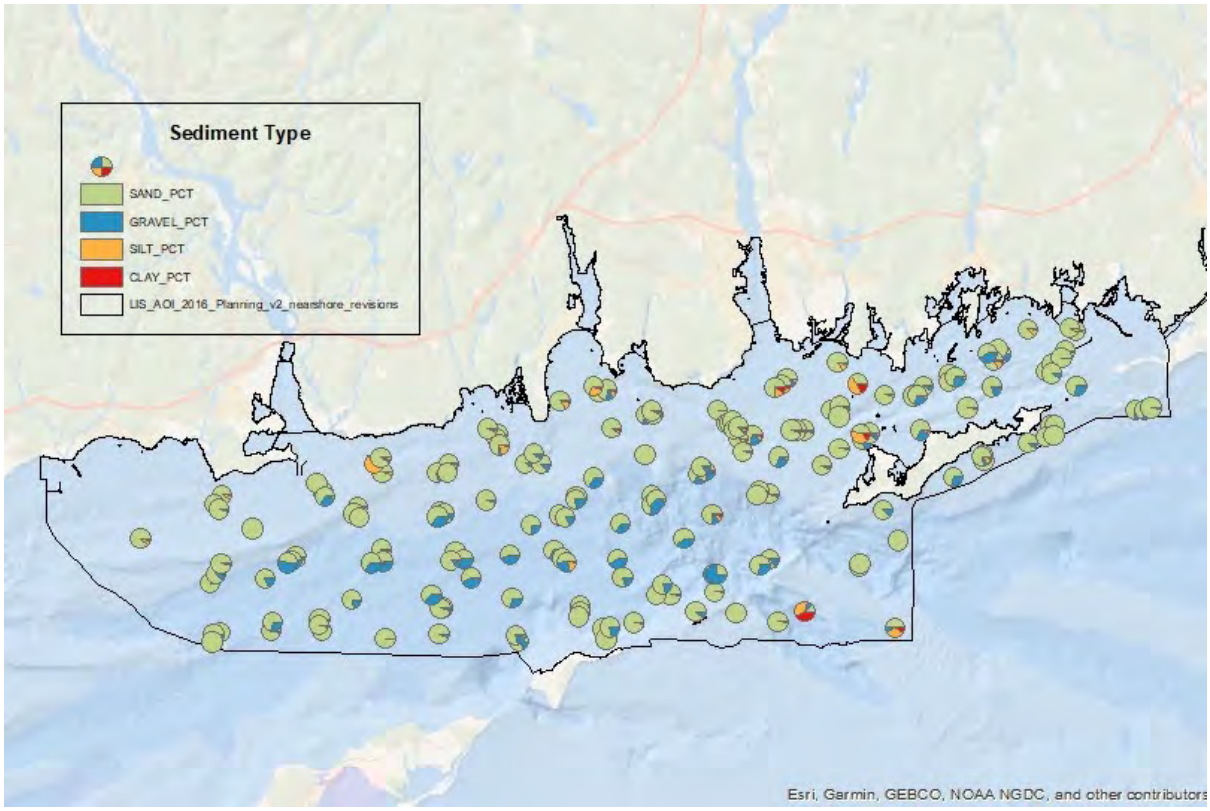

Figure 3.5-5 Map showing the percent (by weight) of the major sediment types in each of the samples collected in both Fall, 2017 and Spring, 2018.

3.5.2 Ecological Characterization – Infauna

Infaunal samples were collected with the 0.1 m^2 modified Van Veen grab on the SEABOSS system. The SEABOSS was lowered to just above the sea floor and then was allowed to drift for several minutes to collect video and still images, after which a grab sample was collected. Of the 179 sediment samples taken, a total of 160 were collected and processed for infauna and results are reported below.

3.5.3 Ecological Characterization – Epifauna

The SEABOSS also recorded digital, geotagged sea-floor images and locations of bottom images acquired with a Nikon D300 digital still camera, GoPro HERO4 Black camera, and Kongsberg Simrad OE1365 video camera. A total of 602 images were utilized for epifaunal analyses from the fall 2017 and 595 images from the spring 2018 campaign. These data were collected and analyzed using ImageJ software and the results are reported below.

3.6 Discussion

In addition to the 179 sediment samples collected by the USGS' SEABOSS during Fall, 2017 and Spring, 2018, the Lamont Doherty Earth Observatory at Columbia University Long Island Sound Mapping collaborative collected additional sediment samples in the Phase II area that were analyzed using both a Beckman Coulter Multisizer and by a Sedigraph. They received a duplicate sediment sample from each of the SEABOSS sediment grabs, however, to date these samples have not been analyzed (Frank Nitsche, personal communication). This does, however, represent a rich dataset of sediment grain size analyses from the Phase II area

derived from three separate analyses methods. This data set could provide the grist for further analysis and cross-comparison of the results to guide future work in Long Island Sound or in other regions conducting similar sediment texture assessments.

3.6 Summary/Conclusions

The LISMaRC Sediment Texture and Grain Size element provided a comprehensive dataset to assist with several other elements of the overall Long Island Sound Cable Fund Habitat Mapping Initiative. These include: 1) acoustic backscatter groundtruth data, 2) sedimentary environments, 3) both infaunal and epifaunal ecological characterization, and 4) additional groundtruth data to assist with the physical oceanography component of the initiative. Furthermore, the USGS Data Release (Ackerman et al., 2020) has already been utilized as part of the data sets assisting the Equinor Corporation with its power cable routing in support of the Beacon Wind offshore windfarm they are permitted to develop.

3.7 References

Ackerman, S.D., Huntley, E.C., Blackwood, D.S., Babb, I.G., Zajac, R.N., Conroy, C.W., Auster, P.J., Schneeberger, C.L., and Walton, O.L., (2020) *Sea-floor sediment and imagery data collected in Long Island Sound, Connecticut and New York, 2017 and 2018: U.S. Geological Survey data release*. https://doi.org/10.5066/P9GK29NM.

Bastami, K. D., Neyestani, M.R., Shemirani, F., Soltani, F., Haghparast, S. and Akbari, A. (2015) Heavy metal pollution assessment in relation to sediment properties in the coastal sediments of the southern Caspian Sea. *Marine Pollution Bulletin*, Volume 92(1–2), 237-243. https://doi.org/10.1016/j.marpolbul.2014.12.035

Galparsoro, I., Borja, Á., Kostylev, V.E., Rodríguez, J.G., Pascual, M. and Muxika, I., 2013. A process-driven sedimentary habitat modelling approach, explaining seafloor integrity and biodiversity assessment within the European Marine Strategy Framework Directive. *Estuarine, Coastal and Shelf Science.* 131, 194-205.

McHugh, C. and T. Kenna. (2015). Sediment grab collection and analysis. section 3.4, p. 65-83 in: *Seafloor Mapping of Long Island Sound – Final Report: Phase 1 Pilot Project*. (Unpublished project report). U. S. Environmental Protection Agency, Long Island Sound Study, Stamford, CT.

McMullen, K.Y., Paskevich, V.F., and Poppe, L.J., (2014). GIS data catalog (ver. 3.0, November 2014), in Poppe, L.J., McMullen, K.Y., Williams, S.J., and Paskevich, V.F., eds., *USGS east-coast sediment analysis: Procedures, database, and GIS data, U.S. Geological Survey Open-File Report 2005-1001*, available online at http://pubs.usgs.gov/of/2005/1001/.

Poppe, L.J., Paskevich, V.F., Moser, M.S., DiGiacomo-Cohen, M.L. and Christman, E.B. (2004) *Sidescan sonar imagery and surficial geologic interpretation of the sea floor off Branford, Connecticut Open-File Report 2004-1003*. https://doi.org/10.3133/ofr20041003

Shepard, F.P., 1954. Nomenclature based on sand-silt-clay ratios. *Journal of Sedimentary Petrology,* 24, 151-158.

U.S. Geological Survey East-Coast Sediment Texture Database (2014). online at URL: http://woodshole.er.usgs.gov/project-pages/sediment/

4.0 SEA FLOOR / HABITAT CHARACTERIZATION

Recommended Citations:

Schneeburger, C. and Zajac, R. N. (2021). Historical Context. Section 4.1 in "Seafloor/Habitat Characterization" p. 47-50 in *The Long Island Sound Habitat Mapping Initiative Phase II – Eastern Long Island Sound – Final Report* (Unpublished project report).

Schneeburger, C. and Zajac, R. N. (2021). Methods. Section 4.1 in "Seafloor/Habitat Characterization" p. 51-53 in *The Long Island Sound Habitat Mapping Initiative Phase II – Eastern Long Island Sound – Final Report* (Unpublished project report).

Schneeburger, C. and Zajac, R. N. (2021). Results. Section 4.1 in "Seafloor/Habitat Characterization" p. 53-62 in *The Long Island Sound Habitat Mapping Initiative Phase II – Eastern Long Island Sound – Final Report* (Unpublished project report).

Schneeburger, C. and Zajac, R. N. (2021). Discussion. Section 4.1 in "Seafloor/Habitat Characterization" p. 63-64 in *The Long Island Sound Habitat Mapping Initiative Phase II – Eastern Long Island Sound – Final Report* (Unpublished project report).

Schneeburger, C. and Zajac, R. N. (2021). References. Section 4.1 in "Seafloor/Habitat Characterization" p. 64-65 in *The Long Island Sound Habitat Mapping Initiative Phase II – Eastern Long Island Sound – Final Report* (Unpublished project report).

4.1 Historical Context

Studies characterizing the geomorphology and sedimentary environments of the seafloor in LIS, as well as benthic ecological studies, have a history going back to the mid-1950s (Zajac, 1998). However, collectively the studies are spatially and temporally disjointed to various degrees, including the area encompassed by the Phase II study area. Early studies of sediment composition indicated that the Phase II study area was primarily comprised of sandy to coarse grained sediments with various mixtures of gravel, and in some shallow depths, small areas that also had sandy silts and clays (Figure 4.1-1). The spatial density, and as such resolution, of the sampling used to develop these initial sedimentary characterizations was low, and as such provided a spatially coarse understanding of sea floor environments (habitats) in this portion of LIS.

Poppe et al. (2000) complied data sets from a variety of studies conducted between the 1970s and 1990s and generated a more comprehensive characterization of the sediment distribution in LIS, including the whole of the Phase II study area (Figure 4.1-2). Their surficial sediment texture map revealed a spatially complex distribution of sedimentary patches of varying sizes comprised of primarily sand, gravelly sand, gravel/bedrock and to a lesser extent silty sand. A few patches of sand-silt-clay and sandy silt were identified in some shallow water areas along coasts and in harbors and bays. Poppe et al.'s (2000) map provides a large-scale depiction of the spatial distribution of general sediment /habitat types in the Phase II area. A related study by Knebel and Poppe (2000) showed that the sedimentary environment in the Phase II area is dominated by large areas of erosion or nondeposition and coarse-grained bedload transport (Figure 4.1-3), as well as geomorphological features such as sand wave and boulder fields.

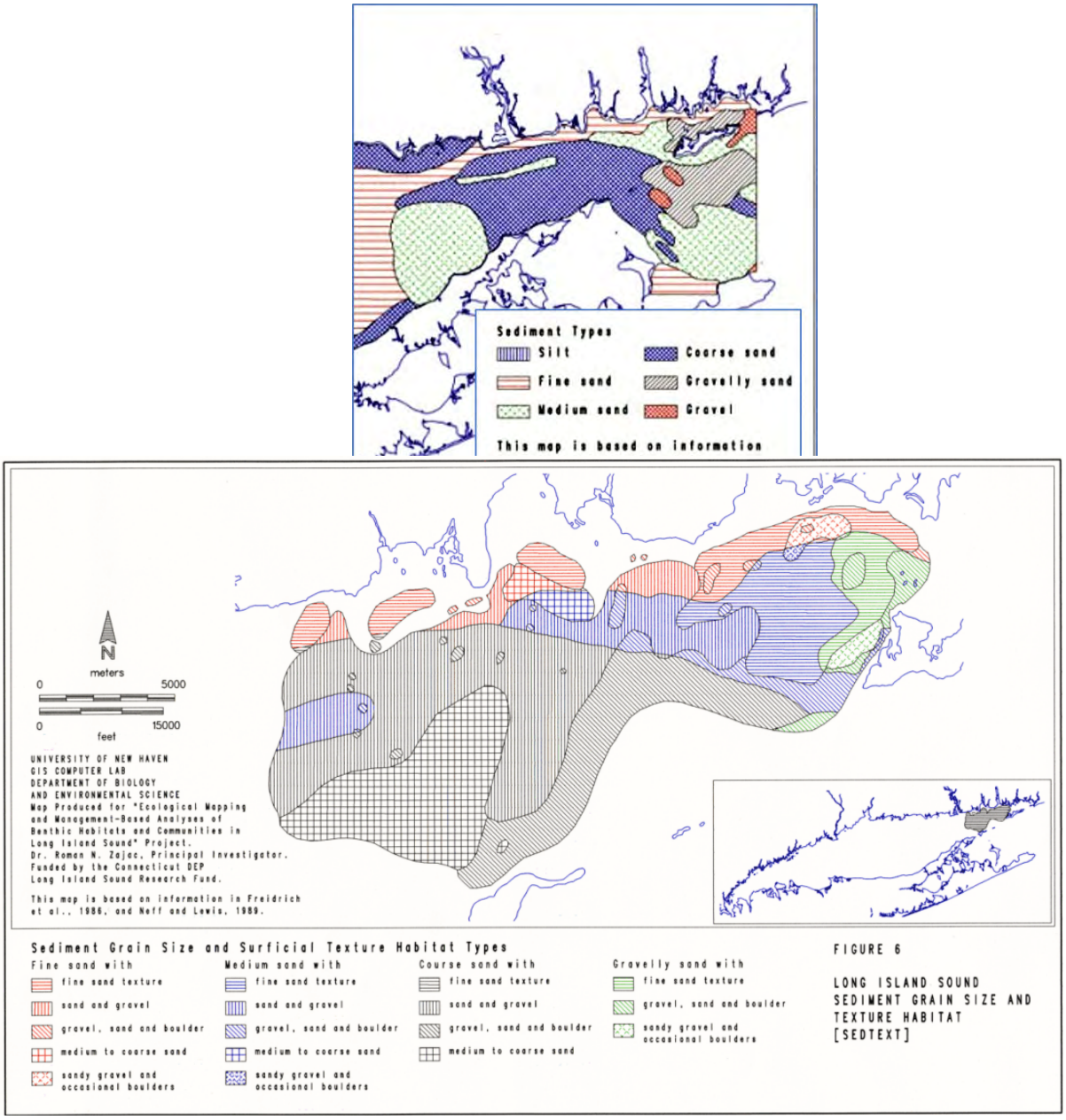

Figure 4.1-1 Examples of early sediment / habitat maps of the Phase II study area. Top: section of map from Freidrich et al. (1986) which reviewed and incorporated information from previous studies to develop a sediment grain-size distribution map. Bottom: Map developed by Zajac (1998) by combining information in Freidrich et al. (1986) and Neff and Lewis (1989) to delineate sedimentary habitats in eastern long Island Sound.

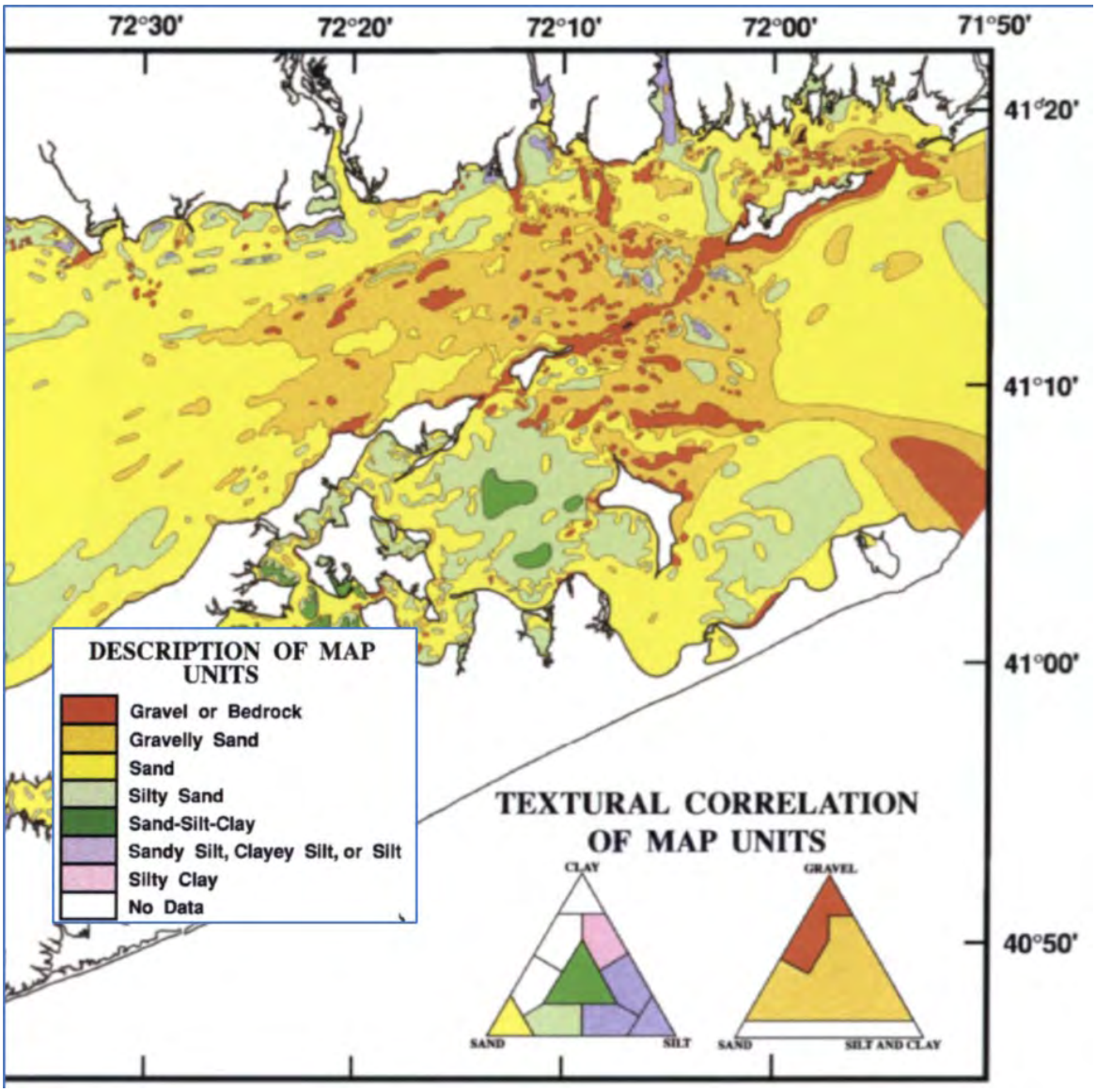

Figure 4.1-2 Portion of sedimentary texture map developed by Poppe et al. (2000) for Long Island Sound showing large-scale distribution of sediment types in the Phase II study area.

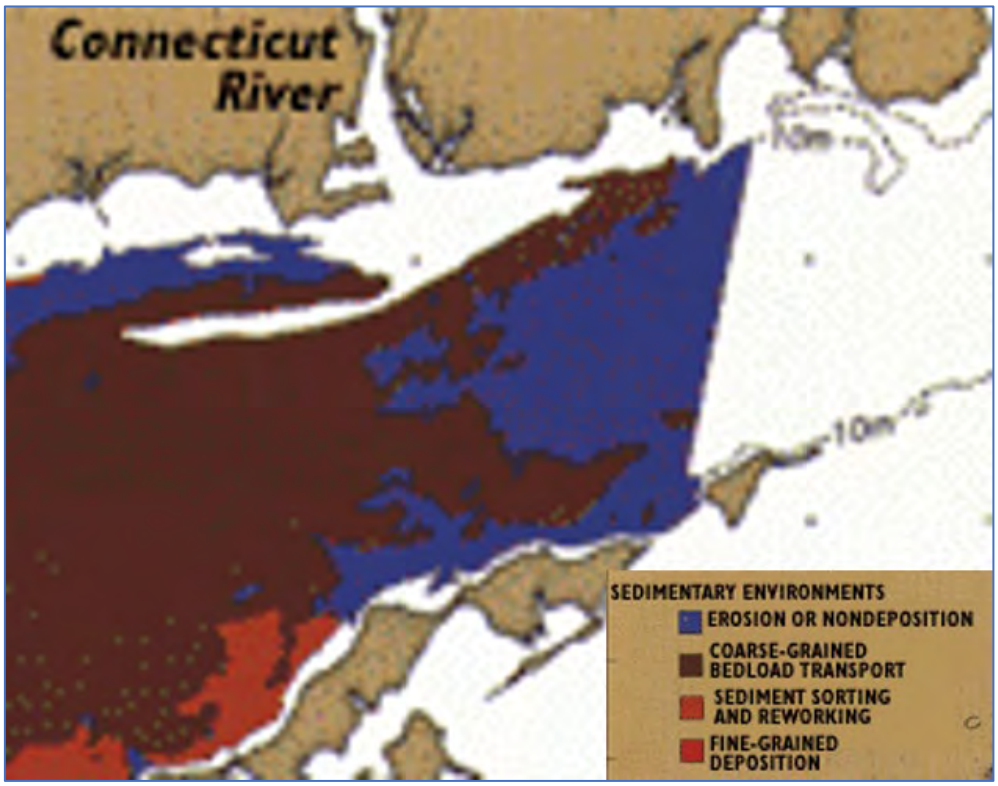

Figure 4.1-3 Sedimentary environments from Knebel and Poppe (2000) in a portion of the Phase II study area.

More spatially detailed studies of specific locations in the Phase II area revealed significant complexity to the sea floor landscape (or benthoscape) at smaller scales. For example, Zajac et al. (2000, 2003) studied a 19.4 km^2 area of the sea floor off the mouth of the Thames River, and found that within large-scale, general sediment-type patches interpreted from a side scan mosaic image, there was significant variation in sediment grain-size composition and biogenic and geomorphologic structural features. There have been several other studies of the sea floor in this region (see for example, https://coastalmap.marine.usgs.gov/regional/contusa/eastcoast/midatl/lis/data.html

Based on these previous studies, the Phase II study is highly dynamic in terms of sedimentary processes, has a complex geomorphology in some areas, and is dominated by primarily sandy and coarser grained sediments, which is supported by the seafloor characterization in the current study. Specific sediment composition and geomorphological characteristics can vary within patches of general sediment types (e.g., those indicated in Figure 4.1-2) and particularly across the many transition zones (e.g. Zajac et al., 2003) from one general sediment type to another that are present in the Phase II area (Figure 4.1-2), as local physical conditions vary across the region.

4.2 Methods

4.2.1 Data Sources Used for Seafloor Characterization

Several types of data representing different seafloor characteristics were used to classify and subsequently characterize the seafloor in the study area. These included a multibeam backscatter mosaic (Figure 4.2-1), bathymetry, seafloor rugosity as measured by the Terrain Roughness Index (TRI), maximum physical bottom stress, and sediment grain-size composition. The backscatter and bathymetric data and subsequent mosaic images created from the backscatter were collected by the National Oceanic and Atmospheric Administration (Batista et al. 2017). The spatial resolution of the backscatter was 2 m per pixel. The TRI for the study area was calculated by Conroy (2021 – this report) and the maximum bottom shear stress projections were developed by O'Donnell et al. (see Chapter 6 of this report). Sediment data at teach bottom sampling site was obtained and processed by the USGS (Ackerman et al., 2020).

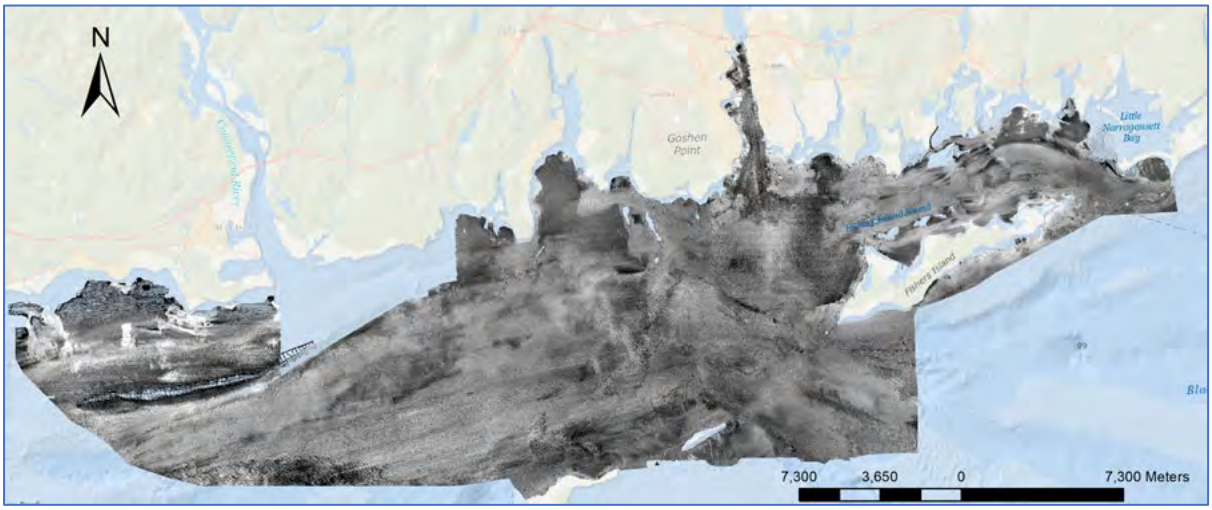

Figure 4.2-1 Acoustic backscatter mosaic of the Phase II study area that was used for seafloor characterization. Darker shades generally represent finer sediments; lighter shades generally represent coarser sediments.

4.2.2 Object-oriented Classification

The integrated backscatter mosaic of the seafloor of the pilot area was analyzed using eCognition Developer 9.4.0 (Trimble, 2019). This software segments the mosaic into meaningful objects (image-objects) of various sizes based on spectral and spatial characteristics (Lucieer, 2008) to perform a multi-segmentation classification to find regions with similar pixel values based on mean pixel brightness. The multiresolution segmentation criteria for this study were modeled based on previous studies on object-based seafloor image classification conducted by Lucieer (2008). Based on eCognition terminology, the mean brightness is equivalent to the mean intensity value of the backscatter pixels. The algorithm for multiresolution segmentation works by producing image objects based on pixel intensity to produce discrete objects that are homogeneous with respect to spectral characteristics (Drăguţ et al., 2010). The multiresolution segmentation was performed several times with different scale parameter segmentations to produce image objects that best represented the backscatter tones. A scale parameter value restricts the objects from becoming too heterogeneous (Trimble, 2019). A low parameter (near 0) would allow for higher heterogeneity and as the scale parameter increases, heterogeneity decreases. It was determined that a scale parameter of 100 worked best for the backscatter image of the Phase

II study area used in this analysis. A homogeneity criterion determines how spatially close the segments will be to one another and is comprised of shape and compactness. Several trials indicated that setting shape / smoothness to 0.9 and compactness to 0.6 were most effective for the backscatter image. The segmentation procedure resulted in an image that differentiated areas with similar pixel properties (Figure 4.2-2)

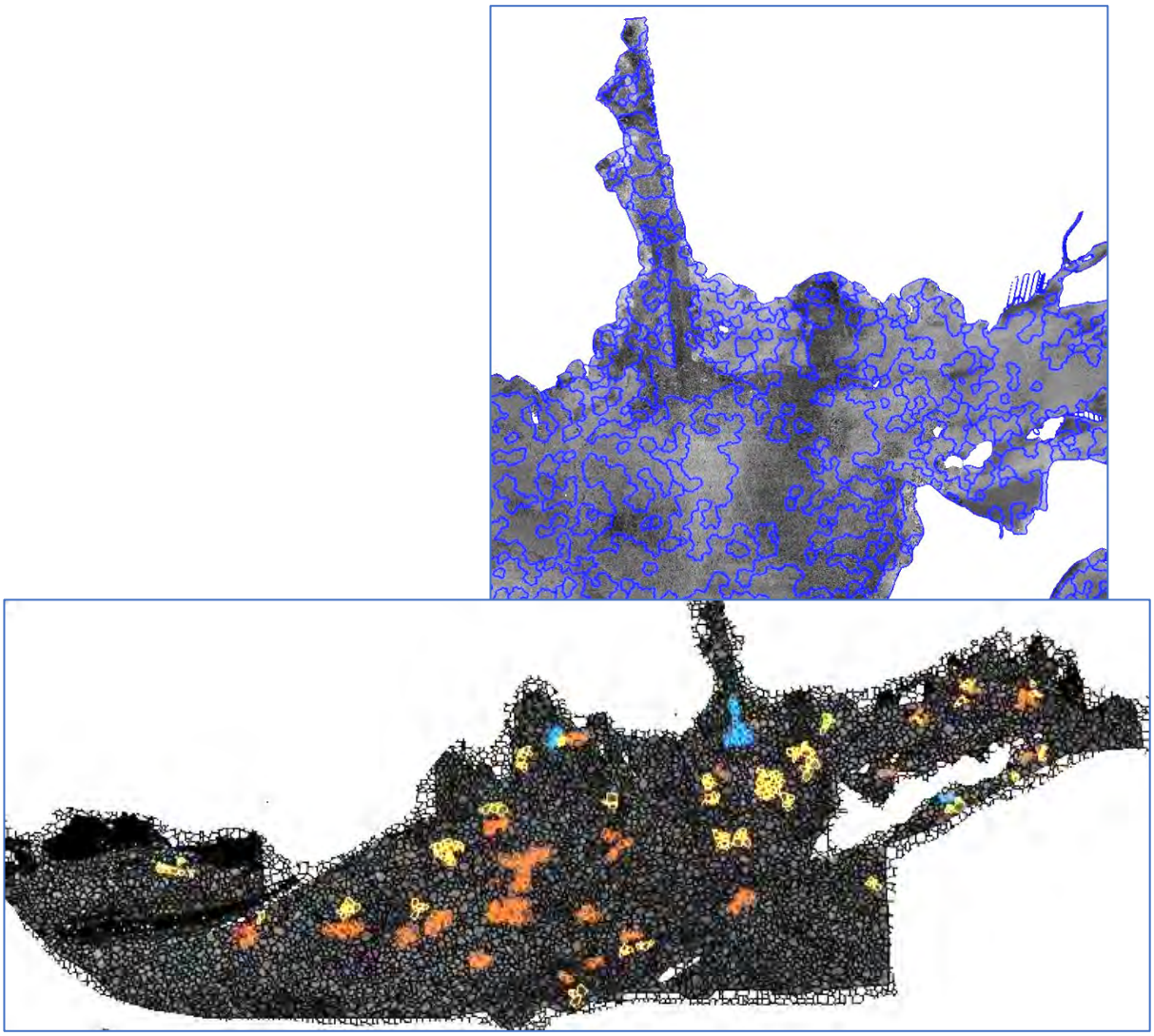

Figure 4.2-2 Examples of images segmentation and class sampling. Top: Results of image segmentation showing closeup around the mouth of the Thames River. Bottom: Sampling different segments to develop classification.

An unsupervised classification was then performed using eCognition by comparing the image objects with the underlying boundaries of pixel tone across the image. Five classes were designated based on general sedimentary groups (gravel, gravelly sediment, sand, silty sand, and sandy silt) used by the USGS for analysis of sediment samples obtained at the Phase II sampling sites (Ackerman et al., 2020). These classes were assigned initial image properties (mean and standard deviation of pixel intensities) by "sampling" visually distinct areas in the segmented backscatter mosaic (Figure 4.2-2). These properties were then adjusted as needed as well as setting nearest neighbor parameters that set how adjacent segments are merged into a specific class based on local homogeneity among neighboring segments and their image

properties or identified as being in different classes. The merging procedure produced 2,425 patches based on the image properties of the backscatter mosaic, and are referred to acoustic patches and assigned to the five, initial, sediment-based classes used in the classification / merging procedure. These acoustic patch types were then analyzed to assess their environmental characteristics and used as the basis for habitat identification and ecological characterization.

After the completion of object-oriented classification, the classified image was exported so that it could be integrated into GIS for further analyses. Using GIS, the classified image was imported as a shapefile and the classes assigned by eCognition were symbolized as separate acoustic patch types. The term acoustic patches refers to seafloor areas that have certain image characteristics (*i.e.*, a specific range of pixel intensities) based on acoustic backscatter data that are related to seafloor properties such sediment type and geomorphology, and were defined through a supervised image classification process. The acoustic patch types represent general habitat areas that have certain environmental characteristics with regard to sediment grain size composition, topographic roughness, and maximum hydrodynamic stresses on the seafloor. These characteristics are potential determinants of the kinds of infaunal and epifaunal communities that may be found within the acoustic patch types. The acoustic patch types can be designated as habitat types, and their mapped distribution forms the basis of an overall habitat map for the Phase II study area. This also forms the framework for subsequent research and surveys that can assess the accuracy of the characteristics of these habitat types as determined in this study and also the extent of the distribution of seafloor habitats in this portion of LIS.

This acoustic patch type data layer was then spatially joined with a file containing the sample points from the 2017 and 2018 surveys and the sediment data from the USGS. Patch analyst (Elkie et al.,1999) was used to run spatial statistics, and derive acoustic patch metrics (e.g. size and area). Sample points were joined with environmental data layers to extract data for bathymetry, TRI and bottom shear stress we All GIS analyses were conducted using ArcGIS 10.5.1. The data base was exported form GIS and used for univariate and multivariate statistical analyses using NCSS 11 (NCSS 2016) and PRIMER7 (Clarke and Gorley, 2015).

4.3 Results

The identified acoustic patches were distributed throughout the Phase II study area (Figure 4.3-1), although there are some generally geographical trends. The most extensive class is patch Type D, which was designated as gravelly sand (Table 4.3-1). It is found throughout the study project area, particularly in the central portion where there is a large continuous section of seafloor of this type. There are 411 patches of Type D, accounting for 45.1% of the study area. The second most extensive class is Type C, designated as sand. The largest areas of this patch type are found along the Connecticut coast, south of the Thames River and along the southern boarders of the project area. Acoustic patch Type C is comprised of 479 patches and makes up 41% of the study area. The three other classes A, B, and E cover smaller portions of the project area making up 0.86%, 11.3%, and 1.7% of the study area, respectively. Types A and E occur as small patches. Type A is classified as sandy silt and found scattered along the northern boundaries and in central areas of the study area. Type B is designated as silty sand, and found in the western section of the project study area and primarily along the coasts of Connecticut, Fishers Island and Long Island. Type E is classified as sandy gravel and patches are primarily found in the west central portion of the Phase II study area.

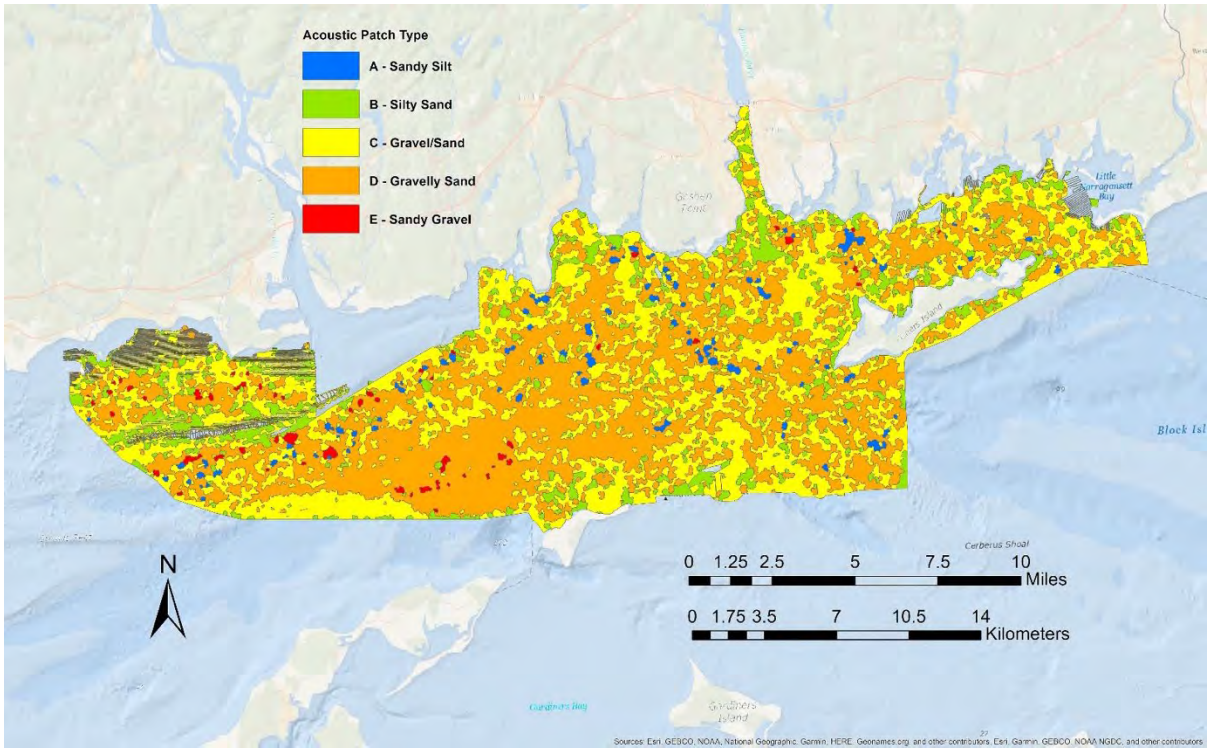

Figure 4.3-1 Acoustic patch types in the Phase II study area.

Table 4.3- 1. General characteristics of acoustic patch types identified in the Phase II study area. The number of samples from which sediment data is available is given as well as general sediment composition (% by weight) as determined by Ackerman et al

	Patch Type A	Patch Type B	Patch Type C	Patch Type D	Patch Type E
Total Area (ha) (% of total area)	780 (1.7%)	5,160.3 (11.3%)	18,650.1 (41%)	20,527 (45.1%)	391.7 (0.86%)
# Sediment Samples	1	15	71	81	1
Sediment class composition Mean % ± 1SE	G: 0.0 S: 35.3 Si: 45.5 C: 19.1	G: 6.6 ± 3.0 S: 82.3 ± 3.6 Si: 8.5 ± 2.5 C: 2.7 ± 0.8	G: 6.4 ± 1.4 S: 88.7 ± 1.6 Si: 3.5 ± 0.7 C: 1.3 ± 0.3	G: 19.9 ± 1.6 S: 75.4 ± 1.8 Si: 3.2 ± 0.7 C: 1.6 ± 0.6	G: 38.4 S: 61.1 Si: 0.4 C: 0.1
Depth Range (m)	8.9 - 9.1	4.95 - 86.8	5.39 - 95.01	6.0 - 89.48	30.54 - 48.0
Tidal Max Stress (Pascal) Range	0.451-0.461	0.191-2.685	0.221-2.052	0.214 - 1.864	0.938 - 0.997
TRI	0.013 -0.141	0.002 – 1.867	0.191 - 2.685	0.003 - 1.662	0.024 - 0.093

Although there were some broad geographical differences in spatial distribution of the acoustic patch types, the fact that each of the types were generally found in all areas of the Phase II study area, suggest that the environmental factors that determine their specific

characteristics are complex and interrelated. Over 85% of the Phase II study area is comprised of sandy sediment, and each acoustic patch type, except Type A, is characterized by over 65% sands by weight (Figure 4.3-2). Using a finer delineation of sediment grain-sizes based on a Phi scale, the acoustic patch types have different sediment compositions (Figure 4.3-3). Acoustic patch type A has the highest fraction of smaller grain sizes, dominated by silts and clays. Acoustic patch types B, C, D and E were dominated by sands, but have increasingly greater proportions of coarser grained sands and gravelly sediments, respectively. Patch types B, C and D had small amounts of silts and clays, whereas acoustic patch type E had almost no fine-grained sediments, but had the most gravel. Based on the sediment grain-size composition, the ND samples (which were not within the backscatter mosaic image area) are likely intermediate between patch type A and B, which is in line with these patch types being generally located in shallower waters (Figures 4.3-1 and 4.3-4). Patch types C, D and E were found in increasingly deeper waters, although there was great variation in depth for these patch types. Terrain roughness was relatively low for patch types A, E and the ND sample sites, and higher for types B, C and D (Fig. 4.3-5). Most notable, was the high variation in TRI for patch Types B, C, and D, indicating that for each of these patch types there are areas that have relatively large variations in local geomorphology, such as sand waves of different sizes and/or boulder fields. Maximum seabed stress increased in patch types A to C, respectively, and is highest in patch types D and E (Figure 4.3-6). As with TRI, bed stress is highly variable in patch types B, C and D.

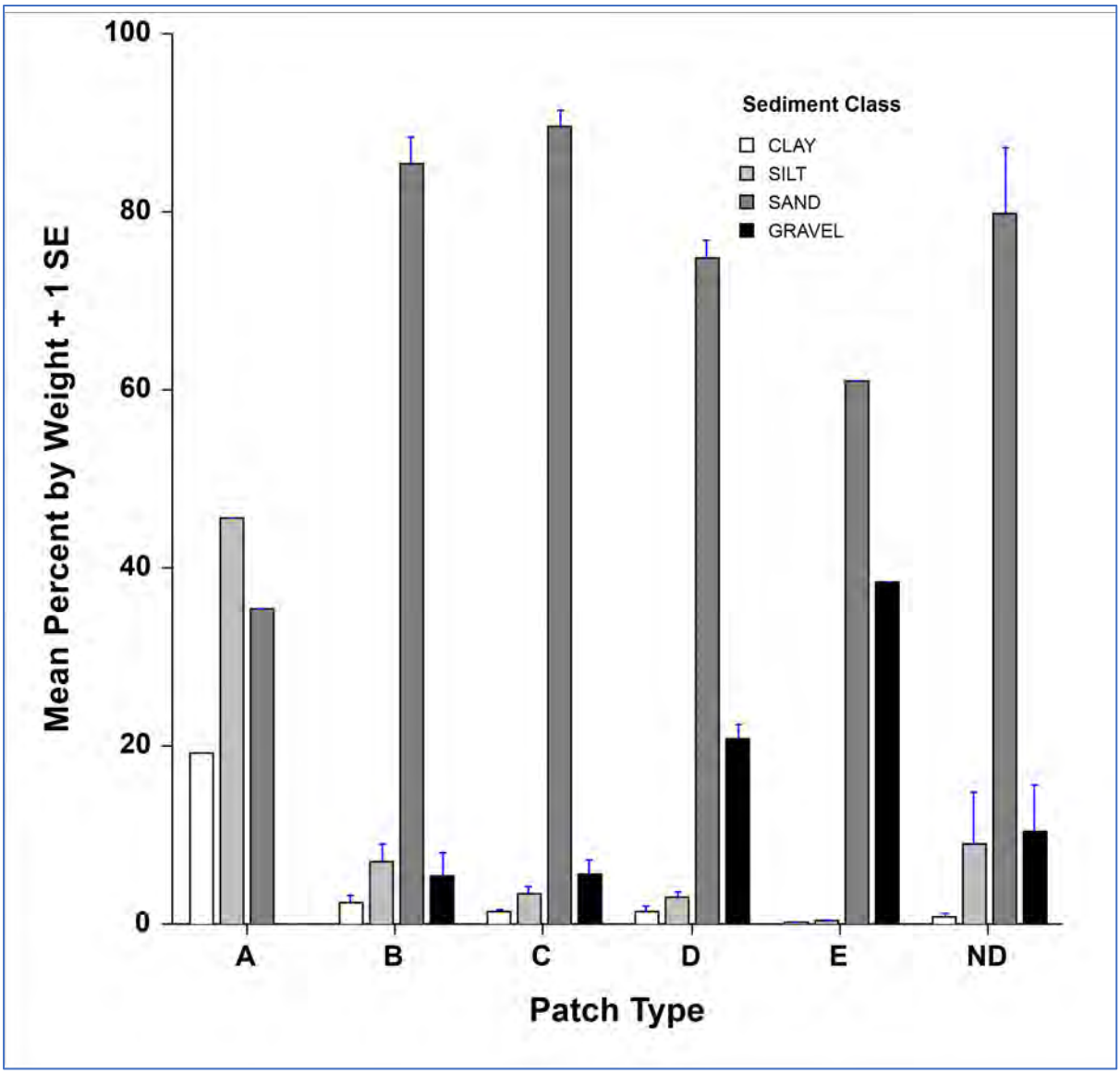

Figure 4.3-2 Mean percent composition (+1 standard error) of different sediment grain-size classes based on USGS classification (see Section 3.0)

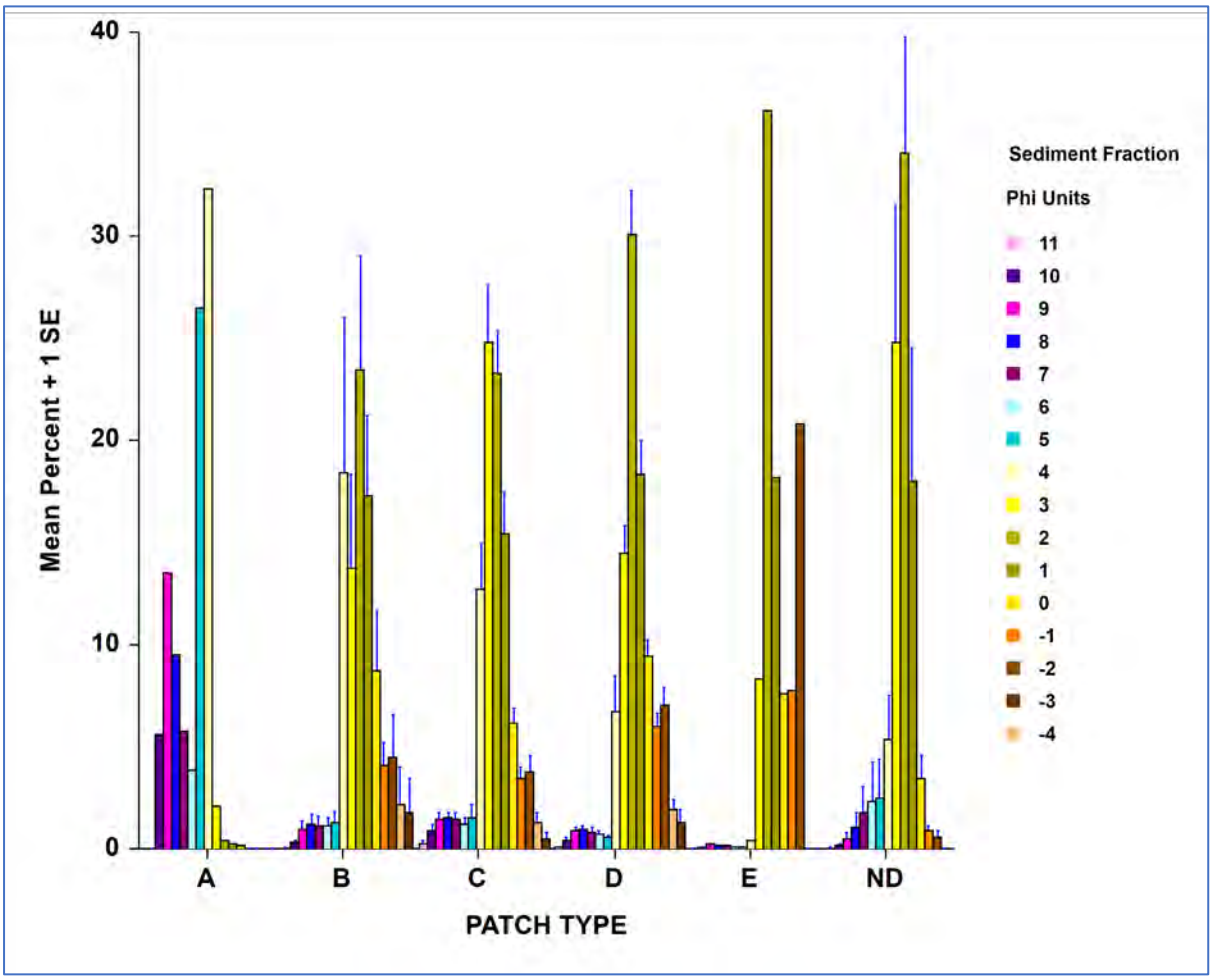

Figure 4.3-3 Sediment grain-size composition in the Acoustic Patch Types identified in the Phase II study area. ND = Not Determined, i.e., sites that were not in the backscatter mosaic image used to classify the patch types. Phi units range: clays, 11 to 8; silts, 8 to 4; sands, 4 to -1; gravels, -1 to -4. Lower phi values in each group indicate coarser sediments in that group. Sediment data was provided by the USGS (see Section 3.0 above).

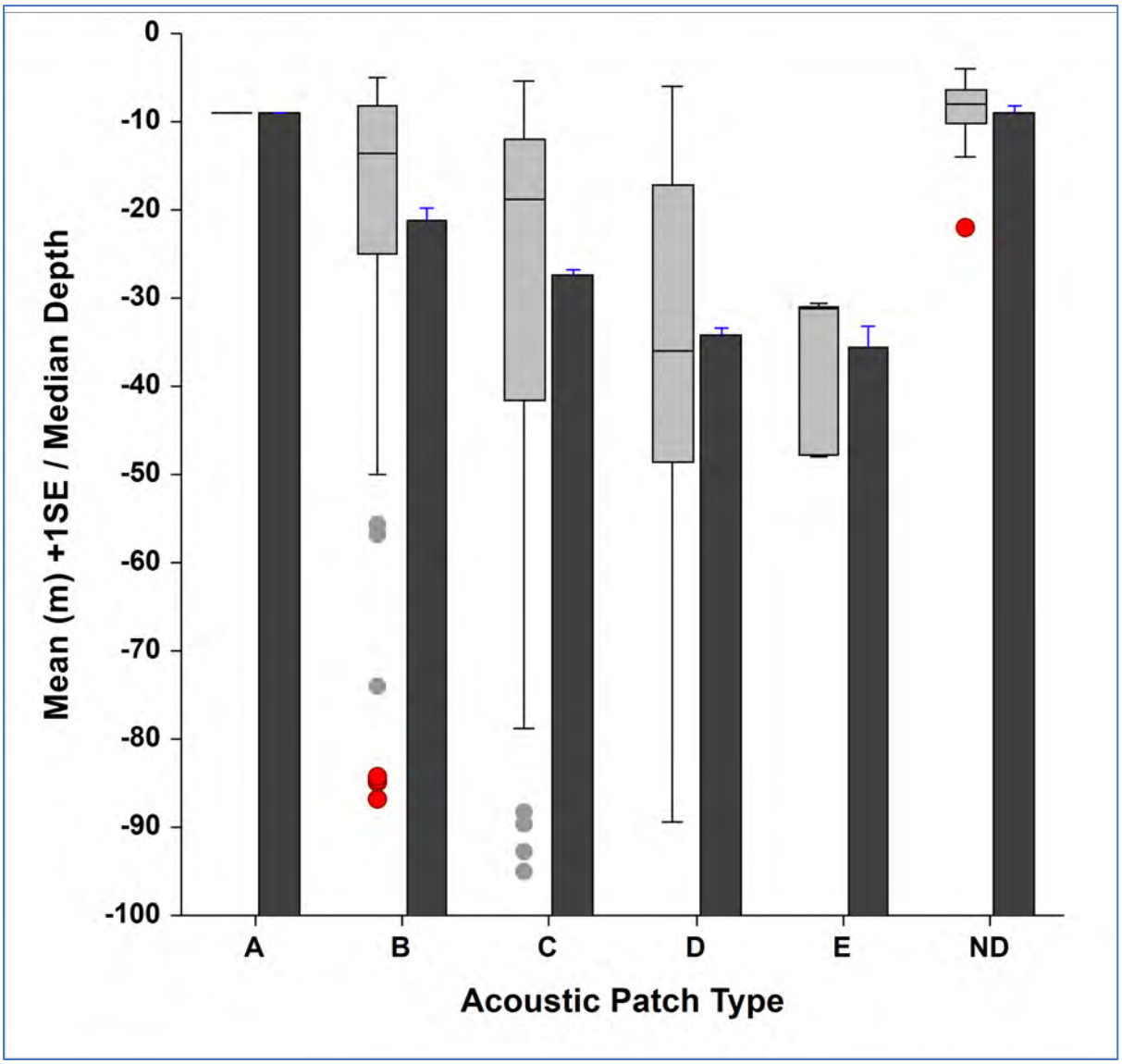

Figure 4.3-4 Depth characteristics of the acoustic patch types identified in the Phase II study area. ND = Not Determined, i.e., sites that were not in the backscatter mosaic image used to classify the patch types. Shown are the mean depth (+1 standard error, SE) and box plots showing the median (median ± 1.57 × (IQR) / √n), the inter-quartile range (IRQ) defined by the upper (75th percentile) and lower 25th percentile ends of the box, whiskers extending to 1.5 * IRQ. Outliers are shown as dots.

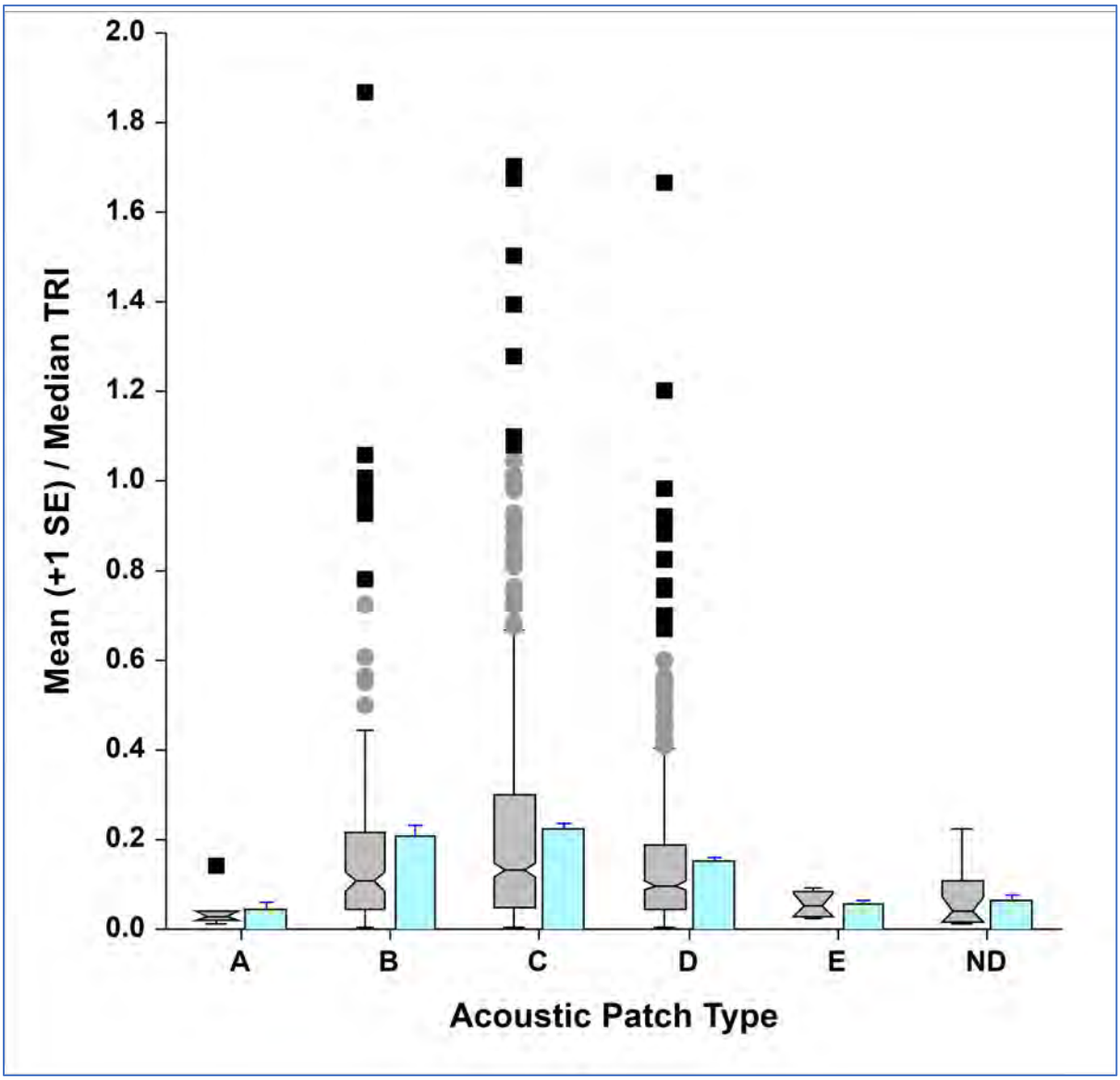

Figure 4.3-5 Terrain roughness (TRI) characteristics of the acoustic patch types identified in the Phase II study area. ND = Not Determined, i.e., sites that were not in the backscatter mosaic image used to classify the patch types. Shown are the mean depth (+1 standard error, SE) and box plots showing the notched median (median ± 1.57 × (IQR) / √n), the inter-quartile range (IRQ) defined by the upper (75th percentile) and lower 25th percentile ends of the box, whiskers extending to 1.5 * IRQ. Outliers are shown as dots.

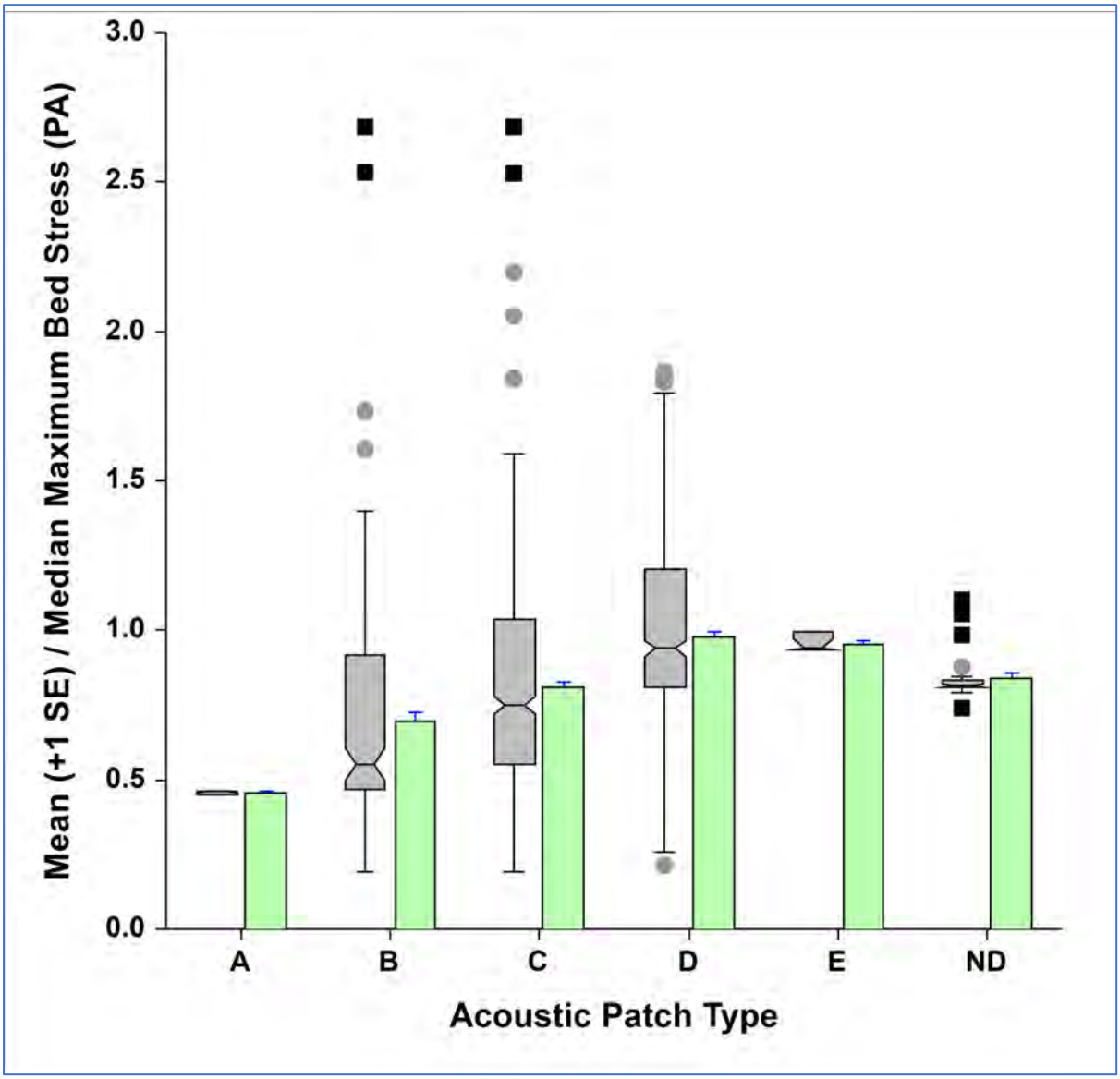

Figure 4.3-6 Maximum bed stress (PA=pascals) characteristics of the acoustic patch types identified in the Phase II study area. ND = Not Determined, i.e., sites that were not in the backscatter mosaic image used to classify the patch types. Shown are the mean depth (+1 standard error, SE) and box plots showing the notched median (median ± 1.57 × (IQR) / √n), the inter-quartile range (IRQ) defined by the upper (75th percentile) and lower 25th percentile ends of the box, whiskers extending to 1.5 * IRQ. Outliers are shown as dots.

Although the acoustic patch types are similar in that they are dominated by sandy sediments, multivariate analyses indicate that, based on all the environmental variables considered jointly, there are statistically significant differences with respect to their overall characteristics (Table 4.3-2). Pair-wise comparisons indicate that differences among patch Types A and B were marginally significantly, and significant differences exist among patch Types C and D, C and A, D and ND, and D and A. PCA ordination indicated that there was relatively high variability (dispersion) within patch Types B and C, and that most patch Type D samples were located closer together in the ordination space (Figure 4.3-7). Many of the Type C samples were separated from the other patch types due to being located in shallower depths and also containing higher proportions of sediments in the Phi 3 and 4 size-classes. Most of the patch type D sites were separated due to being in deeper waters and having coarser grain sizes and increasing maximum seabed stress. The gradient in sedimentary

differences and in the other environmental factors can be seen in the results of a CAP analysis (Figure 4.3-8). The ND and C patch types give way to patch Type D along the CAP2 axis, along a gradient from shallower depths and finer grain sizes to coarser grain sizes and to some extent increases in seabed stress and TRI.

Table 4.3- 2. Results of PERMANOVA analysis of differences among acoustic patch types relative to environmental factors (depth, TRI, maximum tidal stress and sedimentary phi classes). Data were normalized prior to generating a resemblance matrix using Euclidian distance. The analysis used a Type III (partial) sums of squares; fixed effects summed to zero for mixed terms; and 999 permutations of raw data.

PERMANOVA table of results

Source	df	SS	MS	Unique Pseudo-F	P(perm)
Patch Type	5	236.18	47.236	2.7603	0.003
Res	153	2618.2	17.113		
Total	158	2854.4			

Pair-wise tests (significant pairs are highlighted)

Groups	t	P(perm)
B, C	0.744	0.815
B, D	1.241	0.127
B, ND	1.072	0.290
B, E	0.664	0.745
B, A	1.958	0.062
C, D	1.931	0.001
C, ND	1.221	0.169
C, E	0.794	0.617
C, A	2.405	0.034
D, ND	1.930	0.004
D, E	0.652	0.738
D, A	2.971	0.018
ND, E	0.887	0.192
ND, A	2.241	0.190
E, A	No test	

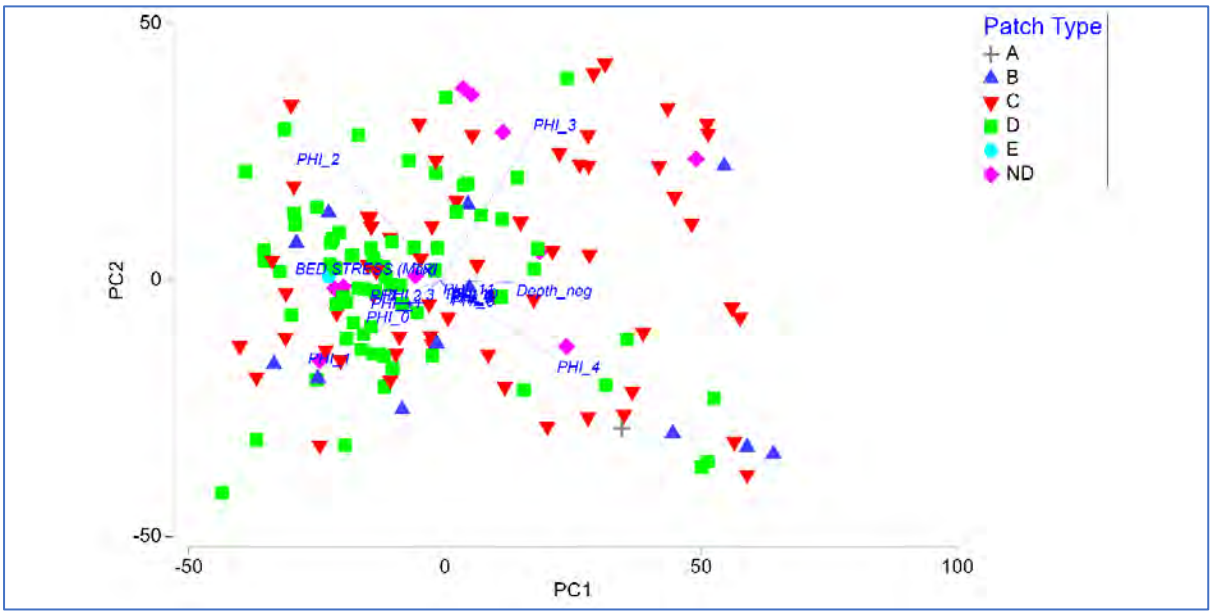

Figure 4.3-7 Principal Components Analysis (PCA) of sample sites in different acoustic patch types using sediment phi sizes, depth, maximum bed stress and TRI as variables. Vectors indicate the direction of separation of the sample sites due to the variables. Principal component axes 1 (PC1) and 2 (PC2) account 59.4 % of the total variation in the data.

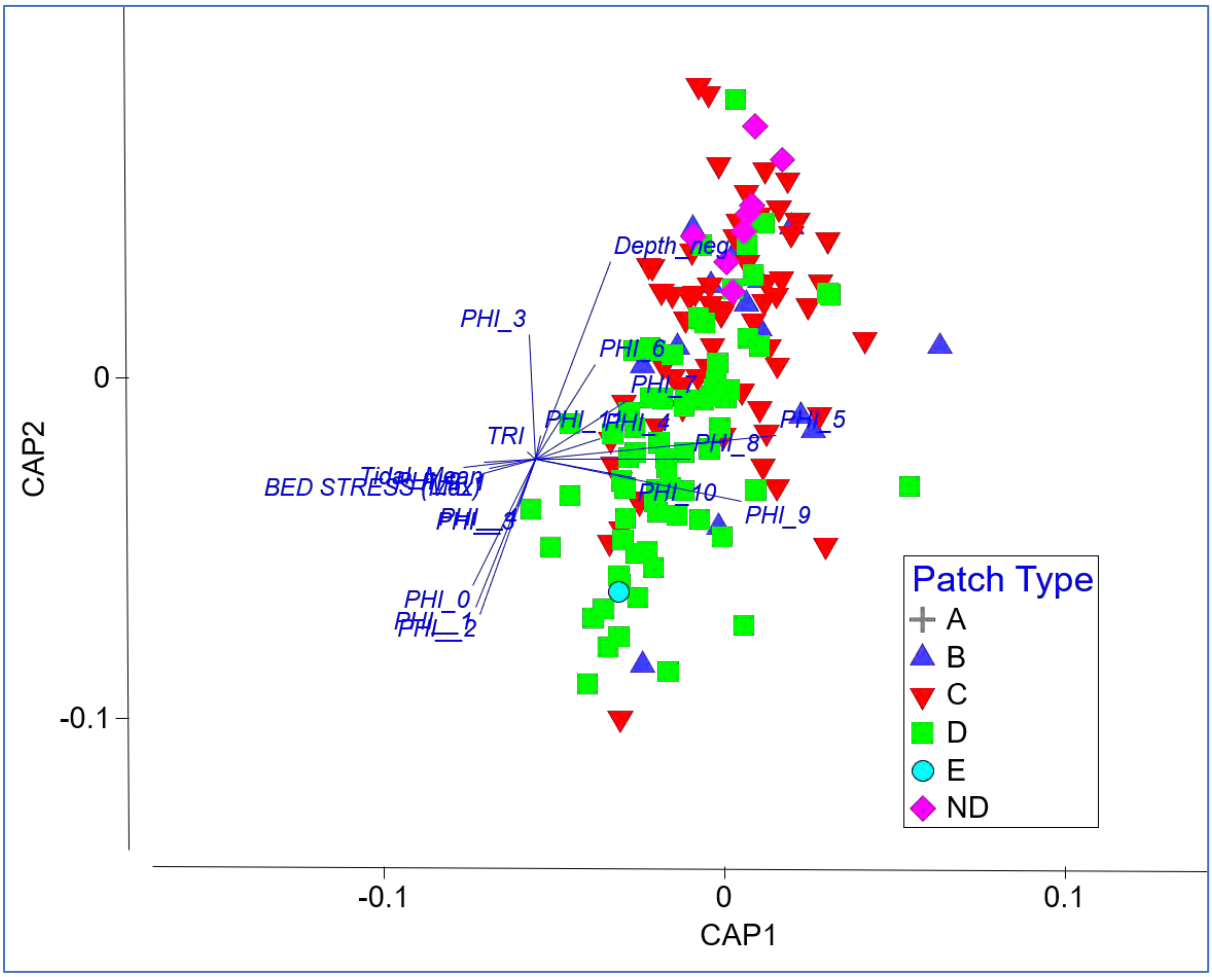

Figure 4.3-8 Results of canonical analysis of principal coordinates (CAP) to discriminate among acoustic patch types.

4.4 Discussion

Although sandy and gravelly sediments dominate 4 of the 5 acoustic patch types, there are distinct differences in the fine-scale composition of sediments in each acoustic patch type, representing a gradient from fine sands and silts to sand to sand/gravel from acoustic patch type A to E, respectively. The distribution of the patch types is spatially complex throughout most of the Phase II study area; however, some broader trends do emerge that are similar to previous mappings of sediment distributions in this portion of LIS. Both the sediment texture map (Figure 4.1-2) and the acoustic patch type map (Figure 4.3-1) indicate finer sediments along the Connecticut shore as well as closer inshore to Fishers Island, and to the north of Plum and Great Gull Islands. Both characterizations indicate a large area of gravelly sand in the central portion Phase II study area, extending from south of the Connecticut River to roughly South of Goshen Point, as well as in the central portions of Fishers Island Sound.

Likewise, both characterizations indicate a complex spatial distribution of patch types running north to south from the Connecticut shore to the area of the Race. One noticeable difference is that the sediment texture map (Figure 4.1-2) indicates a large band of bedrock/gravel extending from Plum Island to all along the southern shore of Fishers Island. The acoustic patch type characterization identifies these areas primarily as gravelly sand and a mix of gravel/sand and silty sand, particularly up against the Fishers Island south shore. This difference is likely due to extrapolations that were done for the sediment texture map and also the inability to collect samples in boulder areas using the sampling equipment for this project. There are boulder areas at a few of our sampling locations but these were not considered within the overall characterization, which was based solely on sediment composition, depth, maximum seabed stress, and topographic roughness. Increasing topographic roughness in patch types C, D and E indicate the presence of larger geomorphological features such as bedrock and boulder fields, as well as sand waves, in these patch types. For example, there are a number of relatively large sand wave fields in the Phase II area, particularly in the western portion (Figure 4.4-1). These sand wave fields increase TRI significantly in these areas and are primarily associated with acoustic patch types C and D, particularly the large field located along the southwest edge of the Phase II study area, which is almost entirely patch Type C.

The seafloor of the Phase II study area as represented by the acoustic patch types provides a framework for identifying benthic habitats and their spatial variation in this portion of LIS. The acoustic patches were identified using the image information in the acoustic backscatter data collected during multibeam surveys, and how that image data was compiled into the overall mosaic (Figure 4.2-1). The initial classification of bottom types was based on tonal differences in the backscatter mosaic. There are tonal differences across the mosaic that are not related to specific bottom type (e.g., in general, darker tones being finer sediments and letter tones being coarser sediments) due to striping where individual data segments were combined, shadowing, and also differences based on when the data was collected. In the segmentation process, differences in image tone across the mosaic may lead potential misclassification of certain areas in terms of one acoustic patch type or another. However, given the fact that much of the area is dominated by sandy sediments, the segmentation and delineation of acoustic patch types did differentiate among areas that had differing compositions of sand and gravel grain sizes. Additional analyses (not provided in this report) indicate that the sediment grain-size composition of each acoustic patch type was fairly consistent from east to west in the study area. The acoustic patch types thus represent general habitat areas that have certain environmental characteristics with regard to sediment grain

size composition, topographic roughness, and maximum hydrodynamic stresses on the seafloor. These characteristics are potential determinants of the kinds of infaunal and epifaunal communities that may be found within the acoustic patch types. However, other environmental and ecological factors can shape the ecological communities that may be present in the acoustic patch types. A more specific discussion of the link between the acoustic patch types and their ecological characteristics is provided in section 5.6.

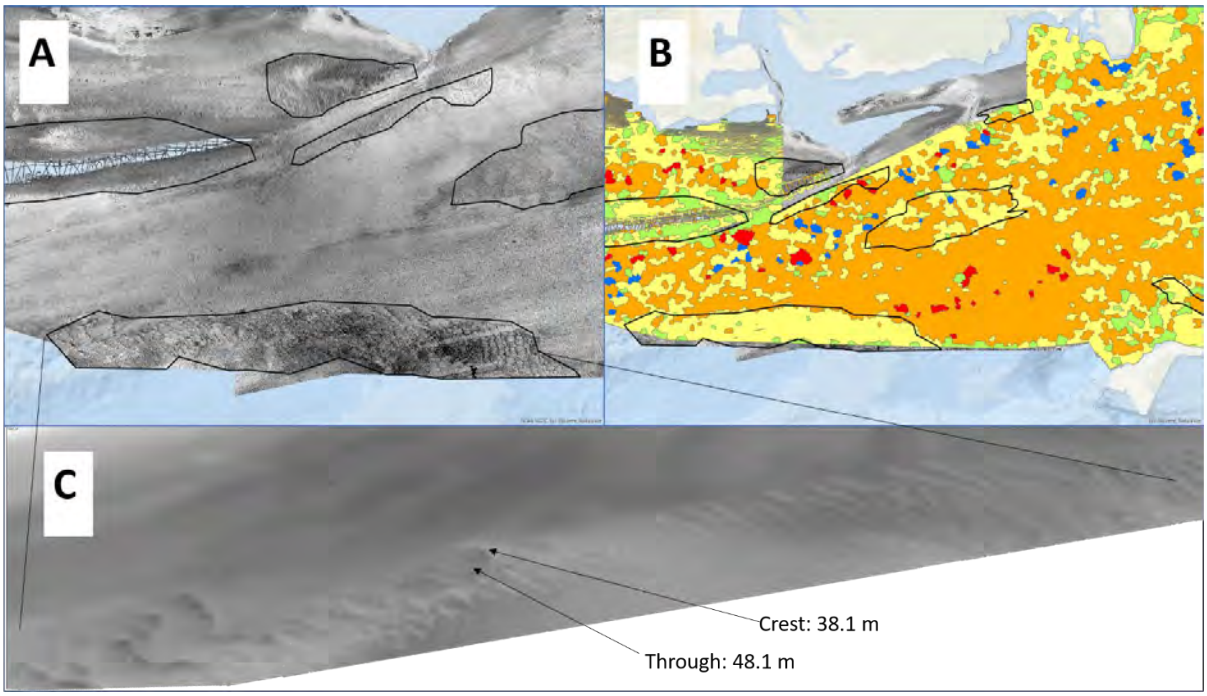

Figure 4.4-1 A: Location of several sand wave fields in the western portion of the Phase II study area. B: Areas of sand wave fields superimposed over acoustic patch types distribution (see Figure 4.6 for key for patch types. C: 3-D close-up of sand wave along the south-western edge of the Phase II study area; values represent depths at a representative crest and through within the sand wave field.

4.5 References - Seafloor Characterization

Ackerman, S.D., Huntley, E.C., Blackwood, D.S., Babb, I.G., Zajac, R.N., Conroy, C.W., Auster, P.J., Schneeberger, C.L., and Walton, O.L., (2020). *Sea-floor sediment and imagery data collected in Long Island Sound, Connecticut and New York, 2017 and 2018: U.S. Geological Survey data release.* https://doi.org/10.5066/P9GK29NM

Battista, T., W. Sautter, and R. Husted. (2017). *Bathymetry, acoustic backscatter, and LiDAR data collected in Long Island Sound for the Phase II Long Island Sound Seafloor Mapping Project 2015 (NCEI Accession 0167531).* NOAA National Centers for Environmental Information. Dataset.
https://www.ncei.noaa.gov/access/metadata/landing-page/bin/iso?id=gov.noaa.nodc:167531

Clarke, K.R. and Gorley, R.N. (2015). *PRIMER v7: User manual/tutorial*. PRIMER-E Plymouth.

Drăguţ, L.; Tiede, D.; Levick, S. (2010). ESP: a tool to estimate scale parameter for multiresolution image segmentation of remotely sensed data. *International Journal of Geographical Information Science.* Vol. 24(6), 859-871.

Elkie, P.C., Rempel. R.S. and Carr, A.P. (1999). *Patch Analyst Users Manual: A tool for quantifying landscape structure.* NWST technical manual TM-002. Ontario.

Freidrich, N.E., McMaster, R.L., Thomas, H.F., Lewis, R.S. (1986). *Non-energy Resources: Connecticut and Rhode Island Coastal Waters.* U.S. Dept. Interior, Minerals Management Service Cooperative Agreement No. 14-12-0001-30115, Final Report FY 1984.

Knebel, H.J. and Poppe, L.J., (2000). Sea-floor environments within Long Island Sound: a regional overview. *Journal of Coastal Research*, 16(3), 533-550.

Lucieer, V.L. 2008. Object-oriented classification of sidescan sonar data for mapping benthic marine habitats. *International Journal of Remote Sensing*. 29(3), 905-921.

NCSS 11 Statistical Software (2016). NCSS, LLC. Kaysville, Utah, USA, https://ncss.com/software/ncss

Neff, N.F., McMaster, R.L., Lewis, R.S., Thomas, H.F., (1988). *Non-energy resources: Connecticut and Rhode Island coastal waters.* U.S. Dept. Interior, Minerals Management Service Cooperative Agreement No. 14-12-0001-30316. Final Report FY 1986.

Poppe, L.J., Knebel, H.J., Mlodzinska, Z.J., Hastings, M.E. and Seekins, B.A., (2000). Distribution of surficial sediment in Long Island Sound and adjacent waters: texture and total organic carbon. *Journal of Coastal Research*. 16(3), 567-574

Trimble (2019). eCognition Developer 9.4.0 https://geospatial.trimble.com/products-and-solutions/ecognition

Zajac, R.N. (1998). A review of research on benthic communities conducted in Long Island Sound and an assessment of structure and dynamics. Chapter 4 in: *Long Island Sound Environmental Studies.* Poppe, L.J and Polloni, C. eds. https://pubs.usgs.gov/of/1998/of98-502/chapt4/rz1cont.htm

Zajac, R.N., Lewis, R.S., Poppe, L.J., Twichell, D.C., Vozarik, J. and DiGiacomo-Cohen, M.L., (2000). Relationships among sea-floor structure and benthic communities in Long Island Sound at regional and benthoscape scales. *Journal of Coastal Research*. 16(3), 627-640

Zajac, R.N., Lewis, R.S., Poppe, L.J., Twichell, D.C., Vozarik, J. and DiGiacomo-Cohen, M.L. (2003). Responses of infaunal populations to benthoscape structure and the potential importance of transition zones. *Limnology and Oceanography* 48, 829-842.

5.0 ECOLOGICAL CHARACTERIZATION

Recommended Citation:

Zajac, R.N., Auster, P.J., Conroy, C.N. (2021). Objectives and Historical Context. Section 5.1 in "Ecological Characterization" p. 66-72 in *The Long Island Sound Habitat Mapping Initiative Phase II – Eastern Long Island Sound – Final Report.* (Unpublished project report).

Zajac, R.N., Walton, O., Schneeberger, C., Govert, N.M. (2021). Infaunal Ecological Characterization. Section 5.2 in "Ecological Characterization" p. 73-117 in *The Long Island Sound Habitat Mapping Initiative Phase II – Eastern Long Island Sound – Final Report.* (Unpublished project report).

Conroy, C.N., Govert, N.M., Auster, P.J., (2021). Epifaunal Ecological Characterization. Section 5.3 in "Ecological Characterization" p. 118- 215 in *The Long Island Sound Habitat Mapping Initiative Phase II – Eastern Long Island Sound – Final Report.* (Unpublished project report).

Conroy, C.N., Govert, N.M., Auster, P.J., Zajac, R.N. (2021). Integrated Ecological Characterization. Section 5.4 in "Ecological Characterization" p. 216-222 in *The Long Island Sound Habitat Mapping Initiative Phase II – Eastern Long Island Sound – Final Report.* (Unpublished project report).

Conroy, C.N., Govert, N.M., Auster, P.J., Zajac, R.N. (2021). Habitat/Seafloor Classification. Section 5.5 in "Ecological Characterization" p. 222-234 in *The Long Island Sound Habitat Mapping Initiative Phase II – Eastern Long Island Sound – Final Report.* (Unpublished project report).

Conroy, C.N., Zajac, R.N. Auster, P.J. (2021). Discussion and Overall Conclusions. Section 5. in "Ecological Characterization" p. 235-238 in *The Long Island Sound Habitat Mapping Initiative Phase II – Eastern Long Island Sound – Final Report.* (Unpublished project report).

5.1 Objectives and Historical Context

The main focus of this portion of the Phase II LIS mapping project was to identify, characterize and map the benthic habitats that comprise the study area and the infaunal and epifaunal communities found in these sea floor habitats at multiple spatial scales. Based on these efforts, information on ecologically significant locations in the Phase II study area can be identified, the information can be used for a variety of marine spatial management efforts, as well as for assessing how the ecological communities and habitats might be affected by future impacts.

Maps depicting sea floor habitats and their ecological communities are critical for many environmental management, conservation, and research activities, and for the growing focus on coastal and marine spatial planning. Such maps depict either separately or in combination the spatial distribution and extent of benthic habitats classified based on physical, geological, geomorphological, and biological attributes and the benthic communities that reside in the

mapped habitats. Additionally, maps can be produced that depict ecological processes across the sea floor. These results and products add to the overall Long Island Sound Cable Fund Seafloor Habitat Mapping project and continue to increase our understanding of Long Island Sound (LIS) and Fishers Island Sound (FIS) in a geospatial context.

5.1.1 Infaunal Communities

Studies of the benthic infaunal ecology in the Phase II area have included both Sound-wide surveys that extended into portions of eastern LIS and FIS, and studies within specific locations. One-time surveys in the mid and late 1970's provided data that helped establish trends in general community composition, diversity and relationships to habitat features (sediment type, depth, see Zajac, 1998; Zajac et al. 2000). In some cases, the spatial resolution was relatively coarse; in another survey (Pellegrino and Hubbard, 1983) the spatial resolution was high but only CT waters were sampled. In the early 1990s and then in the early 2000s a series of benthic samples were taken in LIS in support of the EPA EMAP and NCA programs, respectively. A few of the sample sites were located in the Phase II study area. Some of the general trends that emerge from these studies is that infaunal taxonomic richness generally increases from west to east in the area, ranging from 21 to 60 taxa 0.25 m^{-2}, and that community structure changes as well in the same direction (Figure 5.1-1 and Table 5.1-1). Relatively distinct communities were located just south of the Connecticut River, in deeper waters between the Connecticut River and the mouth of the Thames River, at the mouth of the Thames River and in FIS. Zajac et al. (2003) found smaller scale variation in community types within specific patches of different sediment types and that taxonomic richness could be elevated across transition zones among different sediment types/habitat types. Specific comparisons of taxonomic and community composition between these previous studies and the results from this Phase II project will be represented in the discussion section of the infaunal community characterization section of this report (see below).

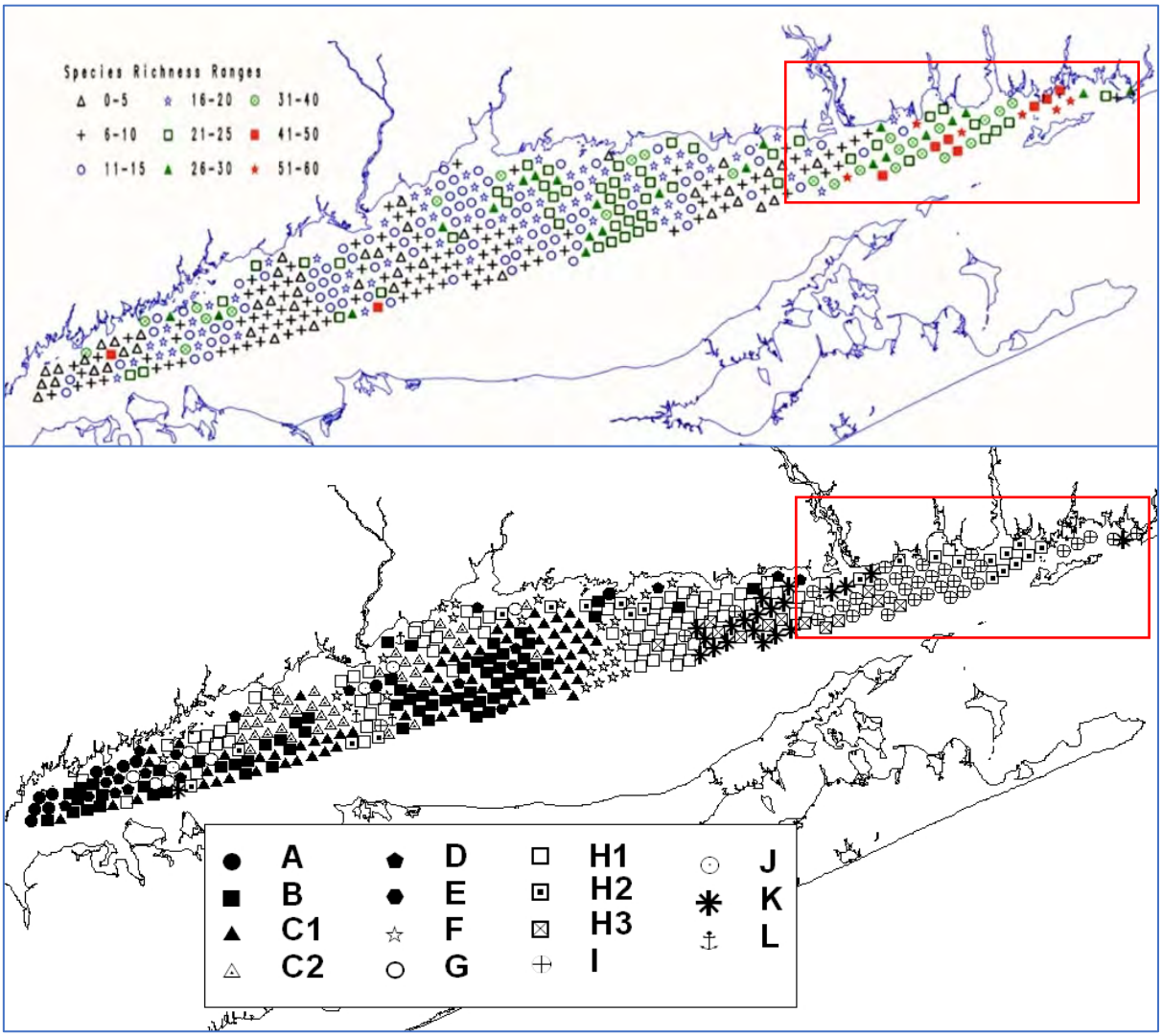

Figure 5.1- 1 Distribution of species richness (Top) and infaunal community types (Bottom) based on analyses by Zajac et al. (2000) from data provided in Pellegrino and Hubbard (1983). Approximate location of the Phase II study area delineated by the red box. Descriptions of the community types are given in Table 5.1.

Table 5.1- 1. Abundances (mean +/- 1SE) per 0.04 m2 of dominant species in each of the community types found in Long Island Sound based on analyses by Zajac et al. (2000) of the data provided in Pellegrino and Hubbard (1983). The community structure analyses were based on the 35 most abundant species found by Pellegrino and Hubbard (1983) throughout Long Island Sound. Community types (A, B, C1, etc.) are given along the top row. P (polychaetes), B (bivalves) and A (arthropods) indicate the beginning of each taxonomic group.

SPECIES	A	B	C1	C2	D	E	F	G	H1	H2	H3	I	J	K
Pectinaria gouldii **P**	0.3 +/-0.2	0.9 +/-0.3	4.7 +/-1.7	0.0 +/-0.0	40.9 +/-11.7	0.4 +/-0.2	10.2 +/-6.5	10.2 +/-2.8	0.5 +/-0.4	0.4 +/-0.4			0.3 +/-0.3	0.0 +/-0.0
Nephtys incisa	0.5 +/-0.3	5.4 +/-0.4	6.4 +/-0.6	6.5 +/-0.6	2.5 +/-0.9	0.8 +/-0.4	11.2 +/-5.2	1.5 +/-0.7	0.6 +/-0.3	1.0 +/-0.6				
Mediomastus ambiseta		1.6 +/-0.4	2.0 +/-0.7	2.6 +/-0.9	4.1 +/-1.8	0.2 +/-0.2	53.3 +/-17.7		1.7 +/-0.6	4.7 +/-3.2				
Polydora websteri		0.0 +/-0.0	0.2 +/-0.2	0.8 +/-0.8	1.9 +/-1.1			0.7 +/-0.7	3.5 +/-1.4	0.2 +/-0.2		2.5 +/-1.5	1.0 +/-0.7	
Ancidea jeffersyii					1.3 +/-1.0		2.4 +/-2.0	1.7 +/-1.2	3.4 +/-0.9	0.0 +/-0.0	2.8 +/-1.1	8.3 +/-4.0		
Prionospio heterobranchia		0.0 +/-0.0			0.6 +/-0.4		0.3 +/-0.3		0.8 +/-0.4	4.5 +/-2.7		14.5 +/-5.7		0.4 +/-0.3
Paraonis fulgens	0.1 +/-0.1	0.4 +/-0.2	0.1 +/-0.1	0.1 +/-0.0		0.6 +/-0.6			0.0 +/-0.0	1.0 +/-0.7	0.2 +/-0.2			
Asabellides oculata		0.1 +/-0.1	0.6 +/-0.4	0.0 +/-0.0	0.3 +/-0.3	0.4 +/-0.2	4.3 +/-1.6	2.7 +/-2.0	12.3 +/-2.1	0.3 +/-0.3			1.0 +/-0.7	
Clymenella zonalis		0.3 +/-0.2	0.7 +/-0.3		0.9 +/-0.7		190.7 +/-45.2	3.5 +/-3.3	5.6 +/-1.6	1.7 +/-0.9	0.4 +/-0.3	2.8 +/-1.7		0.2 +/-0.2
Spiophanes bombyx							0.4 +/-0.4		7.4 +/-1.8	6.4 +/-3.7	0.6 +/-0.4	0.5 +/-0.4	0.5 +/-0.3	1.0 +/-1.0
Cirratulus grandis		0.0 +/-0.0		0.1 +/-0.1	0.3 +/-0.3		0.4 +/-0.4		0.0 +/-0.0	2.5 +/-1.8		35.3 +/-14.6		
Cirratulus cirratus		0.0 +/-0.0							0.2 +/-0.2			8.9 +/-4.6		0.0 +/-0.0
Lepidontus squamatus									0.6 +/-0.4		0.3 +/-0.3	2.4 +/-1.0		0.3 +/-0.2
Steblospio benedicti		0.0 +/-0.0			3.4 +/-2.4		9.7 +/-6.4		0.2 +/-0.1	1.7 +/-1.7				0.1 +/-0.1
Owenia fusiformis					0.3 +/-0.3		1.6 +/-1.1		2.0 +/-1.1					
Nephtys picta					0.3 +/-0.3				3.6 +/-1.2	2.1 +/-2.0	0.8 +/-0.5	0.5 +/-0.3		0.3 +/-0.3
Capitella capitata											2.1 +/-1.7	2.8 +/-1.8		
Ampharete arctica									0.1 +/-0.1	0.6 +/-0.4	1.3 +/-0.9	6.5 +/-2.2		
Prionospio tenuis									0.4 +/-0.4	0.7 +/-0.7		9.9 +/-3.8		
Ampelisca abdita **A**		0.7 +/-0.3	2.2 +/-1.0	0.6 +/-0.5	0.8 +/-0.5		3.1 +/-1.5	1.2 +/-1.2	1.7 +/-0.5	124.2 +/-37.6	0.4 +/-0.4	0.5 +/-0.4		
Unciola irrorata		0.3 +/-0.3	0.1 +/-0.1						1.4 +/-0.4	8.7 +/-4.0	6.0 +/-1.9	1.0 +/-0.4		0.2 +/-0.1
Leptocheirus pinguis									0.2 +/-0.2	9.6 +/-6.3			0.5 +/-0.5	
Ampelisca vadorum		0.0 +/-0.0	0.3 +/-0.3					0.8 +/-0.8	0.1 +/-0.1	21.3 +/-10.4		0.1 +/-0.1	0.3 +/-0.3	
Protohaustorius wigleyi									0.1 +/-0.1		0.3 +/-0.2			24.7 +/-8.1
Ancanthohaustorius millsi										2.0 +/-2.0	0.3 +/-0.3			3.1 +/-1.3
Aeginina longicornis										0.3 +/-0.3	1.1 +/-1.1	11.4 +/-3.5		
Corophium acherusicum					17.4 +/-17.4		3.0 +/-3.0		0.2 +/-0.2	18.5 +/-18.0	0.2 +/-0.2	4.0 +/-1.3		1.0 +/-1.0
Mulinia lateralis **B**	5.3 +/-0.9	11.4 +/-1.2	41.9 +/-5.7	118.2 +/-10.5	15.9 +/-6.0	0.4 +/-0.2	299.6 +/-59.2		0.9 +/-0.4	1.5 +/-1.0				1.0 +/-1.0
Nucula annolata	0.1 +/-0.1	8.6 +/-0.9	125.8 +/-13.9	11.3 +/-2.1	15.3 +/-5.0	3.4 +/-0.9	21.0 +/-7.8	0.7 +/-0.7	0.4 +/-0.3	2.8 +/-1.6		0.3 +/-0.3		
Pitar morrhuana		3.3 +/-0.8	5.2 +/-0.9	5.1 +/-1.3	4.9 +/-2.3		3.3 +/-1.5	3.0 +/-1.4	0.1 +/-0.0	2.8 +/-1.6				
Tellina agilis	0.1 +/-0.1	0.4 +/-0.2	0.7 +/-0.3	0.4 +/-0.3	6.4 +/-4.6		12.8 +/-3.8		8.4 +/-1.1	2.0 +/-1.1		0.3 +/-0.3		0.6 +/-0.3
Yoldia lamatula		0.8 +/-0.2	2.3 +/-0.7	1.6 +/-0.4	0.6 +/-0.5	0.6 +/-0.4	1.2 +/-0.7		0.4 +/-0.4					
Pandora gouldina		0.1 +/-0.1	2.0 +/-1.4	0.3 +/-0.3	0.6 +/-0.6		0.2 +/-0.2		0.1 +/-0.0	0.4 +/-0.4		1.7 +/-1.4		0.2 +/-0.1
Ensis directus		1.0 +/-0.4	0.6 +/-0.3		18.0 +/-9.9	0.2 +/-0.2	0.3 +/-0.3		0.9 +/-0.5	0.6 +/-0.6		0.3 +/-0.3		
Mytilus edulis		0.1 +/-0.1	0.0 +/-0.0	0.1 +/-0.1			0.1 +/-0.1					38.6 +/-38.6		0.0 +/-0.0

5.1.2 Epifaunal Communities

It is noteworthy that there are no historic, spatially comprehensive, studies focused on epifaunal communities in the Phase 2 study region, despite the ecosystem engineering functions played by structure forming fauna dominant in such communities, and their contribution to the biological diversity of the region (i.e., epifaunal species and associates). This is in large part due to the difficulty of directly sampling such communities on hard substratum, in often precipitous topographies, requiring either imaging or some form of hand manipulated sampling gear (e.g., airlift) to collect samples. Pelligrino and Hubbard (1983) did include some characteristic emergent and attached fauna (on small diameter gravels) in grab samples but did not sample substrates that we not amenable to the sampling gear. Seafloor imaging as a component of sidescan and multibeam mapping has been used to qualitatively characterize epifaunal communities and their habitat role in eastern Long Island Sound and FIS (e.g., Poppe et al.,1994, 2013; Langton et al., 1995).

There have been multiple studies that focus on select sites within the Phase 2 area. Welsh and Stewart (1984) characterized benthic macrophyte communities and associated fauna in the Thames River estuary (south to Ledge Light and Black Ledge), using direct quadrat sampling and seafloor imagery, established a baseline for comparison to address changes in human uses of the region. Macrophytes were found to increase habitat complexity with diverse and abundant fauna and utilized year around. Epifauna and associated vagile species were important prey for economically important species. Macrophtyes also served as nursery habitats for juveniles of multiple species. In shallow waters, there is a time series from aerial surveys for seagrass habitats, addressing the changing distribution and status of Zostera marina and associated submerged aquatic vegetation (get ref from EPA habitat project). Moving offshore, monitoring of the New London dredge material disposal site, had included

time series from visual diver transects of seafloor habitat conditions and associated fauna, principally on soft sediments, with a focus on emergent fauna and ecosystem engineering species (e.g., crustacea, burrowing fishes) that modify the seafloor landscape (e.g., Stewart, 1980; Parker and Revelas, 1989). More recent monitoring (AECOM, 2009) has included sediment profiling and plain view imaging to assess, among diverse metrics, surface boundary roughness and conditions that address effects of physical sedimentary transport processes (e.g., producing ripples, sand wave features) and biogenic elements of habitat (e.g., shell, habitat forming species).

Fisheries resource monitoring, linked to seafloor characteristics, have a detailed time series in the LIS region but bounded by the east of LIS, excluding FIS (e.g., Gottschall et al., 2000; Howell et al., 2016). Localized citizen science studies around the Thames River region (Snyder et al., 2019) also provide direct and inferential measures of habitat conditions and change over time. Multiple autecological studies at select sites also provide snapshots of local conditions during earlier periods. For example, Lund et al. (1971) describe seafloor habitat conditions at Ram Island Reef from a study of American lobster ecology. Parry (1981) describe the sponge fauna at select sites in FIS.

The results from Phase II studies of the distribution of emergent and epifaunal communities, with component species, is the first spatially comprehensive assessment for this region and can provide a foundation for linking use of such habitats to diverse human uses of the region today.

5.1.3 Overview of Previous Studies

While certain geologic and ecological characteristics have been mapped in eastern LIS, there remained data gaps that limited the ability to produce contemporary and spatially more comprehensive benthic habitat and ecological maps in the Phase II area. These data gaps are spatial, thematic and temporal in nature, and limited the utility of existing products for resource management applications. Spatial data gaps existed because historical information was generally analyzed at coarse spatial scales, limiting its use for the breadth of management applications, particularly those focused on specific areas. In addition to spatial gaps, there were also thematic and temporal data gaps.

Existing maps of the seafloor are primarily geology based (surficial sediment types and sedimentary environments), and do not incorporate geomorphological, bathymetric, and, perhaps most critically, ecological components of habitat, and particularly epifaunal communities and habitats, and habitat forming species (e.g. mussel beds, oyster reefs, sponge communities, tube mats). There were also no maps that show the distribution and variation of both epibenthic and benthic infaunal communities within defined seafloor patches/habitats, except in some areas based on smaller scale studies (see above). In terms of temporal data gaps, many of the data collected that were used to produce geologically themed seafloor maps currently available, were collected over a time span approaching 80 -100 years in the case of the surficial texture sediment map, and close to 20 years for spatially-coarse side scan data that was used in part to produce the sedimentary environment map. Likewise, no significant ecological sampling of the benthos across the full extent of Long Island Sound, either the epifaunal or infaunal components, nor in shallow or deep waters, over a large spatial scale has been done since the mid-1970s to early 1980s, and no comprehensive sampling in the Phase II study area since 1998. Habitat maps produced using contemporary, and generally more accurate data, are more likely to be utilized for many different

management applications because they contain added information that may be relevant and scalable to a wider array of issues in the marine environment. Furthermore, new management problems cannot always be anticipated (e.g., with respect to climate change), making extracting the maximum amount of information from acoustic imagery potentially important for being prepared to meet the future needs of the coastal and marine management community.

5.1.4 References - Historical Context and Objectives

AECOM. (2009). *Monitoring survey at the New London disposal site, July/ August 2007. DAMOS Contribution No. 180. U.S. Army Corps of Engineers*. New England District, Concord, MA.

Gottschall, K. F., Johnson, M. W., & Simpson, D. G. (2000). *The distribution and size composition of finfish, American lobster, and long-finned squid in Long Island Sound based on the Connecticut Fisheries Division Bottom Trawl Survey, 1984–1994.* NOAA Technical Report NMFS 148.

Howell, P. T., Pereira, J. J., Schultz, E. T., & Auster, P. J. (2016). Habitat Use in a Depleted Population of Winter Flounder: Insights into Impediments to Population Recovery. *Transactions of the American Fisheries Society*. 145(6), 1208-1222.

Langton, R. W., Auster, P. J., & Schneider, D. C. (1995). A spatial and temporal perspective on research and management of groundfish in the northwest Atlantic. *Reviews in Fisheries Science*. 3(3), 201-229.

Lund, W.A., Stewart, L.L., & Weiss, H.M. (1971). *Investigation on the lobster Homarus americanus.* Commercial Fisheries Research Devevelopment Act - Final Report Project No. 3-44-R, Department of Commerce. NOAA, NMFS.

Parker, J.H. and E.C. Revelas. (1989). *Monitoring surveys at the New London disposal site, August 1985 July 1986.* DAMOS Contribution No. 60. SAIC report ; 86/7540&C60 U.S. Army Corps of Engineers, New England District, Concord, MA.

Parry, E.H. (1981). *Ecology of sponges of lower Mystic estuary and Fisheries Island Sound, with emphasis on Cliona celata: distribution, reproduction and winter condition.* M.A. Thesis. Connecticut College, New London.

Pellegrino, P & Hubbard, W. (1983) *Baseline shellfish data for the assessment of potential environmental impacts associated with energy activities in Connecticut's coastal zone.* Vols I & II. Report to the State of Connecticut, Department of Agriculture, Aquaculture Division, Hartford, CT.

Poppe, L.J., Lewis, R., Quarrier, S., Zajac, R., Moffet, A. (1994). *Map showing the distribution of surficial sediments in Fishers Island Sound, New York, Connecticut, and Rhode Island. U.S.* Geological Survey, Miscellaneous Investigations Series Map I-2456.

Poppe, L.J., McMullen, K.Y., Ackerman, S.D., and Glomb, K.A., (2013), *Sea-floor geology and topography offshore in northeastern Long Island Sound: U.S. Geological Survey Open-File Report 2013–1060.* DVD-ROM, http://dx.doi.org/10.3133/ofr20131060.

Snyder, J. T., Whitney, M. M., Dam, H. G., Jacobs, M. W., & Baumann, H. (2019). Citizen science observations reveal rapid, multi-decadal ecosystem changes in eastern Long Island Sound. *Marine Environmental Research.* 146, 80-88.

Stewart, L.L. (1980). *Chronological records of in-situ physical and biological conditions obtained by diver survey at the Central Long Island Sound and New London Disposal Sites.* Second International Ocean Dumping Symposium, Woods Hole, Massachusetts. DAMOS Contribution No. 9. U.S. Army Corps of Engineers, New England District, Concord, MA.

Welsh, B.L. and L. Stewart. (1984). *The effects of energy-related transport activities on benthic marine plants, fish, shellfish and lobsters in the Thames River estuary*. Final Report to Office of Policy and Management, State of Connecticut.

Zajac, R. (1998). A review of research on benthic communities conducted in Long Island Sound and an assessment of structure and dynamics. Chapter 4, in: *Long Island Sound Environmental Studies.* edited by Poppe, LJ. And Polloni, C. USGS Open-File Report 98-502. Available at: https://pubs.usgs.gov/of/1998/of98-502/chapt4/rz1cont.htm

Zajac, R.N., Lewis, R.S., Poppe, L.J., Twichell, D.C., Vozarik, J. and DiGiacomo-Cohen, M.L. (2000). Relationships among sea-floor structure and benthic communities in Long Island Sound at regional and benthoscape scales. *Journal of Coastal Research*. 627-640. Available at:
https://journals.flvc.org/jcr/article/view/80868/78017

Zajac, R.N., Lewis, R.S., Poppe, L.J., Twichell, D.C., Vozarik, J. and DiGiacomo-Cohen, M.L. (2003). Responses of infaunal populations to benthoscape structure and the potential importance of transition zones. *Limnology and Oceanography* 48, 829-842.
https://aslopubs.onlinelibrary.wiley.com/doi/epdf/10.4319/lo.2003.48.2.0829

5.2 Infaunal Ecological Characterization

5.2.1 Objectives

The main focus of this portion of the study was to characterize the infaunal communities across the different sea floor environments found in the Phase II project study area, to assess differences in infaunal community structure among the large-scale acoustic patch types identified through our analyses of the backscatter data (see Section 4.0) and also ecological variability within these patch types. Infaunal communities comprise those organisms that live in seafloor sediments and/or just at the sediment-water interface. The acoustic patch types can be viewed as large-scale (on the order of 10-100s of km^2), general habitat types that have been identified based on reflectance information in the backscatter mosaic image and the characterized based on their sediment composition and associated physical dynamics. These characteristics vary on a relative basis within each acoustic patch type, creating smaller scale habitats with specific sets of characteristics that may support different sets of ecological communities. Based on these efforts, information on ecologically significant locations in the Phase II study area can be identified, as well as how the infaunal community characteristics and habitat distributions might shape future impact assessments and management efforts.

5.2.1 Methods

5.2.1.1 Field Data Acquisition

Samples for ecological characterization were collected during two sampling periods, between November 28 and December 3, 2017 and May 8 and 15, 2018. The sampling design comprised a series of sampling blocks (SB) and sampling sites (NB) that were distributed across the Phase II study area based on acoustic backscatter and bathymetric data that was available prior to the November - December sampling period (See Section 4.2, Figure 4.2-1). The spatial distribution and locations of the sampling locations were selected with the overall objective to sample as many of the different seafloor habitats that were evident in the side scan mosaic that had been previously developed for the study area. These included both areas that were within large-scale sea floor features (acoustic patches) and areas where there are transitions among large scale features. Initial identification of seafloor features was based on previous work conducted in this portion of LIS (Poppe et. al., 2000; Zajac et al., 2000, 2003), visual interpretations of the available side scan mosaic and general information from the literature on sea floor mapping and ecological characterization using acoustic data for habitat identification characterization (e.g. Brown et al., 2012 Kostylev et al., 2001). This planning phase resulted in the selection of 160 sampling locations. Infaunal grab samples were not obtained at several locations due bottom hazards for the sampling equipment and or high currents. Infaunal grab samples were collected using the USGS SEABOSS system (See Section 3.3.1 for details).

The sampling design included taking three randomly located grab samples (generated using ArcGIS) in each SB and one sample at each NB location. Infaunal samples were collected with a 0.1 m^2 modified Van Veen grab. The SEABOSS was lowered to just above the sea floor and then was allowed to drift for several minutes to collect video and still images, after which a grab sample was collected.

5.2.1.2 Infaunal Sample Processing and General Analytical Approaches

In the field, the entire contents of a grab sample obtained at each sampling site was washed on a 1mm sieve using filtered seawater, after a small portion of surficial sediment, approximately 25 cm^2 by 2 cm deep, was removed for sediment analyses. At several locations a 500 µm was used to process the samples to check for mesh size effects. The sieved sample was preserved with 70% ethanol and stained with Rose Bengal. In the lab, samples were sorted under a dissecting microscope and individuals were identified to the lowest possible taxon. A total of 160 samples were processed.

After the data sets were assembled, several sets of statistical and GIS-based analyses were conducted to assess the characteristics of infaunal communities (total abundance [total number of identified organisms per sample], taxonomic/species richness [species richness and taxonomic richness are used interchangeably here and represent the number of taxa that were differentiated to the lowest possible taxonomic level], taxonomic/species diversity [as Shannon Diversity Index, a measure that accounts for both total number of taxa/species and relative proportion/evenness], community composition and related metrics [multivariate analyses measuring similarities and trends within and among samples]) among and within the large-scale acoustic patches that were identified, and to map the spatial trends in community structure and biodiversity relative to sea floor habitat structure.

Community composition and related metrics were analyzed using multivariate analyses, including classification analysis (clustering), non-metric multidimensional scaling (MDS) and canonical analysis of principal coordinates (CAP). These analyses determined community similarities and trends among and within among large-scale acoustic patches. Species contributions to community similarities within acoustic patches and dissimilarities among patches were assessed using similarity percentage analysis (SIMPER). Statistical differences in community structure were assessed using an analysis of similarities (ANOSIM) and permutational analysis of variance (PERMANOVA) procedures. All multivariate procedures were carried out using PRIMER+ PERMOVA software (Clarke and Gorley, 2006). Calculation of several diversity indices were also carried out in PRIMER. Shannon diversity was calculated as:

$$H' = -\sum_{i=0}^{S} (pi \times log10pi)$$

where, S is the total number of species/taxa, pi is the proportion of individuals belonging to the ith species. Higher values of H' indicate greater species diversity.

Differences in total abundance, taxonomic richness, and Shannon diversity among acoustic patch types were tested using analysis of variance (ANOVA) in the NCSS statistical software package (NCSS, 2012). The results of the statistical analyses were used to develop GIS data layers that depicted the spatial distribution of community types and biodiversity across the pilot study area. Details of analytical steps and conditions are provided below as needed.

5.2.3 Results

5.2.3.1 General infaunal community characteristics

A total of 289 infaunal taxa were identified in all the samples collected in the LIS Phase II area. 85% of these were identified to the species level. Two sets of analyses were conducted to assess the general infaunal community characteristics (taxonomic richness, total abundance and diversity): one using the entire data set from both sampling periods and also for each sampling period separately to assess potential seasonal differences among the large-scale patch types. Only one sample was taken in Patch Types A and E; as such, they were excluded from several of statistical tests of general community characteristics among patch types. Tests among samples processed using a 1 mm versus a 500 µm sieve indicated no statistical differences for total abundance, taxonomic richness and diversity, and as such all the samples were combined for subsequent analyses.

Infaunal mean total abundances in the patch types generally ranged from ~ 175 to 225 individuals 0.1 m^{-2} (Figure 5.2-1). The abundance in the one sample taken in Patch Type A was very high, primarily due to a very high number of the slipper shell *Crepidula fornicate* (440) and oligochaetes (72) in the sample. The total abundance in the one sample taken in Patch Type E was lower than the mean values in the other patch types. There were some samples in each of the other patch types that had relatively high total abundances as well, as revealed by the boxplots (Figure 5.2-1). In one case, a sample taken in Patch Type D had close to 1,000 individuals per 0.1 m^{-2}.

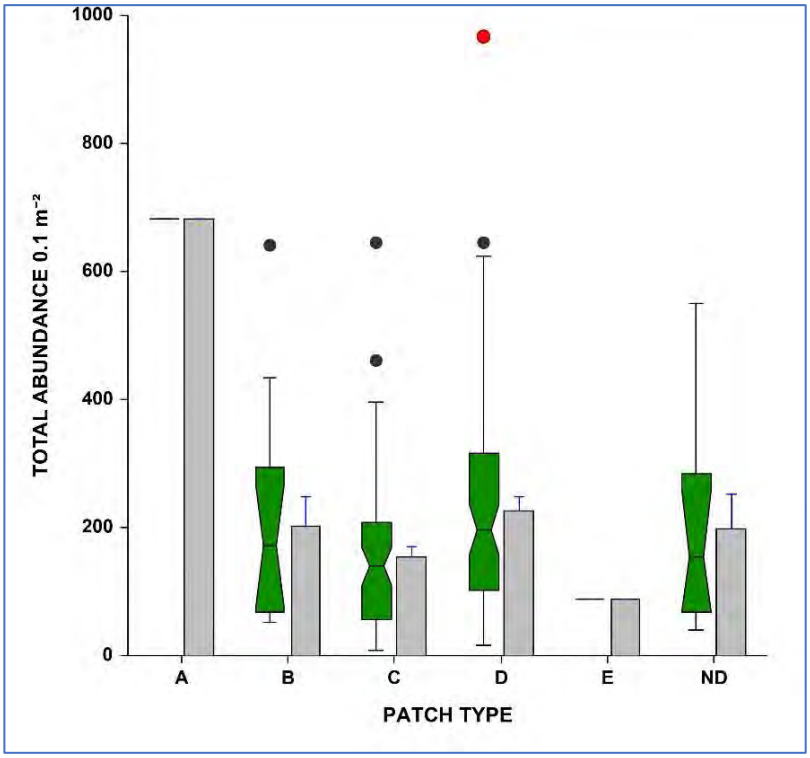

Figure 5.2- 1 Total abundance in the Patch Types in the LIS Phase II Study area. Shown are the mean total abundances (+1 standard error, SE) and box plots showing the notched median (median ± 1.57 × (IQR) / √n), the inter-quartile range (IRQ) defined by the upper (75th percentile) and lower 25th percentile ends of the box, whiskers extending to 1.5 * IRQ. Outliers are shown as dots.

One-way ANOVA indicated that there was a marginally significant difference in mean total abundance among patch types, with a post hoc test indicating that abundances in Patch Type D were greater than in Patch Type C (Table 5.2-1). In general, mean abundances were higher in the November/December samples than in the May samples, particularly in Patch Type B (Figure 5.2-2). Two-way ANOVA indicated that there was a significant difference in mean total abundance among seasons, as well as a significant difference between Patch Types B, C, and D (Table 5.2-1). Individual sample abundance exhibited large spatial variation across the study area (Figure 5.2-4 and Figure 5.2-5). Relatively low abundances were found at most sample sites along the southern boundary of the Phase II study area, as well as in an area to the southeast of the mouth of the Connecticut River. Moderate to high abundances were found throughout the central portion of the study area and in portions of Fishers Island Sound (FIS). Sample sites with locally high abundances were scattered throughout the Phase II area.

Table 5.2- 1. Results of statistical analyses of differences in general community characteristics among patch types in the LIS Phase II study area. Patch types differences tested with one- way ANOVA: patch type and season differences tested with two-way ANOVA.

Total Abundance – Patch types only

Term	DF	Sum of Squares	Mean Square	F-Ratio	Prob Level
Patch Type	3	1.112615	0.3708718	2.5795	0.05567
Within (Error)	154	22.14193	0.1437788		
Adjusted Total	157	23.25455			
Total	158				

Bonferroni (All-Pairwise) Multiple Comparison Test

Group	Count	Mean	Different from Groups
B	14	2.174418	
C	63	2.045596	D
D	71	2.226692	C
ND	10	2.165776	

Total Abundance – Patch types and Season

Term	DF	Sum of Squares	Mean Square	F-Ratio	Prob Level	Power (Alpha=0.05)
Patch Type	2	1.516051	0.7580255	5.61	0.004517*	0.852134
Season	1	1.617094	1.617094	11.97	0.000714*	0.930052
Patch x Season	2	0.3752294	0.1876147	1.39	0.252778	0.294603
S	142	19.18506	0.1351061			
Total (Adjusted)	147	22.04943				
Total	148					

Taxonomic Richness – Patch types only

Model Term	DF	Sum of Squares	Mean Square	F-Ratio	Prob Level
Patch Type	3	0.4506538	0.1502179	3.0061	0.03218
Within (Error)	154	7.69563	0.04997163		
Adjusted Total	157	8.146284			
Total	158				

Bonferroni (All-Pairwise) Multiple Comparison Test

Group	Count	Mean	Different from Groups
B	14	1.340354	
C	63	1.292122	D
D	71	1.40567	C
ND	10	1.306752	

Taxonomic Richness – Patch types and Season

Source Term	DF	Sum of Squares	Mean Square	F-Ratio	Prob Level	Power (Alpha=0.05)
Patch Type	2	13.22823	6.614113	5.22	0.006519*	0.823943
Season	1	12.8402	12.8402	10.13	0.001796*	0.885030
Patch x Season	2	1.396607	0.6983033	0.55	0.577789	0.139724
S	142	180.0695	1.268095			
Total (Adjusted)	147	208.1521				
Total	148					

Diversity (H′): Patch types only

Model Term	DF	Sum of Squares	Mean Square	F-Ratio	Prob Level
Patch Type	3	0.1785805	0.05952685	0.8080	0.49122
Within (Error)	154	11.34503	0.07366905		
Adjusted Total	157	11.52361			
Total	158				

Diversity (H′): Patch types and Season

Source Term	DF	Sum of Squares	Mean Square	F-Ratio	Prob Level	Power (Alpha=0.05)
A: Patch Type	2	0.2395536	0.1197768	1.75	0.176769	0.362893
B: Season	1	0.06691325	0.06691325	0.98	0.323882	0.165983
AB	2	0.1897867	0.09489333	1.39	0.252494	0.294819
S	142	9.695569	0.06827866			
Total (Adjusted)	147	10.51536				
Total	148					

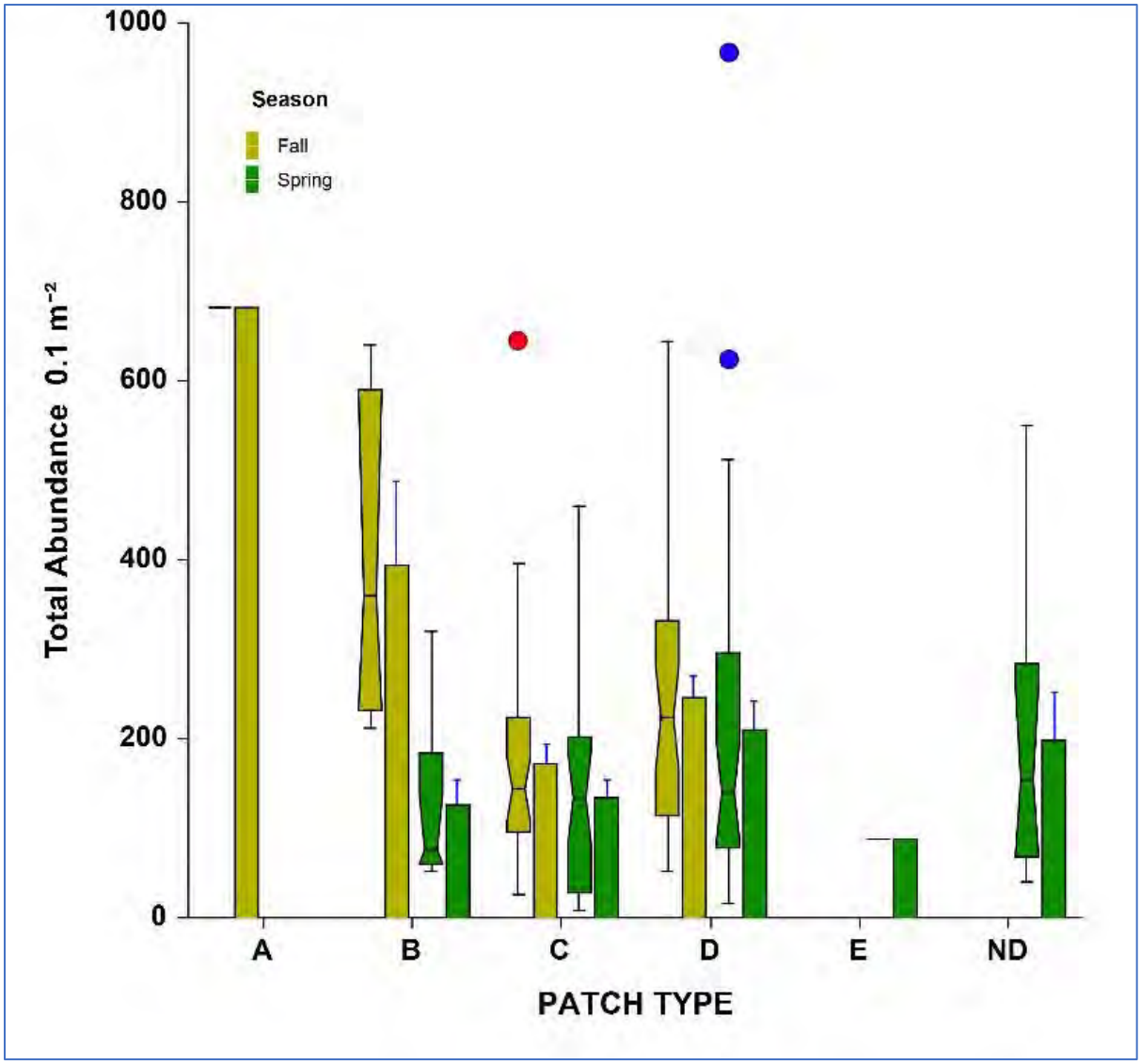

Figure 5.2- 2. Seasonal differences in total abundance in the Patch Types in The LIS Phase II Area. Plot explanation as in Figure 5.2-1.

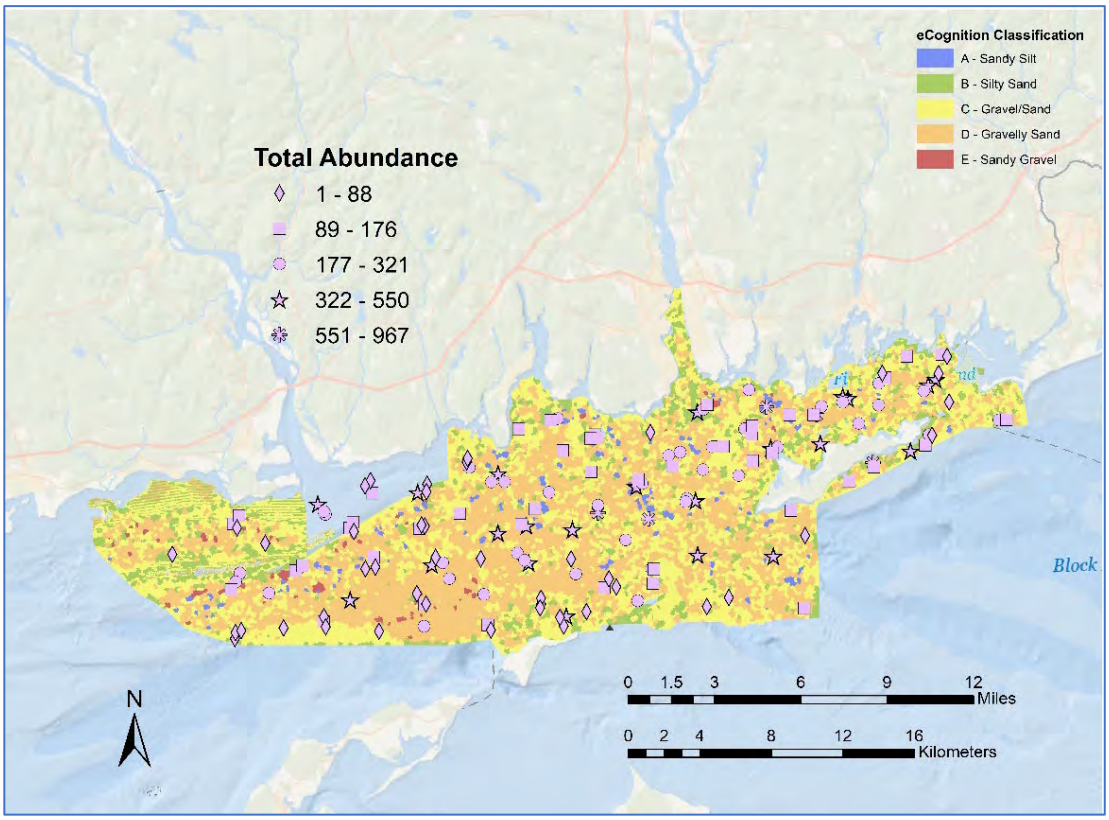

Figure 5.2- 3. Spatial distribution of total abundance of infauna among the sample locations in the LIS Phase II Study Area.

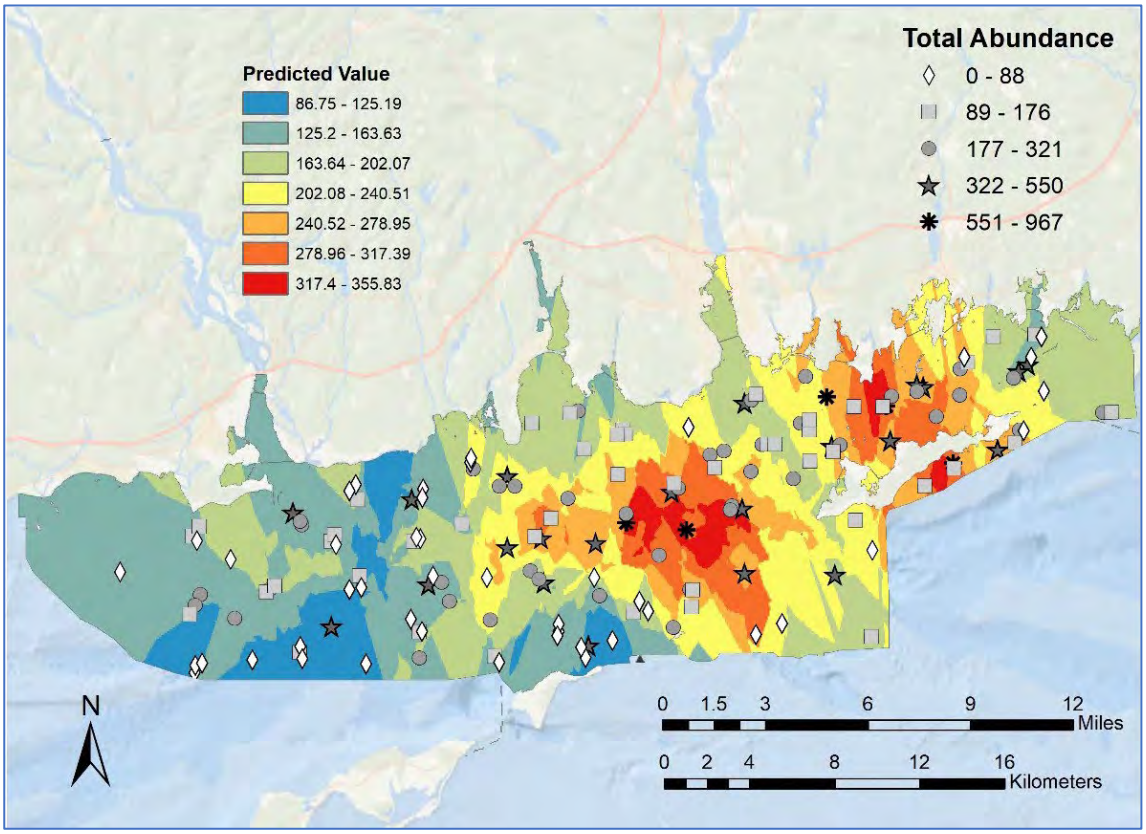

Figure 5.2- 4. Interpolation (using kriging) of total abundance across the LIS Phase II Study Area.

Mean taxonomic richness ranged between 20 and 30 taxa $0.1m^{-2}$ using data from both sampling periods (Figure 5.2-5). The overall range was quite large, with some sites having upwards of 40 to 50 taxa, whereas others had as few as 4 to 5 taxa. There was a statistical difference in taxonomic richness among the acoustic patch types (Table 5.2-1), with post hoc test indicating that richness in Patch Type D was statistically greater than in Patch Type C. More taxa were generally found in samples taken in November – December (fall) than in the May (spring) sampling periods (Figure 5.2-6). Taxonomic richness was higher in fall than in spring for the patch types that were sampled at both times (B, C, and D). In general, the range of the number of taxa found among sampling sites was large and acoustic patch types C and D in both seasons; however, the variation in taxonomic richness among sample sites in Patch Type B was much lower (Figure 5.2-6). Two-way ANOVA indicated significant differences among patch types and seasons but not a significant interaction (Table 5.2-1). Similar to total sample abundance, taxonomic richness was relatively low at sites along the southern portion of the Phase II area (Figure 5.2-7 and Figure 5.2-8). Higher richness was found at sites through the central portion of the area, and also at sites in FIS.

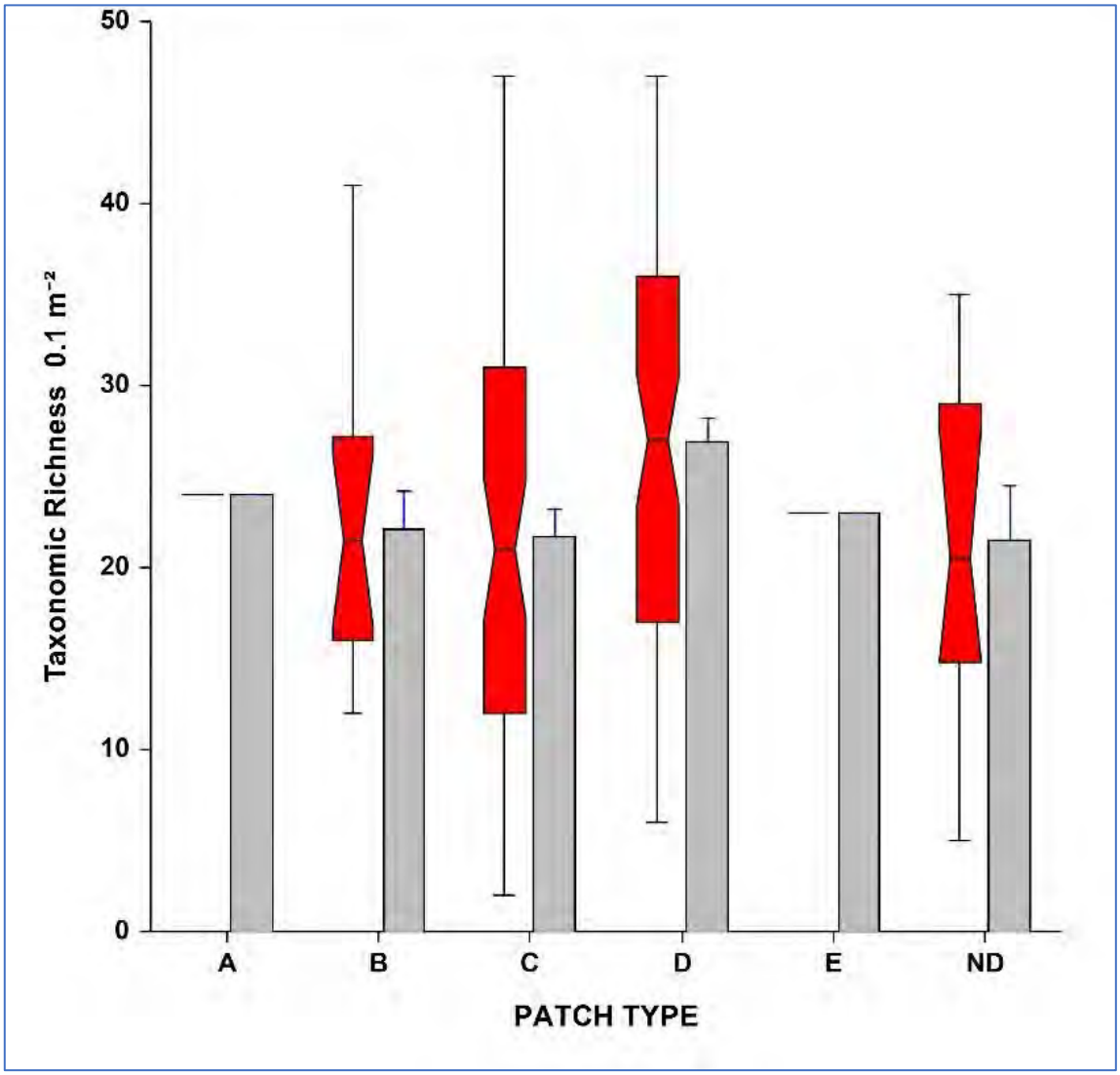

Figure 5.2- 5. Taxonomic richness in the Patch Types in the LIS Phase II Study area. Plot explanation as in Figure 5.2-1.

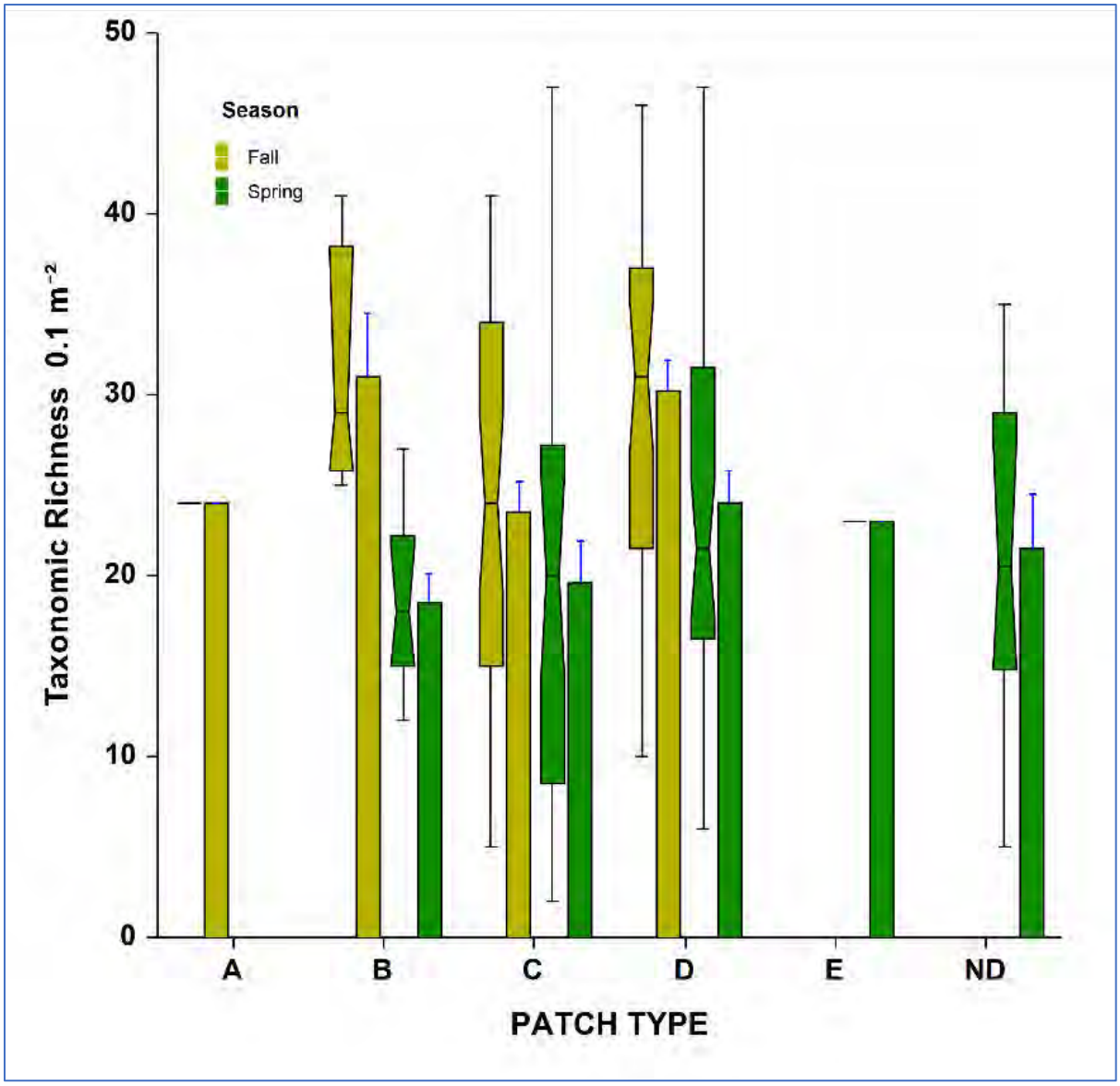

Figure 5.2- 6. Seasonal differences in taxonomic richness in the Patch Types in the LIS Phase II Study area. Plot explanation as in Figure 5.2-1.

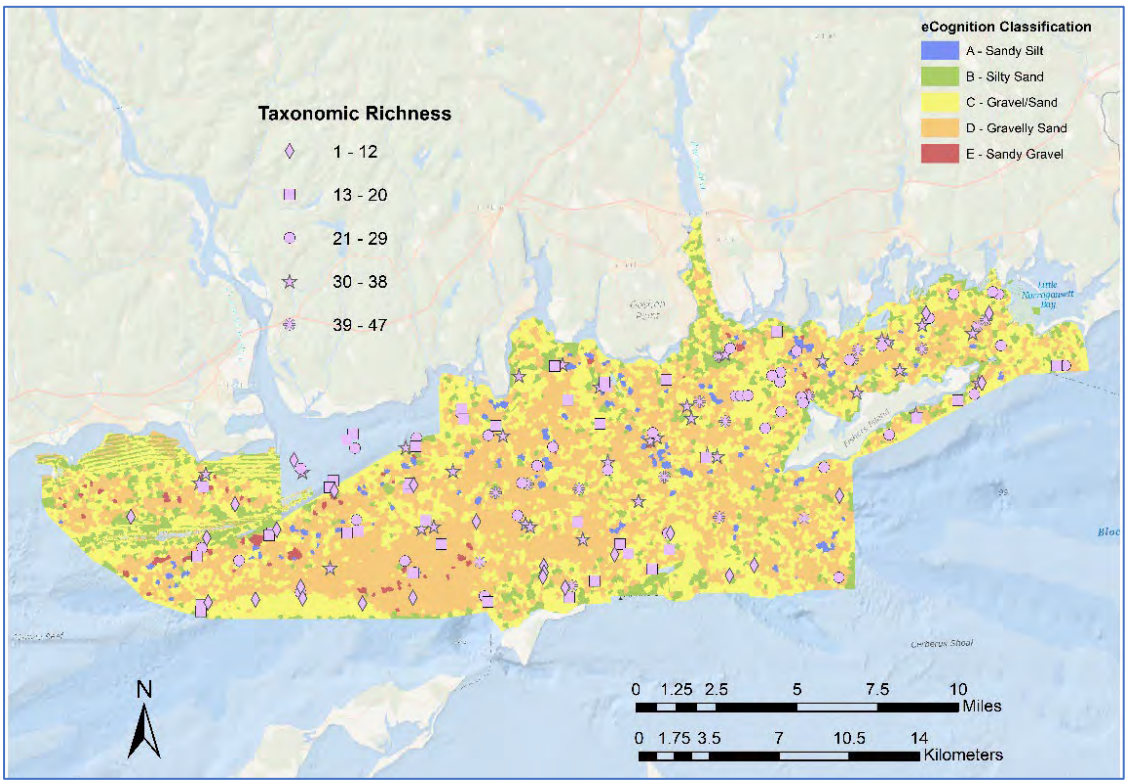

Figure 5.2- 7. Spatial distribution of taxonomic richness of infauna among the sample locations in the LIS Phase II study Area.

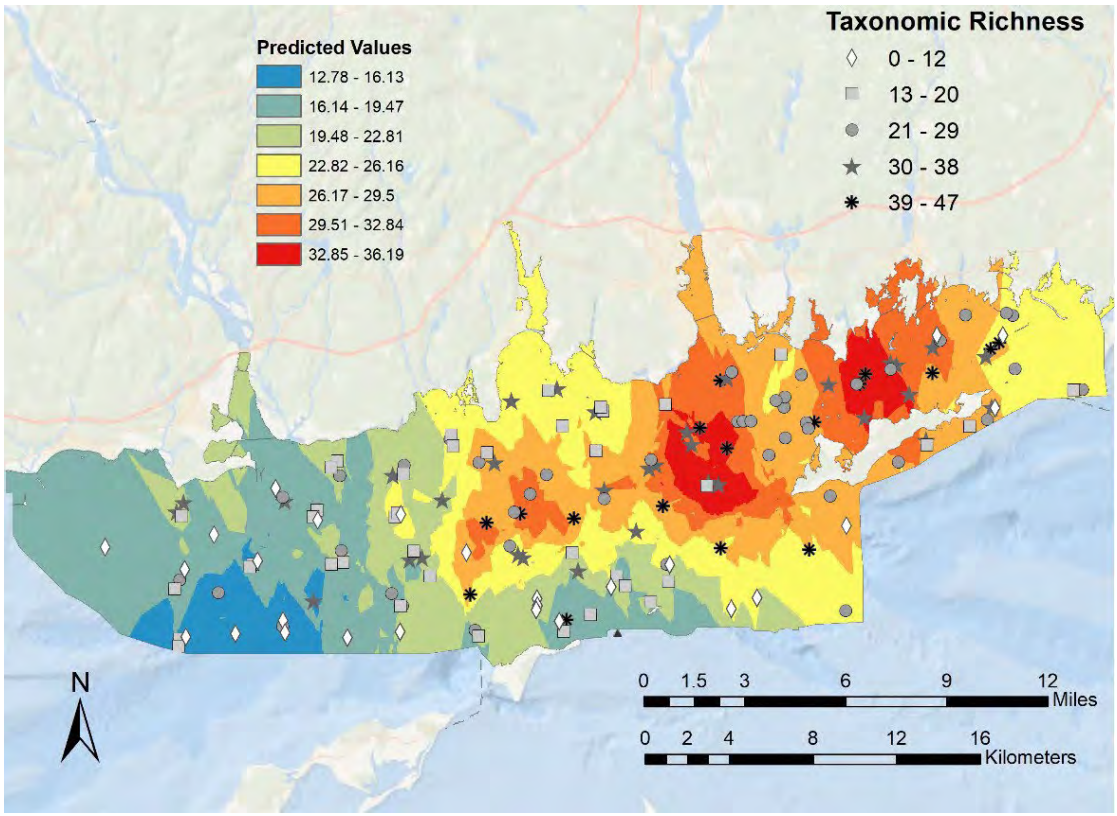

Figure 5.2- 8. Interpolation (using kriging) of taxonomic richness across the LIS Phase II Study Area.

Mean taxonomic diversity, which takes into account both the number of taxa and their proportional abundance and measured by Shannon diversity index H′, ranged from approximately 0.6 to 1.0; although, at some sites it was higher approaching approximately 1.4 (Figure 5.2-9). One-way ANOVA indicated there were no significant differences among patch types in mean Shannon diversity (Table 5.2-1). However, diversity increased in patch types with increasing proportions of coarser sediments (i.e., in the gradient from patch type A to patch type E). This trend has been previously reported when comparing benthic species richness across the whole of LIS (Zajac, 1998) and agrees with previous studies and hypotheses that indicate increasing diversity with increasing sediment grain-size/variability (e.g., Whitlatch, 1981; Etter and Grassle, 1992; Gray, 2002; Thrush et al., 2003). This trend was evident over the small and meso-scale spatial patterns of sediment variation within and among the large-scale acoustic patch types. There were no statistically significant differences among sampling periods (seasons) nor among the acoustic patch types in which seasonal samples were taken (Table 5.2-1). Diversity was somewhat higher in patch types C and D in the fall versus the spring but higher in the spring and patch type B (Figure 5.2-10). Shannon diversity exhibited a somewhat different spatial pattern than taxonomic richness with more spatially constrained areas of high and low diversity (Figure 5.2-11 and Figure 5.2-12). For example, there was relatively high diversity in the areas southeast of the mouth of the Connecticut River and also in the central portion of the Phase II area. There was a particularly large cluster of high diversity in samples taken south of the mouth of the Thames River and into FIS.

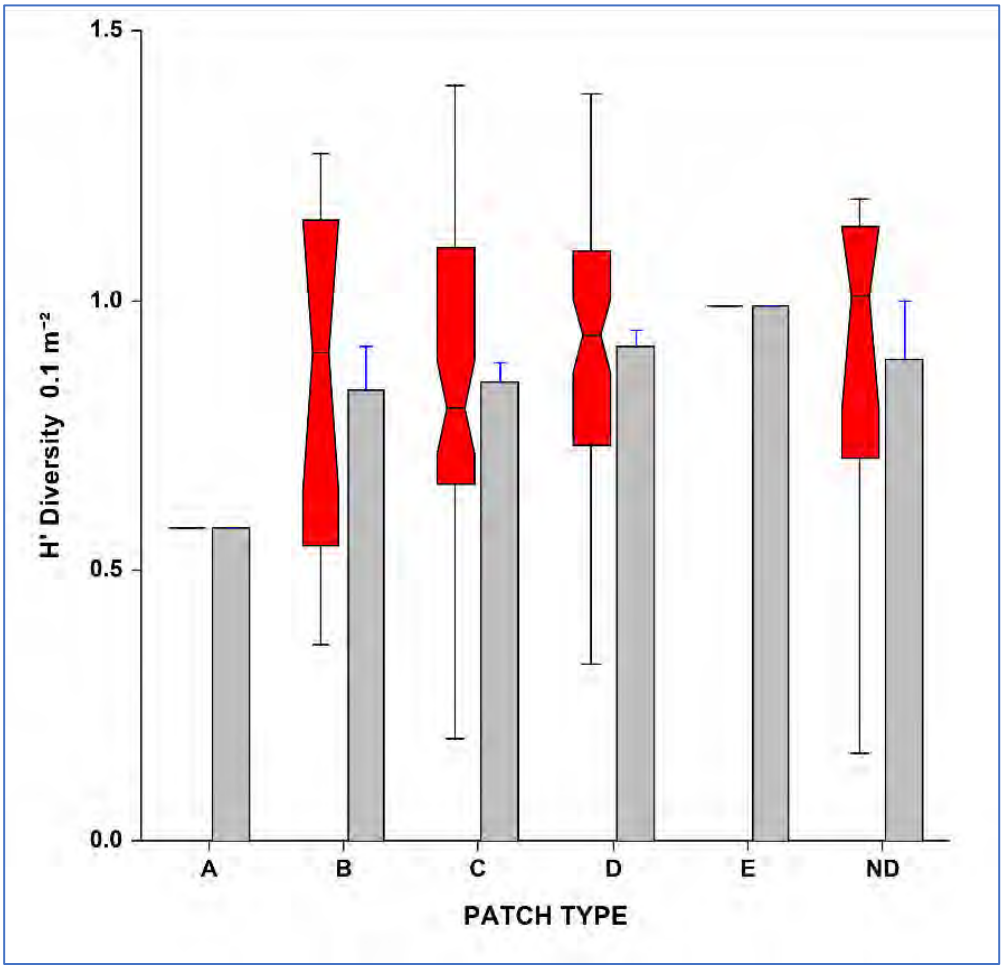

Figure 5.2- 9. Taxonomic diversity in the Patch Types in the LIS Phase II Study area. Plot explanation as in Figure 5.2-1.

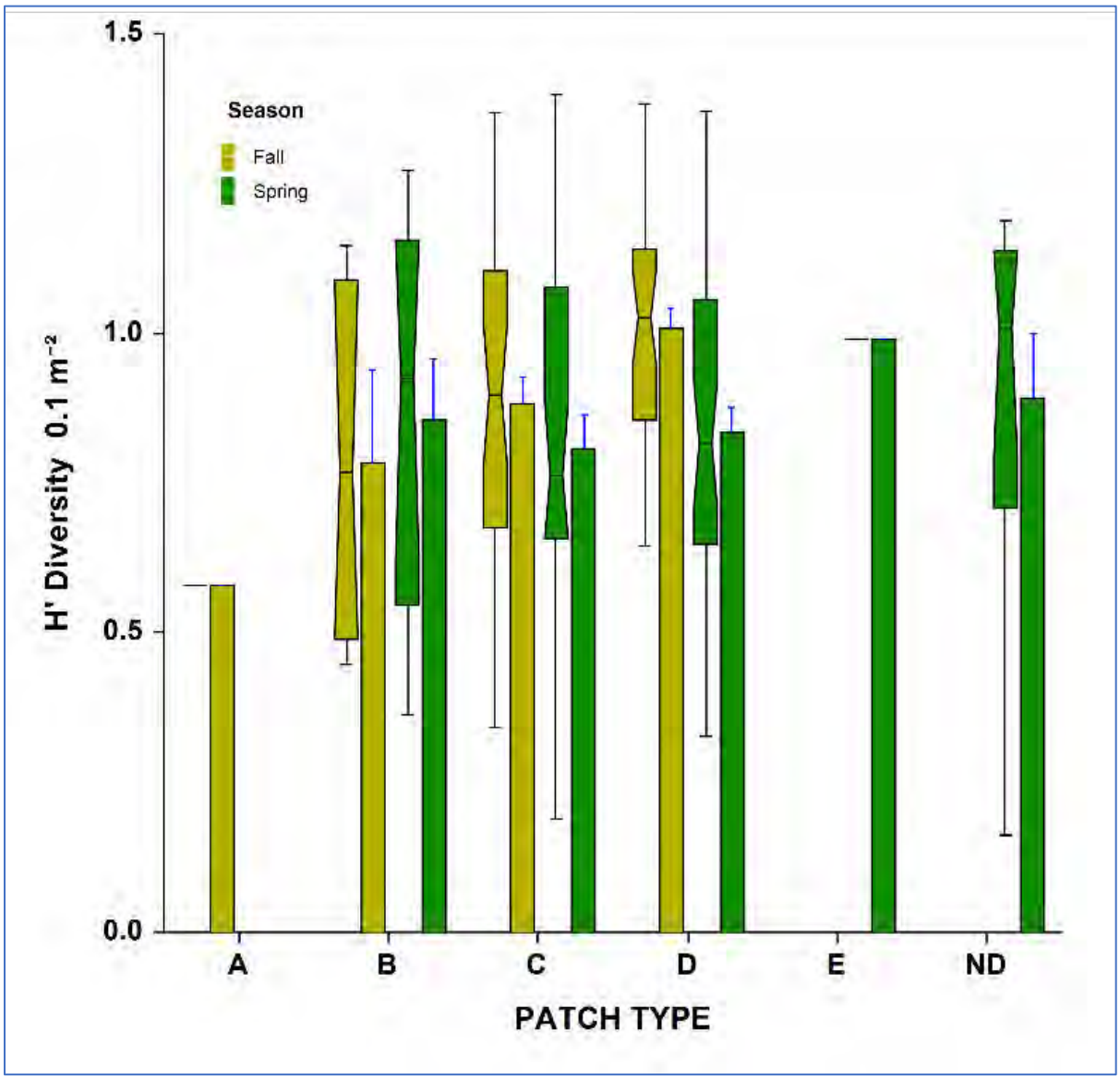

Figure 5.2- 10. Seasonal differences in taxonomic diversity in the Patch Types in the LIS Phase II Study area. Plot explanation as in Figure 5.2-1.

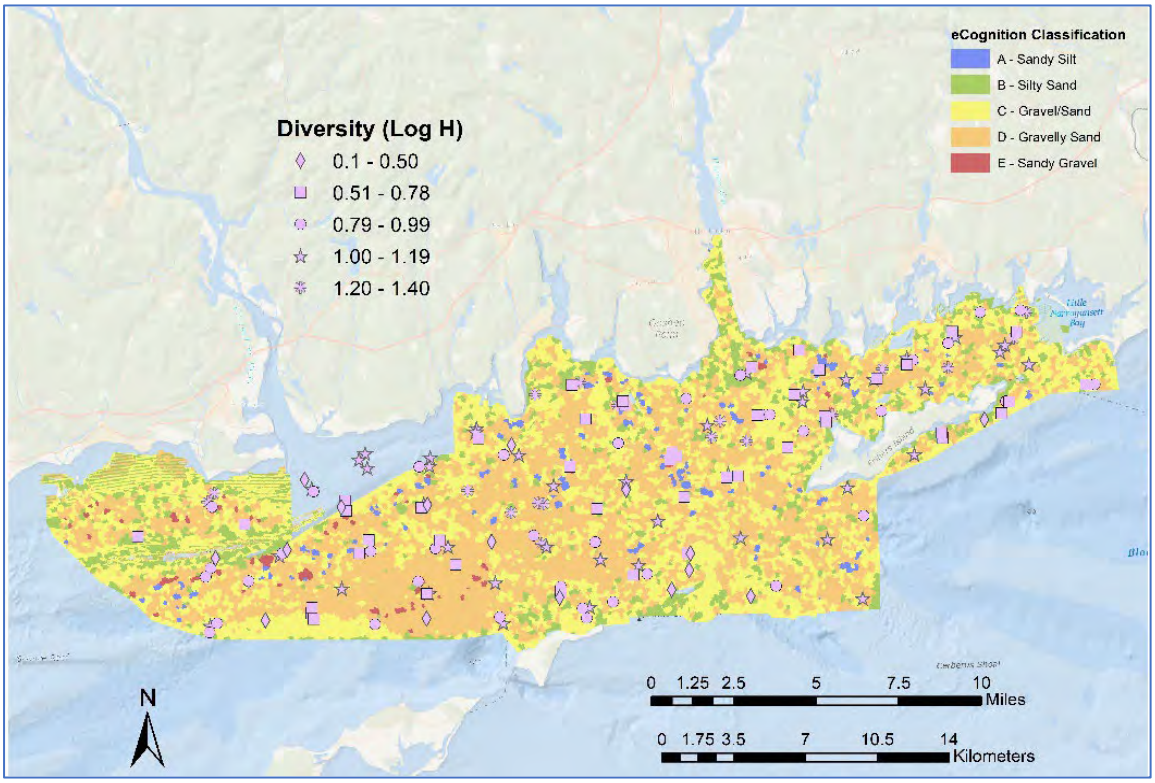

Figure 5.2- 11. Spatial distribution of taxonomic diversity of infauna among the sample locations in the LIS Phase II Study Area.

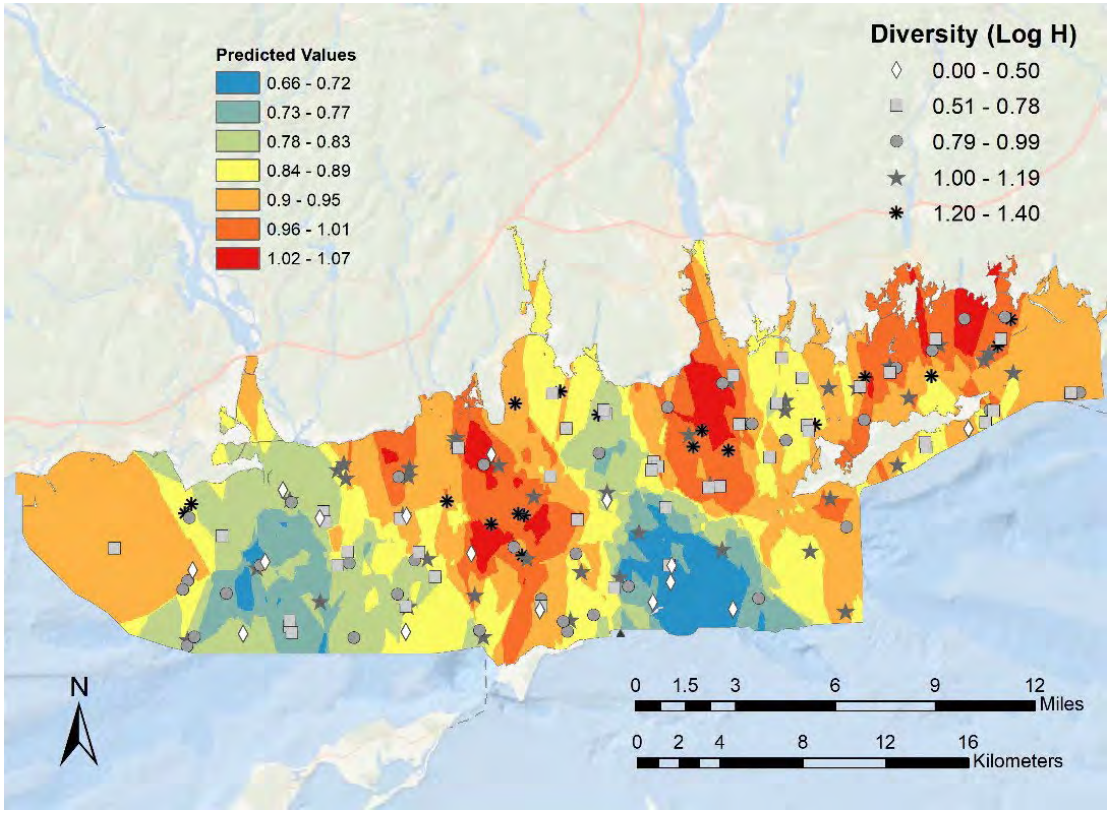

Figure 5.2- 12. Interpolation (using kriging) of taxonomic diversity across the LIS Phase II Study Area.

5.2.3.2 Patterns in infaunal community structure within acoustic patch types

Infaunal community structure is spatially heterogeneous in the Phase II Area. Although there were no sharply distinct community types associated with each of the acoustic patch types identified through the eCognition analysis, there were some notable differences among them (Figure 5.2-13). Community structure was variable within each of the patch types, but there were a set of samples in Patch Type D, which had very similar communities as indicated by their tight clustering in the center of the ordination space. ND samples (collected in shallower water areas along the CT coast where there was no backscatter data) also had relatively similar community structure. Communities in Patch Type C were highly variable, being spread across the entire ordination space; however, there appear to be two subcommunities in this patch type, given the separation of the two clouds of points at either side of the ordination space. Communities in Patch Type B were also variable but were not as varying as those in Patch Type C (Figure 5.2-13). A multivariate index of dispersion analysis indicated that samples in Patch Types D and ND had communities that were relatively more similar as compared to those in patch types B and C (Table 5.2-2). An analogous test of the homogeneity of multivariate dispersions indicated that there were significant differences in within-patch type community variation among patch types, with differences among specific pairs of patch types being mostly significant or marginally significant (Table 5.2-2). An ANOSIM test indicated that overall, there were significant differences in community structure among the different patch types, primarily among Patch Types B, D, C, and ND (Table 5.2-2). A PERMANOVA test to assess differences in community structure among patch types and seasons indicated that both factors had a significant effect on community structure, but that their interaction was not significant (Table 5.2-2). Both patch type and season accounted for about the same level of variation in the data set. These results suggest that community differences among patch types were relatively consistent among the two sampling periods. Pairwise comparisons based on the PERMANOVA test were consistent with the other multivariate analyses, indicating significant differences among patch types B and D, C and D, C and ND, and among D and ND.

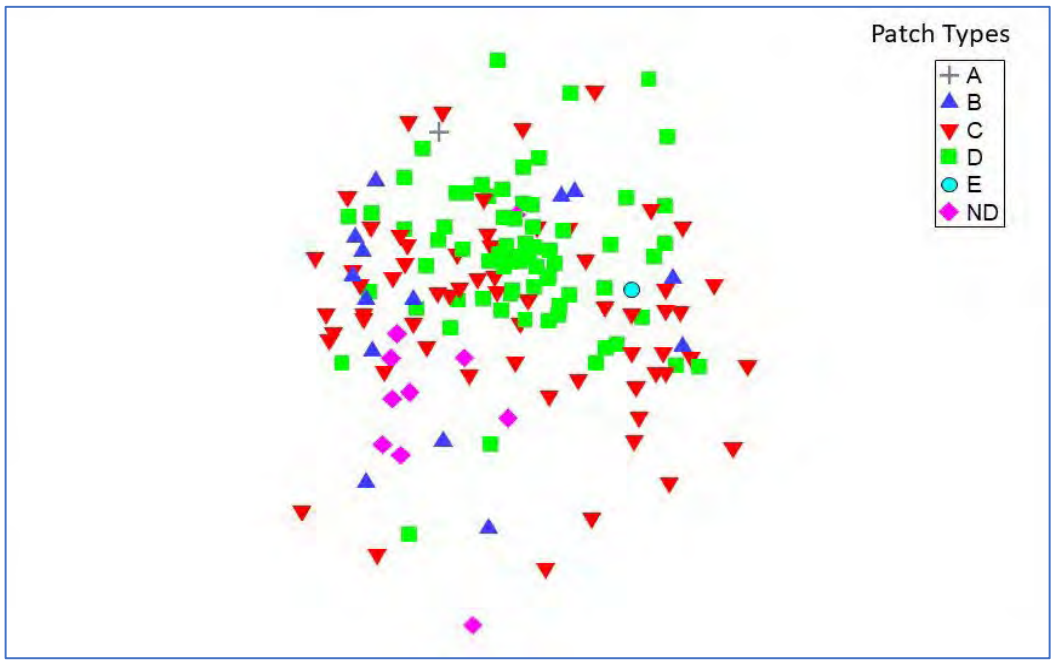

Figure 5.2- 13. nMDS ordination of sample site infaunal communities grouped by their location in the large-scale Patch Types identified in the LIS Phase II study area. (Stress = 0.24, 4th root transformed abundances, Hellinger Distance Similarity Function).

Table 5.2- 2. Results of multivariate statistical tests of patterns in community structure. See above section on Statistical Analyses for details.

Index of Multivariate Dispersion (IMD) for Patch Types

Global Analysis

Factor value	Dispersion
D	0.825
ND	0.887
C	1.214
B	1.261

Pairwise Comparisons

Factor values	IMD
B, C	0.06
B, D	0.427
B, ND	0.386
C, D	0.389
C, ND	0.348
D, ND	-0.079

Distance-based Test for Homogeneity of Multivariate Dispersions among Patch Types
Deviations from Centroid
F: 55.528 df1: 5 df2: 154
P(perm): 0.001

Pairwise Comparisons

Groups	t	P(perm)
(B,C)	1.0239	0.613
(B,D)	1.5249	0.338

(B,ND)	2.2048	0.069
(B,E)	12.366	0.067
(B,A)	12.366	0.056
(C,D)	4.2815	0.001
(C,ND)	3.5428	0.021
(C,E)	12.967	0.017
(C,A)	12.967	0.016
(D,ND)	0.89129	0.674
(D,E)	9.8446	0.018
(D,A)	9.8446	0.009
(ND,E)	11.739	0.098
(ND,A)	11.739	0.072
(E,A)	No test	

ANOSIM Test for Differences Among Patch Types

Global Test
Sample statistic (R): 0.139
Significance level of sample statistic: 0.001%

Pairwise Tests

Groups	R	Significance
B, C	0.034	0.314
B, D	0.33	0.001
B, ND	0.052	0.221
B, E	0.055	0.400
B, A	0.031	0.467
C, D	0.072	0.001
C, ND	0.145	0.052
C, E	-0.084	0.641
C, A	0.201	0.203
D, ND	0.41	0.001
D, E	0.078	0.361
D, A	0.334	0.181
ND, E	0.467	0.182
ND, A	0.527	0.182

PERMANOVA of Differences in Community Structure among Patch Types and Seasons

Source	DF	Sum of Squares	Mean Square	Pseudo-F	P-value
Patch	5	5.4063	1.0813	1.5679	0.001
Season	1	2.0354	2.0354	2.9514	0.001
P x S	2	1.4404	0.72022	1.0443	0.334
Res	151	104.14	0.68964		
Total	159	114.51			

Estimates of components of variation

Source	Estimate	Square root
Patch	0.020293	0.14245
Season	0.035206	0.18763
P x S	0.0014922	0.038629

V(Res)	0.68964	0.83044

PERMANOVA Pair-wise Tests for Patch Type

Groups	t	Significance Level
B, C	1.042	0.269
B, D	1.3341	0.004
B, ND	1.0688	0.212
B, E	1.0293	0.399
B, A	0.9824	0.512
C, D	1.4508	0.002
C, ND	1.4103	0.002
C, E	0.95219	0.686
C, A	1.0654	0.173
D, ND	1.7336	0.001
D, E	0.99741	0.456
D, A	1.114	0.148
ND, E	1.1017	0.195
ND, A	No test	df = 0
E, A	No test	df = 0

Several additional analyses were done to assess differences and relative variabilities of infaunal community structure among the patch types. A CAP was performed to ordinate the samples based on which specific patch type they were taken. The analysis indicates that while there is substantive overlap for some samples, most samples taken in patch types C, D, and ND had relatively more distinct infaunal communities than Patch Type B (Figure 5.2-14). An overlay of environmental factors associated with the samples indicates that increasing depth and coarser sediments grain sizes ($\Phi < 1$) correlated to the separation of patch type D samples from patch type C, which also was correlated with finer sediments. Infaunal communities at the ND sites were quite variable but distinct from the other patch types. They were correlated with somewhat higher latitudes (closer to the CT Shore) and a variable mix of sediment grain sizes. An analysis of rank correlations among communities in the patch types and environmental factors indicated the factors that were most highly correlated with trends community structure among the patch types included longitude, latitude, depth maximum bed stress, terrain roughness, and the $\Phi 1$ sediment grain-size fraction (Table 5.2-3).

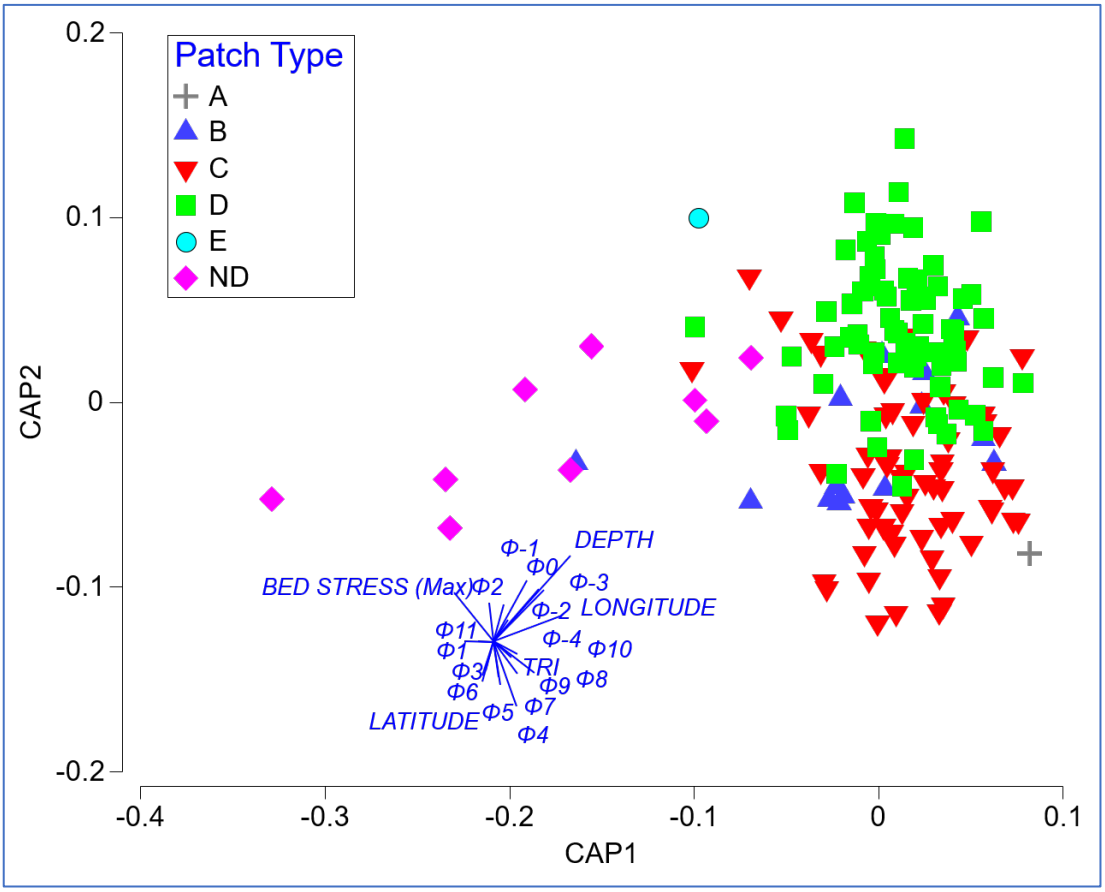

Figure 5.2- 14. CAP analysis to discriminate community structure among a priori groups, in this case Patch Types. Also shown are vectors of correlation to environmental factors and geographic location.

Table 5.2- 3. Results of BVStep stepwise analysis of rank correlations among infaunal communities in different patch types and measured environmental variables. The Best results indicate the environmental variables that resulted in the highest correlation with the infaunal data within the different patch types.

Parameters
Correlation method: Spearman rank
Method: BVSTEP

Global Test
Sample statistic (Average Rho): 0.39
Significance level of sample statistic: 0.1% ($p < 0.001$)

Best results

No.Vars	Correlation	Variables Selected
6	0.390	Longitude, Latitude, Depth, Max Bed Stress, TRI Roughness, Φ1*

* Φ1: 0.5 mm sediment grain size fraction

The relative distinctness of infaunal communities was also borne out in an analysis of mean dispersion among patch types by randomizing (bootstrapping) calculation of centroids in ordination space. As indicted by the results presented above, communities in patch types C and D were relatively more similar than in patch type B in the ND samples which exhibit a much broader 95% envelope (Figure 5.4-15). Also, communities in patch types B and C were more similar relative to that in other patch types.

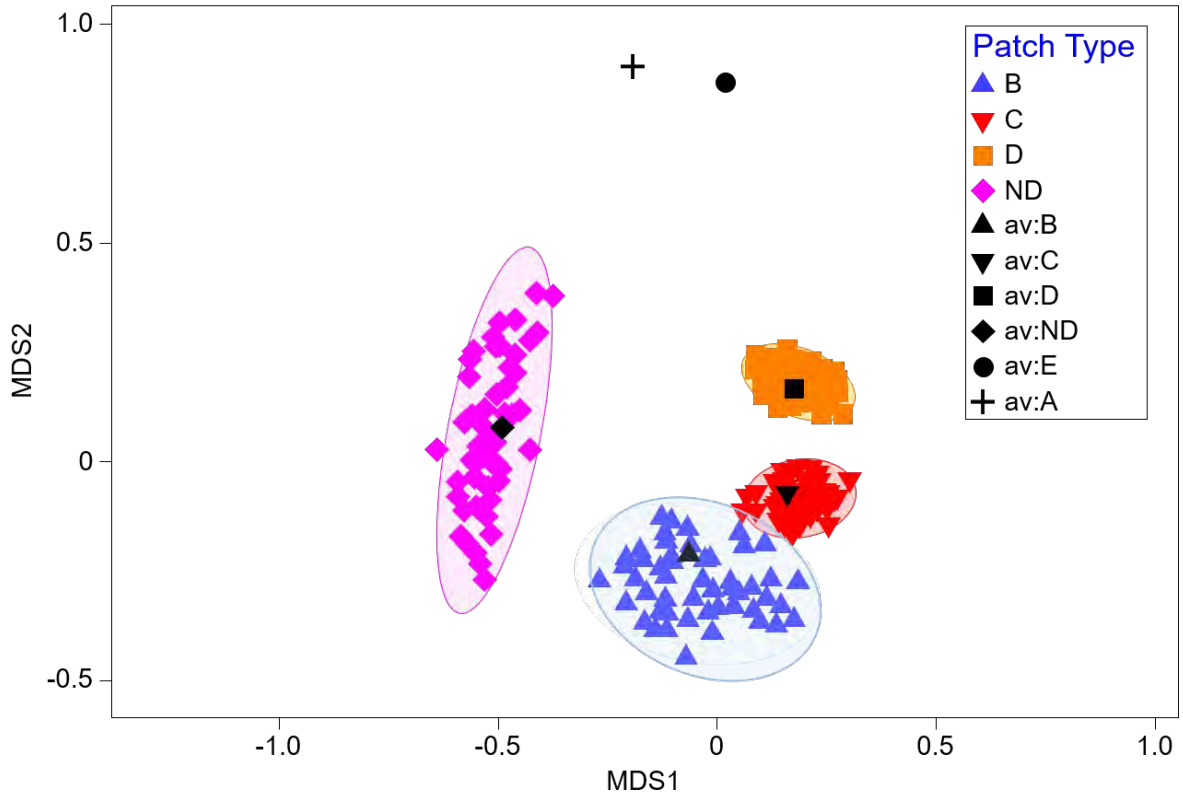

Figure 5.2- 15. Results of bootstrap averages analysis for community structure among patch types in the LIS Phase II study area. This analysis calculates and plots bootstrap averages and confidence regions by bootstrapping centroids of resemblance matrix groups (in this case Patch Types). Shown are the bootstrap centroids and mean (average) centroid and 95% envelopes. Patch Types A and E only had one sample.

The abundances and species composition of the communities that were found in samples among the different patch types was fairly variable (Table 5.2-4). Only one sample was taken in patch type A and it was dominated by a very high abundance of the slipper shell *Crepidula fornicata,* as well as the polychaete *Cirratulus cirratus*, oligochaetes, and corophiid amphipods. In Patch Type B, the dominants were several crustacean taxa including corophiid amphipods, *Ampelisca vadorum*, the hermit crab *Pagurus longicarpus*, and several polychaetes including *Neptys picta* and *Praxillella praetermissa.* Infaunal communities in Patch Type C were dominated by the small bivalve *Astarte* spp, and several polychaete species including *Glycera capitata*, *Spiophanes bombyx* and *Mediomastus ambiseta*. *Pagurus longicarpus* and *Ampelisca vadorum* were also found in relatively high abundances in Patch Type C. The dominant taxa in Patch Type D were *Astarte* spp., corophiid amphipods, *Glycera capitata*, *Spiophanes bombyx* and *Mediomastus ambiseta*, similar to Patch Type C. Only one sample was taken in Patch Type E, and it was dominated by *Astarte* spp., the mussel *Mytilus edulis*, the sand dollar *Echinarachnius parma*, as well as *Crepidula fornicate* and the polychaete *Tharyx acutus.* The ND samples were dominated by several polychaete taxa including *Marenzallaria viridis, Mediomastus ambiseta, Spiophanes bombyx,* and *Nephtys picta* as well as corophiid amphipods. There were also notable differences in the taxonomic composition of less abundant species among the different patch types (Table 5.2-4).

Table 5.2- 4 Results of SIMPER analysis of species contributions to the similarity of community structure within acoustic patch types.

Patch Type A

No analysis - Less than 2 samples in group; given are top 10 species based on abundance in the one sample taken in patch type A

Crepidula fornicata	440
Cirratulus cirratus	92
Oligochaeta	72
Corophium spp.	18
Harmothoe imbricata	9
Anadara transversa	7
Dyspanopeus sayi	7
Idunella clymenellae	6
Crepidula plana	5
Glycera dibranchiata	5

Patch Type B

Average similarity: 20.48

Species	**Av.Abund**	**Av.Sim**	**Sim/SD**	**Contrib%**	**Cum.%**
Corophium spp.	0.90	1.74	0.93	8.50	8.50
Mediomastus ambiseta	0.93	1.70	0.77	8.28	16.78
Ampelisca vadorum	1.43	1.50	0.52	7.31	24.09
Pagurus longicarpus	0.73	1.05	0.51	5.14	29.23
Nephtys picta	0.61	0.90	0.42	4.41	33.64
Praxillella praetermissa	0.78	0.84	0.53	4.09	37.72
Spiophanes bombyx	0.69	0.82	0.53	3.98	41.71
Paraonis fulgens	0.63	0.78	0.42	3.83	45.54
Spiochaetopterus costarum oculatus	0.68	0.78	0.54	3.82	49.36
Arabella iricolor	0.66	0.72	0.53	3.52	52.88
Glycera capitata	0.56	0.57	0.40	2.76	55.65
Ilyanassa trivittata	0.45	0.55	0.35	2.69	58.33
Scalibregma inflatum	0.48	0.54	0.44	2.63	60.97
Cirratulus cirratus	0.36	0.54	0.35	2.62	63.59
Tanaid spp.	0.38	0.44	0.34	2.16	65.75
Astarte spp.	0.79	0.42	0.24	2.07	67.82
Nicomache lumbricalis	0.53	0.42	0.34	2.05	69.87
Magelona papilliformis	0.63	0.41	0.21	2.00	71.87

Patch Type C

Average similarity: 20.38

Species	**Av.Abund**	**Av.Sim**	**Sim/SD**	**Contrib%**	**Cum.%**
Astarte spp.	1.36	2.56	0.73	12.54	12.54
Glycera capitata	0.79	1.69	0.58	8.30	20.84
Spiophanes bombyx	0.86	1.23	0.68	6.05	26.89
Pagurus longicarpus	0.73	1.13	0.65	5.53	32.42
Mediomastus ambiseta	0.69	0.96	0.53	4.70	37.12
Ampelisca vadorum	0.96	0.93	0.42	4.56	41.69
Corophium spp.	0.77	0.89	0.56	4.36	46.05

Paraonis fulgens	0.54	0.79	0.35	3.85	49.90
Praxillella praetermissa	0.64	0.77	0.50	3.76	53.67
Echinarachnius parma	0.46	0.64	0.29	3.13	56.80
Spiochaetopterus costarum oculatus	0.49	0.47	0.41	2.30	59.10
Nicomache lumbricalis	0.49	0.46	0.39	2.26	61.36
Scalibregma inflatum	0.44	0.44	0.39	2.16	63.52
Syllidae	0.43	0.41	0.36	2.03	65.55
Cirratulus cirratus	0.43	0.40	0.33	1.97	67.52
Tharyx acutus	0.48	0.37	0.36	1.83	69.35
Spisula solidissima	0.39	0.35	0.32	1.71	71.06

Patch Type D
Average similarity: 28.27

Species	**Av.Abund**	**Av.Sim**	**Sim/SD**	**Contrib%**	**Cum.%**
Astarte spp.	2.34	4.69	1.41	16.61	16.61
Corophium spp.	1.29	2.04	1.06	7.23	23.83
Glycera capitata	1.05	1.89	0.94	6.69	30.52
Spiophanes bombyx	0.90	1.29	0.77	4.56	35.08
Mediomastus ambiseta	0.91	1.26	0.73	4.46	39.55
Paraonis fulgens	0.77	0.94	0.62	3.32	42.87
Pagurus longicarpus	0.72	0.92	0.63	3.24	46.11
Praxillella praetermissa	0.75	0.83	0.60	2.94	49.05
Nicomache lumbricalis	0.72	0.81	0.60	2.88	51.93
Ampelisca vadorum	0.89	0.73	0.45	2.59	54.53
Crepidula fornicata	0.86	0.73	0.44	2.59	57.12
Astyris lunata	0.70	0.71	0.52	2.50	59.62
Cirratulus cirratus	0.60	0.65	0.49	2.31	61.93
Anadara transversa	0.71	0.63	0.48	2.22	64.15
Syllidae	0.62	0.61	0.51	2.17	66.32
Scalibregma inflatum	0.56	0.60	0.50	2.12	68.44
Crenella	0.49	0.49	0.42	1.75	70.19

Patch Type E: No analysis - Less than 2 samples in group; given are top 10 species based on abundance in the one sample taken in patch type E

Astarte spp.	32
Mytilus edulis	16
Echinarachnius parma	8
Crepidula fornicata	4
Tharyx acutus	4
Glycera capitata	4
Unciola spp.	3
Mediomastus ambiseta	2
Harmothoe imbricata	1
Crepidula plana	1

ND (Patch type not determined)
Average similarity: 25.96

Species	**Av.Abund**	**Av.Sim**	**Sim/SD**	**Contrib%**	**Cum.%**
Marenzallaria viridis	1.96	4.82	1.29	18.56	18.56

Mediomastus ambiseta	1.11	2.35	1.16	9.06	27.62
Corophium spp.	1.09	1.84	0.89	7.07	34.69
Spiophanes bombyx	1.03	1.80	0.87	6.93	41.62
Nephtys picta	0.93	1.76	0.89	6.79	48.41
Pagurus longicarpus	0.94	1.15	0.68	4.43	52.84
Praxillella praetermissa	0.73	0.92	0.52	3.53	56.37
Lepidonotus squamatus	0.58	0.76	0.52	2.94	59.30
Ilyanassa trivittata	0.57	0.69	0.51	2.67	61.97
Paraonis fulgens	0.57	0.66	0.51	2.55	64.53
Ampharete arctica	0.52	0.66	0.51	2.54	67.06
Tellina agilis	0.53	0.59	0.37	2.29	69.35
Protohaustorius wigleyi	0.75	0.57	0.25	2.20	71.55

5.2.3.3 Patterns in community structure across acoustic patch types

Although infaunal communities differed among the large-scale patch types, there was a high degree of variability within patch types and, concurrently, similarity among some samples taken in different patch types (e.g., Figure 5.2-13). Classification (cluster) analysis coupled with a SIMPROF test was used to assess patterns in infaunal community structure across all samples, and identify groupings of samples with similar community structure irrespective of patch type, in order to better understand the distribution and composition of infaunal communities across the Phase II study area (Figure 5.2-16). This resulted in the identification of 13 community types, some of which were relatively distinct from the others, and others that were more similar. Applying the community groupings to the nMDS ordination of the samples reveals that there were six relatively distinct communities (types b, c, d, g, l, and m), whereas the others (a, e, f, h, i, j, and k) exhibited a high degree of overlap (Figure 5.2-17). When three ordination axes are considered, there is greater separation among types j and k. A CAP ordination supports the results from the nMDS analysis, indicating that when the ordination is constrained by community type there are distinct differences in community structure among the types (Figure 5.2-18). Community types c, d, l and m, were most separated from the other types, but exhibited relatively more within community type variation. This assessment is also supported by a bootstrap averages analysis in which the 95% envelopes for the group centroid calculations are broader for these community types (Figure 5.2-19). It is interesting to note that for community type b the 95% envelope was quite large, indicating much more variable community structure within that community type.

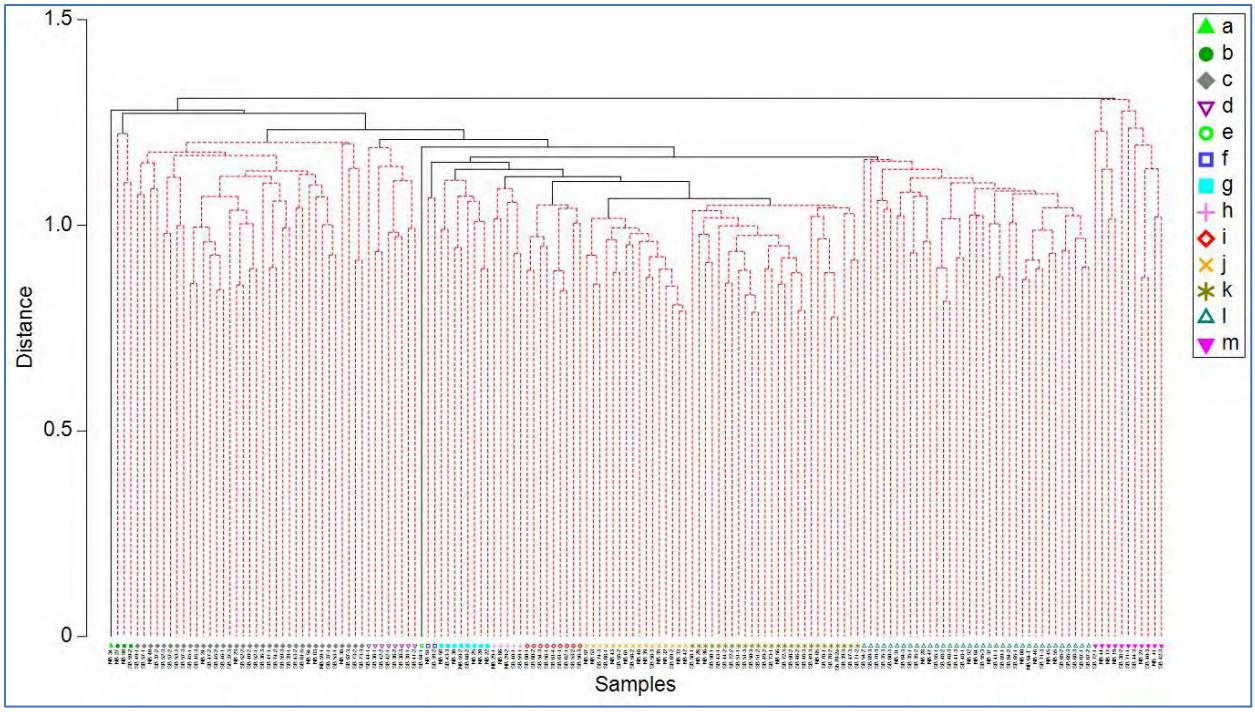

Figure 5.2- 16. Classification dendrogram of infaunal samples in the Phase II study area. Data were 4th root transformed and similarity calculated using Hellinger distance resemblance function. A SIMPROF test was run to identify groups that are significantly different at $p < 0.005$.

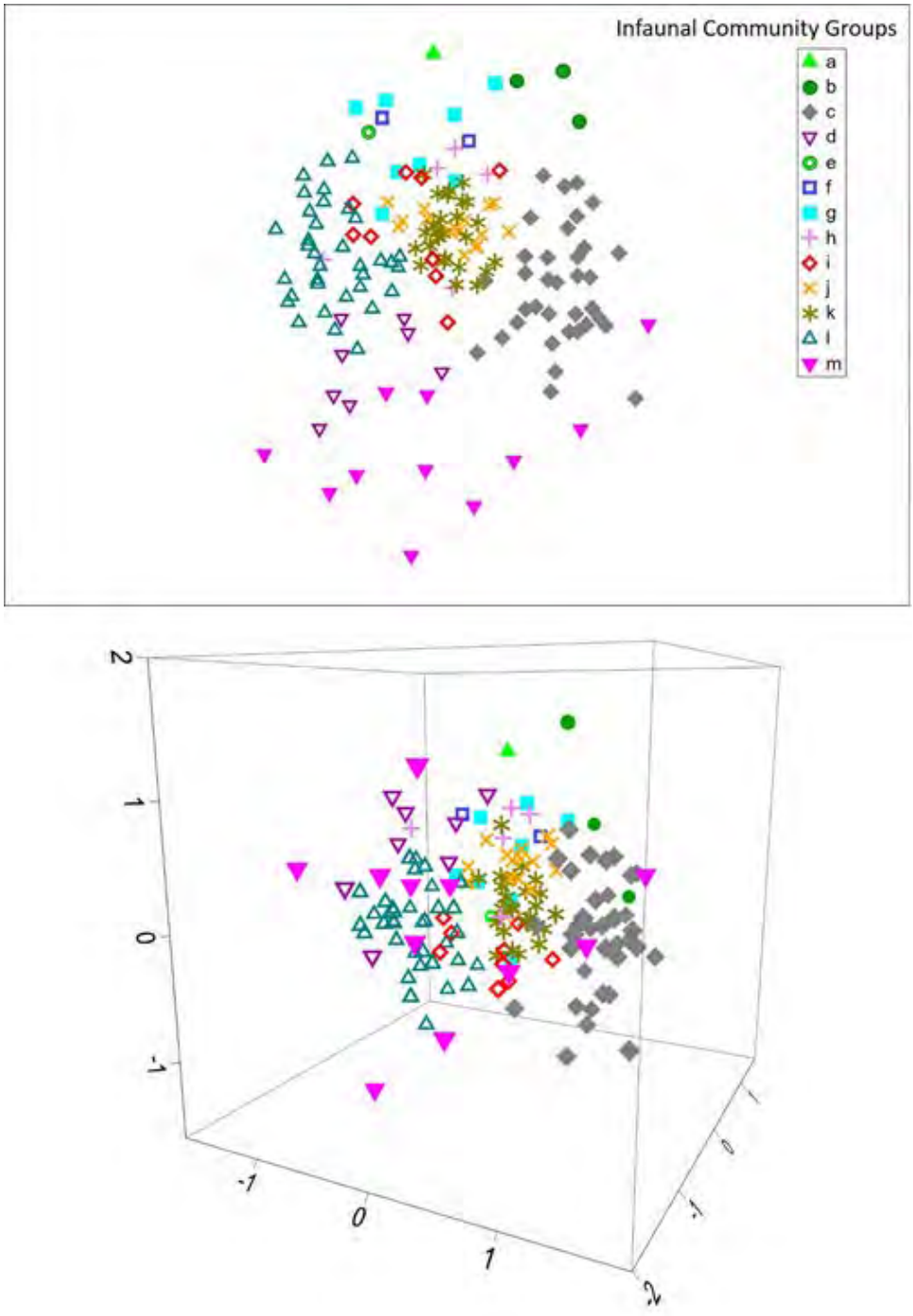

Figure 5.2- 17. TOP: nMDS ordination of sample site infaunal communities grouped by community types as determined by classification and SIMPROF (see Figure 5.2 17) test in the LIS Phase II study area. Stress = 0.24, 4th root transformed abundances, Hellinger Distance Similarity Function. BOTTOM: Same nMDS ordination but showing group separation along 3 axes. Stress = 0.19.

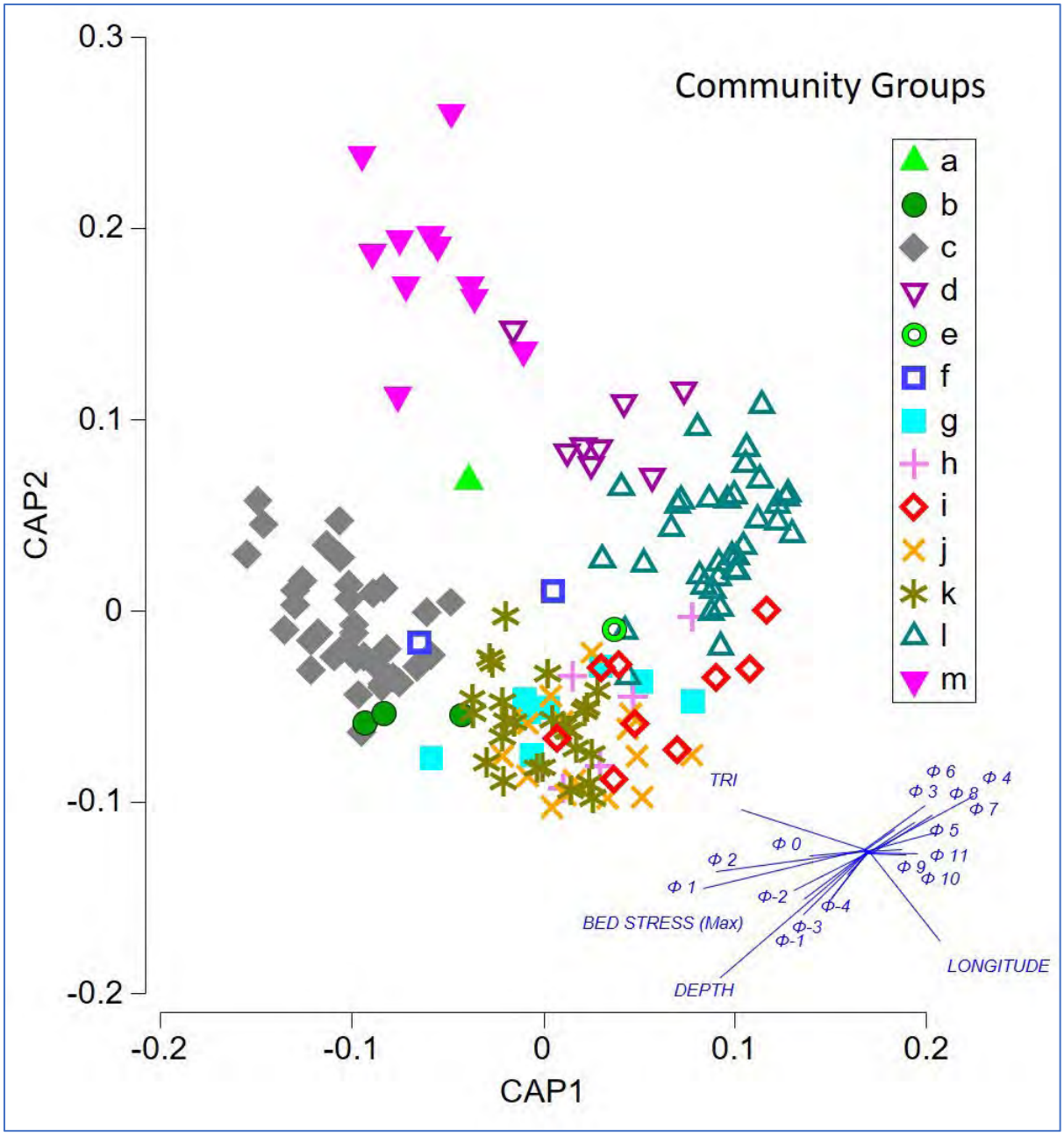

Figure 5.2- 18. CAP analysis to discriminate community structure among a priori groups, in this case Community Types identified by a SIMPROF analysis (see Figure 5.2 17). Also shown are vectors of correlation to environmental factors and geographic location.

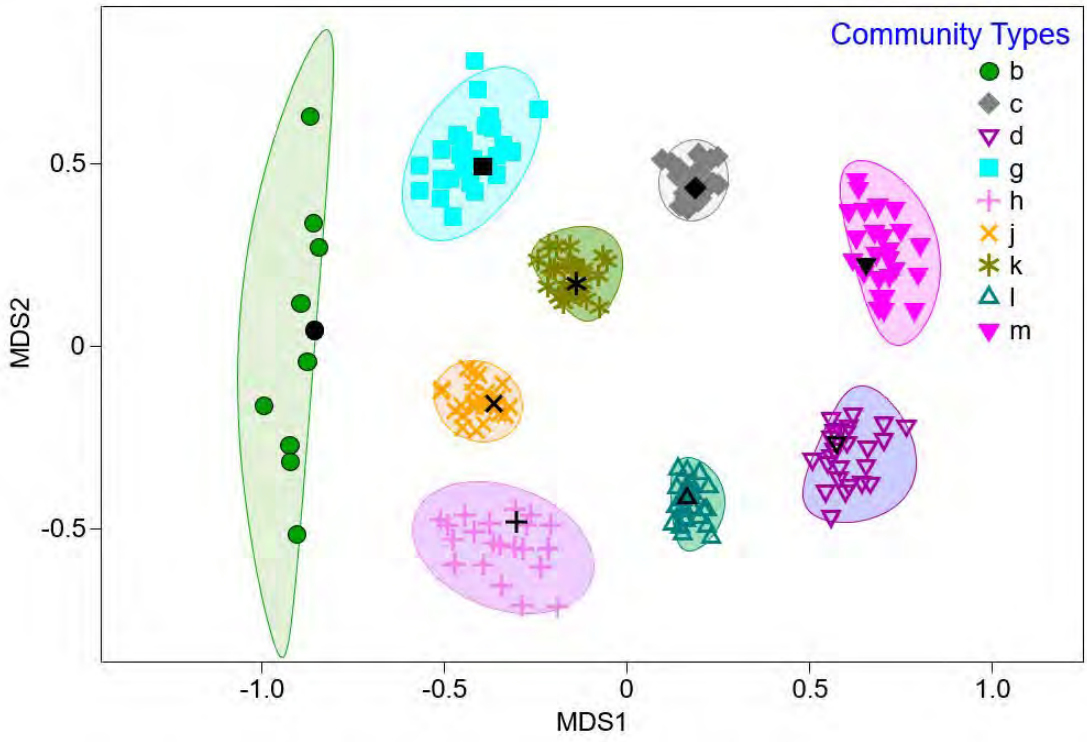

Figure 5.2- 19. Results of bootstrap averages analysis of centroid location within community types in the LIS Phase II study area. This analysis calculates and plots bootstrap averages and confidence regions by bootstrapping centroids of resemblance matrix groups (in this case Community Types). Shown are the bootstrap centroids and mean (average) centroid (black symbol) and 95% envelopes. Community types with less than 4 samples were excluded from the analysis.

Both ANOSIM and PERMANOVA analyses indicated that there were significant differences among community types (Table 5.2-5) and that most pairwise comparisons of the community types were significantly different. SIMPER analysis indicted that some community types were dominated by just a few taxa, whereas others were relatively more diverse in terms of how many taxa contributed to similarity within the community (Table 5.2-6). Community Type b was dominated by just two taxa (the bivalves *Astarte* spp. and *Anadara transversa*), and type c by five taxa (notably also *Astarte* spp., but also several polychaete species and the sand dollar *Echinarachnius parma*). Community type d was dominated by polychaete taxa but also the crustacea *Corophium* spp. *Protohaustorius wigleyi* and *Chiridotea tuftsii*. Community types f and g were dominated by the slipper shell *Crepidula fornicata*; type f also had nigh abundances of *Corophium* spp. and the polychaete *Cirratulis cirratus*; type h also had relatively high abundances of *Corophium* spp but otherwise was dominated by bivalve and crustacean taxa (Table 5.2-5). Community type i had 20 taxa contributing to within-type similarity, with a diverse mix of crustacea, polychaetes and bivalves but also ophiuroids. Community type j also had a relatively large number of taxa contributing to within -type similarity in this community, dominated by *Astarte* spp. and the polychaetes *Ampharete arctica* and *Harmothoe imbricata*. Community type k was similar to type j but had a different mix of polychaete taxa at higher abundances than found in community type j. Community type l was dominated by the amphipod *Ampelisca vadorum* and the maldanid polychaete *Praxillella praetermissa*; there are also relatively high abundances of the hermit crab *Pagurus longicarpus*. Community type m also did not have many taxa contributing to overall community similarity, and was dominated by the Haustoriid amphipod *Phoxocephalus holbolli*, and the polychaete *Nephtys picta*.

Table 5.2- 5. Results of multivariate statistical tests of differences among community types in the Phase II study area.

ANOSIM Test Global Test
Sample statistic (R): 0.576
Significance level of sample statistic: 0.1% (p<0.001)

Pairwise tests –community types pairs that are not significantly different (p < 0.05); are shaded in red; x – not test was performed.

	a	b	c	d	e	f	g	h	i	j	k	l	m
a													
b	0.25												
c	0.028	0.002											
d	0.111	0.006	0.001										
e	x	0.25	0.028	0.111									
f	0.333	0.1	0.002	0.022	0.333								
g	0.111	0.006	0.001	0.001	0.111	0.022							
h	0.167	0.018	0.001	0.001	0.167	0.048	0.002						
i	0.1	0.005	0.001	0.001	0.1	0.018	0.001	0.002					
j	0.059	0.001	0.001	0.001	0.059	0.007	0.001	0.001	0.001				
k	0.037	0.004	0.001	0.001	0.037	0.003	0.001	0.001	0.001	0.001			
l	0.028	0.001	0.001	0.001	0.028	0.002	0.001	0.001	0.001	0.001	0.001		
m	0.083	0.003	0.001	0.005	0.083	0.013	0.001	0.001	0.001	0.001	0.001	0.001	

PERMANOVA results of differences in Community Types

Source	df	SS	MS	Pseudo-F	P(perm)
Co	12	26.645	2.2204	3.7149	0.001
Res	147	87.863	0.5977		
Total	159	114.51			

Estimates of components of variation

Source	Estimate	Square root
S(Co)	0.1426	0.37763
V(Res)	0.5977	0.77311

Table 5.2- 6. SIMPER results for community types found in the Phase II study area.

Group a
Less than 2 samples in group

Group b
Average similarity: 21.93

Species	**Av.Abund**	**Av.Sim**	**Sim/SD**	**Contrib%**	**Cum.%**
Astarte spp.	1.64	12.02	3.91	54.82	54.82
Anadara transversa	0.86	3.46	0.58	15.76	70.58

Group c
Average similarity: 28.21

Species	**Av.Abund**	**Av.Sim**	**Sim/SD**	**Contrib%**	**Cum.%**

Astarte spp.	2.35	9.62	3.18	34.11	34.11
Glycera capitata	1.18	4.76	1.32	16.86	50.98
Echinarachnius parma	0.84	2.22	0.57	7.88	58.85
Paraonis fulgens	0.75	1.79	0.60	6.35	65.20
Astarte castaneum	0.70	1.56	0.56	5.51	70.72

Group d
Average similarity: 30.81

Species	**Av.Abund**	**Av.Sim**	**Sim/SD**	**Contrib%**	**Cum.%**
Marenzallaria viridis	2.16	6.32	2.82	20.51	20.51
Nephtys picta	1.04	2.81	1.55	9.13	29.64
Corophium spp.	1.32	2.33	1.01	7.56	37.20
Spiophanes bombyx	1.06	2.22	1.01	7.20	44.40
Mediomastus ambiseta	1.07	2.02	1.00	6.57	50.97
Protohaustorius wigleyi	0.99	1.30	0.34	4.23	55.20
Praxillella praetermissa	0.85	1.22	0.71	3.97	59.17
Sabellaria vulgaris	1.17	1.14	0.46	3.71	62.88
Magelona papilliformis	0.85	0.94	0.50	3.04	65.91
Tellina agilis	0.60	0.91	0.50	2.95	68.86
Chiridotea tuftsii	0.58	0.83	0.50	2.70	71.57

Group e
Less than 2 samples in group

Group f
Average similarity: 33.20

Species	**Av.Abund**	**Av.Sim**	**Sim/SD**	**Contrib%**	**Cum.%**
Corophium spp.	2.26	6.18	SD=0!	18.62	18.62
Crepidula fornicata	3.10	4.88	SD=0!	14.70	33.32
Nicomache lumbricalis	1.56	3.57	SD=0!	10.75	44.06
Praxillella praetermissa	1.54	3.57	SD=0!	10.75	54.81
Ceriantheopsis americanus	1.09	3.00	SD=0!	9.04	63.85
Cirratulus cirratus	2.05	3.00	SD=0!	9.04	72.89

Group g
Average similarity: 35.68

Species	**Av.Abund**	**Av.Sim**	**Sim/SD**	**Contrib%**	**Cum.%**
Crepidula fornicata	3.10	6.01	2.38	16.85	16.85
Astyris lunata	1.60	3.67	4.30	10.30	27.15
Crepidula plana	1.61	2.90	1.51	8.13	35.28
Corophium spp.	1.54	2.52	1.47	7.06	42.33
Anadara transversa	1.52	2.51	1.56	7.04	49.37
Astarte spp.	1.59	2.50	0.89	7.01	56.38
Pyramidellidae Family	1.48	2.38	1.04	6.66	63.04
Lepidonotus squamatus	1.05	1.50	1.01	4.20	67.24
Pagurus longicarpus	0.99	1.40	1.02	3.92	71.16

Group h
Average similarity: 38.90

Species	Av.Abund	Av.Sim	Sim/SD	Contrib%	Cum.%
Astarte spp.	1.71	5.22	6.68	13.41	13.41
Corophium spp.	1.49	4.61	5.03	11.85	25.26
Mytilus edulis	1.32	3.90	5.74	10.02	35.27
Praxillella praetermissa	1.21	3.73	13.32	9.59	44.86
Spiophanes bombyx	1.00	2.37	1.13	6.10	50.97
Ampharete arctica	1.10	2.17	1.15	5.57	56.54
Pagurus longicarpus	0.80	2.09	1.15	5.38	61.92
Lepidonotus squamatus	0.85	1.49	0.62	3.82	65.74
Nicomache lumbricalis	0.74	1.37	0.62	3.52	69.26
Glycera capitata	0.86	1.23	0.60	3.16	72.42

Group i

Average similarity: 41.52

Species	Av.Abund	Av.Sim	Sim/SD	Contrib%	Cum.%
Corophium spp.	1.70	2.95	7.21	7.10	7.10
Astarte spp.	2.46	2.92	0.98	7.04	14.14
Mediomastus ambiseta	1.79	2.60	1.64	6.25	20.40
Pagurus longicarpus	1.28	1.79	1.69	4.31	24.71
Arabella iricolor	1.15	1.77	1.66	4.27	28.99
Tharyx acutus	1.20	1.73	1.61	4.16	33.15
Lyonsia hyalina	1.10	1.66	1.64	4.00	37.15
Nucula spp.	1.18	1.36	1.07	3.28	40.43
Scalibregma inflatum	1.15	1.33	1.13	3.21	43.64
Anadara transversa	0.85	1.17	1.15	2.81	46.45
Asychis elongatus	1.07	1.15	0.77	2.76	49.21
Spiochaetopterus costarum oculatus	0.89	1.14	1.15	2.74	51.95
Nephtys picta	0.85	1.10	1.16	2.65	54.60
Astarte undata	1.07	1.10	0.81	2.64	57.24
Amphipholis squamata	0.87	1.06	0.83	2.54	59.78
Nicomache lumbricalis	1.01	0.99	0.81	2.38	62.17
Spiophanes bombyx	1.00	0.97	0.80	2.34	64.51
Syllidae	0.84	0.96	0.82	2.30	66.81
Amphipholis abditis	0.85	0.91	0.80	2.19	69.00
Paraprionospio tenuis	0.92	0.79	0.57	1.91	70.91

Group j

Average similarity: 44.84

Species	Av.Abund	Av.Sim	Sim/SD	Contrib%	Cum.%
Astarte spp.	3.00	4.98	3.47	11.10	11.10
Ampharete arctica	1.78	2.78	2.28	6.21	17.31
Harmothoe imbricata	1.34	2.29	2.25	5.11	22.43
Corophium spp.	1.53	2.10	1.59	4.67	27.10
Glycera capitata	1.29	2.03	1.47	4.54	31.64
Spiophanes bombyx	1.18	1.76	1.27	3.93	35.56
Pagurus longicarpus	1.08	1.60	1.06	3.57	39.14
Anadara transversa	1.04	1.55	1.31	3.46	42.60
Nicomache lumbricalis	1.10	1.55	1.28	3.46	46.06
Mediomastus ambiseta	1.02	1.46	1.30	3.25	49.30

Cirratulus cirratus	1.08	1.36	1.03	3.04	52.35
Marenzallaria viridis	0.96	1.27	1.03	2.83	55.17
Marphysa sanguinea	0.78	1.04	0.89	2.32	57.49
Praxillella praetermissa	0.82	1.01	0.89	2.24	59.73
Paraonis fulgens	0.90	0.98	0.74	2.19	61.92
Glycera dibranchiata	0.70	0.97	0.88	2.16	64.08
Mytilus edulis	0.86	0.96	0.69	2.15	66.23
Mulinia lateralis	0.86	0.94	0.74	2.09	68.32
Astarte undata	0.75	0.89	0.75	1.99	70.31

Group k

Average similarity: 41.31

Species	**Av.Abund**	**Av.Sim**	**Sim/SD**	**Contrib%**	**Cum.%**
Astarte spp.	2.74	5.59	3.82	13.54	13.54
Corophium spp.	1.64	3.19	2.59	7.73	21.27
Glycera capitata	1.37	2.83	2.42	6.86	28.13
Mediomastus ambiseta	1.37	2.45	1.59	5.94	34.07
Spiophanes bombyx	1.28	2.26	1.51	5.48	39.55
Paraonis fulgens	1.07	1.67	1.12	4.04	43.59
Tharyx acutus	1.11	1.60	1.10	3.88	47.47
Anadara transversa	1.18	1.58	0.97	3.82	51.29
Syllidae	1.04	1.49	1.12	3.60	54.89
Astyris lunata	1.07	1.33	0.87	3.22	58.10
Cirratulus cirratus	0.90	1.30	0.92	3.14	61.24
Praxillella praetermissa	0.98	1.22	0.82	2.95	64.19
Crepidula fornicata	1.25	1.08	0.60	2.62	66.81
Ampelisca vadorum	0.96	1.08	0.72	2.61	69.42
Pagurus longicarpus	0.84	1.05	0.80	2.55	71.97

Group l

Average similarity: 34.00

Species	**Av.Abund**	**Av.Sim**	**Sim/SD**	**Contrib%**	**Cum.%**
Ampelisca vadorum	2.40	5.44	1.54	16.01	16.01
Praxillella praetermissa	1.31	3.17	1.60	9.31	25.32
Spiophanes bombyx	1.26	2.72	1.48	8.01	33.33
Pagurus longicarpus	1.00	1.97	1.02	5.78	39.12
Corophium spp.	0.99	1.72	0.95	5.05	44.17
Arabella iricolor	0.87	1.65	0.97	4.85	49.02
Spiochaetopterus costarum oculatus	0.90	1.54	0.89	4.53	53.56
Nephtys incisa	0.87	1.27	0.70	3.74	57.30
Nicomache lumbricalis	0.78	1.11	0.66	3.27	60.57
Mediomastus ambiseta	0.77	1.10	0.66	3.23	63.79
Scalibregma inflatum	0.68	1.08	0.72	3.17	66.96
Clymenella torquata	0.79	0.91	0.55	2.67	69.64
Nephtys picta	0.69	0.86	0.52	2.53	72.17

Group m

Average similarity: 17.68

Species	**Av.Abund**	**Av.Sim**	**Sim/SD**	**Contrib%**	**Cum.%**

Phoxocephalus holbolli	1.06	3.35	0.57	18.94	18.94
Nephtys picta	0.72	2.32	0.57	13.10	32.04
Pagurus longicarpus	0.52	1.73	0.45	9.80	41.84
Tellina agilis	0.49	1.58	0.45	8.93	50.78
Paraonis fulgens	0.54	1.55	0.32	8.76	59.54
Glycera capitata	0.53	1.50	0.32	8.49	68.02
Ilyanassa trivittata	0.53	1.39	0.44	7.87	75.89

Several community types were generally found in each of the patch types (Figure 5.2-20, Table 5.2-7). However, there were differences within the community types based on patch type. For example, community type c was found in patch types B, C, D and E, whereas community type k was only found in patch types C, D and ND. Although several community types were found in each patch type, they were primarily comprised by predominantly one community type (Table 5.2-7). In Patch Type B, 50% of the sites were comprised of community type l, in Patch Type C, 60% of the sample sites were comprised of community types c and l, in Patch Type D, 63% of the sites were comprised of community types c, j and k, and in the ND group, 60% of the sites were comprised of community typed. Patch Types C and D had had the most community types across sites that were in those patch types, 10 and 12, respectively. Community types c, l, and m were each found in four patch types.

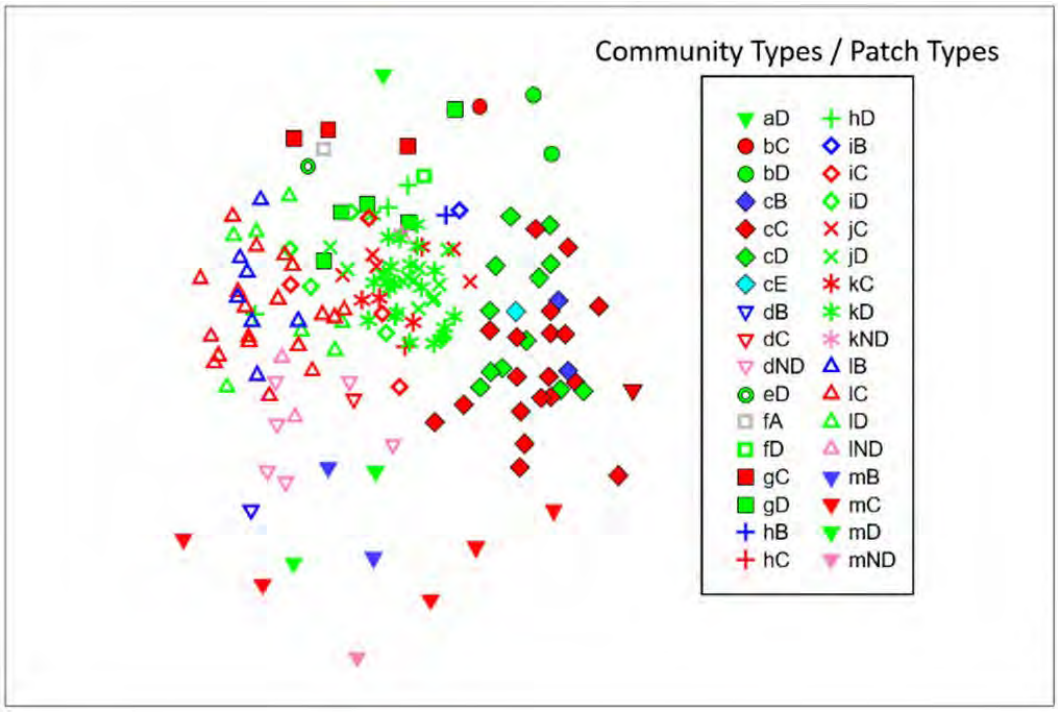

Figure 5.2- 20. nMDS ordination of sample site infaunal communities grouped by community types and patch types in the LIS Phase II study area. (Stress = 0.24, 4th root transformed abundances, Hellinger Distance Similarity Function).

Table 5.2- 7 Frequency of community types in each patch type.

	PATCH TYPES							
COMMUNITY TYPE	A	B	C	D	E	ND	Total Patch Types	Total Sites
a	0	0	0	1	0	0	1	1
b	0	0	1	2	0	0	2	3
c	0	2	19	13	1	0	4	35
d	0	1	1	0	0	6	3	8
e	0	0	0	1	0	0	1	1
f	1	0	0	1	0	0	2	2
g	0	0	3	5	0	0	2	8
h	0	1	1	3	0	0	3	5
i	0	1	4	4	0	0	3	9
j	0	0	5	11	0	0	2	16
k	0	0	4	21	0	1	3	26
l	0	7	19	7	0	2	4	35
m	0	2	6	2	0	1	4	11
Total community types	1	6	10	12	1	4		
Total Sites	1	14	63	71	1	10		160

In general, infaunal community types showed a variety of spatial distributions across the Phase II area (Figure 5.2-21). The most prevalent community types c, j, k, l and m, were found primarily in specific areas of the Phase II area. Community type c was primarily distributed along the southern margins of the Phase II area, and also through the west central area. In relation to environmental conditions, these communities appear to be associated with higher sea floor rugosity (as measured by TRI), sand size-fractions in the range of ~ 1 to 0.25 mm (Φ 0 to1) and for some locations increasing depth (Figure 5.2-18). Community types j and k, which were relatively similar (Figure 5.2-18), were mostly distributed thorough the central portions of the Phase II area, with some j and k communities also found in FIS (Figure 5.2-21). These communities were found at greater depths within the Phase II area and had greater proportions of coarser sediment grain-sizes (~ 2 to 15 mm; Φ -1 to -4). Community type l was found primarily along the northern boundary of the Phase II area, in relatively shallower depths along the Connecticut shore, and were characterized by greater proportions of fine-grained sediments < 1 mm (Φ 3 to 8) (Figure 5.2-18 and Figure 5.2-21). Community type m was primarily found in the western portion of the Phase II area, south of the mouth of the Connecticut River, although there were a few sites with this community type in the eastern portions of the area (Figure 5.2-21). This community type was associated with high seafloor rugosity and mixed sediment grain sizes (Figure 5.2-18). Community type d was distributed primarily thought this area as well. Community types j and k were found in the central portion of, and across the north to south breadth, of the Phase II area. The other community types were somewhat more scattered throughout the Phase II area. The relative similarities amongst the sample sites and their community types were significantly correlated with the geographic distances among the sites (RELATE procedure, average $\rho = 0.186$, $p = 0.009$), consistent with the result that most sites

within a specific community type were geographically closer to each other relative to sites in the other community types.

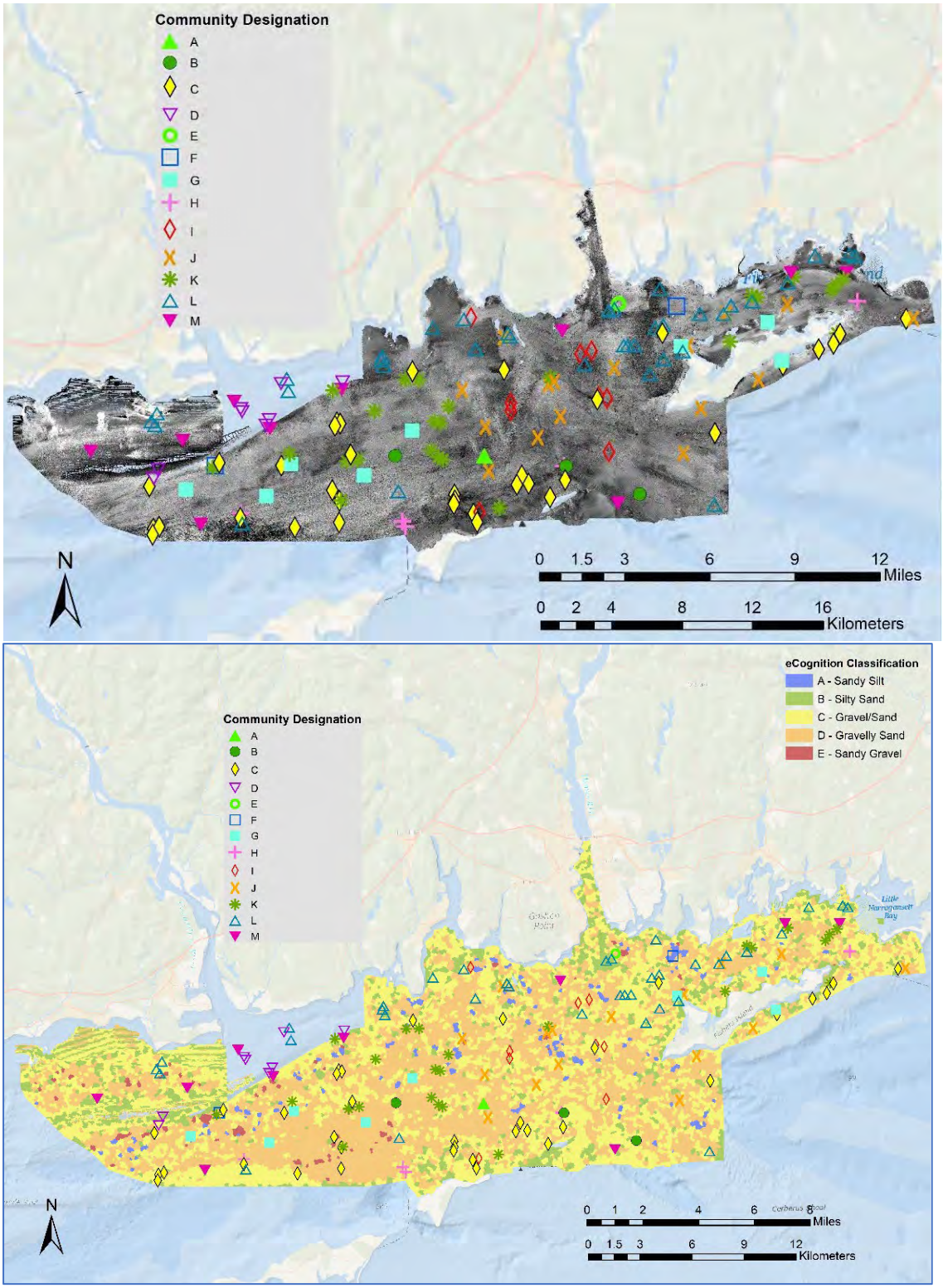

Figure 5.2- 21. Spatial distribution of community types as shown on backscatter mosaic (top) and Patch Types (bottom).

The distributions of the ten most abundant taxa were also spatially variable (Figure 5.2-22 – Figure 5.2-25). Three taxa, the amphipod *Ameplisca vadorum*, the maldanid polychaete *Praxiella praetermissa*, and the spionid polychaete *Marenzellaria viridis*, were most abundant along the northern sections of the Phase II area (Figure 5.2-22). *Ameplisca vadorum* and *Praxiella praetermissa* were also found in relatively high abundances in some of the deeper water sections of the central portion of the Phase II area. *Marenzellaria viridis* was most abundant southeast of the mouth of the CT River, and in FIS.

Five taxa were abundant throughout the deeper sections, as well as in some other locations, of the Phase II area (Figure 5.2-23 and Figure 5.2-24). The capitellid polychaete *Mediomastis ambiseta* was most abundant through the center of the area, along the southern border northwest of Plum Island, and in FIS. Relatively high abundances were also found south of the mouth of the Connecticut River and Niantic Bay. *Spiophanes bombyx*, a small, tube building polychaete, was found in high abundances in the western half of the Phase II area, in a cluster south of the mouth of the Thames River, and in FIS. A small predatory polychaete, *Glycera capitata*, had a similar spatial distribution (Figure 5.2-23). A group of corophiid amphipods, *Corophium* spp., were distributed in high abundance through the central portion of the Phase II area, extending into the area of the Race southwest of Fishers Island and also in FIS. A group of small bivalves within the genus *Astarte*, (designated as *Astarte* spp. as these may be juveniles of several other *Astarte* species that were found; alternatively, these may be *Astarte subaequilatera*) were found in very high abundances throughout the central portion of the Phase II area and also in FIS and south of Fishers Island (Figure 5.2-24).

Two of the dominant taxa found during the study had somewhat more limited spatial distributions. The slipper shell *Crepidula fornicata* was found in high abundance in the western portion of the Phase II area and also in FIS and south of Fishers Island (Figure 5.2-25). No individuals were found in deeper waters of the central portion of the area and southeast towards the Race. The terebellid polychaete *Polycirrus medusa* was found in high densities at several sites in the eastern most portion of the study area in deeper water, as well around the nearshore areas of Fishers Island (Figure 5.2-25).

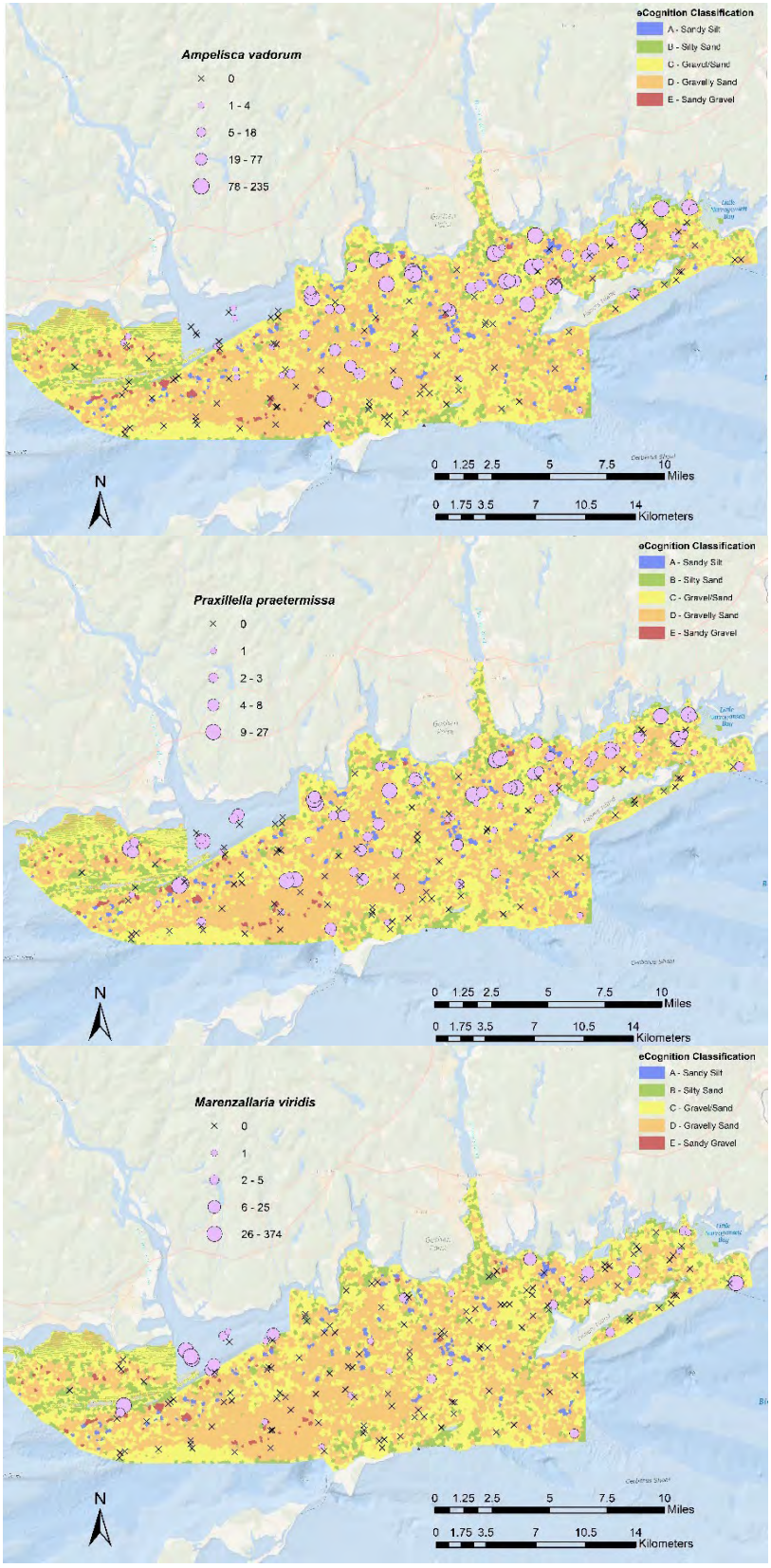

Figure 5.2- 22. Spatial distribution of several dominant infaunal taxa in the Phase II study area.

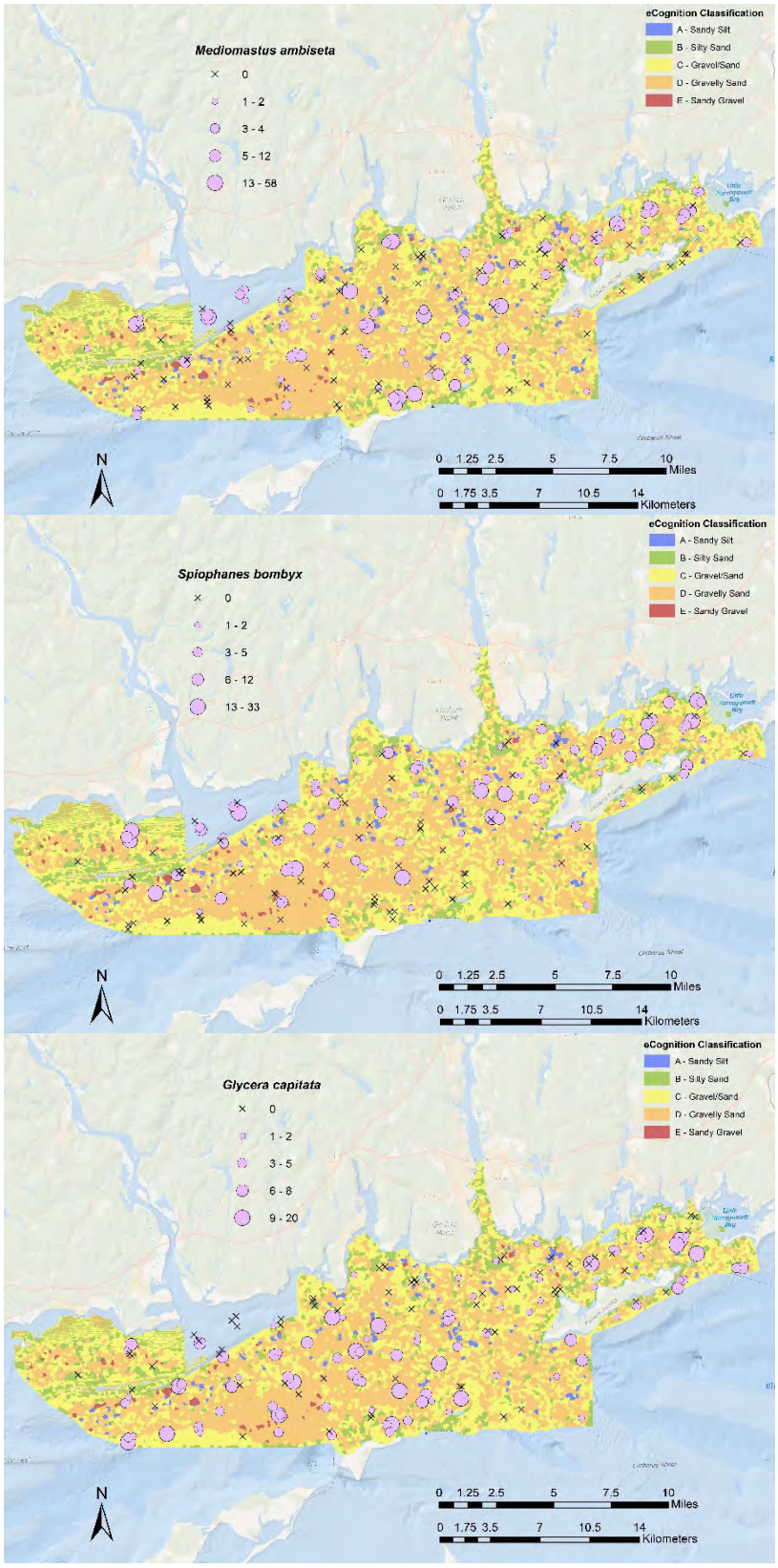

Figure 5.2- 23. Spatial distribution of several dominant infaunal taxa in the Phase II study area.

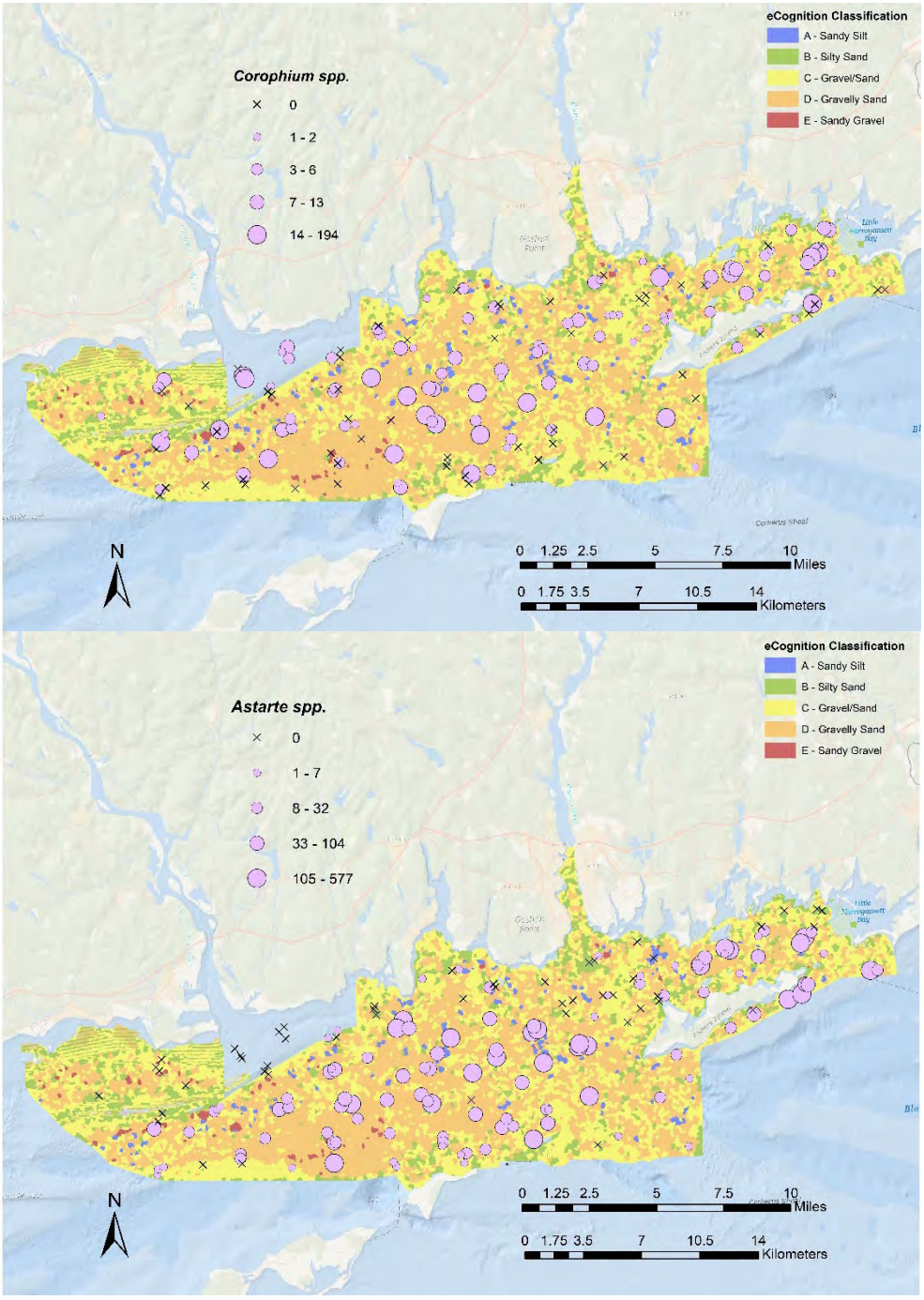

Figure 5.2- 24. Spatial distribution of several dominant infaunal taxa in the Phase II study area.

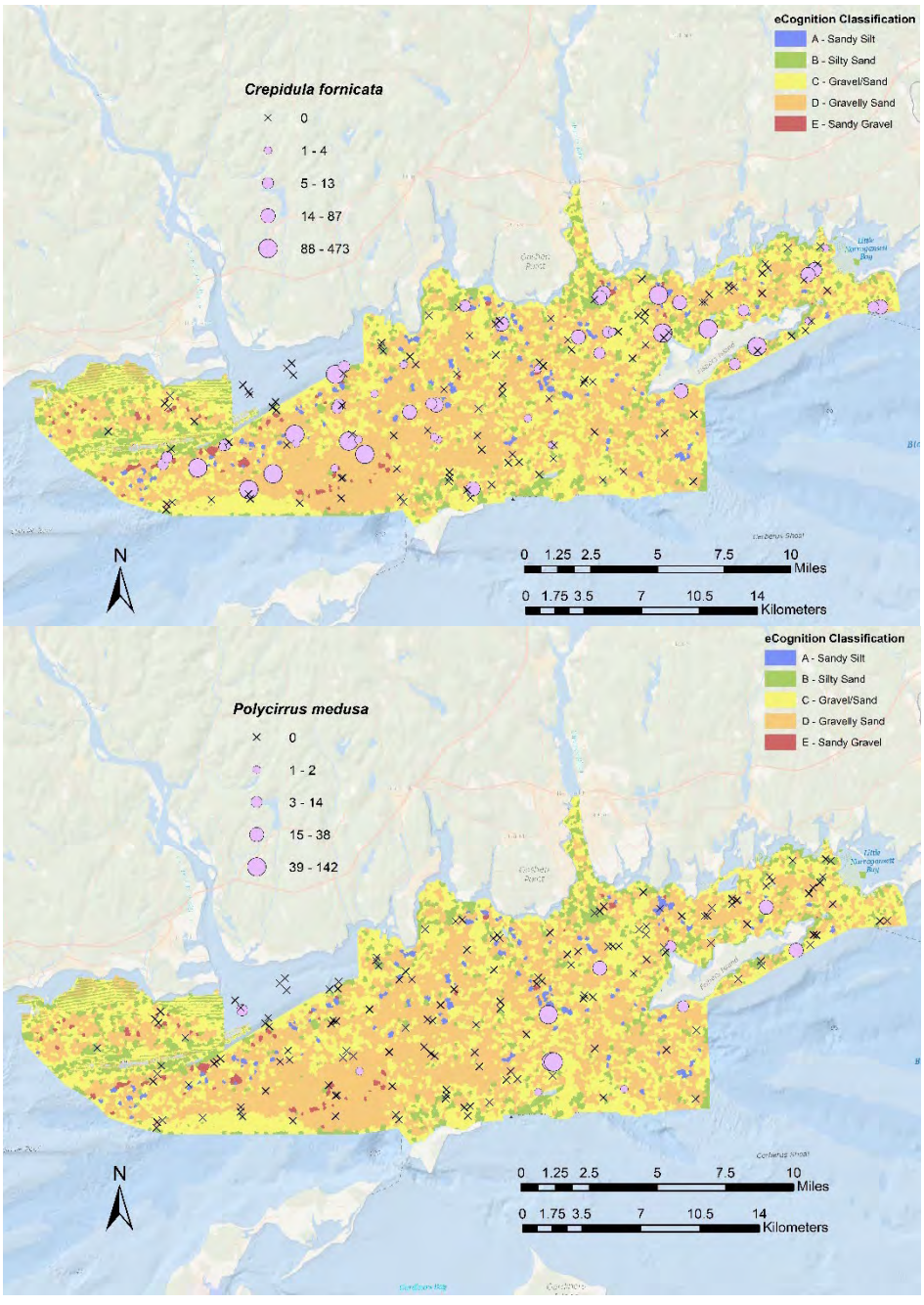

Figure 5.2- 25. Spatial distribution of several dominant infaunal taxa in the Phase II study area.

5.2.4 Discussion

Infaunal community composition and structure varied across the Phase II study area. This variation can likely be attributed, in part, to the environmental differences found among the acoustic patch types and environmental variability within each acoustic patch type relative to the large-scale environmental gradients across this portion of LIS. The ecological characteristics and dynamics of the infauna that are found in this area will also contribute to variations in community structure. These include such factors as life history, seasonality of reproduction and recruitment, differences in local species pools, functional characteristics (e.g., feeding type, motility, etc.), and habitat requirements. However, there are some general trends that can be identified. Total abundance, taxonomic richness, and diversity were highest in the central and eastern portions of the Phase II study area (Figure 5.2-3, Figure 5.2-7 & Figure 5.2-11). High abundances were found in the central portion of FIS and also within a large, deeper water area of the central portion of the study area. High taxonomic richness was found in the western portion of FIS, south of the Thames River, and in central portion of the study area. High taxonomic diversity followed a similar pattern as taxonomic richness although they were not spatially congruent. For example, an area of high diversity south of the Thames River was spatially broader than that of taxonomic richness, whereas diversity extended further to the east in FIS, than taxonomic richness.

These community characteristics were found at relatively low levels in the western portion of the Phase II area. This area is highly dynamic due to the influence of freshwater discharge from the Connecticut River, and hydrodynamic conditions which generate sand wave fields with varying geomorphologies (Bokuniewicz et al., 1977; Fenster et al., 1990)). Although the sand waves are relatively stable over the large-scale (Fenster et al., 1990), they are locally dynamic in terms of sediment flux. These overall conditions in this portion of the Phase II area may reduce habitat suitability for certain infauna. Higher taxonomic richness and diversity in the central and eastern portions of the study area may reflect the number of environmental and ecological conditions. From the central to eastern portions of the area, there is a greater spatial heterogeneity of acoustic patch types, and related small-scale diversity in patch types. Taxonomic richness and diversity in this area may be due in part to increased habitat diversity. These areas are also closer to BIS and areas of tidal change through The Race and eastern FIS, and are thus more likely to have a larger species pool to draw on. High total abundance in many of the samples was due to the presence of a small bivalve, *Astarte* spp., particularly in the general high abundance areas outlined in Figure 5.2-21

Community structure was assessed both with respect to acoustic patch types and in general across the Phase II area. Based on latter assessment, there were three prevalent community types distributed across this portion of LIS. Community type c was found mostly across the western portion of the Phase II study area, along its southern border, north of Plum and Gull islands, and south of Fishers Island (Figure 5.2-21). Taxa with highest average abundance in this community type included the small bivalve *Astarte* spp. (likely *Astarte subaequilatera*, the lentil Astarte), a predatory polychaete annelid (bloodworm) *Glycera capitata,* the sand dollar *Echinarachnius parma,* and the burrowing polychaete *Paraonis fulgens.* Each of these taxa are known to prefer sandy sediments, such as found through much of the western and southern portions of the study area, where acoustic patch types C and D dominated much of the seafloor. With several patches of type E. Community Type c was similar to the composition of numerically dominant taxa identified for acoustic patch types C and D, and to a lesser extent type E. Community Type k was most common across the west-central portion of the

Phase II area and also in the eastern-most portions of FIS (Figure 5.2-21). Dominant taxa included *Astarte* spp., the amphipods *Corophium* spp. and *Glycera capitata,* and the tubiculous polychaete annelids *Mediomastus ambiseta* and *Spiophanes bombyx*. This community had same dominance structure as that identified for acoustic patch type D and was found mostly in this acoustic patch type. Community type l was primarily found in shallower waters along the Connecticut coast both in LIS and through FIS (Figure 5.2-26). It was dominated by the tube building amphipods *Ampelisca vadorum* and *Corophium* spp., the tube building polychaete annelids *Praxillella praetermissa* (a species of bamboo worms) and *Spiophanes bombyx,* and the hermit crab *Pagurus longicarpus*. This set of dominants is very similar to that found for acoustic patch type B and reflects a preference for shallower habitats comprised of finer sediments where many of the Type B patches are located.

The infaunal community patterns discussed above exhibit a number of similarities to those found in previous studies. Data from Pellegrino and Hubbard (1983) indicated a gradient of increasing species richness from the area of the Connecticut River east to FIS (Figure 5.1-1) with an area of elevated species richness in the central portion of the area south of Niantic Bay. These patterns agree with those found in this study for taxonomic richness (Figure 5.2-26). Analysis of community structure using the Pellegrino and Hubbard (1983) by Zajac (1998) resulted in recognizing several community groupings (or types) in ELIS spanning the Phase II area (Figure 5.1-1). The most prevalent was a community designated as Group I (Table 5.2-8), which was found primarily in the west-central portion of the Phase II area but also in FIS. A community group designated as H2 was distributed primarily south of the Thames River and also in some areas westward along the Connecticut coast to the Connecticut River. Just south of the Connecticut River there was a mixture of community groups H2, I, and K. The most prevalent community types in the area surveyed by Pellegrino and Hubbard (1983) that were designated in this study included community types l and k (Table 5.2-9). The taxonomic compositions of the community types designated in both studies were very similar. There was a similar set of tube-building polychaetes among the communities, including *Spiophanes, Prionospio, Ampharete,* and *Clymenella*; although, there was a greater variety of bamboo worms (e.g., *Praxillella,* in the communities designated in this study). There is also a similar set of burrowing polychaetes including *Paraonis, Cirratulis, Nephtys*, and *Mediomastus/Capitella*. However, there is also a greater diversity of these kinds of annelids in the communities designated in this study. The composition of crustaceans was dominated by *Ampelisca* and *Corophium* taxa, and other amphipods. The biggest differences were in the composition of mollusk taxa. *Nucula* and/or *Mulinia* were found in all of the community types; community types l and k designated in the study were dominated by a small clam, *Astarte* spp., and also had locally high abundances of the slipper shell *Crepidula* (Table 5.2-9). Ophiuroids were also common in the community types designated in this study. Differences in the specific overall composition of dominant taxa among the two studies may be due to the seasonality of sampling and differences in the collection and processing of samples. However, generally there are similarities in the overall suites of species with similar life habits and functional characteristics (see also Table 5.2-10). For example, tube-building spionids were prevalent component of all communities, as well as bamboo worms which construct tubes deeper into the sediments. Another significant component in all communities were several different taxa of tube-building amphipods. In terms of burrowing infauna, although, communities were dominated by Cirratulid and Paraonid polychaetes and the carnivorous/omnivorous nephtyid polychaetes.

Table 5.2- 8. Results of PERMANOVA test of differences in community structure.

Factors

Name	Abbrev.	Type	Levels
Patch Type	Pa	Fixed	6
Community BC 4^{th} root	Co	Fixed	13

PERMANOVA table of results

Source	df	SS	MS	Pseudo-F	P(perm)	Unique perms
Pa	5	3.1814	0.63628	1.0763	0.22	996
Co	12	17.905	1.4921	2.524	0.001	993
PaxCo**	16	10.303	0.64394	1.0893	0.046	995
Res	126	74.485	0.59115			
Total	159	114.51				

** Term has one or more empty cells

Details of the expected mean squares (EMS) for the model

Source	EMS
Pa	1*V(Res) + 9.6265*S(Pa)
Co	1*V(Res) + 6.4768*S(Co)
PaxCo	1*V(Res) + 3.8772*S(PaxCo)
Res	1*V(Res)

Construction of Pseudo-F ratio(s) from mean squares

Source	Numerator	Denominator	Num.df	Den.df
Pa	1*Pa	1*Res	5	126
Co	1*Co	1*Res	12	126
PaxCo	1*PaxCo	1*Res	16	126

Estimates of components of variation

Source	Estimate	Sq.root
S(Pa)	0.0046882	0.068471
S(Co)	0.1391	0.37296
S(PaxCo)	0.013615	0.11668
V(Res)	0.59115	0.76886

Table 5.2- 9 Comparison of composition of dominant taxa in the Phase II study area among communities identified by Zajac (1998) and Zajac et al. (2000) based on data in Pellegrino and Hubbard (1983) and this study. See Figure 5.2-1 and Figure 5.2-22 for locations.

Zajac 1998 Type I	**Zajac 1998 Type H2**	**This Study Type L**	**This Study Type K**
Polychaetes			
Prionospio heterobranchia	*Prionospio heterobranchia*	*Prionospio steenstrupi*	
Spiophanes bombyx	*Spiophanes bombyx*	*Spiophanes bombyx*	*Spiophanes bombyx*
Prionospio tenuis	*Steblospio benedicti*	*Marenzallaria viridis*	*Sabellaria vulgaris*
Polydora websteri		*Spiochaetopterus c. oculatus*	*Spiochaetopterus c. oculatus*
Ampharete arctica		*Ampharete arctica*	*Ampharete acutifrons*
Clymenella zonalis	*Clymenella zonalis*	*Clymenella torquata*	*Asychis elongatus*
		Praxillella praetermissa	*Praxillella praetermissa*
		Nicomache lumbricalis	*Nicomache lumbricalis*
	Paraonis fulgens	*Paraonis fulgens*	*Paraonis fulgens*
Cirratulus cirratus		*Magelona papilliformis*	*Cirratulus cirratus*
Cirratulus grandis	*Cirratulus grandis*	*Tharyx acutus*	*Tharyx acutus*
Aricidea jeffersyii	*Mediomastus ambiseta*	*Mediomastus ambiseta*	*Mediomastus ambiseta*
Capitella capitata	*Nephtys incisa*	*Nephtys incisa*	*Glycera capitata*
Nephtys picta	*Nephtys picta*	*Nephtys picta*	*Syllidae*
		Scalibregma inflatum	*Scalibregma inflatum*
		Arabella iricolor	*Arabella iricolor*
			Polygordius spp
			Nereis grayi
Crustaceans			
Ampelisca vadorum	*Ampelisca vadorum*	*Ampelisca vadorum*	*Ampelisca vadorum*
Ampelisca abdita	*Ampelisca abdita*	*Ampelisca verrrilli*	*Corophium* spp.
Corophium acheruscum	*Corophium acheruscum*	*Corophium* spp.	*Pagurus longicarpus*
Lepidontus squamotus	*Leptocheirus pinquis*	*Pagurus longicarpus*	*Lepidonotus squamatus*
Unciola irrorata	*Unciola irrorata*	*Pinnixulala retinens*	*Caprella penantis*
Aeginina longicornis	*Ancanthohaustorius millsi*	*Pinnixa sayana*	*Lysianopsis alba*
			Idunella clymenellae
			Americamysis bigelowi
Mollusks			
Pandora gouldina	*Nucula annulata*	*Astarte* spp.	*Astarte* spp.
Ensis directus	*Pitar morrhuana*	*Mulinia lateralis*	*Mulinia lateralis*
Nucula annulata	*Mulinia lateralis*	*Crepidula fornicata*	*Crepidula fornicata & C. plana*
Tellina agilis	*Tellina agilis*	*Spisula solidissima*	*Anadara transversa*
Mytilus edulis		*Bittiolum alternatum*	*Bittiolum alternatum*
			Nucula proxima
			Pyramidellidae Family
			Astyris lunata
Ophiuroids			
			Amphipholis squamata

A more recent study by Zajac et al. (2003), that used similar seafloor mapping and ecological characterization approaches in a small area south of the mouth of the Thames River found a suite of dominant species similar (Table 5.2-10) to those designated in this study and by Zajac (1998) in that general location.

Table 5.2- 10 Dominant taxa found within a 19.4 km2 area just south of mouth of the Thames River that was surveyed using habitat mapping and ecological characterization approaches similar to those used for this study (Zajac et al., 2000 2003).

	Feeding	**Motility, Sediment Modification**
Polychaetes		
Prionospio steenstrupi	Surface deposit-feeding, Filter feeding	Discretely motile, Tubiculous
Kirkegaardia dorsobranchialis	Surface deposit-feeding	Discretely motile/motile, Sediment bioturbating?
Chaetozone spp.	Surface deposit feeder	Discretely motile
Aricidea catherinae	Herbivore, Surface deposit feeder	Motile, Burrower
Polycirrus exumis	Surface deposit feeder	Discretely motile
Nephtys spp.	Carnivorous, Burrowing deposit feeder	Motile
Clymenella torquata	Subsurface deposit feeder	Sessile, Tubiculous, Bioturbation, Oxygenation
Mediomastus ambiseta	Burrowing deposit feeder	Motile, Pelletization
Amphipods		
Ampelisca vadorum	Surface deposit/ suspension feeder	Tubiculous
Unicola irrorata	Surface deposit/ suspension feeder	Tubiculous
Microduetopus gryllotalpa	Surface deposit/ suspension feeder	Tubiculous
Phoxocephalus holboli	Surface deposit/ suspension feeder	Tubiculous
Exogenes hebes	Herbivore, Surface deposit feeder, Carnivore	Motile, Burrower, Nontubiculous
Bivalve		
Nucula annulata	Subsurface deposit feeder	Discretely motile
Other		
Nemertean	Carnivore	Burrowing
Oligochaete spp.	Burrowing deposit feeder	Motile

5.2.5 References - Infaunal Ecological Characterization

Bokuniewicz, H.J., Gordon, R.B. and Kastens, K.A., (1977). Form and migration of sand waves in a large estuary, Long Island Sound. *Marine Geology*, 24(3), 185-199.

Brown, C.J., Sameoto, J.A. and Smith, S.J. (2012). Multiple methods, maps, and management applications: Purpose made seafloor maps in support of ocean management. *Journal of Sea Research* 72, 1-13.

Clarke, K. and Gorley, R. (2006). PRIMER v6 User manual/tutorial. (*Plymouth Routines in Multivariate Ecological Research*). Plymouth: PRIMER-E.

Fenster, M.S., Fitzgerald, D.M., Bohlen, W.F., Lewis, R.S. and Baldwin, C.T., (1990). Stability of giant sand waves in eastern Long Island Sound, USA. *Marine Geology*, 91(3), 207-225.

Gaston, G.R., McLelland, J.A. and Heard, R.W., (1992). Feeding biology, distribution, and ecology of two species of benthic polychaetes: *Paraonis fulgens* and *Paraonis pygoenigmatica* (Polychaeta: Paraonidae). *Gulf and Caribbean Research*, 8(4), 395-399.

Kostylev, V.E., Todd, B.J., Fader, G.B., Courtney, R., Cameron, G.D. and Pickrill, R.A. (2001). Benthic habitat mapping on the Scotian Shelf based on multibeam bathymetry, surficial geology and sea floor photographs. *Marine Ecology Progress Series* 219, 121-137.

NCSS, LLC. (2012). Statistical Software. Kaysville, Utah, USA. Retrieved from www.ncss.com

Pellegrino, P. E. and Hubbard, W. A. (1983). *Baseline Shellfish Data for the Assessment of Potential Environmental Impacts Associated with Energy Activities in Connecticut's Coastal Zone*. Volumes I & II. Report to the State of Connecticut, Department of Agriculture, Aquaculture Division, Hartford, Connecticut.

Poppe, L.J., Knebel, H.J., Mlodzinska, Z.J., Hastings, M.E. and Seekins, B.A., (2000). Distribution of surficial sediment in Long Island Sound and adjacent waters: texture and total organic carbon. *Journal of Coastal Research*. 567-574.

Zajac, R. (1998). A review of research on benthic communities conducted in Long Island Sound and an assessment of structure and dynamics. Chapter 4, in: *Long Island Sound Environmental Studies*. Poppe, LJ. and Polloni, C. (Eds). USGS Open-File Report 98-502. Retrieved from: https://pubs.usgs.gov/of/1998/of98-502/chapt4/rz1cont.htm

Zajac, R.N., Lewis, R.S., Poppe, L.J., Twichell, D.C., Vozarik, J. and DiGiacomo-Cohen, M.L. (2000). Relationships among sea-floor structure and benthic communities in Long Island Sound at regional and benthoscape scales. *Journal of Coastal Research*: 627-640. Retrieved from: https://journals.flvc.org/jcr/article/view/80868/78017

Zajac, R.N., Lewis, R.S., Poppe, L.J., Twichell, D.C., Vozarik, J. and DiGiacomo-Cohen, M.L. (2003). Responses of infaunal populations to benthoscape structure and the potential importance of transition zones. *Limnology and Oceanography* 48, 829-842. https://aslopubs.onlinelibrary.wiley.com/doi/epdf/10.4319/lo.2003.48.2.0829

Zajac, R.N., Vozarik, J.M. and Gibbons, B.R. (2013). Spatial and temporal patterns in macrofaunal diversity components relative to sea floor landscape structure. *PloS One* 8:e65823.

5.3 Epifaunal Ecological Characterization

5.3.1 Background and Objectives

This element of the project is an extension of studies to develop spatially comprehensive seafloor habitat maps and interpretive products for LIS inclusive of emergent- and epi-faunal elements of seafloor habitats (Zajac et al., 2020). There are inherent difficulties sampling hard substratum habitats upon which epifaunal organisms depend, as well as the fragility of those emergent taxa and biogenic structures that occur on the surface of both hard substratum and fine-grained sediments. Variable life histories make optimal timing for sampling problematic for diverse, short-lived, but ecologically important taxa (Cau et al., 2020). Further, sampling for these taxa is difficult with standard sample gears such as grabs and dredges. For example, the jaws of grab samplers don't close on pebbles and cobbles or are ineffective on boulders and outcrops, while some abundant taxa with weak attachment to the seafloor can be dispersed by the pressure wave in front of sampling gear deployed rapidly from the surface. Specialized sampling tools and approaches for imaging and collection of physical samples (e.g., integrated cameras/grabs, remotely operated vehicles, divers with quadrat cameras, and airlift samplers) can solve some of these issues or at least provide samples to contrast and evaluate those that are more widely applied.

Hard substratum habitats are spatially rare in LIS, especially in deep waters (>10 m) of the central and western basins (Knebel & Poppe, 2000; Poppe et al., 2000), but are more spatially extensive in the eastern part of the region (Poppe et al., 1998, 2006; Langton et al., 1995). Associated structure-forming seafloor communities contribute uniquely to the rich biological diversity of LIS, functioning as physical habitat features and prey for a wide range of vagile species including fish, crustaceans, mollusks, and echinoderms of ecological and economic importance (e.g., Auster et al., 1995, 1997, 1998; Langton et al., 1995; Malatesta & Auster, 1999; Stefaniak et al., 2014; Lindholm et al., 1999; Cau et al., 2020). Further, a number of these species or species groups can serve as sentinels for assessing direct and indirect effects of natural and human-caused events due to their structural fragility or environmental thresholds linked to growth, reproduction, and survival (e.g., turbidity, temperature, salinity, wave energy, trophic interactions). For example, invertebrates with morphologies based on calcium carbonate can exhibit deleterious responses to ocean acidification (e.g., Holcomb et al., 2012 for *Astrangia poculata*), shifts in size and composition of planktonic food resources for filter feeders can shift signs and direction of competitive dominance hierarchies due to the effects of warming (e.g., Thieltges, 2005), and changes in time of reproduction due to warming can influence dispersal patterns based on seasonal changes in oceanographic drivers (Fuchs, et al., 2020). The map products presented here provide a foundation for marine spatial planning and a snapshot in time against which change can be measured. Most importantly, this can serve as a baseline to measure change over time with sufficient temporal resolution in monitoring (e.g., Stefaniak et al., 2014).

The objectives of this project component were to produce: (1) maps of emergent- and epi-faunal community types based on multivariate analyses of faunal data related to physiographic features, (2) maps of faunal and biogenic features richness and diversity, (3) maps of selected species and biogenic habitat features, (4) and in collaboration with other project elements, an integrated habitat map combining infaunal and epifaunal/emergent species diversity.

5.3.2 Image Acquisition and Methods

5.3.2.1 Sample Site Selection and General Cruise Details

Sample locations were selected through a multi-step process. First, sampling effort was spread throughout the geographic extent of the study area across 90 sampling blocks (SB) or sites (NB; Figure 5.3.1). The spatial distribution and locations of the sample areas were selected with the overall objective to sample as many of the different seafloor habitats as possible based on examination of existing seafloor bathymetry and backscatter data to be inclusive of depth and grain size gradients, the presence of transition zones between distinct seafloor features, and efforts to distribute sampling throughout the longitudinal range of the study area. The original plan for the sampling effort was to implement three grab samples and three image transects in blocks and one each at sample sites.

Figure 5.3- 1. Map of the Phase II area, showing the sample blocks (squares) and sample sites (ovals).

The majority of the samples for ecological characterization were collected during 2 sampling periods, between November 28 and December 3, 2017 and May 8 and 15, 2018 using the USGS SEABOSS (Valentine et al., 2000; Figure 5.3-2) for both infaunal grab and epifauna video/photographic samples. Additional sampling details for the SEABOSS cruises are provided in (Ackerman et al., 2020). The R/V *Connecticut* was used to support both cruises.

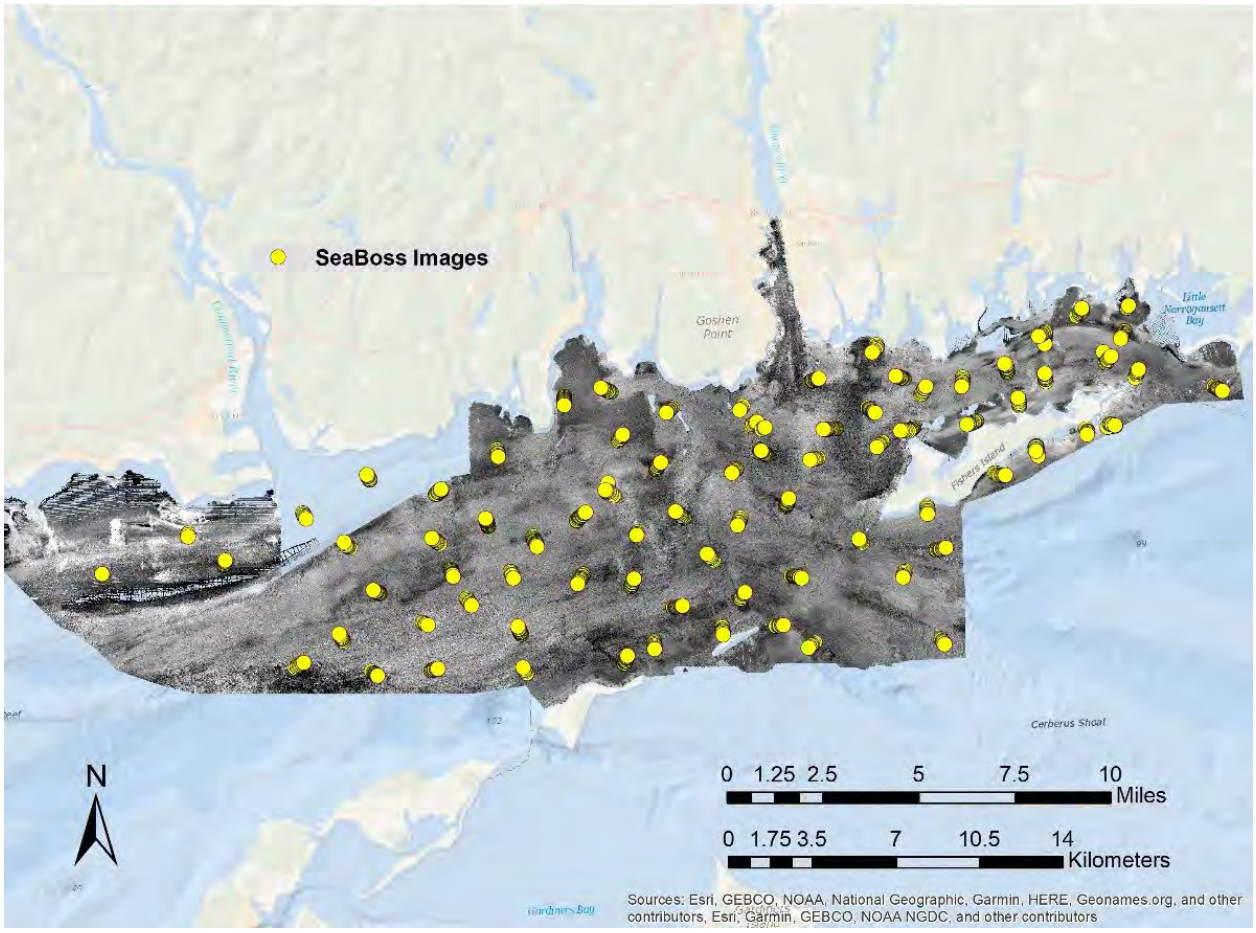

Figure 5.3- 2. Map illustrating the locations of images acquired by the SEABOSS platform.

Locations with high rugosity and complex topographies were sampled via still and video imagery with the Kraken2 ROV during 1 cruise conducted during May 2018, again using the R/V *Connecticut* (Figure 5.3-3). Scuba was employed to collect quadrat camera still images and associated suction samples to assess and contrast patterns of diversity using visual versus direct sample approaches. This wet-diving component of the project was conducted between August 2017 and August 2018 (Figure 5.3-4).

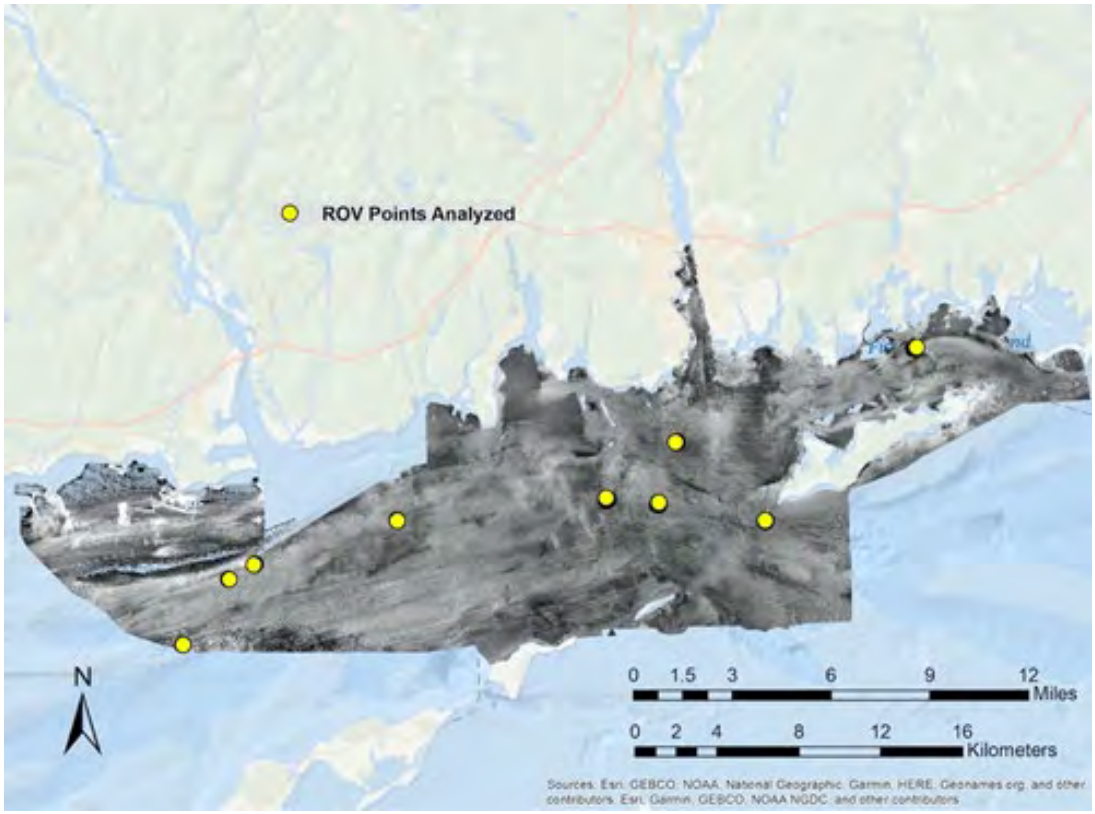

Figure 5.3- 3. Map illustrating the locations of images acquired by the Kraken2 ROV platform.

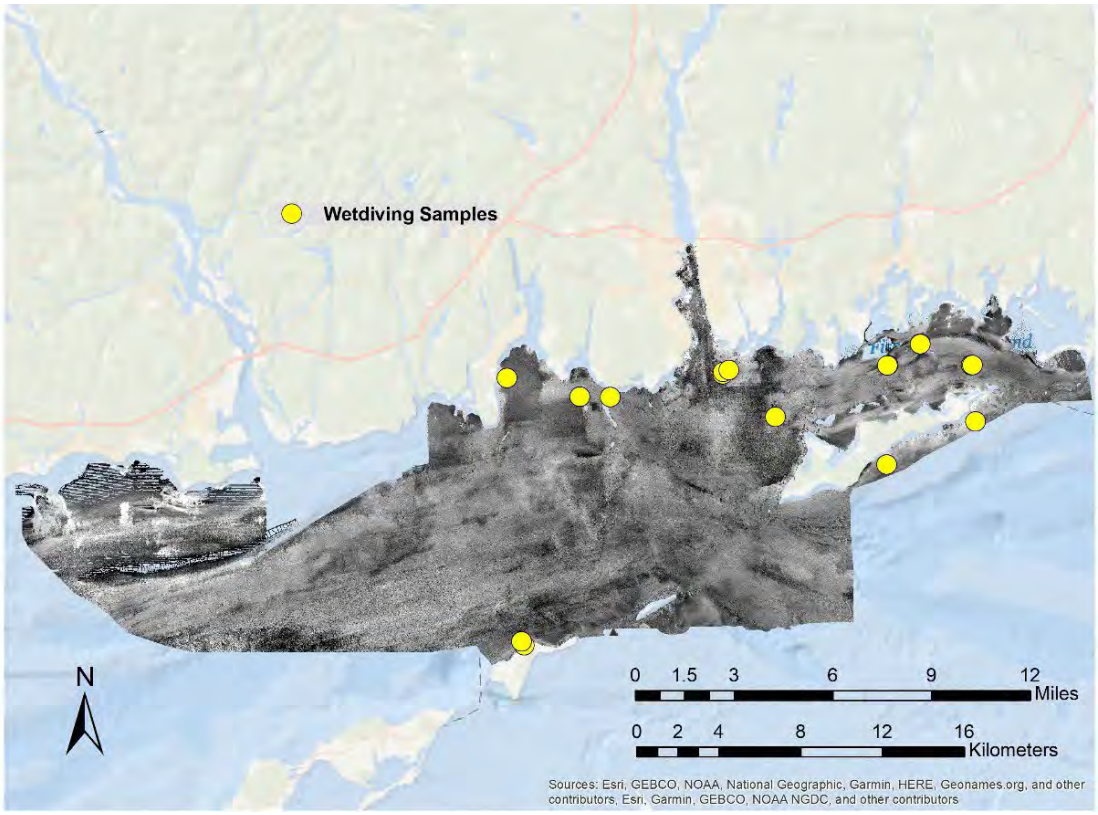

Figure 5.3- 4. Map illustrating the locations of images and suction samples acquired by wet- diving.

5.3.2.2 Epifaunal Sample Design

Epifaunal and emergent seafloor organisms and associated biogenic features were characterized using seafloor imagery and suction sampling by divers. Images were collected during SEABOSS and ROV transects (n = 602 SEABOSS images fall 2017, n = 595 SEABOSS images spring 2018, n = 110 ROV images spring 2018, n = 87 wet-diving images 2017-18). Sampling efforts depended on seafloor characteristics. While most effort was concentrated in the SEABOSS cruises referenced above, select areas with precipitous topographies were sampled via still and video imagery via wet-diving or with the ROV.

Within both sampling blocks and sites, sampling location selection differed based on the sampling method and platform. Trajectories for SEABOSS transects were selected algorithmically. Large numbers of potential transects (n = 1000) with randomized start and end points were randomly generated for each sampling block and site. Transect locations were constrained by simple rules; transects could not be generated within 6.1 m lateral distance (i.e., the beam of the R/V *Connecticut*) of 5 m depth contour or identified obstructions. Bathymetry and backscatter profiles of each randomly generated transect were extracted from acoustic data sets. These profiles were ordered based on the variance and range of bathymetry and backscatter profile data such that transects with the greatest range and highest variance were highest ranked. The highest ranked transects were retained and implemented based on logistic constraints (e.g., ship handling due to wind and wave direction, safety regarding depth and fixed gear such as navigation aids, trap buoys).

This approach was taken since changes in bathymetry and backscatter are key indicators of transition zones (Zajac et al., 2003 & 2020) and sampling transition zones was central to characterizing variation in communities. This algorithmic process was the principle means of efficiently sampling seafloor habitats within blocks and sites across the study region (Figure 5.3-5). This transect selection approach resulted in an overall reduction in the number of transects sampled per sample block (originally planned as n=3, reduced to n=1) and increased the number of sample blocks that were actually sampled during research cruises. Wet-diving locations were determined based on visual assessment of fine scale bathymetric data and were limited to shallow areas <22 m in depth. Trajectories for image and video sampling via ROV were selected using bathymetric data and navigation data from topographically challenging areas identified during SEABOSS transects. Using 3 distinct sampling approaches was necessary to characterize epi- and emergent fauna across available habitats and depths within Phase II area.

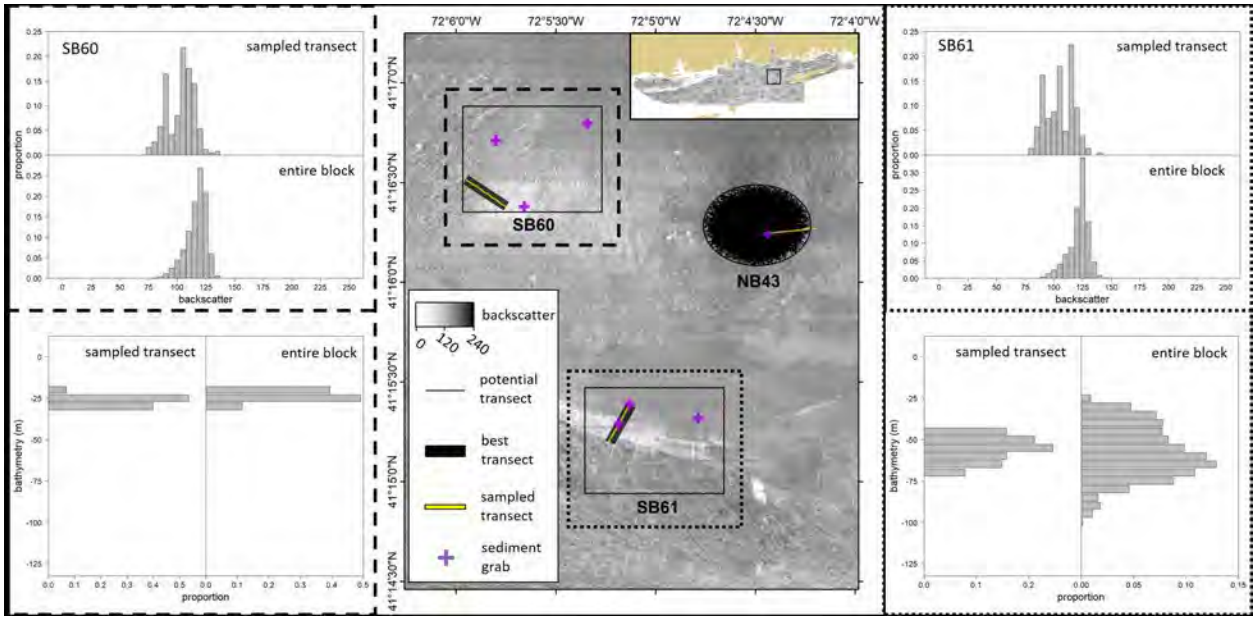

Figure 5.3- 5. Example of approach for selecting transect location. Map depicting sampling blocks SB60 and SB61 and site NB43 (center) with acoustic backscatter base layer. In each sample block and site, yellow line depicts the sampled transects and purple crosses sediment grab locations during fall 2017 (SB60 and SB61) or spring 2018 SEABOSS sampling. Sampled transects were selected a priori from 2000 randomly generated potential transects (depicted as thin black lines at site NB43) as best representing the physical seafloor habitats available in a specific block or site. The range of physical seafloor habitats available in blocks SB60 (left) and SB61 (right) are represented by histograms of backscatter and bathymetry along sampled transects and within entire sample blocks. Note that the distributions of backscatter and bathymetry in the sampled transects largely matches those of the entire sample blocks.

SEABOSS sampling consisted of imaging, video, and sediment grab sampling. Still images were taken using a Nikon D300 camera and Photosea electronic flash set-up for orthogonal imagery (Figure 3.3-2). Video imagery was collected using a GoPro Hero4 for oblique forward-facing field-of-view and a SIMRAD SD video camera mounted for an orthogonal field-of-view. All bottom videos were acquired using a Kongsberg Simrad OE1365 video camera on the SEABOSS. A scientist monitored the real-time bottom video and acquired bottom photographs at approximately 25 s intervals (when the camera was at approximately 1 m off the seafloor) by remotely triggering the Nikon camera shutter. Bottom video was also recorded during the drift from the downward-looking Kongsberg video camera directly to hard drives using an Odyssey7 video recorder. Bottom videos were recorded in MP4 format and a trackline shapefile of the location of the ship for the duration of the video collected during the fall 2017and spring 2018 field activities. A total of 210 sites were occupied within the study area, and bottom videos were acquired at all 210 sites resulting in 218 videos with a total duration of 48 hours 30 minutes and 218 video tracklines with a total length of 41.4 kilometers (Ackerman et al., 2020).

Wet-diving sampling, limited to depths <22 m, consisted of seafloor imaging and suction sampling. Images were taken using either a Sony NEX-5 or Sea & Sea DX-1200HD digital camera with two Sola Video lights mounted on a camera quadropod, set-up for orthogonal imagery (Figure 5.3-6). Images captured 0.5m^2 square area of seafloor. Seafloor samples were collected via suction sampling (Figure 5.3-6). Suction sampling consisted of collecting epifauna within a 0.5m^2 quadrat area using a compressed air suction sampler. Samples were collected in sealable 0.5mm mesh bags connected to the suction sampler then transferred to storage containers and preserved in 70% ethanol for later processing. Specific suction sample locations were imaged prior to and following suction samples.

Figure 5.3- 6. Diver conducting quadrat photo transect (left) and suction sampling (right)

The Kraken2 ROV (Figure 5.3-7) was utilized to acquire imagery in topographically complex and spatially constrained habitats where maneuverability of the camera platform is required to collect adequate image samples. Such areas were difficult to access using SEABOSS.

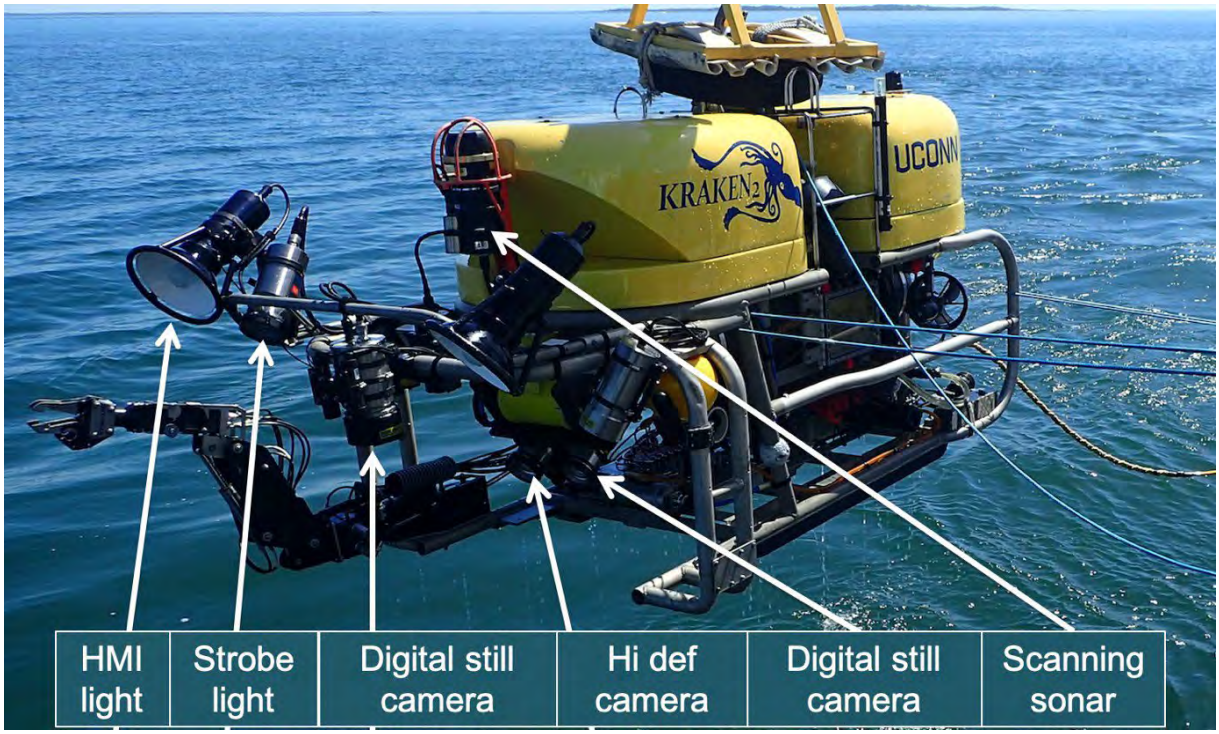

Figure 5.3- 7. The Kraken2 ROV illustrating its still and video imaging and sonar capabilities

ROV sampling consisted of still and video imagery. Still images were recorded using a Nikon E995 digital camera and electronic flash set-up for orthogonal imagery. A Canon PowerShot G11 and electronic flash were also installed for mobile pan-tilt imagery.

All images were taken using artificial lighting (electronic flash or daylight color temperature lighting using HMI or LED sources) to enhance color saturation, edge sharpness, and depth of field. Paired parallel lasers were mounted adjacent to cameras and projected points into each image at 20 cm spacing to facilitate image calibration. All imagery was batch processed using the automated color correction routine in Irfanview software (version 4.50) in order to enhance color saturation and delineate color boundaries to facilitate identification of taxa.

Each image was subsequently examined for clarity and focus. Images with water turbidity that obscured the seafloor or that were out of focus such that identification of all organisms or biogenic features was impeded were rejected. Transects were divided into 50 m segments and images subsampled randomly from each segment, ensuring epifauna along the entire length of each transect would be characterized. Images selected for analysis were approximately 2m apart to preclude analyzing the same areas of the seafloor multiple times. This step produced a total of 1307 processed images for analysis.

Each color corrected image was analyzed for percent cover of all living seafloor species (excluding fish) and biogenic features (e.g., shell, mud tubes, burrows) using ImageJ software (version 1.45s; Abramoff et al., 2004). Percent cover was quantified using a grid of square cells overlaid on each image. The grid featured 280 cells filling the entire image space, but the cells lining the image edge were ignored due to reduced lighting and potential optical distortion caused by the flat port and open aperture of the underwater camera, resulting in a usable grid of 216 cells (Figure 5.3-8).

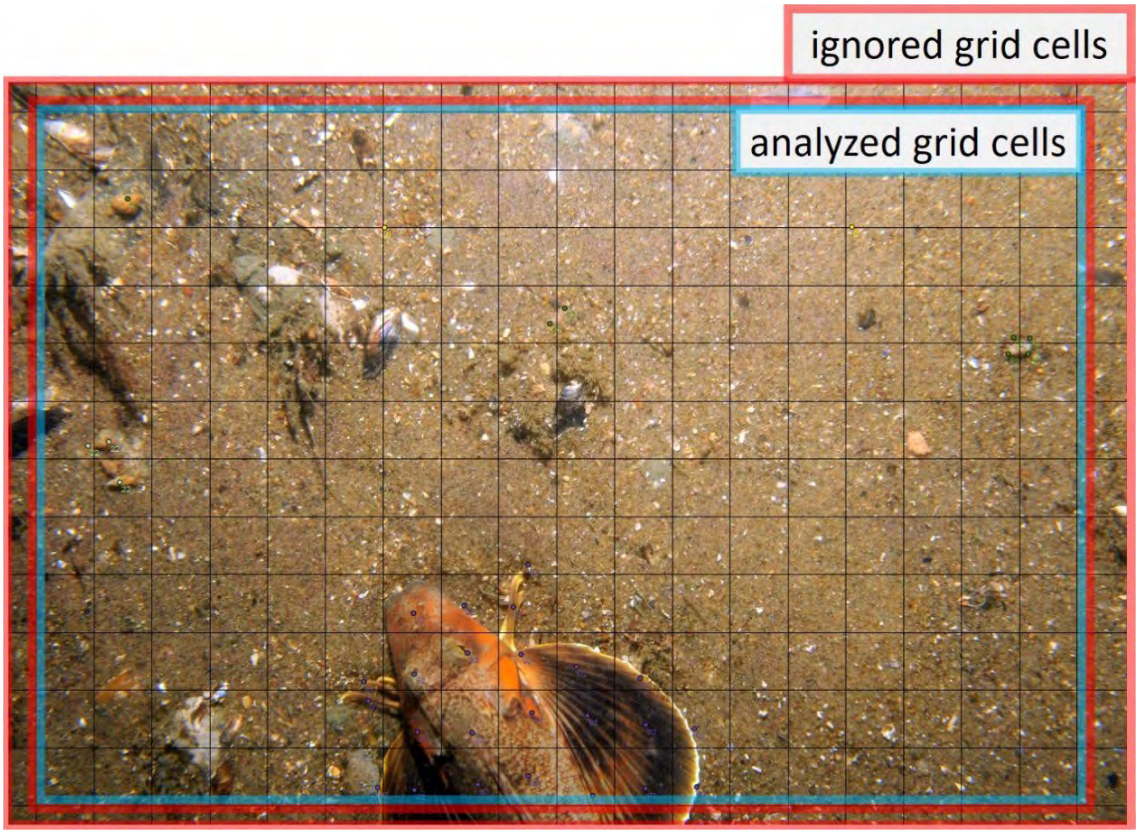

Figure 5.3- 8. Screen capture of grid used for ImageJ analysis

Within each grid square, organisms and biogenic features were identified to lowest possible taxonomic level and marked using the "cell counter" tool in ImageJ. This function displays a mark on each object as selected in the image and, in a separate window, displays counts of each object type. ImageJ only classifies objectives and related numerical counts as a series of undefined "Types" (e.g., Type 1, Type 2, etc.) and does not have a custom naming feature. Therefore, workflow processing of images required a separate record of the identity of "types" for each image and subsequently rectifying counts with actual taxonomic and feature classifications post-processing.

Several counting conventions (i.e., decision rules) were required to address variability in the cover of organisms and biogenic habitat features on the seafloor. Some colonial organisms

(e.g., coral, sponge) and biogenic features occupied multiple grid squares. In addition, some solitary organisms (e.g., mussel, crab, gastropod) also were present in multiple squares. Such individuals were counted in each square to account for the area of coverage in each image. Conversely, more than one organism or biogenic feature could be in a single square and were each counted in order to account for all biological elements within an image. Therefore, the total grid count could be greater than the total number of squares in the grid (but then normalized across images by calculating percent cover, as described below).

Total counts for each taxa or type of biogenic feature from each image were entered into a spreadsheet. All taxa, excluding fish fauna captured in images, and biogenic features were counted from imagery. Taxa and features from the full matrix were parsed for analyses as taxa (i.e., both sessile and mobile invertebrates), taxa and biogenic features (i.e., those structures produced by biota such shell, worm tubes, burrows). Counts were saved and archived as .ROI files (format that saves their position within the image for future analysis). Using the scaling lasers in each image to calibrate length, the width and height of both the image and the grid was measured using the "measure" tool in ImageJ and area of coverage was calculated. Counts were converted to percent cover by dividing the count for each type of organism or feature by the total number of squares for the image. These data were subsequently used in multivariate and univariate analyses to address objectives regarding characterization of communities, variation in patterns of diversity, distribution of habitat features, and seasonality of patterns. Multivariate tests and diversity indices identified in results were implemented using PRIMER-e (v7.0.17, Clarke & Gorley, 2015). Maps, shapefiles, and layer files were created for the % cover of taxa and biogenic features, as well as diversity measures in ArcMap (v10.5).

5.3.3 Results

5.3.3.1 Epifaunal Diversity and Distribution of Communities

Broad scale sedimentary conditions are represented by acoustic patches classified using eCognition (see Section 5.1) and form the basis for delineating communities, patterns in biogenic features, and differential distribution of key taxa and features. Together, these results serve as a part of the foundation for the integrated habitat map (Section 5.4). Patch types A-E follow a general meso-scale gradient of increasing dominance of coarse sediment components. However, all patch types include a degree of coarse stable gravel, (from small patches and minimal representation to more spatially extensive and dominant) that is exposed at the sediment-water interface. These hard substratum surfaces facilitate settlement and survival of epifaunal structure-forming species. However, the composition of hard substratum and surrounding fine-grain sediment communities can be influenced by the interactions of species within and between patch types based on area and circumference mediating interactions such as predation and competition (Fagan et al., 1999; Zajac, 2008). It is noteworthy here that unlike the relatively distinct grain size composition and large spatial scale extent of eCognition acoustic patches in the Phase 1 Stratford Shoals area, exhibited distinct epi- and emergent-faunal dominants in each patch type, the Phase 2 ELIS-FIS region exhibits a high degree of spatial variability between as well as within eCognition acoustic patches.

A total of 119 taxa were identified to the lowest possible taxonomic unit and an additional 33 biogenic features, structures formed by organisms (e.g., shell, tubes, burrows) and used as habitat by vagile fauna were observed in the study region (Table 5-3-1). Multivariate analyses were implemented to test for differences in the composition of taxa and biogenic features based on eCognition patch assignments for image samples. ANOSIM routines identified statistically

significant differences in Global R values for both taxa and biogenic features in fall and spring surveys as well as for live taxa only in the spring 2018 survey (Table 5.3-2). SIMPER comparisons of dissimilarity between eCognition patch types reveals variation in abundance (i.e., patterns of dominance based on cover values from image analysis) but not wholesale differences in composition between patch types (Table 5.3-3A). This pattern in the composition of sedimentary habitats results in a corresponding pattern of gradients in the composition of structure-forming fauna and biogenic structures representative of each eCognition acoustic patch types (Table 5.3-3B). In summary, eCognition patches exhibit significant differences in both taxa and biogenic features such that each class has distinct characteristics useful to differentiate and map elements of habitats.

Table 5.3- 1. List of taxa and biogenic features identified in survey imagery. Organisms were identified to the lowest taxon possible. SFT = Structure-forming taxa and denoted by row as "S."

Taxa	Common name - description	SFT	Major taxonomic group
Ahnfeltia plicata	landlady's wig	S	Rhodophyta
Amphipoda unidentified	unidentified amphipod		Crustacea
Andara spp.	unidentified cockle	S	Mollusca
Anomiidae	jingle shell	S	Mollusca
Anomura unidentified	unidentified crab		Anomura
Anthozoa anemone	unidentified anemone	S	Anthozoa
Arbacia punctulata	purple sea urchin	S	Echinodermata
Argopecten irradians	Bay scallop	S	Mollusca
Ascidacea colonial	Colonial ascidian	S	Tunicata
Ascidacea solitary	Solitary ascidian	S	Tunicata
Ascophyllum nodosum	rockweed, brown alga	S	Ochrophyta
Astarte undata	waved astarte	S	Mollusca
Asteroidea	unidentified seastar		Echinodermata
Astrangia poculata	northern star coral	S	Anthozoa
Astyris lunata	lunar dovesnail		Mollusca
Asterias forbesi	Forbes sea star		Echinodermata
bilvalve siphon	bivalve siphon	S	Mollusca
Bivalvia unidentified	bivalve	S	Mollusca
Botrylloides diegensis	chain sea squirt	S	Tunicata
Brachyura	unidentified brachyuran crab		Decapoda
Bryozoa encrusting	unidentified encrusting bryozoa		Bryozoa
Busyconidae	unidentified whelk		Mollusca
Cancer borealis	Jonah crab		Decapoda
Cancer irroratus	Rock crab		Decapoda
Cancer spp.	Cancrid crab		Decapoda
Caprellidae	skeleton shrimp		Amphipoda
Cardiidae	cockle		Mollusca
Cerastoderma pinnulatum	northern dwarf cockle	S	Mollusca
Ceriantheopsis americana	North American tube anemone	S	Anthozoa
Cerripedia	unidentified barnacle	S	Crustacea
Cheliostomata	calcified bryozoan	S	Bryozoa
Chlorophyta	unidentified green macroalgae	S	Chlorophyta
Chondrus crispus	Irish moss	S	Rhodophyta
Chorda filum	sea lace	S	Ochrophyta
Ciona intestinalis	sea vase	S	Tunicata

Cliona spp.	boring sponge	S	Porifera
Coccotylus truncatus	leaf weed	S	Rhodophyta
Codium fragile	dead man's fingers	S	Chlorophyta
Corallina officinalis	coral weed	S	Rhodophyta
Corymorpha pendula	solitary pendula	S	Hydrozoa
Coryphella verrucosa	aeolid nudibranch		Nudibranchia
Costoanachis lafresnayi	well-ribbed dove snail		Mollusca
Crepidula fornicata	common slipper shell	S	Mollusca
Crucibulum striatum	striate cup-and-saucer	S	Mollusca
Cyclocardia borealis	northern cardida	S	Mollusca
Dendronotidea	dendronotid nudibranch		Mollusca
Desmarestia viridis	sour weed	S	Ochrophyta
Diadumene leucolena	ghost anemone	S	Anthozoa
Dichelopandalus leptocerus	bristled longbeak		Decapoda
Didemnum candidum	white colonial ascidian	S	Tunicata
Didemnum vexillum	sea vomit	S	Tunicata
Echinarachnius parma	common sand dollar		Echinodermata
Ectopleura crocea	pink-mouth hydroid	S	Hydrozoa
epifauna unidentified		S	
Euspira heros	northern moon snail		Mollusca
Fissurellidae	keyhole limpet	S	Mollusca
Fucus vesiculosus	bladder wrack	S	Ochrophyta
Gastropod nudibranch unidentified	unidentified nudibranch		Mollusca
Gastropod unidentified	unidentified snail		Mollusca
Grinellia americana	Grinnell's pink leaf	S	Rhodophyta
Halcampa duodecimcirrata	twelve-tentacle burrowing anemone	S	Anthozoa
Halichondria panicea	breadcrumb sponge	S	Porifera
Haliclona spp.	sponge	S	Porifera
Halisarca spp.	orange sponge	S	Porifera
Henricia sanguinolenta	blood star		Echinodermata
Hidenbrandia rubra	rusty rock	S	Rhodophyta
Holothroidea	sea cucumber		Echinodermata
Homarus americanus	American lobster		Decapoda
Hydroides dianthus	hard tube worm	S	Polychaeta
Hydrozoa-bryozoa erect	erect hydroid-bryozoan aggregate	S	Hydrozoa-Bryozoa
Ilyanassa spp.	mudsnail		Mollusca
Isopoda	Isopod		Crustacea
Laminariaceae	kelp	S	Ochrophyta
Libinia emarginata	spider crab		Crustacea
Libinia dubia	longnose spider crab		Crustacea
Doryteuthis pealeii	longfin squid		Mollusca
Euspira heros	northern moon snail		Mollusca
Macroalgae unidentified	macroalgae	S	Eukaryota
Majidae	crab		Decapoda
Melobesioideae	corallline algae		Rhodophyta
Mercenaria	quahog	S	Mollusca
Metridium senile	frilled anemone	S	Anthozoa

Microciona prolifera	red beard sponge	S	Porifera
Mogula spp.	sea grape	S	Tunicata
Mycale fibrexilis	flabby sponge	S	Porifera
Mysidea	mysid shrimp		Crustacea
Mytilus edulis	blue mussel	S	Mollusca
Nemertean	ribbon worm		Nemertea
Nucella lapillus	dog whelk		Mollusca
Encrusting macroalgae	unidentified encrusting macroalgae		Eukaryota
Paguridae	unidentified hermit crab		Decapoda
Palmaria palmata	dulse	S	Rhodophyta
Penaeidae	shrimp		Decapoda
Phaeophyceae	brown macroalgae	S	Ochrophyta
Placopecten magellancius	giant scallop	S	Mollusca
Polychaeta	polychaete worm	S	Polychaeta
Polyides rotundus	twig weed	S	Rhodophyta
Polymastia robusta	nipple sponge	S	Porifera
Polyplacophora	chiton	S	Mollusca
Polysiphonia spp.	polly	S	Rhodophyta
Porifera spp.	sponge	S	Porifera
Porphyra spp.	nori	S	Rhodophyta
Portunidae	swimming crab		Crustacea
Pycnogonida	sea spider		Arthropoda
Ralfsia verrucosa	tarspot		Ochrophyta
Rhodophyta	red macroalgae	S	Rhodophyta
Sabellid encrusting	featherduster worm	S	Polychaeta
Serpula spp.	tube building annelid	S	Polychaeta
Spirorbis spp.	coiled tube worm	S	Polychaeta
Spisula solidissima	Atlantic surf clam	S	Mollusca
Squilla empusa	mantis shrimp		Crustacea
Strongylocentrotus droebachiensis	green sea urchin		Echinodermata
Terebellida	bristle worm	S	Polychaeta
Tubularia indivisa	oaten pipes hydroid	S	Hydrozoa
Tubulariidae spp.	unidentified hydroid	S	Hydrozoa
Tunicata colonial	colonial tunicate	S	Tunicata
Ulva lactuca	sea lettuce	S	Chlorophyta
Unidentified siphon	emergent siphon	S	
Urosalpinx cinerea	Atlantic oyster drill		Mollusca
Worm-like organism unidentified	unidentified invertebrate		

Biogenic feature	Common name - description	Major taxonomic group
Astrangia poculata skeleton	skeleton of star coral	Anthozoa
biogenic depression	animal formed depression	
biogenic mound	animal formed mound	
biogenic tube unidentified	emergent animal produced tube	
Cirripedia test	attached barnacle test	Crustacea
Chondrichthyes egg case	egg case	Chondrichthyes
Crepidula spp. shell	shell	Mollusca

Crustacea exoskeleton	exoskeleton - molt or death	Crustacea
Diopatra tube	emergent tube	Polychaeta
Echinarachnius parma test	sand dollar test	Echinodermata
encrusting worm tube	encrusting tube	Polychaeta
Euspira spp. egg collar	egg collar	Mollusca
Euspira spp. shell	shell	Mollusca
Gastropod egg case	egg case	Mollusca
Gastropoda shell	shell	Mollusca
Hydroides dianthus tube	worm tube	Polychaeta
large burrow	animal produced burrow	
Macroalgal debris	unattached macroalgae	Eukaryota
medium burrow	animal produced burrow	
Mytilus edulis valve	shell	Mollusca
Nudibranch egg string	egg string	Mollusca
Shell hash	shell	Mollusca
Shell whole-partial	shell	Mollusca
siphon emergent unidentified	emergent bivalve siphon	Mollusca
small burrow	animal produced burrow	
Spirobis worm tube	attached worm tube	Polychaeta
Terrestrial vegetation debris	unattached terrestrial debris	
Urchin test	test	Echinodermata
Whelk shell	shell	Mollusca
Worm castings	coherent sediment in organic	Polychaeta
Worm tube flexible erect	emergent tube from sediment	Polychaeta
Worm tube debris	unanchored worm tube	Polychaeta
Zostera-seagrass debris	unattached seagrass debris	

Table 5.3- 2 Table 5.3-2. Results of ANOSIM procedure for comparisons of taxa and feature cover values based on assignment to eCognition acoustic patches as well as environmental factors (depth, TRI, tau max, longitude). Each cell includes the Global R value for each set of comparisons and significance level. Blocks-sites scale analyses, for aggregated image samples, are based on seasonal and total samples over time. Groups are based on results of hierarchical clustering of community composition (all significant clusters) and results of an iterative aggregation of cluster groups by geospatial adjacencies into four principle sub-areas with data from both seasons.

	2017	2017	2018	2018	2017-18	2017-18
Factors	Taxa/Features	Taxa	Taxa/Features	Taxa	Taxa/Features	Taxa
eCognition	0.077/0.1%	0.013/17.9%	0.077/0.1%	0.035/1.4%		
Depth	0.032/1.3%	0.075/0.1%	(0.037)/98.8%	0.06/0.2%		
TRI	0.075/0.1%	0.044/0.1%	(0.016)/92.7%	0.005/32.9%		
Tau max	0.248/0.1%	0.101/0.1%	0.07/0.1%	0.026/0.5%		
W-E Longitude	0.104/0.1%	0.119/0.1%	0.105/0.1%	0.195/0.1%		
Blocks & Sites						
All Clusters 1%	0.828/0.1%	0.784/0.1%	0.865/0.1%	0.811/0.1%	0.809/0.1%	0.665/0.1%
Cluster 1% 4 Grps					0.339/0.1%	0.364/0.1%

Table 5.3- 3A. Mean cover value, based on percent cover, for select biogenic habitat features and structure-forming taxa from fall 2017/spring 2018 surveys. These features and taxa were selected based on patterns of dominance and occurrence over the study region. Note that patch type A did not have any image samples collected in spring 2018, so cells contain "NA" as not available. (Column abbreviations as follows: SH = whole- partial shell, TB = terrestrial plant debris, ZD = Zostera debris, RH = Rhodophyta, LA = Laminariaceae, HB = hydrozoa/bryozoa, AP = Astrangia poculata, DL = Diadumene leucolena, CS = Crepidula sp., ME = Mytilus edulis, CL = Cliona spp., DS = Didemnum spp., CP = Corymorpha pendula.) B. Ranked order based on max value (from seasonal means). C. Mean, variance, and range of physical habitat characteristics.

A.

		Biogenic Features			Structure-forming Fauna									
eCog	Grain size	SH	TB	ZD	RH	LA	HB	AP	DL	CS	ME	CL	DS	CP
A	Sandy silt	24.7 NA	0 NA	0.5 NA	6.6 NA	0 NA	10.8 NA	0 NA	0 NA	31.7 NA	0 NA	6.4 NA	0 NA	0 NA
B	Silty sand	25.8 20.9	0.2 1.4	1 4.3	6.8 12.9	0.1 0.9	6.7 13.8	0.1 0.1	0.5 2.4	1.8 2.2	0.1 0	<0.1 1	0.1 0.1	0 0.1
C	Gravel- sand	32.4 33.4	0.5 1.6	2.1 2.4	4.4 3.8	0.1 0.8	11.7 26.6	0.4 0.9	5.4 2.6	6 5.7	<0.1 0.3	1.6 0.8	0.7 0.8	0 1.5
D	Gravelly sand	54.8 44.8	0.1 1	1.9 2.4	4.4 4	0 0.7	13 33	2.4 0.7	2.7 4.9	7.4 3.3	0.1 1.4	1.3 1.1	0.9 1.3	0 1.7
E	Gravelly sediment	77 50.3	0 0	0 0	0 0	0 0	22.9 53.4	0 1	0 0	0.5 1	0.3 0	0 0	1 0	0 4.4

B.

	Ranked order			Ranked order fauna									
eCog	SH	TB	ZD	R	LA	HB	AP	DL	CS	ME	CL	DS	CP
A	5	0	4	2	0	5	0	0	1	0	1	0	0
B	4	2	1	1	1	4	4	3	4	4	4	4	4
C	3	1	2	3	2	3	3	1	3	3	2	3	3
D	2	3	3	4	3	2	1	2	2	1	3	1	2
E	1	0	0	0	0	1	2	0	5	2	0	2	1

C.

eCog	Mean Depth	Depth SD	Depth Range	Mean TRI	Depth TRI	TRI Range	Mean Max Tau	Depth Max Tau	Max Tau Range
A	-9	0.1	-9.1 to -8.9	0.047	0.048	0.013 to 0.142	0.46	0.004	0.452 to 0.461
B	-21.4	17.8	-86.8 to -5	0.212	0.294	0.002 to 1.867	0.686	0.386	0.191 to 2.685
C	-27.6	18.9	-95 to -5.4	0.231	0.26	0.004 to 1.703	0.807	0.352	0.191 to 2.685
D	-34.2	18.6	-89.5 to -6.3	0.157	0.183	0.003 to 1.666	0.991	0.311	0.259 to 1.865
E	-34.4	7.1	-47.8 to -30.5	0.059	0.025	0.024 to 0.093	0.952	0.024	0.938 to 0.997

Additional factors, derived from geographically comprehensive data sets of observed and derived metrics within the study area were used to identify proxies to explain additional variation in distribution of taxa and biogenic features (Table 5.3-3C). These factors are depth (from multibeam bathymetry), TRI (derived from variation in bathymetry based on a moving window of surrounding each cell), tau max (value from the model of seafloor stress, see Section 6), and longitude (as an index of west to east variation in site characteristics). Each image sample was classified based on associated eCognition acoustic patch (i.e., A-E) and actual values for each of the environmental factors assigned.

PCA was used to assess the interactions of depth, TRI, tau max, and longitude values for each image sample in explaining variation in image location and coincident eCognition patch assignments. A PCA biplot (Figure 5.3-9) visualizes the PC scores of samples (points) and loadings of variables (vectors). The further away these vectors are from a PC origin, the more influence they have on that PC. Loading plots also provide some inference on which factors correlate with one another, with a small angle between factors indicating a positive correlation while a large angle indicates a negative correlation. A 90° angle indicates no correlation between two factors.

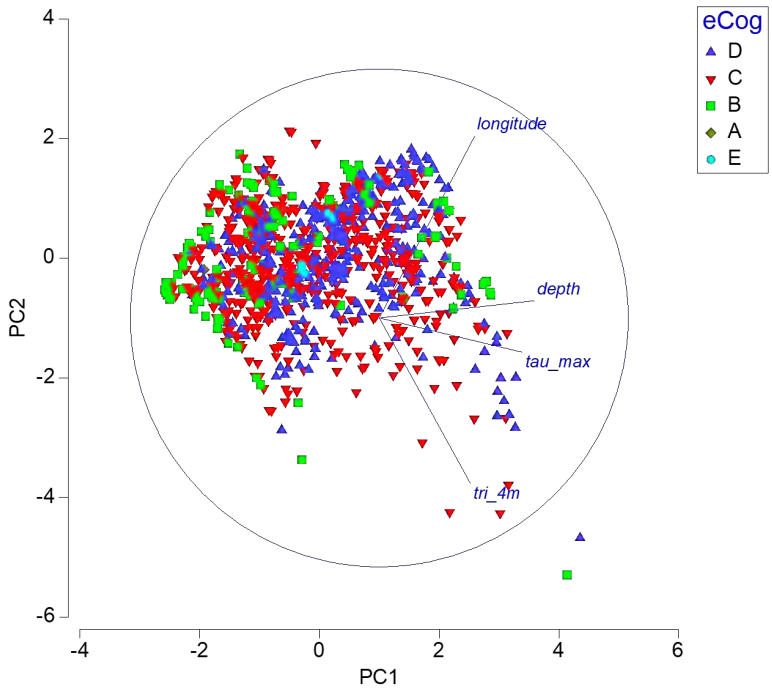

Figure 5.3- 9. PCA biplot of environmental factors (see text for details). Factors are depth, TRI, tau max, and longitude. Factors were normalized for all locations.

Here we find vectors for depth and tau max are separated by a small angle indicating a positive correlation, while TRI and longitude with opposing angles infer a negative correlation. TRI and depth as well as longitude and tau max are at nearly 90° separation indicating little correlation in these paired factors. The first two eigenvectors represent 65.1% of the variation in the data. The sample points in the PCA biplot show some separation and clustering of each eCognition class based on differences in the environmental factors attributed to each image, further indicating fundamental differences in habitat attributes.

An nMDS analysis validates this pattern with a low stress value (Figure 5.3-10). The global R for each environmental factor in results from ANOSIM for each survey (Table 5.3-2) are

generally highly significant. The SIMPER results illustrate that each of the factors is important in quantifying the dissimilarities in pair-wise comparisons by patch type (Table 5.3-4).

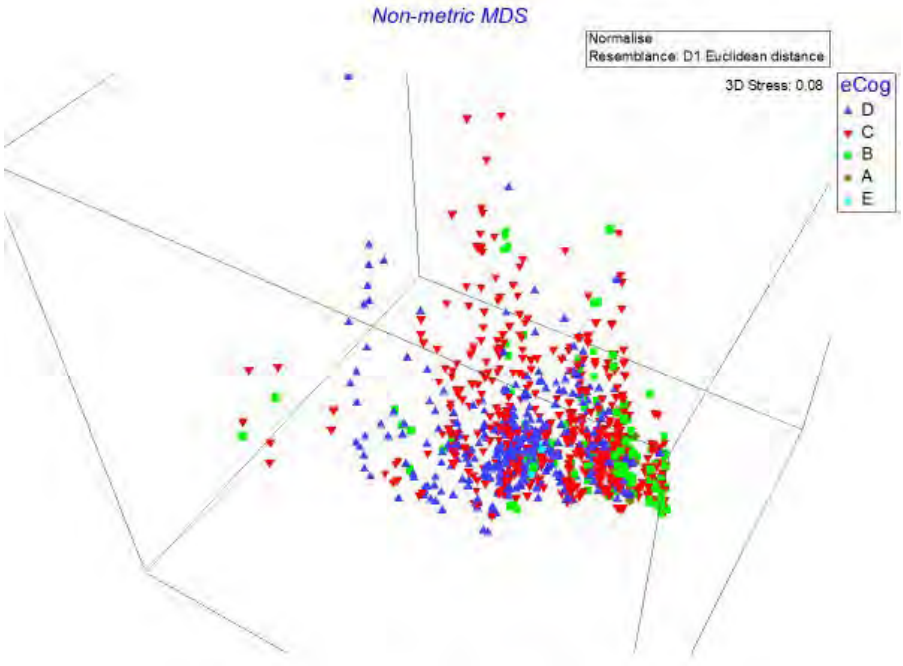

Figure 5.3- 10. A 3-D nMDS plot of the four environmental factors analyzed in the PCA above, classified for each eCognition patch type. Note the low stress value, indicate this plot is realistic representation of differences and similarities between samples (images).

Table 5.3- 4 Table 5.3-4. Results pf SIMPER analyses of faunal and biogenic feature differences across eCognition patch types (A-E). Tables separate seasons (fall, spring) and live taxa only (no features) and taxa with biogenic features.

I. Fall 2017 Live taxa

Groups B & C
Average dissimilarity =87.43

eCog	Group B	Group C				
Species	Av.Abund	Av.Abund	Av.Diss	Diss/SD	Contrib%	Cum.%
Hydrozoa bryozoa erect	14.48	25.27	17.6	0.98	20.13	20.13
gastropod_unidentified	5.31	8.09	9.28	0.71	10.62	30.75
Crepidula fornicata	3.85	12.9	8.5	0.61	9.72	40.47
Rhodophyta	14.75	9.61	7.89	0.52	9.03	49.49
Paguridae	2.86	3.14	7.84	0.52	8.97	58.46
Cirripedia_unstalked	4.43	5.65	7.75	0.64	8.87	67.33
Diadumene leucolena	1.15	11.61	3.88	0.33	4.43	71.76

Groups B & D
Average dissimilarity =85.71

	Group B	Group D				
Species	Av.Abund	Av.Abund	Av.Diss	Diss/SD	Contrib%	Cum.%
Hydrozoa bryozoa erect	14.48	28.16	20.56	1.08	23.99	23.99
Crepidula fornicata	3.85	15.9	9.26	0.68	10.8	34.79
Cirripedia_unstalked	4.43	11.05	8.75	0.71	10.21	45
gastropod_unidentified	5.31	8.9	8.53	0.82	9.95	54.95

Rhodophyta	14.75	9.42	7.64	0.48	8.91	63.85
Paguridae	2.86	2.04	5.19	0.52	6.06	69.91
Chondrus crispus	10.29	4.31	3.63	0.37	4.24	74.15

Groups C & D
Average dissimilarity =83.21

	Group C	Group D				
Species	Av.Abund	Av.Abund	Av.Diss	Diss/SD	Contrib%	Cum.%
Hydrozoa bryozoa erect	25.27	28.16	18.74	1.11	22.53	22.53
Crepidula fornicata	12.9	15.9	9.8	0.71	11.78	34.31
Cirripedia_unstalked	5.65	11.05	7.74	0.69	9.3	43.61
gastropod_unidentified	8.09	8.9	7.4	0.79	8.9	52.51
Rhodophyta	9.61	9.42	6.6	0.5	7.93	60.44
Diadumene leucolena	11.61	5.9	4.75	0.4	5.71	66.14
Paguridae	3.14	2.04	3.98	0.49	4.78	70.93

Groups B & E
Average dissimilarity = 81.13

	Group B	Group E				
Species	Av.Abund	Av.Abund	Av.Diss	Diss/SD	Contrib%	Cum.%
Hydrozoa_bryozoa_erect	14.48	49.5	36.79	1.97	45.35	45.35
Cirripedia_unstalked	4.43	11	9.71	1.25	11.97	57.31
gastropod_unidentified	5.31	10.5	8.08	1.3	9.96	67.28
Paguridae	2.86	9.33	6.8	0.85	8.38	75.66

Groups C & E
Average dissimilarity =76.98

	Group C	Group E				
Species	Av.Abund	Av.Abund	Av.Diss	Diss/SD	Contrib%	Cum.%
Hydrozoa_bryozoa_erect	25.27	49.5	30.06	1.69	39.05	39.05
Cirripedia_unstalked	5.65	11	8.12	1.12	10.54	49.59
gastropod_unidentified	8.09	10.5	6.99	1.13	9.07	58.67
Paguridae	3.14	9.33	5.85	0.76	7.6	66.27
Crepidula fornicata	12.9	1	4.6	0.47	5.97	72.24

Groups D & E
Average dissimilarity = 8.40

	Group D	Group E				
Species	Av.Abund	Av.Abund	Av.Diss	Diss/SD	Contrib%	Cum.%
Hydrozoa_bryozoa_erect	28.16	49.5	23.85	1.43	34.87	34.87
Cirripedia_unstalked	11.05	11	8.28	1.12	12.11	46.98
Crepidula fornicata	15.9	1	5.79	0.58	8.46	55.44
gastropod_unidentified	8.9	10.5	5.59	1.11	8.17	63.61
Paguridae	2.04	9.33	4.95	0.79	7.24	70.85

Table 5.3-4 continued,

Groups B & A
Average dissimilarity =88.99

Species	Group B Av.Abund	Group A Av.Abund	Av.Diss	Diss/SD	Contrib%	Cum.%
Crepidula fornicata	3.85	68.5	30.28	2.21	34.03	34.03
Hydrozoa_bryozoa_erect	14.48	22.33	10.99	1.26	12.35	46.38
Rhodophyta	14.75	14.33	10.63	0.82	11.95	58.32
Grinellia americana	0	18.83	5.74	0.66	6.45	64.78
Porphyra spp	3.49	8.17	5.55	0.66	6.23	71.01

Groups C & A
Average dissimilarity =85.12

Species	Group C Av.Abund	Group A Av.Abund	Av.Diss	Diss/SD	Contrib%	Cum.%
Crepidula fornicata	12.9	68.5	27.02	1.98	31.74	31.74
Hydrozoa bryozoa erect	25.27	22.33	11.13	1.23	13.08	44.81
Rhodophyta	9.61	14.33	8.01	0.81	9.41	54.23
Grinellia americana	0.27	18.83	5.3	0.65	6.22	60.45
Cliona spp.	3.35	13.83	5.28	1.04	6.21	66.66
Porphyra spp.	1.28	8.17	4.51	0.63	5.3	71.96

Groups D & A
Average dissimilarity = 81.26

Species	Group D Av.Abund	Group A Av.Abund	Av.Diss	Diss/SD	Contrib%	Cum.%
Crepidula fornicata	15.9	68.5	24.42	1.89	30.05	30.05
Hydrozoa bryozoa erect	28.16	22.33	11.59	1.09	14.26	44.31
Rhodophyta	9.42	14.33	7.53	0.79	9.26	53.58
Grinellia americana	0.03	18.83	5.05	0.66	6.22	59.8
Cliona spp.	2.73	13.83	4.79	1.16	5.9	65.7
Cirripedia_unstalked	11.05	2.17	4.24	0.58	5.22	70.91

Groups E & A
Average dissimilarity = 80.79

Species	Group E Av.Abund	Group A Av.Abund	Av.Diss	Diss/SD	Contrib%	Cum.%
Crepidula fornicata	1	68.5	24.07	2.21	29.8	29.8
Hydrozoa bryozoa erect	49.5	22.33	18.03	1.3	22.32	52.12
Rhodophyta	0	14.33	5.08	0.98	6.29	58.41
Grinellia americana	0	18.83	5.04	0.68	6.23	64.64
Cirripedia_unstalked	11	2.17	4.9	1.09	6.07	70.71

Table 5.3-4 continued,

II. Fall 2017 Live taxa and biogenic features

Groups B & C
Average dissimilarity = 74.20

eCog	Group B	Group C				
Species	Av.Abund	Av.Abund	Av.Diss	Diss/SD	Contrib%	Cum.%
shell whole piece	55.74	77.03	16.15	1.21	21.77	21.77
shell hash	46.55	48.72	14.09	1.04	18.99	40.76
Hydrozoa bryozoa erect	14.48	25.27	5.93	0.76	7.99	48.75
Rhodophyta	14.75	9.61	3.94	0.47	5.31	54.07
worm castings	9.17	4.15	3.28	0.67	4.42	58.49
Crepidula_fornicata	3.85	12.9	2.7	0.45	3.64	62.13
Mytilus edulis valve	6.45	8.15	2.6	0.52	3.51	65.64
Chondrus crispus	10.29	6.33	2.4	0.39	3.24	68.87
worm tube flexible erect	5.02	4.43	2.2	0.57	2.96	71.83

Groups B & D
Average dissimilarity = 73.72

	Group B	Group D				
Species	Av.Abund	Av.Abund	Av.Diss	Diss/SD	Contrib%	Cum.%
shell whole piece	55.74	118.31	19.66	1.3	26.67	26.67
shell hash	46.55	38.44	11.65	0.99	15.8	42.47
Hydrozoa bryozoa erect	14.48	28.16	5.92	0.9	8.03	50.5
Mytilus edulis valve	6.45	18.61	4.31	0.61	5.85	56.35
Rhodophyta	14.75	9.42	3.61	0.44	4.89	61.24
Crepidula fornicata	3.85	15.9	2.97	0.52	4.02	65.26
worm castings	9.17	1.13	2.45	0.61	3.32	68.59
Cirripedia unstalked	4.43	11.05	2.32	0.63	3.14	71.73

Groups C & D
Average dissimilarity = 67.49

	Group C	Group D				
Species	Av.Abund	Av.Abund	Av.Diss	Diss/SD	Contrib%	Cum.%
shell whole piece	77.03	118.31	15.89	1.22	23.55	23.55
shell hash	48.72	38.44	10.89	0.99	16.13	39.68
Hydrozoa bryozoa erect	25.27	28.16	6.05	1	8.97	48.64
Mytilus edulis valve	8.15	18.61	4.14	0.62	6.13	54.77
Crepidula fornicata	12.9	15.9	3.72	0.58	5.51	60.29
Rhodophyta	9.61	9.42	2.73	0.47	4.04	64.33
Diadumene leucolena	11.61	5.9	2.41	0.39	3.57	67.9
Cirripedia unstalked	5.65	11.05	2.26	0.64	3.35	71.25

Table 5.3-4 continued,

Groups B & E
Average dissimilarity = 73.47

Species	Group B Av.Abund	Group E Av.Abund	Av.Diss	Diss/SD	Contrib%	Cum.%
shell whole piece	55.74	166.33	23.03	1.7	31.35	31.35
Hydrozoa bryozoa erect	14.48	49.5	8.52	1.8	11.59	42.95
shell hash	46.55	5.17	7.87	0.85	10.71	53.66
Mytilus edulis valve	6.45	41.83	7.78	1.29	10.59	64.25
Cirripedia test	1.8	34.67	6.5	2.01	8.84	73.09

Groups C & E
Average dissimilarity = 65.18

Species	Group C Av.Abund	Group E Av.Abund	Av.Diss	Diss/SD	Contrib%	Cum.%
shell whole piece	77.03	166.33	17.44	1.39	26.75	26.75
shell hash	48.72	5.17	7.81	0.86	11.98	38.74
Hydrozoa bryozoa erect	25.27	49.5	7.64	1.78	11.72	50.46
Mytilus edulis valve	8.15	41.83	7.15	1.29	10.97	61.43
Cirripedia test	3.34	34.67	5.71	1.88	8.76	70.19

Groups D & E
Average dissimilarity = 49.51

Species	Group D Av.Abund	Group E Av.Abund	Av.Diss	Diss/SD	Contrib%	Cum.%
shell whole piece	118.31	166.33	10.2	1.08	20.6	20.6
Mytilus edulis valve	18.61	41.83	6.43	1.26	12.99	33.59
Hydrozoa bryozoa erect	28.16	49.5	6.05	1.54	12.22	45.81
shell hash	38.44	5.17	5.73	0.74	11.58	57.39
Cirripedia test	10.74	34.67	4.93	1.73	9.96	67.35
Cirripedia unstalked	11.05	11	2.21	0.96	4.46	71.81

Groups B & A
Average dissimilarity = 82.39

Species	Group B Av.Abund	Group A Av.Abund	Av.Diss	Diss/SD	Contrib%	Cum.%
Crepidula fornicata shell	0.89	55.33	13.32	1.82	16.17	16.17
Crepidula_fornicata	3.85	68.5	12.99	1.69	15.76	31.93
shell whole piece	55.74	36.83	10.04	1.19	12.19	44.11
shell hash	46.55	10	9.34	0.9	11.34	55.45
Hydrozoa bryozoa erect	14.48	22.33	5.01	0.95	6.08	61.53
Rhodophyta	14.75	14.33	4.42	0.66	5.36	66.89
Grinellia americana	0	18.83	3.17	0.68	3.84	70.73

Table 5.3-4 continued,

Groups C & A
Average dissimilarity = 78.56

Species	Group C Av.Abund	Group A Av.Abund	Av.Diss	Diss/SD	Contrib%	Cum.%
Crepidula fornicata	12.9	68.5	11.93	1.62	15.18	15.18
Crepidula fornicata shell	3.21	55.33	11.69	1.78	14.88	30.07
shell whole piece	77.03	36.83	11.56	1.25	14.71	44.78
shell hash	48.72	10	8.99	0.87	11.44	56.22
Hydrozoa bryozoa erect	25.27	22.33	5.31	1.02	6.76	62.98
Rhodophyta	9.61	14.33	3.23	0.78	4.11	67.09
Grinellia americana	0.27	18.83	2.93	0.68	3.73	70.82

Groups D & A
Average dissimilarity = 77.03

Species	Group D Av.Abund	Group A Av.Abund	Av.Diss	Diss/SD	Contrib%	Cum.%
shell whole piece	118.31	36.83	16.53	1.58	21.46	21.46
Crepidula fornicata	15.9	68.5	10.61	1.57	13.77	35.23
Crepidula fornicata shell	3.37	55.33	10.3	1.85	13.37	48.59
shell hash	38.44	10	6.75	0.8	8.77	57.36
Hydrozoa bryozoa erect	28.16	22.33	4.85	1.09	6.3	63.66
Mytilus edulis valve	18.61	0	3.34	0.55	4.33	67.99
Rhodophyta	9.42	14.33	3.08	0.69	4	71.99

Groups E & A
Average dissimilarity = 78.95

Species	Group E Av.Abund	Group A Av.Abund	Av.Diss	Diss/SD	Contrib%	Cum.%
shell whole piece	166.33	36.83	22.07	3.26	27.95	27.95
Crepidula fornicata	1	68.5	9.89	1.69	12.53	40.49
Crepidula fornicata shell	0.67	55.33	9.41	2.49	11.92	52.4
Mytilus edulis valve	41.83	0	7.2	1.4	9.12	61.53
Hydrozoa bryozoa erect	49.5	22.33	6.01	1.59	7.62	69.14
Cirripedia test	34.67	3	5.43	2.09	6.87	76.02

III. 2018 Spring Live taxa
Groups B & D
Average dissimilarity = 86.45
eCog

Species	Group B Av.Abund	Group D Av.Abund	Av.Diss	Diss/SD	Contrib%	Cum.%
Hydrozoa bryozoa erect	29.84	71.28	22.99	1.16	26.59	26.59
Rhodophyta	27.77	8.73	10.02	0.68	11.59	38.18
Phaeophyceae	17.66	8.03	6.72	0.62	7.77	45.95
Paguroidea spp. unidentified	5.96	8.58	5.06	0.59	5.85	51.8

Chorda filum	11.81	6.76	5.04	0.55	5.83	57.63
Tubularia indivisa	6.3	13.78	4.27	0.38	4.94	62.57
Crepidula fornicata	4.76	7.19	3.45	0.43	3.99	66.56
Tubulariidae spp.	3.04	4.6	3.31	0.47	3.82	70.38

Groups B & C
Average dissimilarity = 86.94

	Group B	Group C				
Species	Av.Abund	Av.Abund	Av.Diss	Diss/SD	Contrib%	Cum.%
Hydrozoa bryozoa erect	29.84	57.39	21.82	1.1	25.09	25.09
Rhodophyta	27.77	8.27	10.83	0.68	12.46	37.55
Phaeophyceae	17.66	6.4	7	0.61	8.06	45.6
Paguroidea spp. unidentified	5.96	8.77	5.52	0.55	6.35	51.95
Chorda filum	11.81	5.69	5.38	0.52	6.19	58.14
Crepidula fornicata	4.76	12.27	4.56	0.48	5.24	63.39
Chondrus crispus	6.27	8.23	4.28	0.34	4.92	68.31
Tubulariidae spp.	3.04	4.41	3.81	0.45	4.38	72.68

Groups D & C
Average dissimilarity = 82.86

	Group D	Group C				
Species	Av.Abund	Av.Abund	Av.Diss	Diss/SD	Contrib%	Cum.%
Hydrozoa bryozoa erect	71.28	57.39	26.16	1.21	31.57	31.57
Paguroidea spp. unidentified	8.58	8.77	5.63	0.6	6.8	38.36
Rhodophyta	8.73	8.27	5.13	0.48	6.19	44.55
Crepidula fornicata	7.19	12.27	5.09	0.53	6.15	50.7
Tubularia indivisa	13.78	5.24	4.22	0.4	5.09	55.79
Phaeophyceae	8.03	6.4	3.68	0.52	4.44	60.24
Chorda filum	6.76	5.69	3.58	0.41	4.32	64.56
Tubulariidae spp.	4.6	4.41	3.24	0.44	3.91	68.47
Gastropoda unidentified	6.35	4.29	3.23	0.46	3.9	72.36

Groups B & E
Average dissimilarity = 83.47

	Group B	Group E				
Species	Av.Abund	Av.Abund	Av.Diss	Diss/SD	Contrib%	Cum.%
Hydrozoa bryozoa erect	29.84	115.25	35.08	1.63	42.03	42.03
Rhodophyta	27.77	0	8.06	0.62	9.65	51.68
Phaeophyceae	17.66	0	4.98	0.52	5.97	57.65
Tubularia indivisa	6.3	9.25	4.95	0.66	5.93	63.58
Paguroidea spp. unidentified	5.96	14	4.74	0.89	5.68	69.26
Chorda filum	11.81	0	3.3	0.49	3.96	73.22

Table 5.3-4 continued,

Groups D & E
Average dissimilarity = 72.28

Species	Group D Av.Abund	Group E Av.Abund	Av.Diss	Diss/SD	Contrib%	Cum.%
Hydrozoa bryozoa erect	71.28	115.25	32.59	1.47	45.09	45.09
Tubularia indivisa	13.78	9.25	5.63	0.67	7.79	52.88
Paguroidea spp. unidentified	8.58	14	4.74	0.97	6.56	59.44
Corymorpha pendula	3.77	9.5	3.02	0.7	4.17	63.61
Cerripedia	5.72	4.75	2.76	0.66	3.82	67.43
Tubulariidae spp.	4.6	3.5	2.56	0.62	3.55	70.98

Groups C & E
Average dissimilarity = 75.52

Species	Group C Av.Abund	Group E Av.Abund	Av.Diss	Diss/SD	Contrib%	Cum.%
Hydrozoa bryozoa erect	57.39	115.25	35.76	1.54	47.35	47.35
Paguroidea spp. unidentified	8.77	14	4.93	1.03	6.53	53.89
Tubularia indivisa	5.24	9.25	4.58	0.76	6.06	59.95
Crepidula fornicata	12.27	2.25	3.33	0.46	4.41	64.36
Corymorpha pendula	3.21	9.5	3.1	0.66	4.1	68.47
Tubulariidae spp.	4.41	3.5	2.77	0.59	3.66	72.13

Groups B & NA
Average dissimilarity = 88.91

Species	Group B Av.Abund	Group NA Av.Abund	Av.Diss	Diss/SD	Contrib%	Cum.%
Paguroidea spp. unidentified	5.96	20.75	16.9	0.94	19.01	19.01
Hydrozoa bryozoa erect	29.84	4.44	14.1	0.83	15.86	34.87
Rhodophyta	27.77	1.56	12.1	0.7	13.61	48.48
Phaeophyceae	17.66	0.13	7.39	0.57	8.31	56.79
Tubulariidae spp.	3.04	6.19	6.5	0.64	7.31	64.1
Chorda filum	11.81	0.94	5.49	0.55	6.18	70.27

Groups D & NA
Average dissimilarity = 88.78

Species	Group D Av.Abund	Group NA Av.Abund	Av.Diss	Diss/SD	Contrib%	Cum.%
Hydrozoa bryozoa erect	71.28	4.44	26.57	1.19	29.92	29.92
Paguroidea spp. unidentified	8.58	20.75	15.08	0.86	16.99	46.92
Tubulariidae spp.	4.6	6.19	6.12	0.61	6.89	53.81
Rhodophyta	8.73	1.56	4.18	0.45	4.71	58.52
Tubularia indivisa	13.78	0	3.79	0.34	4.27	62.79
Crepidula fornicata	7.19	1.31	3.59	0.47	4.04	66.83
Gastropoda unidentified	6.35	1	3.49	0.51	3.93	70.76

Table 5.3-47 continued,

Groups C & NA
Average dissimilarity = 89.26

Species	Group C Av.Abund	Group NA Av.Abund	Av.Diss	Diss/SD	Contrib%	Cum.%
Hydrozoa bryozoa erect	57.39	4.44	23.81	1.1	26.67	26.67
Paguroidea spp. unidentified	8.77	20.75	18.4	0.88	20.61	47.28
Tubulariidae spp.	4.41	6.19	7.18	0.6	8.05	55.33
Crepidula fornicata	12.27	1.31	4.97	0.51	5.57	60.9
Rhodophyta	8.27	1.56	4.61	0.45	5.16	66.06
Gastropoda unidentified	4.29	1	3.37	0.48	3.78	69.83
Chorda filum	5.69	0.94	3.3	0.35	3.69	73.53

Groups E & NA
Average dissimilarity = 87.77

Species	Group E Av.Abund	Group NA Av.Abund	Av.Diss	Diss/SD	Contrib%	Cum.%
Hydrozoa bryozoa erect	115.25	4.44	50.2	3.13	57.2	57.2
Paguroidea spp. unidentified	14	20.75	11.78	1.04	13.42	70.62

IV. Spring 2018 Live taxa and biogenic features

Groups B & D
Average dissimilarity = 72.69
eCog

Species	Group B Av.Abund	Group D Av.Abund	Av.Diss	Diss/SD	Contrib%	Cum.%
shell hash	81.68	97.71	12.99	1.14	17.87	17.87
Shell whole partial	45.04	96.87	11.47	1.32	15.79	33.66
Hydrozoa bryozoa erect	29.84	71.28	9.41	1.07	12.94	46.6
Rhodophyta	27.77	8.73	4.63	0.61	6.37	52.97
Phaeophyceae	17.66	8.03	3.07	0.55	4.22	57.19
Tubularia indivisa	6.3	13.78	2.49	0.35	3.43	60.62
Chorda filum	11.81	6.76	2.36	0.53	3.25	63.87
Diadumene leucolena	5.24	10.53	1.85	0.37	2.55	66.42
Mytilus edulis valve	0.5	16.3	1.84	0.43	2.53	68.95
terrestrial vegetation debris	11.05	0.2	1.81	0.26	2.5	71.45

Groups B & C
Average dissimilarity = 73.39

Species	Group B Av.Abund	Group C Av.Abund	Av.Diss	Diss/SD	Contrib%	Cum.%
shell hash	81.68	88.86	14.34	1.11	19.53	19.53
Shell whole partial	45.04	72.11	10.16	1.2	13.84	33.37
Hydrozoa bryozoa erect	29.84	57.39	8.87	0.99	12.08	45.46
Rhodophyta	27.77	8.27	4.94	0.61	6.72	52.18
Phaeophyceae	17.66	6.4	3.17	0.56	4.32	56.5

Chorda filum	11.81	5.69	2.54	0.51	3.46	59.96
terrestrial vegetation debris	11.05	2.54	2.44	0.29	3.33	63.29
worm castings	9.27	9.28	2.16	0.77	2.94	66.22
Chondrus crispus	6.27	8.23	2.14	0.34	2.92	69.15
Crepidula fornicata	4.76	12.27	1.9	0.44	2.6	71.74

Groups D & C
Average dissimilarity = 65.29

Species	Group D Av.Abund	Group C Av.Abund	Av.Diss	Diss/SD	Contrib%	Cum.%
shell hash	97.71	88.86	12.13	1.14	18.58	18.58
Shell whole partial	96.87	72.11	10.87	1.29	16.65	35.22
Hydrozoa bryozoa erect	71.28	57.39	10.19	1.11	15.61	50.83
Mytilus edulis valve	16.3	7.04	2.33	0.52	3.56	54.39
Tubularia indivisa	13.78	5.24	2.23	0.37	3.41	57.8
Rhodophyta	8.73	8.27	2.16	0.43	3.3	61.1
Crepidula fornicata	7.19	12.27	1.98	0.5	3.03	64.14
Diadumene leucolena	10.53	5.52	1.85	0.38	2.84	66.97
worm castings	5.02	9.28	1.65	0.6	2.53	69.51
Paguroidea spp. unidentified	8.58	8.77	1.61	0.84	2.47	71.97

Groups B & E
Average dissimilarity = 71.25

Species	Group B Av.Abund	Group E Av.Abund	Av.Diss	Diss/SD	Contrib%	Cum.%
Hydrozoa bryozoa erect	29.84	115.25	13.93	1.68	19.55	19.55
Shell whole partial	45.04	108.75	12.41	1.79	17.42	36.96
shell hash	81.68	83.25	11.99	1.24	16.83	53.79
Rhodophyta	27.77	0	4.3	0.55	6.04	59.84
Phaeophyceae	17.66	0	2.65	0.46	3.72	63.55
Tubularia indivisa	6.3	9.25	2.22	0.47	3.12	66.67
Paguroidea spp. unidentified	5.96	14	2	0.93	2.8	69.47
terrestrial vegetation debris	11.05	0	1.9	0.27	2.67	72.14

Groups D & E
Average dissimilarity = 56.15

Species	Group D Av.Abund	Group E Av.Abund	Av.Diss	Diss/SD	Contrib%	Cum.%
Hydrozoa bryozoa erect	71.28	115.25	12.37	1.47	22.03	22.03
Shell whole partial	96.87	108.75	10.06	1.41	17.91	39.95
shell hash	97.71	83.25	9.98	1.2	17.77	57.72
Mytilus edulis valve	16.3	14	2.78	0.69	4.95	62.67
Tubularia indivisa	13.78	9.25	2.62	0.51	4.67	67.34
Paguroidea spp. unidentified	8.58	14	1.88	1.05	3.35	70.69

Table 5.3-4 continued,

Groups C & E
Average dissimilarity = 60.25

Species	Group C Av.Abund	Group E Av.Abund	Av.Diss	Diss/SD	Contrib%	Cum.%
Hydrozoa bryozoa erect	57.39	115.25	13.31	1.62	22.09	22.09
shell hash	88.86	83.25	11.44	1.2	18.98	41.07
Shell whole partial	72.11	108.75	10.8	1.55	17.92	58.99
	7.04	14	2.16	0.81	3.58	62.57
Paguroidea spp. unidentified	8.77	14	2.04	1.06	3.38	65.95
Tubularia indivisa	5.24	9.25	1.82	0.61	3.02	68.97
Crepidula fornicata	12.27	2.25	1.49	0.43	2.48	71.45

Groups B & NA
Average dissimilarity = 73.40

Species	Group B Av.Abund	Group NA Av.Abund	Av.Diss	Diss/SD	Contrib%	Cum.%
shell hash	81.68	87.81	13.84	1.2	18.86	18.86
terrestrial vegetation debris	11.05	77.25	12	0.92	16.35	35.21
Shell whole partial	45.04	48.19	8.02	1.21	10.92	46.13
Rhodophyta	27.77	1.56	4.5	0.58	6.13	52.26
Hydrozoa bryozoa erect	29.84	4.44	4.13	0.66	5.63	57.89
Zostera seagrass debris	9.26	23.81	3.83	0.87	5.22	63.11
Paguroidea spp. unidentified	5.96	20.75	3.21	1.27	4.38	67.48
Phaeophyceae	17.66	0.13	2.76	0.48	3.76	71.24

Groups D & NA
Average dissimilarity = 70.03

Species	Group D Av.Abund	Group NA Av.Abund	Av.Diss	Diss/SD	Contrib%	Cum.%
shell hash	97.71	87.81	11.17	1.19	15.95	15.95
terrestrial vegetation debris	0.2	77.25	10.41	0.87	14.87	30.82
Shell whole partial	96.87	48.19	10.3	1.38	14.71	45.53
Hydrozoa bryozoa erect	71.28	4.44	8.76	1.01	12.51	58.04
Zostera seagrass debris	5.21	23.81	3.19	0.76	4.55	62.6
Paguroidea spp. unidentified	8.58	20.75	2.73	1.21	3.9	66.5
worm tube flexible erect	1.74	11.88	2	0.7	2.85	69.35
Mytilus edulis valve	16.3	0.25	1.83	0.42	2.62	71.97

Groups C & NA
Average dissimilarity = 70.60

Species	Group C Av.Abund	Group NA Av.Abund	Av.Diss	Diss/SD	Contrib%	Cum.%
shell hash	88.86	87.81	12.78	1.21	18.1	18.1
terrestrial vegetation debris	2.54	77.25	11.32	0.89	16.03	34.13
Shell whole partial	72.11	48.19	9.14	1.28	12.95	47.08
Hydrozoa bryozoa erect	57.39	4.44	7.79	0.9	11.04	58.12

Zostera seagrass debris	5.27	23.81	3.37	0.78	4.78	62.9
Paguroidea spp. unidentified	8.77	20.75	3.03	1.27	4.3	67.2
worm castings	9.28	8.31	2.28	0.64	3.24	70.44

Groups E & NA
Average dissimilarity = 67.32

Species	Group E Av.Abund	Group NA Av.Abund	Av.Diss	Diss/SD	Contrib%	Cum.%
Hydrozoa bryozoa erect	115.25	4.44	14.81	2.05	22	22
terrestrial vegetation debris	0	77.25	11.04	0.87	16.4	38.4
shell hash	83.25	87.81	10.27	1.2	15.25	53.64
Shell whole partial	108.75	48.19	10.19	1.69	15.14	68.78
Zostera seagrass debris	0	23.81	3.07	0.7	4.57	73.35

5.3.3.2 Patterns of Diversity

SEABOSS and ROV still images were the principal samples for assessing variation in faunal components and biogenic features of habitats across the study area. Species accumulation curves were used for fall 2017 and spring 2018 sample sets to assess the adequacy of sample effort (Figure 5.3-11). Chao 1 and Michaelis-Menton diversity estimation indices were also calculated to estimate the total diversity of taxa in samples based on the accumulation of new taxa in successive samples. They both use different formulas for relationships that describe the number and abundance of species to estimate total species richness with the premise that the rate of new species occurrence is an indicator of total species within the community (see Morris et al., 2014). It is noteworthy that observed richness and estimated richness curves overlap indicating that sampling using this imaging platform and taxonomic classification approach adequately captured the diversity across the landscape. However, as studies in multiple aquatic and terrestrial settings have demonstrated, different sampling methods can yield different patterns. A comparison of SEABOSS and ROV results from 2018 (Table 5.3-5) illustrates differences in diversity between imaging platforms. Indeed, the richness estimates from Chao 1 illustrate that the ROV, with slower speed, greater resolution based on distance to surfaces, yielded greater species richness, although we interpret this to be based in part on ROV sampling in more heterogeneous habitats as well as greater resolution for identifying species to lower taxonomic levels.

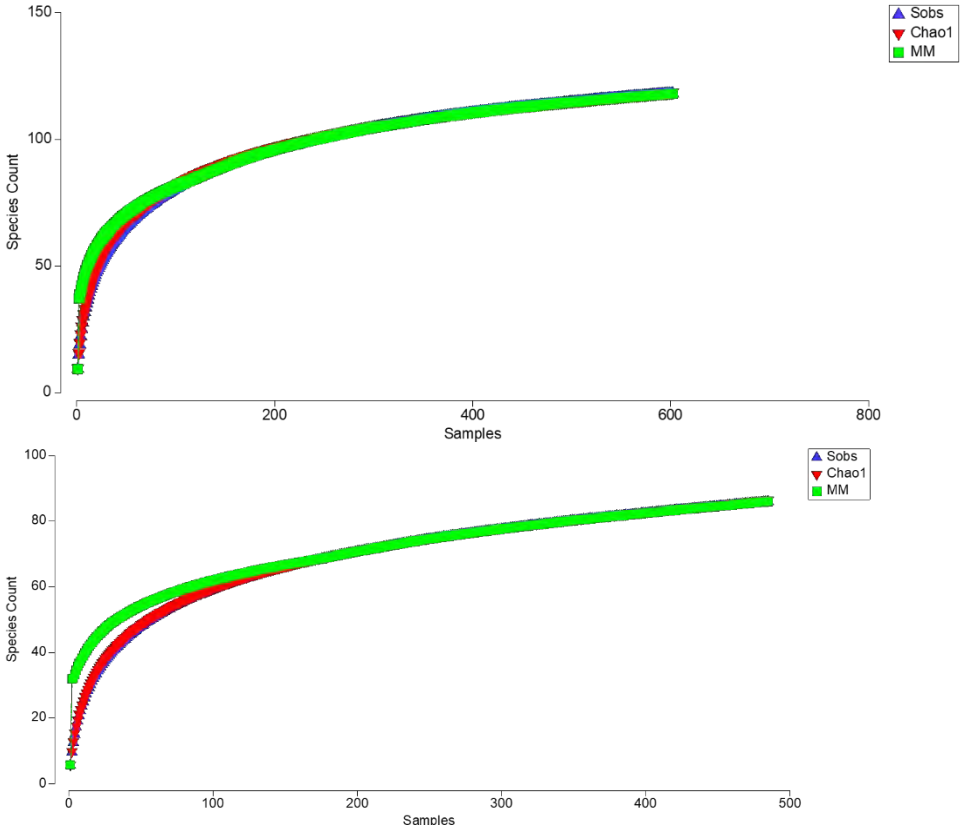

Figure 5.3- 11. Species accumulations curves for 2017 (top) and 2018 (bottom) SEABOSS survey. Each graph includes Sobs (species richness based on observations) as well as Chao1 and Michaelis-Menton (MM) richness estimators based on the relationship between total species richness as samples accumulate (see REF xxxx for details). Each species richness estimator represents a unique approach to predict total richness. Lines are based on 999 (check this) randomizations of sample order.

Table 5.3- 5. Comparison of observed and estimated richness of taxa from 2018 SeaBOSS and ROV surveys.

Samples	S obs	MM	Chao 1
Seaboss	86	86	86.5
ROV	52	54.6	57.6
Combined	120	120	136.2

Image transects in some sample blocks and sites transcended one or more eCognition patch boundaries. This facilitated examination of the role that habitat variability played in enhancing the calculation of local diversity of fauna. Figure 5.3-12 illustrates patterns of accumulated taxon and biogenic feature richness based on linear accumulation of image samples along transects for both fall 2017 and spring 2018 surveys. The two time periods take into account seasonal patterns of recruitment and mortality of benthic fauna with short (annual) life histories. These results indicate that the number of patches and associated transitions have little effect on species richness at this spatial scale. Such patterns, in this ecological setting, can be attributed to the small-scale patchiness of coarse-grained sediments (sand to boulder) within eCognition patches. That is, while large scale patchiness in seafloor maps is attributed to overall patterns of grain size and acoustic reflectivity, small scale patchiness mediates the abundance, but not necessarily diversity, of epifaunal and emergent taxa. Correlating taxa and feature richness at the scale of each image with backscatter value (from multibeam), as a proxy for image scale habitat variation, revealed a similar lack of pattern (Figure 5.3-13).

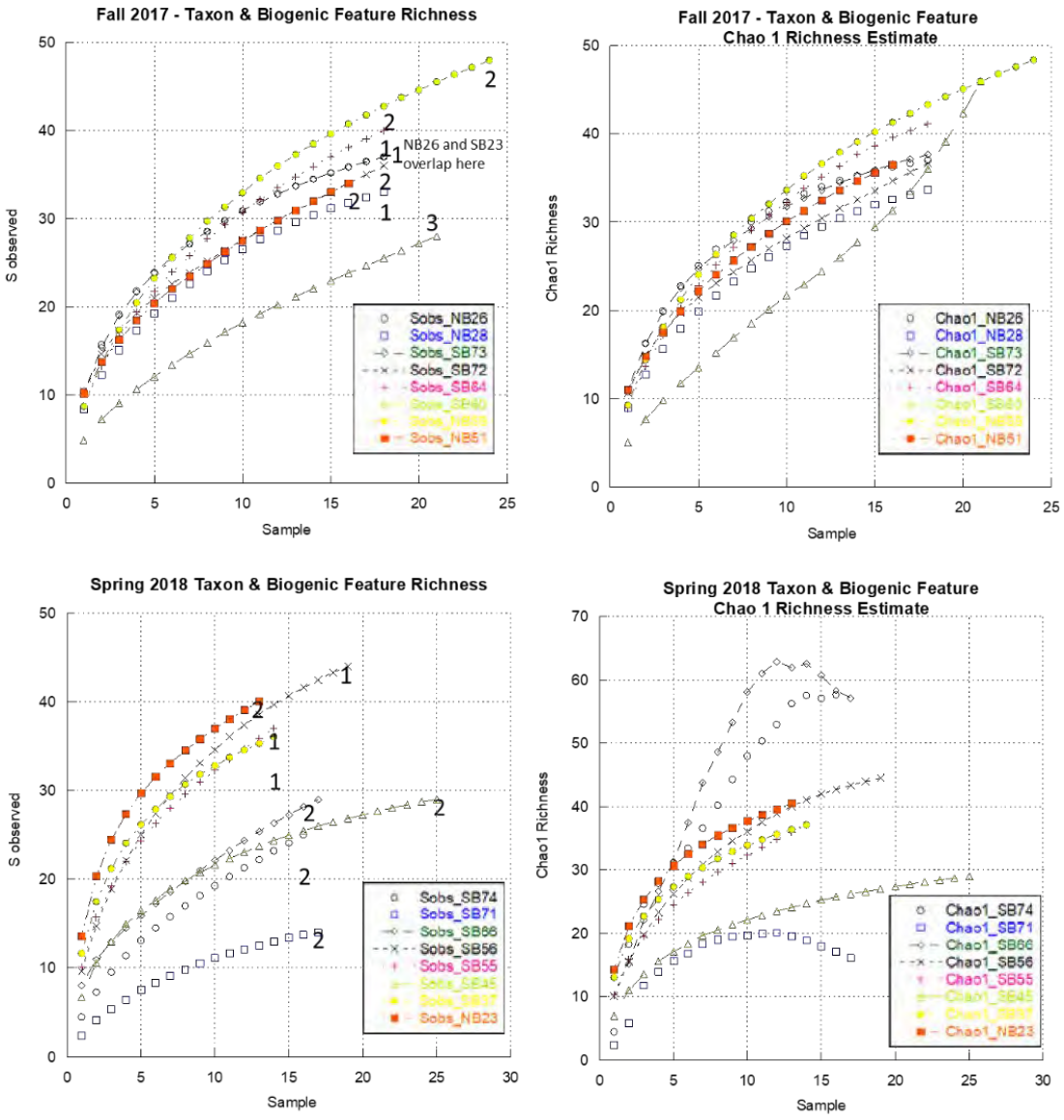

Figure 5.3- 12. Number of eCog patches represented by data from each station with observed richness (left) and richness estimates (right) for 2017 (top) and 2018 (bottom) surveys. (Top) Noteworthy for the 2017 surveys is data from SB60 represents three eCog types and, if linear in arrangement, multiple transitions. In any case, a very different pattern with rising predicted S appears in the Chao1 analysis. Species accumulation curves are based on 999 permutations.

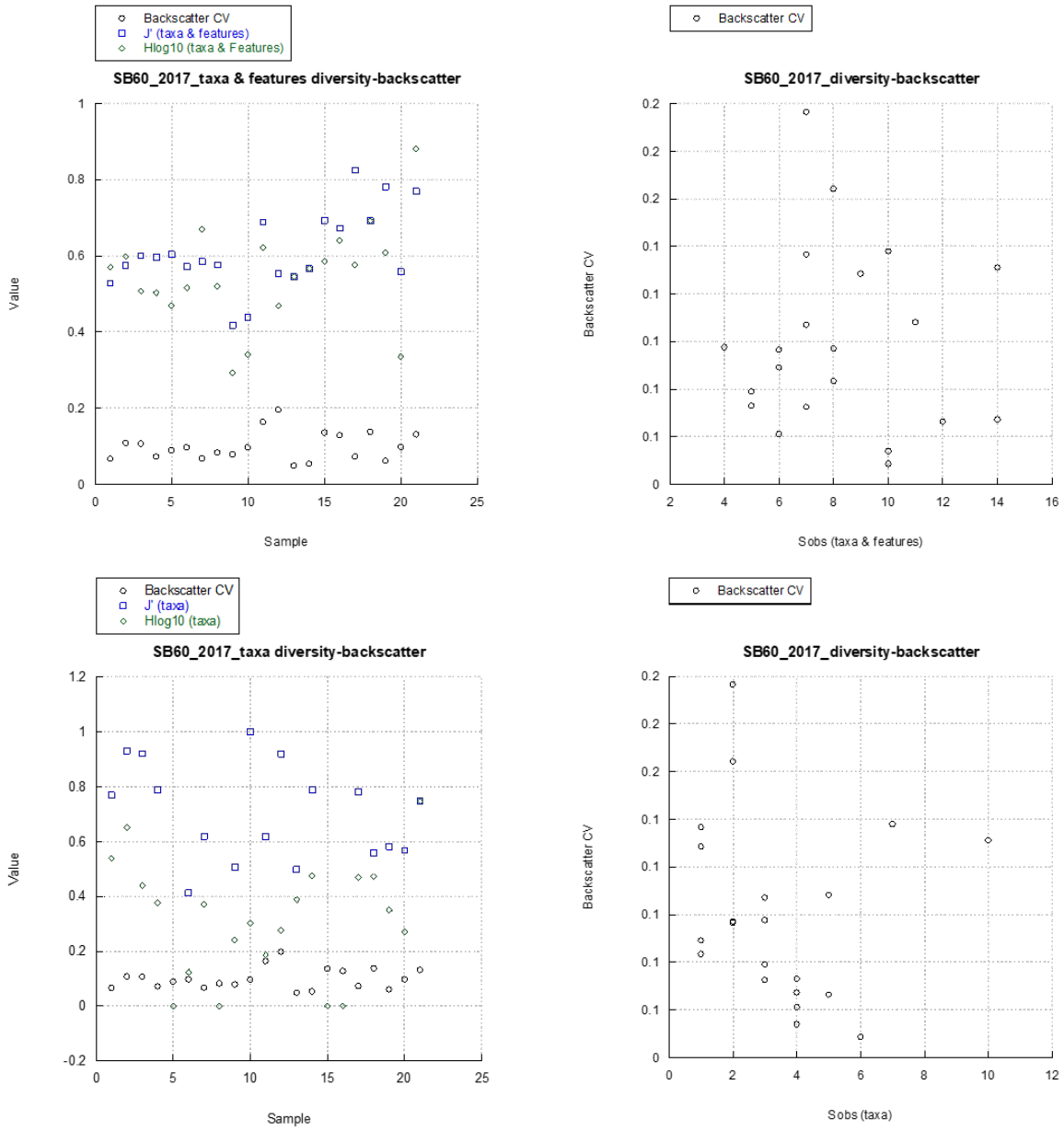

Figure 5.3- 13. Relationship between taxa and features with backscatter for sample block SB60, crossing three eCognition classes. Little discernible relationship between sample-scale (i.e., image-specific) diversity and habitat complexity (as represented by acoustic backscatter).

Image sampling, while facilitating sampling across large areas with efficient use of time and ship resources, limits the ability to identify and assess cryptic species (i.e., those too small, transparent, camouflaged, or sheltered to be represented in images). To conduct an assessment of the degree that images under-sample components of diversity, a limited set of simultaneous image and airlift samples were collected via scuba diving in relatively shallow depths and at multiple sites with complex habitats. A 0.25 m^2 camera quadrapod and airlift were used (see Section 5.3.2.2) over the study period. Image and airlift samples were paired at sites but the entirety of sampling crossed seasons due to logistical constraints. Images identified 35 taxa using while airlift samples collected 130 taxa (Table 5.3-6, Figure 5.3-14). That the sampling was complementary with a total richness of 157 taxa is notable. Image samples were dominated by macroalgae and sponge taxa (Figure 5.3-15) while airlift samples were dominated by arthropods, mollusks, and annelids (Figure 5.3-16). Further, the arthropods were composed of amphipods, decapods, and isopods, all important prey taxa for secondary consumers, including

fish of ecological and economic importance in LIS. An example of the diversity of organisms from a single airlift sample is illustrated with one from Latimer Reef (Table 5.3-7).

Table 5.3- 6. Comparison of taxa richness from quadrapod image and suction samples.

Samples	S obs	MM	Chao 1
Suction	130	177.5	205
Quadrat photo	35	36.4	37
Combined	157	*	*

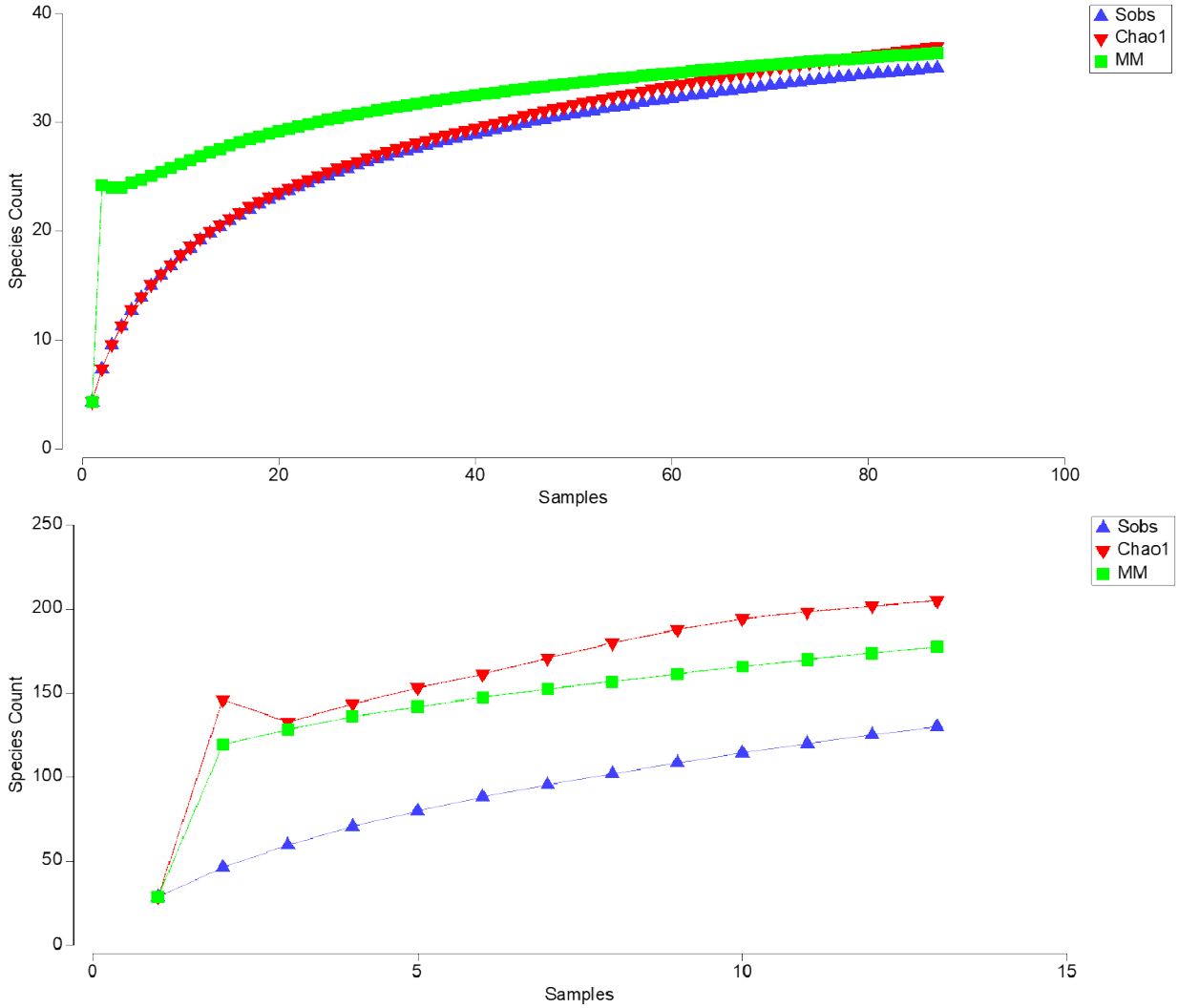

Figure 5.3- 14. Taxa accumulation curves, based on observed richness and Chao1 and Michaelis-Menton richness estimators, for image (top) and airlift (bottom) samples.

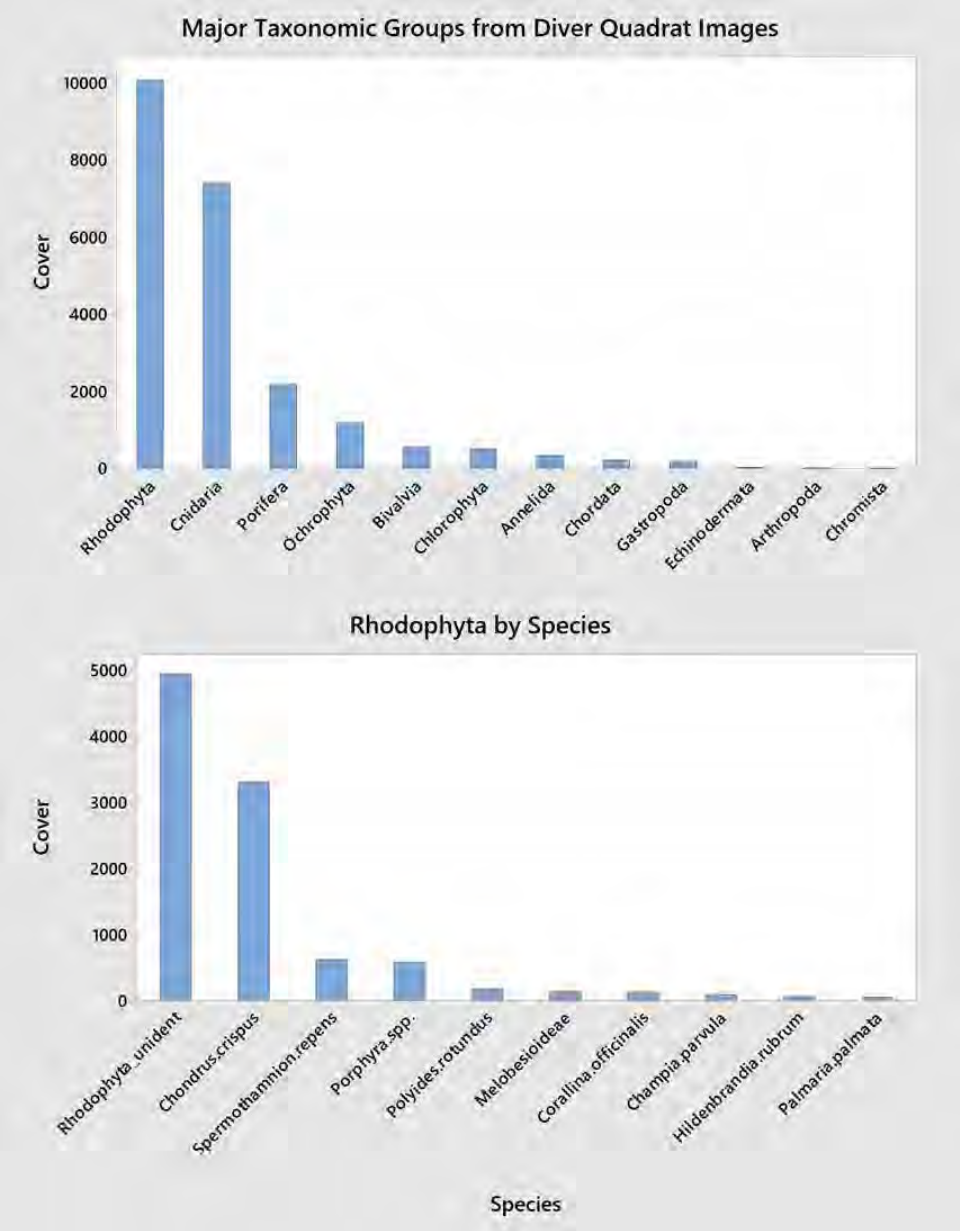

Taxa	Cover
Rhodophyta	10056
Cnidaria	7402
Porifera	2177
Ochrophyta	1179
Bivalvia	548
Chlorophyta	507
Annelida	342
Chordata	222
Gastropoda	189
Echinodermata	30
Arthropoda	19
Chromista	14

Figure 5.3- 15. Results of quadrat images based on cover estimates.

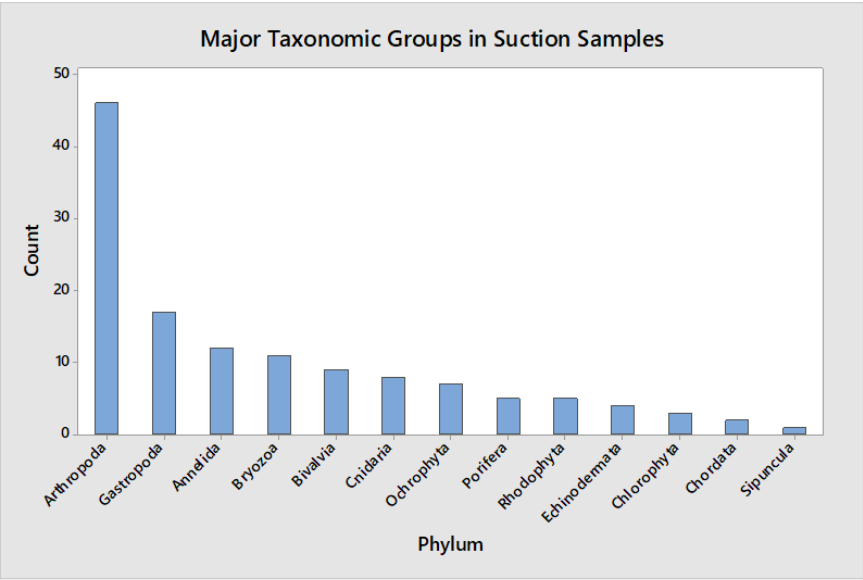

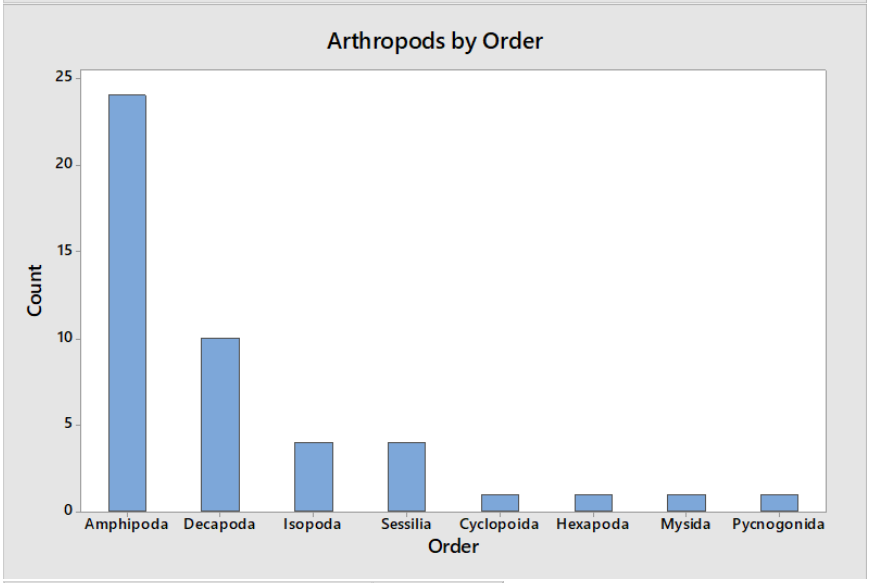

Site	S
Latimer/2018	81
Ellis/2018	42
S of Seaside Pt/2017/S10	17
Black Ledge/2018	41
N of Plum Island/2018	37
Ram Island Reef/2017	37
Two Tree Island	21
S of Seaside Pt/2017/SD09	13
Latimer Reef/2017	12
NW of N Hill Point	7
N of Plum Island	19
Three Ft Rock	17
Ellis Reef	27

Figure 5.3- 16. Results of analysis from airlift samples based on taxon richness.

Table 5.3- 7 Example from Latimer Reef on 15 June 2018 (sample site SD 11).

Site/Year:	Latimer/2018				
Taxonomy					**Total**
Mollusca	Bivalvia	Mytilida	Mytilidea	*Mytilus edulis*	16775
Arthropoda	Malacostraca	Amphipoda	Caprellidae	*Paracaprella tenuis*	643
Arthropoda	Malacostraca	Amphipoda	Caprellidae	Caprellidae	517
Mollusca	Gastropoda	Littorinimorpha	Littorinidae	*Littorina littorea*	473
Arthropoda	Malacostraca	Amphipoda	Caprellidae	*Aeginina longicornis*	397
Mollusca	Gastropoda	Littorinimorpha	Naticidae	*Euspira triseriata*	270
Arthropoda	Hexanauplia	Cyclopoida	Oncaeidae	Oncaeidae	269
Arthropoda	Malacostraca	Amphipoda	Caprellidae	*Caprella linearis*	214
Arthropoda	Malacostraca	Amphipoda	Corophiidae	Corophiidae	192
Arthropoda	Malacostraca	Amphipoda	Amphipoda	Amphipoda	122
Arthropoda	Hexanauplia	Sessilia	Balanidae	Balanus	97
Mollusca	Gastropoda	Neogastropoda	Columbellidae	*Astyris lunata*	93
Mollusca	Gastropoda	Neogastropoda	Columbellidae	*Cotonopsis lafresnayi*	81
Arthropoda	Malacostraca	Amphipoda	Aoridae	Aoridae	78
Annelida	Polychaeta	Sabellida	Serpulidae	*Hydroides dianthus*	63
Annelida	Polychaeta	Phyllodocida	Polynoidae	*Lepidonotus squamatus*	37
Arthropoda	Malacostraca	Amphipoda	Melitidae	Melitidae	35
Arthropoda	Malacostraca	Amphipoda	Stenothoidae	Stenothoidae	30
Arthropoda	Hexanauplia	Sessilia	Archaeobalanidae	*Semibalanus balanoides*	30
Arthropoda	Malacostraca	Amphipoda	Caprellidae	*Caprella penantis*	25
Arthropoda	Malacostraca	Amphipoda	Bateidae	Bateidae	22
Porifera	Calcarea	Leucosolenida	Leucosoleniidae	*Leucosolenia botryoides*	18
Arthropoda	Hexanauplia	Sessilia	Archaeobalanidae	*Chirona hameri*	17
Arthropoda	Malacostraca	Amphipoda	Liljeborgiidae	*Idunella clymenellae*	16
Arthropoda	Malacostraca	Amphipoda	Unciolidae	Unciolidae	15
Arthropoda	Malacostraca	Amphipoda	Gammarellidae	Gammarellidae	14
Echinodermata	Ophiuroidea	Amphilepidida	Amphiuridae	*Amphipholis squamata*	14
Cnidaria	Anthozoa	Actiniaria	Diadumenidae	*Diadumene leucolena*	13
Arthropoda	Malacostraca	Isopoda	Idoteidae	*Idotea balthica*	10

The distribution and abundance of particular taxa (epi- and emergent- fauna) and biogenic features did not follow uniform geographic trends, reflecting the varied seafloor habitats characterized by grain size, seafloor roughness, seafloor stress (from current flows), depth (temperature and light), and west-to-east variation in conditions within the estuary. While multiple spatial patterns were identified that provide important insights, multiple taxa and biogenic habitat features that represent larger gradients and general relationships between epifauna and physical characteristics of seafloor environments within the larger landscape were identified. It is noteworthy that the most diverse sites are to the east in the study area and offshore including eastern FIS, south of Fishers Island, and The Race (Figure 5.3-17).

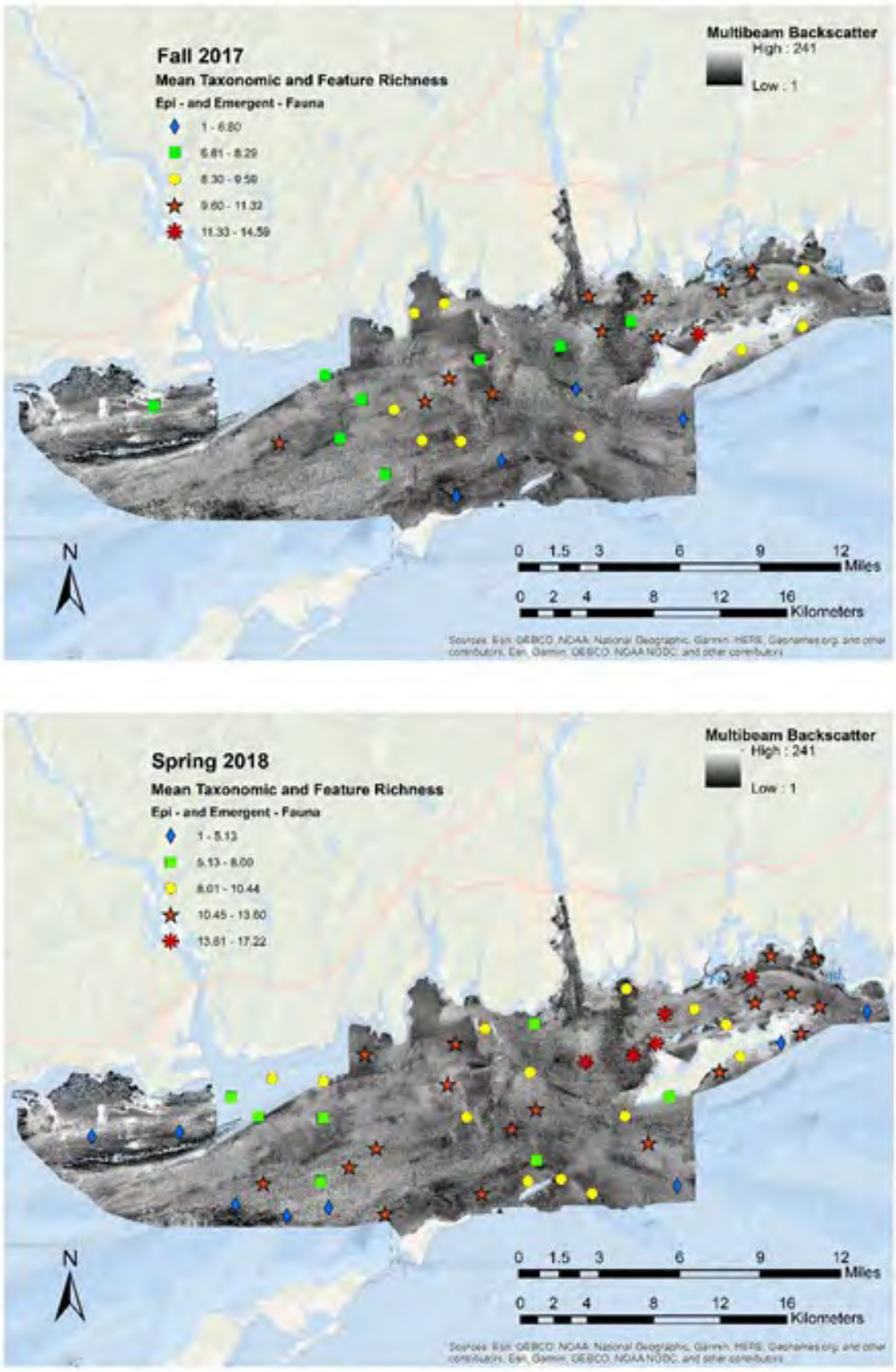

Figure 5.3- 17. Block/site-scale taxonomic and biogenic feature richness as determined during fall (top) and spring (bottom) sampling. Note: the cluster of high richness in the eastern 1/3 of the Phase II study area.

5.3.3.3 Communities at Scale of Blocks and Sites

Image data from all SEABOSS surveys were aggregated to block and site designations and mean values calculated to identify large scale variation in community structure (i.e., images within sites treated as replicates versus samples). Multivariate analyses were implemented with live taxa and biogenic features as well as live taxa only. SIMPROF was used to identify similarities between sites at the 1% threshold level for hierarchical cluster analyses. These groupings were used as a factor for mMDS analysis, where 15 cluster groups were identified (Figure 5.3-19). Results of global ANOSIM, for both features and taxa, and taxa only, were highly significant (Table 5.3-2) as were multiple paired comparisons. SIMPER identified the features and taxa that contributed most to dissimilarity between sites. However, these results when visualized in a geospatial context provided little insight into general patterns of epifaunal and biogenic habitat features across the Phase II map area. A qualitative hierarchical approach for aggregating sites based on geographic proximity and similarity of ecological features was implemented. The most parsimonious was a set of four groupings representing coastal, west, central, and east regions within the map area (Figure 5.3-18). ANOSIM procedures demonstrated that post-hoc groupings were highly significant (Table 5.3-2). Results of SIMPER analyses (Table 5.3-4) demonstrated that the differential cover of biogenic features composed of shell and terrestrial debris as well as structure forming taxa including hydrozoan-bryozoan turfs, *Crepidula*, *Diadumene*, Rhodophyta, and *Chondrus* separated groups of sites at this large scale. These results demonstrate there are differences in community structure across the study region and all similar patch types are not ecologically equivalent.

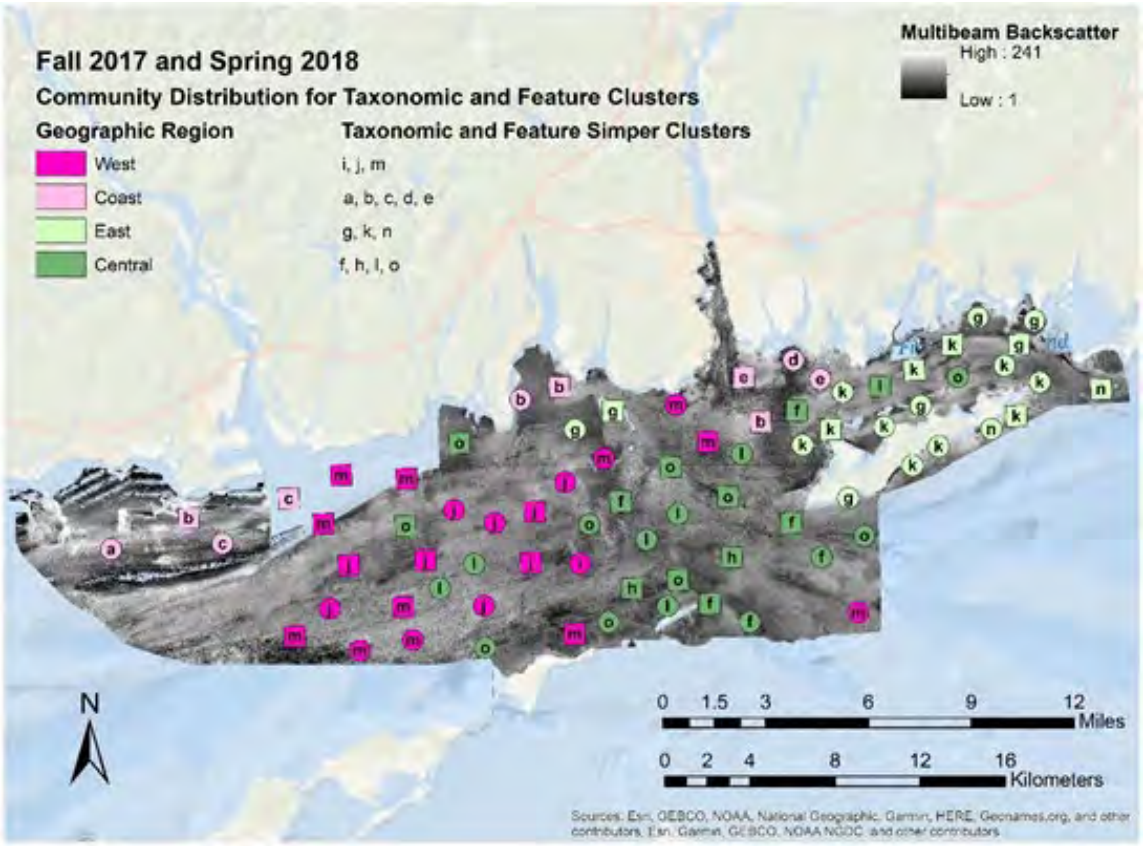

Figure 5.3- 18. Four groupings of site-blocks yield an ecologically significant set of geographically aggregated community types parsing the Phase 2 landscape.

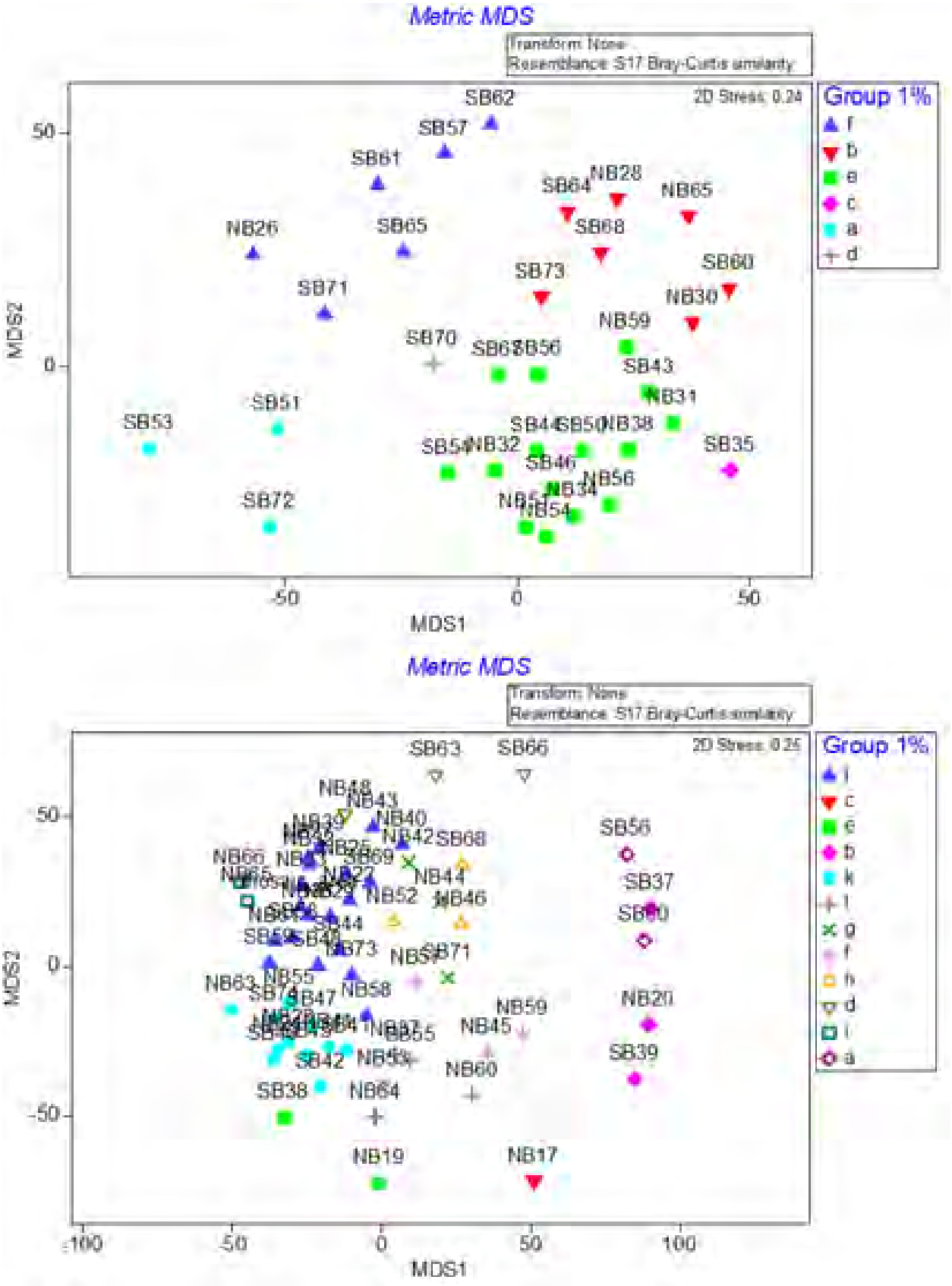

Figure 5.3- 19. mMDS results from SIMPROF analyses based on groupings significant at 1%.

5.3.3.4 Taxon-Biogenic Features and Associations with Environmental Features

The distribution and abundance of taxa and features did not follow uniform geographic trends, reflecting the varied seafloor habitats characterized by eCognition patches as described above. In any case, a number of spatial patterns were identified that provide important insights on this region of LIS. Multiple taxa and biogenic habitat features that represent larger gradients and general relationships with physical characteristics of seafloor environments were identified, as well as ecological responses to on-going changes in local and regional environmental conditions. Some taxa are worthy of specific consideration due to their role as an ecosystem engineer or biogenic habitat, or their vulnerability, conservation status, or dominance in the community. These taxa are: hydrozoan and bryozoan turfs, ghost anemone *Diadumene leucolena*, macroalgal taxa aggregated as Laminariaceae and Rhodopyhta, and the solitary hydroid *Corymorpha pendula* (Figure 5.3-20). Additional taxa are considered jointly as their spatial distributions and patterns of abundance may either represent fundamental changes in seafloor communities, as in blue mussel *Mytilus edulis* and Atlantic slipper shell *Crepidula fornicata*, or interactions between endemic and invasive taxa, as in yellow boring sponge *Cliona* spp., northern star coral *Astrangia poculata,* colonial tunicate *Didemnum vexillum.* Biogenic features that were widely distributed and known to serve as structural attributes of habitat were bivalve shell, seagrass debris, and terrestrial vegetation debris (Figure 5.3-21).

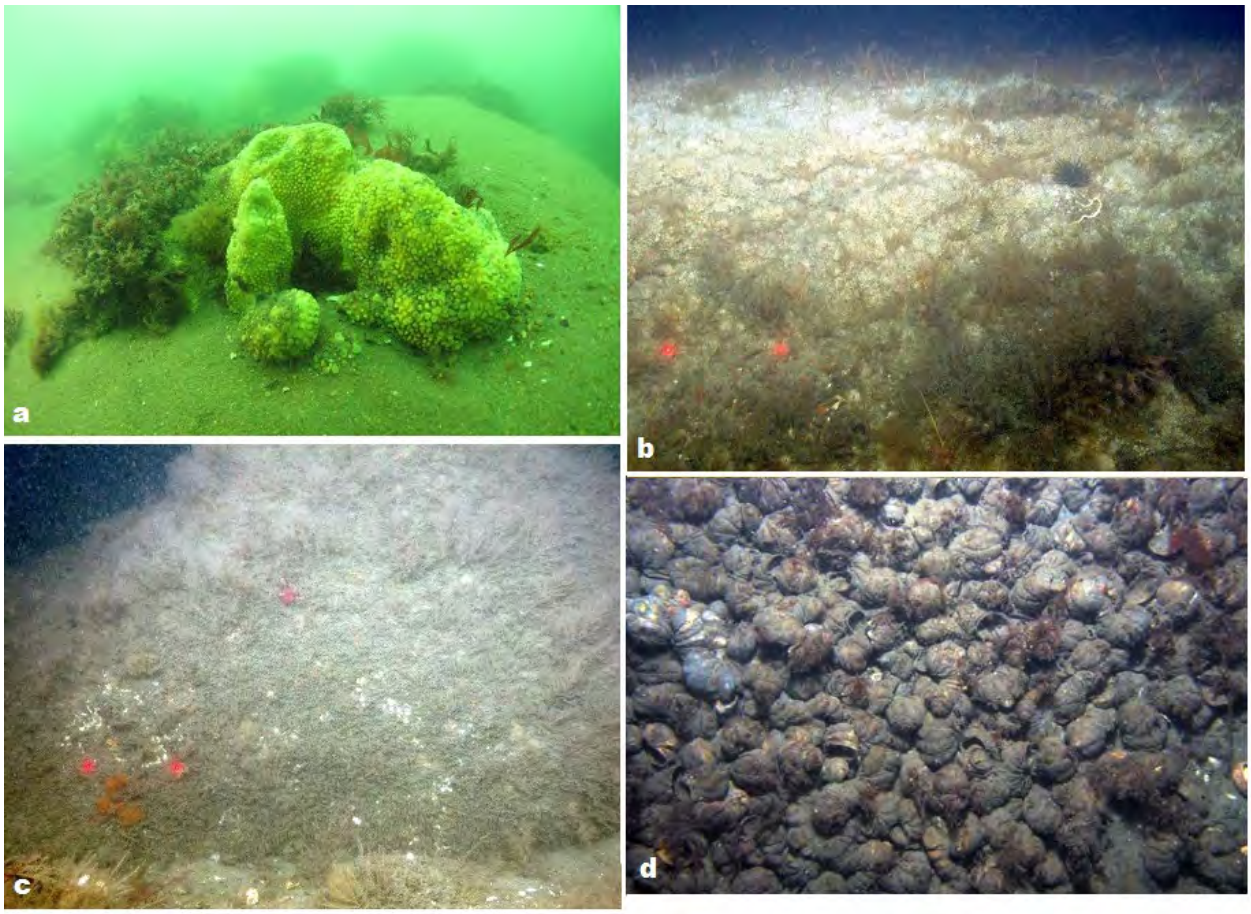

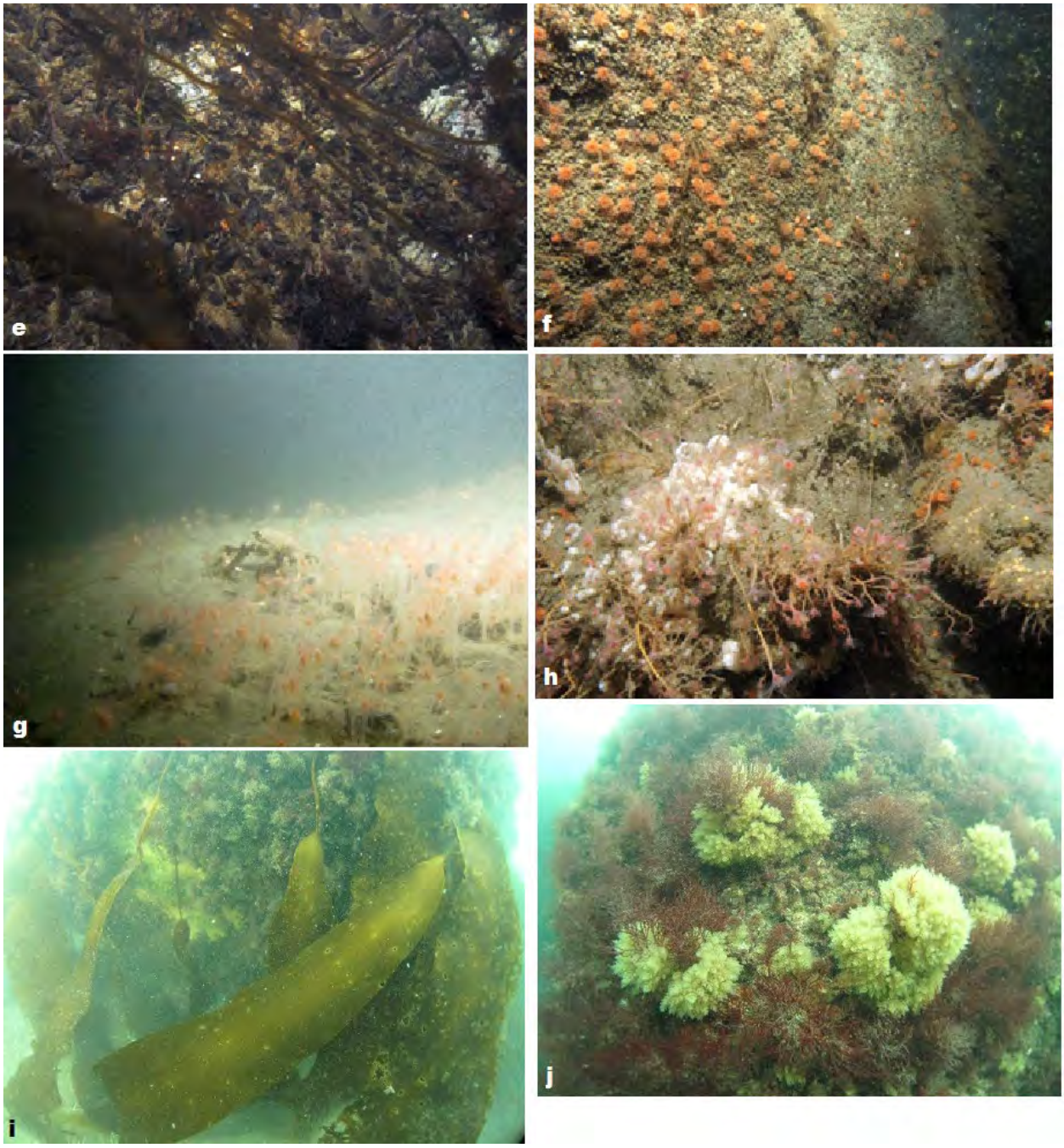

Figure 5.3- 20. Examples of select taxa identified based on analyses for specific attention: (a) Cliona spp. towers at Ellis Reef; (b) massive aggregation of Astrangia poculata at 60m depth located midway between Goshen Point and Great Gull Island; (c) hydrozoan and bryozoan turf on the vertical face of a boulder at 21m depth south of the Thames River; (d) "stacks" of Atlantic slipper shell Credpula fornicata at 18m at the base of Ellis Reef; (e) blue mussel Mytilus edulis in sandy sediments at 11m depth east of Wicopesset Rock; (f) ghost anemones Diadumene leucolena on a vertical boulder face at 13m located midway between Noank and Clay Point in FIS; (g) dense aggregation of solitary hydroids Corymorpha pendula emerging from sand at 47m depth South of Old Saybrook; (h) invasive carpet tunicate Didemnum vexillum (bright white blobs) amongst tubularians at 82m depth in the Race; (i) kelp (Laminariaceae) at <3m depth located on Black Ledge; (j) red algae (Rhodophyta) at 5m depth located on Ramn Island Reef (Peter's photo). Examples of important taxa identified during sampling.

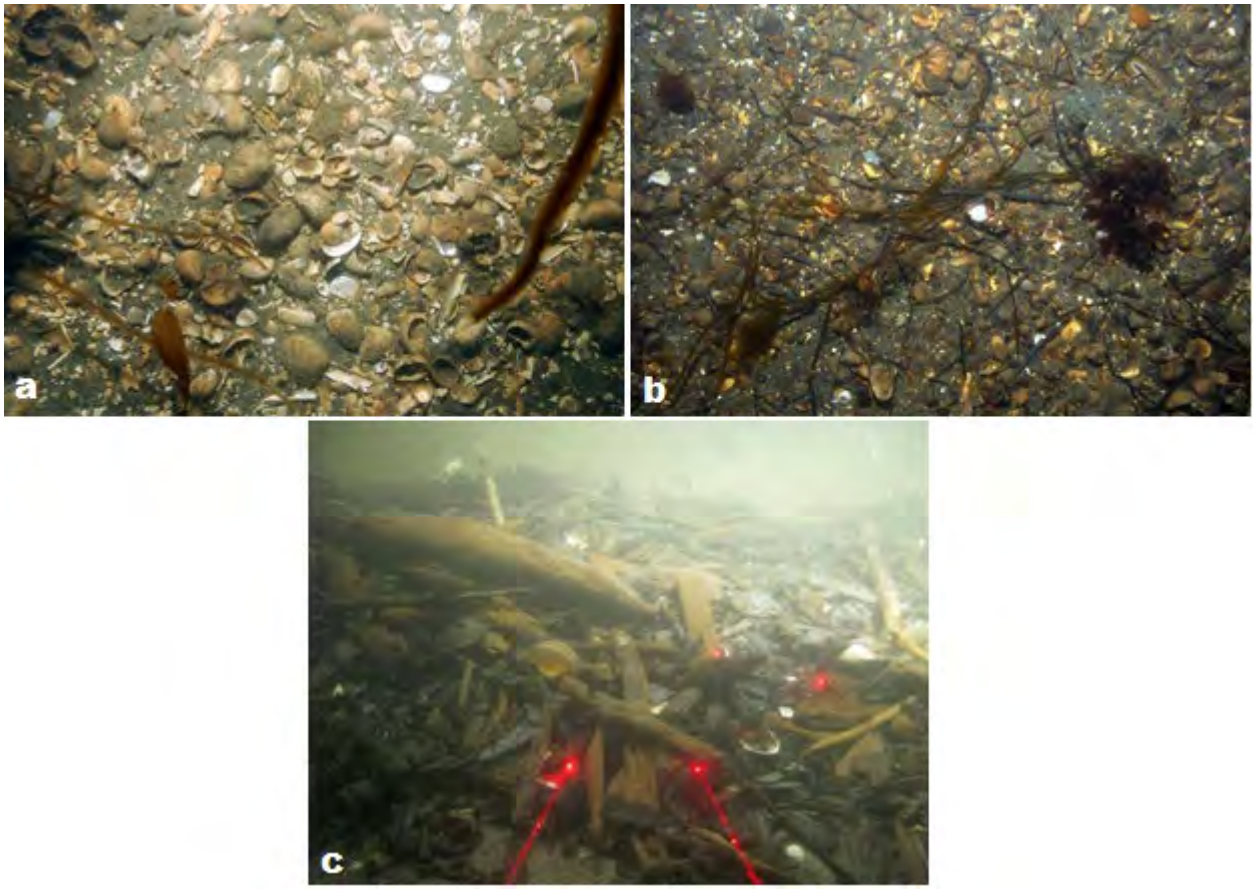

Figure 5.3- 21. (a) Shell valves and pieces covering the seafloor at 24m depth South of Groton Long Point (99% cover); (b) drift seagrass at 22m depth located South of Ellis Reef and East of Ram Island Reef; (c) terrestrial debris at 45m depth located off Old Saybrook, CT.

Here we present a series of maps and brief descriptions that illustrate the distribution and abundance of epifaunal and emergent taxa with diverse life histories as well as biogenic features that fill important functional roles as seafloor habitat. Most of these taxa are structure forming, serving an "ecosystem engineering" role, while the biogenic features are themselves structure. These structures are utilized by vagile fauna for shelter from currents and predators (for physiological benefits and survivorship, respectively) as well as aggregating prey (e.g., amphipods, decapod shrimp) and used as foci for feeding (Cau et al., 2020). In addition, interactions between some benthic fauna and those organisms that influence other organisms and, in part, structure benthic communities are considered in more detail. These summaries are based on the observed distributions and occurrences of these organisms and features and, in the case of the more detailed section on interactions and structuring organisms, mixed effect hurdle models.

Taxa survey datasets often feature an excessive number of null records, or 0 counts where target organisms were not identified, making their analysis using simple linear models difficult (Potts & Elith, 2006). Hurdle modelling separates presence from abundance in distinct models, which both aids model fitting and implicitly acknowledges the unique ecological processes that influence presence and abundance (Ridout et al., 1998; Potts & Elith, 2006). The presence/absence of each taxa were modelled as Bernoulli trials using generalized linear mixed effects models (GLMM) with binomial link functions. When present, natural log transformed taxa abundance was modelled using linear mixed effects models (LMM). Potential fixed effects for all analyses included eCognition patch type, maximum tau (τ), depth (m), TRI, longitude,

and season; interactions were limited to two-way fixed effect crosses featuring eCognition patch type due to the difficulty of interpreting complex interactions. The intercept of sample block/site were included as random effects to account for non-target variation due to geographic heterogeneity. Best fit models were selected using corrected Akaike Information Criteria (AIC), while the contribution of individual model terms was assessed using likelihood ratio tests (LRT). Model effect size was assessed using marginal (fixed effects only) and conditional (fixed and random) effects (Nakagawa & Schielzeth, 2013). Best-fit models were used to predict mean probability of presence (GLMM) and abundance (LMM) as well as 95% confidence intervals across the range of explanatory variables to explore influences on observed patterns of taxa. Tukey's post-hoc pairwise comparisons were used to investigate relationships between taxa presence and abundance and eCognition patches.

5.3.3.4.1 Hydrozoan and bryozoan turfs

Hydrozoan and bryozoan turfs were very common throughout the Phase II study area, occurring in more than 70% of all images analyzed, albeit at varying densities. These turfs were especially dense east of the Connecticut River towards the Race and in western FIS (Figure 5.3-22). Dense turfs were most common in highly structured habitats across available depths, their abundance increasing with both sediment grain size (as represented by eCognition patch; Figure 5.3-22) and bottom complexity (as represented by the TRI; Riley et al., 1999; Figure 5.3-23). Dense turfs were often observed covering hard substrates, where they serve as cover for small sizes of many mobile species. Turfs were also associated with *C. pendula* aggregations. Hydroids exhibit seasonal recruitment due to short life-histories. These taxa also provide structure for small crustacea that are important prey items for vagile fauna like crustacean eating fishes (Cau et al., 2020).

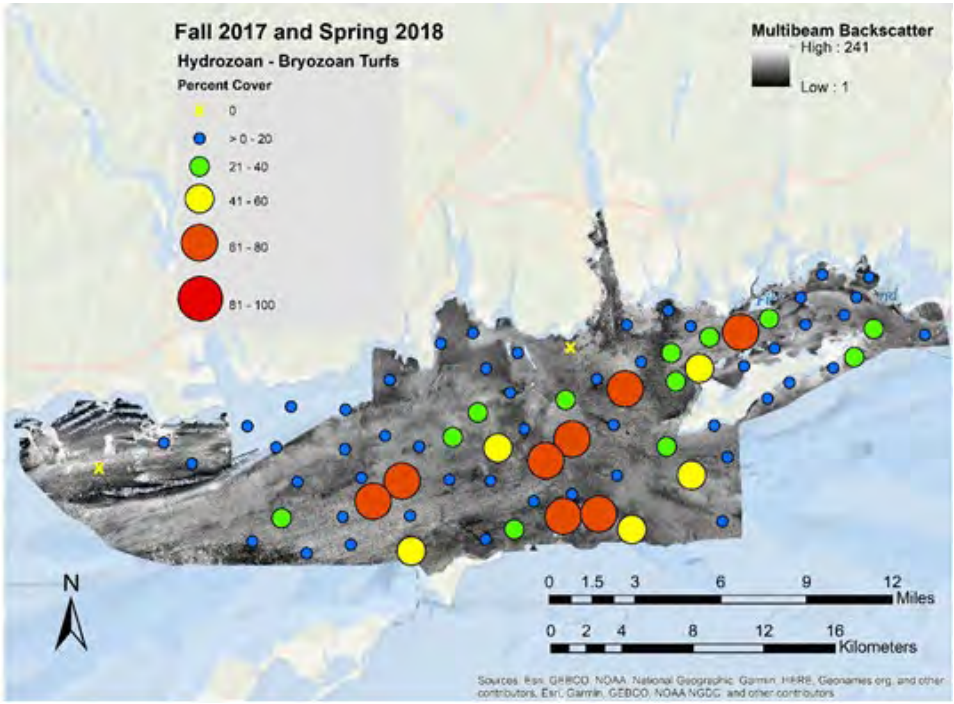

Figure 5.3- 22. Mean percent cover of hydrozoan and bryozoan turfs per block/site sampled.

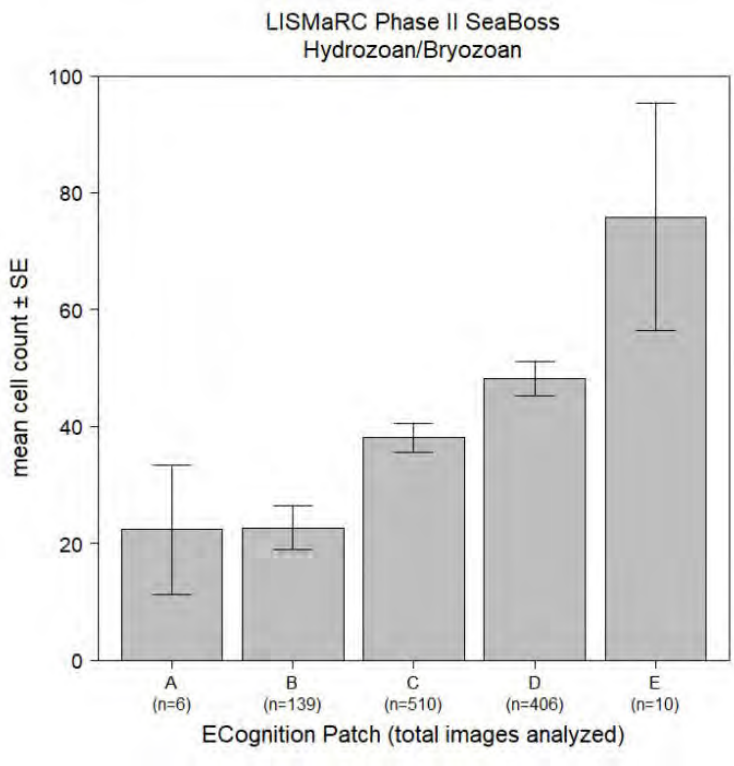

Figure 5.3- 23. Hydrozoan and bryozoan mean abundance by eCognition acoustic patch. Whiskers in mean abundance plot report standard error.

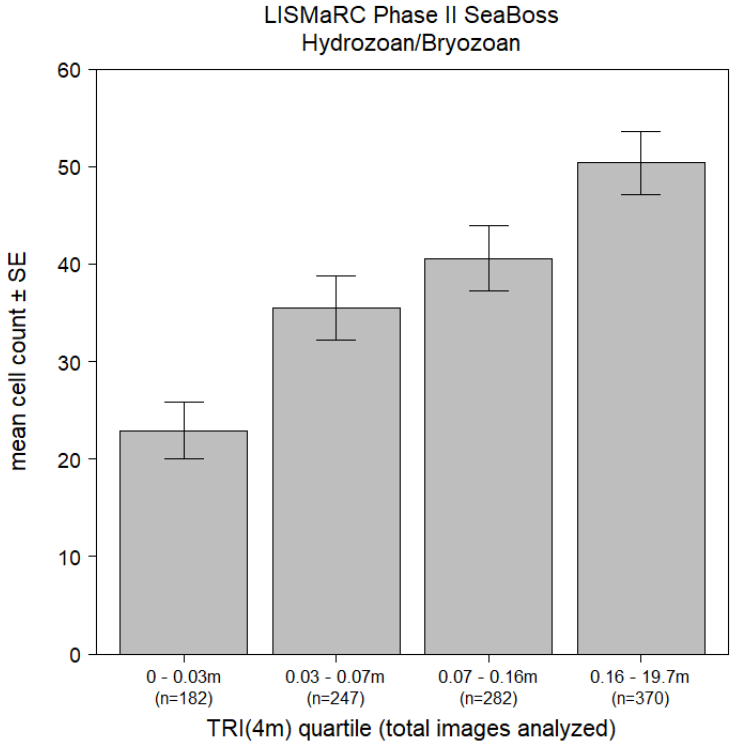

Figure 5.3- 24. Hydrozoan and bryozoan mean abundance by TRI quartile. Whiskers in mean abundance plot report standard error.

5.3.3.4.2 Ghost anemone Diadumene leucolena

Ghost anemone *Diadumene leucolena* were scattered across the eastern 2/3 of the Phase II study area and were most densely concentrated at the Race and to the West of this feature (Figure 5.3-25). Largely limited to highly structured habitats in LIS (as represented by TRI; Figure 5.3-26), ghost anemones attach to hard substrates and are especially dense in areas that experience strong tidal currents (Figure 5.3-27). Despite having toxin-containing nematocysts, ghost anemones are preyed on by gastropods (this is mostly documented in areas where it is invasive; Goddard et al., 2020). Ghost anemones increase the structural complexity of the hard substrates where they attach.

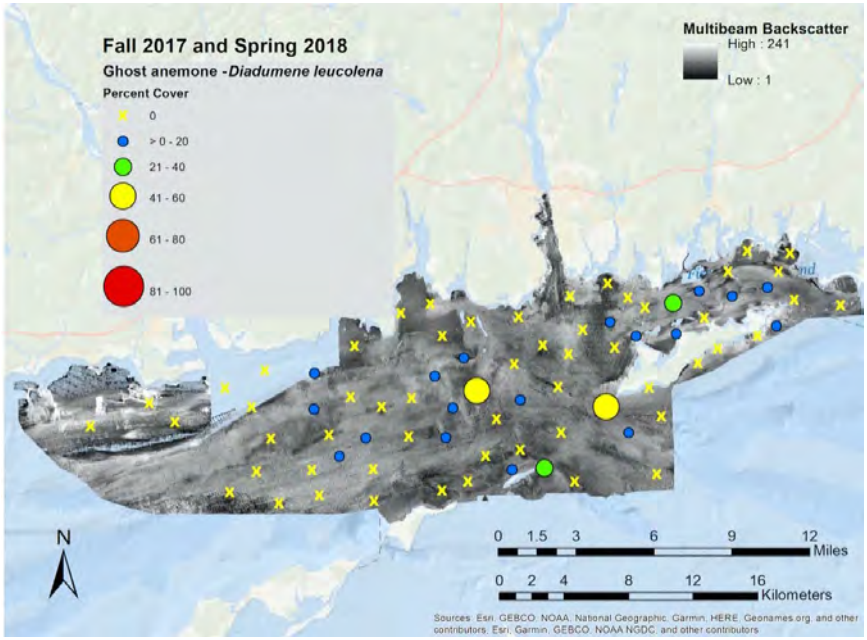

Figure 5.3- 25. Mean percent cover of Diadumene leucolena per Block/site sampled.

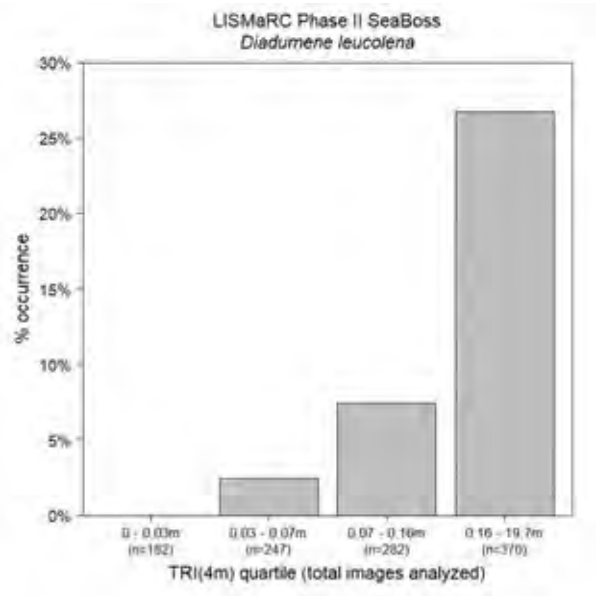

Figure 5.3- 26. D. leucolena % occurrence by TRI quartile. Whiskers in mean abundance plot report standard error.

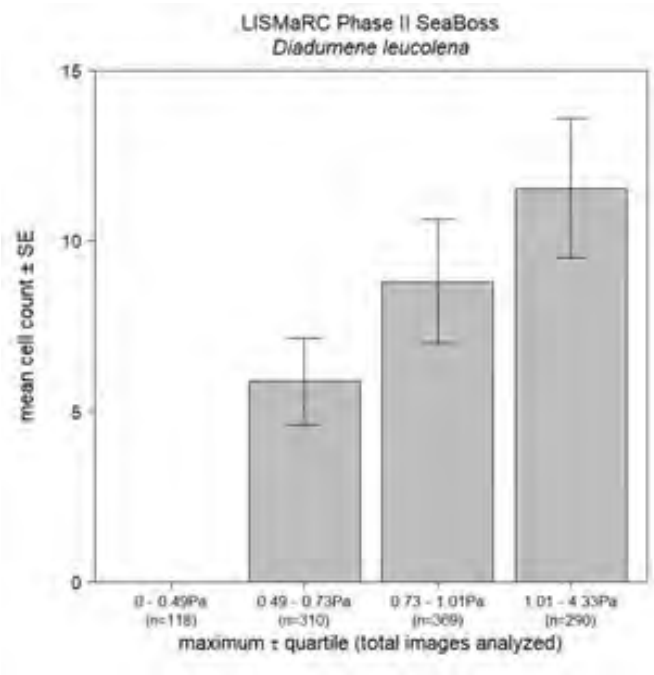

Figure 5.3- 27. D. leucolena mean abundance by maximum monthly bottom stress quartile (maximum □). Whiskers in mean abundance plot report standard error.

5.3.3.4.3 Kelps Laminariaceae

Kelps in the family Laminariaceae (*Laminaria* spp. and *Saccharina* spp.) were observed along the coast, across FIS, along the southern coast of Fishers Island, and at scattered nearshore locations between the Connecticut and Thames Rivers (Figure 5.3-28). Kelp were generally observed in complex hard substrata where they attach to the substrate via a holdfast. This taxon is limited in depth due to the specific characteristics of photosynthetic pigments (Figure 5.3-29). Kelp play important roles in the habitats they define- providing refuge and attachment surfaces for other organisms and promoting productivity and diversity (Steneck et al., 2002). Kelp also play a structuring role when present, limiting light availability to the seafloor and disturbing attached organisms via abrasion due to the movement of their fronds in tidal currents (Jacques et al., 1983; Grace, 2004). The cover provided by kelp species was low across occupied sites in the Phase 2 area. Limited sampling by divers revealed the highest density of kelp found at Black Ledge was <3 m^{-2} during August 2018 (mean cover 35%). Historically, kelp species occurred there at much higher densities, with maximum density of ~300 individuals per m^2 during the same month in 1986 (Egan & Yarish, 1990). These species are at the southern extent of their distributional ranges, but range shifts mediated by temperature trends are less clear due to limited monitoring (Merzouk & Johnson, 2011; Smale, 2020). Sugar kelp, *S. latissima*, has declined in abundance near the southern edge of its range (Witman & Lamb, 2018; Feehan et al., 2019), but partitioning the direct effects of temperature are complicated by indirect effects of elevated temperatures on grazing rates of herbivores, competition for space with turf algae, and settlement of invertebrates on kelp blades that are known to depress populations and impede recovery (Filbee-Dexter et al., 2016, 2018; Witman & Lamb, 2018; Feehan et al., 2019; Smale, 2020).

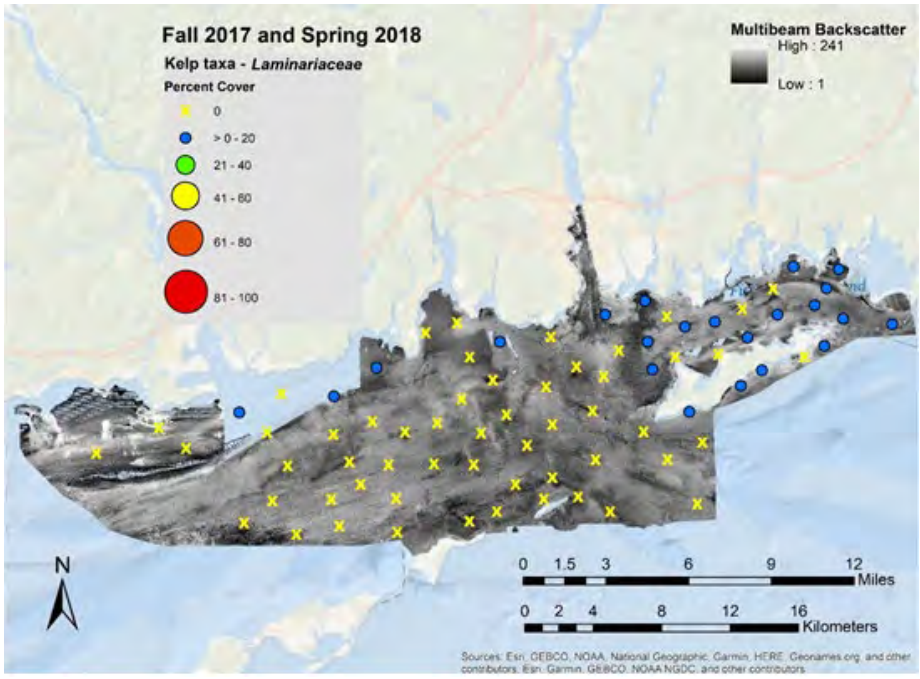

Figure 5.3- 28. Mean percent cover of Laminariaceae per Block/site sampled.

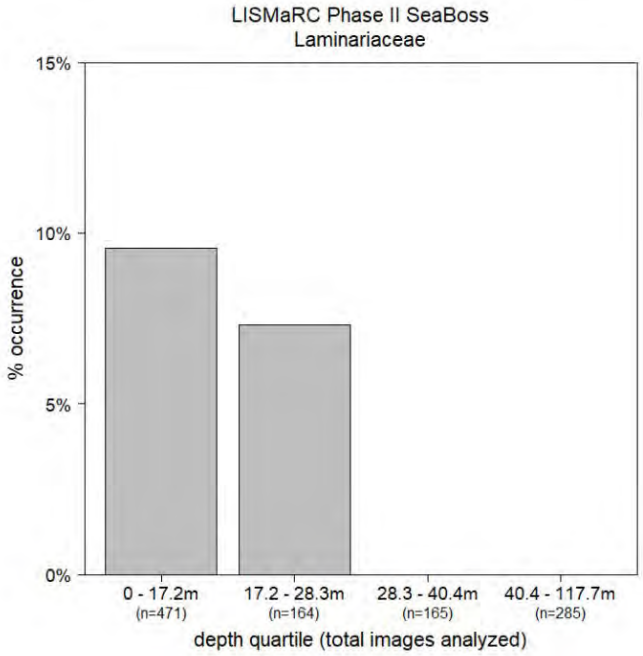

Figure 5.3- 29. Laminariaceae % occurrence by depth quartile. Whiskers in mean abundance plot report standard error.

5.3.3.4.4 Red Macroalgae Rhodophyta

Rhodopyta, red algae, were nearly ubiquitous in shallow nearshore areas across the eastern half of the Phase II study area- from the southern edge of Fishers Island, through FIS, continuing west along the coast to the Connecticut River, and north of Plum and the Gull Islands (Figure 5.3-30). A major characteristic of this taxon is the presence of a pigment that reflects red light and absorbs blue wavelength light, enabling species in this taxon to occur at depths deeper than green or brown macroalgae due to the characteristics of spectral attenuation of light across depths (Figure 5.3-31 and Figure 5.3-32). The distribution of Rhodophyta species in the study area is more widespread than that of kelps, attaching to existing hard stratum materials and

extending into deeper water. While more widespread based on this sampling approach, Rhodophyta were also more closely associated with hard, complex substrates than kelp (Figure 5.3-32). It is notable that Rhodophyta are generally smaller than kelp species and more resistant to effects of drag and dislodgement, so hydrodynamic forces can in part be responsible for some of the variability in distribution (Krumhansl et al., 2015; De Bettignies et al., 2013). Densities were particularly high in FIS and off of Fishers Island. Numerous taxa often co-occurred, including bushy *Polysophonia* spp., thin branching *Ahnfiletia picata* and *Polyides rotundes*, and fairly broad-leafed *Chondrus crispus*. These diverse forms provide refuge for small, mobile organisms.

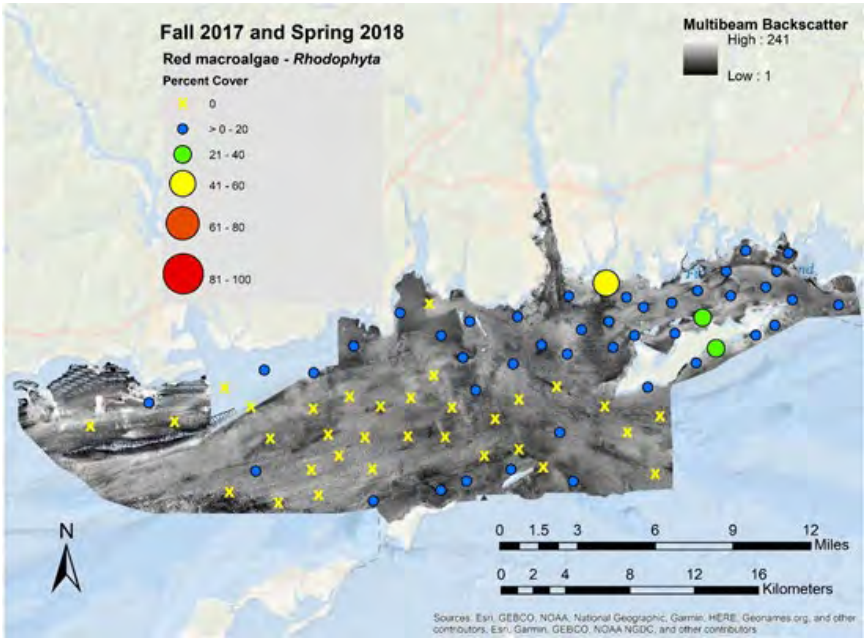

Figure 5.3- 30. Mean percent cover of Rhodophyta per Block/site sampled.

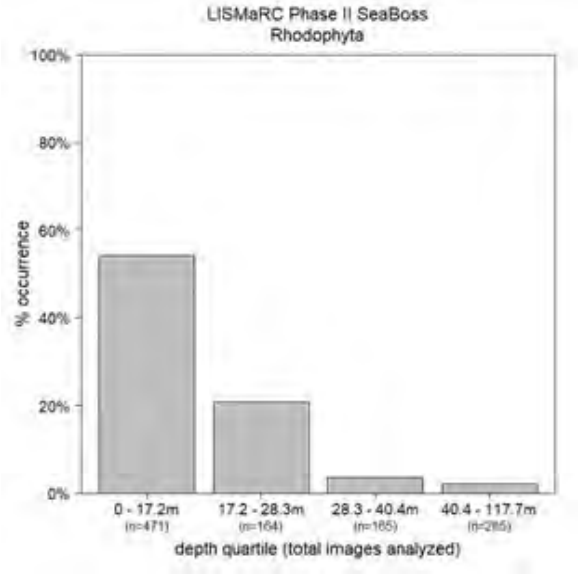

Figure 5.3- 31. Rhodophyta % occurrence by depth quartile. Whiskers in mean abundance plot report standard error.

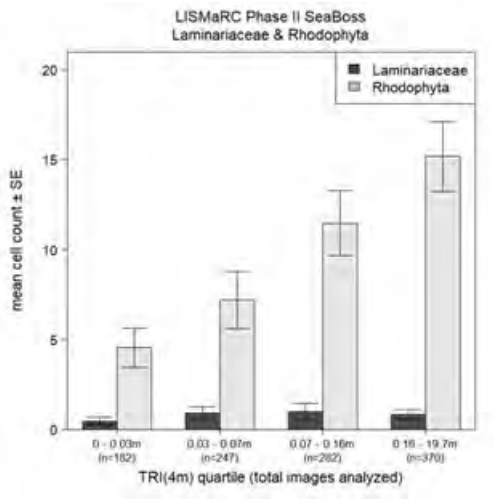

Figure 5.3- 32. Rhodophyta (light gray bars) and Laminariaceae (dark gray bars) % occurrence (top) and mean abundance (bottom) by TRI quartile. Whiskers in mean abundance plot report standard error.

5.3.3.4.5 Solitary Hydroid Corymorpha pendula: Diversity and Spatial Associations with other Fauna

Solitary hydroid, *Corymorpha pendula*, is an ephemeral emergent hydroid found in fine sediment seafloor habitats. The benthic form of this species, the hydroid phase, is present in concentrated patches, but their distribution is dynamic and may change year to year. Following the dispersal of medusae the previously conspicuous hydroids are absent from the Sound by the transition of summer into fall. This species recruits on an annual basis to fine- grain sediment habitats.

When present, corymorphoid hydrozoans may be concentrated in moderately dense aggregations, which play similar ecological roles to those of terrestrial forests (Rossi et al., 2017). These aggregations contrast starkly with the mostly unstructured fine sediments that compose their preferred habitats. Dense aggregations of these erect hydroids can form important habitats for other sessile and mobile organisms (Cau et al., 2020; Byers & Grabowski, 2014; Di Camillo et al., 2017). Hydroids may form the basis of important and unique habitats, both altering the fine sediment environments where they proliferate seasonally (Cerrano et al., 2015) and providing refuge and surfaces that other benthic organisms utilize (Zintzen et al., 2008). During the hydroid phase, benthic biomass in these aggregations increases substantially likely fueled by a combination of factors, conversion of pelagic to benthic biomass via hydrozoan filter-feeding (Gili et al., 1998) and disruption of bottom currents (Hughes, 1978). Additionally, the release of medusae return concentrated biomass to pelagic waters (Gili et al., 1998). Although not as extensively studied as other marine animal forest phenomena, hydroid aggregations also host greater diversity than surrounding sediments (Zintzen et al., 2008).

The factors influencing ephemeral hydroid aggregations, or deciduous animal forests, are unclear and even unstudied for many taxa (Di Camillo et al., 2017), so identifying consistent patterns of conditions coinciding with *C. pendula* observations can provide important insights for their ecology in the LIS. As expected, the benthic hydroid stage of *C. pendula* was present in spring, but not Fall sampling. In spring, this solitary hydroid was found offshore, in deeper waters between the Connecticut and Thames Rivers (Figure 5.3-33). In fact, *C. pendula* was largely absent from the shallowest sampled habitats (< 17.2 m; Figure 5.3-34). *C. pendula* was completely absent from the eastern ¼ of the study area (Figure 5.3-35), which consists of FIS

and nearshore BIS, and sites west of the Connecticut River. The western limit of their distribution is likely an artefact of sampling locations at this end of the study area, which were fairly shallow and close to shore. Since sampling in FIS was extensive, *C. pendula*'s absence is unlikely to be an artefact. The FIS seafloor is variable and includes hard bottom, but much of the available habitat consists of sand or silt, so limitation due to inadequate fine sediments is unlikely. The eastern limit to the distribution of *C. pendula* may be due to competition in the shallow, higher salinity FIS, but at present this is speculative.

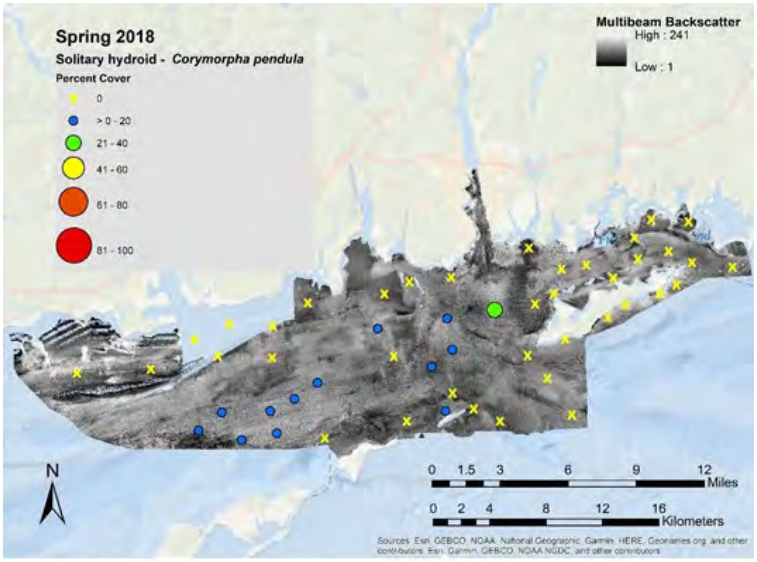

Figure 5.3- 33. Distribution and block/site specific mean percent cover of C. pendula in spring 2018 sampling.

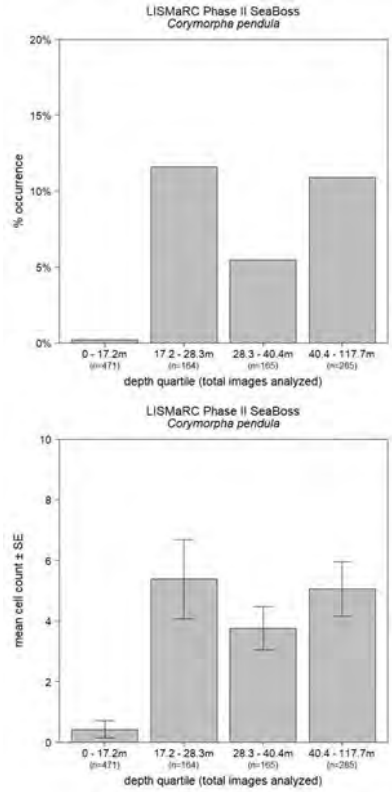

Figure 5.3- 34. C. pendula % occurrence (top) and mean abundance (bottom) by depth quartile. Whiskers in mean abundance plot report standard error.

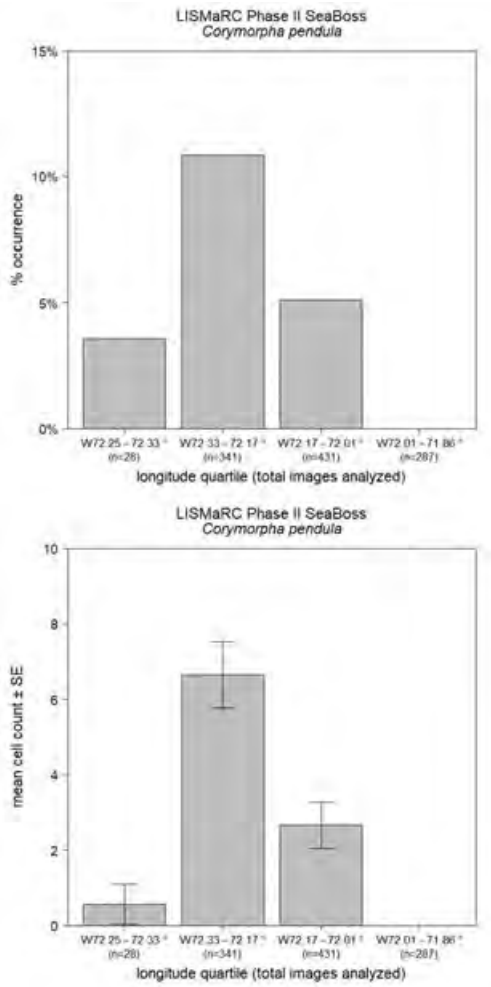

Figure 5.3- 35. C. pendula % occurrence (top) and mean abundance (bottom) by longitudinal section. Whiskers in mean abundance plot report standard error.

Despite its association with fine sediments, *C. pendula* was increasingly common as sediment grain size increased (Figure 5.3-36). Although this appears to run counter to established Genus preferences for finer sediments, it is important to note that *all* of the ECognition- defined habitat types were composed of primarily or substantially sand (Table 5.3-3C). *C. pendula* was also denser (i.e., greater percent cover) in coarser than in finer sediments, but for the most sampled habitat there was a clear separation between sediments featuring silt (patch B) and those that did not (patches C and D), which may belie a preference for sand over mud or silt. Another proxy for sedimentary environments is the complexity, or roughness, of the bottom as measured using derived products of acoustic bathymetry, such TRI (Riley et al., 1999). Courser seafloor tends to feature coarser sediments, including boulder and rock outcroppings. *C. pendula* was rarest in the most complex habitats (i.e., highest TRI quartile; Figure 5.3-37). Similarly, density decreased with increasing habitat complexity, as well. When present *C. pendula* usually covered a substantial proportion of available habitat, between 13.1% (least complex habitats) and 8.3% (most complex habitats) of sample images.

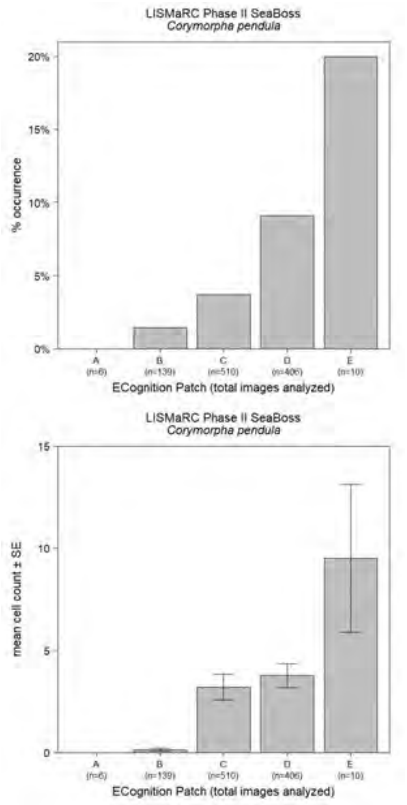

Figure 5.3- 36. C. pendula % occurrence (top) and mean abundance (bottom) by eCognition acoustic patch. Whiskers in mean abundance plot report standard error.

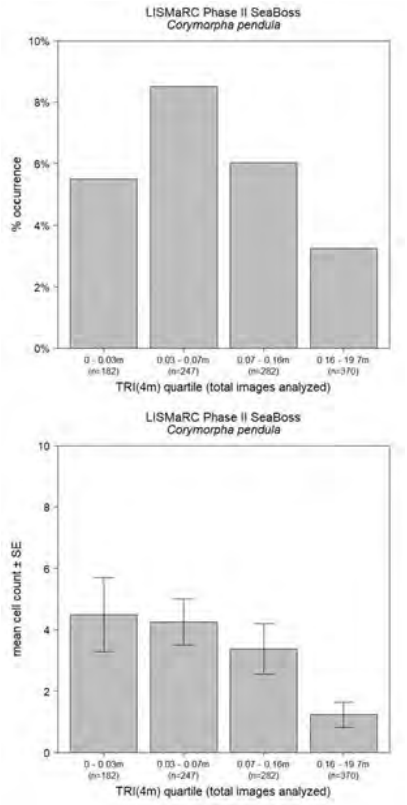

Figure 5.3- 37. pendula % occurrence (top) and mean abundance (bottom) by TRI quartile. Whiskers in mean abundance plot report standard error.

While *C. pendula* was observed in nearly 6% of samples collected in the highest energy habitats and completely absent from areas with the lowest bottom currents, disturbances can greatly

impact this species over relatively short periods of time (i.e., < 1 year; Brooks, 1984; Auster et al., 1996). While seafloor experiencing stronger bottom currents would be more likely to feature more frequent disturbances, the feeding rates and efficiency of solitary hydroids may adapt to such conditions (Dutto et al., 2019). Under low flow conditions, *Corymorpha* hydroids have been observed with hydranths at the sediment surface with stalks bent (Parker, 1917), which may be a less efficient and more energetically costly feeding mode. While absent from habitats with very low bottom currents, *C. pendula* was densest under moderate current conditions (0.49 Pa > τ > 1.01 Pa; Figure 5.3-38). This may indicate a threshold flow rate below which filter feeding may be too costly to support established *C. pendula* aggregations.

Model results suggested depth was the most important factor in the occurrence of *C. pendula*, the hydroid became more common as depth increased. Depth alone explained 8% of the observed variance in the distribution (margin $R^2 = 0.08$), *C. pendula* occurrence increasing with depth. When present, a combination of location, bottom current strength, and seafloor complexity explained nearly 15% of the observed variance in hydroid densities (marginal $R^2 = 0.15$). From east to west, *C. pendula* percent cover increased, while the highest densities occurred in the least complex habitats (i.e., lowest TRI). Despite being absent from areas experiencing the lowest bottom currents, in areas where *C. pendula* did occur the best fit model predicted the densest aggregations in the least dynamic habitats (i.e., lowest maximum τ); it is important to note that since *C. pendula* was absent from seafloor habitats with the lowest flow conditions (τ < 0.49 Pa), so these conditions were excluded from density models.

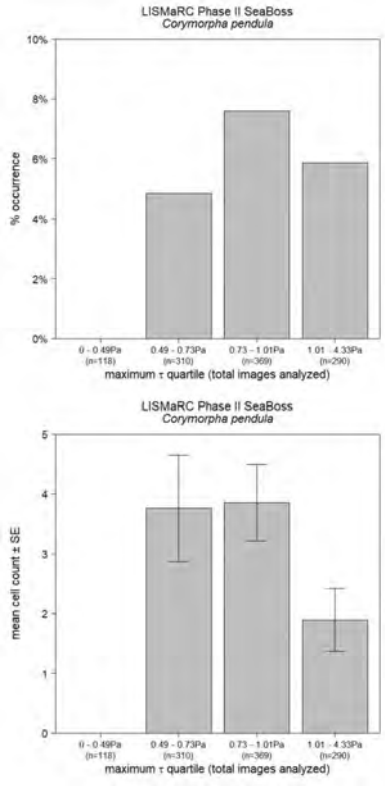

Figure 5.3- 38. C. pendula % occurrence (top) and mean abundance (bottom) by maximum monthly bottom stress quartile (maximum τ). Whiskers in mean abundance plot report standard error.

As observed in some other habitat modifying fauna, *C. pendula* hydroid aggregations were associated with more diverse benthic habitats. There was a clear pattern of decreasing ep- and emergent taxa richness and diversity with distance from *C. pendula* aggregations. The mean number of taxa present reached a maximum in patches of hydroids, decreasing steadily to a distance of 400m, which consisted of relatively few taxa present per sample (Figure 5.3-39).

Shannon diversity was high from aggregations to a distance of 200m, then dropped precipitously the further removed a sample was from *C. pendula* (Figure 5.3-40). There were also specific taxa closely associated with this solitary hydroid. Hydrozoan and bryozoan turfs were far more abundant in the presence of *C. pendula* than at other sampling locations (Figure 5.3-41). The association of *C. pendula* with greater epifaunal diversity and the distribution of specific taxa appears to support this species playing an important role as a habitat modifier and forming the basis of an important, ephemeral marine animal forest in sandy sediment environments throughout ELIS. Additional study is needed to assess the effects of *C. pendula* aggregations on local environmental conditions, local trophic dynamics, and overall productivity, as well as the conditions under which these aggregations form. This is especially important since *C. pendula* may be adversely impacted by physical disturbance, with unknown consequences for associated taxa and benthic diversity. This species may play an important and unrecognized role in fine sediment habitats within the Sound.

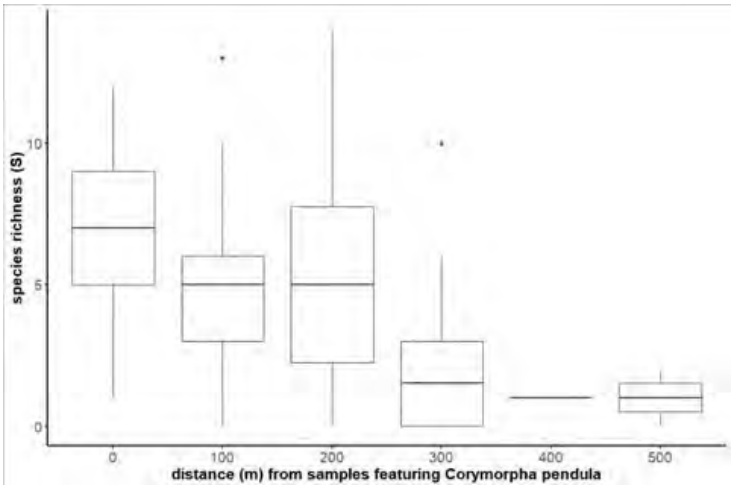

Figure 5.3- 39. Species richness within (distance = 0) and at increasing distances from C. pendula occurrences.

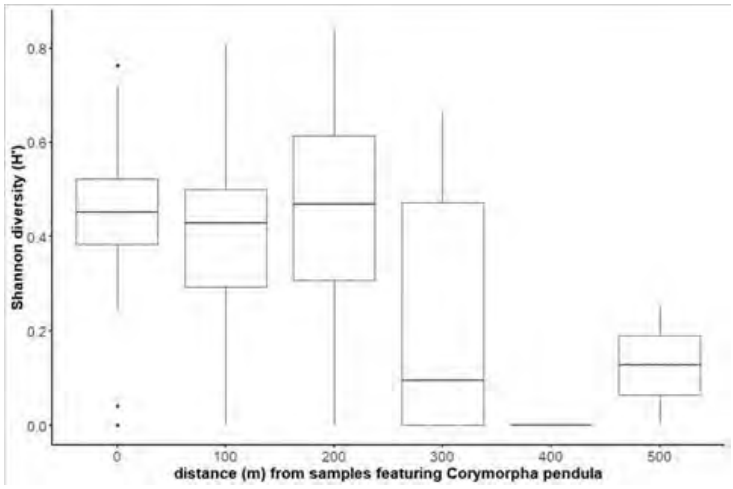

Figure 5.3- 40. Shannon diversity index within (distance = 0) and at increasing distances from C. pendula occurrences.

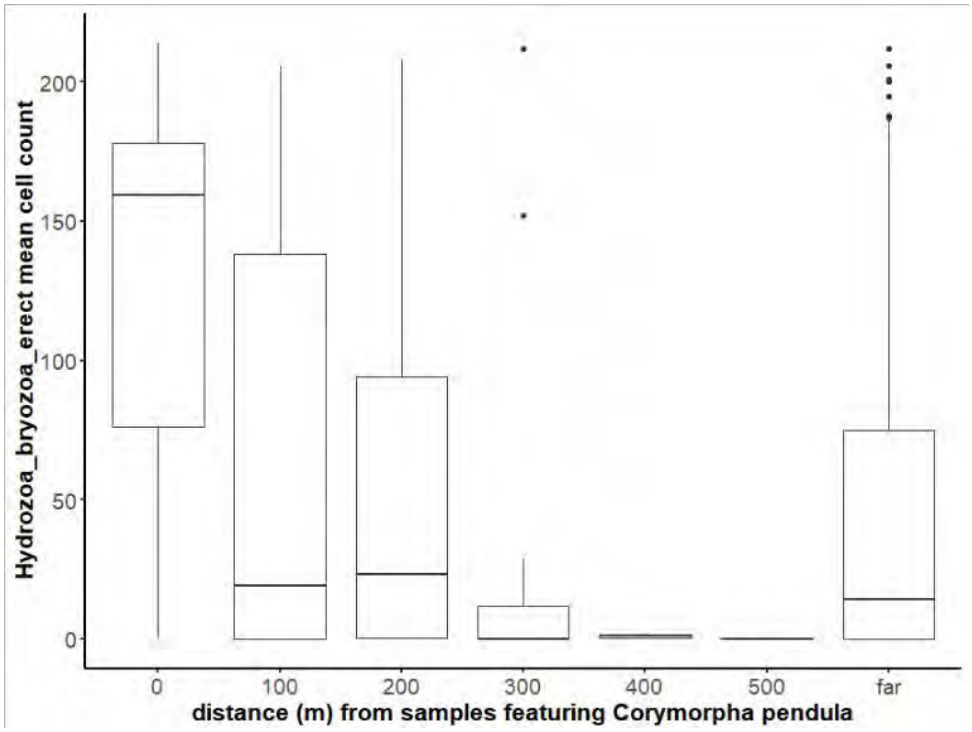

Figure 5.3- 41. Hydrozoan and bryozoan turf abundance within (distance = 0) and at increasing distances from C. pendula occurrences.

5.3.3.4.6 Blue Mussel Mytilus edulis and Atlantic Slipper Shell Crepidula fornicata: A Filter Feeder Regime Shift

Mytilus edulis has long been recognized as an ecologically important species that, in part, structures benthic communities throughout ELIS and FIS (e.g., Langton et al., 1995). In his analysis of data collected over nearly 3 decades, Zajac (1998) identified this filter feeding bivalve as the dominant species in benthic communities between the Connecticut River and Goshen Point in ELIS, as well as throughout central and eastern FIS (Figure 5.3-42). *M. edulis* aggregations enhance complexity to hard substrate seafloor features (e.g., reefs, ledges, gravel pavements) and form connected mats on finer grain sediments (initially settled on shell fragments) forming communities that are more diverse and productive than those in the surrounding sediments (Langton et al., 1995; Norling & Kautsky, 2007; zu Ermgassen et al., 2020). Observed increases in diversity of epifauna and infauna is especially pronounced in fine sediments, where *M. edulis* reefs provides hard substrates for epifaunal recruitment, and alter the characteristics of local sediments through biodeposition (Hatcher et al., 1994; Norling & Kautsky, 2007; zu Ermgassen et al., 2020).

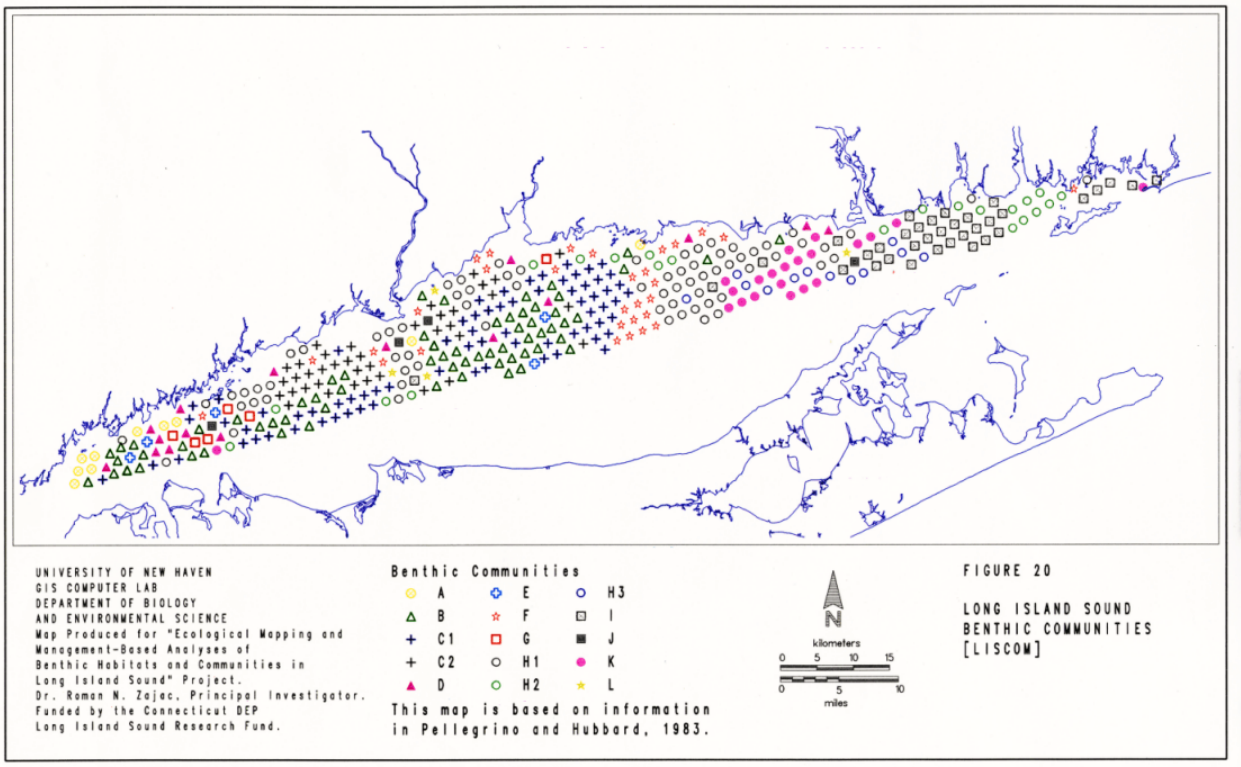

Figure 5.3- 42. Figure 20 in Zajac (1998). Benthic community I, visualized using in the map, was dominated by Mytilus edulis. See Zajac (1998) for analysis methods.

While *M. edulis* played a central role in diverse benthic communities of ELIS in these studies, the filter feeding gastropod *Crepidula fornicata* was not a dominant species in any of the more than dozen described benthic communities (Zajac, 1998). *C. fornicata* attach to hard substrates and form large stacks of conspecifics, which function in part as means of reproduction. In locations dominated by fine substrates, these stacks can form dense aggregations of *C. fornicata*, overlaying surficial sediments with a layer of irregular shell. When densities become very high, these aggregations can become reef-like structures with higher vertical profiles (Ackerman et al., 2015). Similar to *M. edulis* and other structure-forming suspension feeders, *C. fornicata* aggregations are associated with higher benthic diversity than surrounding sediments (de Montaudouin & Sauriau, 1999; de Montaudouin et al., 2018), but that increase in diversity may not match that of other benthic structure-forming suspension feeders (Preston et al., 2020).

Sampling using the SEABOSS platform revealed extensive changes in the distribution and abundance of these structure forming filter feeders. While *M. edulis* was still present from the Connecticut River through FIS, its distribution has decreased substantially since the 1980s (Figure 5.3-43a). Even when present, *M. edulis* was rarely the dominant benthic organism. The only sampling areas where *M. edulis* made substantial contributions to benthic communities (as determined by mean abundances of 5% cover or greater in SEABOSS images; Figure 5.3-44a) were limited to the eastern extent of FIS, where mean cover was 8.8% across all samples. In fact, these were the only sample areas in which *M. edulis* cover exceeded 5% in any single image.

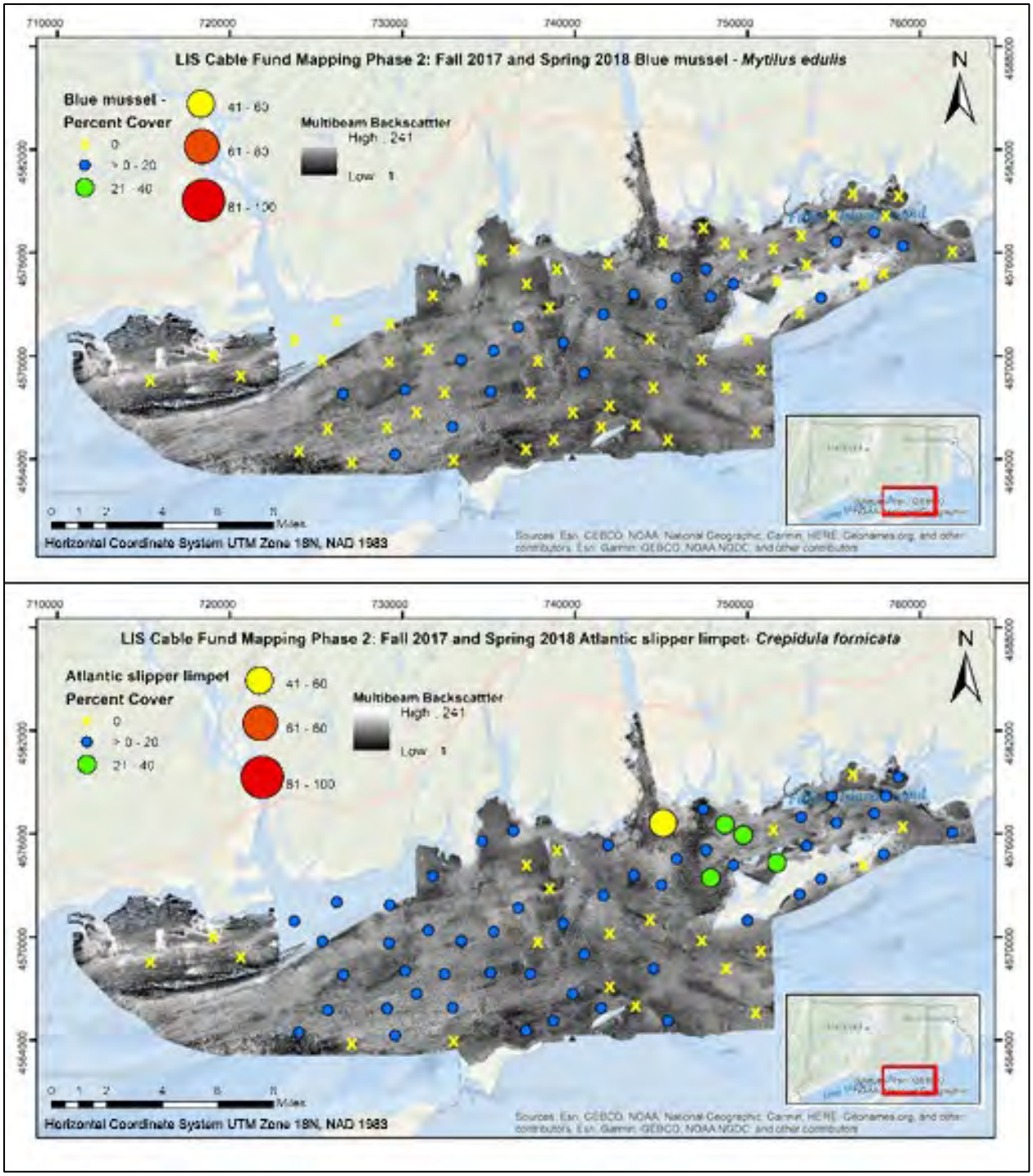

Figure 5.3- 43. Mean percent cover of Mytilus edulis (a – top) and Crepidula fornicata (b – bottom).

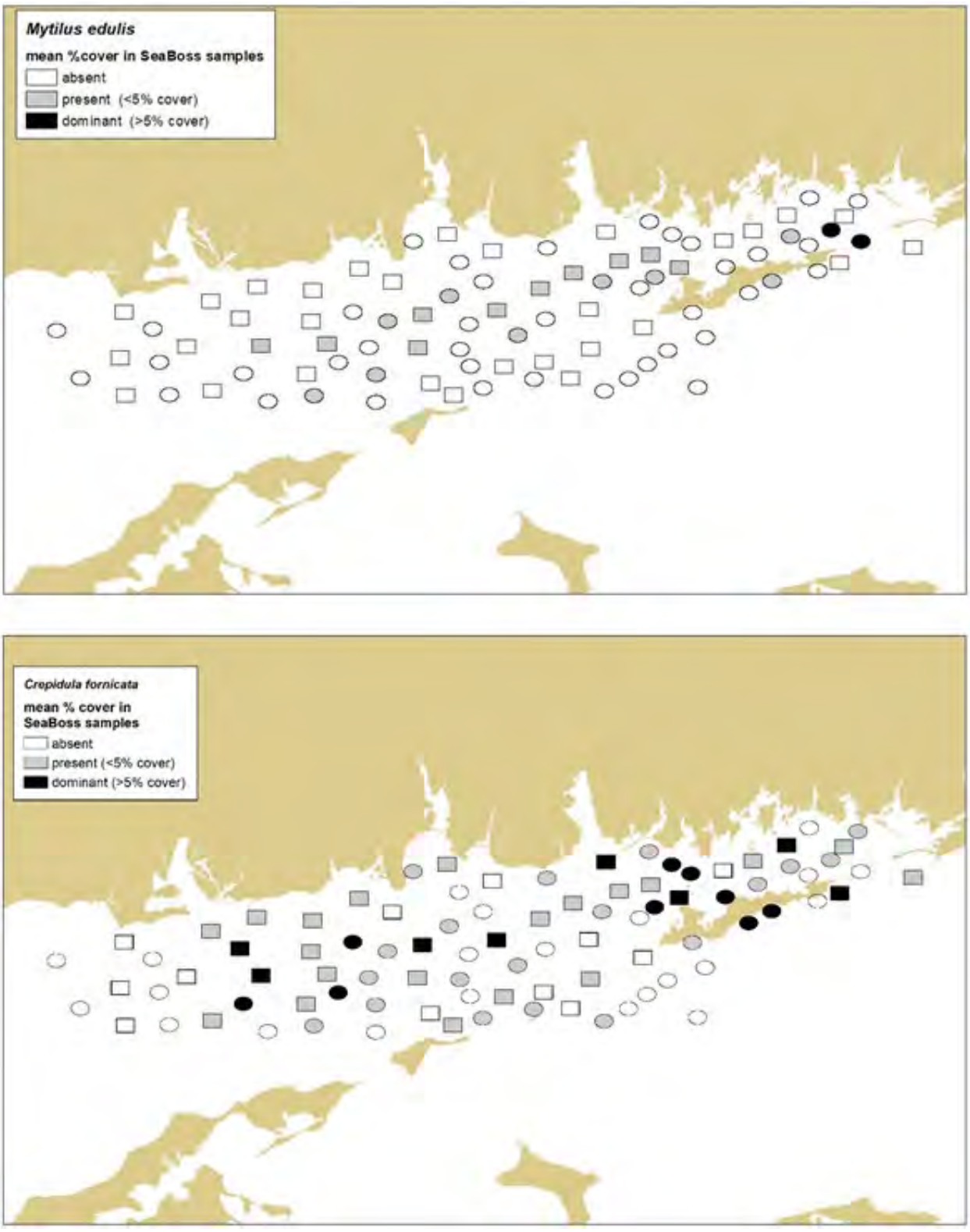

Figure 5.3- 44. Sample areas where Mytilus edulis (a – top) and Crepidula fornicata (b – bottom) were present (gray box) or dominant (black box). Presence defined as mean % cover between 0% and 5%; dominant defined as mean % cover between 5% and 100%.

While *M. edulis* distribution has contracted and its abundance has decreased, *C. fornicata* has expanded substantially (Figure 5.3-43b). *C. fornicata* was distributed throughout the Phase II area, averaging at least 5% cover in more than 20% of sample areas (17 of 77 total sample areas;

Figure 5.3-44b). While direct comparisons with the legacy datasets used in Zajac's (1998) analysis have not been determined (and are beyond the scope of this project), the areas of ELIS and FIS that were previously dominated by *M. edulis* approximately match those areas where *C. fornicata* is newly dominant apart from the eastern edge of FIS. In some locations, *C. fornicata* aggregations now form long, mostly continuous aggregations over fine sediments.

By dividing the Phase II area into 4 equal sections, not only can the wide longitudinal distributions of these species observed in the maps be seen, but also the center of those distributions (Figure 5.3-45). While *C. fornicata* is present throughout, *M. edulis* is completely absent from images in the far western extent of the study region. This includes areas where *M. edulis* had previously been found to be dominant. Additionally, although maximum abundance of *M. edulis* remains in eastern FIS, maximum occurrence (i.e., % of sample images in which *M. edulis* was observed) is much farther west, in the section of the study area extending from the mouth of the Connecticut River to Goshen Point where this species had previously been dominant. This is also the same region where occurrence of *C. fornicata* reaches its maximum, as nearly 50% of sample images contain this species.

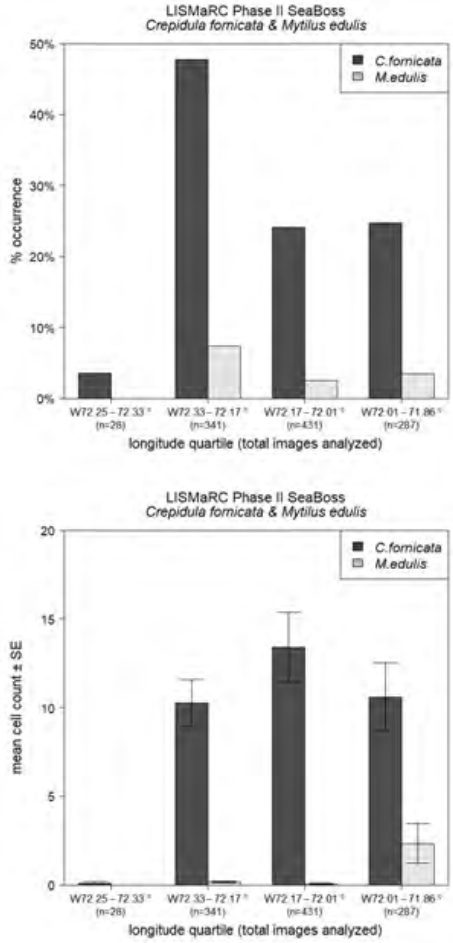

Figure 5.3- 45. M. edulis (light gray bars) and C. fornicata (dark gray bars) % occurrence (top) and mean abundance (bottom) by longitudinal section. Whiskers in mean abundance plot report standard error.

Determining the drivers of this evident shift in benthic community composition using data collected during this project is not feasible, but by focusing on the relationships between both *M. edulis* and *C. fornicata* and available environmental parameters, some insights based on patterns of distribution and abundance can shed some light on these changes. Stark differences in in the abundance of these species were revealed in the context of bottom complexity. While both species were most common on level or near-level seafloor (TRI < 0.07m; Figure 5.3-46),

the greatest densities of *M. edulis* were in the most complex habitats (mean TRI = 0.22 when *M. edulis* cover > 10%). Conversely, *C. fornicata* abundance dropped by nearly half in these same habitats compared to flatter substrates (mean 3.5% cover versus mean 6.2% cover). And while *M. edulis* occurrence peaked in deeper waters, abundance was highest in the shallowest habitats sampled, which include the rocky and highly complex eastern end of FIS (Figure 5.3-47). Similar contrasts were apparent in these both species' apparent relationships with seafloor current strength (maximum monthly bottom stress, tau or τ), a measure of the physical forces exerted on bottom sediments and organisms by tidal currents (Figure 5.2-74). While *M. edulis* was most common and abundant under the most dynamic conditions (i.e., highest maximum bottom stress, τ > 1.01Pa), *C. fornicata* was relatively rare and in lower densities than in areas with less tidal current strength.

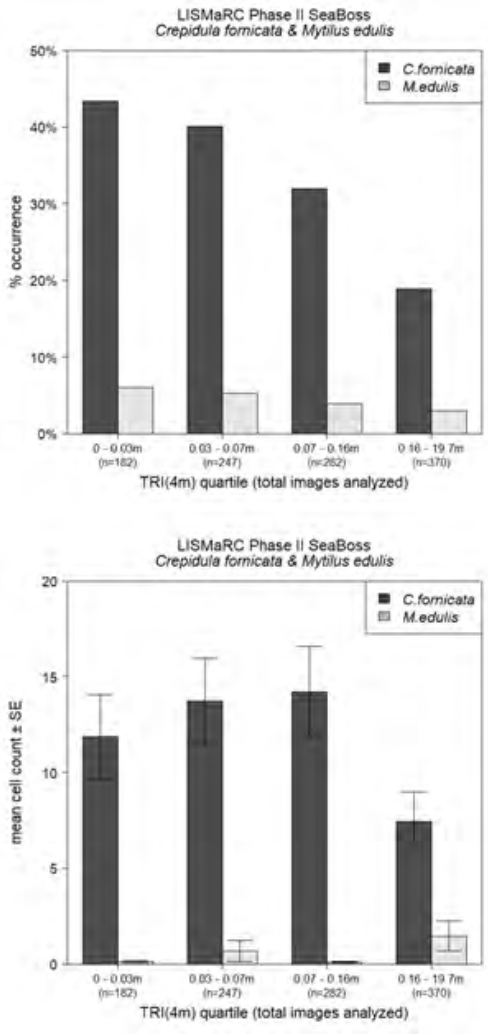

Figure 5.3- 46. M. edulis (light gray bars) and C. fornicata (dark gray bars) % occurrence (top) and mean abundance (bottom) by TRI quartile. Whiskers in mean abundance plot report standard error.

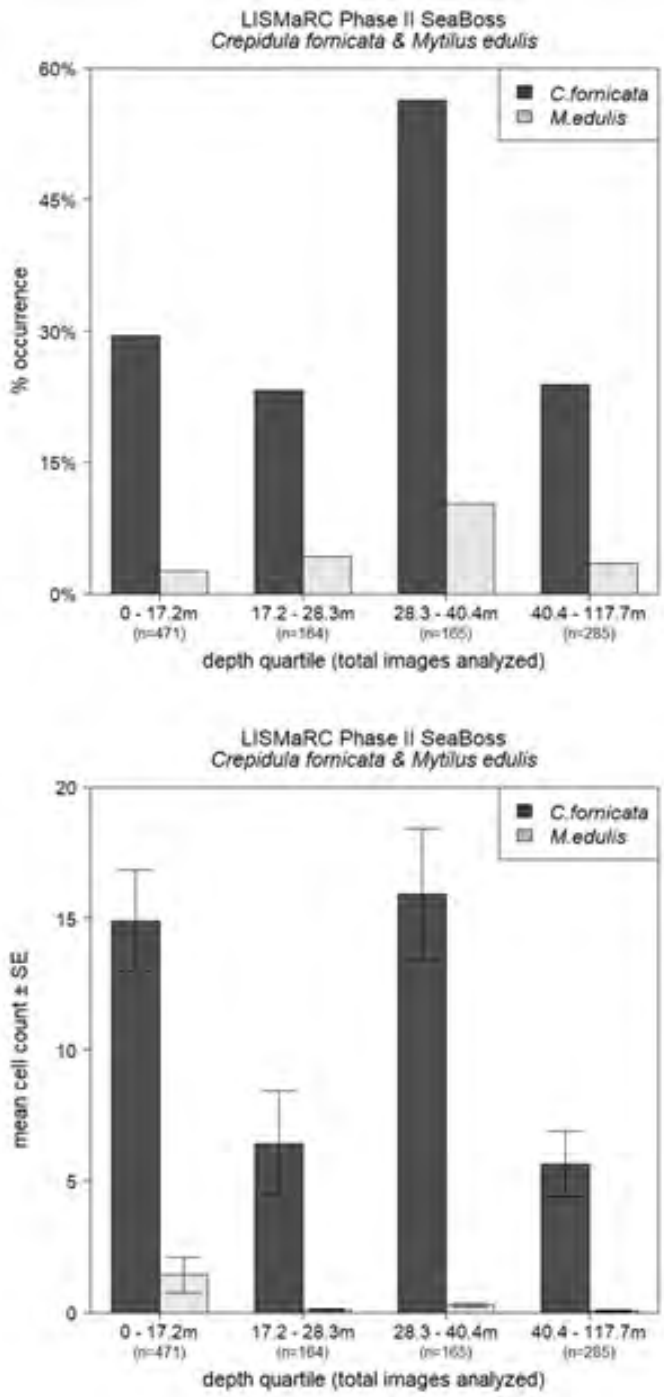

Figure 5.3- 47. M. edulis (light gray bars) and C. fornicata (dark gray bars) % occurrence (top) and mean abundance (bottom) by depth quartile. Whiskers in mean abundance plot report standard error.

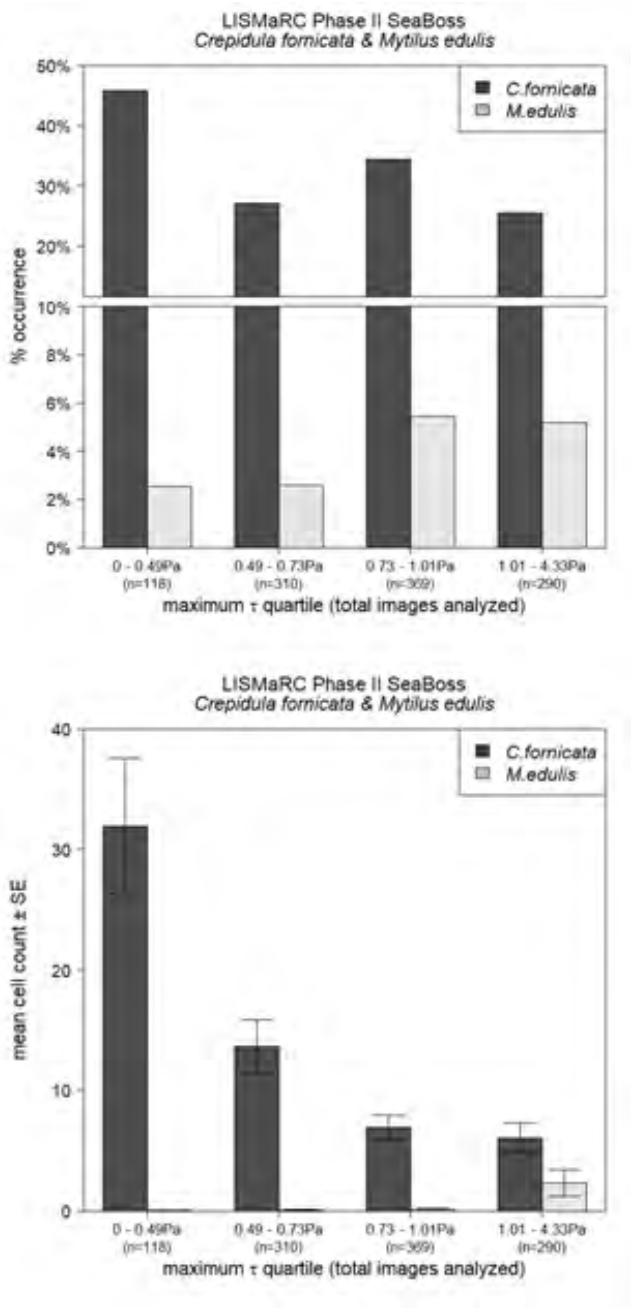

Figure 5.3- 48. M. edulis (light gray bars) and C. fornicata (dark gray bars) % occurrence (top) and mean abundance (bottom) by maximum monthly bottom stress quartile (maximum□□). Whiskers in mean abundance plot report standard error.

While *C. fornicata* was common and abundant in all 5 eCognition patch types compared to other taxa, neither species was evenly distributed across patches (Figure 5.3-49). Of the three heavily sampled patch types, both *M. edulis* and *C. fornicata* were most common in patch D, which is characterized by coarser sediments than either patch B or C (Table 5.3-3A). *M. edulis* was also most abundant in patch D; *C. fornicata* % cover was greater in patch C than in patch D, but these differences were marginal and both substantially exceeded those in patch B. Despite observed differences between patches, *C. fornicata* was one of the most common and abundant organisms in each of the patches. In contrast to *C. fornicata*'s ubiquity, *M. edulis* did not exceed 8% occurrence and did not reach 1% mean cover in any patches.

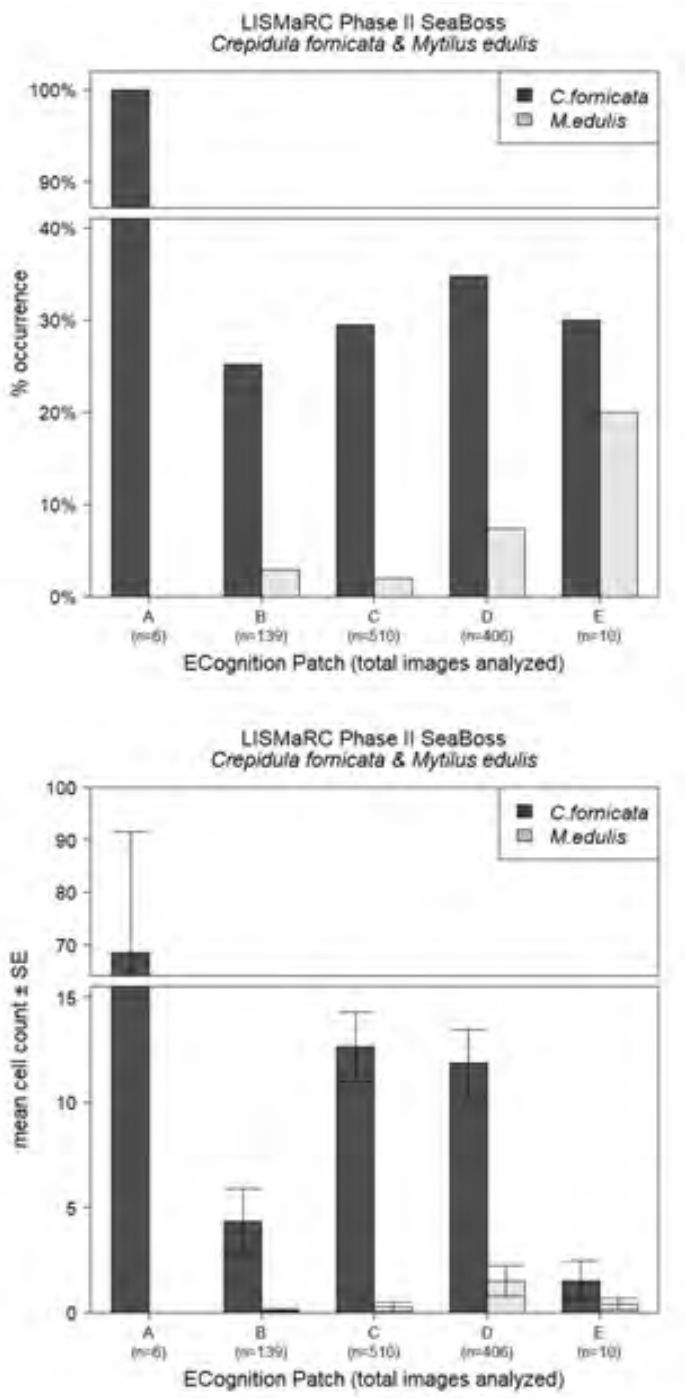

Figure 5.3- 49. M. edulis (light gray bars) and C. fornicata (dark gray bars) % occurrence (top) and mean abundance (bottom) by eCognition acoustic patch. Whiskers in mean abundance plot report standard error.

Combined influences of some environmental, physical, and spatial factors were revealed in the results of GLMM of species occurrence. Bottom complexity (TRI) and depth provided the strongest influence on the observed distribution patterns of both *M. edulis* and *C. fornicata* (i.e., model parameters in the best-fit GLMM's for both species consisted of these factors), with similar effects on both species. Occurrence decreased by more than half for both *M. edulis* (from 6% to 3%) and *C. fornicata* (from 43% to 19%) between the least and most complex bottom habitats (Figure 5.3-46). Occurrences of both species peaked in depths between 28m and 41m, with *C. fornicata* present in more than half of samples (56%; Figure 5.3-47). When considered in total, these results indicate both *M. edulis* and *C. fornicata* were common in deeper, relatively

flat seafloor locations. That the combined effects of TRI and depth did not explain a substantial portion of either *M. edulis*'s (marginal R^2 = 0.05) or *C. fornicata*'s (marginal R^2 = 0.07) occurrence suggests additional influences on these species' distributions.

Multiple factors also influenced the abundance of both species when they were present, as revealed by linear mixed models (LMM) of abundance. *M. edulis* density depended most on geographic location (longitude) and bottom current strength (maximum tau). While *M. edulis* was more than twice as likely to be observed between the Connecticut and Thames Rivers (present in 7.3% of images) than in eastern FIS (3.5% of images; Figure 5.3-45), abundance at the eastern extent of the Phase II area was nearly an order of magnitude greater (mean cover 1.1%) than further west to the mouth of the Connecticut River (mean cover 0.1%). Differences in the density of *M. edulis* at locations with the strongest bottom current conditions (mean cover 1.1%) were similarly much larger than in calmer areas of the seafloor (0.1%; Figure 5.3-48). The influence of longitude and maximum bottom stress explain most of the observed patterns in *M. edulis* abundances (margin R^2 = 0.58).

While the factors strongly affecting *M. edulis* abundances appeared to be clear, *C. fornicata* densities appeared to be the result of a complex mixture of influences including geography and bottom current conditions, as well as bottom complexity (TRI) and eCognition patch type. Where *M. edulis* abundance increased with bottom current strength, *C. fornicata* decreased in number. Under the calmest seafloor conditions *C. fornicata* was nearly 3 times more abundant (mean cover 14.8%) than in more dynamic areas (mean cover 5.2%; Figure 5.3-48). While the overall decrease in density with increasing bottom current strength is clear, *C. fornicata* meets the criterion for "dominance" discussed above in a number of sample areas where bottom currents are consistently strong. *C. fornicata* was most abundant at the eastern edge of LIS (Figure 5.3-45). Between the mouth of the Thames River (north) and the Race (south), *C. fornicata* densities for more than 1/3 greater (mean cover 6.2%) than in the remainder of the Phase II area (mean cover 4.6%). While densities on highly complex seafloor were less than those in flatter habitats (as described above), Tukey post-hoc comparisons of eCogntion-patch-specific *C. fornicata* abundances revealed significantly greater densities in patch C than in patch B (t = 2.97, df = 327; Figure 5.3-50). As might be expected when complex patterns are described by additive combinations of model parameters, the explanatory power of this model was limited (marginal R^2 = 0.08).

What led to the observed shifts in dominant structure-forming suspension feeding organism in large parts of ELIS is not clear based on available sample data and the potentially contributing factors examined during this project. In regions where it is invasive (Northeast Atlantic) and coincident with *M. edulis*, *C. fornicata* attachment to *M. edulis* shells has been shown to reduce growth and survival (Thieltges, 2005). No cases of epibionty were observed with *M. edulis* as the basibiont, but when found in dense aggregations *C. fornicata* were attached to both conspecific and to non-specific shells, so this process could have contributed to the observed changes. Another possible contributing factor could be a change in the quality of food resources. The dynamics of phytoplankton productivity, composition, dominance, and size spectra over recent decades in ELIS, while poorly resolved at this spatial scale (Lopez et al., 2014), could contribute to changes in survival, growth, and competitive interactions between these species. While phytoplankton is a predominant food resource, zooplankton also contributes to nutrition and growth in some ecological settings (Lehane & Davenport, 2006), and Rice et al. (2015) document a decrease in the size of zooplankton in LIS driven in part by temperature. While *M. edulis* feeding efficiency increases with particle size (Strohmeier et al., 2012), *C. fornicata* is not particularly size selective during suspension feeding and is highly

efficient at consuming relatively small phytoplankton (Barillé et al., 2006); Beninger et al., 2007). Although not demonstrated in direct comparisons, the decreased size of available prey in LIS may have influenced competition for seafloor area in ELIS.

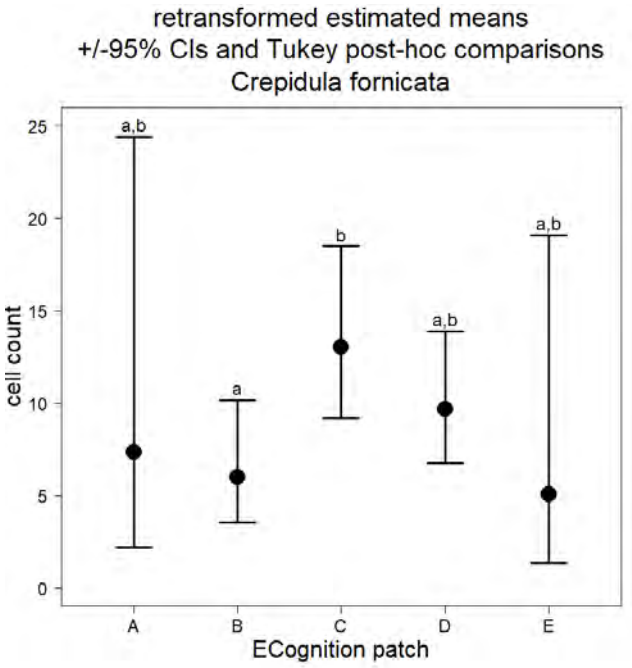

Figure 5.3- 50. LMM-derived estimated marginal means of C. fornicata abundance. Whiskers report standard deviation. Different letters indicate significantly different abundance based on Tukey post-hoc comparisons.

While these species appear to occupy shared habitats, patterns of abundance revealed potentially important distinctions in their responses to specific environmental conditions, albeit at different scales of commonality and abundance. The distinct response of *M. edulis* to the strength of bottom currents, in contrast to *C. fornicata*'s apparent preference for less dynamic habitats, may explain part of the observed spatial patterns of abundance. Most importantly, the small "foot hold" in eastern FIS where *M. edulis* may be considered dominant could result, in part, from the strength of tidal currents flowing through the inlet from BIS. Swift currents may benefit *M. edulis*, providing conditions that lead to higher feeding efficiencies (Dolmer, 2000). Additionally, longitude is merely a proxy for other environmental conditions, including increasingly oceanic conditions in LIS from west to east and large-scale differences in food resources for suspension feeders (Lopez et al., 2014). The eastern end of FIS, where *M. edulis* densities were at their maximum, is heavily influenced by BIS and experiences near-marine conditions (Deignan-Schmidt & Whitney, 2018). This may result in greater availability of larger food, providing *M. edulis* with a food source in the size range allowing for more efficient feeding (see above; (Strohmeier et al., 2012).

As discussed previously, there are important differences in the influences of reef-forming suspension feeders (e.g., *C. fornicata* supports less diversity in surrounding benthic communities than *O. edulis*; Preston et al., 2020). With the spatial distributions of both species in ELIS and FIS mapped and characterized during this project, additional sampling and analysis would be warranted to assess other, possibly related changes in benthic communities.

5.3.3.4.7 Interactions between Hard Substrate and Ecosystem Engineers: Cliona spp., Astrangia poculata, and invasive Didemnum vexillum

Shallow subtidal rocky habitats in LIS are also home to a range of attached and encrusting invertebrates. Among the characteristic species of these attached communities are a number of colonial organisms that can form large masses, including the stony coral *Astrangia poculata*, members of the boring sponge Genus *Cliona*, and the invasive colonial tunicate *Didemnum vexillum*. Each of these taxa are conspicuous when abundant and, to varying extents, form 3-dimensional structures that enhance habitat complexity (Schuhmacher & Zibrowius, 1985 Gittenberger, 2010; Schweitzer & Stevens, 2019). While competition between these taxa has been the focus of previous research in southern New England coastal waters (Grace, 2017), the ability to assess spatial distributions over such a large area that spans a range of habitat types provides the opportunity to gain new insights. This is especially pressing, considering the potential impacts of *D. vexillum*, a recently introduced invasive tunicate which can spread quickly via fragmentation and overgrow other benthic organisms (Daley & Scavia, 2008).

While early evidence of *D. vexillum* effects on benthic communities in LIS suggest either neutral or even positive influence on diversity (Mercer et al., 2009), its impacts on specific benthic taxa can be negative (Grace, 2017). Both coldwater corals and structure- forming sponges were identified as being worthy of special consideration and protection through the LIS Blue Plan, a marine spatial planning process developed under the direction of the State of Connecticut's legislature (CT DEEP, 2019). The Blue Plan identified "ecologically significant areas" (ESAs), locations that feature sensitive or rare habitats or biological communities, based in part on the distribution of key taxa, including *A. poculata* and *Cliona* spp. *D. vexillum* presence and high abundance in the Phase II study area, especially its co-occurrence with *A. poculata* or *Cliona* spp., could provide the groundwork for future targeted studies to resolve consequences of these interactions and ensure the persistence of these benthic organisms.

A. poculata, northern star coral, is a Scleractinian coral distributed along the North American continental shelf from the Gulf of Mexico to Cape Cod. Although ahermatypic (i.e., non-reef building), *A. poculata* is considered constructional (i.e., creates 3-dimensional carbonate structures; Schuhmacher & Zibrowius, 1985) due to the impacts on small-scale, localized complexity of its calcium carbonate "stony" skeleton. While *A. poculata* does host symbiont photosynthetic dinoflagellates, this relationship is facultative. Reliance on heterotrophy increases in conditions of low light availability and low winter temperatures (Dimond & Carrington, 2008; Dimond et al., 2013). Towards the northern limit of their range along the southern coast of New England, growth is limited to spring through fall, primarily relying on polyp feeding rather than endosymbiotic autotrophic sources (Dimond & Carrington, 2007). Although primarily heterotrophic, nearly ¼ of annual growth can be attributed to symbiont photosynthesis in New England waters, highlighting the importance of light availability to the persistence of *A. poculata* (Dimond & Carrington, 2007). Despite the availability of light for photosynthesis in shallow areas, competition for resources, primarily access to light and hard substrates, limits *A. poculata* densities in very shallow waters. Macroalgae outcompete *A. poculata* in these habitats both reducing photosynthesis through consistent shading and even physical abrasion of soft tissue (Jacques et al., 1983; Grace, 2004). Direct competition for space with other epifauna also limits prevalence, as is the case for *A. poculata* with the invasive colonial tunicate *D. vexillum* and boring sponges of the Genus *Cliona* (Grace, 2017).

Members of the Genus *Cliona* are found in marine, estuarine, and freshwater habitats worldwide. Known as boring sponges, these demosponges excavate into calcium carbonate materials- including mollusk shell, coral, and limestone- using a combination of chemical and physical means (Rützler & Rieger, 1973). Clionaid boring sponges take various forms, even within the same species, making them difficult to define taxonomically without microscopic investigation of spicule composition and molecular analyses (Xavier et al., 2010). *Cliona* spp. can be found in boring form, with only oscula visible protruding from mollusk shells, as well as encrusting, as a thin sheet over boulder or bedrock, and massive, forming large masses or towers, forms (Figure 5.3-51); these forms are also referred to as alpha, beta, and gamma stages, respectively, in boring sponges (Rosell & Uriz, 2002). Gamma stage boring sponge can substantially increase substrate complexity, providing important habitat for mobile macrofauna including fish (Miller et al., 2010). Boring sponge infection of commercial aquaculture can result in reduced growth, high mortality, and visible damage precluding commercial value (Carver et al., 2010; Carroll et al., 2015). *Cliona* spp. boring extends beyond bivalves to gastropods (Stefaniak et al., 2005) and corals (Nava & Carballo, 2008).

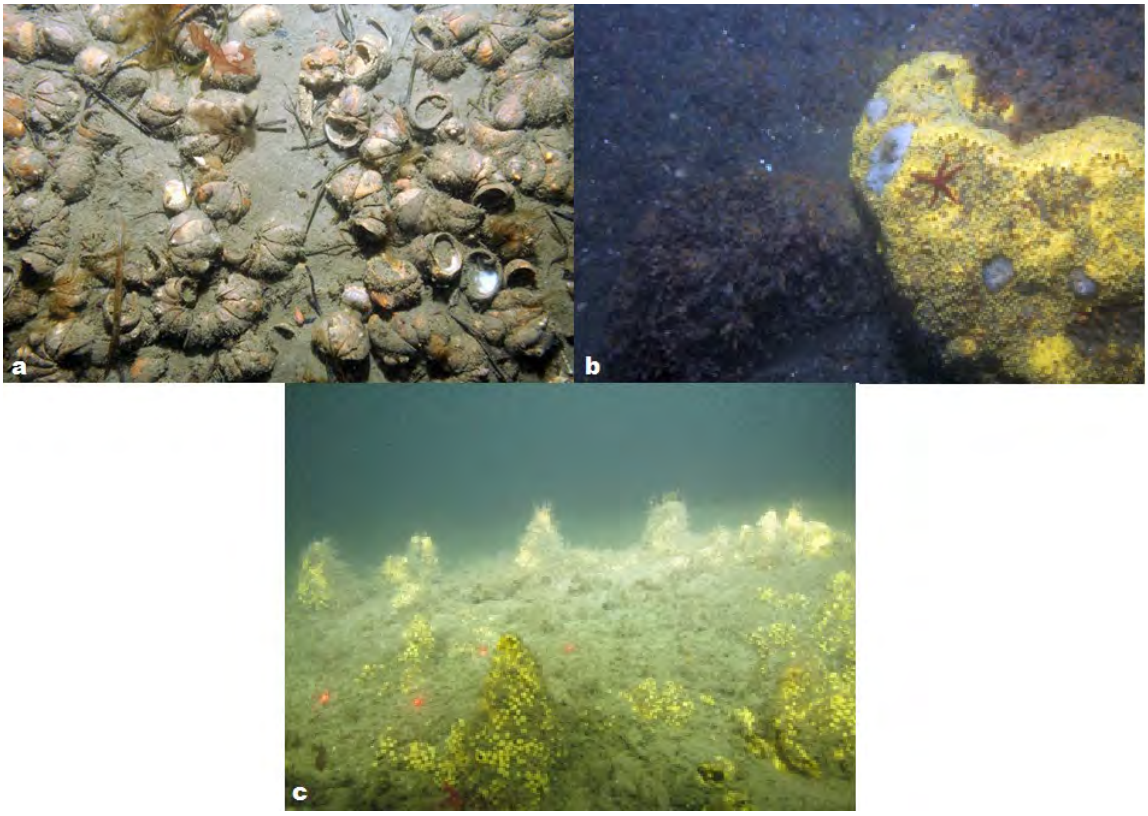

Figure 5.3- 51 Forms of Cliona spp. colonies: (a) alpha-stage visible as yellow oscules in C. fornicata shells (enlarged images below main image); (b) beta-stage colony covering a boulder; and (c) gamma-stage colonies forming towers.

D. vexillum is a colonial ascidian that has reached nearly global distribution in the past 50 years (Lambert, 2009). First observed in LIS less than 2 decades ago, *D. vexillum* colonies form large contiguous masses, overgrowing substrates as well as epibenthos (Mercer et al., 2009). Following its appearance in US waters, the invasive tunicate garnered much attention due to its potential to harm native biological communities (Daley & Scavia, 2008), as well as to its conspicuousness (Auker, 2019).

All three taxa were relatively common occurrences during sampling. *Cliona* spp. were observed in 12.6% of all images, while *A. poculata* was observed in 9.29% and *D.* vexillum 3.56%. To put these values in context, all were in the top 20% of identified taxa based on occurrence. All

were also widely distributed, present in 46% (*Cliona* spp.), 40% (*A. poculata*), and 24% (*D. vexillum*) of all sample areas (blocks or sites). *Cliona* spp. was very common in FIS and northern BIS, appearing in nearly ¾ of the sample areas to the east of the Thames River (20 of 27 sample areas; Figure 5.3-52). At the scale of each sample image, *Cliona* spp. became increasingly common moving east from the mouth of the Connecticut River into FIS, where boring sponges were observed in nearly 1/5 of all images (Figure 5.3-53). Mean abundance was highest in the eastern half of the Phase II area. *A. poculata* had 2 distinct spatial centers of their distribution-Fisher's Island Sound and west of the Race between Goshen Point/Niantic Bay and Plum Island (Figure 5.3-54). In this latter area *A. poculata* also reached its peak abundance, accounting for >12% of each sample image in which it was observed. While less common than *A. poculata*, *D. vexillum* was also observed more in this region than in any other and covered 13% of the substrate in sample images on average (Figure 5.3-55).

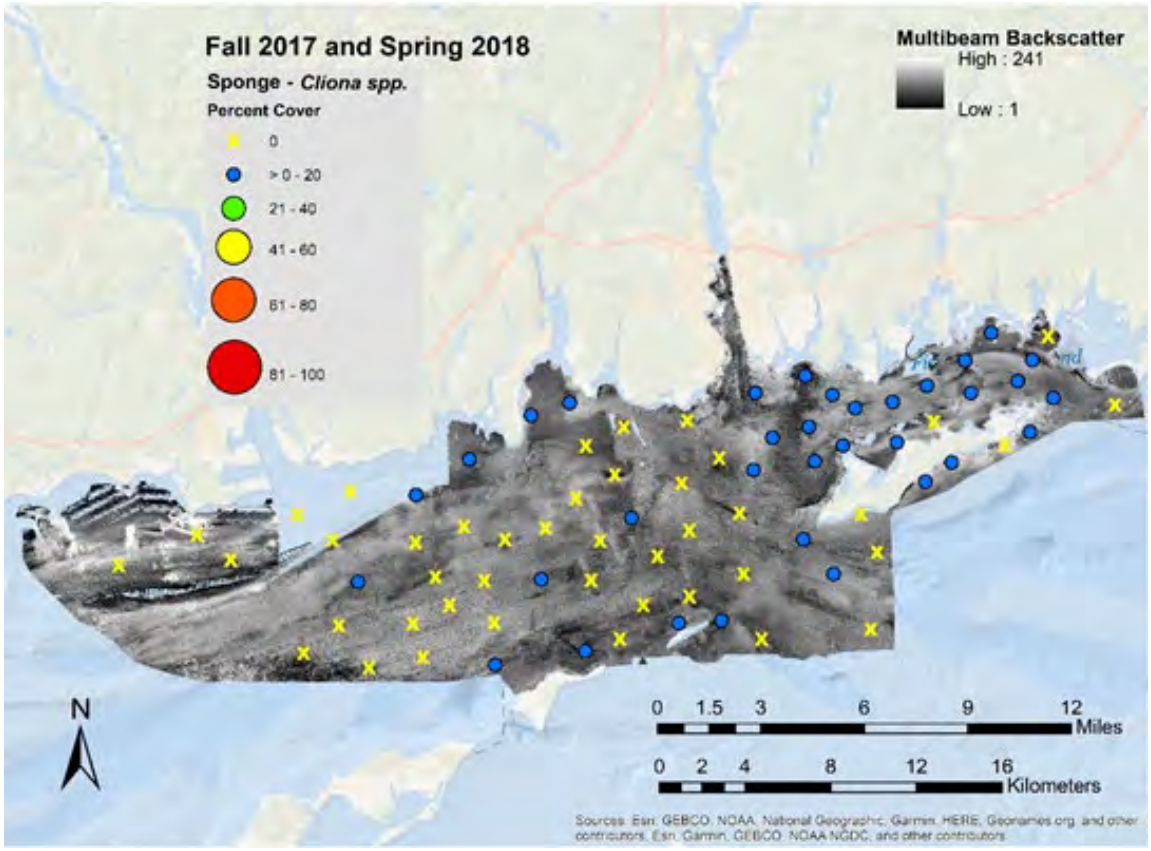

Figure 5.3- 52. Mean percent cover of Cliona spp. per Block/site sampled.

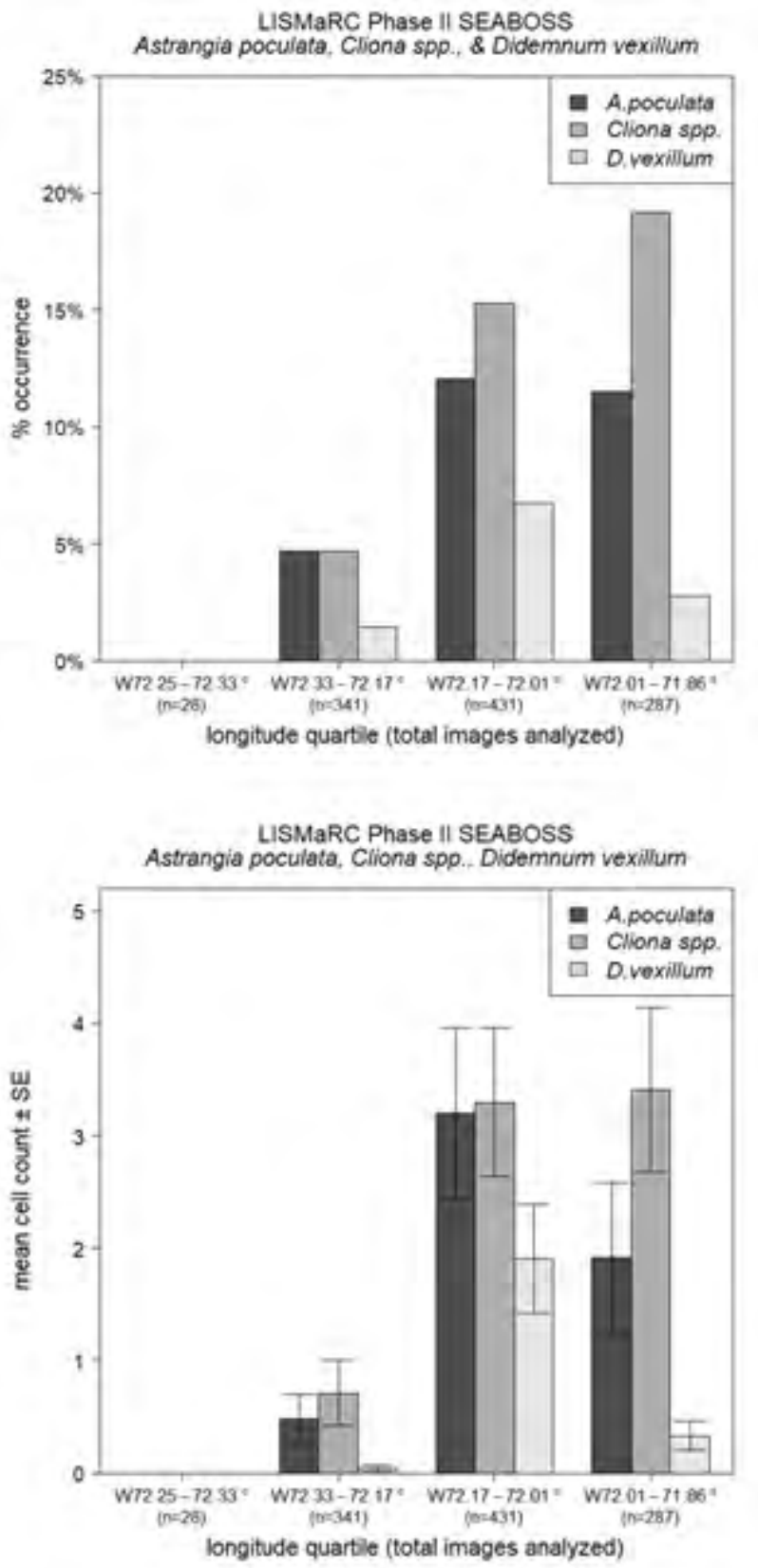

Figure 5.3- 53. A. poculata (dark gray bars), Cliona spp. (light gray bars), and D. vexillum (white bars) % occurrence (top) and mean abundance (bottom) by longitudinal section. Whiskers in mean abundance plot report standard error.

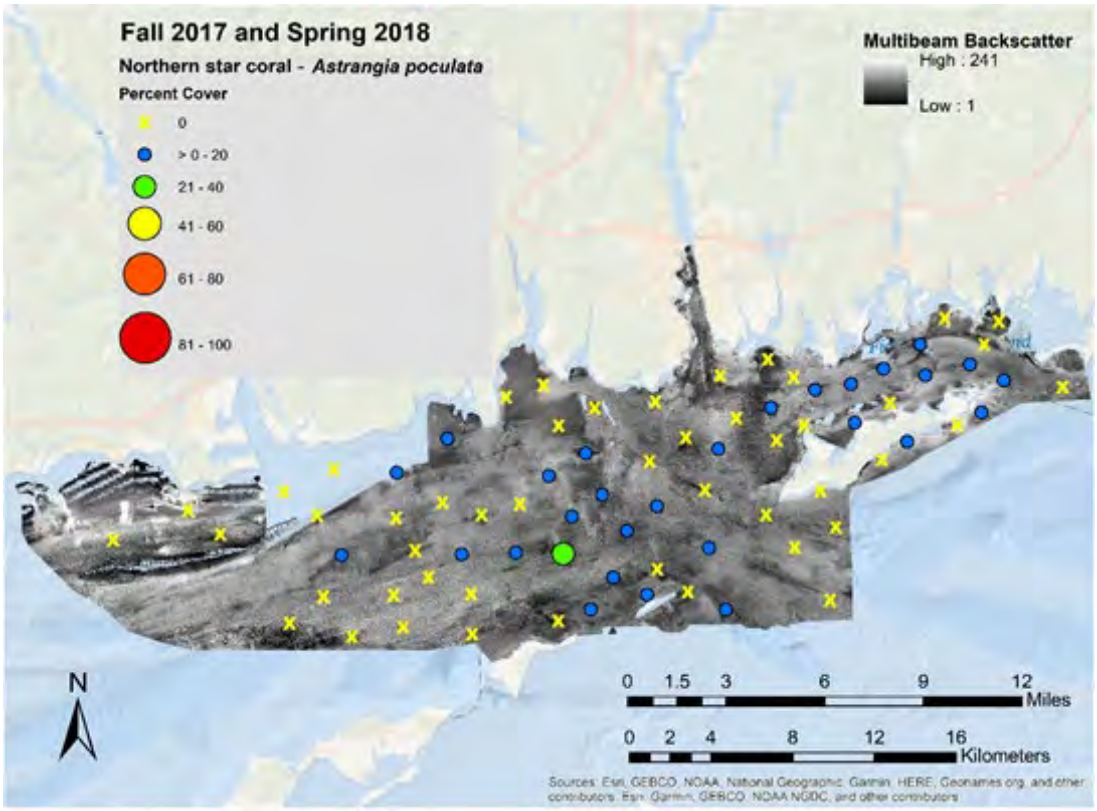

Figure 5.3- 54. Mean percent cover of A. poculata per Block/site sampled.

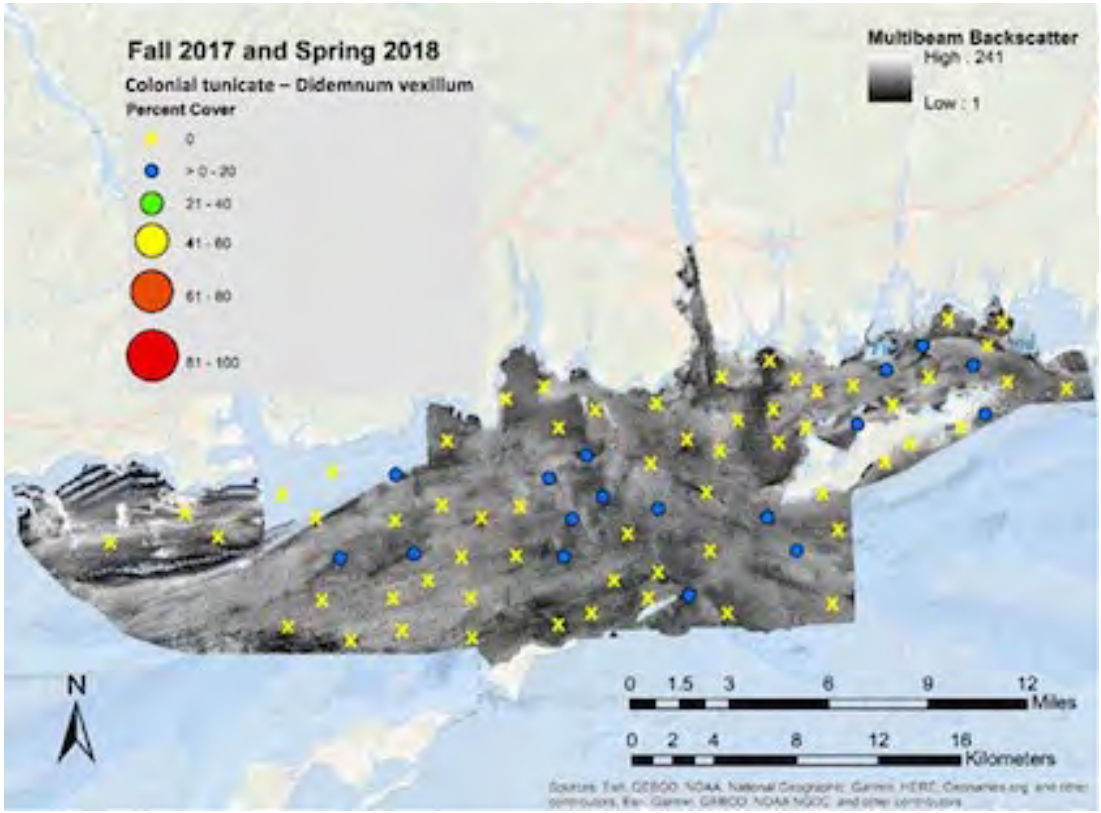

Figure 5.3- 55. Mean percent cover of D. vexillum per Block/site sampled.

A. poculata, *Cliona* spp., and *D. vexillum* share important characteristics, such as the need for solid surfaces for attachment and reliance on filter-feeding. These similarities likely drove some of the observed patterns in presence and abundance, such as the occurrences and

abundances of all three taxa increasing with substrate complexity (i.e., TRI; Riley et al., 1999; Figure 5.3-56). Greater spatial complexity, as measured using derivatives of bathymetric data like TRI, are proxies for hard substrates. Another characteristic of these taxa was how often they were observed as large aggregations covering much of the visible substrate. When present, *A. poculata* exceeded 10% cover in 22% of sample images, *Cliona* spp. exceeded this threshold in 28% of occurrences, and *D. vexillum* did so in 1/3 of its observed occurrences. Although an imperfect measure, this 10% coverage value does serve as a useful threshold for instances where these organisms may strongly influence benthic communities (e.g., *Cliona* spp. impacts on mollusk communities; Coleman, 2014) and attract mobile macrofauna.

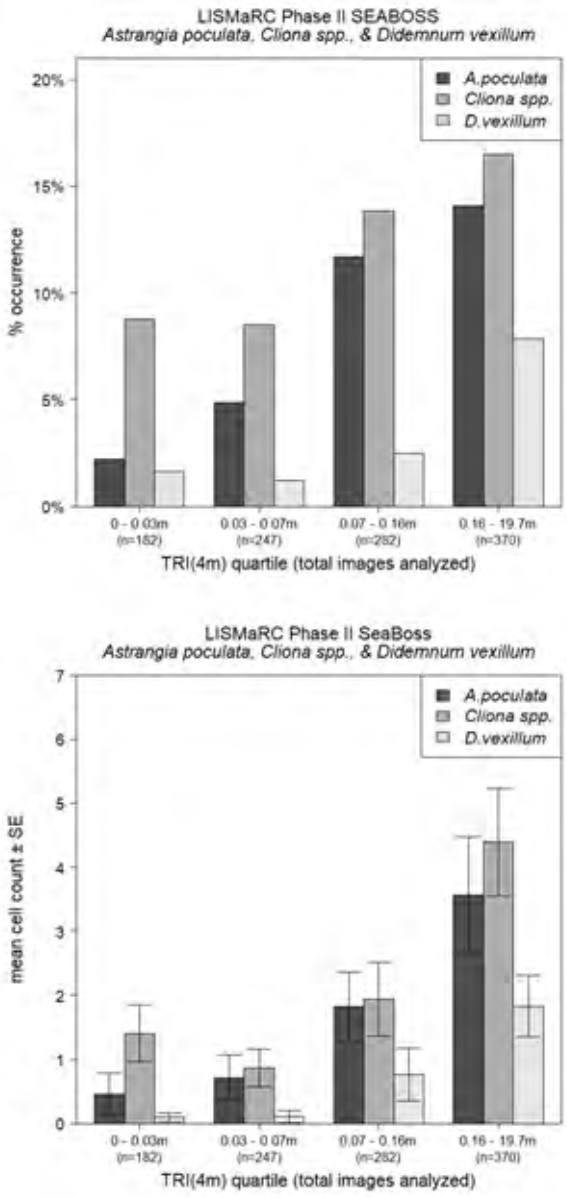

Figure 5.3- 56. A. poculata (dark gray bars), Cliona spp. (light gray bars), and D. vexillum (white bars) % occurrence (top) and mean abundance (bottom) by TRI quartile. Whiskers in mean abundance plot report standard error.

Perhaps unsurprisingly, *Cliona* spp. and *A. poculata* were commonly observed in close proximity- boring sponge appears in 25% of the images where *A. poculata* was identified (15 of 60 images). Both of these organisms attach to hard substrates, so their co-occurrence could be expected. While *A. poculata* was mostly limited to hard geological substrates (i.e., mostly

boulders), *Cliona* spp. was observed in finer substrates both as alpha stage sponges usually within large slipper shell beds and as gamma stage towers that likely began as alpha stage within bivalves. *D. vexillum* was less often found along the other two taxa, present in 8% and 9% of the images, respectively, featuring *A. poculata* and *Cliona* spp. Although *D. vexillum* was less widely distributed in comparison to *A. poculata* and *Cliona* spp., some tunicate colonies may have gone undetected in SEABOSS sampling. *D. vexillum* was observed on the lateral faces of boulders and rocky outcroppings during ROV and wet-diving sampling efforts (Figure 5.3-57) where they were far less likely to be capture by orthogonal imaging from the SEABOSS system.

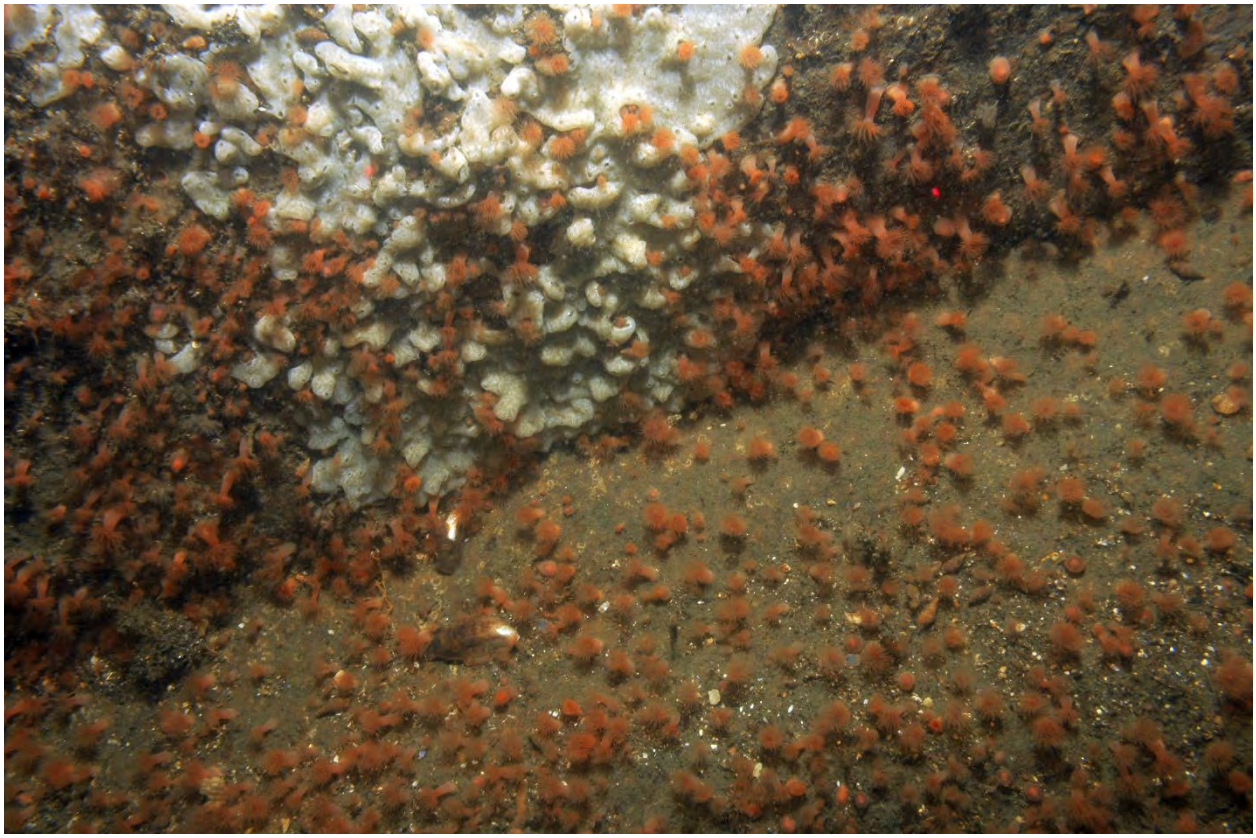

Figure 5.3- 57. D. vexillum colony on a vertical rock face (LISMaRC_Fall2017_DSC_IrfColCor_3129).

While their similar ecology did lead to the above similarities, there were some interesting divergences in occurrence and abundance. The depths at which these organisms were most common differed, as *Cliona* spp. appeared in more than 1/5 of sample images taken in the shallowest areas sampled by SEABOSS (to 17m) and *A. poculata* was nearly as common in moderately deeper habitats (17m - 28m). *D. vexillum* was most common below 40m (Figure 5.3-58). Abundance peaked for these taxa in these same depths. *A. poculata*'s limited distribution on the shallowest hard substrates has been observed previously, and most likely is a consequence of competition for both substrate with other attached fauna and access to light with macroalgae (Jacques et al., 1983; Grace, 2004). While *D. vexillum* has been observed in shallow habitats during its worldwide expansion, there is some evidence of limits on its distribution induced by other fauna in places it has invaded, both in the form of direct competition with other epifauna for space (Grace, 2017) as well as predation (Forrest et al., 2013). While not documented in the LIS, similar interspecific interactions may control *D. vexillum* abundance and distribution.

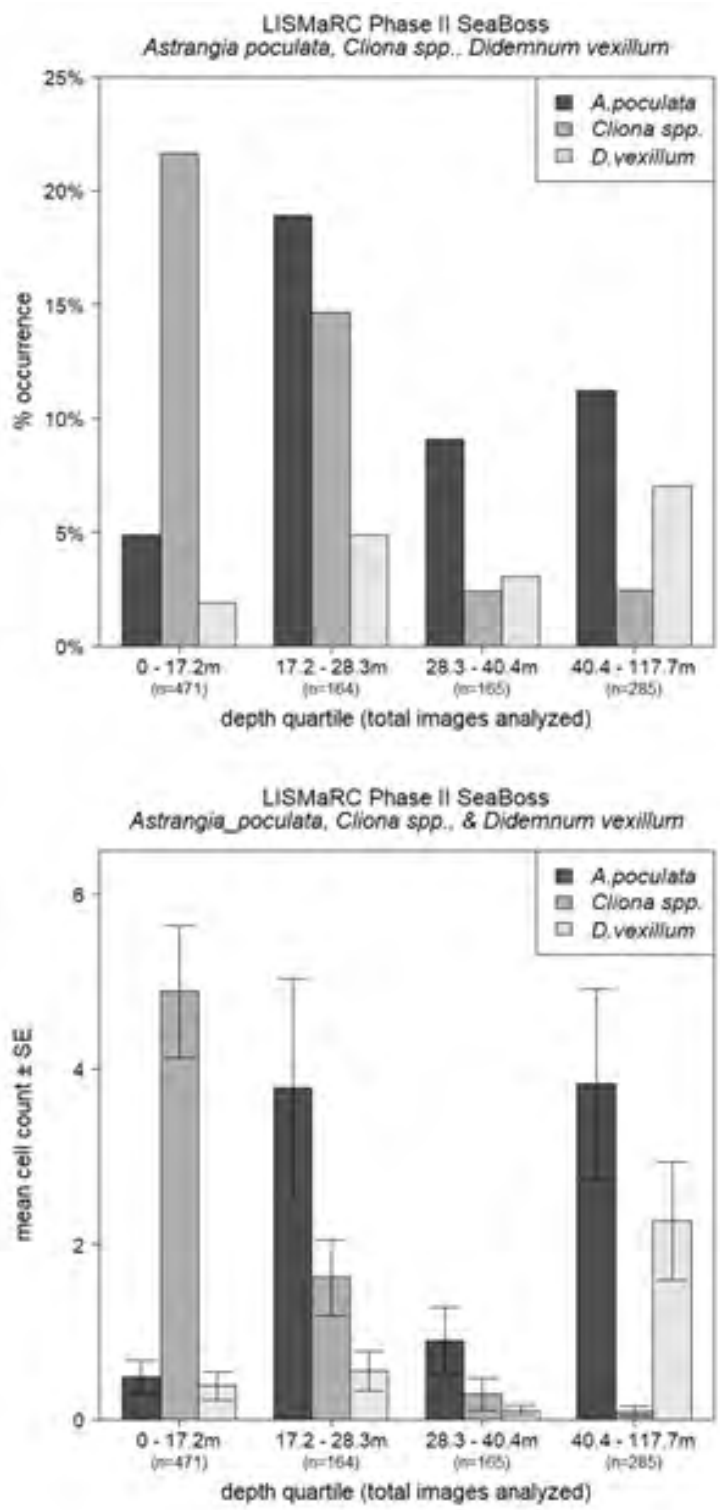

Figure 5.3- 58. poculata (dark gray bars), Cliona spp. (light gray bars), and D. vexillum (white bars) % occurrence (top) and mean abundance (bottom) by depth quartile. Whiskers in mean abundance plot report standard error.

These three taxa also diverged in their apparent response to tidal currents (tau). While *A. poculata* was evenly distributed across areas experiencing a wide range of bottom current conditions, the coral was entirely absent from the lowest energy habitats (Figure 5.3-59). Boring sponges were observed more than four times as often in the less energetic half of the Phase II sample area as compared to the higher energy half (present in 23.3% and 5.6% of sample images, respectively). Although far less common overall, *D. vexillum* was nearly four

times more common in areas that experience the strongest bottom currents (5.5%) than the remainder of the sample area (1.4%) and, like *A. poclulata*, was completely absent from areas with weak bottom current conditions. Slow currents are associated with higher sedimentation rates, which can negatively impact corals like *A. poculata* and may, in part, explain their absence from particularly low energy patches of seafloor (Baynes & Szmant, 1989). *D. vexillum* abundance in areas experiencing strong bottom currents is more surprising, as this colonial tunicate is associated with low energy areas in other locations where it is invasive (Vercaemer et al., 2015).

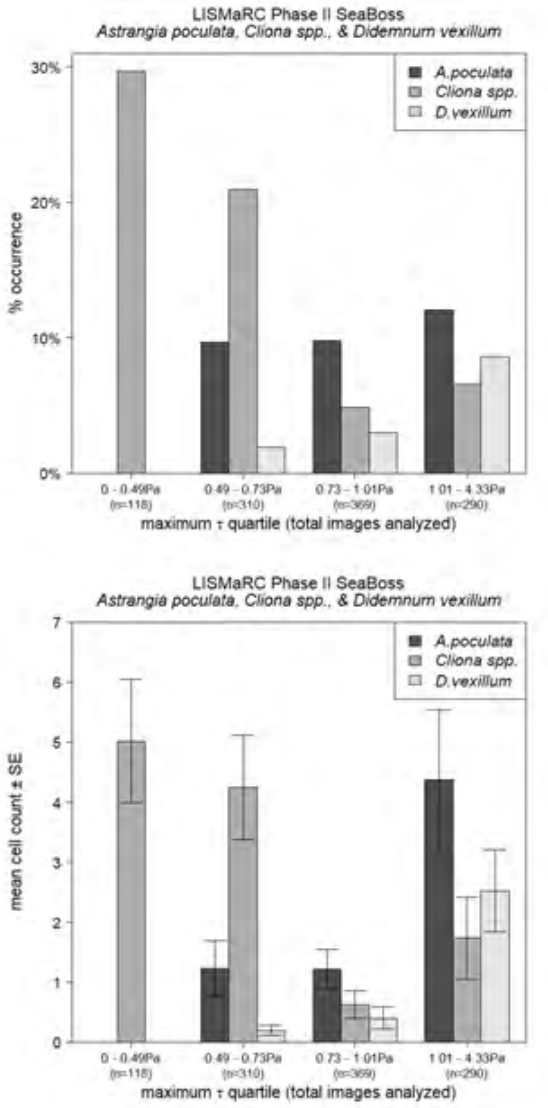

Figure 5.3- 59. A. poculata (dark gray bars), Cliona spp. (light gray bars), and D. vexillum (white bars) % occurrence (top) and mean abundance (bottom) by maximum monthly bottom stress quartile (maximum τ). Whiskers in mean abundance plot report standard.

Both *A. poculata* and *D. vexillum* were increasingly common in areas featuring coarser substrates (as represented by eCognition patches; Figure 5.3-60). Although no eCognition patch types were characterized as primarily consisting of hard substrates, neither organism would be expected in the fine sediments characterizing much of the Phase II area and represented by patch types A and B. While *Cliona* spp. similarly require hard substrates, boring sponges were most common and abundant in Patch Type C, which is primarily composed of gravelly sand. Interestingly, mean abundance of *C. fornicata* was also high in Patch Type C.

Alpha-stage *Cliona* spp. were almost exclusively observed in *C. fornicata* beds, which may underlie the relatively high mean abundance of boring sponges in gravelly sand.

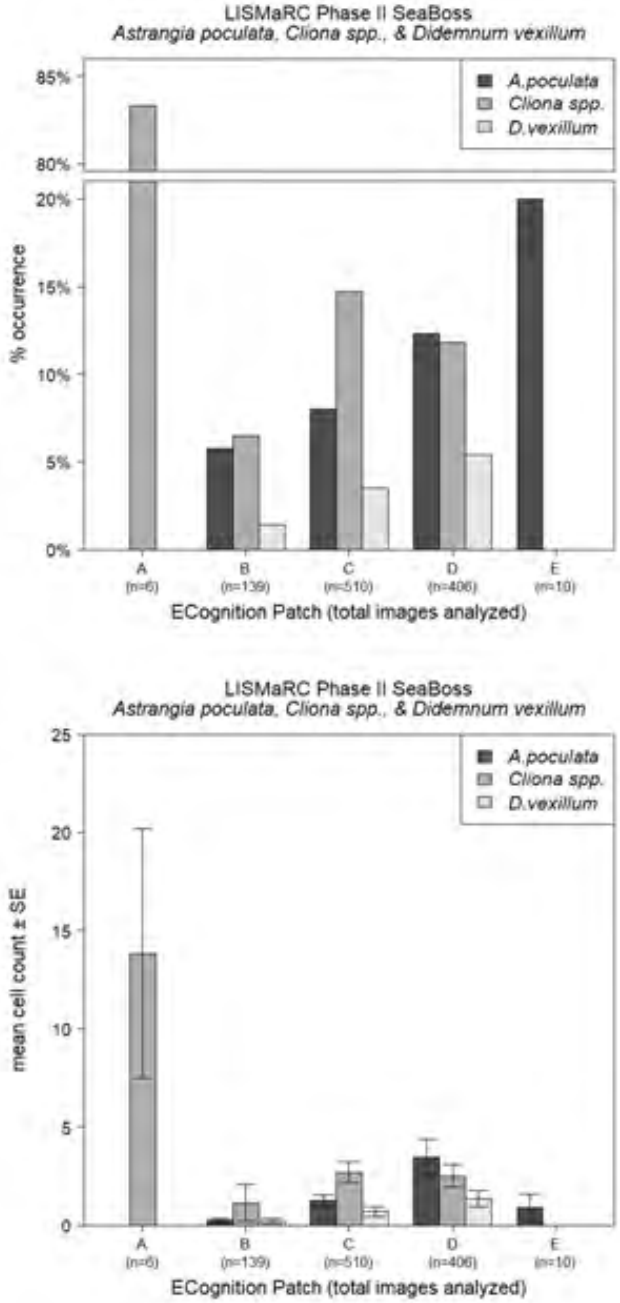

Figure 5.3- 60. A. poculata (dark gray bars), Cliona spp. (light gray bars), and D. vexillum (white bars) % occurrence (top) and mean abundance (bottom) by eCognition acoustic patch. Whiskers in mean abundance plot report standard error.

Modeling results of occurrence confirmed the importance of substrate to *A. poculata*, as the best fit model was limited to TRI as the lone factor influencing occurrence. The combined influence of TRI and depth explained some of the observed distribution of *Cliona* spp. in the study area. While the best-fit model for *A.* poculata accounted for less than 1% of observed variance (marginal $R^2 < 0.01$), the combination of substrate complexity and depth explained 8% of *Cliona* spp. occurrences. Interestingly, no combination of explanatory factors exceeded the null model in describing *D. vexillum* occurrences. Both *A. poculata* abundance also varied with TRI and longitude, both more abundant as TRI increases but differing in longitudinal patterns, *A. poculata* increasing east to west and *Cliona* spp. west to east. Linear relationships

with longitude proved to be fairly weak, explaining 3% of *A. poculata* and 1% of *Cliona* spp. abundance. *D. vexillum* abundance increased with both increasing current strength and from west to east, explaining 18% of variance in abundances.

5.3.3.4.8 Shell biogenic habitat

Biogenic shell debris, including both whole valves and pieces of shell, were almost ubiquitous, absent from only a single block/site (Figure 5.3-61). Present in more than 9 of 10 images analyzed (92.6%), shell cover varied throughout the sample area. In some places, shell consisted of several scattered valves over fine sediment habitats, while in others the seafloor was completely covered by shell debris. In limited areas, shell deposits were concentrated in troughs or depressions in finer sediments, which was also observed in Phase I area sampling (Stefaniak & Auster, 2015) as well as in other regions (Auster et al., 1996). Shell debris is present in areas featuring gastropods, but can also aggregate shell at the base of steep slopes with fine grained sediments, in the roughs of sand waves, and in flow refuges when sorted by tidal currents and storm energy. Once deposited, shell may be further transported by currents, be covered by shifting sediments, or remain as an intact habitat for centuries. East of the Connecticut River mean shell cover was nearly 4 times greater than west of the river mouth (Figure 5.3-62). Shell covered more of the substrate in deeper areas, where it may have accumulated in deposits due to current-mediated transport. Shell cover did increase in areas with stronger bottom currents (as represented by maximum tau; Figure 5.3-63), and shell deposits in areas that experience strong bottom currents may either be covered by shifting sediments or undergo further transport. Shell density increased with sediment grain size (as represented by eCognition patch; Figure 5.3-64). Shell deposits increase the amount of hard substrate available for epifauna and flora (e.g., sponges, Nicol & Reisman, 1976), serve as refuge from predation (e.g., recently settled bivalves, Glaspie & Seitz, 2018; crustaceans, Auster, 1995; juvenile fish, Auster et al., 1995, Langton et al., 1995, and Scharf et al., 2006), and increase diversity across habitat mosaics (Thrush et al., 2006). The presence of shell can also limit emergent infaunal communities that prefer fine sediments (e.g., tube worms, Raineault et al., 2012).

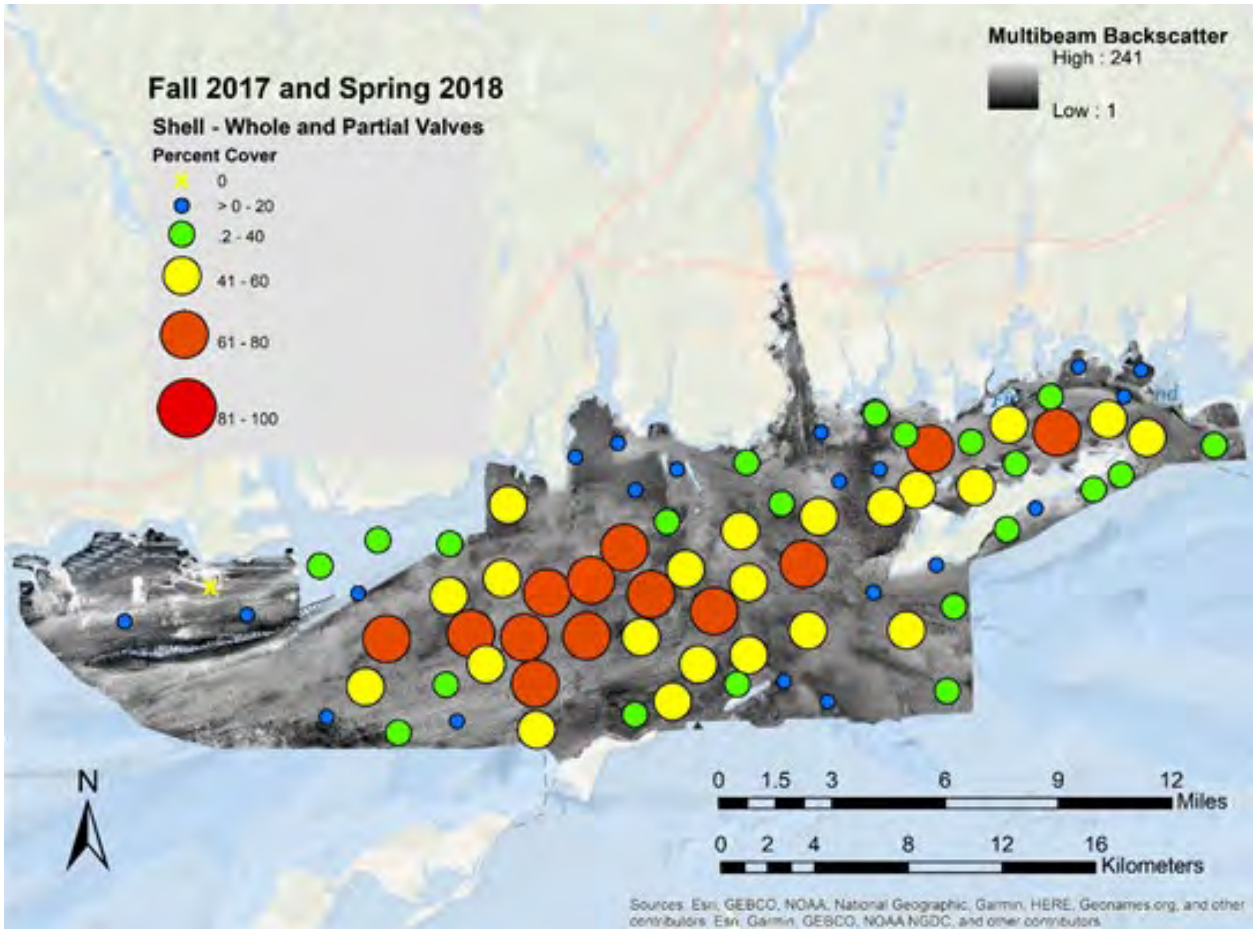

Figure 5.3- 61. Mean percent cover of whole and partial shell.

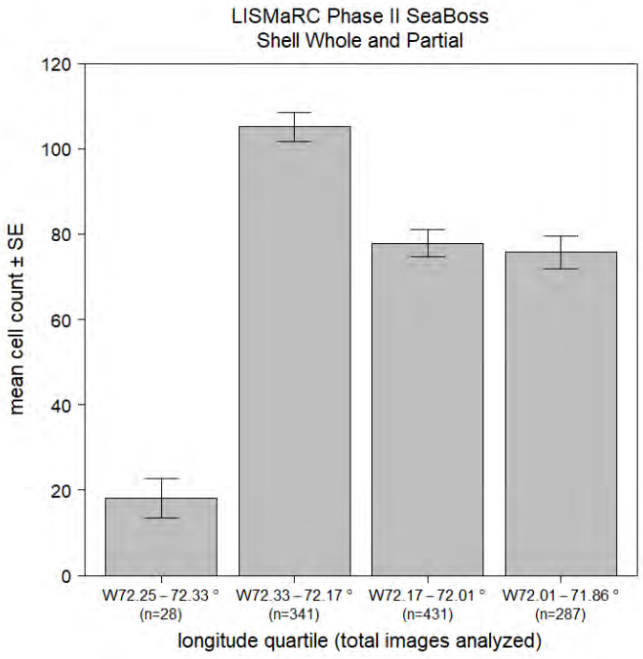

Figure 5.3- 62. Shell mean abundance by longitudinal section. Whiskers in mean abundance plot report standard error.

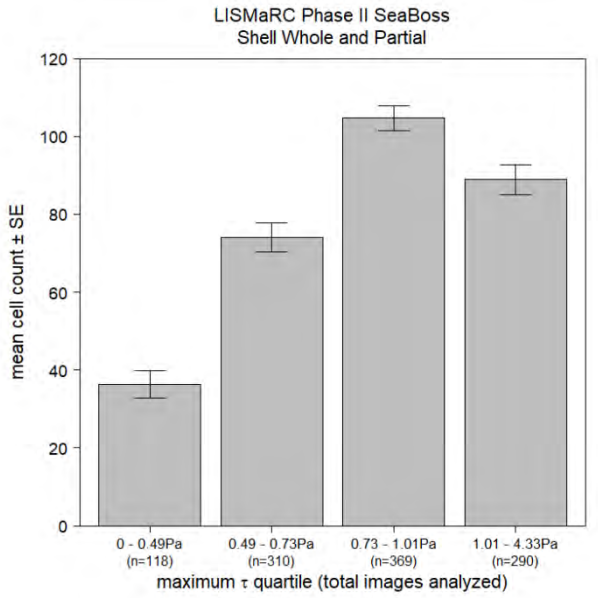

Figure 5.3- 63. Shell mean abundance by maximum monthly bottom stress quartile (maximum τ). Whiskers in mean abundance plot report standard error.

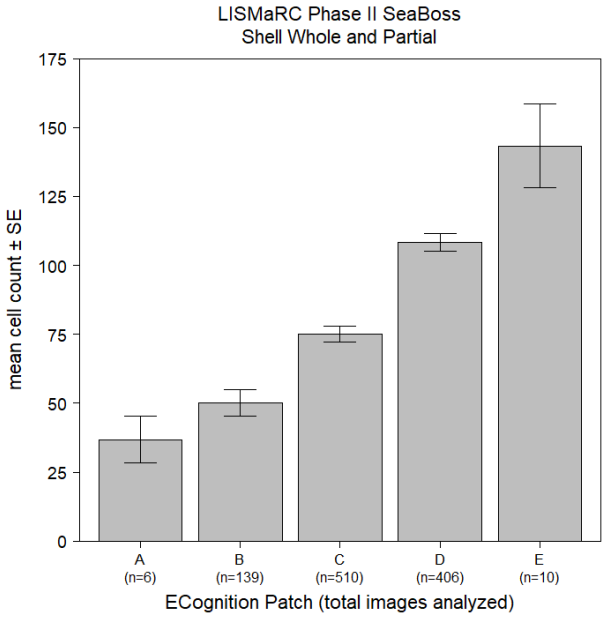

Figure 5.3- 64. Shell mean abundance by eCognition acoustic patch. Whiskers in mean abundance plot report standard error.

5.3.3.4.9 Drift Seagrass (Zostera marina) and Terrestrial Debris

While shell valves was the most widespread and abundant biogenic debris present in the Phase II area, other organic material was available and abundant at sites specific sites. Drift seagrass (*Zostera marina*) was observed throughout the study in low quantities but was particularly concentrated in two areas–FIS and at the mouth of the Connecticut River (Figure 5.3-65). While persistent in the eastern portion of the study area (Figure 5.3-66), from the Connecticut River west drift seagrass increased dramatically from fall (mean cover 2%) to spring (mean cover 29%). Seagrass was most common and abundant in shallow (Figure 5.3-67), low energy (as represented by maximum bottom stress, tau; Figure 5.3-68) habitats.

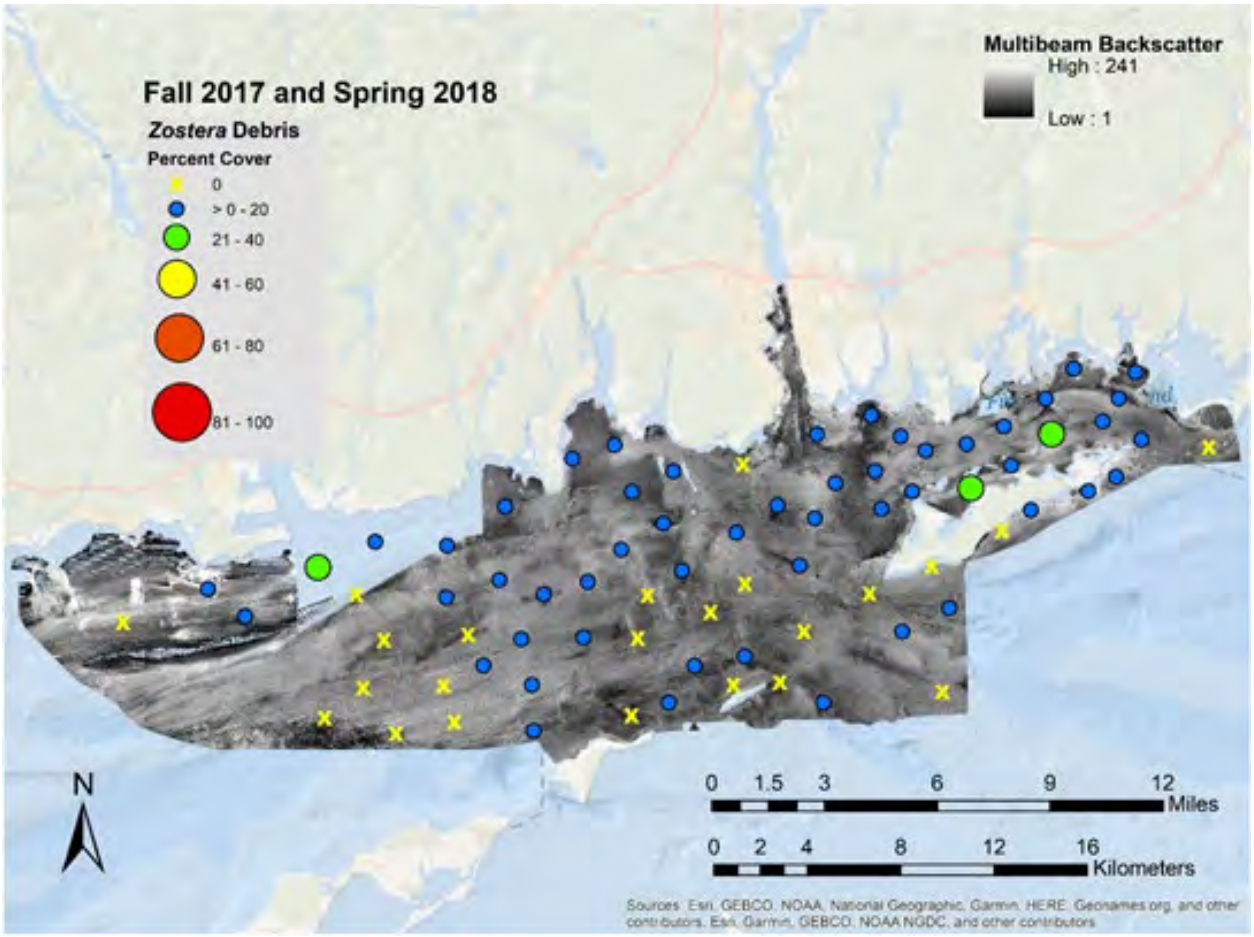

Figure 5.3- 65. Mean percent cover of drift seagrass Zostera marina.

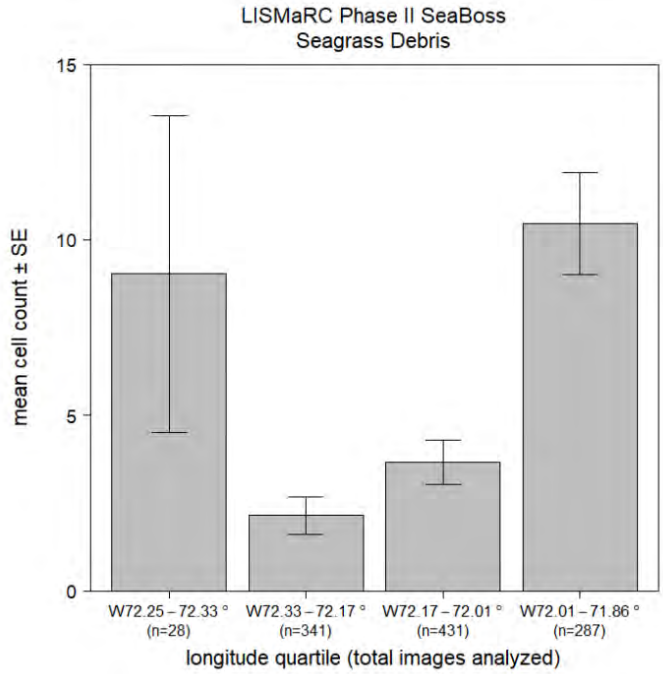

Figure 5.3- 66. Drift seagrass mean abundance by longitudinal section. Whiskers in mean abundance plot report standard error.

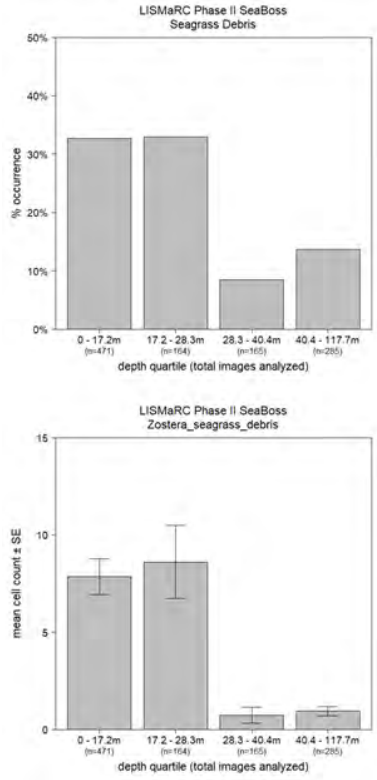

Figure 5.3- 67. Drift seagrass % occurrence (top) and mean abundance (bottom) by depth quartile. Whiskers in mean abundance plot report standard error.

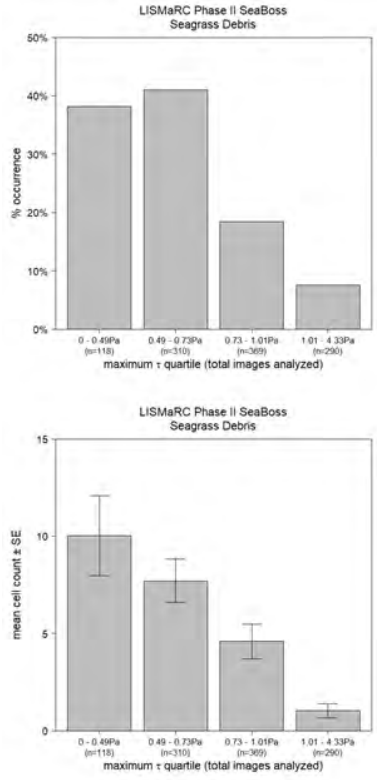

Figure 5.3- 68. Drift seagrass % occurrence (top) and mean abundance (bottom) by maximum monthly bottom stress quartile (maximum τ). Whiskers in mean abundance plot report standard error.

Organic material from terrestrial sources was less widespread than seagrass but nearly ubiquitous near the Connecticut River during spring sampling (Figure 5.3-69). Organic

terrestrial debris mostly consisted of leaf litter, branches, and other plant material that originated from the Connecticut River. More than ¾ of the nearly 30,000 km^2 Connecticut River watershed is forested (Clay et al., 2006), contributing seasonal inputs of plant material as the spring thaw, snow melt, and seasonal increases in precipitation greatly increase both river flow rates and terrestrial inputs.

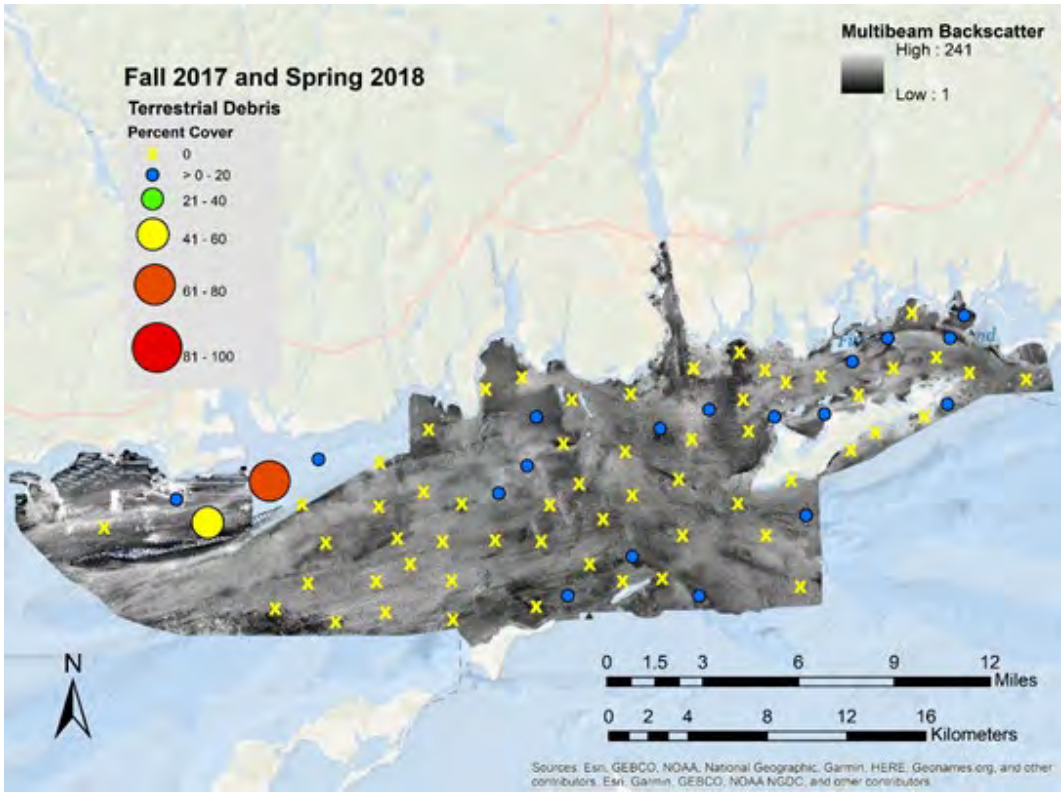

Figure 5.3- 69. Mean percent cover of terrestrial debris.

Where abundant in the study area, terrestrial debris covered much of the bottom and was easily disturbed, highlighting its ephemeral impacts to physical habitats. Terrestrial vegetation was most common and abundant in nearshore shallows (Figure 5.3-70) but, unlike seagrass litter, appeared to aggregate in higher energy habitats (Figure 5.3-71). Aggregation in areas with stronger bottom currents may have had different drivers depending on setting and conditions. Near the mouth of the Connecticut River where leaf litter and other terrestrial debris were often mobile during sampling, abundance was due to the continuous supply of new material from the river itself while in off-shore areas troughs and depressions in the sediment experienced much lower flow rates than the surrounding area, limiting transport of light terrestrial vegetation.

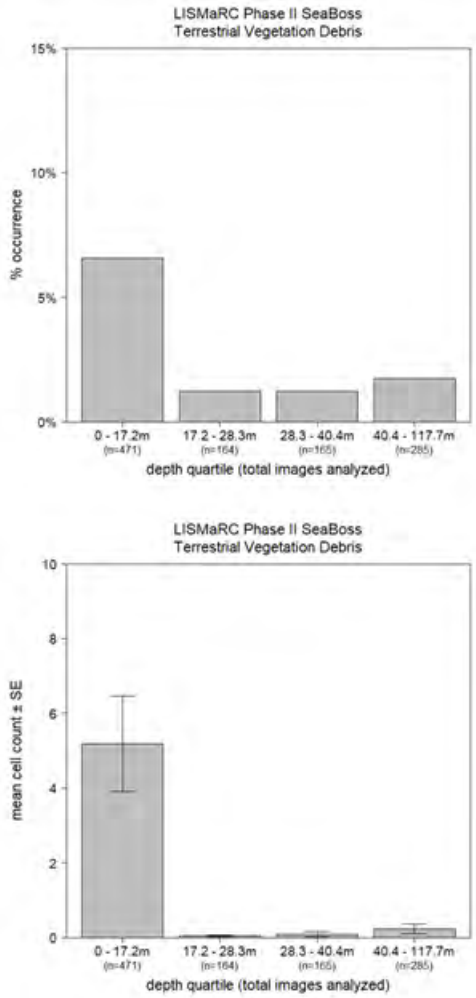

Figure 5.3- 70. Terrestrial vegetation debris % occurrence (top) and mean abundance (bottom) by depth quartile. Whiskers in mean abundance plot report standard error.

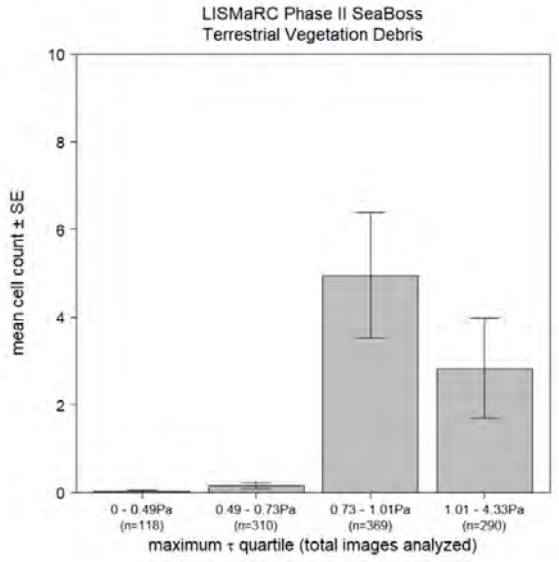

Figure 5.3- 71. Terrestrial vegetation debris mean abundance by maximum monthly bottom stress quartile (maximum τ). Whiskers in mean abundance plot report standard error.

Despite the short duration of seagrass litter and terrestrial vegetation in marine habitats, this debris may have important impacts on local habitats over both the short and long term. Visibility

was greatly decreased at the mouth of the Connecticut River when terrestrial vegetation was most abundant, likely influencing predation, and instances of organisms taking refuge in larger woody debris piles was observed as well. Seagrass litter also provided structure and surfaces to which organisms attached. Leaf litter and drift seagrass are also available as forage for benthic organisms; although, these materials are unlikely to form a major component of diet for most organisms (Beddingfield & McClintock, 1999). Beyond these apparent and temporary contributions to LIS habitats, seagrass litter and terrestrial debris also contribute both particulate and dissolved organic material and nutrients to the marine benthos. In addition to larger materials, rivers contribute substantial amounts of both natural and anthropogenic particulate and dissolved nutrients to coastal marine systems (Meybeck, 1982), impacting ecological processes. The residence time of both seagrass and terrestrial vegetation debris in the benthic habitats of LIS remains unclear, and may be highly variable.

5.3.4 Select Site Accounts

During this study multiple sites with notable biological and geological features were identified. Here each site location is briefly described and associated imagery is included to visualize local conditions.

5.3.4.1 Ellis Reef (SB-71)

Ellis Reef (Figure 5.3-72) is composed of a shallow platform and steep slope declining in depth westward to a deeper natural channel. Along the slope is a narrow rockfall with boulder-cobble substrate. Currents keep the hard substratum surfaces clear of fine sediments and facilitate extensive epifaunal cover that is dominated by *Cliona* spp. sponge and northern star coral, *Astrangia poculata*. Notable are sponge-coral tower or stack formations. Interstices of boulder piles and under boulder-sediment margins provide cover for shelter seeking vagile fauna (cunner *Tautogolabrus adspersus*), tautog (*Tautoga onitis*), black sea bass (*Centropristis striatus*), and American lobster (*Homarus americanus*). Red and brown macroalgae are common in the shoaler portions of the formation. At the base of the steep slope is a coarse grain sediment step and then a deeper sloping mixed sand cobble sediment with an extensive cover of *Crepidula fornicata* with epibionts.

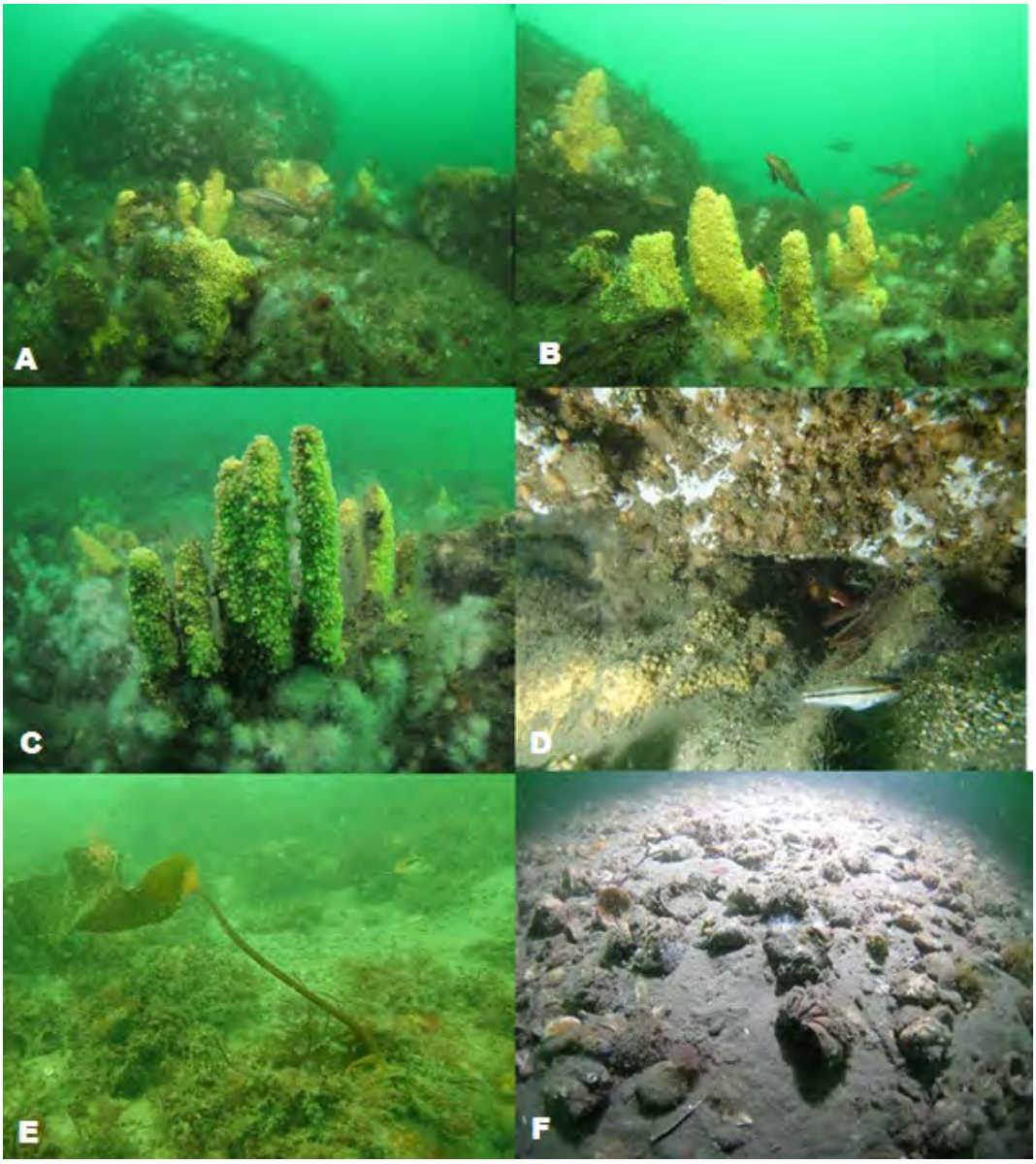

Figure 5.3- 72. Ellis Reef (SB-71). A. Rock fall region along the slope of Ellis Reef with gravel-boulder substrate. Extensive epifaunal coverage is dominated by Cliona spp. sponge and star coral Astrangia poculata; B. The habitat formed by geologic and biologic elements are used by wide size classes of rock reef species, including black sea bass (Centropristis striata) and cunner (Tautogolabrus adspersus) as in image; C. Notable are sponge-coral towers or stack formations; D. Interstices of boulder piles and at boulder-sediment margin provide cover for shelter seeking vagile fauna; E. Red and brown macroalgae are common in the shallower portions of the upper slope and platform of the formation; F. At the base of the steep slope is a coarse grain sediment step and then a deeper shallow sloping mixed sand cobble sediment with an extensive cover of Crepidula with diverse epibionts including star coral.

5.3.4.2 Ram Island Reef (SB-70)

Ram Island Reef (Figure 5.3-73), to the south of Ram Island, is composed of a silt-coarse sand substrate with scattered and piled boulders to approximately 2 m longest diameter. The area is characterized by a central channel bounded by dual boulder crests reaching less than 2 m depth at the peak. Boulder-cobble substrate slopes downward towards the center of the crests. Current velocity is enhanced due to topography and facilitates clearing of rock surfaces for settlement and growth of diverse macroalgae and attached invertebrates.

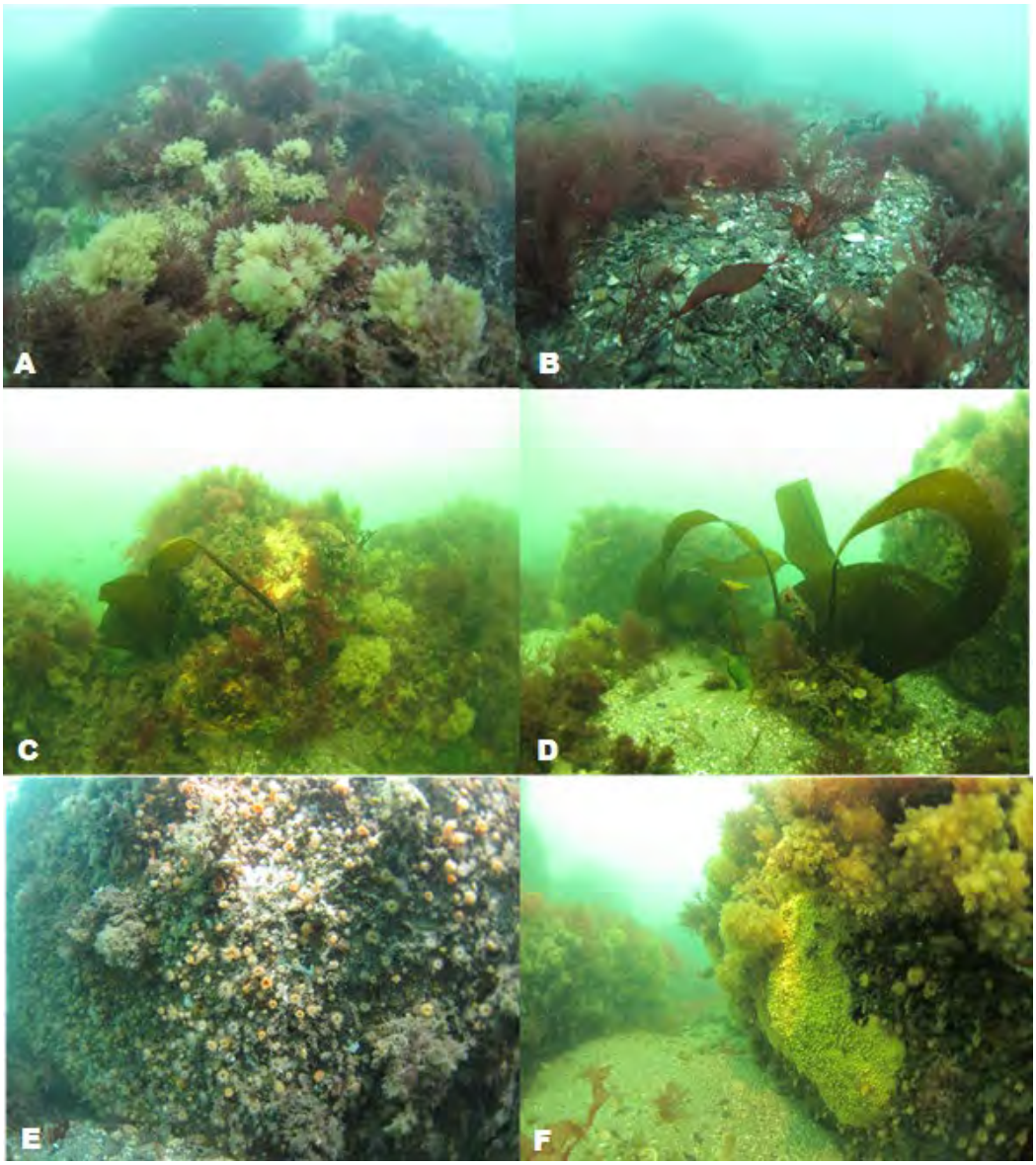

Figure 5.3- 73. Ram Island Reef (SB-70). A. Mixed red macroalgae (Rhodophyta), tufted bryozoans (Bugula turrita), and other invertebrates beneath the algal-bryozoan canopy on boulder surfaces; B. Shell debris in a small sediment basin at the base of a boulder slope; C. Kelp (Saccahrina) attached to hydrozoan-bryozoan tufts on a boulder; D. Kelp attached to cobble-pebble in coarse sand; E. Anemones Diadumene leucolena and associated invertebrates on a boulder surface shaded from direct sunlight and canopy of macroalgae above the top of this image; F. Extensive Cliona spp. colony and associated invertebrates at an undercut location shielded from direct sunlight and free of macroalgae.

5.3.4.3 Black Ledge (Shallow water mapping site)

Black Ledge (Figure 5.3-74) is shallow coarse sediment and gravel-boulder platform located approximately 1 km offshore and to the southeast of the mouth of the Thames River. The shallow peak, with a portion exposed at low water to approximately 4 m, covers an area of about 1 km^2 and is exposed to high current velocities (Egan & Yarish, 1990, this report). Nearly monthly observations of Atlantic kelp *Saccharina longicruis* density from 1985-1987 (Egan & Yarish, 1990) found seasonal variation based on recruitment and growth patterns. Observations during this study (August 2018) demonstrate density is significantly lower (mean density < 3 blades m^{-2}) compared to approximately 300 blades m^{-2} in the 1980s.

Figure 5.3- 74. Black Ledge (Shallow water mapping site). Top: Dense but patchy stand of Saccharina longicruis, surrounded by algal tufts; Bottom: Single kelp blades attached to invertebrate tufts and not to underlying boulder surface. Such attachment increases susceptibility to dislodgement from high storm generated surge and current.

5.3.4.4 Varved Lake Clays and Deltaic Deposits (SB-39)

An area off the Connecticut River with varved lake clays and deltaic deposits exposed at the sediment surface (Figure 5.3-75; see Lewis & Stone, 1991 for an extensive treatment of seafloor structure due to post-glacial processes).

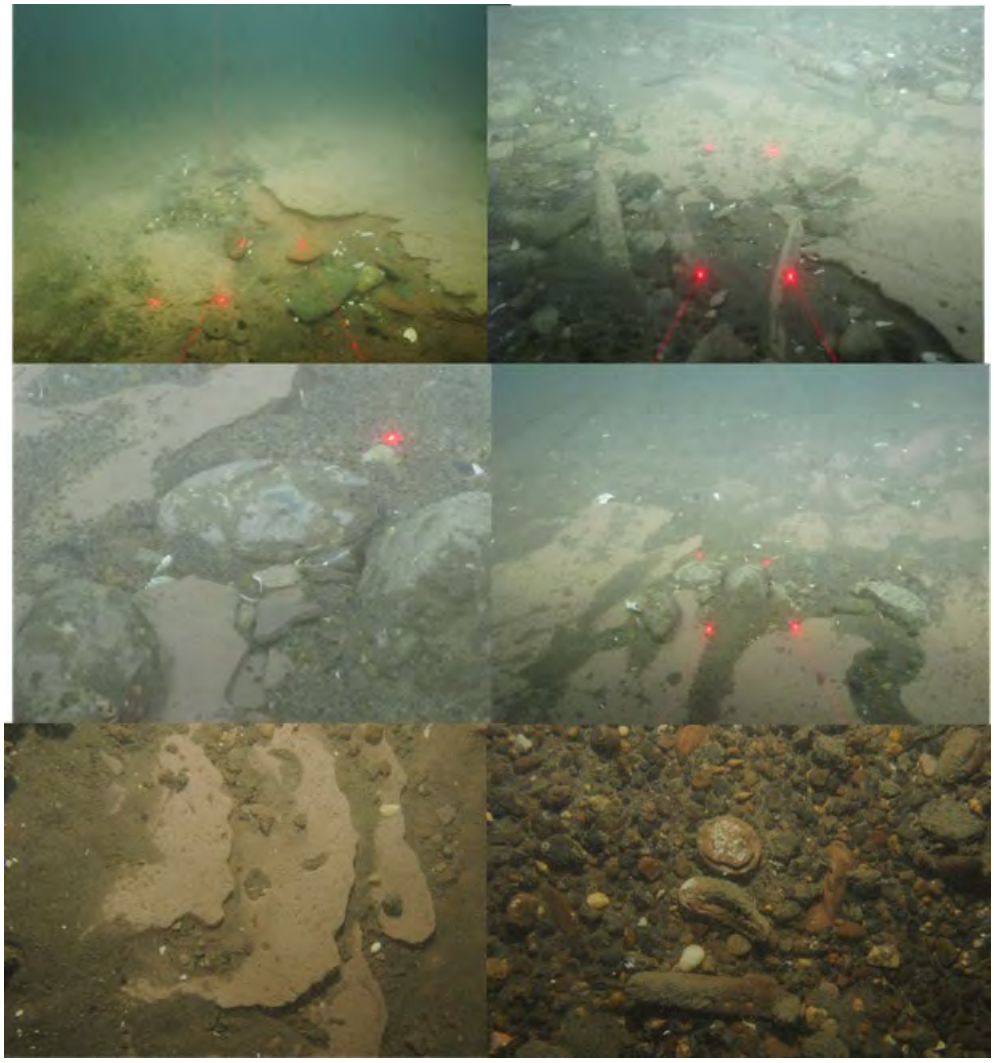

Figure 5.3- 75. Varved clay and deltaic deposits off the mouth of the Connecticut River (SB-39). Exemplars of exposed deposits.

5.3.4.5 Deep Boulder Moraines (NB-42 and SB-56)

Boulder dominated habitats were formed by glacial transport processes and can be part of moraines from the last glaciation (Figure 5.3-76 and Figure 5.3-77; see Lewis & Stone, 1991). Boulder and more extensive gravel surfaces serve as sites for diverse epifaunal communities with composition influenced by angle to the seafloor (i.e., from horizontal to vertical) and angle to dominate currents.

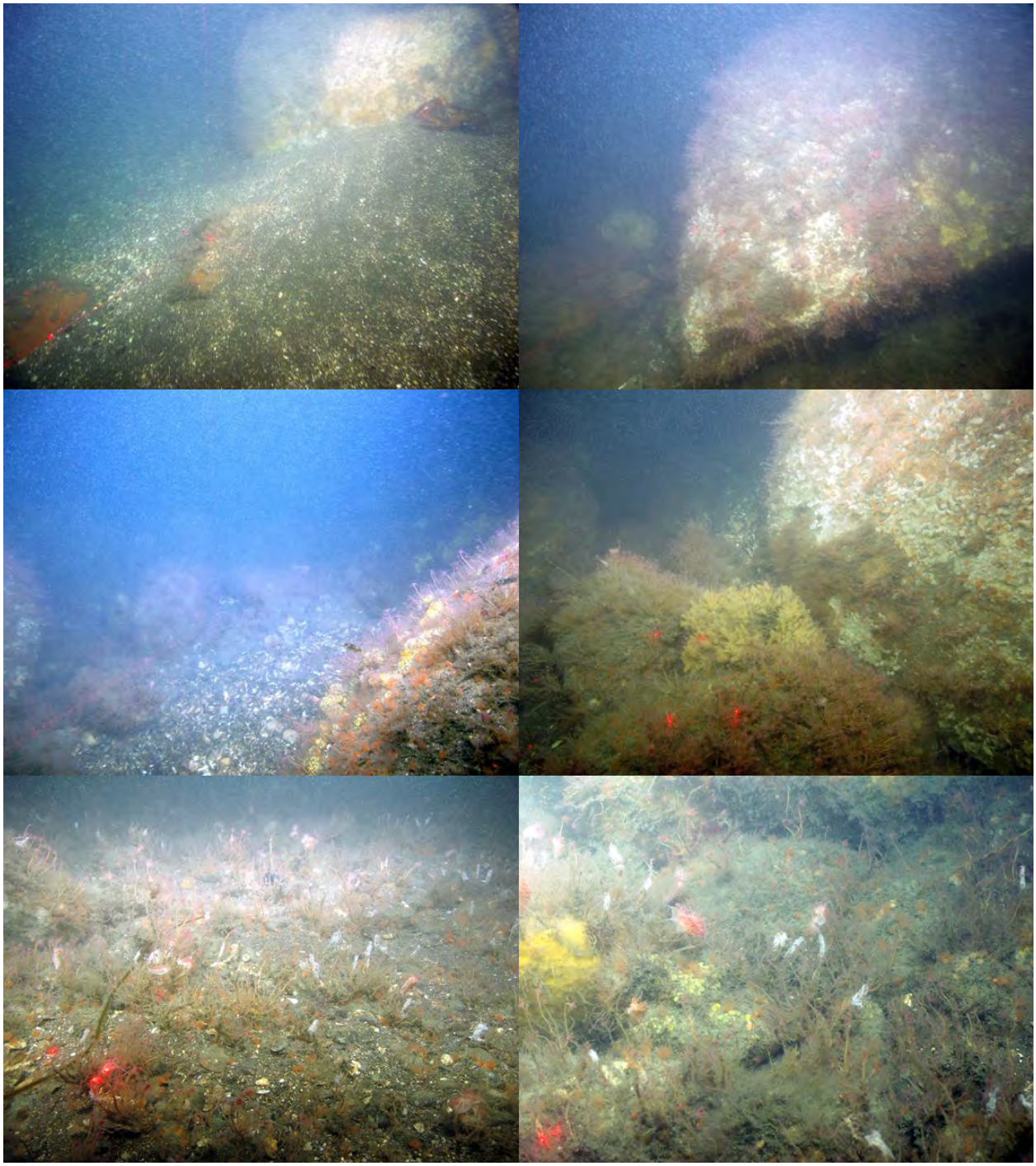

Figure 5.3- 76. Images from NB-42 illustrating the glacial boulder-dominated landscape and associated fauna in deep mid-Sound region.

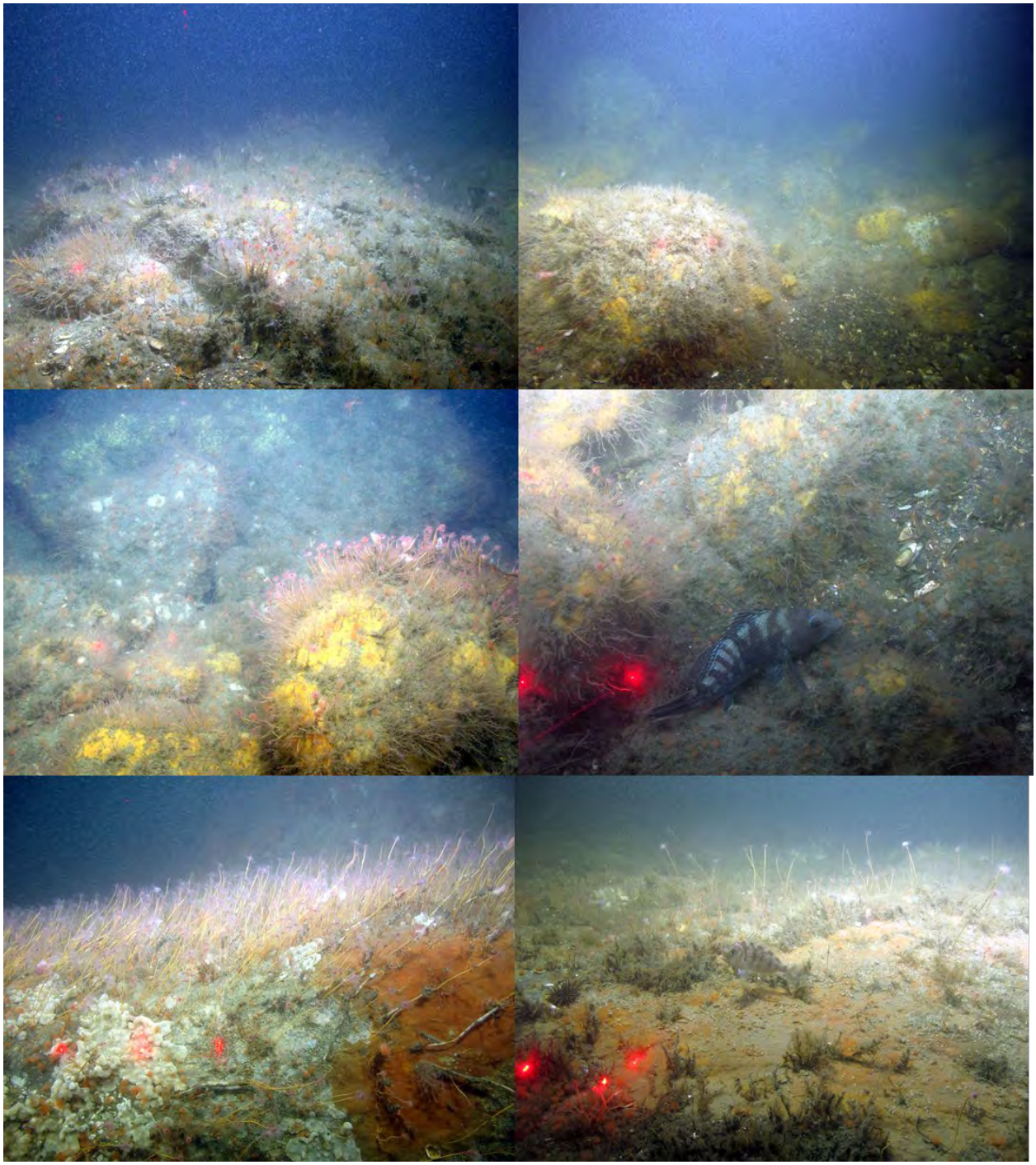

Figure 5.3- 77. Images from SB-56 illustrating the glacial boulder-dominated landscape and associated fauna in deep mid-Sound region.

5.3.4.6 South of The Race (SB-66)

The Race, a depression along a moraine segment that stretches from Orient Point to Fishers Island, is inferred to be the extant form of the spillway for glacial Lake Connecticut and is the eastern opening to LIS (Figure 5.3-78; see Poppe et al., 2006 and references therein). The area has been described as a complex habitat of steep sedimentary habitats with boulder-gravel deposits and extreme current velocities. The circulation through The Race, in part influenced by the rapid changes in depth and constriction of west and east walls of the sloping seafloor and

between landforms, produces a tidal forcing. This forcing produces larger scale gyres that transport offshore water from BIS westward through the Race and along the north shore of LIS and brackish estuarine water from the western sound eastward along the southern shoreline. These conditions transport propagules from communities over a wide region and deliver them to a diversity of seafloor habitats based on sediment and outcrop characteristics and orientations. Hard rock surfaces were densely colonized along the transect site on the east slope.

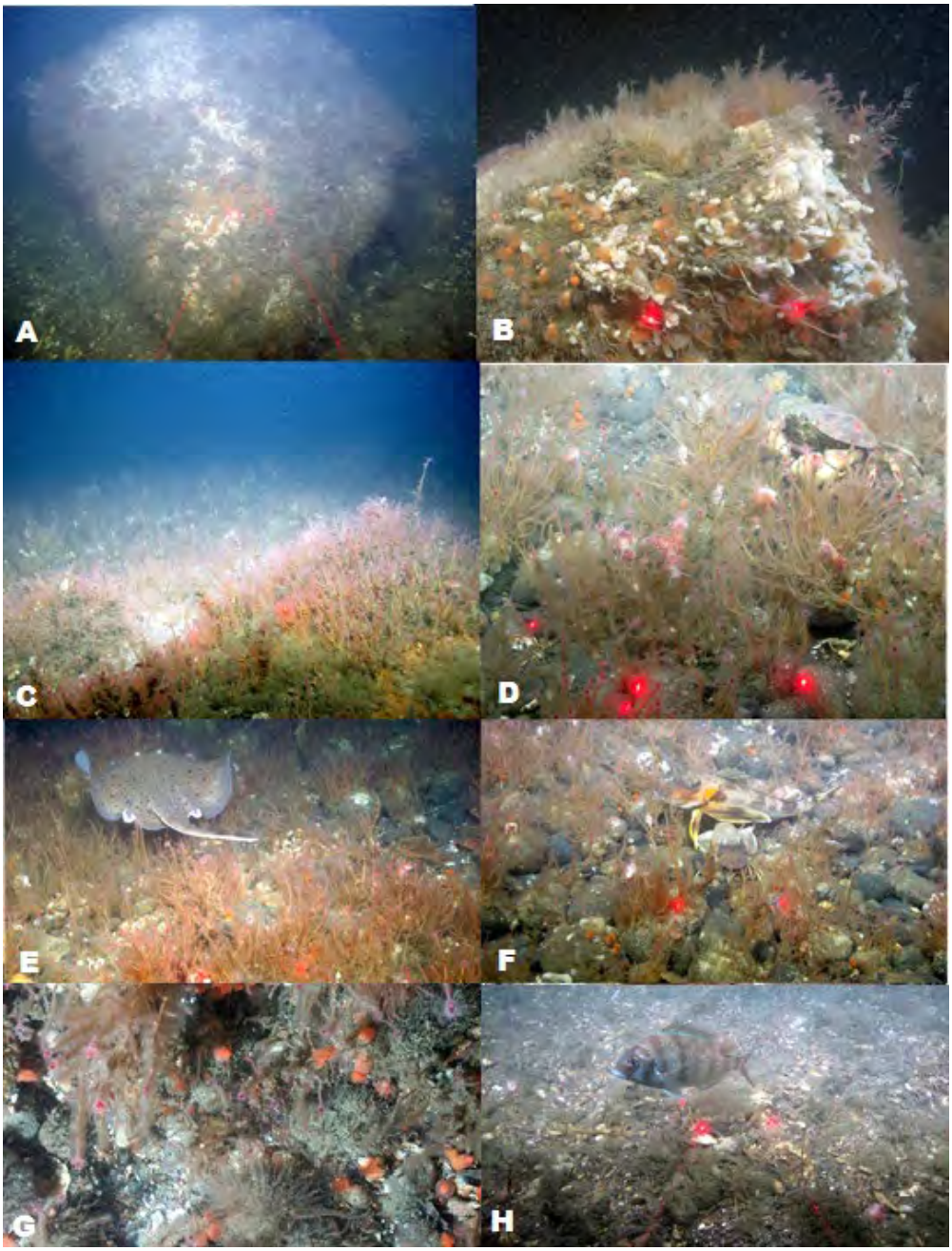

Figure 5.3- 78. South of Race Rock (SB-66). A-C. Boulders and coarse gravel with high cover of hydroids and bryozoans characteristic of this area; D-G. Diverse vagile species utilize this habitat for shelter and to forage for prey; H. A young-of-year fish typically using the gavel-biogenic habitat for shelter from currents and predators.

5.3.4.7 South of Fishers Island (SB-39)

Boulder deposits on the south side of Fishers Island are the southern extent of a glacial moraine. The hard rock surfaces are within depths to sustain photosynthesis and support extensive macroalgal and invertebrate communities (Figure 5.3-79).

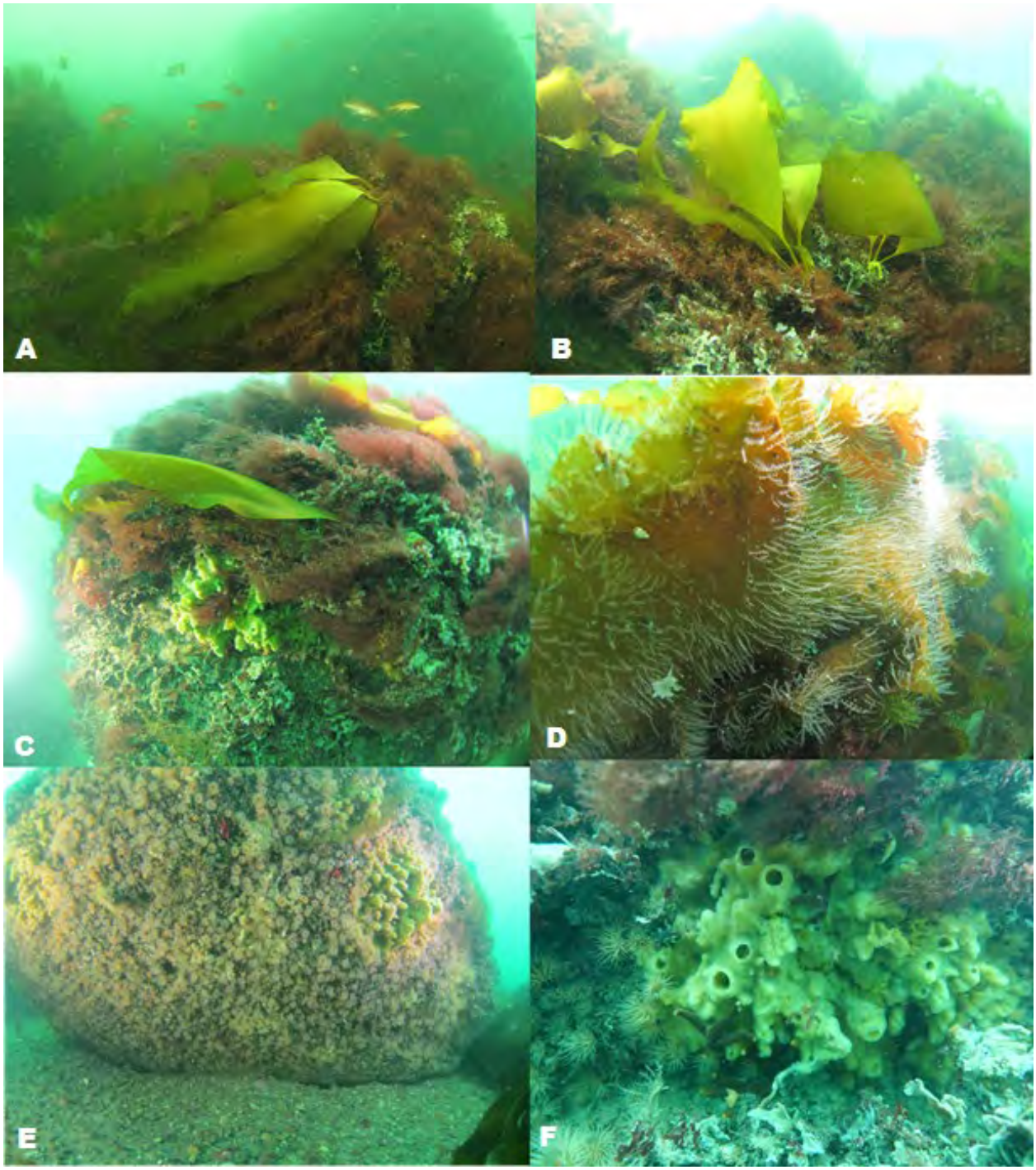

Figure 5.3- 79. South of Fishers Island (SB-39). A-C. Kelp blades streaming in the direction of current, shading understory macroalgae and invertebrates; D. Epifaunal hydroids attached to kelp blade; E-F. Understory and shaded epifauna.

5.3.5 References - Epifaunal Ecological Characterization

Abramoff, M.D., Magalhaes, P.J., and Ram, S.J. (2004). "Image Processing with ImageJ". *Biophotonics International 11(*7), 36-42.

Ackerman, S.D., Pappal, A.L., Huntley, E.C., Blackwood, D.S., and Schwab, W.C. (2015). *Geological Sampling Data and Benthic Biota Classification—Buzzards Bay and Vineyard Sound, Massachusetts*: U.S. Geological Survey Open-File Report 2014–1221, 30 p., http://dx.doi.org/10.3133/ofr20141221.

Ackerman, S.D., Huntley, E.C., Blackwood, D.S., Babb, I.G., Zajac, R.N., Conroy, C.W., Auster, P.J., Schneeberger, C.L., and Walton, O.L. (2020). *Sea-floor sediment and imagery data collected in Long Island Sound, Connecticut and New York, 2017 and 2018*: U.S. Geological Survey data release, https://doi.org/10.5066/P9GK29NM

Auker, L.A. (2019). A decade of invasion: changes in the distribution of *Didemnum vexillum* (Kott 2002) in Narragansett Bay, Rhode Island, USA, between 2005 and 2015. *BioInvasions Records*, 8(2), pp.230-241.

Auster, P.J, Malateta, R.J., and LaRosa, S.C. 1995. Patterns of microhabitat utilization by mobile megafauna on the southern New England (USA) continental shelf and slope. *Marine Ecology Progress Series*. 127: 77-85.

Auster, P.J., Malatesta, R.J., Langton, R.W., Watling, L., Valentine, P.C., Donaldson, C.L.S., Langton, E.W., Shepard, A.N. and Babb, I.G. (1996). The impacts of mobile fishing gear on seafloor habitats in the Gulf of Maine (Northwest Atlantic): Implications for conservation of fish populations, *Reviews in Fisheries Science*, 4:2, 185-202, DOI: 10.1080/10641269609388584.

Auster, P.J., Malatesta, R.J. and Donaldson C.L.S. (1997). Distributional responses to small-scale habitat variability by early juvenile silver hake, *Merluccius bilinearis*. *Environmental Biology of Fishes* 50:195-200.

Auster, P. J., Michalopoulos, C., Page, C. V., & Malatesta, R. J. (1997). Delineating and monitoring habitat management units in a temperate deep-water marine protected area. In N. P. Munro, & J. H. Martin Willison (Ed.), *Linking Protected Areas with Working Landscapes, Conserving Biodiversity: Proceedings of the Third International Conference on Science and Management of Protected Areas* (pp. 169-185). Wolfville, Nova Scotia: Science and Management of Protected Areas Association.

Auster, P. J., Heinonen, K. B., Witharana, C., & McKee, M. (2009). *A habitat classification for the Long Island Sound region. Long Island Sound Study Technical Report.* Stamford, CT: EPA Long Island Sound Office.

Abramoff, M.D., Magalhaes, P.J. and Ram, S.J. (2004). Image processing with ImageJ. *Biophotonics International* 11(7):36-42.

Barillé, L., Cognie, B., Beninger, P., Decottignies, P. and Rincé, Y., (2006). Feeding responses of the gastropod *Crepidula fornicata* to changes in seston concentration. *Marine Ecology Progress Series*, 322, 169-178.

Barnes R.S.K., Coughlan J. and Holmes N.J. (1973). A preliminary survey of the macroscopic bottom fauna of the Solent, with particular reference to *Crepidula fornicata* and *Ostrea edulis*. *Proceedings of the Malacological Society of London* 40, 253–275.

Baynes, T.W. and Szmant, A.M. (1989). Effect of current on the sessile benthic community structure of an artificial reef. *Bulletin of Marine Science*, 44(2), 545-566.

Bell J.J. (2004). Evidence for morphology-induced sediment settlement prevention on the tubular sponge *Haliclona urceolus*. *Marine Biology* 146, 29–38.

Bell J.J. (2007). The ecology of sponges in Lough Hyne Marine Nature Reserve (south-west Ireland): past, present and future perspectives. *Journal of the Marine Biological Association of the United Kingdom* 87, 1655–1668.

Bell J.J., Burton M., Bullimore B., Newman P.B. and Lock K. (2006). Morphological monitoring of subtidal sponge assemblages. *Marine Ecology Progress Series* 311, 79–91.

Beninger, P.G., Decottignies, P., Guiheneuf, F., Barillé, L. and Rincé, Y. (2007). Comparison of particle processing by two introduced suspension feeders: selection in *Crepidula fornicata* and *Crassostrea gigas*. *Marine Ecology Progress Series*, 334, 165-177.

Brooks, A.L. (1984). *A Study of the Benthic Macrofauna at the Central Long Island Sound Disposal Site*. Naval Underwater Systems Center, New London, CT. 44 pp.

Byers, J.E. and Grabowski, J.H. (2014). Soft-sediment communities. in *Marine Community Ecology*. Sinauer, pp.227-249.

Carroll, J. M., O'Shaughnessy, K. A., Diedrich, G. A., & Finelli, C. M. (2015). Are oysters being bored to death? Influence of Cliona celata on Crassostrea virginica condition, growth and survival. *Diseases of Aquatic Organisms, 117*(1), 31-44.

Carver, C. E., Thériault, I., & Mallet, A. L. (2010). Infection of cultured eastern oysters *Crassostrea virginica* by the boring sponge Cliona celata, with emphasis on sponge life history and mitigation strategies. *Journal of Shellfish Research, 29*(4), 905-915.

Cau, A., Mercier, A., Moccia, D., & Auster, P. J. (2020). The nursery role of marine animal forests. In S. Rossi, & L. Bramanti (Eds.), *Perspectives on the Marine Animal Forests of the World* (pp. 309-331). Switzerland AG: Springer Nature. Retrieved from https://doi.org/10.1007/978-3-030-57054-5_10#DOI

Cerrano, C., Bianchelli, S., Di Camillo, C. G., Torsani, F., & Pusceddu, A. (2015). Do colonies of *Lytocarpia myriophyllum, L*. 1758 (Cnidaria, Hydrozoa) affect the biochemical composition and the meiofaunal diversity of surrounding sediments? *Chemistry and Ecology, 31*(1), 1-21.

Clarke, K. R., & Gorley, R. N. (2006). PRIMER v6: User Manual/Tutorial. *(Plymouth Routines in Multivariate Ecological Research)*. Plymouth: PRIMER-E.

Clarke, K. R., and Warwick, R.M. 2001. Change in Marine Communities: an Approach to Statistical Analysis and Interpretation. PRIMER-E Ltd, Plymouth, U.K.

Clay, C., Deininger, M., & Hafner, J. (2006). *The Connecticut River Watershed: Conserving the Heart of New England.* The Trust for Public Land.

Coleman, S. E. (2014). *The effects of boring sponge on oyster soft tissue, shell integrity, and predator-related mortality.* M.Sc. Thesis, University of North Carolina at Chapel Hill.

Connecticut Department of Energy and Environmental Protection. (2019). *Long Island Sound Blue Plan.* Hartford, CT.

Daley, B. A., & Scavia, D. (2008). *An Integrated Assessment of the Continued Spread and Potential Impacts of the Colonial Ascidian, Didemnum sp. A, in U.S. Waters.* Technical Memorandum NOS NCCOS 78, NOAA, National Centers for Coastal Ocean Science.

De Bettignies, T., Wernberg, T., & Lavery, P. S. (2013). Size, not morphology, determines hydrodynamic performance of a kelp during peak flow. *Marine Biology, 160*(4), 843-851.

de Montaudouin, X., & Sauriau, P.-G. (1999). The proliferating Gastropoda *Crepidula fornicata* may stimulate macrozoobenthic diversity. *Journal of the Marine Biological Association of the United Kingdom, 79*(6), 1069-1077.

de Montaudouin, X., Blanchet, H., & Hippert, B. (2018). Relationship between the invasive slipper limpet *Crepidula fornicata* and benthic megafauna structure and diversity, in Arcachon Bay. *ournal of the Marine Biological Association of the United Kingdom, 98*(8), 2017-2028.

Deignan-Schmidt, S. R., & Whitney, M. M. (2018). A model study on the summertime distribution of river waters in Long Island Sound. *Estuaries and Coasts, 41* (4), 1002-1020.

Di Camillo, C. G., Bavestrello, G., Cerrano, C., Gravili, C., Piraino, S., Puce, S., & Boero, F. (2017). Hydroids (Cnidaria, Hydrozoa): a neglected component of animal forests. *Marine Animal Forests*, 397–427.

Dijkstra J.A., Lambert W.J. and Harris L.G. (2012). Introduced species provide a novel temporal resource that facilitates native predator population growth. *Biological Invasions* DOI 10.1007/s10530-012-0339-1.

Dimond, J. and Carrington, E., (2008). Symbiosis regulation in a facultatively symbiotic temperate coral: zooxanthellae division and expulsion. *Coral Reefs*, 27(3), 601-604.

Dimond, J.L., Kerwin, A.H., Rotjan, R., Sharp, K., Stewart, F.J. and Thornhill, D.J., (2013). A simple temperature-based model predicts the upper latitudinal limit of the temperate coral *Astrangia poculata*. *Coral Reefs*, 32(2), 401-409.

Dolmer, P., (2000). Feeding activity of mussels *Mytilus edulis* related to near-bed currents and phytoplankton biomass. *Journal of Sea Research*, 44(3-4), 221-231.

Dutto, M. S., Carcedo, M. C., Nahuelhual, E. G., Conte, A. F., Berasategui, A. A., Garcia, M. D., and Hoffmeyer, M. S. (2019). Trophic ecology of a corymorphid hydroid population in the Bahía Blanca Estuary, Southwestern Atlantic. *Regional Studies in Marine Science*, 31, 100746.

Ellis J. and Solander D. (1786) The natural history of many curious and common zoophytes collected from various parts of the globe. London: Benjamin White and Son.

Egan, B. and Yarish, C. (1990). Productivity and life history of *Laminaria longicruris* at its southern limit in the Western Atlantic Ocean. *Marine Ecology Progress Series*, 67, 263-273.

Fagan, W.F., Cantrell, R.S. and Cosner, C., (1999). How habitat edges change species interactions. *The American Naturalist*, 153(2), 165-182.

Feehan CJ, Grace SP, Narvaez CA. (2019). Ecological feedbacks stabilize a turf-dominated ecosystem at the southern extent of kelp forests in the Northwest Atlantic. *Scientific Reports* 9(1) 1-10.

Fell P.E. (1974). Diapause in the gemmules of the marine sponge *Haliclona loosanoffi* with a note on the gemmules of *Haliclona oculata*. *Biological Bulletin* 147, 333–351.

Fell P.E. (1978). Variation in the time of annual degeneration of the estuarine sponge, *Haliclona loosanoffi*. *Estuaries* 1(4), 261–264.

Fell P.E., Parry E.H., and Balsamo A.M. (1984). The life histories of sponges in the Mystic and Thames estuaries (Connecticut), with emphasis on larval settlement and post larval reproduction. *Journal of Experimental Marine Biology and Ecology* 78, 127–141.

Forrest, B.M., Fletcher, L.M., Atalah, J., Piola, R.F. and Hopkins, G.A. (2013). Predation limits spread of *Didemnum vexillum* into natural habitats from refuges on anthropogenic structures. *PLoS One*, 8(12), p.e82229.

Filbee-Dexter K, Feehan CJ, Scheibling RE. (2016). Large-scale degradation of a kelp ecosystem in an ocean warming hotspot. *Marine Ecology Progress Series* 543, 141–152.

Filbee-Dexter K, Wernberg T. (2018). Rise of turfs: a new battlefront for globally declining kelp forests. *BioScience* 68, 64–76.

Fuchs, H. L., Chant, R. J., Hunter, E. J., Curchitser, E. N., Gerbi, G. P., & Chen, E. Y. (2020). Wrong-way migrations of benthic species driven by ocean warming and larval transport. *Nature Climate Change, 10*(11), 1052-1056.

Gili, J. M., Alvà, V., Coma, R., Orejas, C., Ribes, M., Zabala, M., . . . Hughes, R. G. (1998). The impact of small benthic passive suspension feeders in shallow marine ecosystems: the hydroids as an example. *Zoologische verhandelingen, 323*(8), 99-105.

Ginn B.K. 1(997.) *Ecology, systematics, and feeing rate of sponges on subtidal hard substrates in Little Letite Passage, Deer Island, New Brunswick*. Masters Thesis, University of New Brunswick, Fredericton, Canada.

Gittenberger, A., (2010). *Risk analysis of the colonial sea-squirt Didemnum vexillum Kott, 2002 in the Dutch Wadden Sea, a UNESCO World Heritage Site*. *GiMaRIS*. 32pp.

Glaspie, C.N. and Seitz, R.D., (2018). Habitat complexity and benthic predator-prey interactions in Chesapeake Bay. *PloS one*, 13(10), p.e0205162.

Goddard, J. H., Goddard, W. M., and Goddard, Z. E. (2020). Benthic Heterobranch Sea Slugs (Gastropoda: Heterobranchia) from Santa Barbara County, California. *Proceedings of the California Academy of Sciences* Series 4. 66(10),, 275-298.

Grace, S.P., (2004). *Ecomorphology of the temperate scleractinian Astrangia poculata: coral-macroalgal interactions in Narragansett Bay.* Doctoral Disssertation, University of Rhode Island.

Grace, S., (2017). Winter quiescence, growth rate, and the release from competition in the temperate scleractinian coral *Astrangia poculata* (Ellis and Solander 1786). *Northeastern Naturalist*, 24, B119-B134.

Grant R.E. (1826). Notice of a New Zoophyte (*Cliona celata* Gr.) from the Firth of Forth. Edinburgh *New Philosophical Journal* 1, 78–81.

Gray, J.S. (2000). The measurement of marine species diversity, with an application to the benthic fauna of the Norwegian continental shelf. *Journal of Experimental Marine Biology and Ecology* 250, 23-49.

Hartman W.D. (1958). Natural history of the marine sponges of southern New England. *Bulletin of the Peabody Museum Yale University* 12, 1–155.

Holcomb, M., Cohen, A.L. and McCorkle, D.C. (2012). An investigation of the calcification response of the scleractinian coral *Astrangia poculata* to elevated pCO 2 and the effects of nutrients, zooxanthellae and gender. *Biogeosciences*, 9(1), 29-39.

Houziaux J., Haelters J. and Kerckhof, F. (2007). *Facts from history – the former ecological value of the gravel grounds in Belgian marine waters: their importance for biodiversity and relationship with fisheries.* ICES SGBIODIV Report, Annex 4: Biodiversity science: a case study from Belgian marine waters.

Howell P. and Auster P.J. (2012). Phase shift in a estuarine finfish community associated with warming temperatures. *Marine and Coastal Fisheries*: *Dynamics, Management, and Ecosystem Science* 4(1), 481–495.

Hughes, R.G. (1978). Life-histories and abundance of epizoites of the hydroid *Nemertesia antennina* (L.). *Journal of the Marine Biological Association of the United Kingdom*, 58(2), 313-332.

Jaques T.G., Marshall N. and Pilson M.E.Q. (1983). Experimental ecology of the temperate scleractinian coral Astrangia danae II. *Marine Biology* 76, 135–148.

Kaandorp J.A. (1999). Morphological analysis of growth forms of branching marine sessile organisms along environmental gradients. *Marine Biology* 134, 295–306.

Knebel H.J. and Poppe L.J. (2000). Sea-floor environments within Long Island Sound: a regional overview. *Journal of Coastal Research* 16, 533–550.

Kluijver M.J. de and Leewis R.J. (1994). Changes in the sublittoral hard substrate communities in the Oosterschelde estuary (SW Netherlands), caused by changes in the environmental parameters. *Hydrobiologia* 282/283, 265–280.

Koopmans M. and Wijffels R.H. (2008). Seasonal growth rate of the sponge *Haliclona oculata* (Demospongiae: Haplosclerida). *Marine Biotechnology* 10, 502–510.

Koopmans M., Martens D. and Wijffels R.H. (2009). Towards commercial production of sponge medicines. *Marine Drugs* 7, 787–802.

Krumhansl, K.A., Demes, K.W., Carrington, E. and Harley, C.D. (2015). Divergent growth strategies between red algae and kelps influence biomechanical properties. *American Journal of Botany*, *102*(11), 1938-1944.

Lambert, G. (2009). Adventures of a sea squirt sleuth: unraveling the identity of *Didemnum vexillum*, a global ascidian invader. *Aquatic Invastions*, 4(1), 5-28.

Langton, R.W., Auster, P.J. and Schneider, D.C. (1995). A spatial and temporal perspective on research and management of groundfish in the northwest Atlantic. *Reviews in Fisheries Science* 3, 201-229.

Lehane C, Davenport J. (2006). A 15-month study of zooplankton ingestion by farmed mussels (*Mytilus edulis*) in Bantry Bay, Southwest Ireland. *Estuar Coast Shelf* Sci 67, 645–652.

Lewis, R.S. and Stone, J.R. (1991). Late Quaternary stratigraphy and depositional history of the Long Island Sound basin: Connecticut and New York. *Journal of Coastal Research,* 1-23.

Lindholm, J.B., Auster, P.J. and Kaufman, L.S. 1999. Habitat-mediated survivorship of juvenile (0-year) Atlantic cod *Gadus morhua*. *Marine Ecology Progress Series*, 180, 247-255.

Linnaeus C. (1758). Systema Naturae per regna tria naturae, secundum classes, ordines, genera, species, cum characteribus, differentiis, synonymis, locis. Tomus I. Editio decima, reformata. Holmiae: Laurentius Salvius.

Lopez, G., Carey, D., Carlton, J.T., Cerrato, R., Dam, H., DiGiovanni, R., Elphick, C., Frisk, M., Gobler, C., Hice, L. and Howell, P. (2014). Biology and Ecology of Long Island sound. In *Long Island Sound* (pp. 285-479). Springer, New York, NY.

Lough R.G., Valentine P.C., Potter D.C., Auditore P.J., Bolz G.R. Neilson J.D. and Perry R.I. (1989). Ecology and distribution of juvenile cod and haddock in relation to sediment type and bottom currents on eastern Georges Bank. *Marine Ecology Progress Series* 56, 1-12.

Malatesta, R.J. and Auster, P.J. (1999). The importance of habitat features in low-relief continental shelf environments. *Oceanologica Acta* 22, 623-626.

Mercer, J. M., Whitlatch, R. B., & Osman, R. W. (2009). Potential effects of the invasive colonial ascidian (Didemnum vexillum Kott, 2002) on pebble-cobble bottom habitats in Long Island Sound, USA. *Aquatic Invasions, 4*(1), 133-142.

Merzouk, A., & Johnson, L. E. (2011). Kelp distribution in the northwest Atlantic Ocean under a changing climate. *Journal of Experimental Marine Biology and Ecology, 400*(1-2), 90-98.

Meybeck, M. (1982). Carbon, nitrogen, and phosphorus transport by world rivers. *American Journal of Science, 282*(4), 401-450.

Miller, A. N., Strychar, K. B., Shirley, T. C., & Rützler, K. (2010). Effects of heat and salinity stress on the sponge Cliona celata. *International Journal of Biology, 2*(2), 3-16.

Mittermayr, A., Legare, B., & Borrelli, M. (2020). Applications of the coastal and marine ecological classification standard (CMECS) in a partially restored New England salt marsh lagoon. *Estuaries and Coasts*, 1-12.

Morris, E.K., T. Caruso, F. Buscot, M. Fischer and C. Hancock. (2014). Choosing and using diversity indices: insights for ecological applications from the German Biodiversity Exploratories. *Ecology and Evolution* 4, 3514-3524.

Müller O.F. (1776). Zoologiae Danicae prodromus : seu Animalium Daniae et Norvegiae indigenarum ; characteres, nomina, et synonyma imprimis popularium Havniae: Typis Hallageriis.

Nakagawa, S. and Schielzeth, H., (2013). A general and simple method for obtaining R^2 from generalized linear mixed-effects models. *Methods in Ecology and Evolution*, 4(2), 133-142.

NASA (2013) http://earthobservatory.nasa.gov/IOTD/view.php?id=52059&src=eorss-iotd (downloaded 7 March 2013)

Nava, H. and Carballo, J.L. (2008). Chemical and mechanical bioerosion of boring sponges from Mexican Pacific coral reefs. *Journal of Experimental Biology*, 211(17), 2827-2831.

Norling, P. and Kautsky, N. (2007). Structural and functional effects of *Mytilus edulis* on diversity of associated species and ecosystem functioning. *Marine Ecology Progress Series*, 351, 163-175.

Parker, G.H. (1917). The activities of *Corymorpha*. *Journal of Experimental Zoology*, 24(2), 303-331.

Patrizzi B.J. (2010). *The distribution and diet of the scleractinian coral Astrangia poculata in Long Island Sound.* Masters Thesis, Southern Connecticut State University, New Haven, USA.

Poppe, L.J., DiGiacomo-Cohen, M.L., Smith, S.M., Stewart, H.F. and Forfinski, N.A.,(2006). Seafloor character and sedimentary processes in eastern Long Island Sound and western Block Island Sound. *Geo-Marine Letters*, 26(2), 59.

Poppe L.J., Knebel H.J., Mlodzinska Z.J., Hastings, M.E. and Seekins B.A. (2000). Distribution of surficial sediment in Long Island Sound and adjacent waters: texture and total organic carbon. *Journal of Coastal Research* 16, 567–574.

Poppe, L.J., Lewis, R.S., Denny, J.F., Parolski, K.F. and DiGiacomo-Cohen, M.L. (1998). *Sidescan sonar image, surficial geologic interpretation, and bathymetry of the Fishers Island Sound sea floor*. Connecticut, New York, and Rhode Island: US Geological Survey Geologic Investigations Map Series Survey Number 5, U.S. Geological Survey.

Poppe L.J., Ackerman, S.D., Doran E.F., Beaver A.L., Crocker J.M. and Schattgen P.T. (2006). *Interpolation of Reconnaissance Multibeam Bathymetry from North-Central Long Island Sound.* U.S. Geological Survey Open-File Report 2005-1145.

Potts, J.M. and Elith, J. (2006). Comparing species abundance models. *Ecological modelling*, 199(2), 153-163.

Preston, J., Fabra, M., Helmer, L., Johnson, E., Harris-Scott, E. and Hendy, I.W., (2020). Interactions of larval dynamics and substrate preference have ecological significance for benthic biodiversity and *Ostrea edulis* Linnaeus, 1758 in the presence of *Crepidula fornicata*. *Aquatic Conservation: Marine and Freshwater Ecosystems*, 30(11), 2133-2149.

Raineault, N.A., Trembanis, A.C. and Miller, D.C., (2012). Mapping benthic habitats in Delaware Bay and the coastal Atlantic: acoustic techniques provide greater coverage and high resolution in complex, shallow-water environments. *Estuaries and Coasts*, 35(2), 682-699.

Rice, E., Dam, H.G. and Stewart, G., (2015). Impact of climate change on estuarine zooplankton: surface water warming in Long Island Sound is associated with changes in copepod size and community structure. *Estuaries and Coasts*, 38(1), 13-23.

Ridout, M., Demétrio, C.G. and Hinde, J., (1998, December). Models for count data with many zeros. *Proceedings of the XIXth international biometric conference* 19, 179-192. Cape Town, South Africa: International Biometric Society Invited Papers.

Riley, S.J., DeGloria, S.D. and Elliot, R., (1999). Index that quantifies topographic heterogeneity. *Intermountain Journal of Sciences*, 5(1-4), 23-27.

Rosell, D. and Uriz, M.J., (2002). Excavating and endolithic sponge species (Porifera) from the Mediterranean: species descriptions and identification key. *Organisms Diversity & Evolution*, 2(1), 55-86.

Rützler, K. and Rieger, G., (1973). Sponge burrowing: fine structure of *Cliona lampa* penetrating calcareous substrata. *Marine Biology*, 21(2), 144-162.

Scharf, F.S., Manderson, J.P. and Fabrizio, M.C., (2006). The effects of seafloor habitat complexity on survival of juvenile fishes: species-specific interactions with structural refuge. *Journal of Experimental Marine Biology and Ecology*, 335(2), 167-176.

Schuhmacher, H. and Zibrowius, H., (1985). What is hermatypic?. *Coral Reefs*, 4(1), 1-9.

Schweitzer, C.C. and Stevens, B.G., (2019). The relationship between fish abundance and benthic community structure on artificial reefs in the Mid-Atlantic Bight, and the importance of sea whip corals *Leptogorgia virgulata*. *PeerJ*, 7, p.e7277.

Shield C. and Witman J. (1993). The impact of Henricia sanguinolenta predation on the finger sponges, *Isodictya* spp. *Journal of Experimental Marine Biology and Ecology* 166, 107–133.

Smale, D.A., (2020). Impacts of ocean warming on kelp forest ecosystems. *New Phytologist*, *225*(4), 1447-1454.

Stefaniak, L.M., McAtee, J. and Shulman, M.J., (2005). The costs of being bored: effects of a clionid sponge on the gastropod *Littorina littorea* (L). *Journal of Experimental Marine Biology and Ecology*, 327(1), 103-114.

Stefaniak, L.M., Auster, P.J. and Babb, I.G., 2014. Loss of an erect sponge on a rock reef in Long Island Sound (north-west Atlantic). *Marine Biodiversity Records*, 7, 1-6.

Stefaniak, L.M. and P. J. Auster. (2015) Emergent and epi-fauna Characterization. Section 5.5, In: *Seafloor Mapping of Long Island Sound – Final Report: Phase 1 Pilot Project.* (p.268-375). (Unpublished project report). U. S. Environmental Protection Agency, Long Island Sound Study, Stamford, CT.

Steneck, R.S., Graham, M.H., Bourque, B.J., Corbett, D., Erlandson, J.M., Estes, J.A. and Tegner, M.J., (2002). Kelp forest ecosystems: biodiversity, stability, resilience and future. *Environmental Conservation*, 29(4), 436-459.

Strohmeier, T., Strand, Ø., Alunno-Bruscia, M., Duinker, A. and Cranford, P.J., (2012). Variability in particle retention efficiency by the mussel *Mytilus edulis*. *Journal of Experimental Marine Biology and Ecology*, 412, 96-102.

Thieltges, D.W., (2005). Impact of an invader: epizootic American slipper limpet *Crepidula fornicata* reduces survival and growth in European mussels. *Marine Ecology Progress Series*, *286*, 13-19.

Thrush, S.F., Gray, J.S., Hewitt, J.E. and Ugland, K.I., (2006). Predicting the effects of habitat homogenization on marine biodiversity. *Ecological Applications*, 16(5), 1636-1642.

USGS. (2013). Waterdata http://waterdata.usgs.gov/nwis/rt (downlaoded 7 March 2013).

Valentine, P.C., Blackwood, D. and Parolski, K.F., (2000). *Seabed observation and sampling system* (No. 142-00). US Geological Survey.

Vercaemer, B., Sephton, D., Clément, P., Harman, A., Stewart-Clark, S. and DiBacco, C., (2015). Distribution of the non-indigenous colonial ascidian Didemnum vexillum (Kott, 2002) in the Bay of Fundy and on offshore banks, eastern Canada. *Management of Biological Invasions*, 6(4), 385.

Wang Y., Bohlen W.F. and O'donnell J. (2000). Storm enhanced bottom shear stress and associated sediment entrainment in a moderate energetic estuary. *Journal of Oceanography* 56, 311–317.

Webster N.S. (2007). Sponge disease: a global threat? *Environmental Microbiology* 9, 1363–1375.

Whitney M.M. (2010). A study on river discharge and salinity variability in the Middle Atlantic Bight and Long Island Sound. *Continental Shelf Research* 30, 305–318.

Witman JD, Lamb RW. (2018). Persistent differences between coastal and offshore kelp forest communities in a warming Gulf of Maine. *PLoS ONE* 13: e0189388.

Wulff J.L. (2006). Ecological interactions of marine sponges. *Canadian Journal of Zoology* 84, 146–166.

Xavier J.R., Rachello-Dolmen P.G., Parra-Velandia F., Schönberg C.H.L., Breeuwer J.A.J. and van Soest R.W.M. (2010). Molecular evidence of cryptic speciation in the "cosmopolitan" excavating sponge *Cliona celata* (Porifera, Clionaidae). *Molecular Phylogenetics and Evolution* 56, 13–20.

Zajac, R., (1998). *Spatial and temporal characteristics of selected benthic communities in Long Island Sound and management implications*, Final Report, Long Island Sound Research Fund Grant CWF-317-R. Hartford, CT: Connecticut Department of Environmental Protection, Office of Long Island Sound Programs.

Zajac, R.N., Lewis, R.S., Poppe, L.J., Twichell, D.C., Vozarik, J. and DiGiacomo-Cohen, M.L., (2003). Responses of infaunal populations to benthoscape structure and the potential importance of transition zones. *Limnology and Oceanography*, 48(2), 829-842.

Zajac, R.N., (2008). Challenges in marine, soft-sediment benthoscape ecology. *Landscape Ecology*, 23(1), 7-18.

Zajac, R.N., Stefaniak, L.M., Babb, I., Conroy, C.W., Penna, S., Chadi, D. and Auster, P.J., (2020). An integrated seafloor habitat map to inform marine spatial planning and management: A case study from Long Island Sound (Northwest Atlantic). In P. Harris a d E. Baker (Eds.) *Seafloor Geomorphology as Benthic Habitat* (Second ed., 199-217). Elsevier.

Zintzen, V., Norro, A., Massin, C. and Mallefet, J., (2008). Temporal variation of *Tubularia indivisa* (Cnidaria, Tubulariidae) and associated epizoites on artificial habitat communities in the North Sea. *Marine Biology*, 153(3), 405-420.

zu Ermgassen, P.S., Thurstan, R.H., Corrales, J., Alleway, H., Carranza, A., Dankers, N., DeAngelis, B., Hancock, B., Kent, F., McLeod, I. and Pogoda, B., (2020). The benefits of bivalve reef restoration: A global synthesis of underrepresented species. *Aquatic Conservation: Marine and Freshwater Ecosystems*, 30(11), 2050-2065.

5.4 Integrated Ecological Characterization

5.4.1 Overview and approach

The ecosystem dynamics of the seafloor and bottom waters are shaped by both the infaunal and epifaunal communities that are found in any particular habitat/bottom type. Both sets of organisms are critical in seafloor and demersal food webs, and are often key ecosystem engineers generating a variety of habitats, both when live and dead (e.g., shell hash from bivalves) that are critical to different life stages of the full biotic diversity of the seafloor. Thus, being able to determine patterns of joint infaunal and epifaunal community structure can provide insights into ecosystem function and also assessments for conservation and management.

In order to show the joint trends in several community characteristics for both infauna and epifauna in the Phase II study area, mean taxonomic richness and mean diversity were calculated at the sampling block (SB) and single sample site (NB) levels and plotted those together in GIS. For the epifaunal data, the mean from all the image data taken along the transect at a particular SB and NB was calculated. For infauna, at the SB sites means were calculated based on the three samples taken within the SB; for the NB sites the value for the one sample taken at that site was used. Abundances were not jointly assessed due to the difference in how the number of total individuals within a sample was measured for the infauna (number per sample area) and epifauna (percent occurrence).

5.4.2 Taxonomic Richness

Up to 47 different taxa were found in the infaunal samples compared to approximately 11 for epifauna in the images analyzed. These differences reflect how data was collected from either the sediment or image samples (see Section 5.2.2 and Section 5.2.3 for detailed methodologies). As such, these integrated characterizations reflect the relative values given the sampling differences. There were several sections of the Phase II study area where both infaunal and epifaunal taxonomic richness was high; these included areas around Fishers Island, just south of the Thames River, within and south of Niantic Bay and an area just north of Plum Island (Figure 5.4-1). Areas that had high epifaunal taxonomic richness and relatively low infaunal richness included an area in the eastern portion of Fishers Island Sound, and in the central – southern portion of the study area. Areas that had low taxonomic richness for both community types were located within the Race in the southeast corner of the study area, and also south of the Connecticut shore between the Connecticut River and Niantic Bay extending into the central portions of the Phase II area. There were also several single locations with both low epifaunal and infaunal taxonomic richness such as in the sand wave fields along the southwest border of the study area.

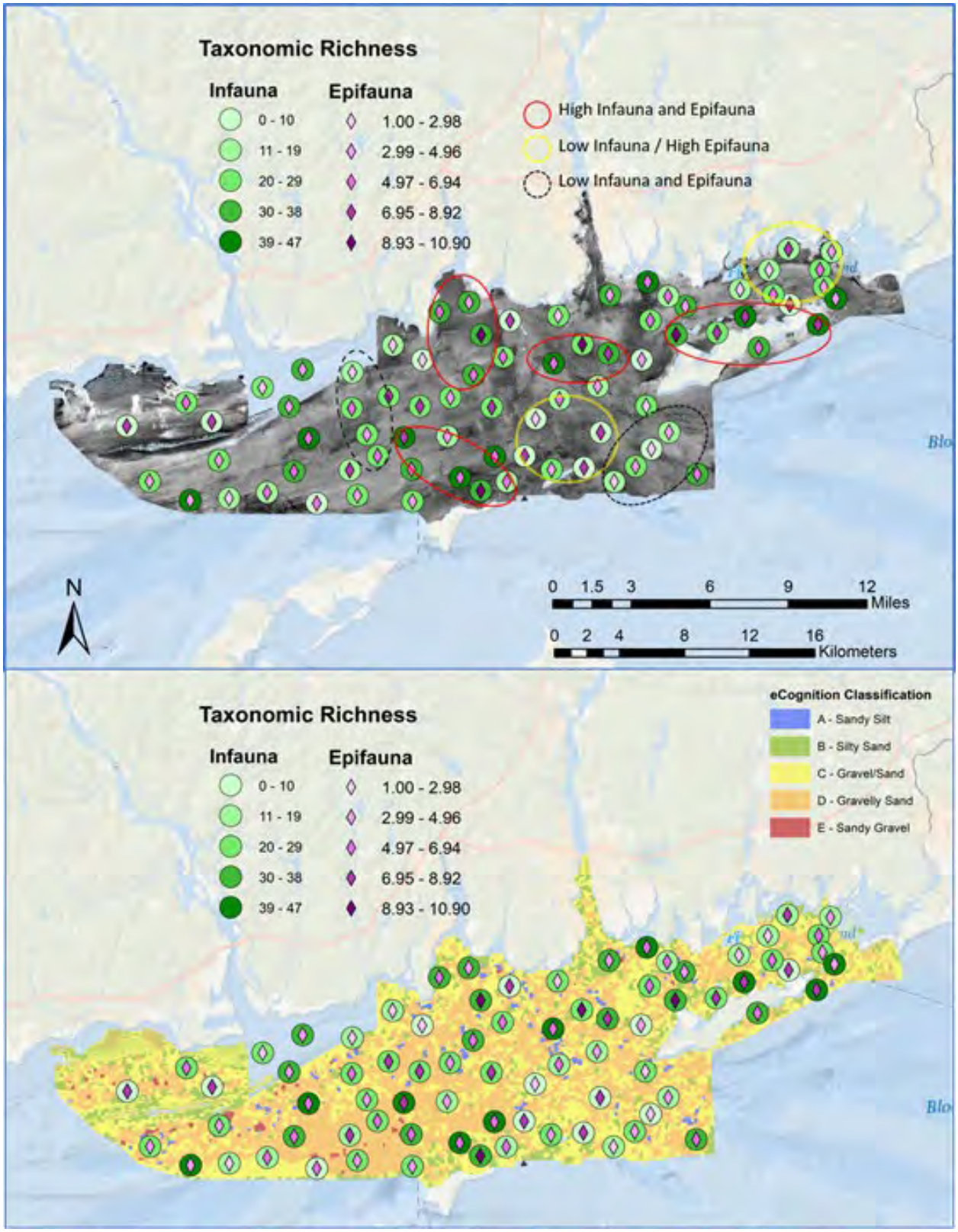

Figure 5.4- 1. Comparisons of infaunal and epifaunal taxonomic richness in the Phase II study area in ELIS. Enclosed areas indicate general trends in taxonomic richness. Both figures show the same data with the top using the backscatter mosaic as a background and the lower using the distribution of acoustic patch types. Trend polygons removed from lower figure for clarity. See text for details.

5.4.3 Diversity

The Shannon diversity index, H', which was calculated for both communities is a metric that assesses both species richness and relative abundance of the taxa found within the sample. The values generally range from <1 in less diverse communities to ~3 in highly diverse communities. As such, diversity values for infauna and epifauna are relatively more comparable than the taxonomic richness values assessed above. Overall, diversity values were relatively low for both the infauna and epifauna (Figure 5.4-2). There were several portions of the study area that had both relatively high infaunal and epifaunal diversity, which were similar to that for taxonomic richness (Figure 5.4-1) but generally covered a larger area−for example, that around Fishers Island and south of the Thames River. There is also a large area in the central portion of the study area. Epifaunal diversity was relatively high compared to infaunal diversity generally in the southeast portion of the Phase II study area. Locations where diversity was low for both infauna and epifauna included the eastern portion of FIS, and several areas in the western most portion of the study area, where large sand wave fields are located.

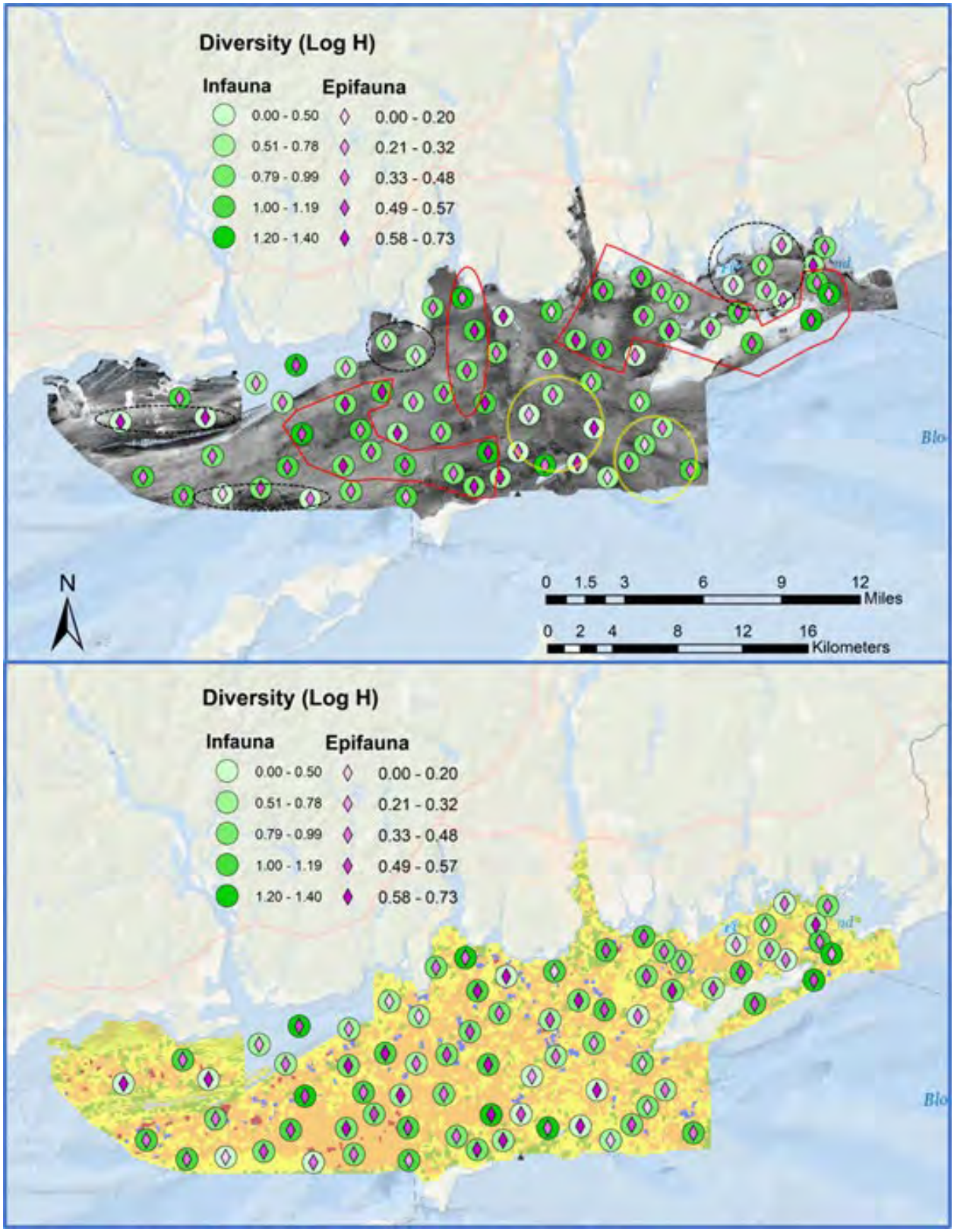

Figure 5.4- 2. Comparisons of infaunal and epifaunal taxonomic richness in the Phase II study area in ELIS. Enclosed areas indicate general trends in taxonomic richness; symbology as in Figure 5.2 106. Both figures show the same data with the top using the backscatter mosaic as a background and the lower the distribution of acoustic patch types. Trend polygons removed from lower figure for clarity. See text for details.

5.4.4 Integrated Habitat Map

An integrated habitat map (Figure 5.4-3) links acoustic patch types to generalized physical and the defining ecological characteristics of biogenic features, infauna, and epi- and emergent fauna. It is notable that the faunal response to the general gradient in grain size from patch types A to E (i.e., finer to coarser sediments) along with the concomitant physical gradient. The ecological pattern in this area comports with the similarity of sediment composition (a gradient of sand-gravel) such that patterns of diversity and dominance shift across patches but are drawn from a similar species pool. Depth, tidal stress, and related measures are correlated with such changes, but species life-histories will be important for predicting the effects of ecological disturbance to human-caused impacts and patterns of resilience (e.g., acute versus chronic stresses and small versus large spatial scales; (Auster & Langton, 1999; Grabowski et al., 2014).

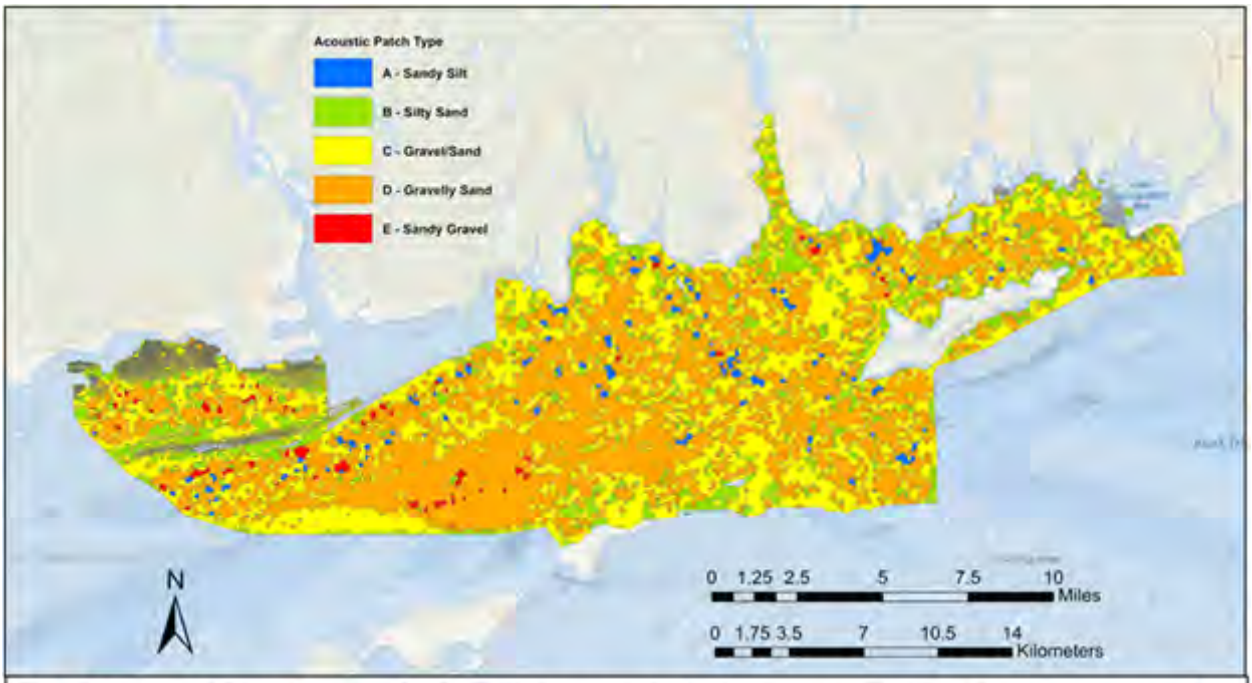

Patch type A - *Physical:* Generally shallow, low complexity, low energy. *Biogenic:* Lowest coverage of shell, low *Zostera* debris; *Infaunal taxa:* Tube building and burrowing fauna, molluscs, *Ampelisca*, bamboo worms, burrowing anemones; *Epi- emergent- taxa:* Low hydrozoan-bryozoan turf, high *Crepidula*, high *Cliona*, high Rhodophyta (some shallow sites).

Patch type B - *Physical:* Moderate depths, moderate to high complexity, low to moderate energy. *Biogenic:* Low-mod shell coverage, moderate *Zostera* and terrestrial debris; *Infaunal taxa:* Tube building and burrowing fauna, hermit crabs, amphipods, bamboo worms, burrowing worms, sand dollars; *Epi- emergent- taxa:* Low-mod hydrozoan-bryozoan turf, low *Astrangia*, low *Crepidula*, low *Mytilus*, *Diadumene*, *Corymorpha* (winter-spring), *Cliona*, high Rhodophyta cover at some shallow sites.

Patch type C - *Physical:* Deepest, highest complexity, moderate to high energy; *Biogenic:* Moderate shell coverage, moderate *Zostera* and terrestrial debris; *Infaunal Taxa*: Tube building and burrowing Fauna, molluscs, *Astarte* spp., amphipods. bamboo worms, burrowing worms, sand dollars; *Epi- emergent- taxa:* Moderate hydrozoan-bryozoan turf, moderate *Astrangia*, moderate *Crepidula*, moderate *Mytilus*, *Diadumene*, moderate *Corymorpha* (winter-spring), *Cliona*, moderate *Rhodophyta* (some shallow sites).

Patch type D - *Physical:* Deep, moderate complexity, highest energy; *Biogenic:* Mod-high shell coverage, low *Zostera* and terrestrial debris; Infaunal Taxa: Molluscs, *Astarte* spp., tube building and burrowing fauna, amphipods, bamboo worms, sand dollars. *Epi- emergent- taxa:* Moderate-high to highest *Astrangia*, moderate *Crepidula*, high *Mytilus*, high *Diadumene*, moderate *Corymorpha* (winter-spring), *Cliona*, moderate *Rhodophyta* (some shallow sites).

Patch type E - *Physical*: Shallow to moderate depths, low complexity, high energy; *Biogenic:* Highest coverage of shell; *Infaunal taxa:* Molluscs, *Astarte* spp. tube building and burrowing fauna, ophiuroids, sand dollars; *Epi- emergent- taxa*: Highest hydrozoan-bryozoan turf, high *Astrangia*, low *Crepidula*, moderate *Mytilus*, high *Corymorpha* (winter-spring).

Figure 5.4- 3. Integrated Habitat Map for the Phase II study area. Descriptors below summarize the main habitat and ecological characteristics of each acoustic patch type.

5.4.5 References - Integrated Ecological Characterization

Auster, P. J., & Langton, R. W. (1999). The effects of fishing on fish habitat. In American Fisheries Society Symposium 22, 150-187.

Grabowski, J. H., Bachman, M., Demarest, C., Eayrs, S., Harris, B. P., Malkoski, V., ... & Stevenson, D. (2014). Assessing the vulnerability of marine benthos to fishing gear impacts. Reviews in Fisheries Science & Aquaculture, 22(2), 142-155.

5.5 Seafloor/Habitat Classification

5.5.1 Overview and Classification Approach for the Phase II Area

Over the past decade there have been considerable efforts to integrate information from seafloor mapping and associated geological and ecological studies to develop and apply habitat/ecological classification systems (Greene et al., 1999; Mumby & Harborne, 1999; Allee et al., 2000; Auster et al., 2009; Verfaillie et al., 2009; Guarinello et al., 2010; FGDC, 2012). The overarching goal of such systems is to provide a common, hierarchical typology that classifies sea floor habitats and ecological systems across a broad spectrum of spatial scales, from 1000's of km^2 to the spatial extent of a single sample, and in turn provide a consistent framework for assessment and management of sea floor environments.

In 2012, CMECS was adopted by the Federal Geographic Data Committee (FGDC). This system is comprised of multiple classification components within the context of Biogeographic and Aquatic Settings (Figure 5.5-1). These include Water Column, Geoform, Substrate, and Biotic components, each of which can have a number of modifiers (Figure 5.5-2 and Figure 5.5-3) providing specific descriptors. Together these form a biotope for the specific setting.

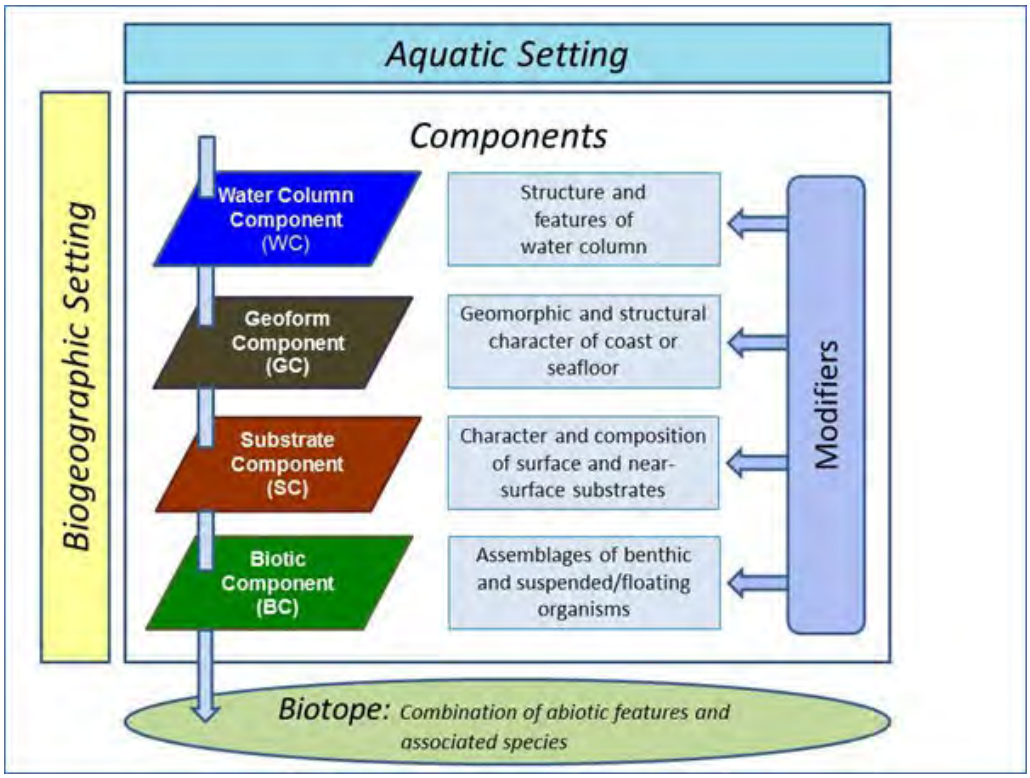

Figure 5.5- 1. Overall organization of CMECS including hierarchical components and their modifiers.

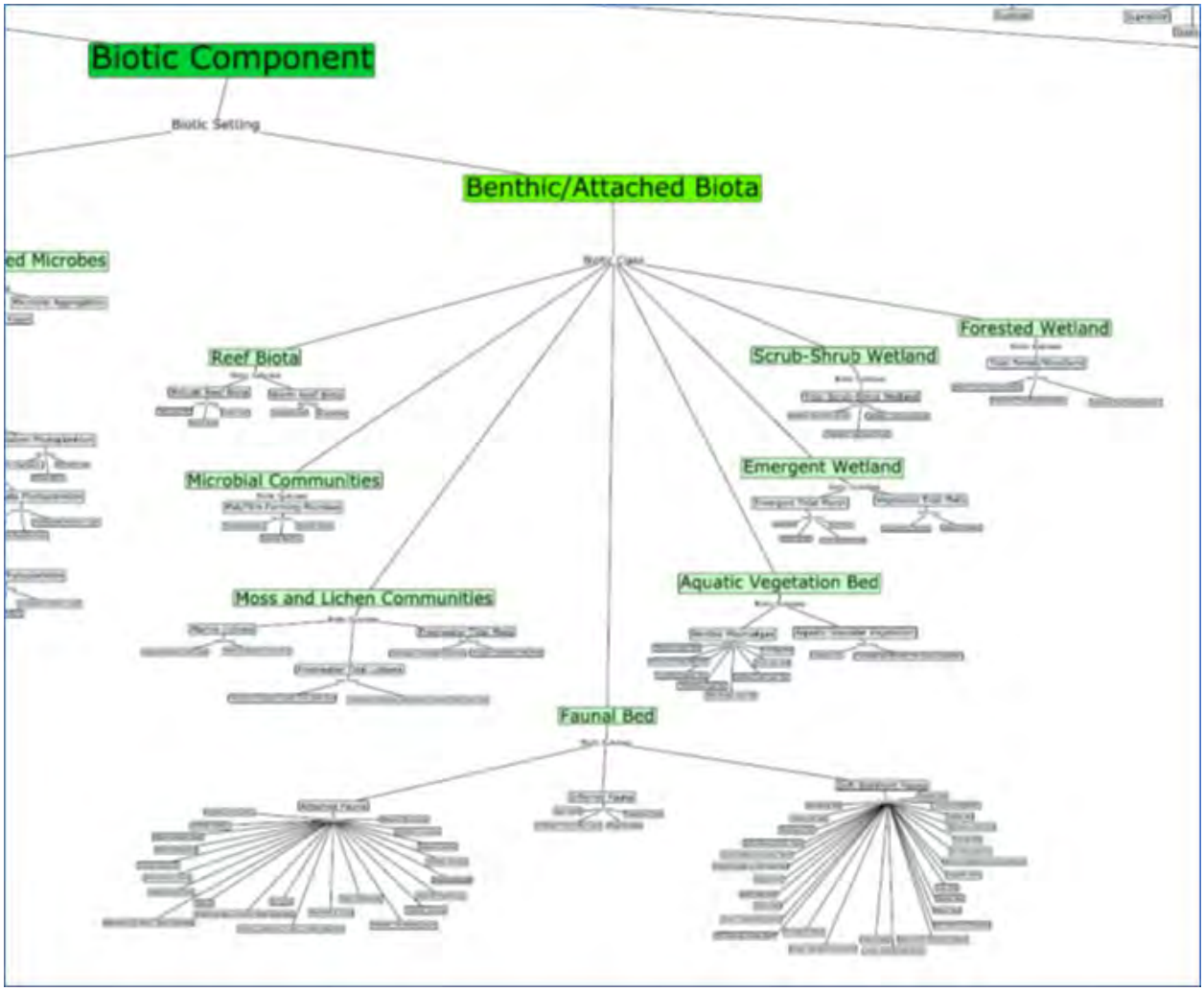

Figure 5.5- 2. Biotic component modifiers in the CMECS classification system for the Benthic/Attached Biota biotic setting.

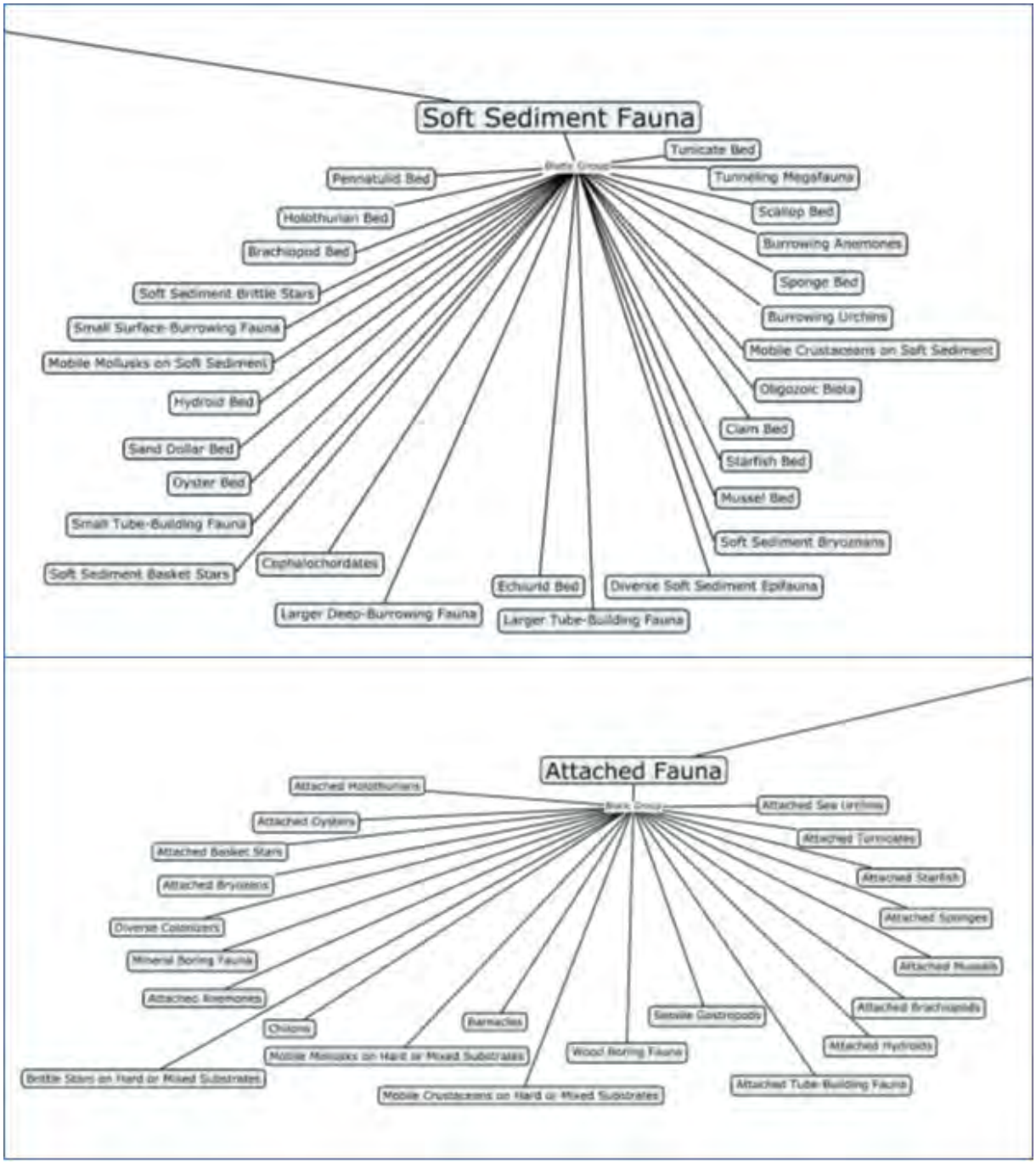

Figure 5.5- 3. Detailed view of Biotic Sub-classes for the Attached Fauna and Soft Sediment Fauna for the Faunal Bed Biotic Class in the CMECS Classification system showing suggested modifiers.

CMECS has been applied and assessed for a variety of marine environments (e.g. Keefer et al., 2008; Ackerman et al., 2015; Bassett et al., 2017; Mittermayr et al., 2020A; Mittermayr et al. 2020B). These studies demonstrate the utility of CMECS, and collectively add to the catalogue of seafloor environments that have been classified using this standard. They also provide suggestions on how to improve CMECS and recognize that the component subgroups and modifiers need to be flexible so that the environmental and ecological characteristics of a specific area can be effectively portrayed at different spatial scales and be relevant to management efforts.

Sub-components and modifiers included in the CMECS documentation do not necessarily apply in all seafloor environments, which was recognized by its developers, so our approach

was to adhere to the extent possible to CMECS modifiers but also to define our own as necessary to accurately describe biotic components specific to the Phase II area. Our selections of sub-components and modifiers for the classification are based on the in-depth analyses conducted of the infaunal (Section 5.2.2) and epifaunal (Section 5.2.3) communities, as well as the analyses of the sediment and environmental data associated with characterization of the seafloor patch structure (Section 5.1).

We developed CMECS classifications at two levels of resolution, at the sample level and at the acoustic patch level. At the sample level this included CMECS classifications for both infauna (based on analyses of grab samples) and epifauna (based on analyses of digital images). Having classifications for both groups of biota provides for more detailed information at the scale of a sample site (infauna) and image transect location (epifauna). At the acoustic patch level, we integrated these 2 sets of data to provide an overall CMECS class at this greater spatial resolution.

5.5.2 Infauna

The CMECS classification for each infaunal sample site includes several standard CMECS component modifiers and study-specific, Biotic Group modifiers for the Biotic Sub-class (Table 5.5-1 and Table 5.5-2). The Biotic Group modifiers (types) in Table 5-22 were based on data for each of the samples and were developed by assessing the dominant taxa and their general functional characteristics. Also included are two additional components, Biotic Community and Other Elements. The Biotic Community component lists the specific and or common names of the dominant taxa making up the community at that sample location. These are given in decreasing relative abundance. The Other Elements component provides some additional information regarding taxa of interest, such as deep burrowing crustaceans, and other information such as low overall abundance in the sample.

Table 5.5- 1 CMECS classification components for infaunal communities in the Phase II study area in ELIS.

Physical Setting	Sound: Long Island Sound is a sound
Geoform	Basin: The system-scale geologic form of LIS is a basin
Substrate	Varied sediment classes: Types is based on general sediment classification acoustic within which the sample was found[#]
Biotic Setting	Benthic / Attached Biota: CMECS based
Biotic Class	Faunal Bed: CMECS based
Biotic Sub-class	Soft Sediment Fauna: CMECS based
Biotic Group	Varied: Based on dominant taxa in the sample and their functional characteristics; See Table 5-22 for specific descriptions
Biotic Community	Dominant Taxa found given in order of decreasing abundance*
Other Elements	Other taxa of note found in samples / relevant other information

In the Infaunal Communities Phase II GIS shapefile detailed data on sediment composition at each infaunal sample site is also provided including percent composition by weight of general sediment classes (gravel, sand, silt, clay) as well as detailed sediment composition by Wentworth scale phi values

* In the Infaunal Communities Phase II GIS shapefile, there is a column (field) that provides the community type designation (a-m) based on multivariate analyses of the infaunal data; see Section 5.2.2 of this report for details.

Table 5.5- 2 Modifiers for the biotic group component of the CMECS classification for infaunal sample sites in the Phase II study area in ELIS. Modifiers were developed based on the data for each infaunal sample location.

Biotic Groups	
Clam Bed	Sample dominated by bivalves
Clam Bed / Burrowing Fauna	Sample dominated by bivalves and burrowing fauna, generally polychaetes
Clam Bed / Small Tube Building Fauna	Sample dominated by bivalves and small tube builders, generally spionid polychaetes
Clam Bed / Tube Building and Burrowing Fauna	Sample dominated by bivalves with tube building and burrowing polychaetes of varied sizes
Faunal Bed	No evident dominant taxa
Large Tube Building Fauna	Mostly large tube building fauna such as bamboo worms
Mollusk Bed	Sample dominated by both bivalves and other mollusks
Mollusk Bed / Burrowing Fauna	Sample dominated by both bivalves and other mollusks and burrowing polychetes
Mollusk Bed / Burrowing Fauna /Motile Fauna	as above but with surface motile taxa
Mollusk Bed / Tube Building and Burrowing Fauna	Sample dominated by bivalves and other mollusk with tube building and burrowing polychaetes of varied sizes
Mollusk Bed / Tube Building Fauna	Sample dominated by bivalves and other mollusk with tube building polychaetes
Motile Crustaceans	Sample dominated by surficial motile crustaceans
Motile Gastropods and Crustacea	Sample dominated by gastropods and crustaceans
Motile Surface Fauna	sample with surface motile fauna but no dominant taxa
Ophiuroids / Clam Bed	Brittle stars and bivalves
Sand Dollar Bed	Sample with large numbers of sand dollars
Sessile and Mobile Mollusks	Sample with gastropods and mix of sessile mollusks
Small & Large Tube Building Fauna	Sample dominated by large and small builders such as spionids and bamboo worms
Small Surface-Burrowing Fauna	Sample dominated by small polychaetes usually living just below the surface of the sediment
Small Tube Building Fauna	Sample dominated by tube building polychaete such as spionids
Tube Building Fauna	Sample dominated by a variety of tube building polychaetes
Tube Building and Burrowing Fauna	Sample dominated by a variety of tube building and burrowing fauna
Tube Building and Burrowing Fauna / Clam Bed	Sample dominated by a variety of tube building and burrowing fauna and bivalves
Tube Building and Burrowing Fauna / Mollusk Bed	Sample dominated by a variety of tube building and burrowing fauna and mollusks

Examples of the CMECS classification for several infaunal sample sections are shown in Figure 5.5-4 and Figure 5.5-5. These CMECS classifications are included in the Infaunal Communities Phase II GIS shapefile, which also contains data for total abundance, taxonomic richness, and Shannon Diversity, as well as community type designations. Environmental data (e.g., sediment grain size distributions, depth) are also included in that GIS shapefile.

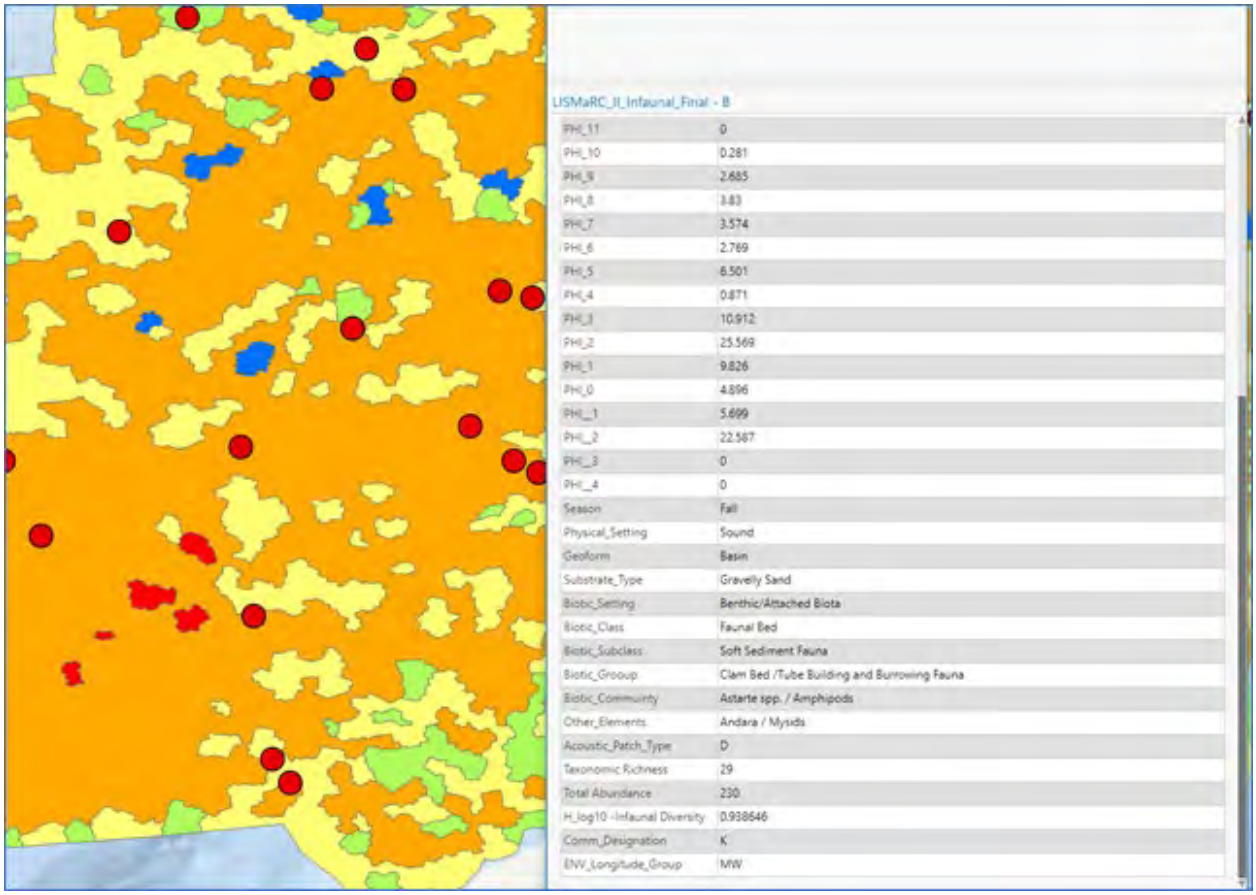

Figure 5.5- 4. Example of GIS query of database associated with the Infaunal Community Phase II shapefile showing CMECS classification (in black box) for sample SB51-1. Arrow points to sample location in the middle of the Phase II study area.

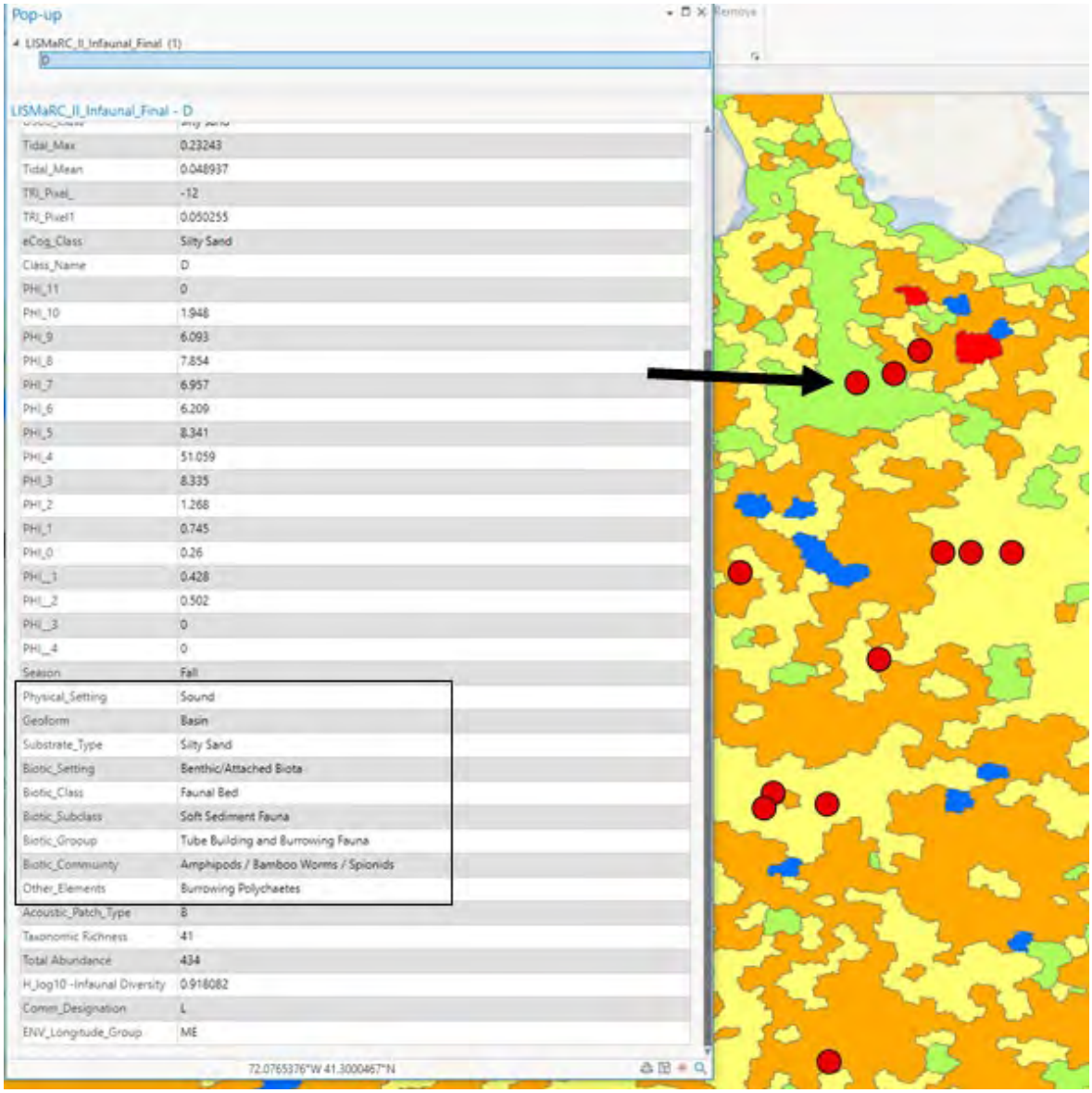

Figure 5.5- 5. Example of GIS query of database associated with the Infaunal Community Phase II shapefile showing CMECS classification (in black box) for sample SB64-3. Arrow points to location of sample just south of the mouth of the Thames River.

5.5.3 Epifauna

The CMECS classification for emergent and epifaunal images includes several standard CMEC component modifiers and study-specific, Biotic Group modifiers for the Biotic Sub-class (Table 5.5-3 and Table 5.5-4). The Biotic Group modifiers (types) in Table 5.5-4 were based on data for each of the image sets for each acoustic patch type and were developed by assessing the dominant taxa, features, and the physical setting in which they occur and their general functional characteristics. These classes were then assigned to each image and the associated acoustic type. The taxa and feature composition for each image sample are associated with the CMECS hierarchical classes.

Examples of the CMECS classification for several image sample sections are shown in Figure 5.5-6 and Figure 5.5-7.

Table 5.5- 3 CMECS classification components for epifaunal communities in the Phase II study area in ELIS.

Physical Setting	Sound: Long Island Sound is a sound
Geoform	Basin: The system-scale geologic form of LIS is a basin
Substrate	Varied sediment classes: Types is based on general sediment classification acoustic within which the sample was found[#]
Biotic Setting	Benthic / Attached Biota: CMECS based
Biotic Class	Faunal bed/aquatic vegetation bed (some shallow patches): CMECS based
Biotic Sub-class	Attached fauna/soft sediment fauna/benthic macroalgae (some shallow patches): CMECS based
Biotic Group	Varied: Based on dominant taxa across sample site and their functional characteristics; See Table 5-24 for specific descriptions

Table 5.5- 4 Modifiers for the biotic group component of the CMECS classification for infaunal sample sites in the Phase II study area in ELIS. Modifiers were developed based on the data for each infaunal sample location.

Biotic Groups	
Clam Bed	Sample dominated by bivalves
Clam Bed / Burrowing Fauna	Sample dominated by bivalves and burrowing fauna, generally polychaetes
Clam Bed / Small Tube Building Fauna	Sample dominated by bivalves and small tube builders, generally spionid polychaetes
Clam Bed / Tube Building and Burrowing Fauna	Sample dominated by bivalves with tube building and burrowing polychaetes of varied sizes
Faunal Bed	No evident dominant taxa
Large Tube Building Fauna	Mostly large tube building fauna such as bamboo worms
Mollusk Bed	Sample dominated by both bivalves and other mollusks
Mollusk Bed / Burrowing Fauna	Sample dominated by both bivalves and other mollusks and burrowing polychetes
Mollusk Bed / Burrowing Fauna /Motile Fauna	as above but with surface motile taxa
Mollusk Bed / Tube Building and Burrowing Fauna	Sample dominated by bivalves and other mollusk with tube building and burrowing polychaetes of varied sizes
Mollusk Bed / Tube Building Fauna	Sample dominated by bivalves and other mollusk with tube building polychaetes
Motile Crustaceans	Sample dominated by surficial motile crustaceans
Motile Gastropods and Crustacea	Sample dominated by gastropods and crustaceans
Motile Surface Fauna	sample with surface motile fauna but no dominant taxa
Ophiuroids / Clam Bed	Brittle stars and bivalves
Sand Dollar Bed	Sample with large numbers of sand dollars
Sessile and Mobile Mollusks	Sample with gastropods and mix of sessile mollusks
Small & Large Tube Building Fauna	Sample dominated by large and small builders such as spionids and bamboo worms
Small Surface-Burrowing Fauna	Sample dominated by small polychaetes usually living just below the surface of the sediment
Small Tube Building Fauna	Sample dominated by tube building polychaete such as spionids
Tube Building Fauna	Sample dominated by a variety of tube building polychaetes
Tube Building and Burrowing Fauna	Sample dominated by a variety of tube building and burrowing fauna
Tube Building and Burrowing Fauna / Clam Bed	Sample dominated by a variety of tube building and burrowing fauna and bivalves
Tube Building and Burrowing Fauna / Mollusk Bed	Sample dominated by a variety of tube building and burrowing fauna and mollusks

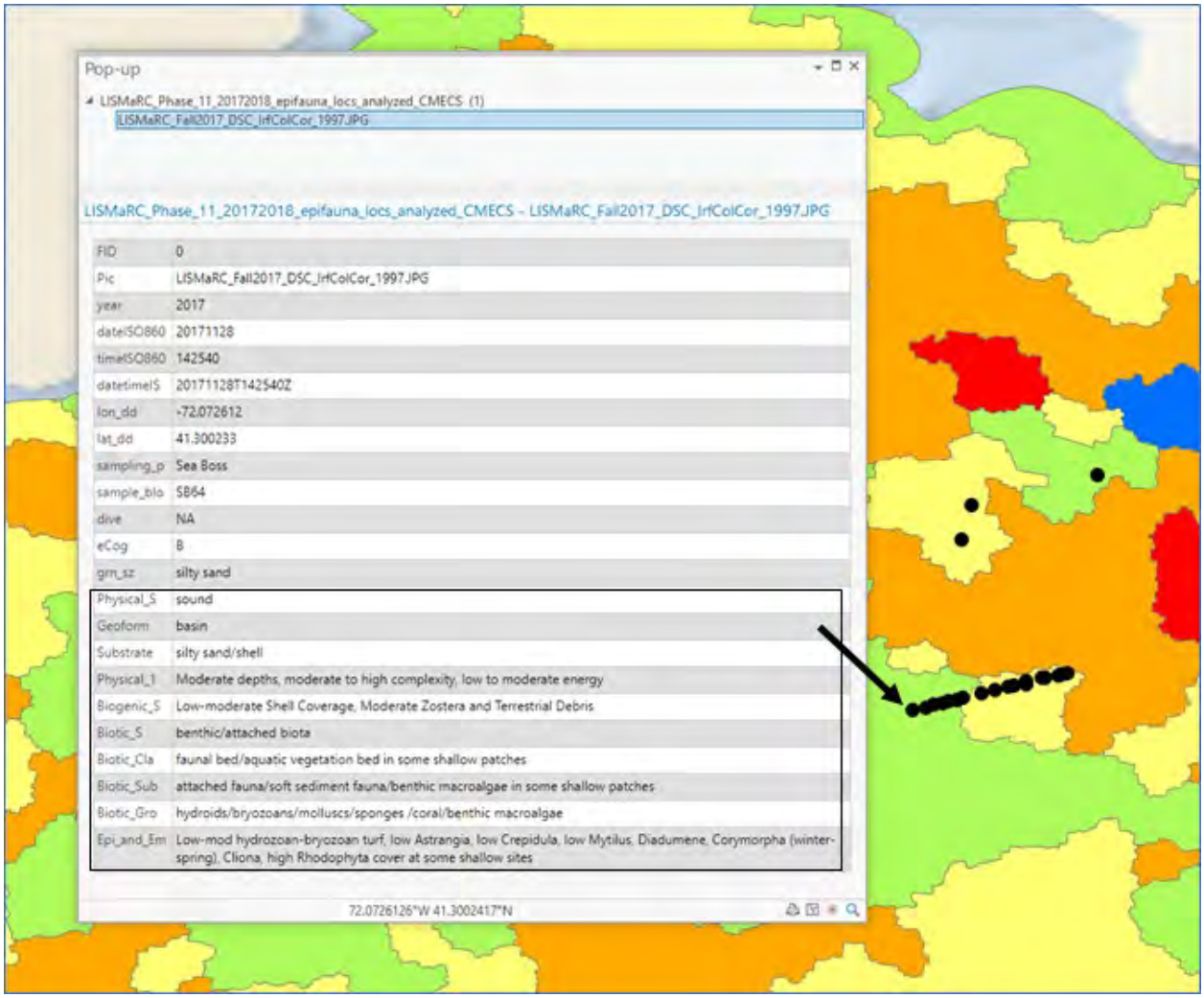

Figure 5.5- 6. Example of GIS query of database associated with the Epifaunal Community Phase II shapefile showing CMECS classification (in black box) for sample SB64-3. Arrow points to locations of images.

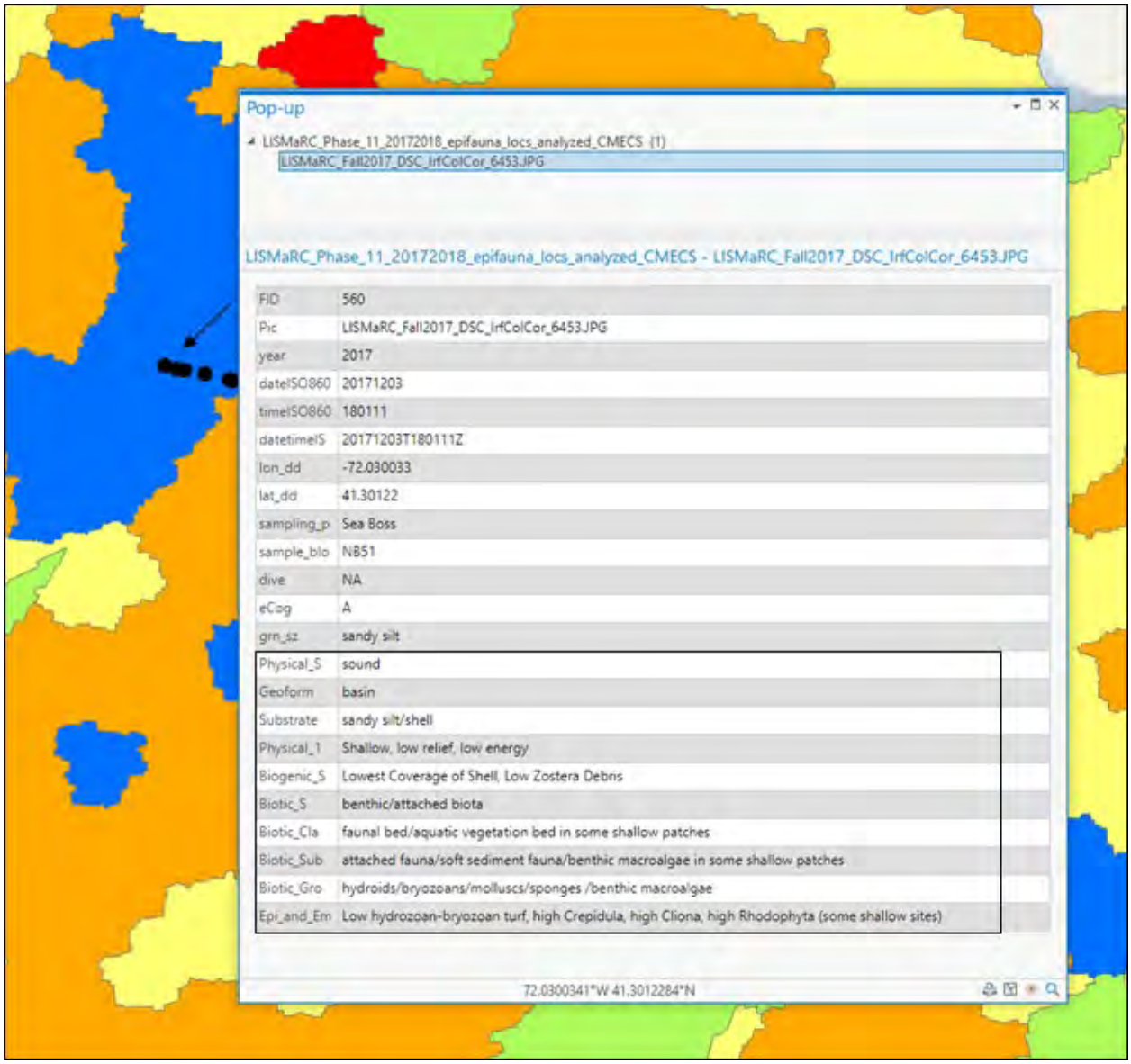

Figure 5.5- 7. Example of GIS query of database associated with the Epifaunal Community Phase II shapefile showing CMECS classification (in black box) for sample NB51. Arrow points to locations of images within the acoustic patch.

5.5.4 Acoustic Patch Level CMECS Classification

The CMECS classifications of the acoustic patch types summarize the results from the analyses of both the infaunal and epifaunal communities and associated environmental characteristics, such as surficial features that are ecologically relevant (see Section 5.2.2 and Section 5.2.3). Several classification levels were added to provide details about the habitat and ecological characteristics in the acoustic patch types (Table 5.5-5). To provide more in-depth environmental information about each acoustic patch type two additional classes were added including Physical Setting Notes and Biogenic Surface Features. The Biotic Group class was split into Epi- and Emergent Fauna and Infauna, with both classes having a Notes class to provide information on specific taxa that were dominant in each acoustic patch type. The modifiers in each of these classification levels attempt to encompass both the primary characteristics of biotic communities in the acoustic patch types and, to the extent possible, their variability.

An example of a query showing the CMECS classification for an acoustic patch type is shown in Figure 5.5-8. In some sense the acoustic patch types may be considered as Biotopes as they are classified across all the CMECS components and indeed cover areas larger than that of a grab or photographic sample location. It is important to note that although each patch of a particular acoustic patch type has the same CMECS classification, there is variation in the specific community types and other ecological characteristics found across the Phase II study area. The CMECS classification for the acoustic patch types attempts to capture their general attributes across the Phase II study area. As such, it should be used as a starting point for a more detailed consideration of ecological characteristics in any specific portion of the area using the more in-depth analyses presented in Section 5.2.2 and Section 5.2.3, and their associated GIS databases.

Table 5.5- 5 CMECS classification components for acoustic patch types in the Phase II study area in ELIS.

Physical Setting	Sound: Long Island Sound is a sound
Geoform	Basin: The system-scale geologic form of LIS is a basin
Substrate	Varied sediment classes: Types are based on general sediment classification of the acoustic patch types but also includes information on surficial features found in photographs, such as the presence of shell
Physical Setting Notes	General characteristics in terms of depth, topographic complexity and bottom stress energy
Biogenic Surface Features	General incidence of surface features created or deposited by biota and other features that occur in some of the patches of this acoustic patch type
Biotic Setting	Benthic / Attached Biota: CMECS based
Biotic Class	Faunal Bed: CMECS based, noting variations, such as vegetation beds in some shallow areas
Biotic Sub-class fauna	CMECS based: combination of attached fauna / soft sediment/benthic macroalgae depending on patch type and how these may vary by depth
Biotic Group Epi-Emergent Fauna	Varied: General types of dominant taxa in the specific acoustic patch types as determined by analyses (see Section 5.3)
Epi- and Emergent Fauna Notes	General abundance levels of specific epifaunal taxa, noting any seasonality
Biotic Group Infauna	Varied: General types of dominant taxa in the specific acoustic patch types as determined by analyses (see Section 5.2)
Infauna Notes	General abundance levels of specific taxa

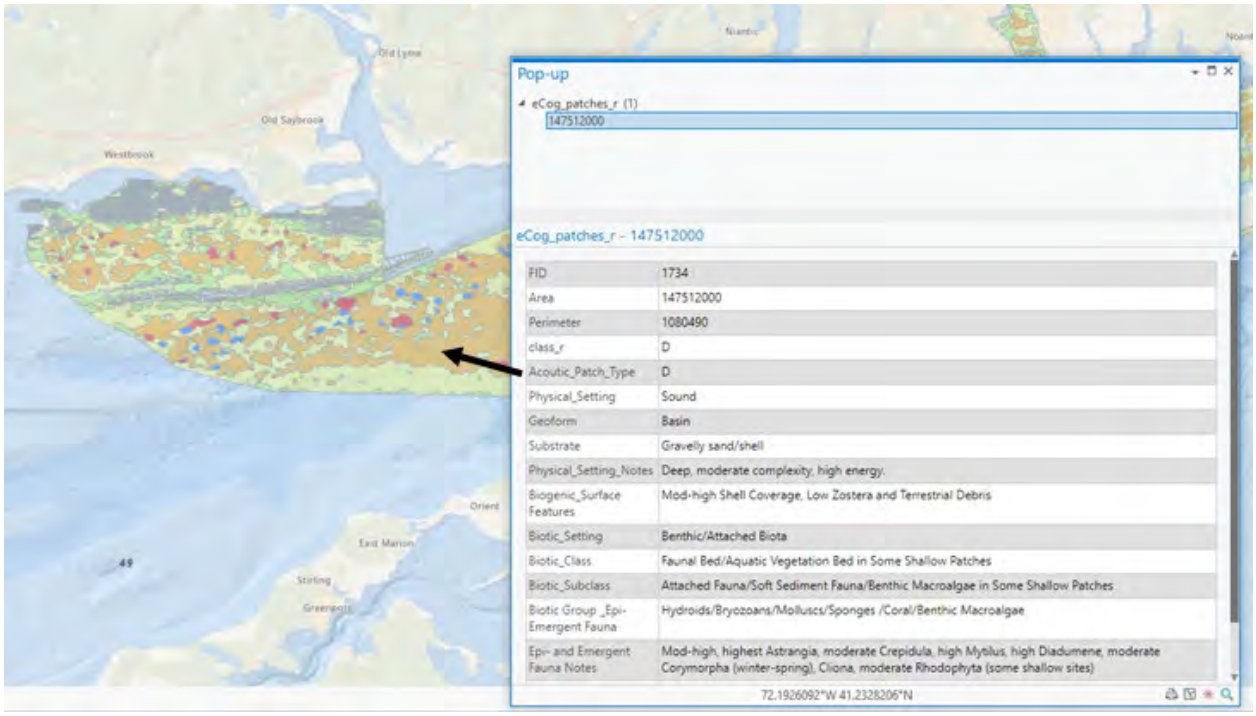

Figure 5.5- 8. Example of GIS query of database associated with the Infaunal Community Phase II shapefile showing CMECS classification for acoustic patch D in the central portion of the study area. Arrow points to the acoustic patch being queried.

5.5.5 References - Seafloor/Habitat Classification

Ackerman, S.D., Pappal, A.L., Huntley, E.C., Blackwood, D.S. and Schwab, W.C., (2015). *Geological Sampling Data and Benthic Biota Classification: Buzzards Bay and Vineyard Sound, Massachusetts*. Open File Report 2014-1221, U.S. Geological Survey. Retrieved from https://pubs.er.usgs.gov/publication/ofr20141221.

Allee, R.J., Dethier, M., Brown, D., Deegan, L., Ford, R.G., Hourigan, T.F., Maragos, J., Schoch, C., Sealey, K., Twilley, R. and Weinstein, M.P., (2000). *Marine and estuarine ecosystem and habitat classification*. NOAA Technical Memorandum NMFS-F/SPO-43 U.S. Department of Commerce, National Oceanic and Atmospheric Administration, National Marine Fisheries Service.

Auster, P.J., Heinonen, K.B., Witharana, C. and McKee, M. (2009) *A habitat classification scheme for the Long Island Sound region.* Long Island Sound Study Technical Report. EPA Long Island Sound Office, Stamford, Connecticut.

Bassett, R.D., M. Finkbeiner, and P.J. Etnoyer. (2017). *Application of the Coastal and Marine Ecological Classification Standard (CMECS) to Deep-Sea Benthic Surveys in the Northeast Pacific: Lessons from Field Tests in 2015*. NOAA Technical Memorandum NOS NCCOS 228, NOAA National Ocean Service, Charleston, SC 29412, 49.

Federal Geographic Data Committee (FGDC). (2012). FGDC-STD-18-2012. Coastal and Marine Ecological Classification Standard. Reston, VA Federal Geographic Data Committee.

Greene, H.G., Yoklavich, M.M., Starr, R.M., O'Connell, V.M., Wakefield, W.W., Sullivan, D.E., McRea Jr, J.E. and Cailliet, G.M., (1999). A classification scheme for deep seafloor habitats. *Oceanologica acta*, 22(6), 663-678.

Guarinello, M.L., Shumchenia, E.J. and King, J.W., (2010). Marine habitat classification for ecosystem-based management: a proposed hierarchical framework. *Environmental Management*, 45(4), 793-806.

Keefer, M.L., Peery, C.A., Wright, N., Daigle, W.R., Caudill, C.C., Clabough, T.S., Griffith, D.W. and Zacharias, M.A., (2008). Evaluating the NOAA coastal and marine ecological classification standard in estuarine systems: a Columbia River estuary case study. *Estuarine, Coastal and Shelf Science*, 78(1), 89-106.

Mittermayr, A., Legare, B. and Borrelli, M., (A 2020). Applications of the coastal and marine ecological classification standard (CMECS) in a partially restored New England salt marsh lagoon. *Estuaries and Coasts*, 1-12.

Mittermayr, A., Legare, B.J., Kennedy, C.G., Fox, S.E. and Borrelli, M., (B 2020). Using CMECS to create benthic habitat maps for Pleasant Bay, Cape Cod, Massachusetts. *Northeastern Naturalist*, 27(10), 22-47.

Mumby, P.J. and Harborne, A.R., (1999). Development of a systematic classification scheme of marine habitats to facilitate regional management and mapping of Caribbean coral reefs. *Biological Conservation*, 88(2), 155-163.

Verfaillie, E., Degraer, S., Schelfaut, K., Willems, W. and Van Lancker, V., (2009). A protocol for classifying ecologically relevant marine zones, a statistical approach. *Estuarine, Coastal and Shelf Science*, 83(2), 175-185.

5.6 Overall Discussion and Conclusions

5.6.1 Habitat Mapping

The seafloor environment in the Phase II study area is spatially complex, reflecting the mix of large-scale hydrodynamic and geomorphological features that influence its features. In the eastern portion of the study area the major flux of water occurs through the Race, creating strong currents throughout much of the Phase II area and overall erosional/non-depositional and coarse-grained bedload transport sedimentary environments (Knebel & Poppe, 2000). Along the Connecticut shore, outflow from the Connecticut River carries sediment and organic matter into the western portion of the Phase II area and adds complexity to this area's hydrodynamics. The Thames River also is a source of sediment and affects the hydrodynamics of the area south of its mouth and the western portion of FIS, which is also affected by fluxes of water that occur at its eastern end. The influence of these features leads to the sand and coarse sediments that comprise most of the Phase II area (see Section 4.3), and also geomorphological features such as extensive sand waves of various spatial scales in some locations and areas dominated by large rocks and boulders. Areas with finer sediments are generally confined to just south of the mouths of the Connecticut and Thames rivers and in embayments such as Niantic Bay.

The dominance of sands and coarser sediments in the Phase II study area is evident in the backscatter mosaic that was used for the characterization of sea floor habitat structure. Much of the mosaic has a complex pattern of image characteristics that are primarily associated with sandy/harder sediments than that of muddy/finer sediments. This is in contrast to the Phase I area where there are large areas of muddy sediments that were distinct features in the backscatter mosaic. Sea floor characterization, which can be used as a basis for habitat mapping, can be difficult in an area such as eastern LIS. Difficulties stem from the subtle differences in backscatter returns in an environment that is primarily comprised of sands/coarse sediments and their varied geomorphologies such as flat beds, sand waves, cobble/ boulder fields, and mixtures of these. Montereale-Gavazzi et al. (2019) found that water column conditions (e.g., complex current patterns) and shifting geomorphology could cause significant backscatter variability, particularly in dynamic sandy and muddy areas.

Testing of several supervised classification approaches for backscatter mosaics indicated overall accuracies of around 50% and limitations in discriminating subtle differences between sediment types with only fractional differences in sediment composition at small spatial scales (Diesing et al., 2020). Acknowledging these and other possible image collection, processing and analysis issues that can affect the interpretation of backscatter mosaics, the acoustic patch types identified in this study represent a set of seafloor conditions that have relatively distinct attributes in terms of ecological habitats. Each acoustic patch type has a different overall distribution of sediment grain-sizes and other environmental characteristics (Figure 4.3-3–Figure 4.3-6), despite being comprised primarily of sandy / coarse sediments. Although there was overlap in their characteristics, there is a trend of acoustic patch types A to E, respectively, being comprised of progressively coarser sediments, and higher maximum bed stress (Figure 4.3-6) and other features such as shell hash, and certain other surficial features (Table 5.3-3A). While there was some variation in sediment composition within each acoustic patch type, analyses indicated relatively consistent sediment grain-size composition in acoustic patch types B, C, and D when separated into groups spanning the west to east gradient in the study area.

The acoustic patch types can be designated as habitat types, and their mapped distribution forms the basis of an overall habitat map for the Phase II study area (Figure 4.3-1) and see below). This also forms the framework for subsequent research and surveys that can assess the accuracy of the characteristics of these habitat types as determined in this study, and also the extent of the distribution of seafloor habitats in this portion of LIS. Based on the analyses and resultant habitat map (Figure 5.4-3) produced in this study, there are several areas that should be studied in additional detail. More samples should be taken in acoustic patch types A and E, as only one grab sample was collected in these two patch types. The sediment data collected by the LDEO group in this study could be used to provide more detail as to sediment composition in the acoustic patch types, and as a test of the characterization presented in Section 4.3. Unfortunately, these data were not available in a final form in time to be used in our analyses within the period of project completion.

5.6.2 Infaunal Communities

Infaunal community characteristics vary across the Phase II study area, but there are some general trends, notably higher total abundance and taxonomic richness from west to east. There are several areas of relatively high diversity throughout the study area. Infaunal community composition for each acoustic patch type, is relatively distinct, but variable within acoustic patch types, predominantly due to changes in taxonomic dominance. The relative mix of sediment grain-sizes within each acoustic patch type, particularly the dominant sand fractions, are not different to the extent that they support distinct sets of communities. Analysis of community structure without grouping by acoustic patch type revealed that differences were most notable between the south/central, and north coastal portions of the Phase II area. The eastern central portion of the study area is comprised of a variable mix of community types but their similarity is relatively high (Figure 5.2-21). Each acoustic patch type was found to support a variety of these community types, although there was generally one dominant type (Table 5.2-7). As such, the determinants of infaunal community composition across the Phase II study area include the habitat characteristics of the acoustic patch types and specific seafloor characteristics that may be found in a particular area, such as bottom stress conditions and/or differences in geomorphology (e.g., sand dunes or featureless bottom areas).

Due to sequence of designing the field surveys relative to availability of information and related analyses, only one sample was collected in acoustic patch types A (sandy silts) and E (gravelly sand). Any future surveys should collect more samples in these areas to fully characterize the community types that they may support. Also, there was a set of samples taken in areas where there was no backscatter available at the time the sampling design was being developed. These are designated as ND and were located along the Connecticut shore. These have sedimentary characteristics that are intermediate to patch types A and B, and had relatively distinct communities from the other acoustic patch types. Future surveys of infauna community structure should also include more detailed sampling of these nearshore areas and also classification of the seafloor based on approaches used in this study.

Apart from the community types that were indicated by the analyses, and the dominant species, there are portions of the Phase II study area that support infauna that occur in low numbers but can have important ecological functions and can be considered as indicators of relatively un-impacted environmental conditions. These include taxa such as ophiuroids, deep burrowing shrimp, sand dollars and large polychaetes. The presence of these at each of the infaunal sampling locations are noted in the CMECS classifications generated in the study.

5.6.3 Epifaunal Communities

The communities of attached and emergent taxa associated with each acoustic patch type were distinct principally based on changes in dominance and not wholesale differences in composition. As with infaunal community characteristics linked to sediment size fractions, epi- and emergent taxa were associated with multiple grain-sizes differentially represented within each acoustic patch type. That is, epifaunal taxa that require stable sites for attachment (i.e., cobble to boulder size rocks) occurred in all patch types, but the frequency of occurrence of these size fractions of gravel differed along a gradient (i.e., patch types A-E). Indeed, the spatial variation of taxa occurred at much finer spatial scales than could be resolved in the map products, although larger scale patterns were clearly identified based on acoustic patches and regions within the study area (i.e., communities at sample site scale, Section 5.3.3.3).

5.6.4 Management Considerations and Implications

The habitat and ecological characterization of the Phase II study area can inform managers, stakeholders, and policymakers about several important issues related to assessing risk and benefits of human activities in this region. These include:

1. Our results indicate complexity in the distribution of taxa at multiple spatial scales. That is, distributions of specific taxa varied within acoustic patches, between acoustic patches and between regions with multiple acoustic patch types. This infers complexity across the landscape of the ecological drivers that mediate recruitment and survival of multiple taxa. Such drivers can have direct (e.g., depth, grain size, bottom stress) and indirect roles (e.g., predation, competition) in mediating distribution. Put simply, and despite similarity in grain size distribution (sands-gravels) across the study region, all areas are not ecologically equal and assessing risks and benefits of particular projects that result in disturbance should address impacts at multiple scales.
2. The maps and data products represent a snapshot in time. Results for both infauna and epifauna have identified particular differences in composition and functional roles of taxa, and based on the two sampling periods, some temporal changes were found. However, while the general spatial differences in ecological characteristics determined in this study may be relatively consistent over time, they do not incorporate the full extent of the temporal changes that occur within the study area. The benthic fauna in Long Island Sound can exhibit significant seasonal fluctuation (e.g., Zajac, 1998), and such potential fluctuations should be considered within the scope of management activities.
3. In addition to the seasonal differences in benthic communities observed over the duration of Phase II, comparing results to past studies and sampling efforts reveal longer-term changes in seafloor ecology. Previously documented benthic communities and dominant taxa were found to have changed on the scale of decades, likely responding to larger regional disturbances such as changing seafloor conditions and the influence of non-native species. While the differences in community structure found across the study area can be used to gauge their relative susceptibility and resilience to disturbances and their abilities to recover to a previous state, these community characteristics remain uncertain. Due to the nature of the habitats and communities in this portion of LIS, models of benthic response to and patterns of recovery after disturbances developed in other portions of the Sound (e.g., Rhoads et al., 1978) where there are different sedimentary environments and benthic communities, may not be applicable, and alternative recovery pathways and scenarios may occur (Zajac, 2001). Additionally, community responses within eastern LIS will likely

change over time, as longer term shifts in community composition continue, necessitating periodic sampling in order to characterize recovery.

4. The integrated habitat map, diversity, community, and taxon-specific maps, and the aggregate of supporting analyses, can inform decisions related to the spatial and temporal extent of potential impacts from human activities. The spatial extent of habitats, associated communities, and particular taxa can be used to assess the localized uniqueness of the natural resources and, along with the life histories of the taxa, can be used to estimate potential for recovery and resilience from disturbances.

5.6.5 References - Overall Discussion and Conclusions

Diesing, M., Mitchell, P.J., O'Keeffe, E., Gavazzi, G.O. and Bas, T.L., (2020). Limitations of predicting substrate classes on a sedimentary complex but morphologically simple seabed. Remote Sensing, 12(20), 3398.

Montereale-Gavazzi, G., Roche, M., Degrendele, K., Lurton, X., Terseleer, N., Baeye, M., Francken, F. and Van Lancker, V., (2019). Insights into the short-term tidal variability of multibeam backscatter from field experiments on different seafloor types. *Geosciences*, 9(1), p.34.

Rhoads, D.C., McCall, P.L. and Yingst, J.Y., 1978. Disturbance and Production on the Estuarine Seafloor: Dredge-spoil disposal in estuaries such as Long Island Sound can be managed in ways that enhance productivity rather than diminish it. American Scientist, 66(5), 577-586.

Zajac, R., (1998). *Spatial and temporal characteristics of selected benthic communities in Long Island Sound and management implications,* Final Report, Long Island Sound Research Fund Grant CWF-317-R,. Hartford, CT: Connecticut Department of Environmental Protection, Office of Long Island Sound Programs.

Zajac RN (2001). Organism–sediment relations at multiple spatial scales: implications for community structure and successional dynamics. In, Aller J., Aller R. and Wooden S.A., Eds. *Organism-Sediment Interactions*. (Belle W. Baruch Library in Marine Science Series No. 21., pp. 119-140). University of South Carolina Press.

6.0 PHYSICAL OCEANOGRAPHIC CHARACTERIZATION

Recommended Citation:

O'Donnell, J., McCardell, G., Howard-Strobel, M.M. (2021). "Physical Oceanographic Characterization" p. 239-261 in "The Long Island Sound Habitat Mapping Initiative Phase II – Eastern Long Island Sound – Final Report" (Unpublished project report).

6.1 New Data Acquisition

We executed springtime and wintertime deployments of bottom tripods with an array of instruments measuring temperature, salinity, currents, and stresses and executed two ship surveys in which we measured salinity, temperature, density structure and current patterns.

Tripod-style bottom-frames were deployed in and near Fishers Island Sound to collect measurements for determining bottom stresses, current structure, wave characteristics, salinity, and temperature. Three frames were deployed in spring 2017 and five during winter 2018. Tables 6.1-1 and 6.1-2 summarize the frame deployments for fall 2017 and winter 2018, respectively; Figs. 6.1-1 and 6.1-2 show the frame deployment locations for fall 2017 and winter 2018, respectively. These observations supplement previous data from eastern Long Island Sound.

The moored instrument array configuration for the frames is shown in Figure 6.1-3. Each frame was equipped with an RDI acoustic Doppler current profiler (ADCP) with wave sampling enabled located 1.5 meters above bottom, a Nortek Aquadopp 2 kHz High-Resolution phase coherent profiler looking downward at 0.75 meters above the bottom, and a Sea-Bird Model 37 SMP measuring salinity, temperature and pressure also at 0.75 meters above bottom. The RDI ADCP sampled currents every 15 minutes and waves once per hour. The Nortek Aquadopp sampled every hour, and the Sea-Bird CT/P sensor sampled every 15 minutes.

Transect and station data were collected during fall 2017 and spring 2018 cruises. During both cruises, a single transect was continually and repeatedly sampled during a 12-hour period with a ship-mounted acoustic Doppler current profiler (ADCP). Stations along the transect were also repeatedly sampled with a Sea-Bird Model 19+ CTD (conductivity, temperature, depth). During the fall 2017 cruise, four stations were sampled. During the spring 2018 cruise, additional stations were added to look at cross-bathymetric contours in the eastern half and the eastern entrance to Fishers Island Sound, and near the western limit of the study area south of Clinton Harbor. Cruise data collection summaries are presented in Tables 6.1-3 and 6.1-4. Location details of the cruise sampling stations are shown in the appendix. Table 6.1-5 shows the timeline of the data collection effort.

Table 6.1- 1. Spring 2017 Moored Frames - Station Location and Deployment Summary.

Station ID	Latitude	Longitude	Sensors	Deploy Date (2017)	Recovery Date (2017)	Water Depth (m)	Deployment Length (days)
SOW1	41.303300°	-71.903817°	-AQD 2 kHz HR -SBE37 CT/P -ADCP 600 kHZ	30 MAR	7 JUN	22.6	70
EID2	41.325933°	-71.927667°	-AQD 2 kHz HR -SBE37 CT/P -ADCP 1200 kHz	28 MAR	7 JUN	4.6	72
WID3	41.310900°	-71.968917°	-AQD 2 kHz HR -SBE37 CT/P -ADCP 1200 kHz	28 MAR	8 JUN	5.5	73

Table 6.1- 2. Winter 2017-2018 Moored Frames - Station Location and Deployment Summary.

Station ID	Latitude	Longitude	Station Depth (meters)	RDI ADCP SN/Freq	SBE 37 SN	AQD SN
SOW1	41 18.1977	-71 54.2284	21.5	1094/600	9695	8445
EID2	41 19.5557	-71 55.6593	3.9	10463/1200	9673	8455
WID3	41 18.6537	-71 58.1355	4.8	10462/1200	9696	8432
WFW4	41 17.4727	-72 02.2383	10.3	6615/600	9694	8438
SFW5	41 16.2218	-71 58.3172	6.3	11708/1200	9674	8554

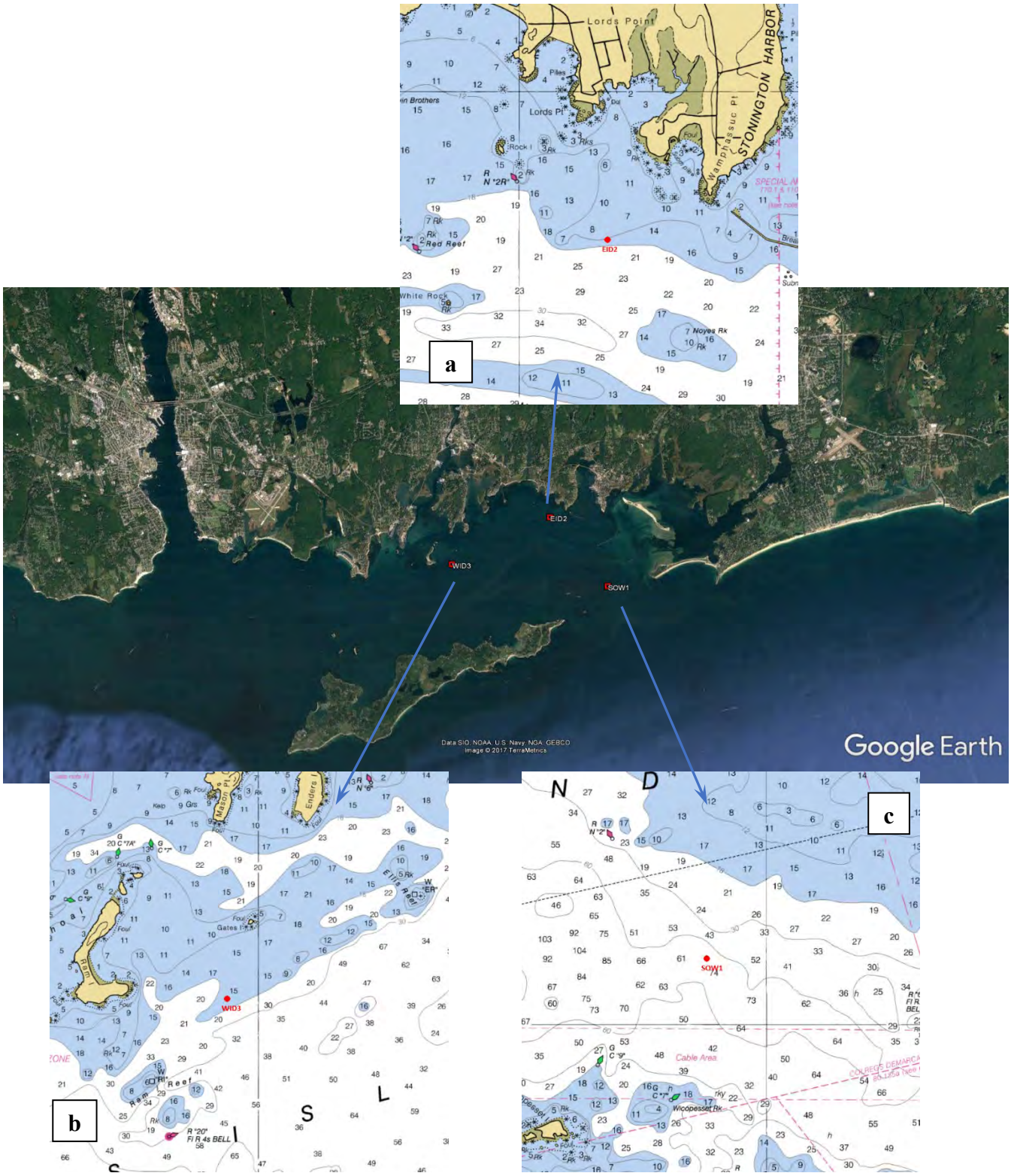

Figure 6.1- 1 Location of the three frames deployed in Fishers Island Sound during Spring of 2017, a) detail of bathymetry (in feet) near EID2 - the Eastern Inside Dissipative station, b) bathymetry (in feet) at WID3 - Western Inside Dissipative station, c) bathymetry (in feet) at SOW1 - Southern Outside Wave station.

Figure 6.1- 2. Location of the five bottom moored frames in Fishers Island Sound for the Winter 2017-2018 data collection campaign. Yellow stations were occupied during the Spring 2017 campaign, the two red stations are new locations.

Figure 6.1- 3 Frame deployed at SOW1 – all frames were equipped similarly, with a) Nortek High Resolution downward looking Aquadopp profiler, b) Sea-Bird Instruments Model 37 SMP Conductivity/Temperature/Pressure sensor, and c) RD Instruments acoustic Doppler current profiler with wave array firmware.

Table 6.1- 3. CTD 12 Hour Survey – Winter 2017 - Station Locations.

Station ID	Latitude	Longitude	Station Depth (meters)	N Casts
N1-1	41 17.9177	72 05.0212	6.1	5
N1-2	41 17.1696	72 05.4720	10.9	10
N1-3	41 16.4313	72 05.9873	20.1	10
N1-4	41 15.5349	72 06.5856	33.5	6
N2-1	41 18.1732	72 10.7515	9.8	6
N2-2	41 17.3729	72 10.7154	14.0	12
N2-3	41 16.5301	72 10.6272	17.7	12
N2-4	41 15.5604	72 10.5426	32.6	7
N3-1	41 17.1089	72 14.6969	16.5	6
N3-2	14 16.1559	72 14.6969	17.4	11
N3-3	41 15.2662	72 14.6969	28.0	11
N3-4	41 14.3049	72 14.6969	33.8	6
N4-1	41 15.5647	72 20.4353	5.8	6
N4-2	41 15.0995	72 19.6817	8.5	11
N4-3	41 14.5568	72 18.7853	32.3	11
N4-4	41 13.9125	72 17.7541	36.6	6
N5-1	41 17.7994	72 02.5349	9.1	8
N5-2	41 16.8567	72 02.5349	12.5	8
N5-3	41 17.3042	72 00.0604	14.0	8
N5-4	41 18.1633	72 00.0604	9.8	9

Table 6.1- 4. CTD 12 Hour Survey - Spring 2018 - Station Locations.

Station ID	Latitude	Longitude	Station Depth (meters)	N Casts
N0-1	41 17.6108	71 51.4745	21.1	7
N0-2	41 17.0093	71 53.4086	22.0	7
N0-3	41 16.3598	71 53.0402	42.9	7
N0-4	41 17.0412	71 51.0424	36.7	8
N1-1	41 18.8733	71 55.3366	9.5	8
N1-2	41 18.8733	71 57.3814	16.4	8
N1-3	41 18.0035	71 57.3814	19.4	8
N1-4	41 18.0035	71 55.3366	20.0	8
N21-1	41 17.9177	72 05.0212	6.1	7
N21-2	41 17.1696	72 05.4720	10.9	12
N21-3	41 16.4313	72 05.9873	20.1	13
N21-4	41 15.5349	72 06.5856	33.5	7
N22-1	41 18.1732	72 10.7515	9.8	6
N22-2	41 17.3729	72 10.7154	14.0	11
N22-3	41 16.5301	72 10.6272	17.7	12
N22-4	41 15.5604	72 10.5426	32.6	6
N23-1	41 17.1089	72 14.6969	16.5	6
N23-2	14 16.1559	72 14.6969	17.4	12
N23-3	41 15.2662	72 14.6969	28.0	12
N23-4	41 14.3049	72 14.6969	33.8	7
N24-1	41 15.5647	72 20.4353	5.8	6
N24-2	41 15.0995	72 19.6817	8.5	12
N24-3	41 14.5568	72 18.7853	32.3	12
N24-4	41 13.9125	72 17.7541	36.6	7
N6-1	41 14.7994	72 31.4255	9.8	7
N6-2	41 13.8567	72 31.4255	26.1	13
N6-3	41 13.3042	72 31.4255	32.5	13
N6-4	41 12.1633	72 31.4255	17.2	7

Table 6.1- 5. Data Collection Timeline.

2017	
28 March	Deploy WID3, EID2 in Fishers Island Sound
30 March	Deploy SOW1 east entrance FIS
07 June	Recover SOW1, EID2
08 June	Recover WID3
28 Nov-3 Dec	SeaBoss cruise -> underway ADCP
28-29 Nov	12 hour CTD survey stations N1-1, N1-2, N1-3, N1-4
29-30 Nov	12 hour CTD survey stations N2-1, N2-2, N2-3, N2-4
30 Nov-1 Dec	12 hour CTD survey stations N3-1, N3-2, N3-3, N3-4
01-02 Dec	12 hour CTD survey stations N4-1, N4-2, N4-3, N4-4
02-03 Dec	12 hour CTD survey stations N5-1, N5-2, N5-3, N5-4
21 Dec	Deploy WID3, EID2, SOW1, SFW5, WFW4
2018	
19 March	Recover WID3, EID2, SOW1, SFW5, WFW4
08-15 May	SeaBoss cruise -> underway ADCP and mTSG
08-09 May	12 hour CTD survey stations N1-1, N1-2, N1-3, N1-4
09-10 May	12 hour CTD survey stations N21-1, N21-2, N21-3, N21-4
10-11 May	12 hour CTD survey stations N22-1, N22-2, N22-3, N22-4
11-12 May	12 hour CTD survey stations N23-1, N23-2, N23-3, N23-4
12-13 May	12 hour CTD survey stations N24-1, N24-2, N24-3, N24-4
13-14 May	12 hour CTD survey stations N6-1, N6-2, N6-3, N6-4
14-15 May	12 hour CTD survey stations N0-1, N0-2, N0-3, N0-4

6.2 Model Implementation

The Long Island Sound (LIS) FVCOM model was initially developed with support from the Connecticut Sea Grant College Program and the collaboration of Professor C. Chen of the University of Massachusetts, Dartmouth. The domain of the model and the resolution are shown in Figure 6.2-1. We developed an implementation of FVCOM (Chen et al., 2007) at UCONN and designed it to use the results of the operational northwest Atlantic regional model, operated as the Northeast Coastal Forecast System (NECOFS) to provide ocean boundary conditions. This 'nesting' approach is computationally efficient since it allows the effect of the larger-scale processes to be simulated at coarse resolution through NECOFS and allows UCONN computing resources to focus on the smaller-scale structures in LIS and Block Island Sound (BIS). Our FVCOM implementation uses GOTM (Burchard, et al., 1999) to model vertical turbulent mixing. O'Donnell et al. (2015b) found that a bottom roughness value of z_0=1 cm provided the best representation of bed stresses within LIS in the FVCOM model and this value was used throughout the domain.

LIS-FVCOM was initialized using a temperature and salinity climatology data set derived via objective interpolation of CTDEEP station data as described by O'Donnell et al. (2015b), and the data in the NOAA archive described by Codiga and Ullman (2011). In order to be input

into the FVCOM model, these OI fields were linearly interpolated to a set of standard depths. The 2018 model runs were initialized using end-of-year conditions from 2017.

LIS-FVCOM is forced at the seaward boundaries by sea level variations and salinity and temperature. The sea level is initially prescribed using tidal constituents derived from the global tidal model (Egbert et al., 1994). The amplitudes and phases of the major constituents were then iteratively adjusted to achieve an optimal representation of the amplitude and phase at each tidal frequency using NOAA tidal height observations at Montauk (NY), New London (CT), New Haven (CT), Bridgeport (CT), and King's Point (NY). Subtidal fluctuations at the open boundary are incorporated from the NECOFS system by de-tiding and low-pass filtering the NECOFS solution at the open boundary locations using t-tide (Pawlowicz et al., 2002) and a 25-hour raised cosine low-pass filter. The model's subtidal performance was further optimized by removing the low-passed error in the NECOFS subtidal forcing as determined by comparing the NECOFS solution with NOAA sea-surface height (SSH) gauges at Newport, RI and Atlantic City, NJ. These stations are near the open boundary of the LIS model. The de-tided and adjusted NECOFS subtidal solution was then combined with the time series of tidal heights generated using the optimized tidal constituents as described above.

Freshwater enters the LIS FVCOM domain through seven model cells corresponding to the locations of the Thames, Connecticut, Niantic, Quinnipiac, Housatonic, and Hudson rivers and New York City wastewater treatment plants (WWTP). These fluxes are based on gauged flows measured by the USGS at Thompsonville, CT, and lagged by one day to account for the distance between the head of the Connecticut River in our model and Thompsonville. Each river, R_i, is adjusted using the USGS Thompsonville data as $R_i = 1.20 \frac{R_{CT}}{\overline{R_{CT}}} \overline{R_i}$ where R_{CT} is the day-specific Connecticut River flow, $\overline{R_{CT}}$ is the mean Connecticut River flow, and $\overline{R_i}$ is the mean flow for river *i*. The factor of 1.20 follows from the salt budget of Gay et al. (2004) and accounts for the portion of the watersheds of the rivers below the USGS gauges. A fixed input of 40 m^3s^{-1} was added to the East River to represent the freshwater discharged from the New York WWTPs.

Domain-variable winds derived from the Weather Research and Forecasting model (WRF) run as hindcasts at UMass, Dartmouth are used for the LIS-FVCOM surface wind forcing. The LIS-FVCOM model originally used heat fluxes also obtained from the UMass WRF model. However, the UMass WRF heat fluxes substantially underestimate the wintertime cooling at LIS locations. To correct this issue, we assimilated sea surface temperatures (SSTs) into the model using NASA MODIS Aqua 8-day composited and de-clouded (level 3) satellite data. Because the NASA SST product has poor coverage in cells that are close to the coast, we pre-screened the entire dataset to keep only data from cells that had at least 86.7% coverage for the entire year (i.e. we removed all data from those cells with 7 or more missing 8-day SSTs out of the total of 45 8-day products for the 2017 year). The remaining SST data was then linearly interpolated in time to fill any temporal gaps and then spatially interpolated to 100% coverage using the nearest spatial neighbor with good coverage. The net effect of this pre-screening and interpolation methodology is that values in cells at the coast where coverage is poor are replaced with the values from the nearest offshore cell.

Figure 6.2-1 shows time-series of the model to data temperature comparisons both with and without SST temperature assimilation. Note that the improvement in the bottom temperatures (panels a, b) is similar to the improvement in the surface temperatures (panel

c,d), indicating that the model is capturing the downward heat fluxes within the water column adequately.

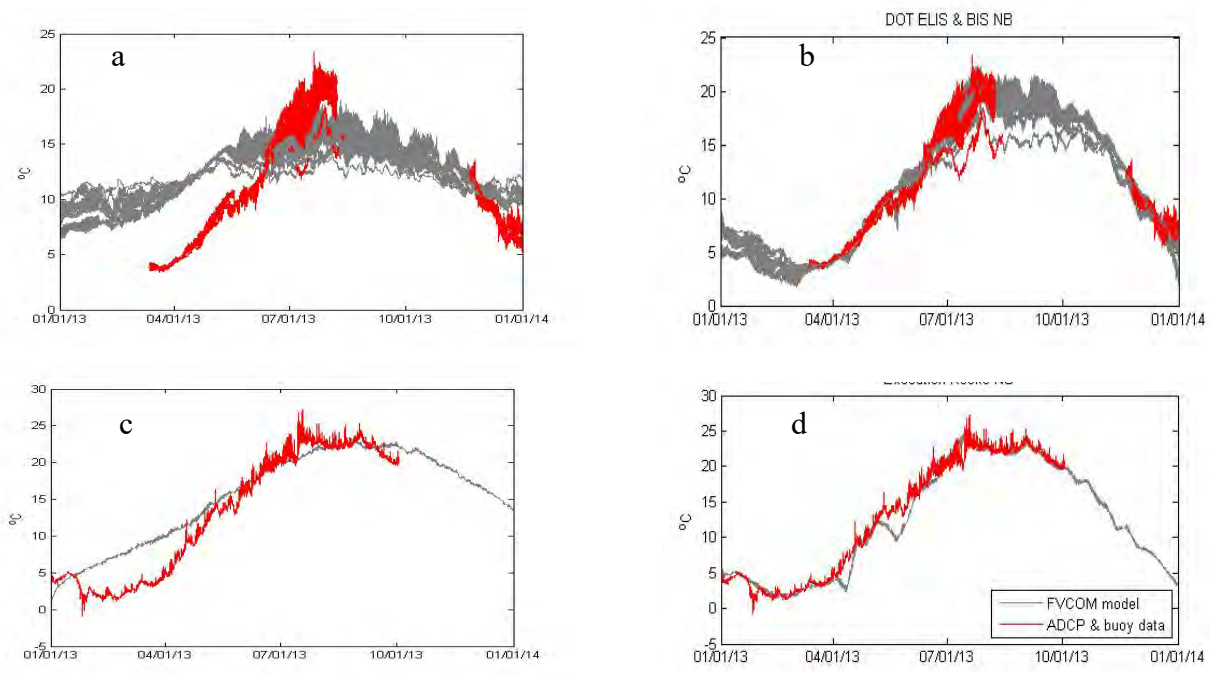

Figure 6.2- 1 Comparison of model temperature predictions (gray) with observations (red) in LIS during 2013 with and without SST data assimilation. (a,c) show comparisons when the model is forced using only WRF heat fluxes; (b,d) show the comparisons when MODIS-a SST is also assimilated into the model. (a,b) show comparisons of near-bottom temperatures at seven locations in the ELIS and BIS during 2013 (See O'Donnell et al., 2015a); (c,d) show comparisons of near-surface temperatures at the LISICOS Execution Rocks buoy.

6.3 Model Skill Assessment

To evaluate the model performance we use the 'skill', s, statistic defined as:

$$s = 1 - \frac{\left\langle \left(f_m - f_d \right)^2 \right\rangle}{\left\langle \left(f_d - \left\langle f_d \right\rangle \right)^2 \right\rangle} \qquad (1)$$

where f_m and f_d represent the model and data values (e.g. f represents sea level (η) or temperature (T), etc.) and the $\langle\ \rangle$ notation represents the mean of the argument over the simulation interval (i.e. $\langle f_d \rangle$ is the mean of the data) (von Storch and Zwiers, 1999).
The Long Island Sound model skill assessment using this metric is described in O'Donnell et al (2015). Since the time of that report, the model has been improved by Dr. McCardell. Most notably, the model now assimilates sea surface temperatures (SST) from the NASA MODIS Aqua satellite.

6.3.1 Sea Surface Height Skills

Table 6.3-1 shows the model sea-surface-height (SSH) skill (Equation 1) from the 2017 simulation compared to hourly measurements at the four NOAA tidal gauges in LIS: New London, New Haven, Bridgeport, and King's Point. The first row shows the skills when simulated sea surface heights (relative to MSL) are compared to the raw observations. The second and third rows shows the skills when the model and data series are divided into tidal and weather components using harmonic analysis (Pakolwicz et al, 2002). The errors in the simulation of tides are small - the skills all exceed 93%. The errors in the simulation of the total water level (SSH) mainly arise from the errors in the simulation of the meteorologically driven motions and are to some extent due to inadequacies in the atmospheric model used to prescribe winds.

Table 6.3- 1 Table 6.3.1: Model skills (Eq. 1) when model elevations are compared to NOAA gage data at New London, New Haven, Bridgeport, and Kings Point. The first row (Total SSH skill), shows the skills when sea-surface heights (relative to MSL) are compared, the the second row shows the skills at tidal frequencies, the third row shows the skills for the subtidal residuals.

	New London	New Haven	Bridgeport	King's Point
Total SSH skill	91%	92%	93%	93%
Tidal skill	94%	93%	94%	94%
Subtidal skill	77%	75%	77%	54%

Figure 6.3-1 shows a comparison of the spectral power density obtained from the NOAA record at the four LIS gauges with that from the LIS-FVCOM model at these locations. Note that although the model does a good job at capturing the M2 amplitudes and M4 harmonics, it significantly underestimates the M6 harmonics.

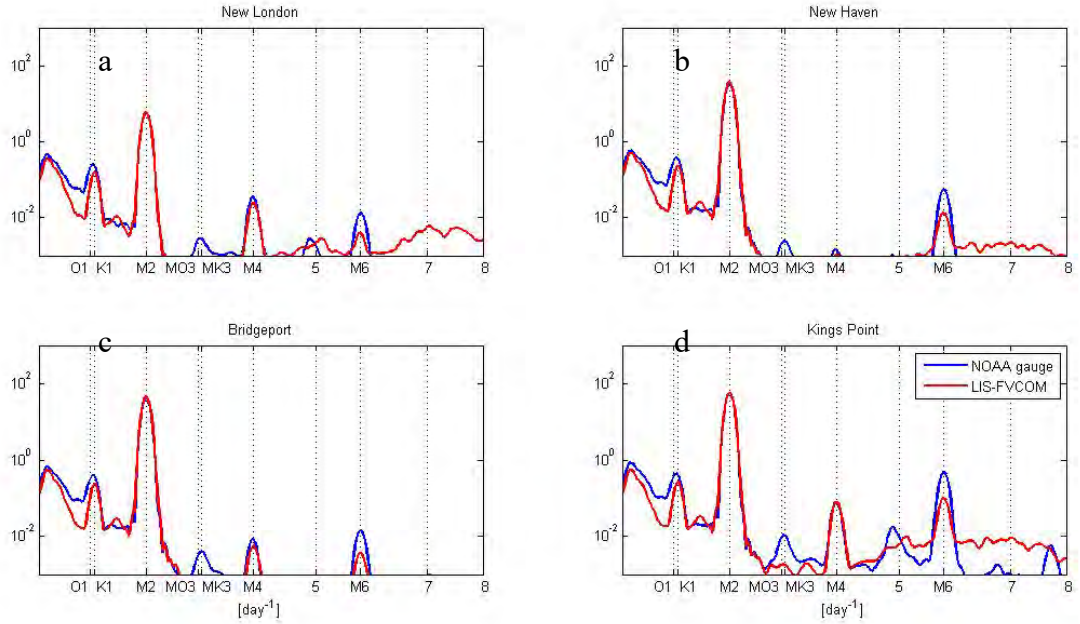

Figure 6.3- 1 Comparison of the power spectral density (PSD) of the SSH records from the NOAA gauges (blue) at New London (a), New Haven (b), Bridgeport (c), and Kings Point (d) with those from the FVCOM-LIS model (red) estimated using the Welch method with non-overlapping 10-day windows.

6.3.2 Temperature and Salinity Skills

Figure 6.3-2 shows a comparison of surface and bottom model temperatures with monthly climatologies derived from 1993-2015 CTDEEP surveys and the 2017 CTDEEP surveys. These data are described by Kaputa and Olson (2000) and O'Donnell et al. (2014). The skills listed in the panels were calculated by combining the individual station scores using the mean square methodology described in Ganju et al. (2016).

For comparison, the surface and bottom traditional skills from runs that only used the WRF heat flux forcing (did not use the SST assimilation) were in the 0.70-0.90 range. Note that the CTDEEP dataset used to evaluate the temperature skills shown in Figure 6.3.2 was not what was assimilated into the model. The high skill scores are thus indicative of both the success of the data assimilation itself and of excellent agreement between the screened remote sensing temperature data and the in situ temperature measurements made by the CTDEEP.

As shown in Figure 6.3-3, the near-surface and near-bottom traditional salinity skills are 0.15, and 0.19, respectively. Figure 6.3-3 indicates that much of the salinity error is due to a bias error. This was removed prior to creating the interpolated map products.

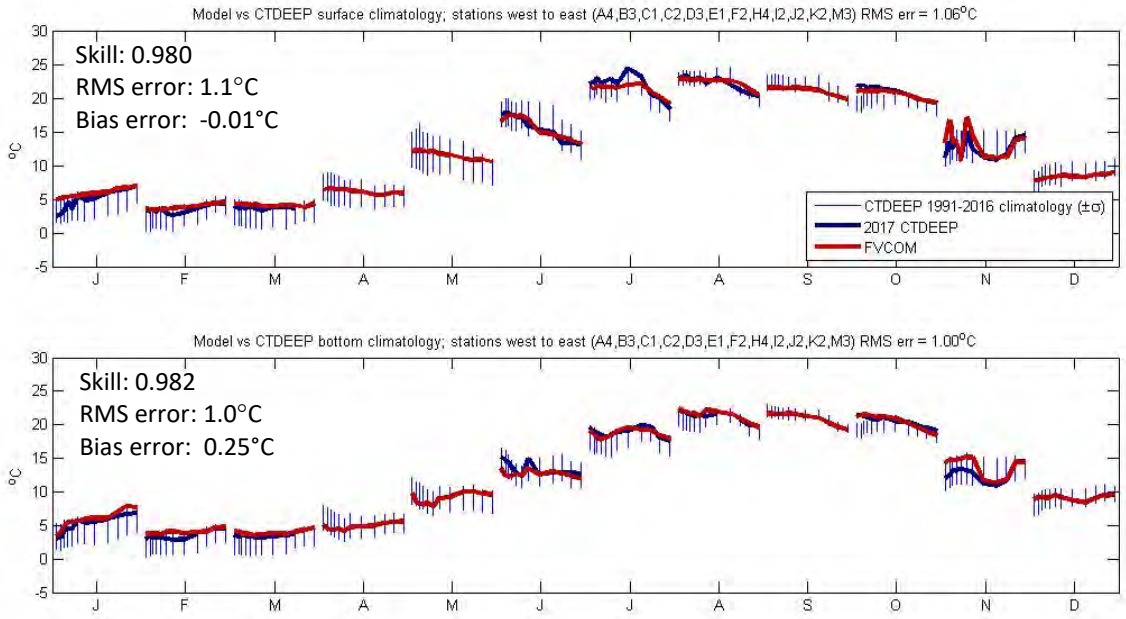

Figure 6.3- 2. Plots by month showing surface (top panel) and bottom (bottom panel) temperature comparisons between model predictions (red lines) and monthly climatologies from 1993-2016 CTDEEP survey data (thin vertical blue bars, ±σ) and the 2017 CTDEEP surveys (thick blue lines). Within each month, the CTDEEP stations are plotted by longitude from west to east.

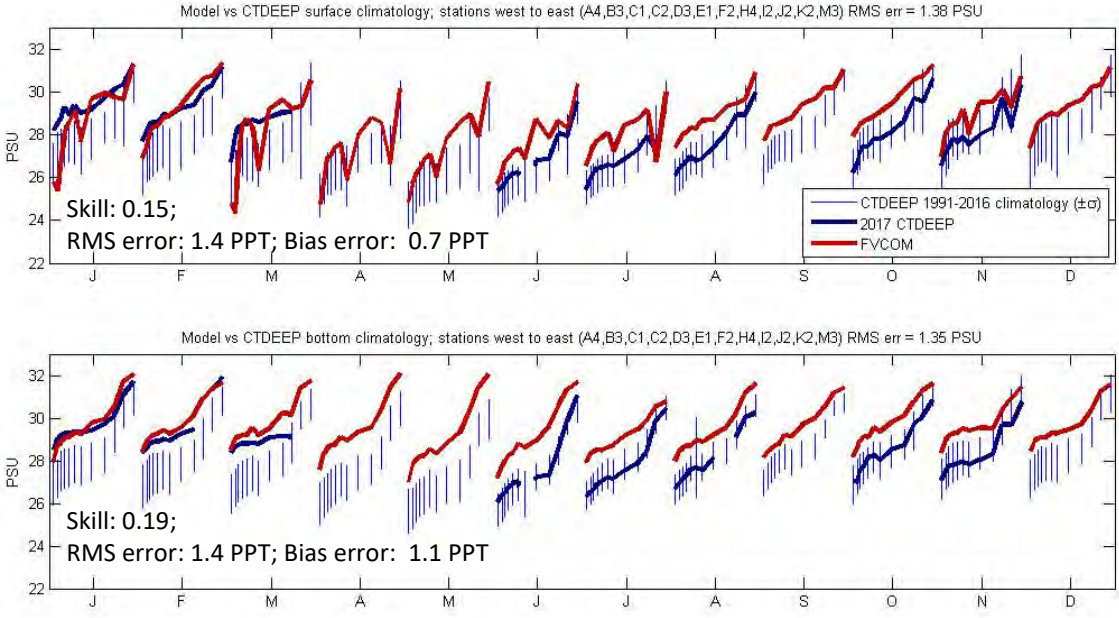

Figure 6.3- 3 Figure 6.3-3. Plots by month showing surface (top panel) and bottom (bottom panel) salinity comparisons between model predictions (red lines) and monthly climatologies from 1993-2016 CTDEEP survey data (thin vertical blue bars, ±σ) and the 2017 CTDEEP surveys (thick blue lines). Within each month, the CTDEEP stations are plotted by longitude from west to east.

6.4 Fisher's Island Sound (FIS) comparisons

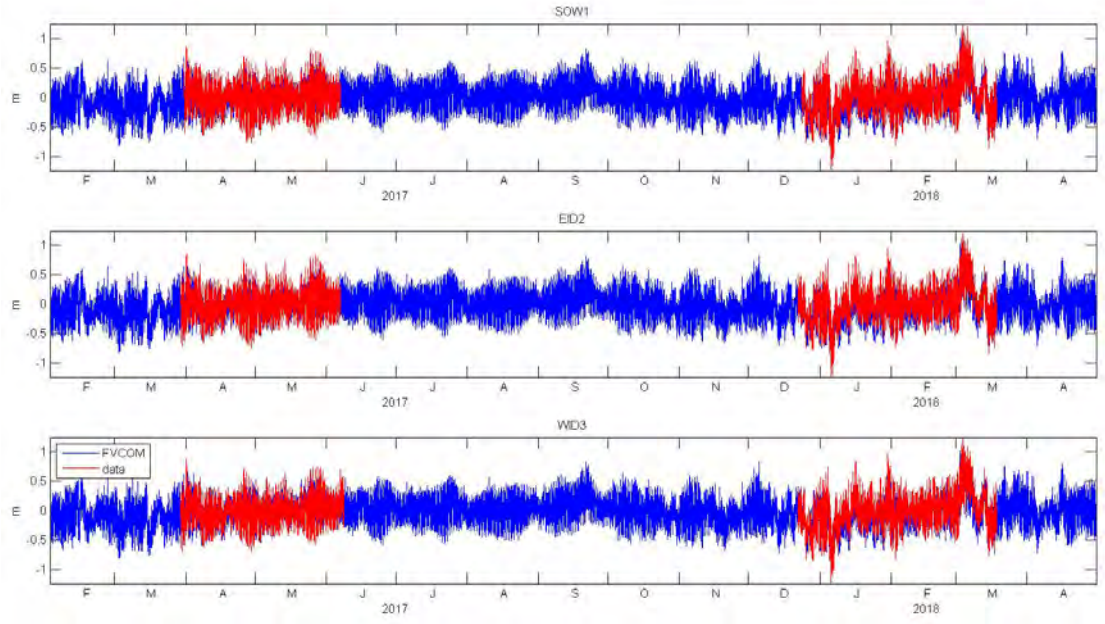

Figure 6.4- 1. Time-series plots of SSH at the three FIS bottom-mooring deployment locations comparing the FVCOM predictions (blue) with measurements from the moored instruments (red).

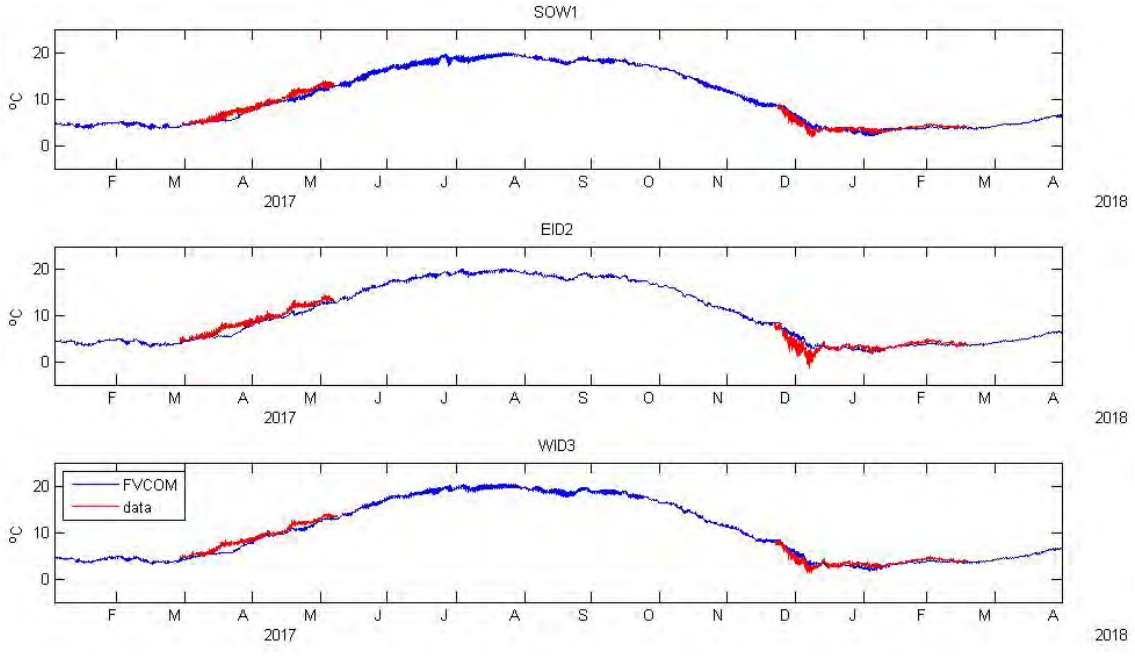

Figure 6.4- 2. Time-series plots of near-bottom temperatures at the three FIS bottom mooring deployment locations comparing the FVCOM predictions (blue) with measurements from the moored instruments.

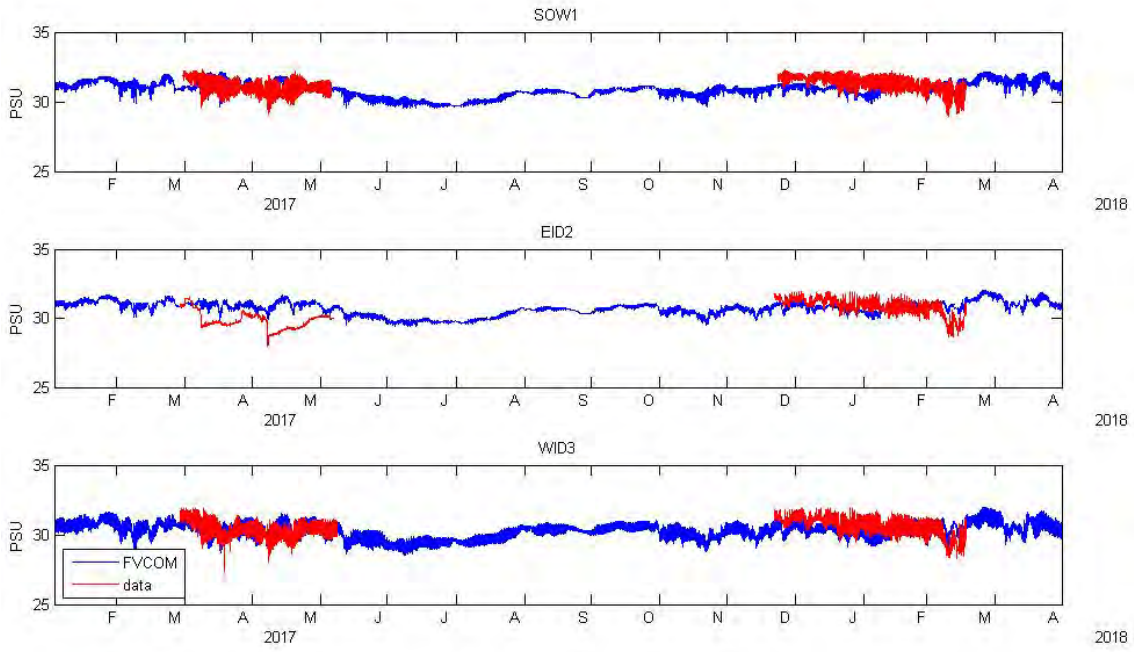

Figure 6.4- 3. Plots of near-bottom salinities at the three FIS bottom mooring deployment locations comparing the FVCOM predictions (blue) with measurements from the moored instruments.

6.5 Acoustic surveys along-track MSL reference heights

The model was used to produce estimates of along-track MSL and water heights to support the acoustic surveys conducted by Roger Flood, Stony Brook University as well as provide further validation of the model results. These surveys took place in Dec 2017, January 2018, and March 2018. Soundings were made at approximately 60k locations and times. Figure 6.5-1 shows the location of these surveys. Figures 6.5-2 and 6.5-3 show the times of the surveys in dark grey at the bottom of the top panel.

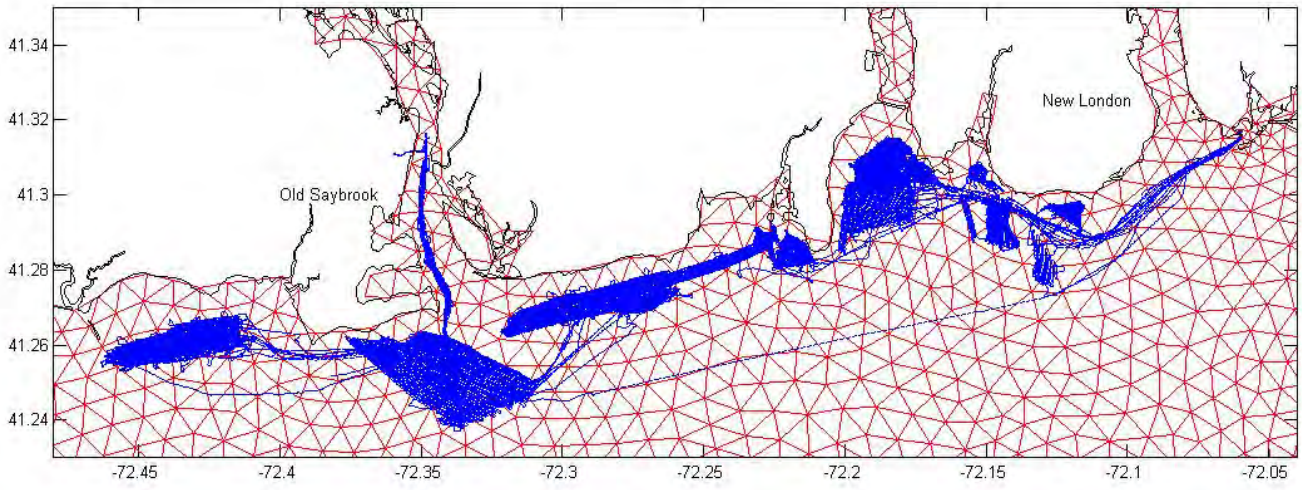

Figure 6.5- 1 Figure 6.5-1. Acoustic survey tracks (blue) for Dec 2017 through Mar 208 surveys, the FVCOM LIS model grid (red), and the CT coastline (black).

In order to remove known errors from the model predictions, the hourly FVCOM LIS SSH solution was compared to the NOAA hourly observations at New London and New Haven and the USGS observations at Old Saybrook. Prior to these comparisons, both the model results and the observations were detided using t_tide (R. Pawlowicz, et al, 2002). The

subtidal and tidal model results were then corrected using the 3-station mean model-observational discrepancy as shown in Eq.2.

$$\eta_{corrected}{}_i^j = \eta_{pred}{}_i^j + \frac{1}{3} \sum_{i=[\,i_{NLN}, i_{HVN}, i_{OS}]} \left(\eta_{obs}{}_i^j - \eta_{pred}{}_i^j \right) \quad (2)$$

where $\eta_{pred}{}_i^j$ are the model SSH predictions at locations $i = [1, \ldots, N]$ and hourly times $j = [1, \ldots, M]$ and $\eta_{obs}{}_i^j$ are the SSH observations at the three gauge locations $i = [i_{NLN}, i_{HVN}, i_{OS}]$ and hourly times $j = [1, \ldots, M]$.

The corrected hourly model results were then temporally interpolated to the 60k unique acoustic survey times using t_tide for the tidal portion and a linear interpolation for the subtidal portion. These time-interpolated results (at the acoustic survey times) were then spatially interpolated from the 200-500 m FVCOM grid to the 60k unique acoustic survey locations. The observations at the three tidal gauges significantly corrects the subtidal model error (which is highly spatially correlated) and, to a lesser extent, the tidal model error, while preserving the spatial gradients in the model. Table 6.5-1 shows the tidal and subtidal skills and RMS errors for both uncorrected and corrected model results.

Also included in table are the skills and errors for a corrected null model. A null model that is corrected by the mean error at the three stations is the mean SSH of the three stations. Because of the high correlation in subtidal SSH in the local region of the three gauges, the corrected null model performs well for subtidal SSHs, particularly at Old Saybrook which is located midway between New London and New Haven. The corrected null model does a poor job with the tides, however.

The results were referenced to NAVD88 by looking at the long-term bias differences between the subtidal model results and the subtidal observations at New London and Old Saybrook, both of which were referenced to NAVD88. Because the model is expected to be able to capture the long-term mean SSH gradients, this also provides a means of comparing the NAVD88 reference for the New London NOAA record with the NAVD88 reference for the USGS Old Saybrook record. There appears to be about a 5 cm difference between these two references. Because the model predicts only a 2 mm difference in the long-term wintertime mean between Old Saybrook and New London, we chose the mean of the NAVS references at these two locations as the “zero” reference and adjusted the model results by a fixed offset accordingly.

Table 6.5- 1. Skills (1-[model-obs]^2⁄var[obs]) and RMS errors (cm) at the three tidal stations for uncorrected model, corrected model, and corrected null model for the period from 1 Dec 2017 through 31 Mar 2018.

			New London	New Haven	Old Saybrook
Tidal	Skill	uncorrected	94.7%	95.2%	90.6%
		corrected	93.6%	99.2%	99.7%
		corrected null	33.0%	81.4%	97.4%
	RMS error (cm)	uncorrected	6.5	14.6	11.0
		corrected	7.2	5.9	2.1
		corrected null	23.3	28.5	5.8
Subtidal	Skill	uncorrected	59.2%	48.0%	57.2%
		corrected	94.0%	93.6%	97.7%
		corrected null	93.9%	95.0%	99.0%
	RMS error (cm)	uncorrected	14.9	18.4	15.5
		corrected	5.7	6.5	3.6
		corrected null	6.1	5.7	2.4
Overall	Skill	uncorrected	80.6%	89.1%	80.5%
		corrected	93.7%	98.5%	99.1%
		corrected null	57.5%	83.0%	98.1%
	RMS error (cm)	uncorrected	16.2	23.4	19.0
		corrected	9.2	8.8	4.0
		corrected null	24.0	29.3	5.9

Figure 6.5-2 shows a comparison of the uncorrected model results with the observations for the period of the March acoustic surveys, while Figure 6.5-3 shows the comparison with the corrected model results. Also shown in the bottom panels of Figs 6.5-2 and 6.5-3 are the model-observation residuals, i.e. the model error. Figure 6.5-2 indicates that this error is highly correlated between the three stations. Since the model is corrected by removing the mean of this error, the remaining error in the corrected model (Fig. 6.5-3) is no longer positively correlated.

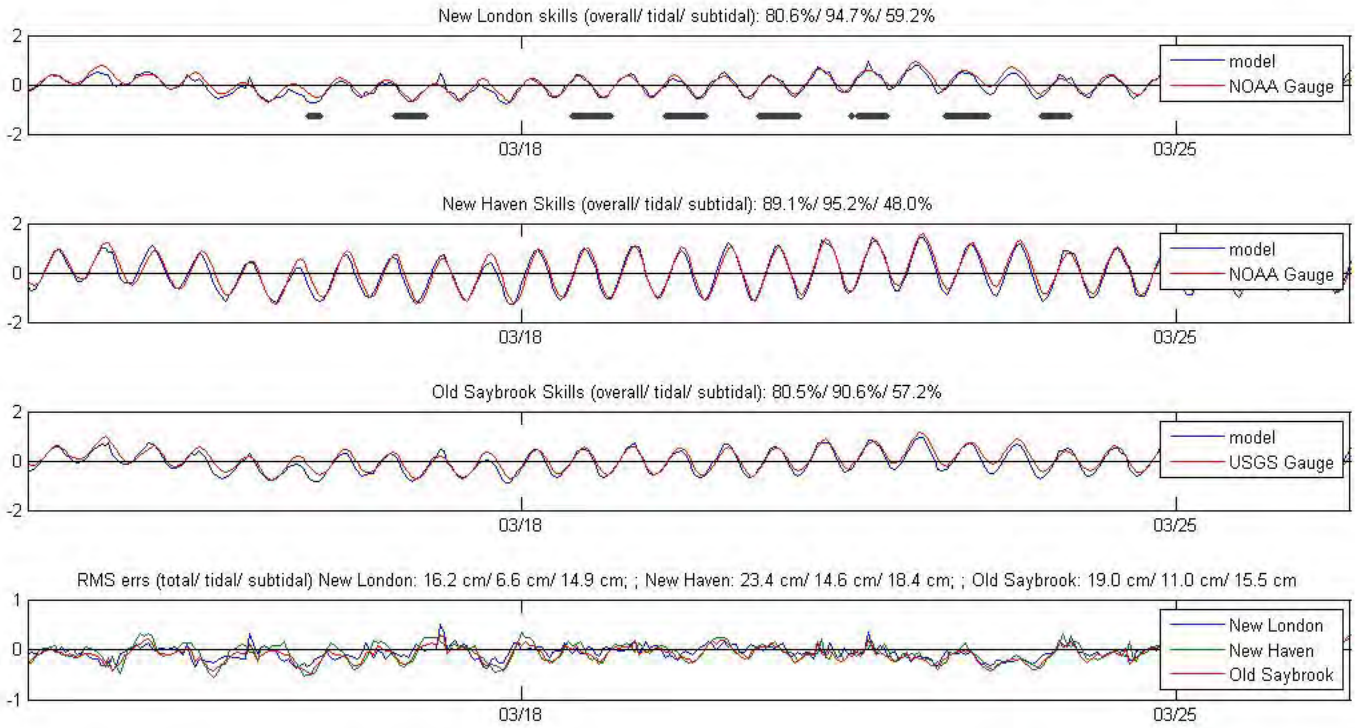

Figure 6.5- 2. Comparison of uncorrected model results (blue) with NOAA gauged observations at New London (top panel) and New Haven (second panel) and with USGS gauged observations at Old Saybrook (3rd panel). The grey dots/ bars in the top panel show the acoustic survey times. The bottom panel shows the differences between the model predictions and the observations for all three stations. Note that these errors are highly correlated.

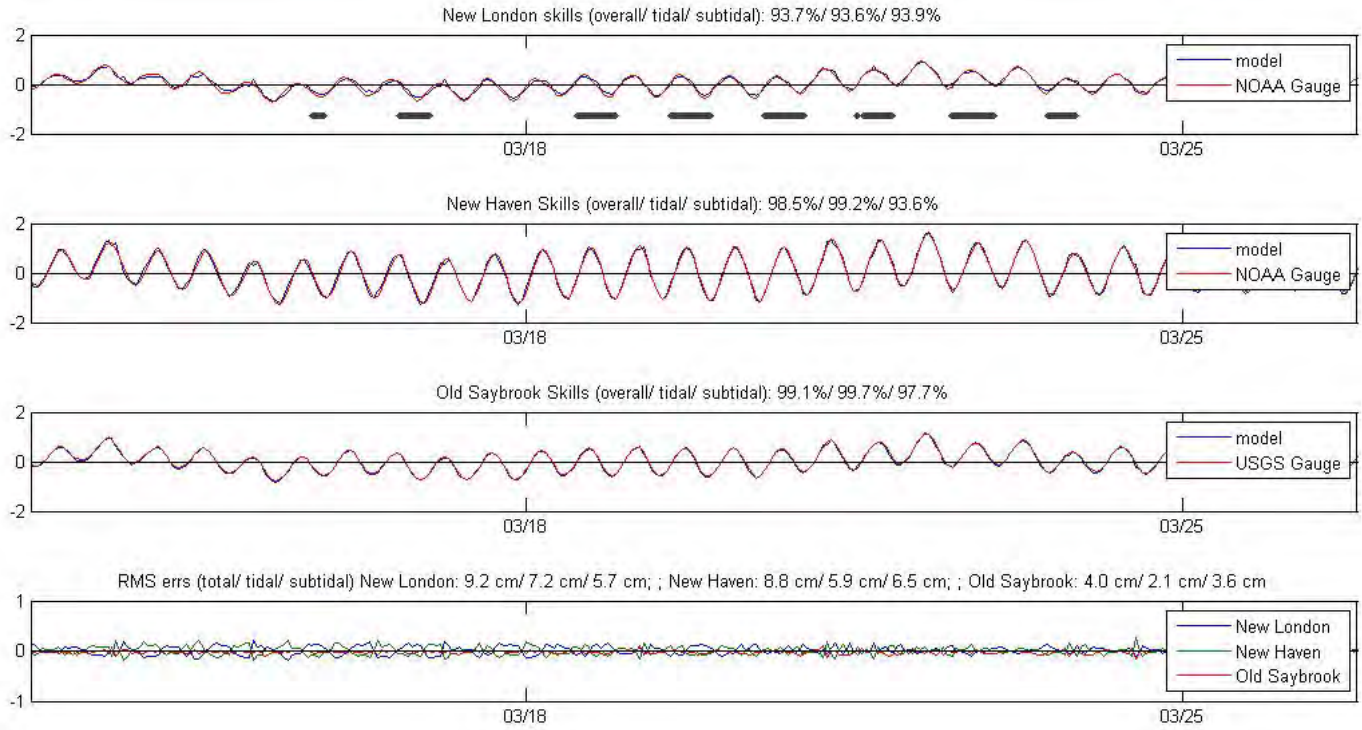

Figure 6.5- 3. Comparison of corrected model results (blue) with NOAA gauged observations at New London (top panel) and New Haven (second panel) and with USGS gauged observations at Old Saybrook (3rd panel). The grey dots/ bars in the top panel show the acoustic survey times. The bottom panel shows the differences between the model predictions and the observations for all three stations. Note that these errors are no longer highly correlated since the correlated error has been removed.

6.6 Physical Oceanographic Products

The model was used to produce maps of:

1. the bottom temperature distributions throughout the study area for each month
2. the bottom salinity distributions throughout the study area for each month
3. the spatial structure of the maximum bottom stress magnitude due to (mainly) tidal currents
4. the spatial structure of the mean bottom stress magnitude due to (mainly) tidal currents
5. tidal and the subtidal currents as (u,v) velocity components where u is the east-west component and v is the north-south component.

These fields were rasterized into GIS format and transferred to the map server to distribute the results. Products are best viewed through that interface. As examples, Figure 6.6-1 shows estimates of mean near-bottom temperatures in the study area during July of 2017, Figure 6.2-2 shows estimates of the maximum bottom stresses due to tidal currents and Figure 6.2-3 depicts the tidal U (east-west) current amplitude. These parameters greatly influence benthic fauna. Note that the magnitude of the spatial gradients predicted by the model far exceeds the estimates of the model error.

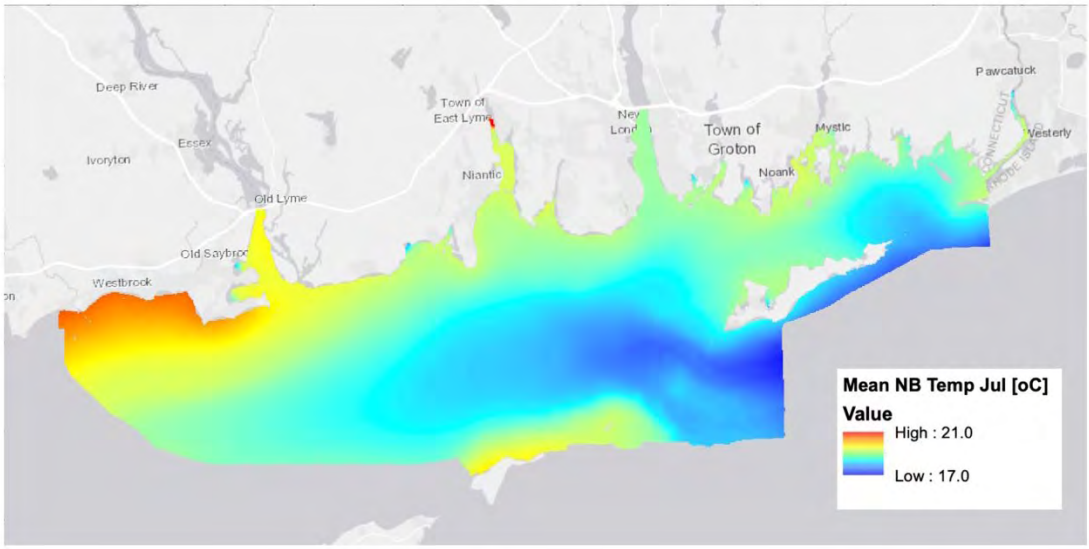

Figure 6.6- 1. Example map product showing mean bottom temperatures during July, 2017.

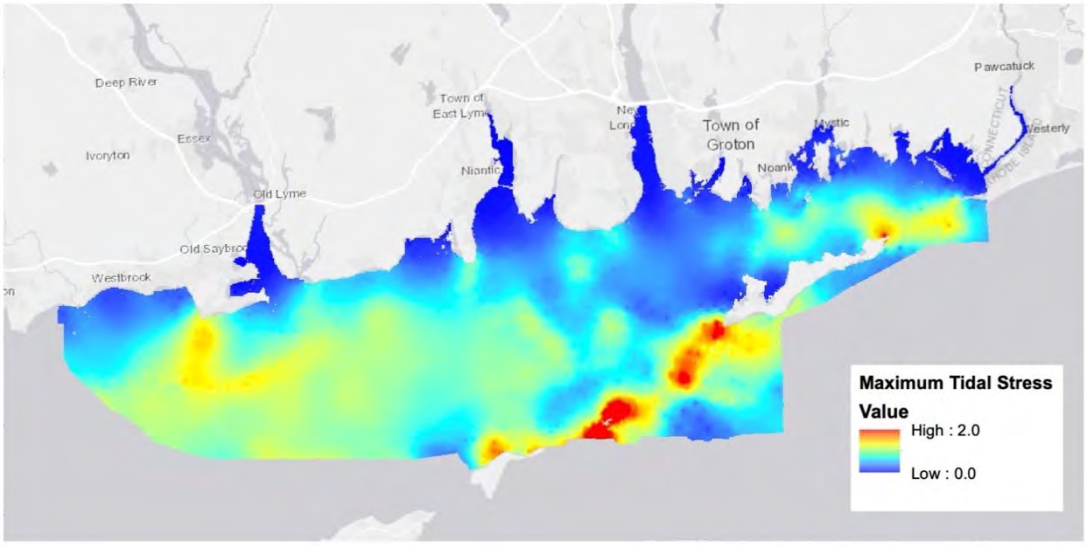

Figure 6.6- 2 Example map product showing maximum bottom stresses due to tides.

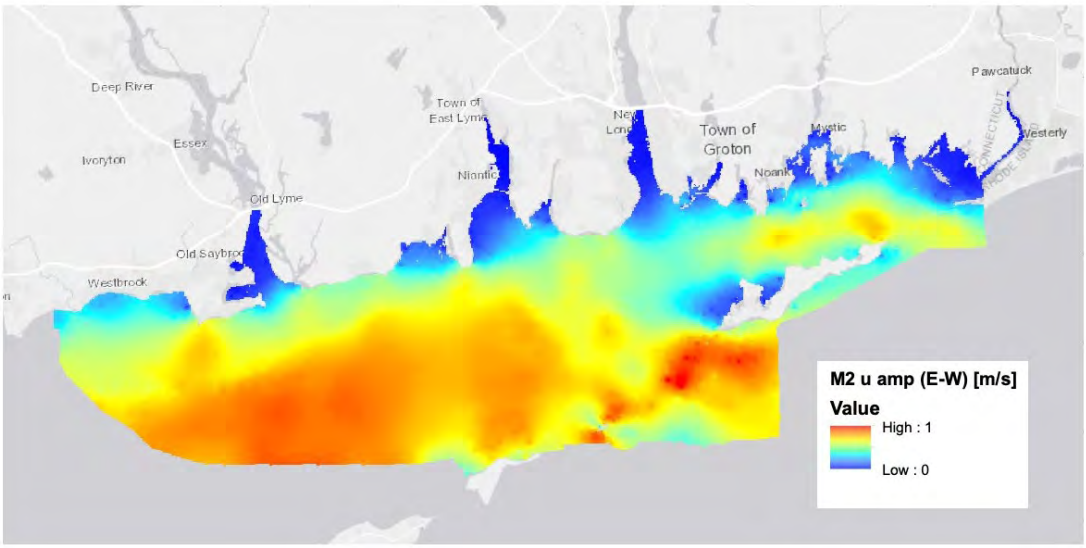

Figure 6.6- 3 Example of map product of mean subtidal currents shown for the u (East-West) component.

6.7 Summary and Conclusions

We report the results of a numerical model to estimate the distributions of ecologically relevant characteristics of the near bottom environment. Using the model, we developed GIS-format map products with information that span the domain. Figure 6.6-1 shows an example. Others are included in the Appendix One.

A limited measurement program was executed to acquire salinity, temperature, and current distributions so that the performance of the model in describing the small-scale spatial variations and the seasonal scale evolution of the variables could be critically assessed. The comparison of the model simulations to observed temperatures is excellent. In the study region, model temperatures were generally well within ±1°C of measured values (See Figure 6.3-2 and 6.4.2). Salinities are generally within ±1 ppt (Figure 6.3-3 and 6.4.3). That the spatial and temporal structures of the temperature, salinity, and velocity fields captured by the model show excellent agreement with the field studies clearly supports the model's use as a tool to interpolate spatially between the observations for the purpose of making maps of the ecologically important characteristics of the bottom environment.

The mean temperature and salinity maps were generated for each month and provide insights into the temporal and spatial variability of these measures within the Phase II area. It is well known that LIS experiences some of the largest seasonal variation in water temperature, which is supported by the model results, with a mean low of 3.5° C occurring particularly in the western regions of the area in the months of February and March. The same western area experiences high water temperature (23°C) in August. Salinity was not surprisingly more stable over the course of the year, with higher salinities occurring in the eastern end of the area and lower salinities near the mouth of the Connecticut during the spring and summer months.

Water currents directly affect benthic organisms through bottom stress, which is a measure of the force the current creates over the seabed. Bottom stress maps were generated for tidal mean, maximum tidal and overall maximum and in each case illustrated similar patterns, with highest values in and around the Race, eastern Fishers Island Sound and to some degree west of the mouth of the Connecticut River. Bottom stress is a key factor in the distribution of sediment types through scouring in high current areas and deposition in lower current regimes. Additionally, bottom stress influences rates of recruitment and feeding by benthic taxa, can impact attachment to the substrates and survivorship during storm events. For these reasons the bottom stress map products were utilized by the Ecological Characterization team as a critical element in the development of the Integrated Habitat Map product.

6.8 References

Bennett, D. C., J. O'Donnell, W.F. Bohlen and A.E. Houk, (2010). Tides and Overtides in Long Island Sound. *Journal of Marine Research*, 68(1), 1-35.

Blumberg, A.F. , L.A. Khan and J. P. St. John, (1999). *Three-Dimensional Hydrodynamic Simulations of the New York Harbor, Long Island Sound and the New York Bight*, Journal of Hydraulic Engineering, 125 799-816.

Bogden, P. S., O'Donnell, J., (1998). Generalized inverse with shipboard current measurements: Tidal and nontidal flows in Long Island Sound. *Journal of Marine Research* 56 (5), 995.

Bokuniewicz, H. J. and R. B. Gordon, (1980a).: Sediment transport and deposition in Long Island Sound. *Advances in Geophysics*, 22, 69-106.

Chen, C.H. Huang, R.C. Beardsley, H. Liu, Q. Xu and G. Cowles, (2007). A finite-volume numerical approach for coastal ocean circulation studies: comparisons with finite difference models. *Journal of Geophysical Research*, 112, C03018, doi:10.1029/2006JC003485.

Crowley, H., (2005). *The seasonal evolution of thermohaline circulation in Long Island Sound*. PhD Dissertation, Marine Sciences Research Center, Stony Brook University, Stony Brook, NY, 142 pp.

Fribance, D. B., J. O'Donnell, *and* A. Houk *(*2013*),* Residual circulation in western Long Island Sound*, Journal of Geophysical Research, Oceans,* 118*,* 4727–4745*, doi:*10.1002/jgrc.20329.

Ganju, N. M. J. Brush, B. Rashleigh, A.L. Aretxabaleta, P. del Barrio, J.S. Grear, L.A. Harris, S.J. Lake, G. McCardell, J. O'Donnell, D.K. Ralston, R.P. Signell, J.M. Testa and J.M.P. Vaudrey. (2016). Progress and Challenges in Coupled Hydrodynamic-Ecological Estuarine Modeling. *Estuaries and Coasts*. 39(2), 311-332.

Hao, Y. , (2008). *Tidal and residual circulation in Long Island Sound*. PhD Dissertation, Marine Sciences Research Center, Stony Brook University, Stony Brook, NY, 70 pp.

Kaputa, N. P. and C. B. Olsen, (2000). State of CT. Dept. of Env. Protection, Long Island Sound Ambient Water Quality Monitoring Program: Summer Hypoxia Monitoring Survey '91-'98 Data Review

Kenefick, A.M., (1985). Barotropic M2 tides and tidal currents in Long Island Sound: a numerical model. *Journal of Coastal Research*, v. 1, 117-128.

Murphy, D.L., (1979). *A Numerical Investigation into the Physical Parameters which Determine the Residual Drift in Long Island Sound*. Ph.D. Dissertation, Dept. of Marine Sciences, The University of Connecticut.

O'Donnell, J. and W.F. Bohlen, (2003). *The structure and variability of the residual circulation in Long Island Sound.* Final Report, Connecticut Department of Environmental Protection, Hartford, CT. Grant CWF 325-R, 303 p. Available at: (http://www.lisrc.uconn.edu/DataCatalog/DocumentImages/pdf/Odonnell_Bohlen_2003.pdf)

O'Donnell, J., R. E. Wilson, K. Lwiza, M. Whitney, W. F. Bohlen, D. Codiga, T. Fake, D. Fribance, M. Bowman, and J. Varekamp (2013). The Physical Oceanography of Long Island Sound. In *Long Island Sound: Prospects for the Urban Sea.* Latimer, J.S., Tedesco, M., Swanson, R.L., Yarish, C., Stacey, P., Garza, C. (Eds.), ISBN-13: 978-1461461258

R. Pawlowicz, B. Beardsley, and S. Lentz, (2002), Classical tidal harmonic analysis including error estimates in MATLAB using T_TIDE, *Computers and Geosciences* (28), 929-937.

Rivera Lemus, E. R., (2008). *Wind waves in central Long Island Sound : a comparison of observations to an analytical expression*. Masters Thesis, Department of Marine Sciences, University of Connecticut.

Schmalz, R.A., Devine, M.F., and Richardson, P.H., (1994). *Residual circulation and thermohaline structure, Long Island Sound Oceanography* Project Summary Report, Volume 2, NOAA Technical Report NOS-OES-003, National Oceanic and Atmospheric Administration, Rockville, MD.

Shchepetkin, A. F. and J. C. McWilliams, (2005). Regional Ocean Model System: a split-explicit ocean model with a free-surface and topography-following vertical coordinate. *Ocean Modelling,* 9, 347–404.

Signell, R., J. List and A. Farris, (2000). Bottom currents and sediment transport in Long Island Sound: a modeling study, *Journal of Coastal Research* 16, 551–566.

Swanson, R.L., (1976). Tides. MESA New York Bight Atlas Monograph, 4. New York Sea Grant Institute. Albany, New York.

Valle-Levinson, A. and R.E. Wilson, (1994a). Effects of Sill Bathymetry, oscillating barotropic forcing and vertical mixing on estuary ocean exchange, *Journal of Geophysical Research,* 99(C6), 12667-12681.

Valle-Levinson, A., and R. E. Wilson, (1994b). Effects of sill processes and tidal forcing on exchange in eastern Long Island Sound, *Journal of Geophysical Research*, 99(C6), 12667-12681Valle-Levinson et al. (1995)

Wilson, R.E. and R.L. Swanson. (2005). A perspective on bottom water temperature anomalies in Long Island Sound during the 1999 Lobster Mortality event. *Journal of Shellfish Research,* 24, 825–830.